AD-A172 467 BLAST TRAUMA THE EFFECT ON HEARING(U) TEXAS UNIV AT DALLAS CALLIER CENTER FOR COMMUNICATION DISORDERS R P HAMERNIK ET AL. JUL 83 DAMD17-80-C-0133 1/4

UNCLASSIFIED F/G 6/19 NL

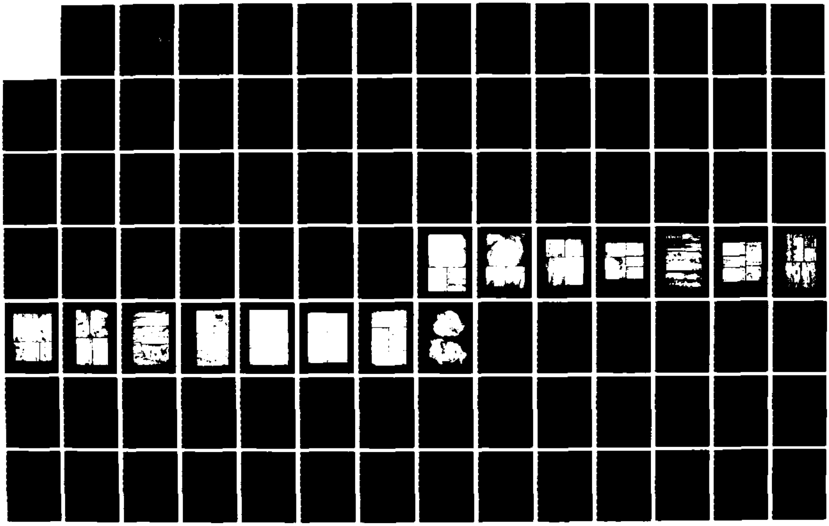

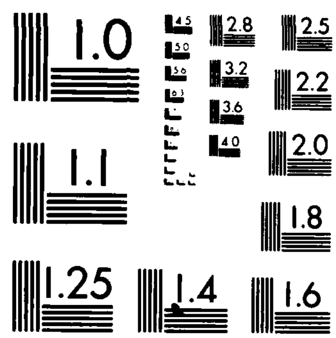


MICROCOPY RESOLUTION TEST CHART
NATIONAL BUREAU OF STANDARDS 1963-A

PHOTOGRAPH THIS SHEET

AD-A172 467

DTIC ACCESSION NUMBER

LEVEL

BLAST TRAUMA:
THE EFFECT ON HEARING
JULY 1983

INVENTORY

(1)

DOCUMENT IDENTIFICATION

DISTRIBUTION STATEMENT A
Approved for public release;
Distribution Unlimited

DISTRIBUTION STATEMENT

QUALITY INSPECTED 1

| ACCESSION FOR | | |
|---|---|---|
| NTIS | GRA&I | ☑ |
| DTIC | TAB | ☐ |
| UNANNOUNCED | | ☐ |
| JUSTIFICATION | | |
| BY | | |
| DISTRIBUTION / | | |
| AVAILABILITY CODES | | |
| DIST | AVAIL AND/OR SPECIAL | |
| A-1 | 23 | 2 |

DISTRIBUTION STAMP

DTIC
ELECTE
OCT 0 3 1986
S D
D

DATE ACCESSIONED

DATE RETURNED

86 10 [illegible]

DATE RECEIVED IN DTIC

REGISTERED OR CERTIFIED NO.

PHOTOGRAPH THIS SHEET AND RETURN TO DTIC-DDAC

DTIC FORM 70A DEC 83

DOCUMENT PROCESSING SHEET

PREVIOUS EDITION MAY BE USED UNTIL STOCK IS EXHAUSTED.

# DISCLAIMER NOTICE

AD-A172 467

AD ________________

# BLAST TRAUMA: THE EFFECT ON HEARING

ANNUAL/FINAL

Roger P. Hamernik, Ph.D.
Richard J. Salvi, Ph.D.
Donald Henderson, Ph.D.

July 1983

Supported by

U.S. ARMY MEDICAL RESEARCH AND DEVELOPMENT COMMAND
Fort Detrick, Frederick, Maryland 21701-5012

Contract Number DAMD17-80-C-0133

University of Texas at Dallas
Dallas, Texas 75235

SECURITY CLASSIFICATION OF THIS PAGE

# REPORT DOCUMENTATION PAGE

| | |
|---|---|
| 1a. REPORT SECURITY CLASSIFICATION<br>Unclassified | 1b. RESTRICTIVE MARKINGS |
| 2a. SECURITY CLASSIFICATION AUTHORITY | 3. DISTRIBUTION / AVAILABILITY OF REPORT<br>Approved for public release;<br>distribution unlimited |
| 2b. DECLASSIFICATION / DOWNGRADING SCHEDULE | |
| 4. PERFORMING ORGANIZATION REPORT NUMBER(S) | 5. MONITORING ORGANIZATION REPORT NUMBER(S) |
| 6a. NAME OF PERFORMING ORGANIZATION<br>University of Texas at Dallas<br>6b. OFFICE SYMBOL (If applicable) | 7a. NAME OF MONITORING ORGANIZATION |
| 6c. ADDRESS (City, State, and ZIP Code)<br>Dallas, TX 75235 | 7b. ADDRESS (City, State, and ZIP Code) |
| 8a. NAME OF FUNDING / SPONSORING ORGANIZATION U.S. Army Medical Research & Development Command<br>8b. OFFICE SYMBOL (If applicable) | 9. PROCUREMENT INSTRUMENT IDENTIFICATION NUMBER<br>DAMD17-80-C-0133 |
| 8c. ADDRESS (City, State, and ZIP Code)<br>Fort Detrick, Frederick, MD 21701-5012 | 10. SOURCE OF FUNDING NUMBERS<br>PROGRAM ELEMENT NO. 62773A<br>PROJECT NO. 3E162.773A819<br>TASK NO. 00<br>WORK UNIT ACCESSION NO. 039 |

11. TITLE (Include Security Classification)
(U) Blast Trauma: The Effect on Hearing

12. PERSONAL AUTHOR(S)
Roger P. Hamernik, Ph.D., Richard J. Salvi, Ph.D., and Donald Henderson, Ph.D.

| 13a. TYPE OF REPORT | 13b. TIME COVERED | 14. DATE OF REPORT (Year, Month, Day) | 15. PAGE COUNT |
|---|---|---|---|
| Annual/Final | FROM 8/1/80 TO 7/31/83 | July 1983 | |

16. SUPPLEMENTARY NOTATION

| 17. COSATI CODES | | |
|---|---|---|
| FIELD | GROUP | SUB-GROUP |
| 06 | 10 | |
| 20 | 01 | |

18. SUBJECT TERMS (Continue on reverse if necessary and identify by block number)
Blast trauma; impulse noise; hearing loss; tuning curves; auditory nerve; cochlea; hair cells; evoked response.

19. ABSTRACT (Continue on reverse if necessary and identify by block number)
The purpose of this research was to study the effects of impulse noise (blast trauma) on auditory function. The impulse noise was produced by a compressed air-driven shock tube; the exposures were varied to produce a range of cochlear lesions. The effects of impulse noise was studied by measuring: (1) changes in pure tone thresholds and tuning curves obtained behaviorally or with the auditory evoked response, (2) changes in the thresholds and tuning curves of single auditory nerve fibers, (3) changes in cochlear anatomy as determined by light and electron microscopy. The goal of the study was to relate the audiometric and physiological data with the cochlear pathologies in order to understand the nature of auditory pathologies produced by exposure to blast waves.

| | |
|---|---|
| 20. DISTRIBUTION / AVAILABILITY OF ABSTRACT<br>☐ UNCLASSIFIED/UNLIMITED ☒ SAME AS RPT. ☐ DTIC USERS | 21. ABSTRACT SECURITY CLASSIFICATION |
| 22a. NAME OF RESPONSIBLE INDIVIDUAL<br>Mrs. Virginia Miller | 22b. TELEPHONE (Include Area Code) 301-663-7325<br>22c. OFFICE SYMBOL SGRD-RMI-S |

DD FORM 1473, 84 MAR

83 APR edition may be used until exhausted.
All other editions are obsolete.

SECURITY CLASSIFICATION OF THIS PAGE

## Summary

The purpose of this projects was to determine how high intensity blast waves (impulse noise) affect the auditory system. Audiometric, physiological and anatomical measurements were obtained from chinchillas that were exposed to impulses of 155-160 dB peak sound pressure level. The traumatic effects of the exposures were quite variable; some animals were essentially unaffected while others showed large threshold shifts and significant hair cell losses. At frequencies where the exposure caused a hearing loss there was also a loss of frequency selectivity as determined by either evoked response or psychophysical tuning curves (PTC). After exposure, the tips of the psychophysical and evoked response tuning curves were frequently displaced to higher or lower frequencies by as much as an octave. The thresholds of single auditory nerve fibers with characteristic frequencies corresponding to the hearing loss were also elevated; the neural threshold shifts were often larger than those predicted from the hearing loss data. Units with elevated thresholds had abnormally broad tuning curves (TC). Sometimes the thresholds in the tail of the tuning curve were <u>hypersensitive</u> and lower than the threshold at the characteristic frequency; consequently, the tuning curves were "W" shaped. The phenomenon of tail hypersensitivity may contribute to the displacement of the tips of psychophysical and evoked response tuning curves. The loss of cochlear hair cells was, in general, correlated with neural and behavioral threshold shifts; however, sometimes there were slight threshold elevations in the absence of any significant hair cell loss. Damage to the cochlea as a result of exposure to blast trauma has been thought to result from direct mechanical damage to the tissue as well as subtle damage resulting form metabolic depletion. Direct mechanical damage to the cochlea (e.g., tearing and ripping of the organ of Corti from the basilar membrane) was shown to occur immediately after impulse noise exposure. Even when animals were exposed to the same type of blast wave, there was considerable variability in the degree and pattern of hearing loss, the changes in tuning, and the pattern of cochlear histopathologies.

## Foreward

The authors wish to acknowledge the technical assistance of Ron Milone, Fred Farzi, and George Turrentine who helped to collect and analyze much of the data. Special thanks are given to Harley Willett, Perry Mobley, and Mark Phillips of Technical Services who designed, fabricated, and repaired many of the pieces of instrumentation used in the experiments. The authors are also extremely grateful to Dr. William Ahroon for his efforts in organizing and developing much of the computer software used in the experiments and for his help in collecting some of the data.

## Table of Contents



## List of Figures

3.3.52 Chinchilla 366: cochleogram
3.3.53 Chinchilla 459: AER audiogram
3.3.54 Chinchilla 459: 0.5 kHz AER TC
3.3.55 Chinchilla 459: 1.0 kHz AER TC
3.3.56 Chinchilla 459: 2.0 kHz AER TC
3.3.57 Chinchilla 459: 4.0 kHz AER TC
3.3.58 Chinchilla 459: 8.0 kHz AER TC
3.3.59 Chinchilla 459: 11.2 kHz AER TC
3.3.60 Chinchilla 459: 0.5 kHz single unit TC
3.3.61 Chinchilla 459: 1.0 kHz single unit TC
3.3.62 Chinchilla 459: 2.0 kHz single unit TC
3.3.63 Chinchilla 459: 4.0 kHz single unit TC
3.3.64 Chinchilla 459: 8.0 kHz single unit TC
3.3.65 Chinchilla 459: 11.2 kHz single unit TC
3.3.66 Chinchilla 459: single unit TC
3.3.67 Chinchilla 459: cochleogram
3.3.68 Chinchilla 510: AER audiograms
3.3.69 Chinchilla 510: 0.5 kHz AER TC
3.3.70 Chinchilla 510: 1.0 kHz AER TC
3.3.71 Chinchilla 510: 2.0 kHz AER TC
3.3.72 Chinchilla 510: 4.0 kHz AER TC
3.3.73 Chinchilla 510: 8.0 kHz AER TC
3.3.74 Chinchilla 510: 11.2 kHz AER TC
3.3.75 Chinchilla 510: cochleogram
3.3.76 Chinchilla 543: AER audiograms
3.3.77 Chinchilla 543: 0.5 kHz AER TC
3.3.78 Chinchilla 543: 1.0 kHz AER TC
3.3.79 Chinchilla 543: 2.0 kHz AER TC
3.3.80 Chinchilla 543: 4.0 kHz AER TC
3.3.81 Chinchilla 543: 8.0 kHz AER TC
3.3.82 Chinchilla 543: 11.2 kHz AER TC
3.3.83 Chinchilla 543: 0.5 kHz single unit TC
3.3.84 Chinchilla 543: 1.0 kHz single unit TC
3.3.85 Chinchilla 543: 2.0 kHz single unit TC
3.3.86 Chinchilla 543: 4.0 kHz single unit TC
3.3.87 Chinchilla 543: 8.0 kHz single unit TC
3.3.88 Chinchilla 543: 11.2 kHz single unit TC
3.3.89 Chinchilla 543: cochleogram
3.3.90 Chinchilla 547: AER audiograms
3.3.91 Chinchilla 547: 0.5 kHz AER TC
3.3.92 Chinchilla 547: 1.0 kHz AER TC
3.3.93 Chinchilla 547: 2.0 kHz AER TC
3.3.94 Chinchilla 547: 4.0 kHz AER TC
3.3.95 Chinchilla 547: 8.0 kHz AER TC
3.3.96 Chinchilla 547: 11.2 kHz AER TC
3.3.97 Chinchilla 552: AER audiograms
3.3.98 Chinchilla 552: 0.5 kHz AER TC
3.3.99 Chinchilla 552: 1.0 kHz AER TC
3.3.100 Chinchilla 552: 2.0 kHz AER TC
3.3.101 Chinchilla 552: 4.0 kHz AER TC
3.3.102 Chinchilla 552: 8.0 kHz AER TC
3.3.103 Chinchilla 552: 11.2 kHz AER TC
3.3.104 Chinchilla 552: 0.5 kHz single unit TC
3.3.105 Chinchilla 552: 1.0 kHz single unit TC

| | | |
|---|---|---|
| 3.3.106 | Chinchilla 552: | 2.0 kHz single unit TC |
| 3.3.107 | Chinchilla 552: | 4.0 kHz single unit TC |
| 3.3.108 | Chinchilla 552: | 8.0 kHz single unit TC |
| 3.3.109 | Chinchilla 552: | 11.2 kHz single unit TC |
| 3.3.110 | Chinchilla 557: | AER audiograms |
| 3.3.111 | Chinchilla 557: | 0.5 kHz AER TC |
| 3.3.112 | Chinchilla 557: | 1.0 kHz AER TC |
| 3.3.113 | Chinchilla 557: | 2.0 kHz AER TC |
| 3.3.114 | Chinchilla 557: | 4.0 kHz AER TC |
| 3.3.115 | Chinchilla 557: | 8.0 kHz AER TC |
| 3.3.116 | Chinchilla 557: | 11.2 kHz AER TC |
| 3.3.117 | Chinchilla 603: | AER audiograms |
| 3.3.118 | Chinchilla 603: | 0.5 kHz AER TC |
| 3.3.119 | Chinchilla 603: | 1.0 kHz AER TC |
| 3.3.120 | Chinchilla 603: | 2.0 kHz AER TC |
| 3.3.121 | Chinchilla 603: | 4.0 kHz AER TC |
| 3.3.122 | Chinchilla 603: | 8.0 kHz AER TC |
| 3.3.123 | Chinchilla 603: | 11.2 kHz AER TC |
| 3.3.124 | Chinchilla 603: | 0.5 kHz single unit TC |
| 3.3.125 | Chinchilla 603: | 1.0 kHz single unit TC |
| 3.3.126 | Chinchilla 603: | 2.0 kHz single unit TC |
| 3.3.127 | Chinchilla 603: | 4.0 kHz single unit TC |
| 3.3.128 | Chinchilla 603: | 8.0 kHz single unit TC |
| 3.3.129 | Chinchilla 603: | 11.2 kHz single unit TC |
| 3.3.130 | Chinchilla 603: | cochleogram |
| 3.3.131 | Chinchilla 607: | AER audiograms |
| 3.3.132 | Chinchilla 607: | 0.5 kHz AER TC |
| 3.3.133 | Chinchilla 607: | 1.0 kHz AER TC |
| 3.3.134 | Chinchilla 607: | 2.0 kHz AER TC |
| 3.3.135 | Chinchilla 607: | 4.0 kHz AER TC |
| 3.3.136 | Chinchilla 607: | 8.0 kHz AER TC |
| 3.3.137 | Chinchilla 607: | 11.2 kHz AER TC |
| 3.3.138 | Chinchilla 607: | 0.5 kHz single unit TC |
| 3.3.139 | Chinchilla 607: | 1.0 kHz single unit TC |
| 3.3.140 | Chinchilla 607: | 2.0 kHz single unit TC |
| 3.3.141 | Chinchilla 607: | 4.0 kHz single unit TC |
| 3.3.142 | Chinchilla 607: | 8.0 kHz single unit TC |
| 3.3.143 | Chinchilla 607: | 11.2 kHz single unit TC |
| 3.3.144 | Chinchilla 607: | cochleograms |
| 3.3.145 | Chinchilla 750: | AER audiograms |
| 3.3.146 | Chinchilla 750: | 0.5 kHz AER TC |
| 3.3.147 | Chinchilla 750: | 1.0 kHz AER TC |
| 3.3.148 | Chinchilla 750: | 2.0 kHz AER TC |
| 3.3.149 | Chinchilla 750: | 4.0 kHz AER TC |
| 3.3.150 | Chinchilla 750: | 8.0 kHz AER TC |
| 3.3.151 | Chinchilla 750: | 11.2 kHz AER TC |
| 3.3.152 | Chinchilla 750: | cochleogram |
| 3.3.153 | Chinchilla 820: | AER audiograms |
| 3.3.154 | Chinchilla 820: | 0.5 kHz AER TC |
| 3.3.155 | Chinchilla 820: | 1.0 kHz AER TC |
| 3.3.156 | Chinchilla 820: | 2.0 kHz AER TC |
| 3.3.157 | Chinchilla 820: | 4.0 kHz AER TC |
| 3.3.158 | Chinchilla 820: | 8.0 kHz AER TC |
| 3.3.159 | Chinchilla 820: | 11.2 kHz AER TC |

3.3.160 Chinchilla 820: cochleograms
3.3.161 Chinchilla 852: AER audiograms
3.3.162 Chinchilla 852: 0.5 kHz AER TC
3.3.163 Chinchilla 852: 1.0 kHz AER TC
3.3.164 Chinchilla 852: 2.0 kHz AER TC
3.3.165 Chinchilla 852: 4.0 kHz AER TC
3.3.166 Chinchilla 852: 8.0 kHz AER TC
3.3.167 Chinchilla 852: 11.2 kHz AER TC
3.3.168 Chinchilla 852: 1.0 kHz single unit TC
3.3.169 Chinchilla 852: 2.0 kHz single unit TC
3.3.170 Chinchilla 852: 4.0 kHz single unit TC
3.3.171 Chinchilla 852: cochleogram
3.3.172 Chinchilla 860: AER audiograms
3.3.173 Chinchilla 860: 0.5 kHz AER TC
3.3.174 Chinchilla 860: 1.0 kHz AER TC
3.3.175 Chinchilla 860: 2.0 kHz AER TC
3.3.176 Chinchilla 860: 4.0 kHz AER TC
3.3.177 Chinchilla 860: 8.0 kHz AER TC
3.3.178 Chinchilla 860: 11.2 kHz AER TC
3.3.179 Chinchilla 860: 0.5 kHz single unit TC
3.3.180 Chinchilla 860: 1.0 kHz single unit TC
3.3.181 Chinchilla 860: 2.0 kHz single unit TC
3.3.182 Chinchilla 860: 4.0 kHz single unit TC
3.3.183 Chinchilla 860: 8.0 kHz single unit TC
3.3.184 Chinchilla 860: 11.2 kHz single unit TC
3.3.185 Chinchilla 860: cochleogram
3.3.186 Chinchilla 925: AER audiograms
3.3.187 Chinchilla 925: 0.5 kHz AER TC
3.3.188 Chinchilla 925: 1.0 kHz AER TC
3.3.189 Chinchilla 925: 2.0 kHz AER TC
3.3.190 Chinchilla 925: 4.0 kHz AER TC
3.3.191 Chinchilla 925: 8.0 kHz AER TC
3.3.192 Chinchilla 925: 11.2 kHz AER TC
3.3.193 Chinchilla 925: 0.5 kHz single unit TC
3.3.194 Chinchilla 925: 1.0 kHz single unit TC
3.3.195 Chinchilla 925: 2.0 kHz single unit TC
3.3.196 Chinchilla 925: 4.0 kHz single unit TC
3.3.197 Chinchilla 925: 8.0 kHz single unit TC
3.3.198 Chinchilla 925: 11.2 kHz single unit TC
3.3.199 Chinchilla 925: cochleogram
3.3.200 Chinchilla 940: AER audiograms
3.3.201 Chinchilla 940: 0.5 kHz AER TC
3.3.202 Chinchilla 940: 1.0 kHz AER TC
3.3.203 Chinchilla 940: 2.0 kHz AER TC
3.3.204 Chinchilla 940: 4.0 kHz AER TC
3.3.205 Chinchilla 940: 8.0 kHz AER TC
3.3.206 Chinchilla 940: 11.2 kHz AER TC
3.3.207 Chinchilla 940: 0.5 kHz single unit TC
3.3.208 Chinchilla 940: 1.0 kHz single unit TC
3.3.209 Chinchilla 940: 2.0 kHz single unit TC
3.3.210 Chinchilla 940: 4.0 kHz single unit TC
3.3.211 Chinchilla 940: 8.0 kHz single unit TC
3.3.212 Chinchilla 940: cochleogram

## List of Appendices

1. Salvi, R. J., Ahroon, W. A., Perry, J. W., Gunnarson, A. D., and Henderson, D. (1982). "Comparison of psychophysical and evoked-potential tuning curves in the chinchilla." Am. J. Otolaryngol., 3, 408-416.

2. Shaddock, L. C., Hamernik, R. P., Axelsson, A. (1983). "Vascular and sensory cell changes in the cochlea induced by elevated temperature and noise." Submitted Hearing Res.

3. Shaddock, L. C., Hamernik, R. P., Axelsson, A. (1983). "The effect of high-intensity impulse noise on the vascular system of the chinchilla cochlea." Submitted Ann. Oto. Rhino. Laryngol.

4. Hamernik, R. P., Turrentine, G., Salvi, R., Henderson, D., Roberto, M. (1983). " Scanning electron microscopic study of impulse noise induced mechanical damage in the cochlea." J. Acoust. Soc. Amer. 73, S81(A).

## 1.0 Introduction

Military personnel are frequently exposed to brief acoustic transients of high intensity (blast waves) which are particularly hazardous to hearing. It has proved exceedingly difficult to determine which impulse noise exposures are "safe" because the amount of hearing loss resulting from a particular impulse noise exposure is highly variable both within and across subjects (Luz and Hodge, 1971; Blakeslee, et al., 1978). Furthermore, impulse noise behaves much differently than continuous noise in terms of the growth of hearing loss with stimulus level (Walker, 1970; McRobert and Ward, 1973; Eames et al., 1973) and the recovery of hearing following exposure (Luz and Hodge, 1971; Henderson et al., 1974). The problems involved in developing a realistic damage risk criteria for impulse noise are compounded by the fact that relatively little is known about how impulse noise affects the auditory system.

Earlier investigations have suggested that impulse noise might affect the anatomical structures of the cochlea in two different ways depending on the stimulus intensity. At low levels, metabolic changes such as atrophy of the vascular supply, depletion of enzymes, swelling of nerve endings, etc. would be the primary mechanism for cochlear destruction. High intensity impulses, on the other hand, would tend to produce immediate structural changes such as tears in the reticular lamina and rupture of tight cell junctions (Luz and Hodge, 1971). Although the proposed mechanisms of cochlear damage resulting from impulse noise exposure are interesting, there have been few comprehensive attempts at understanding what effects the various cochlear histopathologies have on hearing performance and on neural activity in the cochlea. Furthermore, there is little direct evidence on the mechanical effects that impulse noise has on the cochlea, particularly immediately after exposure. Until the underlying mechanisms of impulse noise induced hearing loss are better understood in terms of anatomical, physiological and audiometric changes, it may be difficult to develop a satisfactory damage risk criteria for impulse noise exposure.

The purpose of this project was to develop a comprehensive understanding of the effects that blast wave exposure has on the auditory system. The approach was to assess the audiometric effects of impulse noise exposure by obtaining pre- and post-exposure measures of threshold and frequency selectivity. At the end of the audiometric testing , the animals were prepared for single unit recordings from auditory nerve fibers. Estimates of each unit's threshold, frequency selectivity, and spontaneous activity were obtained from a large sample of auditory nerve fibers. Since most fibers in the auditory nerve innervate a single hair cell, the response of each fiber reflects the output of a limited region of the basilar membrane. At the end of the physiological experiments, the cochleas were fixed and analyzed by light or scanning electron microscopy to determine the pattern of hair cell loss and the other types of structural abnormalities in the cochlea. The goal of this project was to correlate the audiometric and physiological changes with the histopathologies in the cochlea. Additional anatomical studies were carried out to determine what types of histological changes occur immediately after impulse noise exposure, i.e., structural or metabolic changes.

## 2.0 Methods

### 2.1 Subjects

Adult chinchillas were used as subjects. The chinchillas that were used for behavioral and evoked response testing were anesthetized (sodium pentobarbital 50 mg/kg I.P.) and made monaural by surgical destruction of the left cochlea. Those animals that were used exclusively for anatomical studies were binaural.

### 2.2 Behavioral Testing

Behavioral testing was based upon a shock avoidance conditioning paradigm (Blakeslee et al., 1978; Salvi et al., 1978). The animal's head was placed in a restraining yoke and was held in a standing position in the sound field. The animal registered a response by slight upward motion of the body which closes a microswitch. A modified tracking procedure was used to estimate the pure tone thresholds and the tone-on-tone masked thresholds. A stimulus trial consisted of a train of eight tone bursts (20 ms on, 5 ms rise-fall time, 2 bursts/sec). A response between bursts one and four was recorded as a Hit and was followed by a safety light (7.5 sec). If the animals failed to respond by the fifth burst the trial was scored as a Miss and pulsed shock (1-5 mA) was delivered to the animal's tail except near threshold.

Pure tone threshold testing began at a clearly audible level and the intensity was reduced by 10 dB after a correct response or increased in 10 dB after a Miss. After the second reversal, the step size was decreased to 5 dB and 4 additional threshold crossings were obtained and used to estimate threshold. A total of 48-72 threshold crossings were used to estimate threshold.

The procedures for obtaining psychophysical tuning curves have been described previously (Salvi et al., 1982). A continuous masking tone was used to mask the probe tone. The probe tone (same as for threshold testing) was presented at 15 dB sensation level (SL) and introduced at random intervals. The animals were trained to ignore the continuous masker and respond only when the probe tone was presented. A modified tracking procedure was used to estimate the level of the continuous masker necessary to mask the probe tone. The masker level was initially varied in 10 dB steps and after the second reversal the step size was reduced to 5 dB.

### 2.3 Evoked response testing

Chronic electrodes were implanted in the vicinity of the inferior colliculus using procedures outlined previously (Henderson et al., 1973; Salvi et al., 1982). The animals were tested using the same restraining yoke and acoustic equipment as that employed in the behavioral experiments. The acoustic signals for evoked response testing were identical to those used in the behavioral experiments except that the probe tone was presented at a rate of 10/s.

The electrical potentials were filtered (300-1500 Hz), amplified (20,000 to 50,000 times) and led to a signal averager with artifact reject capability. The data were sampled at 25 kHz over 512 points to obtain a 20.48 ms analysis window. Normally, 512 samples were collected; however, if a clear response was present the averaging process was terminated earlier. No effort was made to measure the actual amplitude of the response since only the transition from the presence to the absence of the evoked response was used to make a judgement regarding the absolute or masked thresholds.

Pure tone threshold testing began at a level that produced a clear evoked response and then the level was reduced in 10 dB steps until the response was just above the background noise. The step size was then reduced to 5 dB and additional samples were taken. Threshold was the point midway between the highest intensity where a response was absent and the lowest intensity where a response was present.

Evoked response masked thresholds were determined with the intensity of the probe tone 15 dB above the evoked response threshold (see Salvi et al., 1982 for details). A continuous pure tone masker was then introduced and increased in level until the evoked response produced by the probe was nearly obliterated. Then the intensity of the masker was varied in 5 dB steps and additional samples were taken. Masked threshold was the intensity midway between the lowest intensity where a response was absent and the highest intensity where a response was present. Masked threshold was determined using masker frequencies above and below the probe frequency in order to obtain a tuning curve.

### 2.4 Single unit recordings

Details of the experimental procedures can be found in earlier reports (Salvi et al., 1978; Salvi et al., 1979; Salvi et al., 1982). The animals were anesthetized with Dial in urethane and tracheotomized. A ball electrode was place on the round window to monitor the compound action potential. Then the auditory nerve was exposed by a posterior fossa approach. Glass microelectrodes (3 M NaCl, 15-40 Mohms) were used to record the activity of single fibers. Spontaneous acitivity was sampled from each fiber for 10 to 15 seconds and then tuning curves were measured using a computer automated threshold tracking procedure which uses a 1 spike difference between the tone and no-tone interval as the criterion for threshold (Liberman, 1978; Salvi et al., 1982).

## 2.5 Cochleograms

At the end of the physiological experiments, the animals were killed by decapitation. Their cochleas were fixed in cold, 2.5% veronal acetate buffered glutaraldehyde (pH 7.3) and post-fixed in 1% veronal acetate buffered $OsO_4$. If the animal had: (1) suffered a sizeable threshold shift or if significant changes in tuning had occured, and (2) if a large sample of single unit thresholds were obtained, then the cochlea was embedded in Spurr's Low Viscosity Resin to allow a more detailed analysis of the cochlea. Otherwise the sensory epithelium was dissected out of the cochlea and mounted in glycerin. With both procedures, a cochleogram was plotted using hair cell counts averaged over 0.24 mm intervals of the organ of Corti. A hair cell was counted as present if the cell-body cuticular plate complex was intact.

## 2.6 Scanning electron microscopy

The animals that were prepared for scanning electron microscopy were killed by decapitation. The bullae were quickly removed and the cochlea widely exposed. The round window membrane was punctured and the stapes was removed. Cold 5% glutaraldehyde in veronal acetate buffer at pH 7.3 (630 mOs) was gently perfused through the cochlea through the round window with a fine pipette. The fixed cochleas were stored overnight in a refrigerator. On the following day the cochleas were post-fixed with a glutaraldehyde/osmium mixture in a 5:2 ratio. The gluteraldehyde was prepared as in the initial fixation and the osmium was a 2% aqueous solution. The cochleas were post-fixed for 15 minutes then dehydrated with cold 35% ETOH and dissected down to the desired turn. During the dissection, the stria vascularis and spiral ligament were removed to roughly the level of the spiral prominence. The basilar membrane was left attached to the bony modiolus and the outer bony capsule. Reissner's membrane was also removed. The remaining cochlea was then rapidly dehydrated in a cold graded ETOH series (50, 70, 80, 95, 100%). The cochleas were then critical point dried with liquid $CO_2$ following standard procedures, except that no rapid pressure changes were allowed. Depressurization was over in a 10-15 minute period. The specimens were then placed in a Denton DV502 vacuum evaporator and gently brought under vacuum. Gold or gold-paladium was sputtered onto the specimens using the Denton DSM-5A triode (cold) sputtering head. Specimens were brought to ambient pressure using dry nitrogen and mounted on to a stub using conductive paint. The cochleas were then viewed using a JEOL JSM-35 Scanning Electron Microscope. Sixteen chinchillas followed this protocol at post-exposure survival times of 0 days (i.e., immediately after exposure), 1 day, 5 days, 10 days and 30 days.

## 2.7 Blast wave exposures

The animals were exposed to impulses generated by a compressed air-driven shock tube. The blast wave is delivered through a six foot exponential horn and delivered into an anechoic enclosure. The blast wave has a Friedlander pressure-time profile. The top panel in Figure 2.7.1 shows a typical pressure-time profile of the blast wave. The non-reverberant wave has a A-duration of 1 to 1.5 ms. The botton panel of Figure 2.7.1 shows the amplitude spectrum of the impulse. Much of the energy of the impulse is located at the low frequencies, i.e., below 300 Hz. The animals in the audiological and physiological experiments were exposed at grazing incidence. A total of 50 impulses were presented to each animal at the rate of one per minute. The impulses were presented at either 155 dB or 160 dB. The animals that were used in the electron microscopy studies were exposed to 100 impulses (160 dB) at the rate of two per minute at normal incidence.

## 3.0 Results

The results section has been divided into three sections that reflect the major advances made during the project. The first section deals with methodological advances. The second section is a scanning electron microscopic (SEM) investigation that is concerned with the growth and development of cochlear histopathologies resulting from impulse noise exposure. The third section examines the anatomical effects that occur after impulse noise exposure and attempts to relate these changes to the audiometric and physiological measures obtained from the same animal.

## 3.1 Methodological advances

Auditory evoked response tuning curves: Psychophysical tuning curves (PTC) have been used extensively in human studies to obtain estimates of frequency selectivity in normal and hearing impaired listeners (Chistovich, 1957; Small, 1959; Wightman et al., 1977). Psychophysical tuning curves can also be collected from animals (McGee et al., 1976; Salvi et al., 1982); unfortunately, many months of training may be needed to obtain a sample of four to six tuning curves. At the start of this project, we had collected psychophysical tuning curves from approximately eight chinchillas, but over half of the animals died from unknown causes before the anatomical and physiological measurements could be obtained. Consequently, a great deal of time and effort was expended without accomplishing our objective. At this point, we realized that we needed a more efficient method of obtaining tuning curves from the chinchilla if we were to achieve the objectives of the grant. A review of the literature suggested that it might be possible to obtain estimates of frequency selectivity using the evoked response of the chinchilla (Henderson et al., 1973; Mitchell and Fowler, 1980; Klein and

Mills, 1981).

The procedures for collecting evoked response tuning curves are outlined in the method section and in a recent publication (Salvi et al., 1982). Briefly, a probe tone at 15 dB above the evoked response threshold is used to elicit a clear evoked potential. Then a continuous pure tone masker is introduced and increased in intensity until it just abolishes the evoked response elicited by the probe tone. When the masking procedure is carried over a range of frequencies surrounding the probe frequency one obtains an evoked response tuning curve. The masked thresholds are lowest in the vicinity of the probe and rapidly increase with increasing separation between probe and masker frequency.

A comprehensive comparison between the evoked response and behavioral tuning curves has been published and a reprint can be found in Appendix 1 (Salvi et al., 1982). Briefly, the evoked response tuning curves have nearly the same shape as those obtained behaviorally; the only systematic difference between the two set of data was that the evoked potential tuning curves were elevated 5-15 above the psychophysical tuning curves. When the two types of tuning curves were normalized at their tips to account for the difference in sensitivity then there was virtually no difference between the tuning curves obtained with the two methods. In terms of effort expended, a set of six tuning curves requires about three to four weeks to obtain with the evoked response method while it takes approximately 6 months using behavioral conditioning methods.

In summary, it appears that the evoked potential tuning curves may provide a reasonably accurate substitute for the rather time-consuming psychophysical tuning curves, particularly when small differences in sensitivity are not considered important. This is especially true in studies of acoustic trauma where one is primarily interested in the changes in tuning rather than the absolute estimates of tuning.

## 3.2 Inner ear pathologies following blast wave exposure

This section will review the anatomical results of blast wave exposures in the chinchilla that were obtained using the scanning electron microscope (SEM). Two fundamentally different lesion patterns are discussed: (1) lesions that are produced by severe "mechanical" damage to the organ of Corti and (2) lesions that are more limited in extent and consist primarily of missing sensory cells with the structural elements of the organ of Corti remaining essentially intact. The progressive development of the lesion is followed over a period of 30 days. Based upon descriptive anatomy, the case is made that the severe "mechanical" type lesions produce a somewhat different pattern of sensory and supporting cell loss that has consequences for the mechanical transduction processes which take place in the cochlea. (Section 3.3 will attempt to relate the psychophysical and physioloigcal results to the different lesion patterns. Some animals discussed in Section 3.3, such as chinchilla 60 and 366, have cocnleas typical of the mechanical type lesions while other animals, such as chinchillas 459 and 820, have cochleas typical of the limited "non-mechanical" types of lesions). A number of papers have been published on the development of cochlear lesions following acoustic trauma. These papers have made a distinction between noise-induced direct mechanical damage to the cochlea and a pattern of damage that is primarily the result of metabolic processes (Beagley, 1965a-b; Stockwell et al., 1969; Voldrich, 1972; Voldrich and Ulenlova, 1980). There are comparatively few micrographs in the literature that convincingly document a true stress failure of the cochlear partition and the subsequent effects of such a lesion on the sensory elements.

3.2.1 Background: Blast waves, because of their very short duration (on the order of milliseconds), and high peak intensities, produce a mechanical impulse, $\int F\,dt$, which results in an extremely high stress loading on the vibrating cochlear partition. These excessive stresses result in a failure of the tight cell junctions and subsequent damage to the organ of Corti as a result of the intermixing of endolymph and perilymph. The following micrographs illustrate the sequence of events that take place on the organ of Corti when segments of the organ are destroyed by blast waves.

The SEM, because of its suitability for viewing the surface structure of large areas of tissue, was chosen to document the progressive development of the blast wave induced lesion. A detailed protocol for all the histological procedures is presented in the Method section.

3.2.2 Results from normal, control animals: Figure 3.2.1 illustrates several views of the sensory elements of the normal organ of Corti. Plate A in Figure 3.2.1 is a low magnification view of the cochlea, dissected down to approximately the first turn. This is the area in which the majority of the blast wave lesions were found, and is the location in which the greatest mechanical damage originated. The arrows in plate A in Figure 3.2.1 indicate the spiralling area of the organ of Corti (note the uniform appearance and texture of the tissue; compare with Figure 3.2.2). Plates B, C, and D in Figure 3.2.1 are enlargements showing areas of sensory cells from the cochlea shown in plate A. Note the regular arrangements of the inner hair cells (IHC) and outer hair cells (OHC) in plate B, and the "W" shaped and erect appearance of OHC stereocilia (plate C) and the linear shape and erect appearance of the IHC stereocilia typical of the normal organ of Corti.

3.2.3 Mechanical damage of the organ of Corti after blast wave exposure:

Immediately after blast wave exposure (Figure 3.2.2 and 3.2.3):

In plate A in Figure 3.2.2 the organ of Corti (*) is torn loose from its attachments along the basilar membrane and forms a "snake-like" mass of degenerating cells which floats freely in the endolymphatic fluid of the scala media. The tissue that is torn loose consists of all the outer hair cells and their supporting cellular network. A fracture line which follows the line of attachment between the second and third row of outer hair cells extends into viable areas of the organ of Corti (plate B, Figure 3.2.2). Visible in plate B and C of Figure 3.2.2 in the area of the lesion are the outer pillar cell processes (P) and the disturbed cells of Claudius (C), as well as a variety of swollen sensory cells (S) and other supporting cellular elements of the organ of Corti, such as the Dieters cells (D). The inner hair cells (I) appear to be surprisingly intact in the most severe area of the lesion (compare their appearance to those in the control micrograph of Figure 3.2.1, plate B and D). Figure 3.2.3, plate A, illustrates a curious phenomenon that in the area of the main lesion all of the outer hair cells have been ripped from their cuticular plate attachments medial to a fracture line that runs between the second and third row of outer hair cells. The cuticular plate is left in the supporting matrix of the reticular lamina. Figure 3.2.3, plate B shows that the outer hair cell cilia in the region of the main lesion display a variety of pathologies including broken cilia (C), fused cilia ($C_2$), and disrupted cilia ($C_3$). Basalward to the main lesion the organ of Corti is intact (Figure 3.2.3, B and C), there are numerous defects in the reticular lamina (R). Further basalward (Figure 3.2.3, plate D), the organ of Corti is generally intact, but the cilia of the first row of outer hair cells are disrupted and there are numerous cytoplasmic extrusions (E) along the inner hair cell array. The second and third row of outer hair cells appears relatively normal.

<u>One day after exposure (Figure 3.2.4 and 3.2.5):</u> In Figure 3.2.4, plate A and B, remnants of the "snake-like" dislodged coil of the organ of Corti (*) are still visible, loose in the endolymphatic space. The individual cellular elements are much less distinct. The degeneration of the outer hair cells in areas adjoining the main lesion is more advanced (Figure 3.2.4, plate C and E) and there are very few intact outer hair cells left over a considerable extent of the organ of Corti. There are still numerous holes (H) into the perilymphatic spaces (plate C and E). However, many inner hair cells in area of the main lesion (plate B) still look surprisingly normal, while further basalward of the main lesion where the overall cell loss is less severe (plate D), the inner hair cell cilia (I) are greatly disturbed.

Scar formation in the area of the main lesion is becoming evident (S) (Figure 3.2.5, plate A). The inner hair cell cilia are still comparatively normal. The inset shows inner hair cell cilia basalward to the lesion where there was no actual hair cell loss at one day after exposure. The inner hair cell cilia are severely disturbed and fused. Some phagocytic types of cells (P) are seen at this time on the organ of Corti (Figure 3.2.5, plate

B), but they are comparatively infrequent. In areas where the "snake" was formed (Figure 3.2.5, plate C), large crevices (arrows) into the perilymphatic spaces have not yet been completely sealed off by scar tissue. Again, note the relatively normal inner hair cell cilia (I).

Five days after exposure (Figure 3.2.6 and 3.2.7): In Figure 3.2.6, plate A, the free floating "snake-like" portion of the organ of Corti has essentially disappeared (*) and scar formation (Figure 3.2.6, plate B) appears advanced. Elements of the reticular lamina and of the outer hair cells are still visible (O). The remaining inner and outer hair cell cilia (Figure 3.2.6, plate D) are severely disturbed in regions removed from the main lesion, and there is no consistent pattern or preference for damage in any particular row of outer hair cells. (Note: regions of the second row in plate A appear quite normal.) Inner hair cell cilia (I) in the region of the main lesion (Figure 3.2.6, plate C and D) do not appear fused or agglutinated as they are in the outer hair cell cilia; however, there are numerous cytoplasmic extrusions present along the inner hair cell array and the cilia of many inner hair cells are bent (arrow), most often toward the outer hair cells. Giant cilia are not frequently seen. In the animals sacrificed five days after exposure, phagocytic cell types (P) begin to appear more frequently (Figure 3.2.6, plate E).

Figure 3.2.7 illustrates a number of inner hair cell anomalies in the region of the main lesion aside from cilia defects. In Figure 3.2.7, plate A and B, an ejection of the cuticular plate of one inner hair cell (arrow) can be seen. In Figure 3.2.7 plate A, the cilia are severely damaged while in plate B, the cilia are surprisingly normal in appearance. Adjoining inner hair cells and their cilia often look completely normal even in areas where inner hair cells are found to be completely missing (M), as in Figure 3.2.7 plate C. The pattern of outer hair cell defects can abruptly change from primarily third row damage (plate D) to only the third row being intact (see $O_3$ in plate E).

Ten days after exposure (Figure 3.2.8 and 3.2.9): The damaged inner hair cell cilia (I) in Figure 3.2.8, plate A, are in a more advanced stage of degeneration in many localized areas of the main lesion. Figure 3.2.8, plates B and D, illustrate that scar tissue (S) originating from the area of the Claudius cells and Hensen cells has nearly completely sealed off the endolymphatic space from the perilymphatic space, except for some small narrow rifts (H). In Figure 3.2.8, plate C and D, considerable debris (D) and phagocytic (P) activity can still be found on the reticular lamina.

Figure 3.2.9, plate A and B shows that while some areas of the lesion have appeared to stabilize, i.e., there is a nearly complete layer of scar tissue (S), other localized areas still show large openings into the perilymphatic space (Figure 3.2.9 C and D) in areas where elements of the organ of Corti are still degenerating. Note the relatively normal looking inner hair cell cilia in Figure 3.2.9, plate C, in an area where the pillar heads are severely damaged.

Thirty days after exposure (Figure 3.2.10 and 3.2.11): Figure 3.2.10 illustrates the appearance of the surface of the organ of Corti one month after exposure. The organ of Corti still appears to be undergoing degenerative changes. While the lesion is nearly completely stabilized by scar tissue, there are still some restricted areas (arrows and inset) where there may be some communication between endolymph- and perilymph-containing spaces. The amount of debris (D) has been greatly reduced, but not entirely, and the cilia are still extensively disrupted over wide areas of the remaining organ of Corti.

In the area of the main lesion (Figure 3.2.11, plate A and B), many inner hair cells appear grossly abnormal and phagocytic activity (P) is still evident. Basalward to the lesion (Figure 3.2.11, plate C and D), inner and outer hair cell cilia are extremely damaged with the usual range of anomalies, e.g., fusion ($C_1$), giant cilia ($C_2$) and disrupted cilia ($C_3$). At this late post-exposure period, the cilia disturbances may represent a permanent state for the damaged sensory epithelia or these cells may continue to degenerate over a much longer period than one would anticipate based upon data from threshold shift recovery curves.

3.2.4 Non-"mechanical" sensory cell lesions after blast wave exposure: Figure 3.2.12, 3.2.13 and 3.2.14 illustrate the appearance of the organ of Corti at post-exposure times of 0 hours, one day and 30 days respectively for animals that sustained a lower level of sensory cell damage from the blast wave exposures (Cochleograms such as those from chinchillas 543R, 349R and 607R in Section 3.3 would be typical of such a level of trauma). Variability following impulse noise exposure is very great, and the different classes of lesions described in this section reflect this variation. All animals prepared for the SEM received the same blast wave exposure. Immediately after exposure (Figure 3.2.12), the most noticeable changes in the sensory cell population are the disturbances of the cilia (arrows), cytoplasmic extrusions (E) along the inner hair cell array, and occasional damaged sensory cells with communicating holes in the reticular lamina (*). One day after exposure (Figure 3.2.13), the outer hair cell (O) degeneration is well advanced and while the appearance of the inner hair cells (I) is somewhat variable, they do not appear extensively damaged. Thirty days after survival (Figure 3.2.14), the outer hair cells (O) appear to have completely degenerated in some areas (Figure 3.2.14, plate B, arrows), while in other areas, the OHC loss is partial (Figure 3.2.14, plate A) and the OHC appear to still be degenerating. The areas of missing sensory cells are covered by scar tissue (S). In some areas, the outer hair cell loss is accompanied by severely damaged inner (I) hair cells (Figure 3.2.14, plate C) and in some cases, very restricted lesions (arrows) with complete loss of all sensory and supporting cells. Even at this late date, debris (D) is still evident on the organ of Corti. (Tissue in some lesioned areas is weakened and thus fractured during preparation. A = artifact.)

3.2.5 Lesions of the conductive system: While the variability seen in the effects of blast waves on hearing can not be completely explained, one definite contributing factor is a change in the conductive properties of the middle and external ear. In this SEM study, all animals were examined immediately after exposure. In approximately 45% of the upstream ears (i.e., tympanic membrane perpendicular to the shock tube), a rip in the tympanic membrane was found. The typical appearance of the tears is illustrated in Figure 3.2.15. Associated with the tears was bleeding between the epithelial layers of the tympanic membrane and the formation of hemotomas. Often animals without tears also showed the bleeding indicating excessive stress in the tympanic membrane.

3.2.6 Conclusions: A variety of lesions were obtained from the 160 dB blast wave exposures, but in general, they could be broken down into two types: (a) severe mechanically-induced damage associated with the "snake-like" ribbon of detached sensory and supporting cells, and (b) sensory cell lesions (predominantly outer hair cells) that are not produced by any obvious mechanical disruption of the reticular lamina.

A noise-induced mechanical separation of the outer hair cells from their medial attachments to the pillar cell heads serves to protect the inner hair cells in those same areas of the organ of Corti. Large numbers of IHC with intact cilia survive to the 30 day post-exposure point, while basalward of the "snake-like" lesion, not only are the OHCs severely damaged, but IHC cilia show severe disturbances within the first day after exposure. Changes in the mechanical coupling of traveling wave mechanisms in the denuded areas of the organ of Corti are hypothesized to account for the limited protection afforded the IHC. This pattern of inner hair cell degeneration is much different from that seen following continuous noise or low-level impulse noise exposures where large segments of the OHC are seldom ripped away from the rest of the organ of Corti. The degenerative changes on the organ of Corti following impulse noise exposure have not stopped after 30 days, while the indications from audiometry are that hearing thresholds have stabilized by 30 days after exposure.

3.3 Psychophysical, physiological and anatomical correlates

As stated earlier, one of the goals of this project was to determine the audiological, physiological and anatomical changes that occur as a result of blast wave exposures. Since the traumatizing effects of these exposures vary considerably from one animal to the next, it is not particularly useful to "average" the results across groups of animals. Thus, this segment of the report will focus on the anatomical, physiological and audiometeric changes that occur within individual animals and an effort will be made to study the interrelationships between the three sets of measures.

At the outset of the project, a considerable amount of time was spent collecting behavioral audiograms and tuning curves from approximately eight chinchillas. Unfortunately, before the physiological experiments could be carried out most of the animals died at about the same time; autopsies on several animals failed to reveal the cause of death. This was a serious setback for the grant because a substantial amount of time was invested in obtaining the behavioral data. Rather than collect additional data using the time consuming behavioral techniques, we chose to use the more efficient evoked potential method for obtaining estimates of thresholds and tuning curves from a second group of animals (see Section 3.1 above). Thus, most of the data presented below comes om animals tested with the evoked response technique; however, some data were available from a few behaviorally trained animals.

A total of 19 animals were exposed to either 155 dB or 160 dB peak SPL blast waves. The varialbe nature of the lesions allowed the data to be organized around four basic lesions types regardless of exposure conditions. The four lesions and animals in each category are :

(A) Severe mid-cochlear to basal lesions. Animals 603, 59, 60, 366, 750, 510, 459, 852.

(B) Large but scattered losses across the whole cochlea. Animal 820.

(C) Narrow focal lesions. Animals 543, 607, 925.

(D) Little or no cell loss. Animals 117, 940, 860.

In addition to these animals, limited data are presented on four additional animals that did not complete the experimental protocol because they died prematurely for various reasons. These animals are 118, 547, 552, and 557. Of the nineteen animals exposed to blast waves only 11 animals completed the entire protocol which included audiometric testing, single unit recordings from auditory nerve fibers and cochlear anatomy. The data from each animal are briefly discussed below.

### 3.3.1 Chinchilla 59:

Psychophysical results: Chinchilla 59 was exposed to 50 impulses having a peak SPL of 160 dB and an A-duration of 1 ms. The pre- and post-exposure audiogram obtained with tone bursts of 20 ms duration are shown in Figure 3.3.0. The animal developed a 30 to 40 dB hearing loss at the probe tone frequencies used to collect the psychophysical tuning curves. The psychophysical tuning curves obtained at 0.5 and 1.0 kHz (Figure 3.3.1-3.3.2) have become much more broadly tuned as a result of the exposure. The tuning curves lack a sharply tuned tip region due to a greater loss of sensitivity in the tip of the curve than in the tail. That is, the tuning curves have been transformed from band pass to low pass filters. One noteworthy point is the relationship between the intensity of the probe relative to a masker of similar frequency. Masker and probe intensities are nearly equal before exposure, but after exposure much higher masker levels are required to mask the probe. It is not clear why this occurs, but perhaps it is related to the abnormally broad excitation pattern along the cochlear partition or to "off-frequency" listening cues such as beats and combination tones (Weber et al., 1980).

The tuning abnormalities for chinchilla 59 were most pronounced at 2 kHz (Figure 3.3.3) where the post-exposure tuning curve is "W" shaped due to two distinct threshold minima; the first at the probe frequency of 2 kHz and a second and lower minima located at 1 kHz. One interpretation of these results is that the 2 kHz probe tone is being detected by neurons innervating the 1 kHz region of the cochlea rather than those at the 2 kHz region. This could occur because the thresholds at the low frequencies are less than those near 2 kHz; thus the spectral spread of energy from the probe would be more likely to activate units having characteristic frequencies (CFs) near 1 kHz. An alternative explanation is that neurons with CFs near 2 kHz have "W" shaped tuning curves, but are actually more sensitive to tones near 1 kHz than at CF (Liberman and Kiang, 1978; Salvi et al., 1982). Unfortunately, this issue could not be explored physiologically because the animal died before further testing could be completed.

The psychophysical tuning curves obtained at 4, 8, and 11.2 kHz (Figure 3.3.4-3.3.6) also showed a greater loss in sensitivity in the tip of the tuning curve than in the tail following exposure. While the tips of the tuning curves are generally broader, the curves at 4 and 11.2 kHz still have a remnant of a short, narrow tip near CF.

Cochleogram: Figure 3.3.8 shows the pattern of hair cell loss in chinchilla 59. There is a substantial loss of OHC between the 0.7 and 2.8 kHz regions of the cochlea plus a small secondary loss of OHC near the 4.0 kHz region. The changes in sensitivity and tuning below 4.0 correlated reasonably well with the pattern of hair cell loss; however, there is a discrepancy at 4.0 kHz and above. At the high frequencies, there is a loss of tuning and sensitivity yet little or no hair cell. It is difficult to account for this discrepancy; it could be due to measurement error (e.g., a change in the animal's criterion) or it might be due to subtle histopathologies in the basal region of the cochlea that are not detected in the simple cochleogram. Since the cochlea was embedded in plastic, the latter hypothesis can be investigated in more detail by sectioning the cochlea and studying the region by electron or high power light microscopy.

### 3.3.2 Chinchilla 60:

Psychophysical results: Chinchilla 60 was also exposed at the rate of 1 per minute to 50 impulses having a peak SPL of 160 dB. Figure 3.3.8 shows the pre- and post-exposure behavioral thresholds obtained with 20 ms tone bursts. There is little loss in sensitivity at 0.5 kHz; however, there is a 30 to 50 dB elevation of the thresholds between 1.0 and 11.2 kHz. The post-exposure psychophysical tuning curve obtained at 0.5 kHz (Figure 3.3.9) shows approximately a 10 dB upward shift, but the shape of the tuning curve is nearly the same as before the exposure, i.e., there is little change in tuning. The post-exposure tuning curves obtained at 1 kHz (Figure 3.3.10), 4 kHz (Figure 3.3.12), 8 kHz (Figure 3.3.13) and 11.2 kHz (Figure 3.3.14) all show a drastic loss of sensitivity in the tip region so that the curves are extremely broad following exposure. The most profound change in tuning, however, took place at 2 kHz (Figure 3.3.11). The 2 kHz tuning curve was extremely broad and failed to show a high pass cutoff over the range of frequencies tested. The lowest point on the tuning curve was at 5 kHz, over an octave above the probe; one interpretation of these results is that the 2 kHz probe tone is activating neurons associated with the 5 kHz region of the cochlea. This interpretation is consistent with the fact that the 4-5 kHz region is the most sensitive point on the audiogram. It is also interesting to note that large segments of the tuning curves obtained at 2, 8 and 11.2 kHz match or rather closely suggesting that the three probe stimuli may be exciting similar regions of the cochlea.

Single unit data: It is difficult to make a direct comparison between the neural and behavioral data due to the potential effects of anesthesia and surgery (Hawkins et al., 1978) and also because of acoustic differences (especially from 2-6 kHz) introduced by the outer ear transfer function (von Bismark, 1967). Nevertheless there are interesting relationships between the two sets of data. Unit 54 (Figure 3.3.15) is typical of units with CFs near 0.6 kHz; the tuning curve is nearly as sharp as that observed behaviorally at 0.5 kHz although the two curves are not identical. The tuning curves become more distorted at higher frequencies. The lowest point on the tuning curve of unit 4 (Figure 3.3.16) is near 0.17 kHz; however, the CF was estimated to be at 0.8 kHz near the notch which is present near the high frequency cutoff of the tuning curve. Relative to the psychophysical tuning curve, the neural tuning curve has a much lower threshold in the low frequency tail; thus, the neural and psychophysical curves have somewhat different shapes. No units were encountered in the 1.5-2.5 kHz region; this would appear to be consistent with the lack of a tip and high frequency cutoff for the 2.0 kHz psychophysical tuning curve. Few high-CF units were encountered and most of these had CFs around 4 and 5 kHz. Unit 25 (Figure 3.3.19) has a very high threshold and is so broadly tuned that it is difficult to assign a CF. A reasonable estimate of the CF of unit 25 is 2.8 kHz, since this is near the high frequency cutoff of the tuning curve; however, it is possible that the original CF of the unit may actually be much higher because of damage to the cochlea (Robertson et al., 1980). Unit 24 had a tip of about 15 dB in depth near 4 kHz and a very high threshold. The neural tuning curves in the 3-5 kHz region bear some resemblance to the psychophysical tuning curves at 4 and 8 kHz. The tuning curve of unit 43 (Figure 3.3.19) was one of the most distorted; in fact, it was not possible to estimate the CF (probably near 16 kHz) since the high frequency slope could not be measured in the 14-20 kHz region due to the limited output of our acoustic system.

Anatomical data: Figure 3.20 shows the degree of inner (IHC) and outer hair cell (OHC) loss as a function of location in the cochlea and as a function of frequency (Eldredge, 1977). There is nearly a complete loss of OHC from the base to the 0.9 kHz region of the cochlea and a 20-40% loss extending up to the apex. There is also a substantial loss of IHC from 1.5-3.5 kHz and from 5.5-10 kHz. The lack of IHC and OHC is correlated with the absence of nerve fibers with CFs between 1.5-3.5 kHz and between 6-10 kHz. There are a few units near 5 kHz which presumably innervate the remaining IHC from this cochlear region; however, almost no unit with identifiable CFs were found at higher frequencies even though IHCs were present. It is interesting that the lowest point on the psychophysical tuning curves obtained at 2, 4, 8 and 11.2 kHz is near 5 kHz, i.e., a narrow region where IHC and active nerve fibers were found. The smallest loss (10-30%) of hairs cell was found below 1 kHz; not surprisingly, the unit thresholds and tuning curves were relatively normal in this region. Except for the region above 10 kHz, there is reasonably good correspondance between the anatomical, physiological and psychophysical data.

### 3.3.3 Chinchilla 117:

Psychophysical data: Chinchilla 117 was exposed to 50 impulses having a peak SPL of 160 dB. In contrast to the preceeding animals, there was essentially no change in the psychophysical thresholds as a result of the exposure (Figure 3.3.21). Furthermore, most of the psychophysical tuning curves (Figures 3.3.22-3.3.27) show rather minor changes in shape as a result of the exposure. The only exception occurs at 8 kHz where the tuning curve is shifted upward and the tip of the tuning curve is truncated.

Single unit data: Representative single unit tuning curves that span most of the audiogram are shown in Figures 3.3.28-3.3.32. The minimum thresholds of the units are relatively low and the tuning curves are for the most part narrowly tuned. The threshold of unit 68 (CF near 0.5 kHz), however, is elevated somewhat and the tuning curve is slightly broader than normal.

It was our impression that some of the low frequency units with CFs in the 0.4-1.5 kHz range showed somewhat abnormal tuning and sensitivity, but this was not an overwhelming effect. In general, the blast wave exposure seemed to have little effect on the single fiber activity in chinchilla 117.

Anatomical data: Figure 3.3.33 contains the cochleogram of chinchilla 117. This animal sustained little or no hair cell loss as a result of the exposure. The lack of any significant histopathologies is consistent with the behavioral and physiological data which indicated that the auditory system was nearly normal after exposure

3.3.4 Chinchilla 118:

Psychophysical data: Chinchilla 118 was exposed to 50 impulses having a peak SPL of 160 dB. This animal died of unknown causes before the post-exposure protocol could be completed, consequently only limited data are available. The audiogram in Figure 3.3.34 shows a low threshold region at 4.0 kHz where the loss in sensitivity is only 10 dB; the thresholds at higher (8.0 kHz) and lower (1.0, 2.0 kHz) frequencies were elevated roughly 20 to 30 dB. The previous results from chinchilla 59 suggest that this low threshold island might result in tuning curves with displaced tips.

The 1.0 kHz tuning curve (Figure 3.3.35) shows a greater loss in sensitivity in the tip of the tuning curve than in the tail; the tip of the curve has become extremely broad and the most effective masking frequency has shifted downward from 1.0 kHz. Presumably the response to the probe tone is now being mediated primarily from the 0.4 kHz region of the cochlea rather than from the 1.0 kHz region. More severe changes in tuning occured at 2.0 kHz (Figure 3.3.36); the tip of the curve has shifted downward to 1.0 kHz and the tip is extremely broad and irregular. It is somewhat surprising that the tip of the tuning curve was not displaced toward higher frequencies since the sensitivity and tuning in the 4.0 kHz region is reasonably good as shown in Figure 3.3.37. The tuning curve at 8.0 kHz (Figure 3.3.38) is simply shifted upward in the tip region with almost no change in sensitivity in the low frequency tail. Unfortunately no single unit or anatomical data are available since the animal died before the data could be collected.

3.35 Chinchilla 366:

Evoked potential data:

The evoked response audiograms of chinchilla 366 are shown in Figure 3.3.39. There was a 15 dB loss near 0.5 kHz which increased to 40-50 dB at 1.0 and 2.0 kHz. At the highest frequencies (8.0 and 11.2 kHz), the thresholds were nearly normal. The low frequency tail of the 0.5 kHz tuning curve

(Figure 3.3.40) showed little change in sensitivity; however, the tip region was elevated approximately 15 dB and thresholds along the high-frequency leg were elevated by as much as 40-60 dB. Consequently, the bandwidth of the tuning curve was not substantially altered even though there was a loss in sensitivity. The large threshold elevations along the high-frequency slope are probably related to the mid-frequency hearing loss, i.e., after the exposure, few mid-frequency units (1.0-2.0 kHz) contribute to the response elicited by the probe and therefore the high-frequency leg of the tuning curve is shifted toward lower frequencies. In the region of maximum hearing loss, there were significant alterations in tuning. Both the 1.0 and 2.0 kHz tuning curves (Figure 3.3.41-3.3.42) were extremely broad and there was only a small remnant of a tip at the probe frequency. The 4.0 kHz tuning curve (Figure 3.3.43) showed a loss in sensitivity of 15-20 dB near the tip and little or no change at other frequencies. Relatively insignificant changes in tuning were seen at the 8.0 and 11.2 kHz tuning curves (Figures 3.3.44-3.45).

Single unit data: The single unit thresholds, for the most part, followed the contour of the evoked response audiogram. Units with CFs near 0.5 kHz had slightly elevated thresholds and showed little or no change in tuning (Figure 3.3.46.). The tuning curves near 1.0 kHz had extremely broad but discernable tips and high thresholds (Figure 3.3.47). Units with CFs near 4.0 kHz had "W" shaped tuning curves with hypersensitive tails. The minimum threshold of unit 4 (Figure 3.3.48), for example, is approximately 64 dB at 1.2 kHz; however, the threshold at the CF (approximately 3.0 kHz) is roughly 12 dB higher. It is important to note that the threshold near 1.0 kHz for unit 4 is roughly 10-15 lower than that of unit 45 (Figure 3.3.47) whose CF is near 1 kHz. Furthermore, the thresholds in the tail (near 1 kHz) of this 3 kHz unit are comprarable to the evoked response thresholds near 1 kHz. Thus, in pathological ears, high CF units may make a significant contribution to the neural and/or behavioral responses obtained with low frequency signals. Among the high-CF units, the tip of the tuning curve was segregated from the tail region by a significant high threshold notch as illustrated in units 127 (Figure 3.3.50) and 126 (Figure 3.3.51). This notch was absent in the evoked response tuning curves; however, the discrepancy may not be as serious as it seems since the evoked potential tuning curves would also show a notch in the 2-5 kHz region if correction was made for the outer ear transfer function (von Bismark, 1967). Also note that the thresholds in the tail of the tuning curve are as low as 60-70 dB near 1-2 kHz; again, this illustrates that the high-CF units could contribute to the responses obtained with low frequency signals.

Anatomical data: The cochleogram of chinchilla 366 (Figure 3.3.52) showed a significant loss of OHC and a mild loss of IHC from about the 0.9 to 6.0 kHz region of the cochlea; only a few hair cells were missing in other regions. The region of outer hair cell loss is in reasonably good agreement with the pattern of threshold shift seen in Figure 3.3.39. Furthermore, the changes in tuning are most severe in the region of outer hair cell loss. It interesting that there is little or no hair cell loss above the 6 kHz region of the cochlea; however, the single unit tuning curves from this region have a high threshold notch between the tip and tail region and the thresholds in the tail of the tuning curve actually appear to be more sensitive than normal (i.e., hypersensitive). In the middle of the cochlea there is complete loss of OHC extending over about two octaves with little loss of IHC. Units presumably innervating the region devoid of OHCs showed significant threshold shifts; in addition, their tuning curves were frequently "W" shaped (e.g., Figure 3.3.48) with the thresholds in the tail being lower than in the tip.

### 3.36 Chinchilla 459:

Evoked potential data: Chinchilla 459 was exposed to 50 impulses having a peak SPL of 160 dB at the rate of 1 per minute. As a result of the exposure, the animal sustained a threshold shift of 40-50 dB at 8 and 11.2 kHz and little or no loss at lower frequencies (Figure 3.3.53). There were only slight changes in tuning at 0.5 and 1.0 kHz (Figure 3.3.54-3.3.55) after exposure; however, the 2 kHz tuning curve (Figure 3.3.56) showed some peculiar changes. The masked thresholds at 2 kHz (Figure 3.3.56) were elevated somewhat on either side of the tip, but not at the tip itself; consequently the tip region was actually narrower after exposure. It is not clear whether these unusual changes in tuning were real or due to measurement error. The small loss in sensitivity at 4 kHz was correlated with a slight elevation in the tip of the 4 kHz tuning curve (Figure 3.3.57). At 8 kHz where the loss was more substantial, the tip of the tuning curve was shifted downward to 6 kHz and the tip of the curve was wider than normal (Figure 3.3.58). There was also a substantial loss in sensitivity at 11.2 kHz and the masked thresholds were extremely high near 11 kHz. Due to a technical error, the remainder of the tuning curve was not measured; however, it seems likely that the tip of the 11.2 kHz would have been displaced toward lower frequencies similar to what occured at 8 kHz.

Single unit data: The auditory nerve fibers from units with CFs below 4.0 kHz had relatively low thresholds and their tuning curves were narrowly tuned as illustrated in Figure 3.3.60-3.3.63. However, just above 4.0 kHz there was a drastic change in tuning. Unit 14 (Figure 3.3.64), for example, has a CF near 5.0 kHz and a very sharp tip; however, the thresholds at CF are as much as 20 dB above those in the tail of the tuning curve. As a result, the tuning curve has a "W" shape with a minimum threshold near 1.8 kHz. The tuning curve of unit 133 (Figure 3.3.65) has a broad "U" shape making it difficult to assign a CF to the unit; since the high frequency cutoff of the tuning curve is near 9.0 kHz it is reasonable to assume that the CF of the unit was rougly 7-8 kHz. The tuning curve of unit 60 (Figure 3.3.66) has two segments, one with a threshold minima near 1.5 kHz. However, it is unlikely that this is a low CF unit since other units in this region were quite sensitive. Furthermore, the unit responded to a narrow range of frequencies near 12.0 kHz. Unit 60 presumably is a high frequency unit, but one cannot accurately assign a CF since the tuning curve is poorly defined over the range of intensities used to test the unit.

Anatomical data:

The cochlea of chinchilla 459 (Figure 3.3.67) shows little or no hair cell loss up to about the 4.0 kHz region of the cochlea. However, in the region between 4.0 and 16.0 kHz there is a substantial loss of OHC and a small loss of IHC. The location of the lesion correlates extremely well with frequencies that show a loss of sensitivity in the evoked response audiogram. The auditory nerve fibers that innervate the region of hair cell loss show a significant loss in sensitivity and abnormal tuning. One interesting finding is that units with CFs corresponding to the low-frequency edge of the lesion have "W" shaped tuning curves similar to that shown in Figure 3.3.64, i.e., the thresholds near the CF are much higher than those in the tail and there is a distinct notch between the tip and tail segements of the tuning curve. Other units with CFs within the lesion had "U" shaped tuning curves.

### 3.3.7 Chinchilla 510:

Evoked response data: Chinchilla 510 was exposed at the rate of 1 per minute to 50 impulses having a peak SPL of 160 dB. After the exposure the animal developed a hearing loss of approximately 40 dB at 2 kHz and a relatively small loss at other frequencies (Figure 3.3.68). At 0.5, 1.0, 4.0, 8.0, and 11.2 kHz (Figures 3.3.69, 3.3.70, 3.3.72, 3.3.73, and 3.3.74) where the thresholds were nearly normal, the evoked response tuning curves showed little or no change in frequency selectivity. On the other hand, at 2 kHz where the threshold is elevated, the post-exposure tuning curve is extremely broad so that the tip is nearly flat for more than two octaves (Figure 3.3.71). In addition, the high pass cutoff of the tuning curve is shifted toward higher frequencies; this suggests that regions of the cochlea basalward to the 2 kHz region of the cochlea may be contributing to the response. This animal died after the post-exposure evoked potential tuning curves were collected; consequently, single unit data are not available.

Anatomical data: Figure 3.3.75 contains the cochleogram of chinchilla 510. There is an extensive loss of OHC between the 1.0 and 4.0 kHz regions of the cochlea. The location of the lesion correlates with a significant loss of tuning and loss of sensitivity at 2 kHz. Other frequencies showed losses in sensitivity of approximately 5-10 dB; however, there was little or no hair cell loss related to the change in sensitivity.

3.3.8 Chinchilla 543:

Evoked potential data: Chinchilla 543 was exposed to 50 impulses having a peak SPL of 160 dB. After exposure, the thresholds were elevated 20 to 40 dB at 8 and 11.2 kHz; the low frequency thresholds, on the other hand, were nearly normal (Figure 3.3.76). The tuning curves at 0.5, 1.0, 4.0 and 8.0 showed little change as a result of the exposure (Figures 3.3.77, 3.3.78, 3.3,80, 3.3.81). The 2.0 kHz tuning curve (Figure 3.3.79) was shifted upwards and showed some anomalies in the tip region which is surprising given the small threshold shift at this frequency. The most significant changes in tuning occured at 11.2 kHz (Figure 3.3.82) where the hearing loss was greatest. The tip of the 11.2 kHz tuning curve was lost and the lowest point on the curve was shifted downward to 7 kHz. Thus, the high frequency hearing loss was again correlated with a significant loss in tuning.

Single unit data: Most of the units with CFs below 4.0 kHz had relatively low thresholds and showed reasonably good tuning; these results are in keeping with the lack of threshold shift observed in the evoked response at these frequencies (Figures 3.3.83-3.3.85). The tuning curves became progressively abnormal as the CF increased above 4.0 kHz. Although unit 83 (Figure 3.3.86) has a relatively normal tip near 4.0 kHz, there is a high threshold notch in the tail of tuning curve. Unit 115 (Figure 3.3.87) has a CF near 8 kHz and the tuning curve is much broader than those seen at lower frequencies. The tuning curve of unit 128 (Figure 3.3.89) has two tips, one at 10.0 kHz, near the high pass cutoff, and a second more sensitive tip near 3 kHz which is separated from the CF by a high threshold notch. Thus, the single unit tuning curves show the same variation across frequency as the evoked response tuning curves.

Anatomical data: The cochleogram of chinchilla 543 is shown in Figure 3.3.89. There is only a small scattered loss of hair cells below the 7.0 kHz region of the cochlea. However, from about the 7.0 to 17.0 kHz region of the cochlea there is a significant loss of OHC. The location of this lesion in the high frequency region of the cochlea is well correlated with the pattern of threshold shift observed with the evoked response and single fibers. Furthermore, in regions where the evoked response and single unit thresholds were elevated there was a significant loss of tuning in the evoked response and single unit data.

3.3.9 Chinchilla 547:

Evoked potential data: Chinchilla 547 was exposed to 50 impulses having a peak SPL of 160 dB. The evoked response audiograms (Figure 3.3.90) indicate that there was a mild hearing loss at 8 and 11.2 kHz, but little or no loss in sensitivity at other frequencies. The post-exposure tuning curves obtained at 0.5, 1.0 and 4.0 kHz showed little or no change in tuning (Figures 3.3.91, 3.3.92, and 3.3.94). The 2.0 kHz post-exposure tuning curve, on the other hand, was shifted upward and is slightly different from the pre-exposure curve. The most significant change in tuning occurred at 8.0 kHz where the hearing loss was greatest. The tip of the tuning curve was shifted downward from 8.0 to 6.0 kHz; in addition, there was a notch along the high frequency edge of the tuning curve. The effects of the high frequency hearing loss can also be seen at 11.2 kHz where the tip of the tuning curve is nearly lost as a result of the exposure. The evoked potential results appear to be quite similar to those seen with animal 543. Unfortunately, animal 547 died and we were unable to obtain either the anatomical or physiological data.

### 3.3.10 Chinchilla 552:

Evoked potential data: Chinchilla 552 was exposed to 50 impulses having a peak SPL of 160 dB. As shown in Figure 3.3.97, the animal showed a loss in sensitivity after the exposure of approximately 5-15 dB across the range of frequencies. The tuning curves obtained at 0.5, 1.0, 2.0 and 11.2 kHz (Figures 3.3.98, 3.3.99, 3.3.100, and 3.3.102) were in general shifted upward a small amount without much change in the shape of the tuning curve. The tuning curves obtained at 4.0 and 8.0 (Figures 3.3.101 and 3.3.102) showed a slight shift in the location of the tip of the tuning curve after exposure. In general, however, the exposure seemed to have limited effect on the thresholds and tuning curves of chinchilla 552.

Single unit data: The units with CFs below 2.0 kHz generally had low thresholds and relatively narrowly tuned frequency threshold curves (Figures 3.3.104 and 3.3.105). The units with CFs between 2.0 and 6.0 kHz, however, had thresholds that were elevated slightly and tuning curves that had rather broad tips (Figure 3.3.106 and 3.3.107) often with a blunt "W" shape. Many units with CFs above 8.0 kHz (Figure 3.3.108 and 3.3.109) showed reasonably good tuning; however, the thresholds of the units were somewhat higher than normal and higher than one might expect based on the evoked response thresholds. The poor sensitivity among the high CF units is more than likely the result of trauma induced either by surgery or anesthesia.

Anatomical data: The cochleogram is unavailable for this animal due to fixation artifacts which made it impossible to obtain valid data.

### 3.3.11 Chinchilla 557:

Evoked potential data: Chinchilla 557 was exposed to 50 impulses having a peak SPL of 160 dB. The animal died before the physiological and anatomical data could be collected; however, evoked response thresholds and tuning curves are available. Figure 3.3.110 shows that the animal sustained a loss in sensitivity of approximately 10 to 20 dB at 2 kHz and below while sensitivity remained unchanged at the higher frequencies. This type of low frequency hearing loss was seldom seen with the blast waves used in this experiment. Little or no changes were noted in the tuning curves obtained between 2.0 and 11.2 kHz (Figures 3.3.113-3.3.116). At 0.5 and 1.0 kHz, where the threshold shifts were greatest, the tuning curves (Figure 3.3.11 and 3.3.12) were in general displaced upward 10-20 dB with only a slight broadening of the tip of the tuning curve.

3.3.12 Chinchilla 603:

Evoked potential data: Chinchilla 603 was exposed to 50 impulses having a peak SPL of 160 dB. As a result of the exposure, the animal sustained a hearing loss of approximately 40 dB at 2 kHz and below while the thresholds at the higher frequencies showed little or no change from their pre-exposure values (Figure 3.3.117). The tuning curves obtained at 0.5 and 1.0 kHz were extremely wide (Figures 3.3.118 and 3.3.119); furthermore, the high frequency leg of the tuning curve tended to roll over at high intensities making the high frequency slope of the curves rather shallow. One interpretation of these results is that the response to the probe results from units not only at the probe frequencies, but also from units of higher CF. This point is made more dramatically using the 2.0 kHz tuning curve (Figure 3.3.120); the tip of the tuning curve has shifted from 2.0 kHz to approximately 4.0 kHz as a result of the exposure. These results suggest that the response to the 2.0 kHz tone is actually being mediated by neurons with CFs near 4.0 kHz. Thus, the sensitivity (or threshold shift) of the 2.0 kHz region of the cochlea is probably significantly underestimated by the audiogram. The tuning curves at 4.0, 8.0 and 11.2 kHz (Figures 3.3.121-3.3.123) are shifted upward slightly and there is some detuning (Figure 3.3.121) particularly at 4.0 kHz.

Single unit data: The thresholds of units with CFs below 4.0 kHz were higher than normal. The thresholds of units with CFs near 2.0 kHz were extremely high and the tuning curves were broad and quite distorted. For example, in Figure 3.3.126, it is unclear whether the CF is 1.9, 1.4, or 0.8 kHz. The units with CFs near 0.5 and 1.0 kHz (Figures 3.3.124 and 3.3.125) also showed significant threshold shifts; in spite of this, the tips of the tuning curves were relatively narrow. It is interesting to note that the high frequency slopes of the low frequency tuning curves fail to roll over at high intensities as was the case with the evoked response tuning curve. The differences presumably arise from the fact that the curves obtained with evoked response arise from a population of units along the cochlear partition whereas the curve for a single unit represents the output of a limited segment of the basilar membrane. The tuning curves with CFs near 4.0 kHz were typically "W" shaped. As shown in Figure 3.3.127, the thresholds in the tail of some 4.0 kHz tuning curves were similar to the evoked response thresholds near 1.0-2.0 kHz. Thus, in noise exposed animals, there is a propensity for high frequency neurons to contribute to responses obtained with low frequency tones. Many of the tuning curves obtained from units with CFs above 4.0 kHz showed reasonably good sensitivity and sharp tuning suggesting that the high frequency region of the cochlea was relatively unaffected by the exposure.

Anatomical data: Figure 3.3.130 contains the cochleogram of chinchilla 603. The animal had a large lesion of inner and outer hair cells centered at the 5 kHz location of the cochlea. The apical 50% of the cochlea was essentially normal. These data are unusual in that they do not correspond with the single unit or evoked response data. The physiological and evoked response data both agree in showing a low frequency loss (30 dB) between 0.5 and 2 kHz while the high frequencies (4-11.2 kHz) were essentially normal. This represents the only instance in which the anatomy was in total disagreement. At present we cannot account for this discrepancy.

### 3.3.13 Chinchilla 607:

Evoked potential data: Chinchilla 607 was exposed to 50 impulses having a peak SPL of 160 dB. The exposure produced little or no change in threshold (Figure 3.3.131) and little or no change in the evoked response tuning curves (Figures 3.3.132-3.3.137). This animal was the least affected by the 160 dB exposure.

Single units data: This particular animal had some of the lowest single unit thresholds and sharpest tuning curves of any of the animals used in this study as illustrated in Figure 3.3.138-3.3.143. In many cases, the difference in threshold for frequencies in the tip and tail of the tuning curve were as great as 60-70 dB and the threshold of a number of units approached 0 dB SPL. Thus, the blast wave exposure seemed to have little effect on single unit activity in this animal.

Anatomical data: The cochleogram of chinchilla 607 (Figure 3.3.144) shows that the blast wave exposure produced little hair cell loss except perhaps for a small patch of OHC in the 3.0 kHz region of the cochlea.

### 3.3.14 Chinchilla 750:

Evoked potential data: Chinchilla 750 was exposed to 50 impulses having a peak SPL of 155 dB. As a result of the exposure, the animal sustained a hearing loss of at least 15 dB at all frequencies except 11.2 kHz (Figure 3.3.145). The maximum loss was approximately 50 dB at 2 kHz. The tuning curves obtained at 0.5, 1.0, 2.0 and 8.0 (Figures 3.3.146, 3.3.147, 3.3.148 and 3.3.150) were shifted upward to varying degrees depending on the loss in sensitivity at the probe frequency. The most significant changes in tuning occurred at 2.0 kHz where the tuning curve consists of two tips. The 8.0 kHz tuning curve also became substantially broader after the exposure. There was relatively little change in the 4.0 kHz tuning curve (Figure 3.3.149) which is rather surprising given the fact that there was about a 15 dB loss in sensitivity at this frequency. No single unit data is available since the animal died before these experiments could be carried out.

Anatomical data: The cochleogram of chinchilla 750 is shown in Figure 3.3.152. The cochlea of this animal was rather interesting in that there was a mild 5-20% loss of IHC and OHC throughout most of the cochlea except for the region from 1.0 to 4.0 kHz where there was a significant loss of OHC. This loss of OHC corresponds to the region of greatest hearing loss and detuning. Unfortunately, the changes in threshold observed at other frequencies are not well correlated with the hearing loss, e. g., at 0.5 and 8.0 kHz.

### 3.3.15 Chinchilla 820:

Evoked potential data: Chinchilla 820 was exposed to 50 impulses having a peak SPL of 155 dB. After exposure, the animal showed a threshold shift of 10-30 dB at 1.0 and 2.0 kHz (Figure 3.3.153) and little loss in sensitivity at other frequencies. The 1.0 kHz tuning curve (Figure 3.3.155) was shifted upward after the exposure and there was a moderate loss of tuning. The 2.0 kHz tuning curve (Figure 3.3.156) was grossly abnormal with the tip of the tuning curve displaced from the 2.0 to the 4.0 kHz region of the cochlea. The 4.0 kHz tuning curve (Figure 3.3.157) was also displaced upward; this is somewhat surprising given the lack of threshold shift at this frequency. Other tuning curves (Figures 3.3.154, 3.3.158, and 3.3.159) were nearly unchanged. Single unit data is not available since the animal died before the physiological measurements could be obtained.

Anatomical data: The cochleogram of chinchilla 820 is shown in Figure 3.3.160. Throughout most of the cochlea there is a mild loss of IHC and OHC. However, near the 0.5, 1.2, 5.0 and 9.0 kHz regions of the cochlea there are relatively large, but narrow lesions of IHC and/or OHC. The locations of the lesions are in general agreement with the frequencies where the evoked potential thresholds and tuning curves are abnormal; however, the changes appear to be somewhat greater than one would expect on the basis of the size of the lesion.

### 3.3.16 Chinchilla 852:

Evoked potential data: Chinchilla 852 was exposed to 50 impulses having a peak SPL of 155 dB. After the exposure, the thresholds from 0.5 to 4.0 kHz were elevated approximately 15-35 dB with the greatest loss occurring at 2.0 kHz (Figure 3.3.161). The 0.5 and 4.0 kHz tuning curves were shifted upward after the exposure, but the tips of the curves were still relatively sharp. Significant changes occurred in the 1.0 and 2.0 kHz tuning curves (Figures 3.3.162 and 3.3.164). The tips of the tuning curves were shifted upwards to the 5 kHz region and the tips of the curves were extremely broad. The 4.0 and 8.0 and 11.2 kHz tuning curves, on the other hand, either showed no change or were shifted upwards slightly (Figure 3.3.165-3.3.167).

Single unit data: Approximately a dozen units were obtained on this animal before the experiment ended. Thus, comparisons with anatomy and evoked response data are limited. Figures 3.3.165 and 3.3.166 are tuning curves from units with CFs near 1-2 kHz; both units have extremely high thresholds and are relatively broadly tuned. The thresholds of units near 4.0 kHz were also elevated, but to a lesser degree than those of lower CF; nevertheless, the tuning curves of these mid-frequency neurons were relatively broad. The tuning curve of unit 3 (Figure 3.3.170), for example, is interesting since the thresholds in the tail of the tuning curve are lower than those with CFs around 1-3 kHz; furthermore, the tail thresholds approximate the evoked response thresholds measured at the low frequencies. These results suggest that the mid-frequency neurons may be mediating the response to low-frequency tone bursts.

Anatomical data: Figure 3.3.171 contains the cochleogram of chinchilla 852. There is nearly a complete loss of OHC from about the 0.8 to 6.0 kHz regions of the cochlea. The loss in sensitivity and changes in tuning in the evoked potentials are roughly correlated with the location of the lesion; however, the changes appear to be somewhat smaller than those observed with lesions located more basally. The single unit data follows the general contour of the lesion; however, the changes in threshold seem to be somewhat greater than those observed with the evoked response.

### 3.3.17 Chinchilla 860:

Evoked potential data: Chinchilla 860 was exposed to 50 impulses having a peak SPL of 155 dB. The exposure produced only a small 10-15 dB threshold shift at the high frequencies (Figure 3.3.172). None of the evoked response tuning curves showed any significant changes as a result of the exposure (Figures 3.3.173-3.3.178).

Single unit data: Figures 3.3.179-3.3.184 are typical single unit tuning curves from chinchilla 860. The tuning curves generally have low thresholds and are narrowly tuned. However, the thresholds of some units with CFs above 10 kHz were slightly higher than normal.

Anatomical data: The cochleogram of chinchilla 860, which is shown in Figure 3.3.185, shows little or no hair cell loss with the exception of a few missing hair cells in the extreme basal region of the cochlea. In summary, the 155 dB blast wave exposure had little or no effect on the evoked potential and single unit measures and produced virtually no damage in the cochlea.

### 3.3.18 Chinchilla 925:

Evoked potential data: Chinchilla 925 was exposed to 50 impulses having a peak SPL of 155 dB. The exposure resulted in a small threshold shift above 3.0 kHz of approximately 5-15 dB (Figure 3.3.186). Only minor changes in tuning were noted; generally the tuning curves were displaced upward on the order of 5-10 dB (Figures 3.3.187-3.3.192). Thus, the 155 dB exposure produced little or no change in the evoked potential thresholds and tuning curves.

Single unit thresholds: The single unit tuning curves of most units from chinchilla 925 had relatively low thresholds at CF and the tips of the tuning curves were quite narrow as illustrated by Figures 3.3.193-3.3.198. Apparently, the noise exposure had little effect on the response patterns of these nerve fibers.

Anatomical data: Figure 3.3.199, which contains the cochleogram of chinchilla 925, shows little or no hair cell loss throughout most of the cochlea except for a punctate lesion of both IHC and OHC near 4.0 kHz. This lesion did not seem to have a significant effect on either the evoked response or single unit response.

### 3.3.19 Chinchilla 940:

Evoked potential data: Chinchilla 940 was exposed to 50 impulses having a peak SPL of 155 dB. The animal sustained little or no hearing loss as a result of the exposure (Figure 3.3.200) and there were only minor or insignificant changes in the evoked response tuning curves (Figures 3.3.201-3.3.206).

Single unit data: A somewhat sample of 65 units was obtained before the experiment was terminated. Most of the units that were studied, however, had relatively low thresholds and tuning curves with relatively sharp tips as illustrated in Figures 3.3.207-3.3.212. The units with very low or very high CFs had thresholds that were slightly higher than normal; however, only a few such units were obtained and it seems likely that more sensitive units would have been found if the experiment had continued. Although the sample is limited, the data suggests that the exposure had little effect on auditory nerve fiber activity.

Anatomical data: The cochleogram of chinchilla 940 in Figure 3.3.212 shows an extremely small and scattered losses of OHC. Thus, there is little evidence that the blast wave exposure had any effect on the cochlea.

## 4.0 Discussion

The blast wave exposures used in this study produced a diverse set of audiometric, physiological and anatomical changes. As one would expect, the 155 dB blast wave exposure produced less traumatic effects than the 160 dB blast wave exposure. Only three of the six animals exposed to the 155 dB exposure showed a noticeable hair cell loss and/or change in sensitivity, while nine of the thirteen animals exposed to the 160 dB impulse showed a significant loss of hair cells and a change in sensitivity. Furthermore, the largest cochlear lesions and the most pronounced changes in threshold and tuning were observed in the animals exposed to the 160 dB impulse.

The pattern of damage varied widely across animals exposed to essentially the same blast wave level. The extreme range of variability can be appreciated by comparing the results from chinchillas 60 and 607. Chinchilla 607 was virtually unaffected by the 160 dB blast wave whereas chinchilla 60 showed nearly a complete loss of IHC and/or OHC over the basal two-thirds of the cochlea and significant threshold shifts and changes in tuning over all but the lowest frequency. The range of variability was much less in the group of animals exposed to the 155 dB blast wave. The wide range of variability produced by the blast wave exposures, especially in the 160 dB group, may be partially accounted for by the ruptures seen in the tympanic membrane (anatomy section 3.2.5). If the ruptures were to occur early in the exposure, then the input to the inner ear would be attenuated and the cochlea would be protected from further damage. Ruptures of the tympanic membrane were more prevalent in animals exposed to the 160 dB blast wave than those exposed at 155 dB; this may account for the wider range of damage seen in the former group, although other factors may also play an important role.

Besides the enormous variability in the overall level of damage, there were also large differences in the pattern of damage along the cochlear partition. In one case, the width of the lesion extended from the 1.0 to 17.0 kHz region while in other animals there was only a small punctate lesion. Frequently, the lesion was located near the middle of the cochlea with relatively normal areas of the cochlea on either side; however, there were several cases where the lesion was located in more basal regions of the cochlea. Thus, the focal point of the lesion may vary even though the acoustic spectrum of the impulse has not changed. In general, the OHC lesions were wider and more severe than the IHC lesions.

When there was a significant loss of OHC or IHC in a particular region of the cochlea, then the behavioral or evoked response thresholds associated with that region were generally elevated approximately 20 to 60 dB. The magnitude of the hearing loss was influenced somewhat by the location of the test frequency relative to the lesion. Test frequencies that were centered on the lesion seemed to show greater threshold shifts than other frequencies that were located on the border of the lesion (e.g., chinchilla 750, Figure 3.3.145). The frequencies bordering the lesion presumably show less threshold shift than those near the center of the lesion because the excitation pattern has a greater likelihood of spilling over into normal regions of the cochlea adjacent to the lesion. This would be particularly true if the high frequency regions basal to the lesion were normal. The degree of threshold shift also seemed to be related to the location of the lesion; the threshold shifts associated with apical lesions seemed to be less than those associated with the base. The spread of excitation towards the base of the cochlea could be one factor contributing to this difference.

Single auditory nerve fibers with CFs corresponding to the lesion also had abnormally high thresholds; however, the threshold shifts obtained by individual units were typically larger than those measured with the evoked response or behaviorally. When the lesion included both IHC and OHC, then it was never possible to locate fibers having CFs corresponding to the lesion. However, if the lesion involved just OHC, then it was generally possible to find units with CFs corresponding to the location of the lesion (e.g., chinchilla 366, Figure 3.3.48). Units with CFs located in the region of OHC had grossly abnormal tuning curves and it was sometime difficult to accurately assign CFs to these units. Furthermore, the tuning curves were often "W" shaped with the threshold in the tail being lower than that in the tip.

In a few instances there was a slight elevation of threshold in the absence of any significant hair cell loss (e.g., chinchilla 510 and 543). These slight threshold increases could be the result of subtle cochlear pathologies which are not detected with a conventional cochleogram. Alternatively, the threshold shifts could be the result of measurement errors, e.g., one might fail to record from the most sensitive nerve fibers associated with a particular region of the cochlea or the evoked response tracings might be extremely noisy during a test session.

There were a variety of changes in the evoked potential and behavioral tuning curves following exposure to the blast waves. The changes in tuning were most profound in regions where the hearing loss and hair cell loss were greatest. The most fundamental and common change in tuning was a simple elevation in the tip of the tuning curve which resulted in an overall broadening of the tuning curve. In some cases, however, the tips of the tuning curves were displaced either above or below the probe frequency. Tuning curves with tips displaced towards higher frequencies generally occurred with mid-cochlear or low-frequency hearing loss (or apical or mid-cochlear lesions). The tip is presumably displaced because neurons with CFs above the tip are as sensitive or more sensitive to the probe frequency than those located at the probe frequency. Thus, the masked-threshold tuning curve may map out the response of units located above the probe (e.g., chinchilla 603).

Tuning curves tips were sometimes displaced toward lower frequencies when the evoked response or behavioral thresholds below the probe frequency were substantially better than those near the probe. The downward displacement generally occurred for probe frequencies located on the low-frequency border of a high-frequency hearing loss (e.g., cinchilla 543 and 459). The downward shift in the tip of the tuning curve was generally much less than the upward shift. One obvious reason for this difference is that the mechanical response of the basilar membrane spreads more rapidly towards the basal or high frequency region of the cochlea than towards the apical or low frequency area.

The single unit tuning curves showed relatively systematic changes depending on the location of the unit's CF relative to the lesion. If the CF was located basalward of a cochlear lesion, the threshold of the unit was relatively normal at CF. However, the threshold in the tail of the tuning curve was often lower than normal (hypersensitive) and the tip and tail regions were separated by a high threshold notch. Furthermore, the tuning curves were "W" shaped (e.g., unit 126, Figure 3.3.51). When the CF was centered on a significant OHC lesion, the threshold at CF was generally quite high while the thresholds in the tail of the tuning curve were not as severely affected. In some cases there was a high threshold notch between the tip and tail region (e.g., unit 4, Figure 3.3.48), consequently, some of the tuning curves were "W" shaped. However, in many cases the tuning curves failed to show a pronounced threshold minima at any frequency and the tuning curves assumed a broad "U" shape (e.g., unit 133, Figure 3.3.65) or "V" shape. "W" shaped tuning curves were also found if the CF was located along the apical border of a lesion; again, it was common to find a sharp notch separating the tip from the tail of the tuning curve (e.g., unit 14, Figure 3.3.64).

The <u>hypersensitive</u> thresholds that occured in the low-frequency tails of some units with "W" shaped tuning curves are potentially important for understanding the relationship between the magnitude of hair cell loss and the amount of threshold shift measured behaviorally or with the evoked response. The frequencies that were hypersensitive in the tails of the single unit tuning curves were often associated with regions of the cochlea with large cochlear lesions. The thresholds of the units with CFs corresponding to the location of the lesion in turn had elevated thresholds; the thresholds at CF were often higher than the thresholds found in the hypersensitive tails of units with CFs located above the lesion. For example, the threshold at 1.0 kHz of unit 12, which has a CF = 4.0 kHz (Figure 3.3.127) is lower than that of unit 28, which has a CF = 1.0 kHz (Figure 3.3.125). Furthermore, the threshold in the tail of unit 12, which has a CF of 4.0 kHz, closely approximates the evoked response threshold at 1.0 kHz (Figure 3.3.117). These results clearly illustrate how low frequency thresholds can be mediated by units with CFs located above the lesion. The net effect is that the pure tone audiogram can grossly underestimate the threshold shift and anatomical damage corresponding to a particular location along the basilar membrane. The hypersensitive tails also help to explain why the tips of psychophysical and evoked response tuning curves (e.g., Figure 3.3.120) are displaced toward higher frequencies.

Using SEM analysis of blast wave lesions, a distinction was made between lesions which seemed to be the result of direct mechanical damage to the organ of Corti versus lesions that seemed to result from metabolic factors. A qualitative comparison can be made of the single unit tuning curves obtained from chinchillas 60 and 366 that sustained "mechanical" lesions versus chinchilla 459 that sustained a "non-mechanical" lesion. The tuning curves obtained from these animals did not seem to differ significantly even though the underlying lesions appear to have been induced in a different way. Thus, one might conclude that the manner in which the lesion is induced does not seem to significantly influence the physiological results. However, this view needs to be interpreted cautiously. First, rather limited physiological data are available from animals with mechanical-type lesions. Second, the data were obtained at least 2 months post-exposure so that the lesion had resolved itself into a stable scar configuration. The physiological results from the two types of lesions might have been fundamentally different during the early stages of trauma when there is likely to be significant intermixing of fluids from the mechanical ruptures (e.g., Figure 3.2.2). It would be important to study the physiological responses during the early stages of cochlear trauma.

## Bibliography


Beagley, H.A. (1965a). Acoustic trauma in the guinea pig. I. Electrophysiology and Histology. Acta Oto-Laryng. 60: 437-451.

Beagley, H.A. (1965b). Acoustic trauma in the guinea pig. II. Electron microscopy including morphology of cell junction in the organ of Corti. Acta Oto-Laryng. 60: 479-495.

von Bismark, G. 1967. The sound pressure transformation from free-field to the eardrum of the chinchilla. M. S. Thesis, Massachusetts Institute of Technology, Cambridge, Mass..

Blakeslee, E. A., Hynson, K., Hamernik, R. P. and Henderson, D. (1978). Asymptotic threshold shift in chinchillas exposed to impulse noise. J. Acoust. Soc. Amer. 63, 876-882.

Chistovich, L. A. (1957). "Frequency characteristics of masking effect." Biofizika 2, 749-755.

Eames, B. L., Hamernik, R. P., and Henderson, D. (1975). The role of the middle ear in acoustic trauma from impulses. Laryngoscope, 85, 1582-1592.

Eldredge, D.H., Miller, J.D., Bohne, B.A., and Clark, W.W. 1977. Frequency-position maps for the chinchilla cochlea. J. Acoust. Soc. Amer. 62, S-35.

Hawkins, J. E., Cazals, Y., Erre, J. P., and Aran, J. M. 1978. Selective elevation of cochlear whole-nerve thresholds for high frequencies recorded acutely in guinea pigs. J. Acoust. Soc. Amer. 64, Suppl. 1.

Henderson, D., Hamernik, R. P., Woodford, C., Sitler, R. and Salvi, R. J. (1973). Evoked response audibility curve of the chinchilla. J. Acoust. Soc. Amer. 54, 1099-1101.

Klein, A. J., and Mills, J. H. (1981). "Physiological (waves I and V) and psychophysical tuning curves in human subjects." J. Acoust. Soc. Am. 69, 760-768.

Liberman, M. C. (1978). Auditory-nerve response from cats raised in a low-noise chamber. J. Acoust. Soc. Amer. 63, 442-455.

Liberman, M.C. and Kiang, N.Y.S. 1978. Acoustic trauma in cats. Cochlear pathology and auditory-nerve activity. Acta Otolaryngol. Suppl. 358, 11-64.

Luz, G. A. and Hodge, D. C. (1971). Recovery from impulse-noise induced TTS in monkeys and men: A descriptive model. J. Acoust. Soc. Amer., 49, 1770-1779.

McGee, T., Ryan, A. and Dallos, P. (1976). "Psychophysical tuning curves of chinchillas." J. Acoust. Soc. Amer. 60, 1146-1150.

McRobert. H. and Ward, W. D. (1973). Damage risk criteria: The trading relation between intensity and the number of non-reverberant impulses. J. Acoust. Soc. Amer. 53, 1297-1300.

Mitchel., C., and Fowler, C. (1980). "Tuning curves of cochlear and brainstem responses of the guinea pig." J. Acoust. Soc. Amer. 68, 896-900.

Robertson, D., Cody, A. R., Bredberg, G., and Johnstone, B. M. 1980. Response properties of spiral ganglion neurons in cochleas damaged by direct mechanical trauma. J. Acoust. Soc. Amer. 67, 1295-1305.

Salvi, R. J., Hamernik, R. P., and Henderson, D. (1978). Discharge patterns in the cochlear nucleus of the chinchilla following noise induced asymptotic threshold shift. Exp. Br. Res. 32, 301-320.

Salvi, R. J., Henderson, D. and Hamernik, R. P. (1979). Single auditory nerve fiber and action potential latencies in normal and noise-treated chinchillas. Hearing Res. 1, 237-251.

Salvi, R. J., Perry, J., Hamernik, R. P., and Henderson, D. (1982). "Relationships between cochlear pathologies and auditory nerve and behavioral responses following acoustic trauma." In: New perspectives on noise-induced hearing loss. edited by R. P. Hamernik, D. Henderson and R. J. Salvi (Raven Press, New York).

Salvi, R. J., Ahroon, W. A., Perry, J., Gunnarson, A. D. and Henderson, D. (1982) Comparison of psychophysical and evoked-potential tuning curves in the chinchilla. Am J. Otolaryngol., 3, 408-416.

Small, A. M. (1959). "Pure tone masking." J. Acoust. Soc. Amer. 31, 1619-1625.

Stockwell, C.W., Ades, H.W. and Engstrom, H. (1969). Patterns of hair cell damage after intense auditory stimulation. Ann. Otol. 78: 1144-1168.

Voldrich, L. (1972). Experimental acoustic trauma. Part I. Acta Otolaryng. 74: 392-397.

Voldrich, L. and Ulehlova (1980). Comparative method for the study of structural damage in acoustic trauma. Laryngoscope 90: 1887-1891.

Walker, J. G. (1970). Temporary threshold shift from impulse noise. Am. Occup. Hyg. 13, 51.

Weber, D. L., Johnson-Davies, D. and Patterson, R. D. 1980. The use of psychophysical tuning curves to measure frequency selectivity. In: Psychophysical physiological and behavioral studies in hearing, edited by G. van Den Brink and F. A. Bilsen (Delft University Press, Netherlands).

Wightman, F. L., McGee, T., and Kramer, M. (1977). "Factors influencing frequency selectivity in normal and hearing impaired listeners." In: Psychophysic and physiology of hearing, edited by E. F. Evans and J. P. Wilson (Academic Press, London), pp. 295-306.

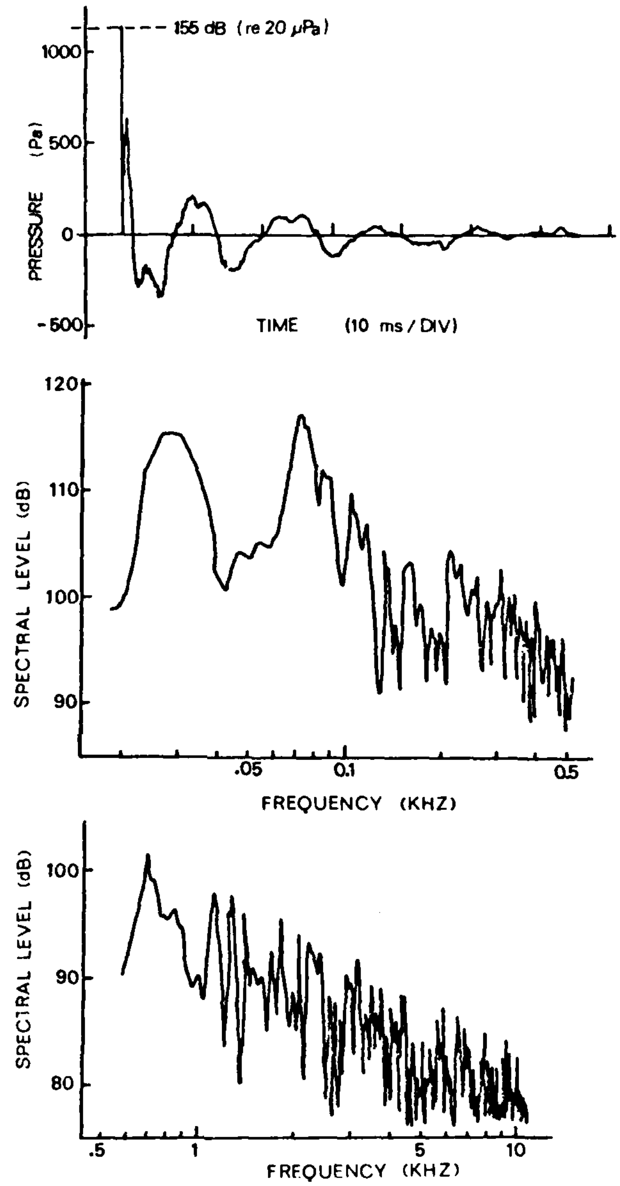


Figure 2.7.1: Pressure-time waveform and spectrum of the blast wave

Figure 3.2.1

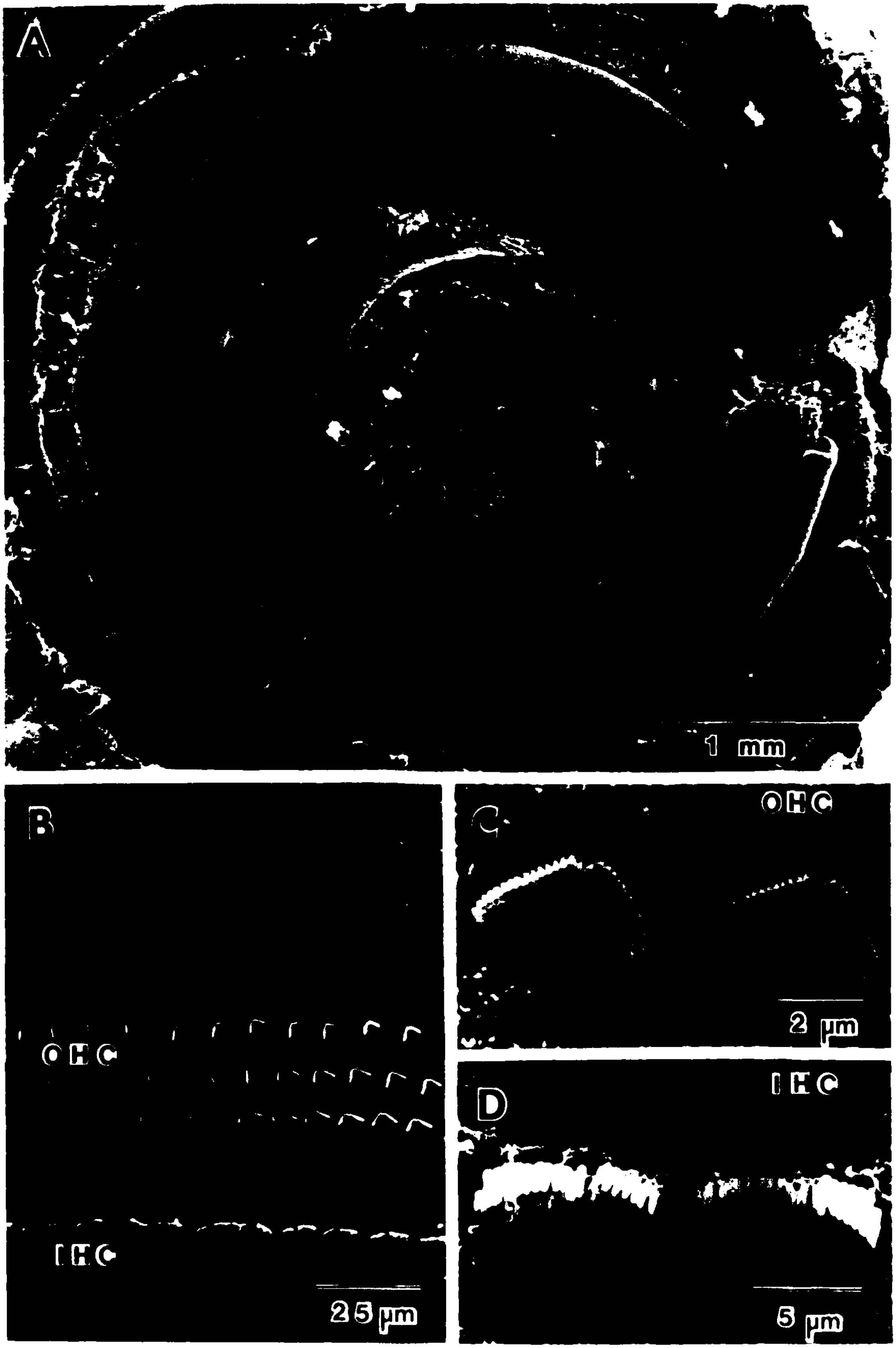

Figure 3.2.2

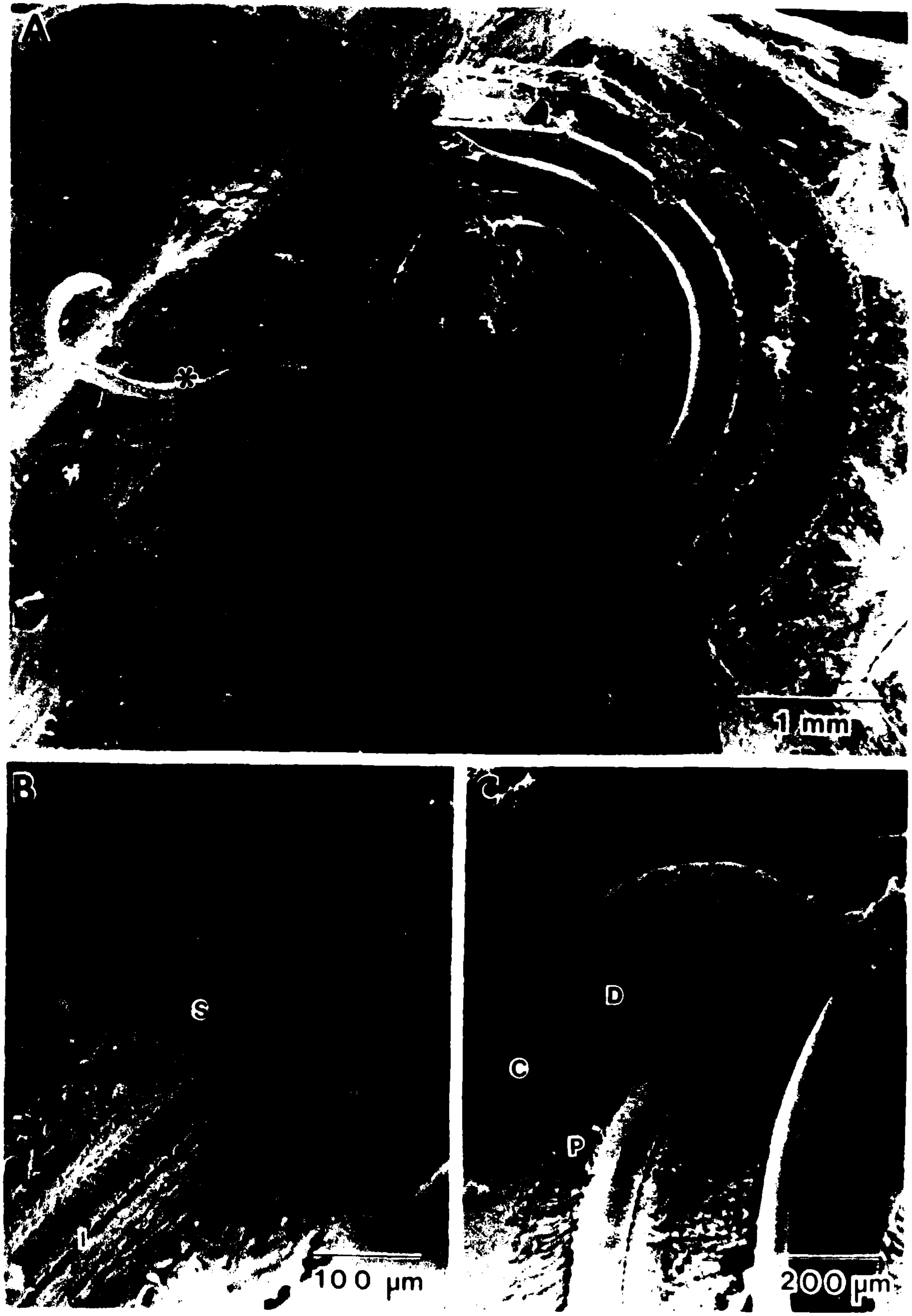

Figure 3.2.3

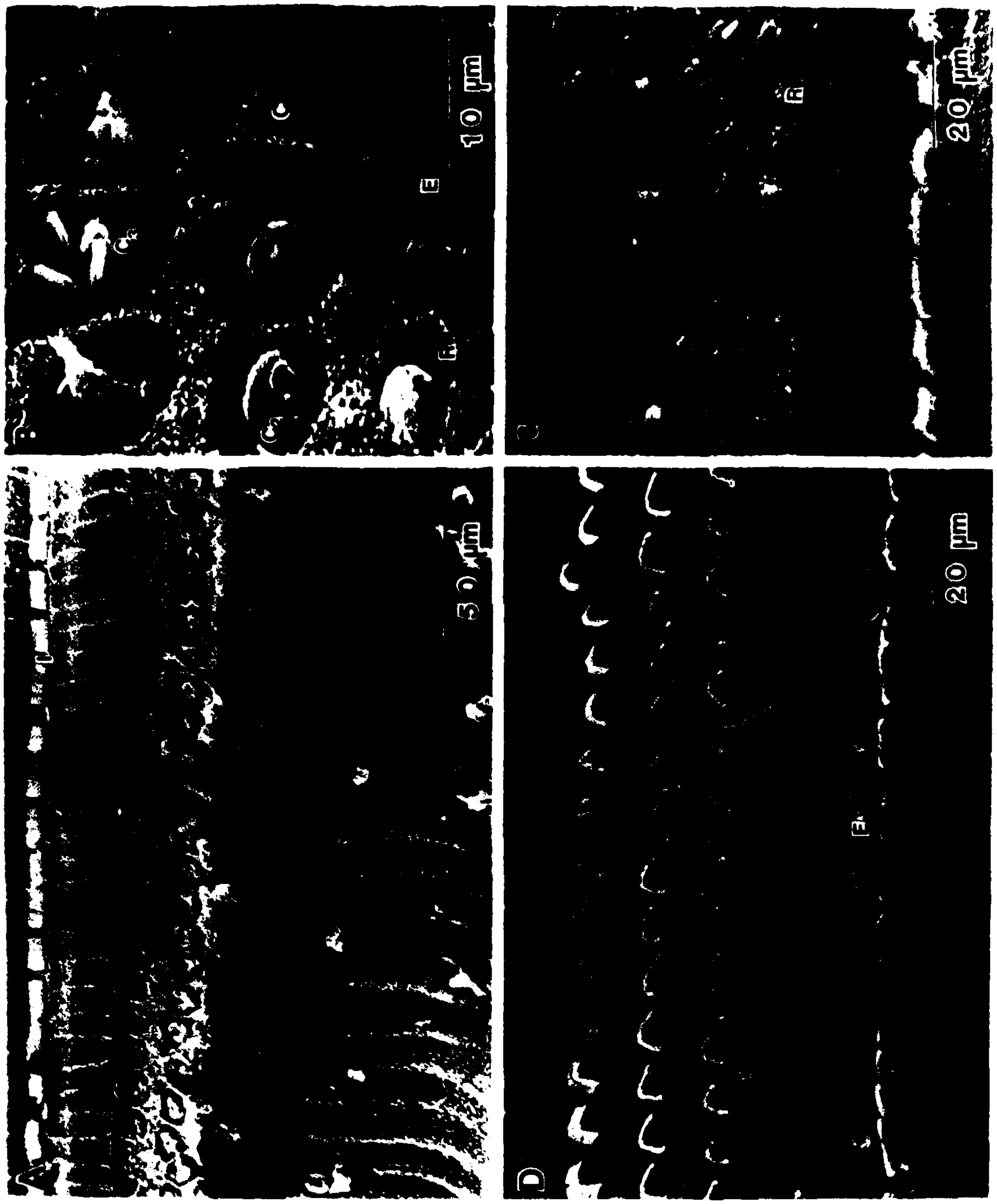

Figure 3.2.4

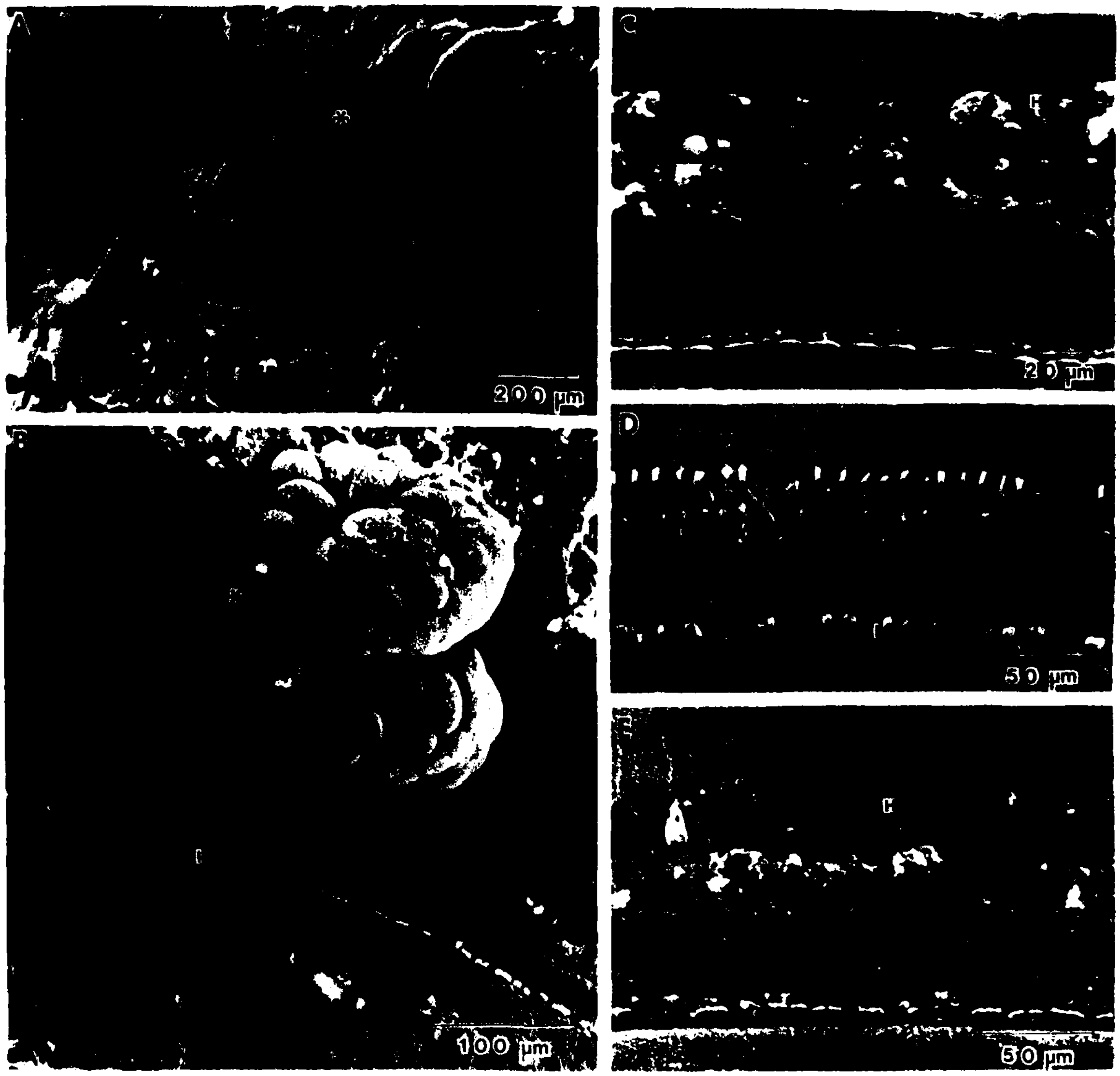

Figure 3.2.5

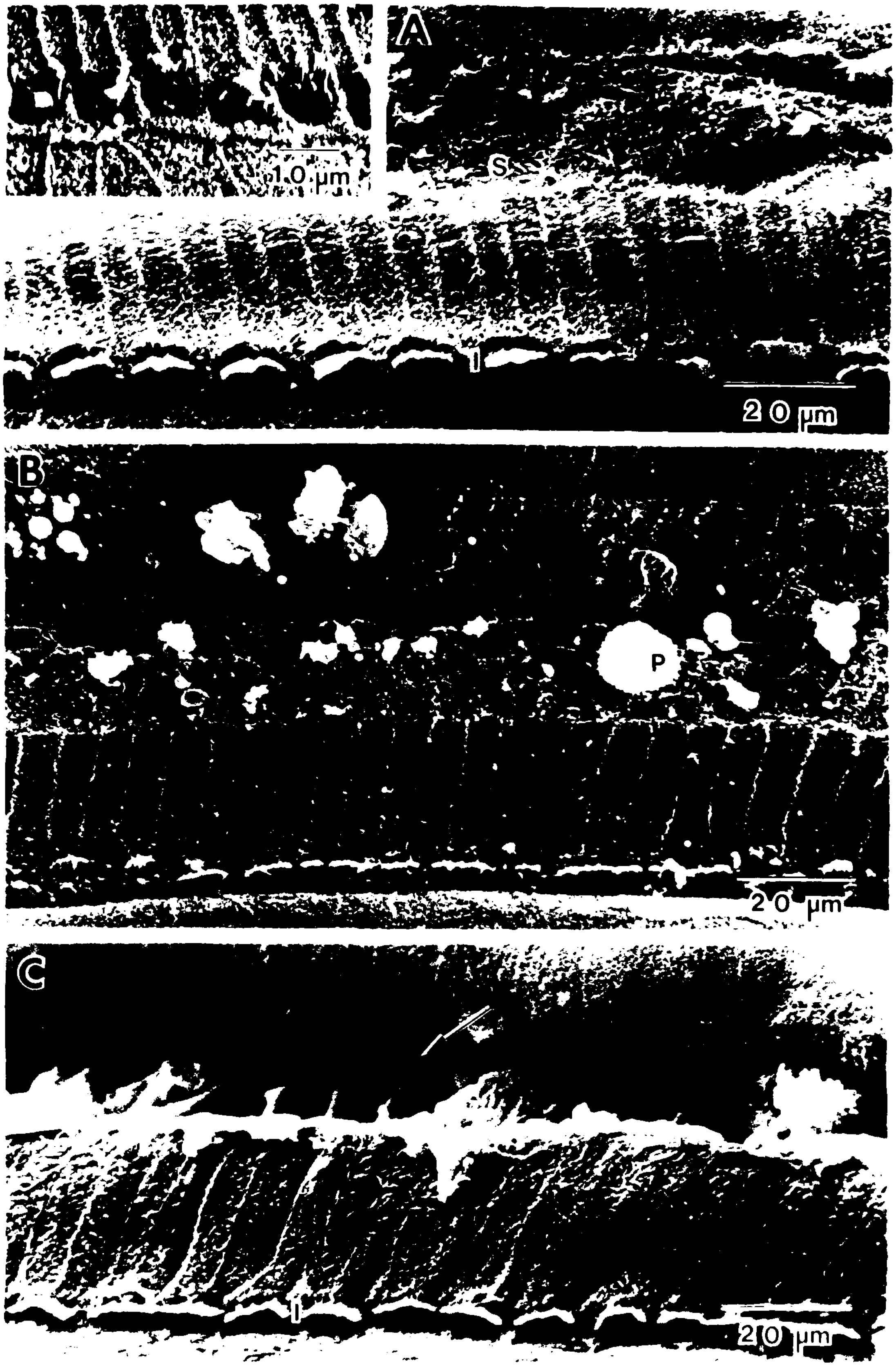

Figure 3.2.6

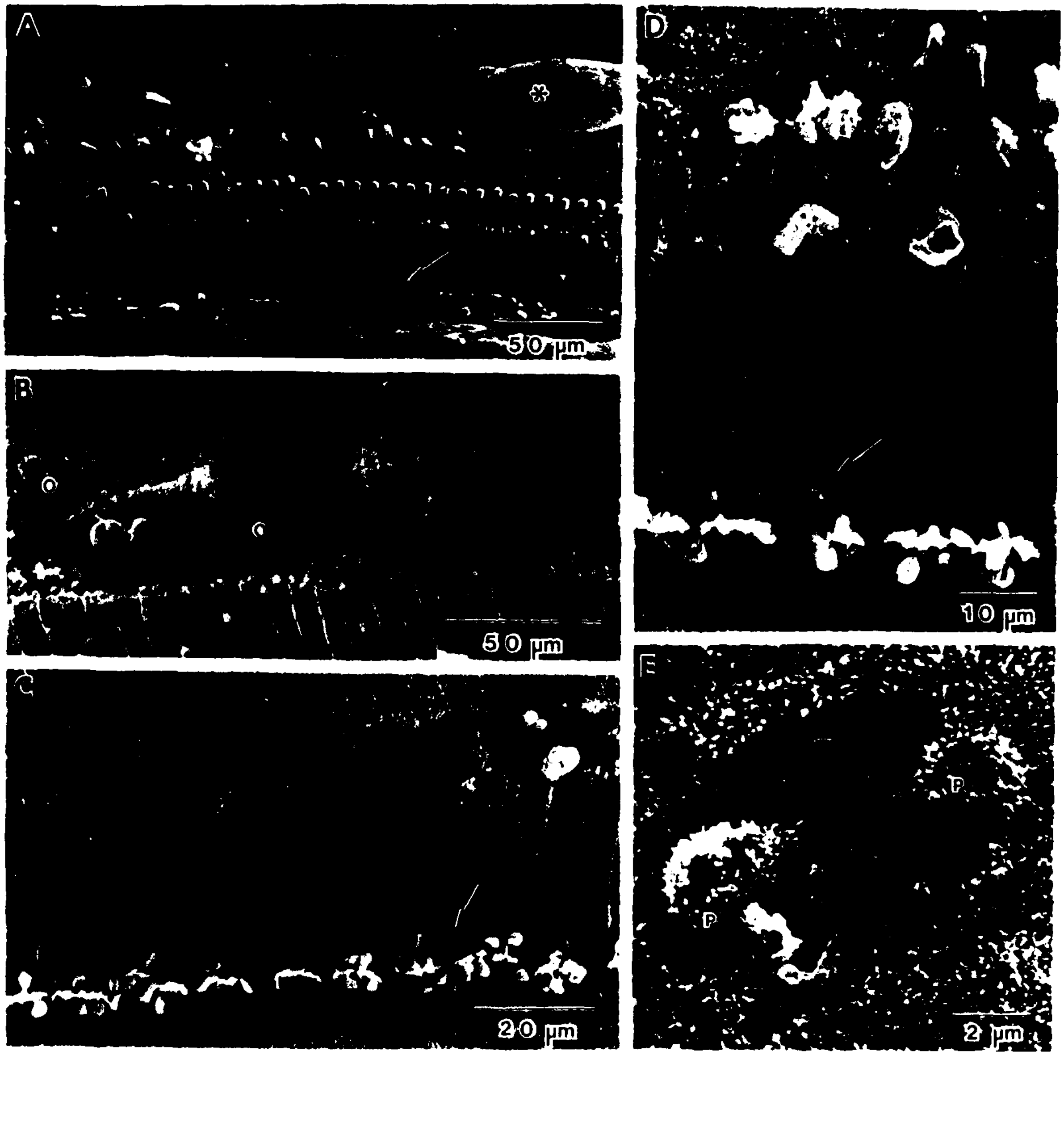

Figure 3.2.7

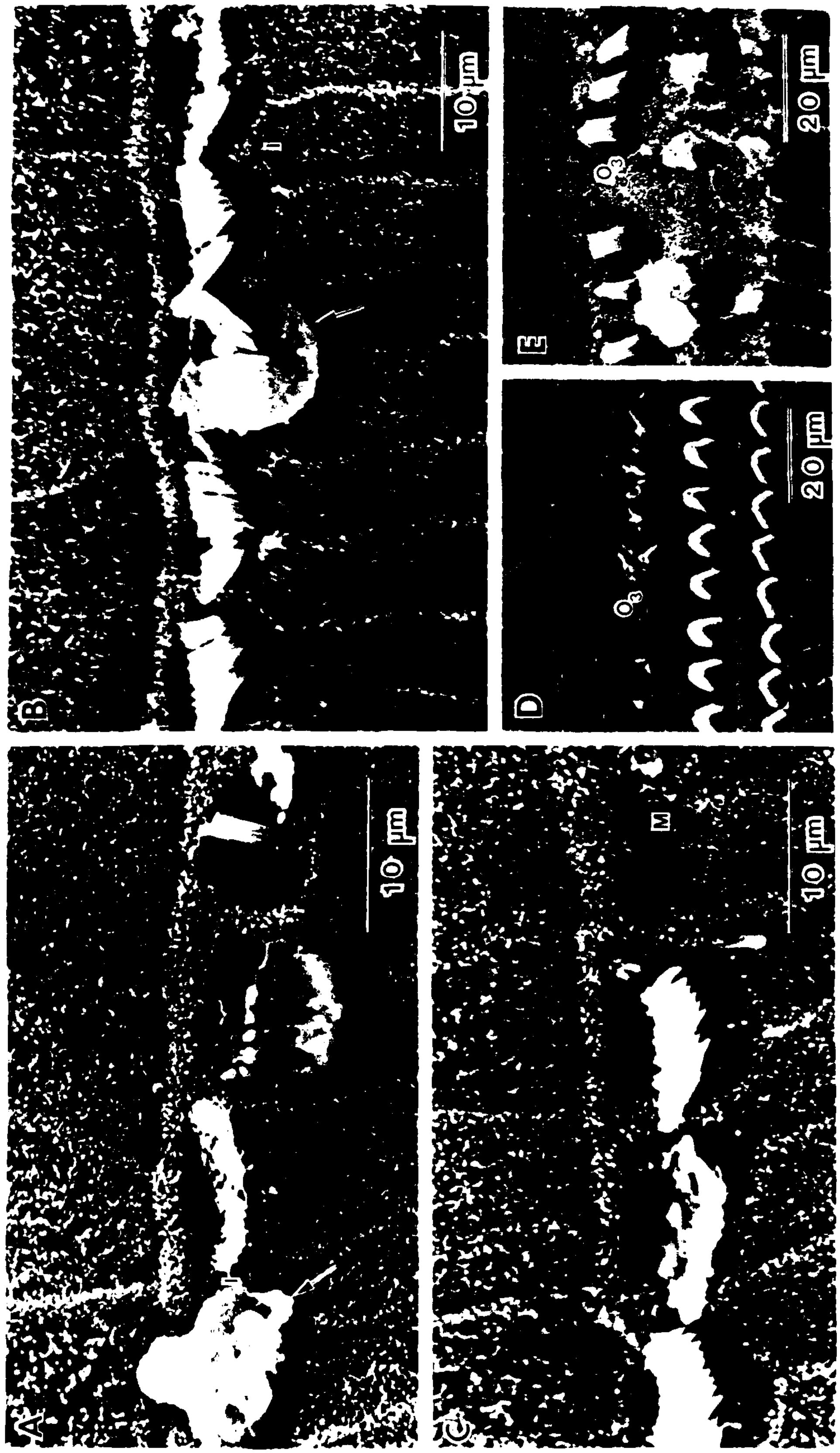

Figure 3.2.8

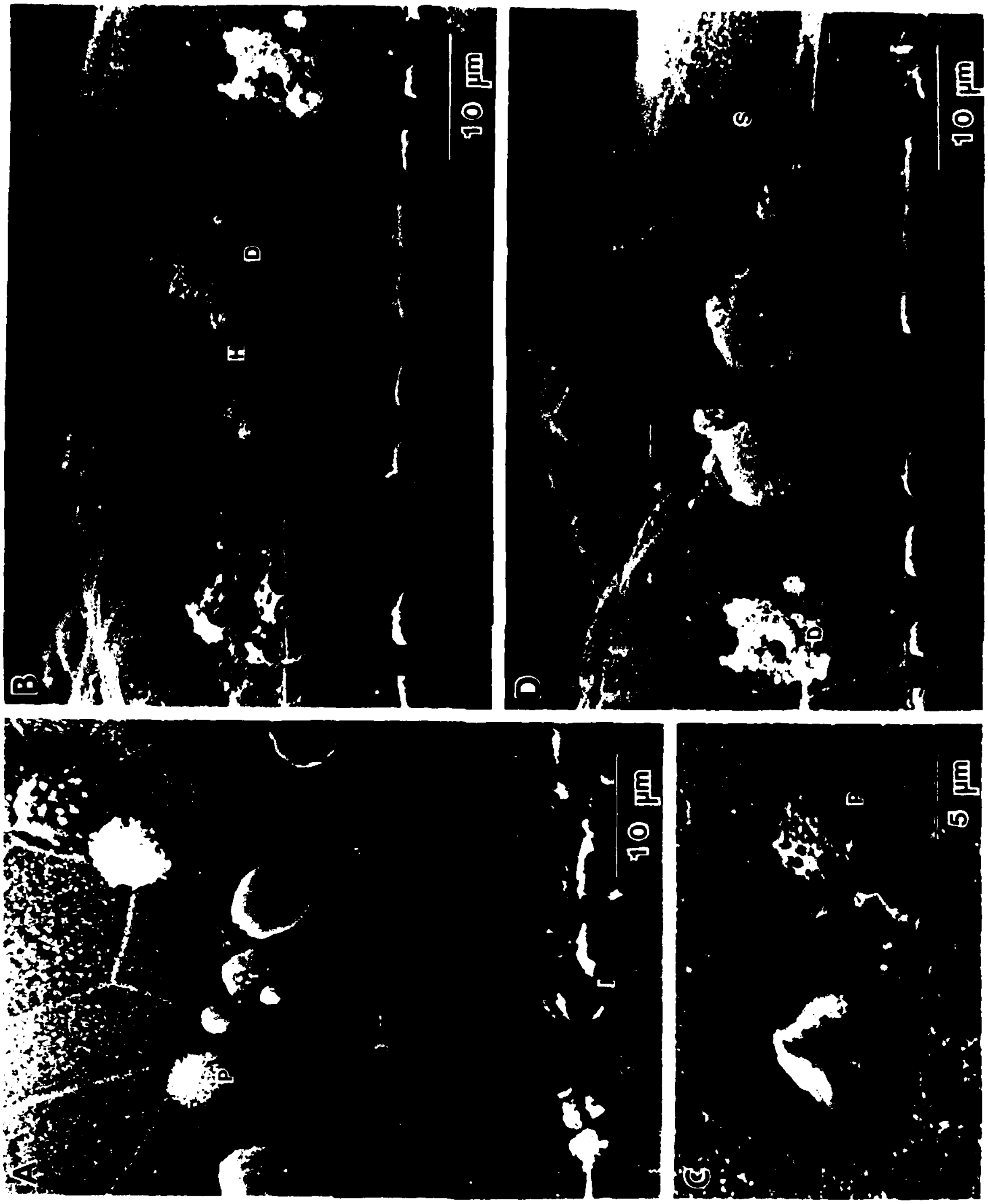

Figure 3.2.9

Figure 3.2.10

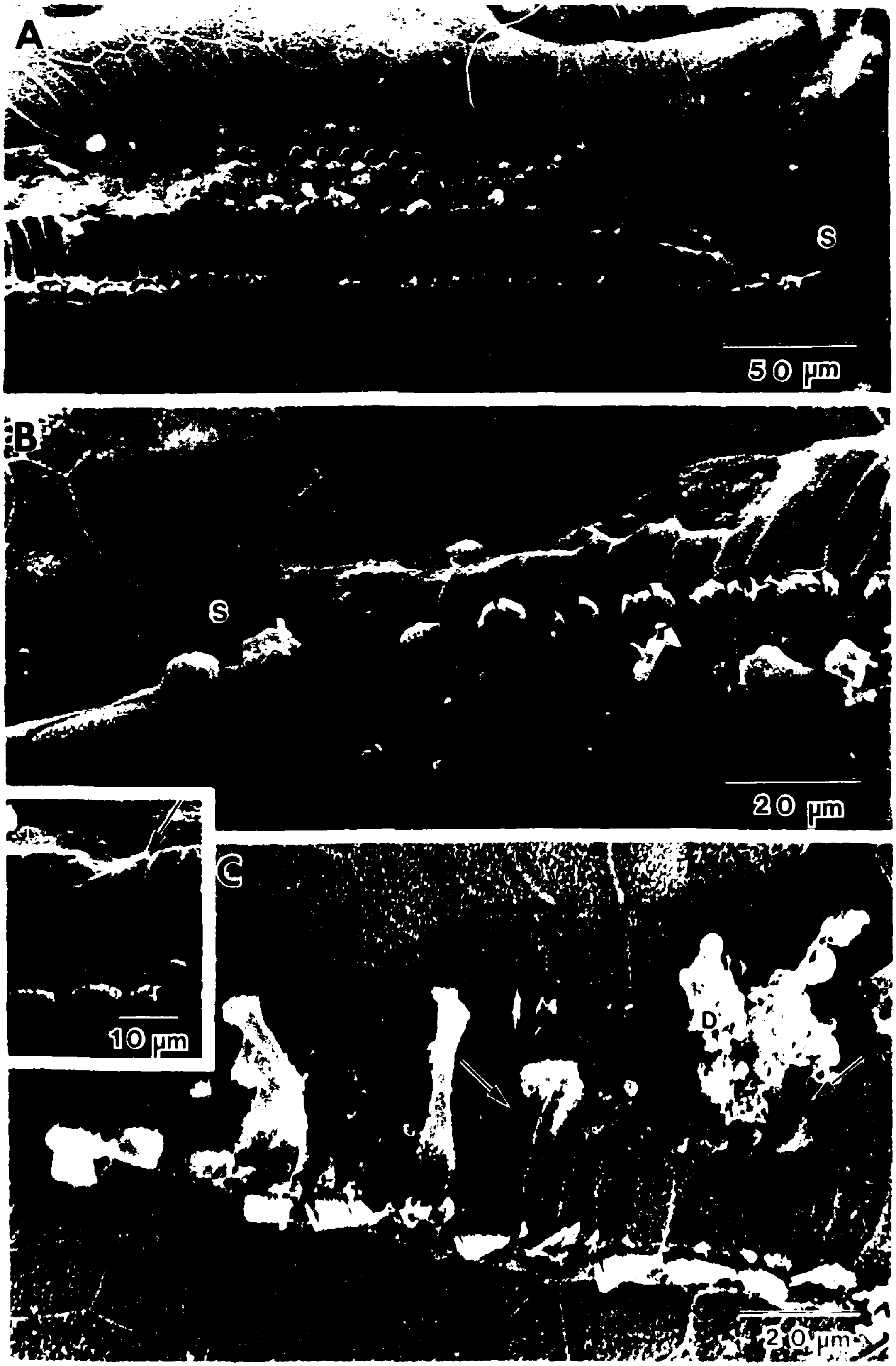

Figure 3.2.11

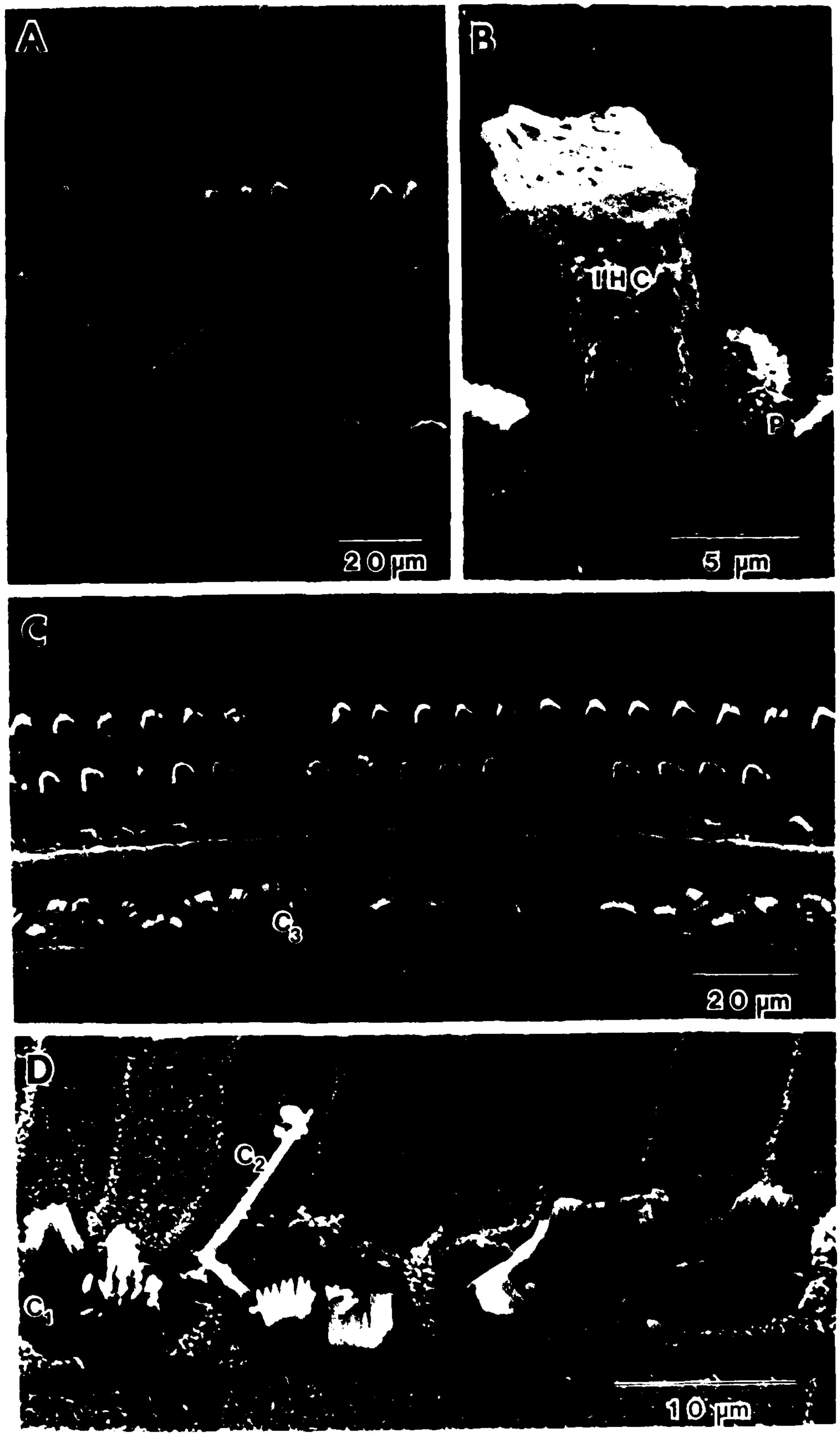

Figure 3.2.12

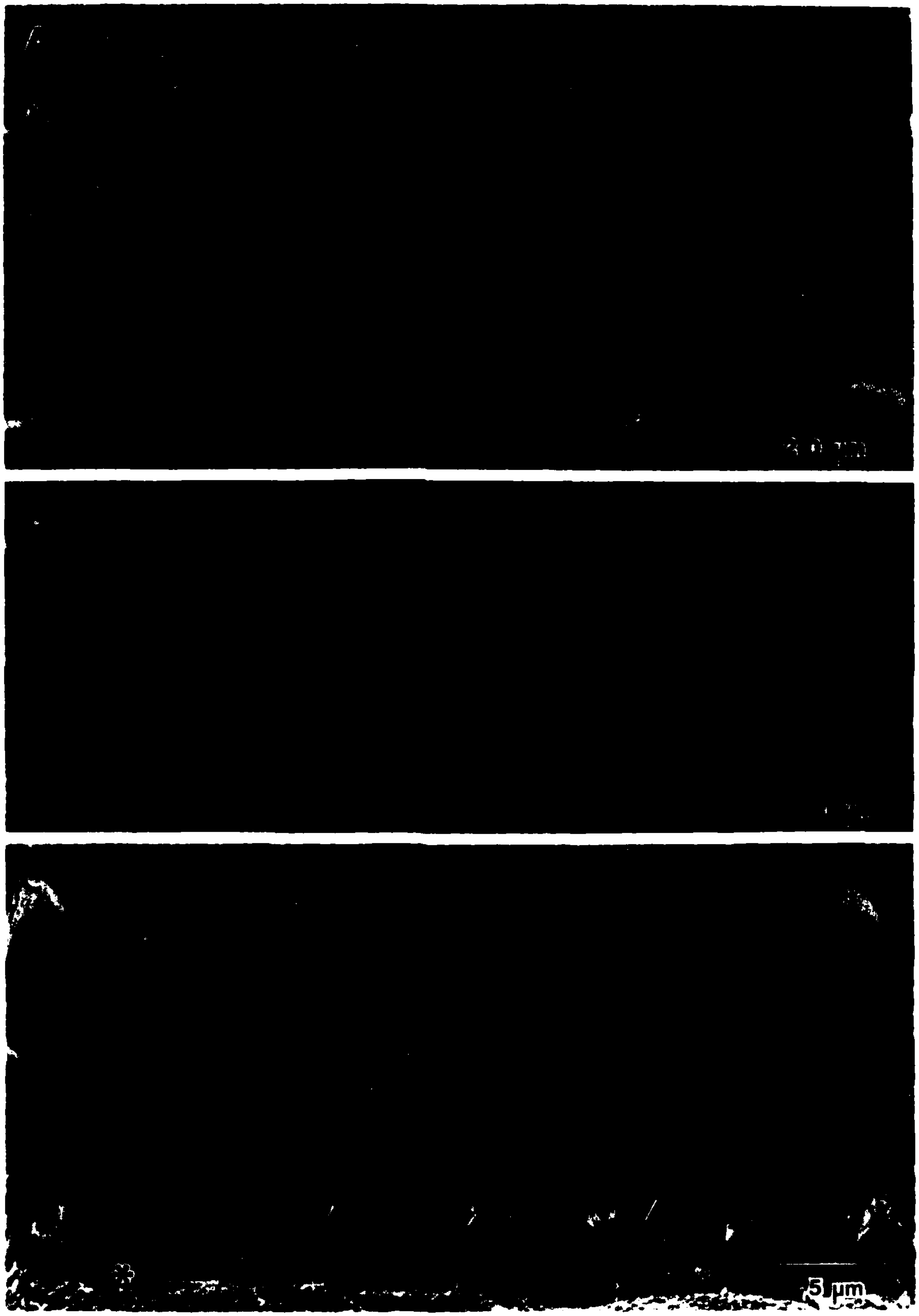

Figure 3.2.13

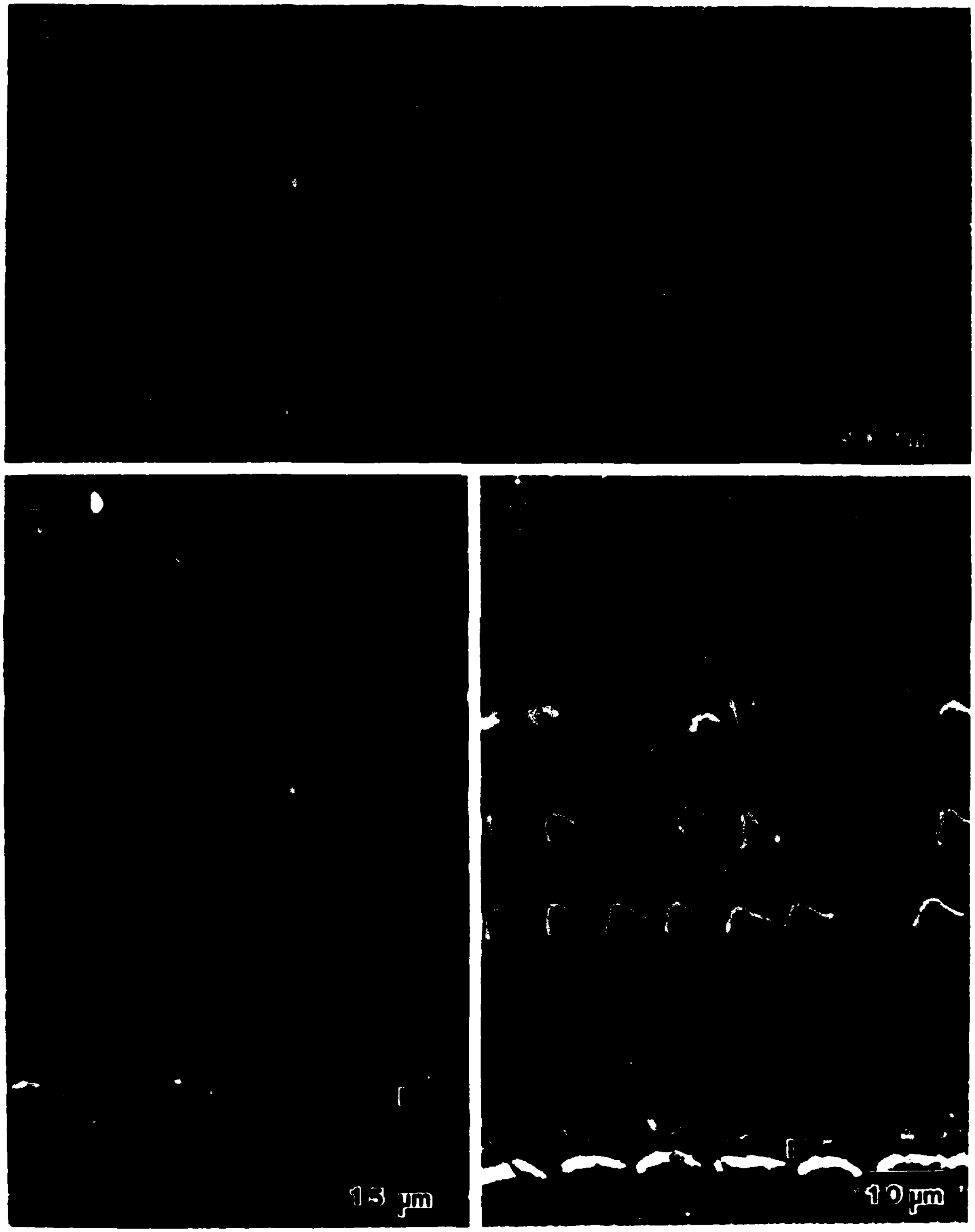

Figure 3.2.14

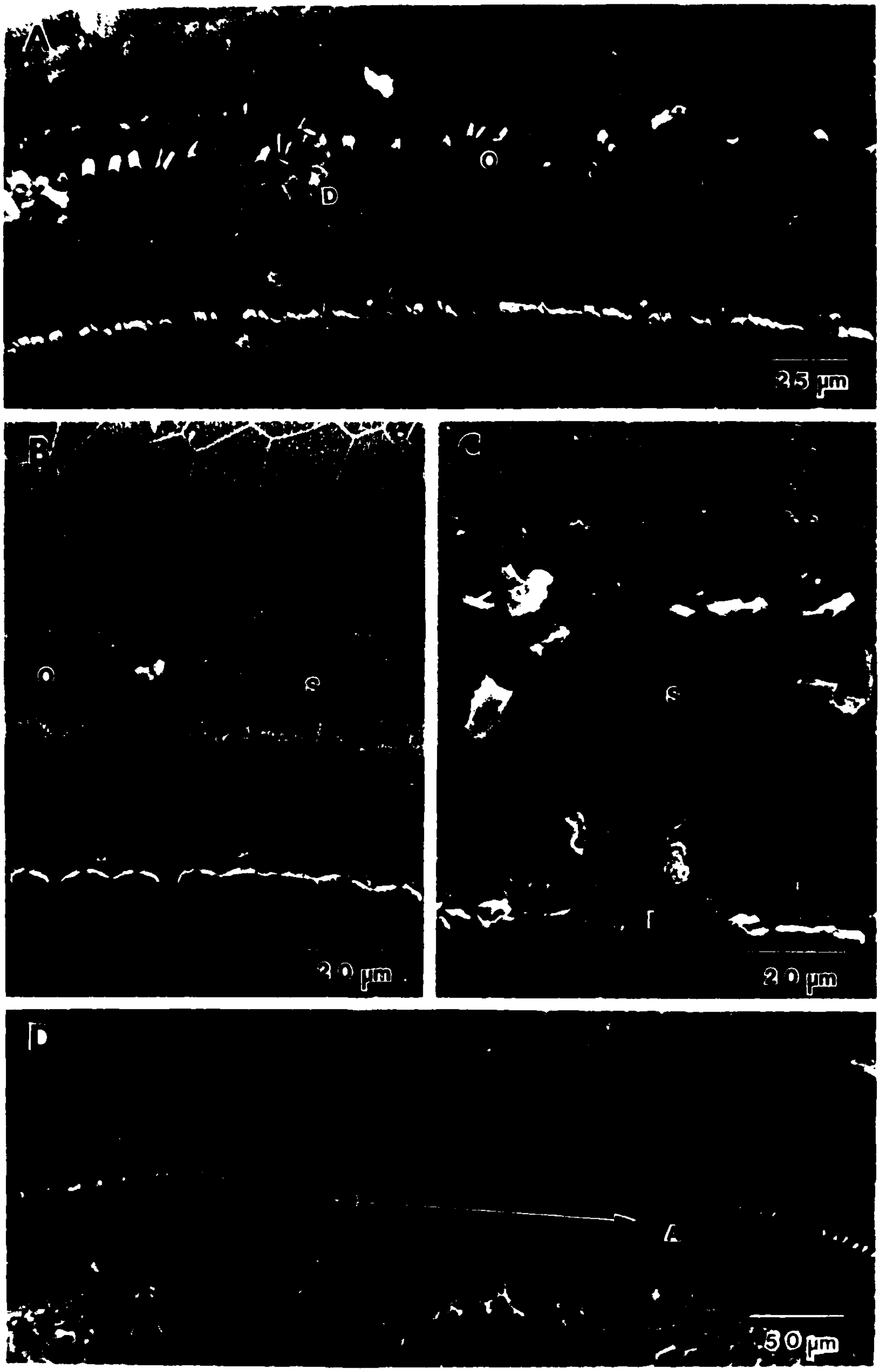

Figure 3.2.15

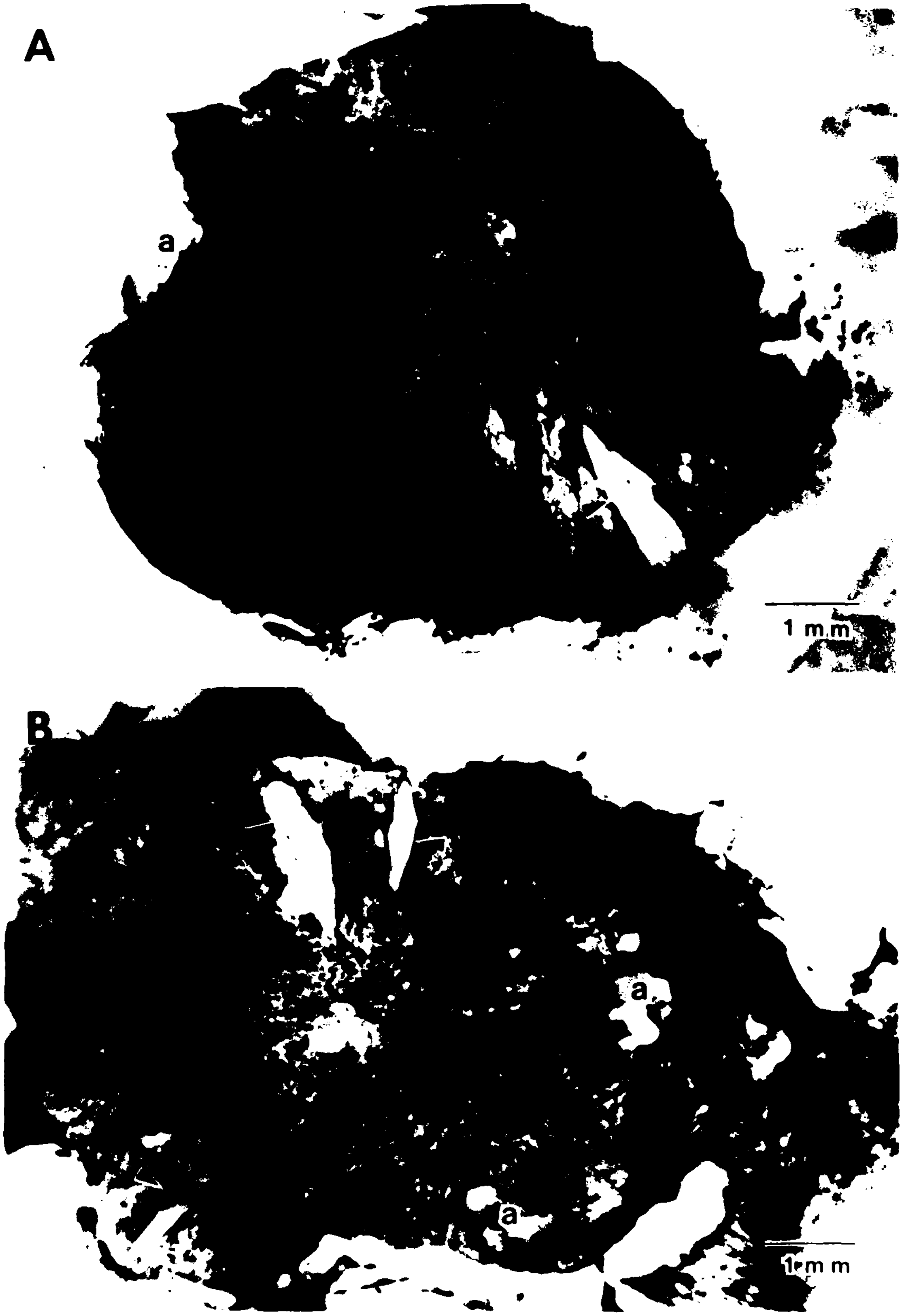

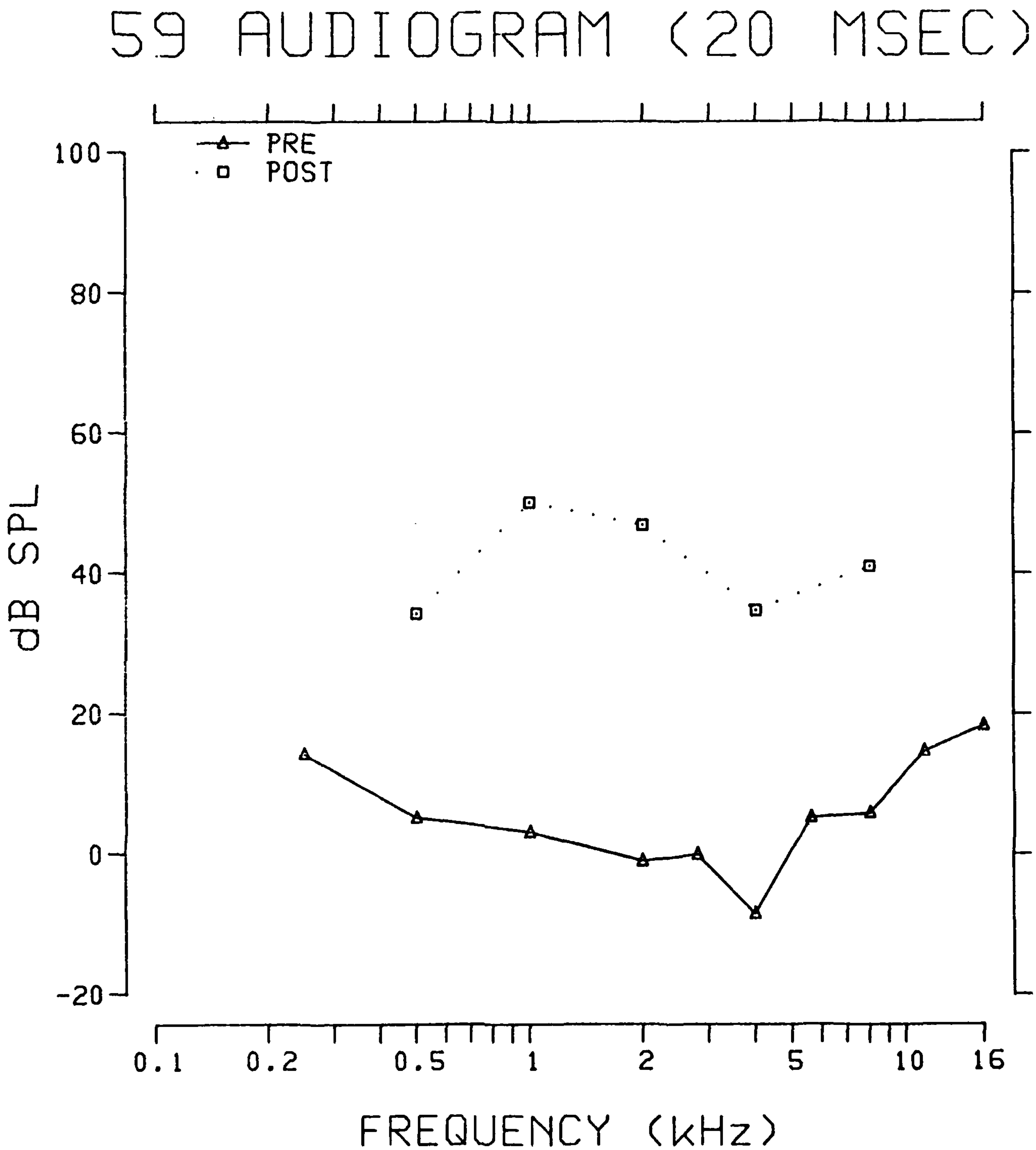


Fig. 3.3.0: Pre- and postexposure behavioral thresholds of chinchilla 59.

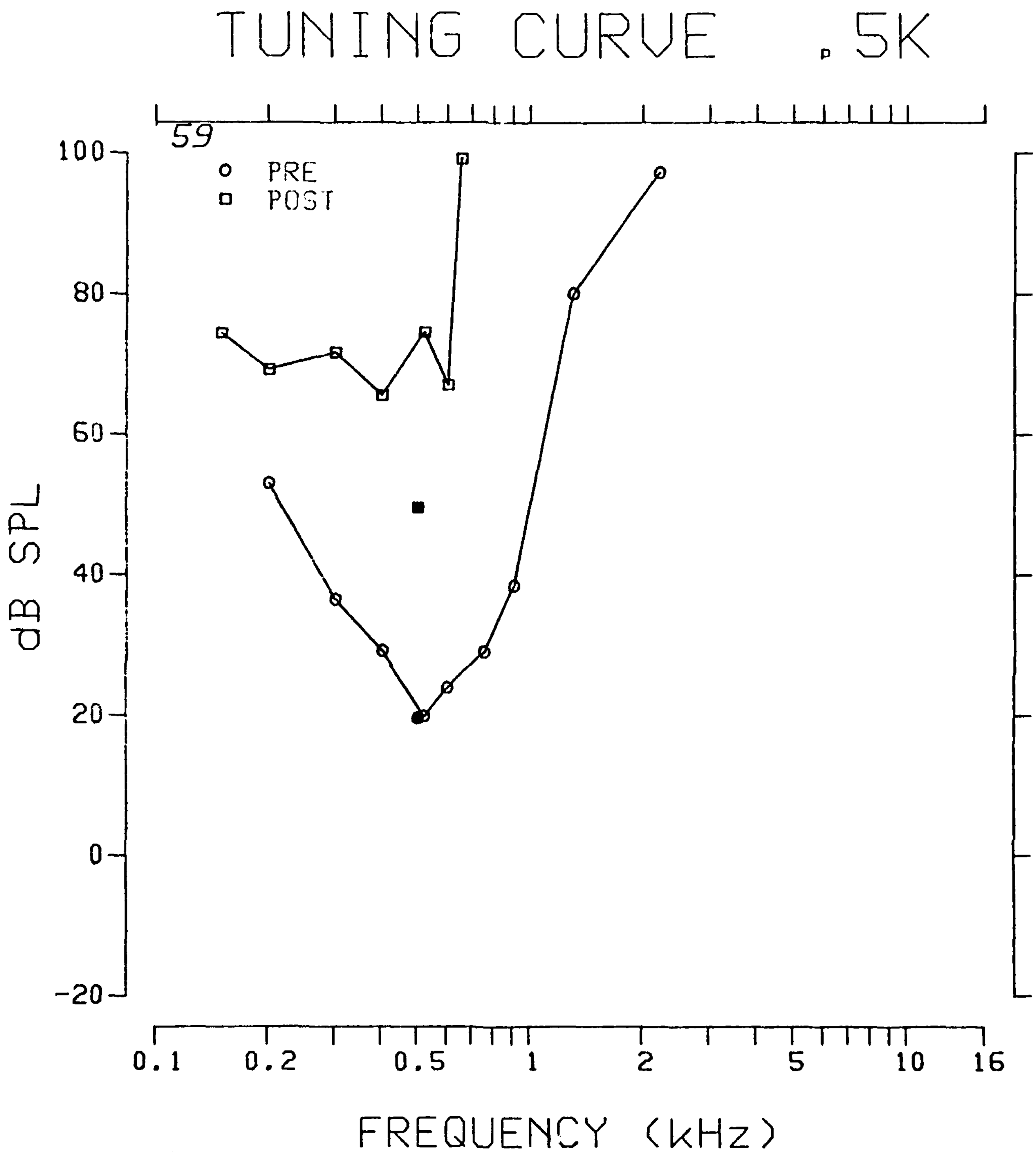


Fig. 3.3.1: Pre- and postexposure psychophysical tuning curve at 0.5 kHz for chinchilla 59.

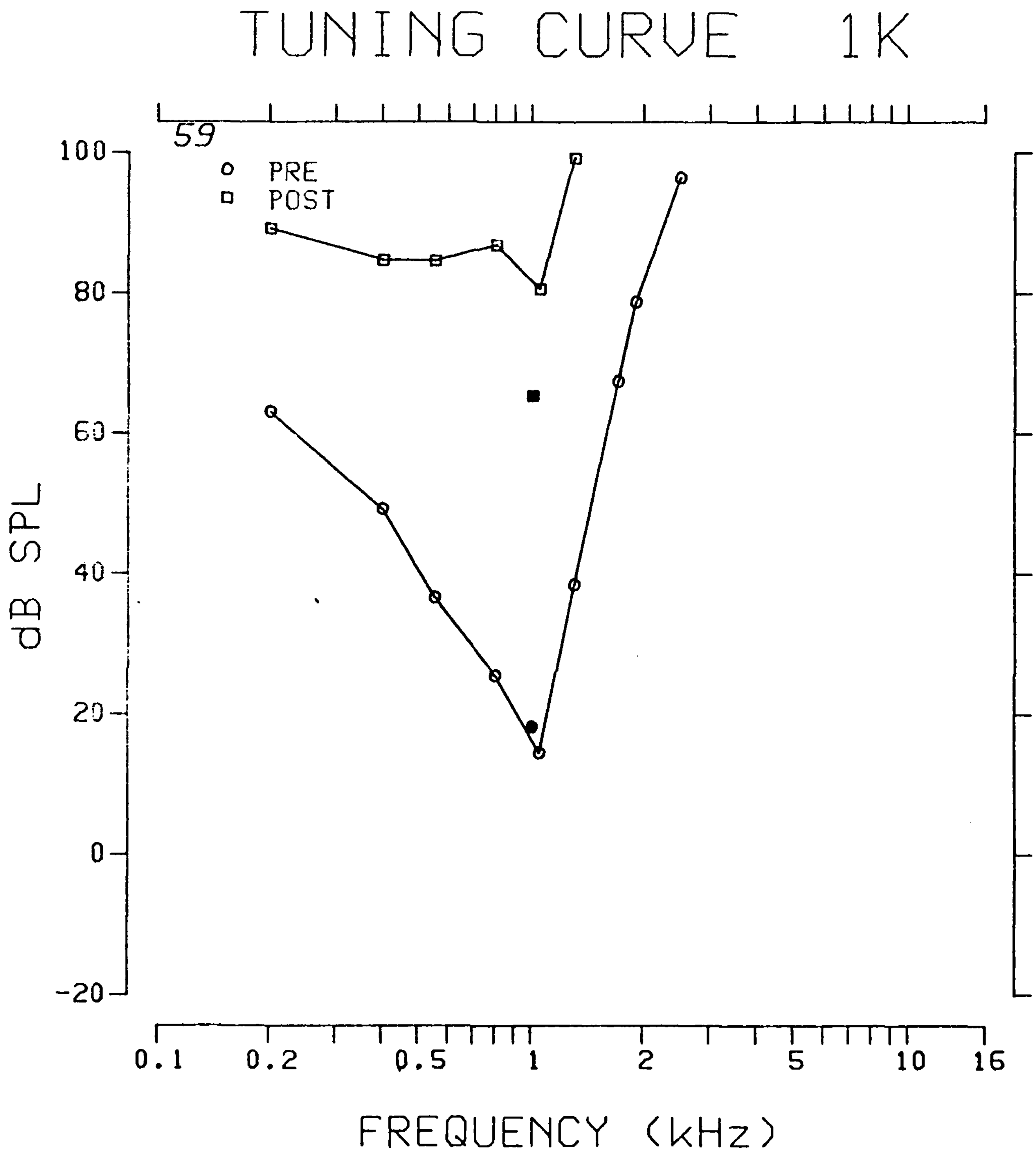


Fig. 3.3.2: Pre- and postexposure psychophysical tuning curve at 1.0 kHz for chinchilla 59.

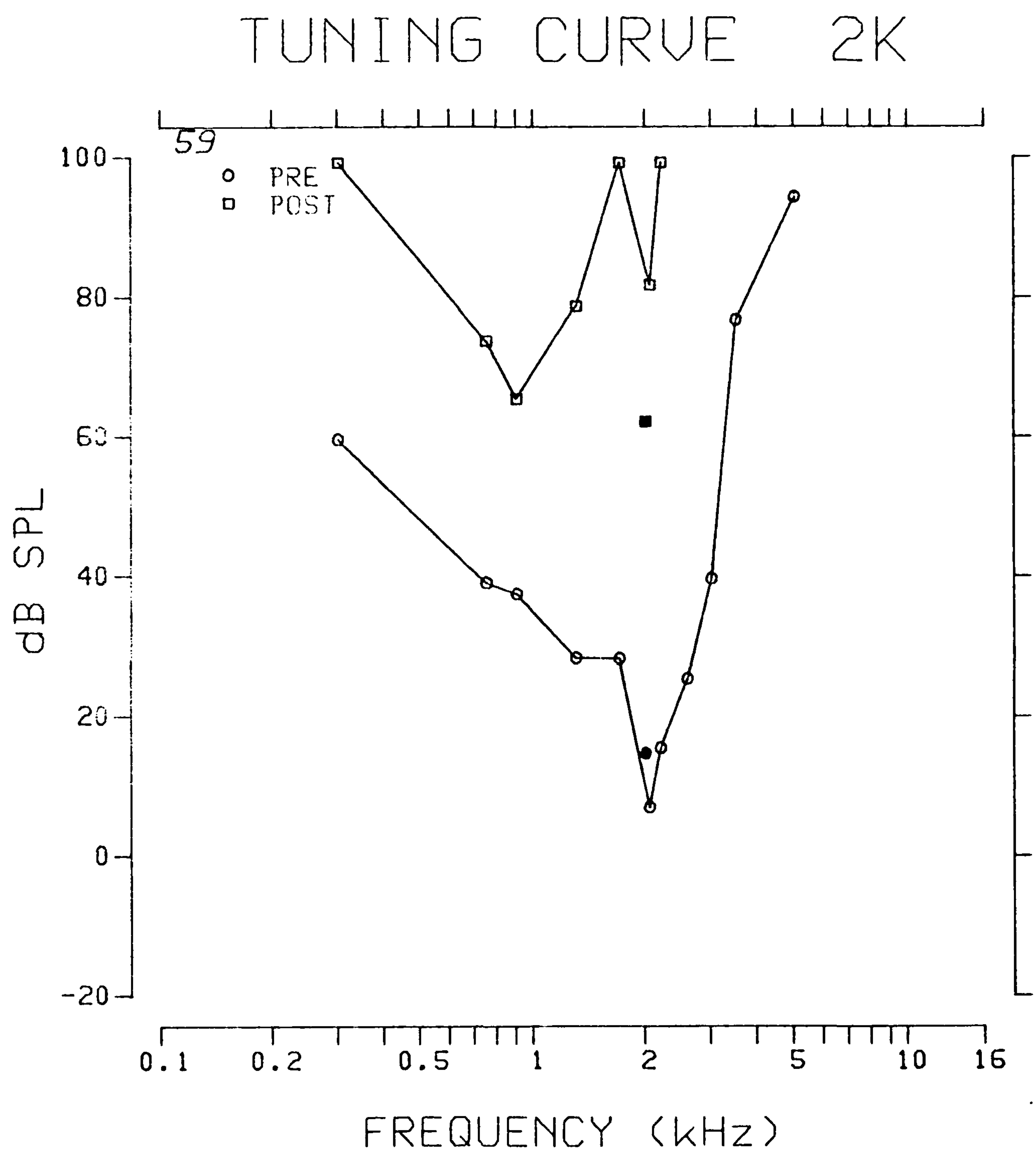


Fig. 3.3.3: Pre- and postexposure psychophysical tuning curve at 2.0 kHz for chinchilla 59.

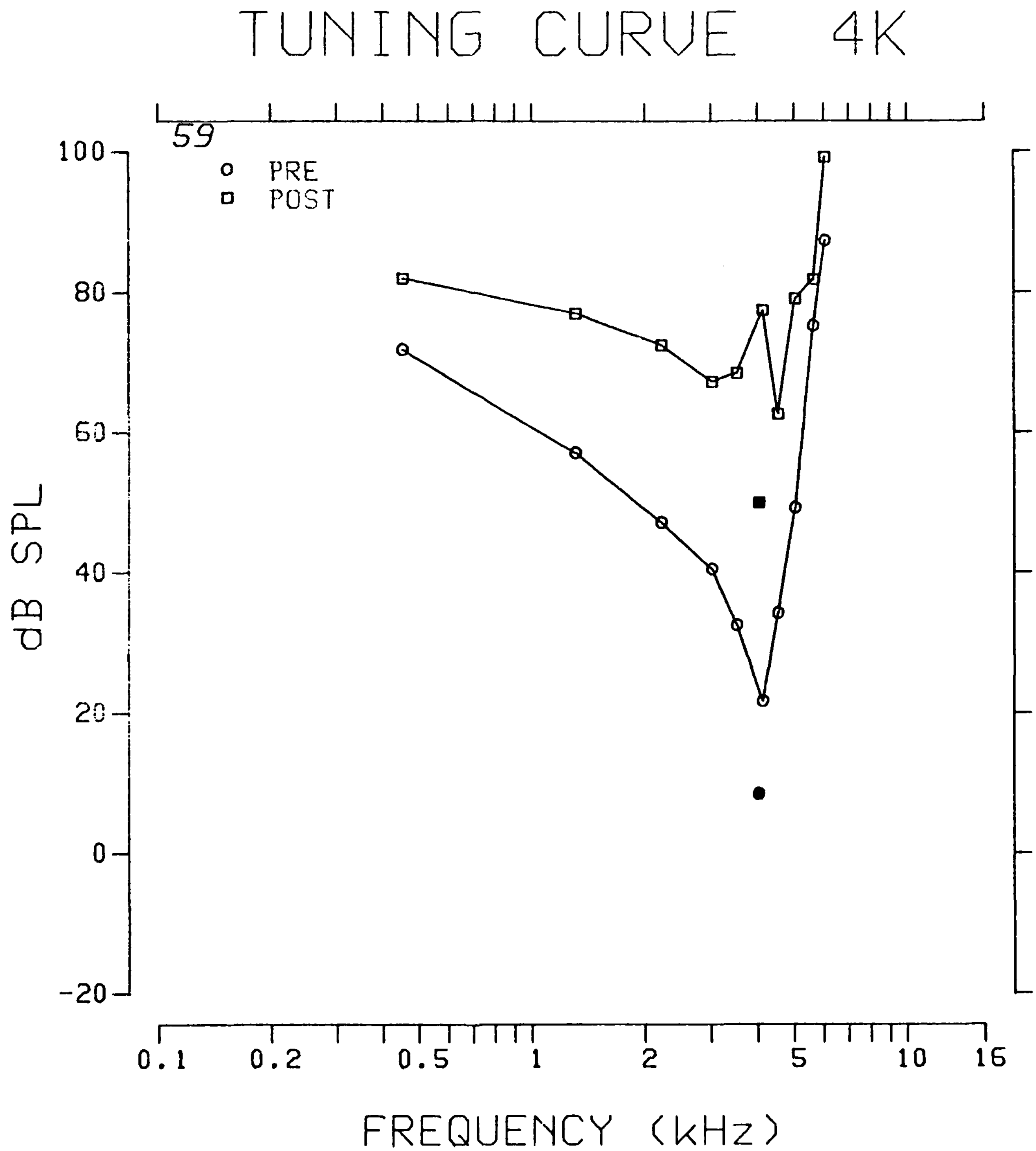


Fig. 3.3.4: Pre- and postexposure psychophysical tuning curve at 4.0 kHz for chinchilla 59.

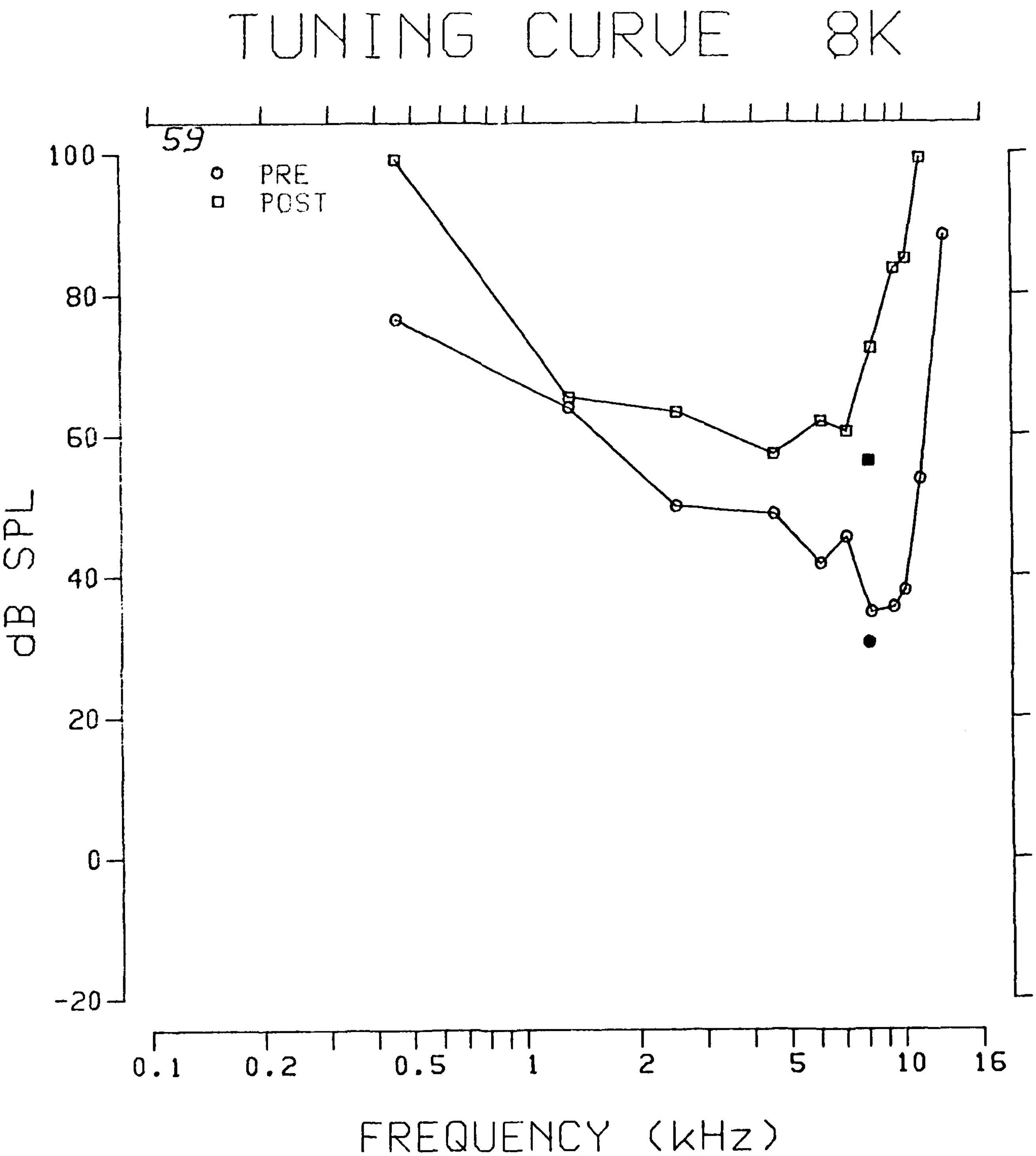


Fig. 3.3.5: Pre- and postexposure psychophysical tuning curve at 8.0 kHz for chinchilla 59.

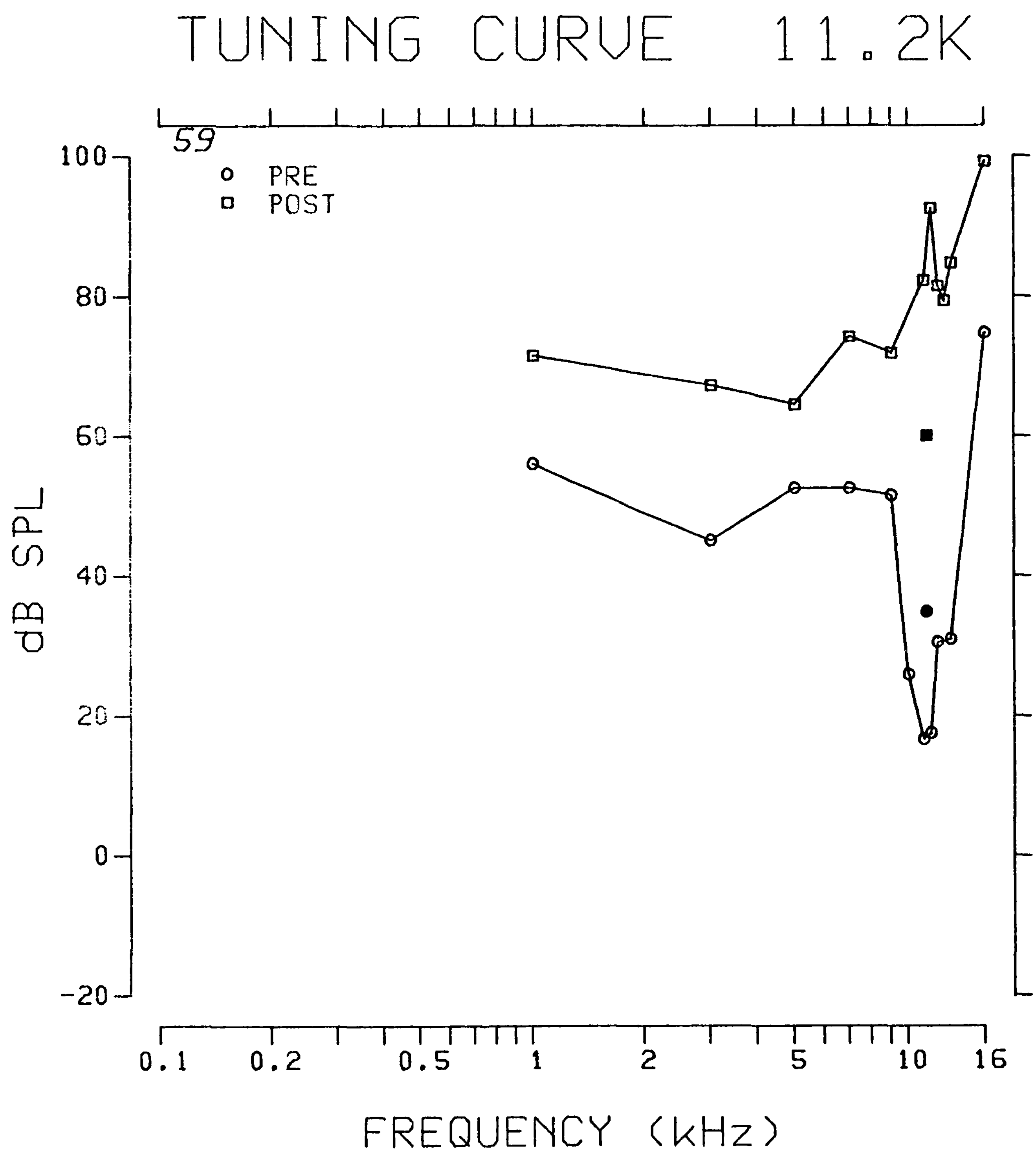


Fig. 3.3.6: Pre- and postexposure psychophysical tuning curve at 11.2 kHz for chinchilla 59.

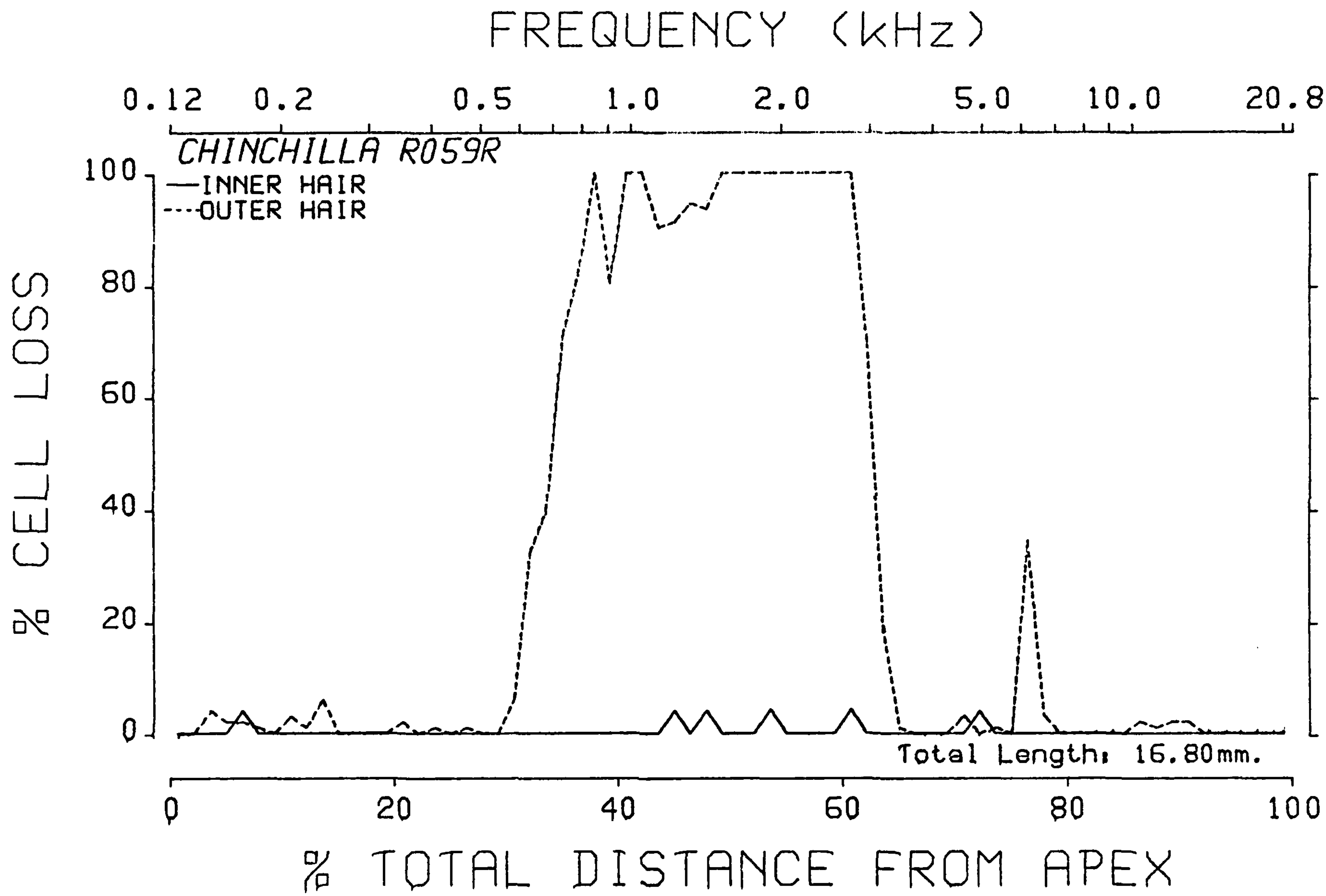


Fig. 3.3.7: Cochleogram of chinchilla 59.

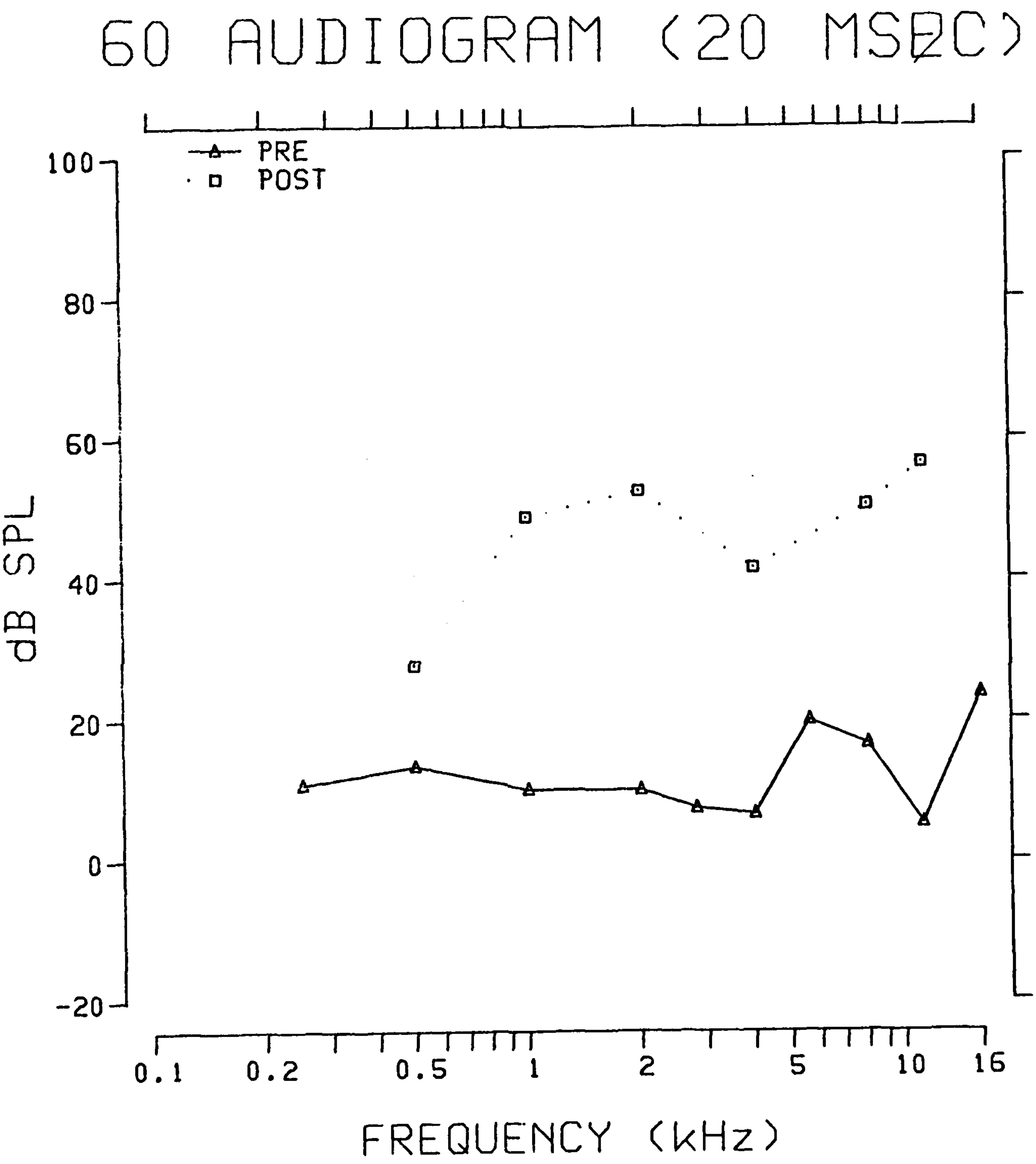


Fig. 3.3.8: Pre- and postexposure behavioral thresholds of chinchilla 60.

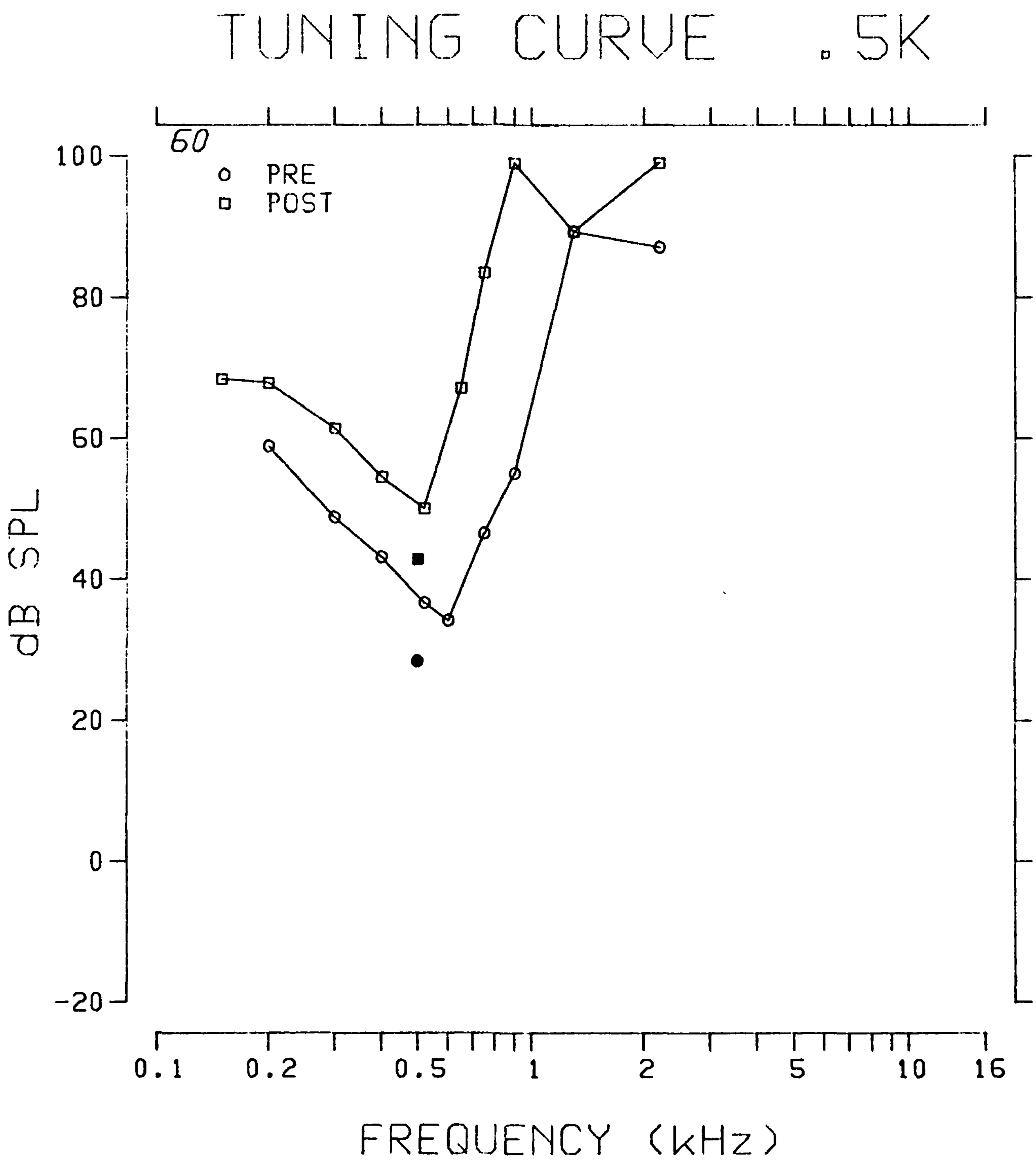


Fig. 3.3.9: Pre- and postexposure psychophysical tuning curves at 0.5 kHz of chinchilla 60.

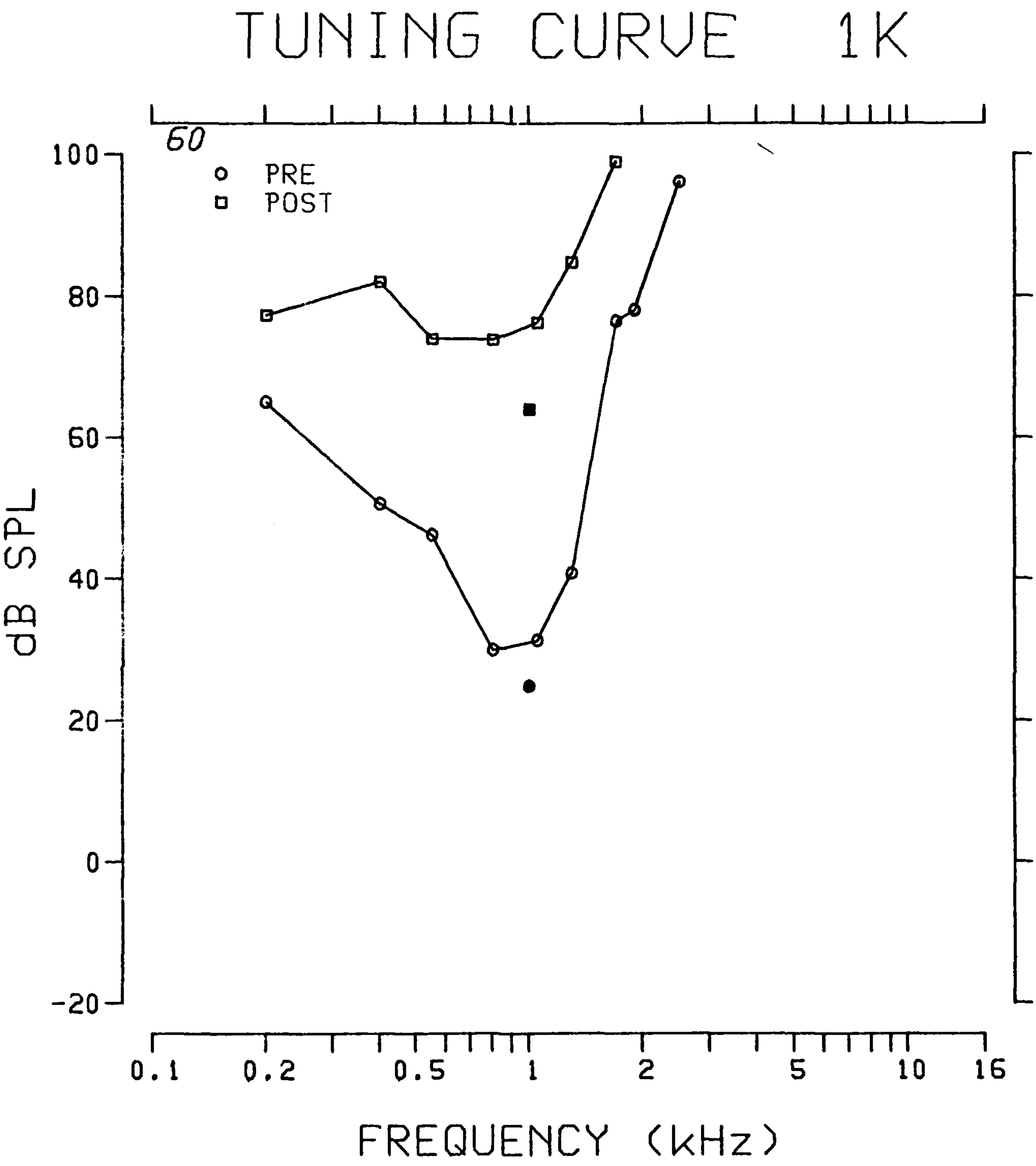


Fig. 3.3.10: Pre- and postexposure psychophysical tuning curves at 1.0 kHz of chincnilla 60.

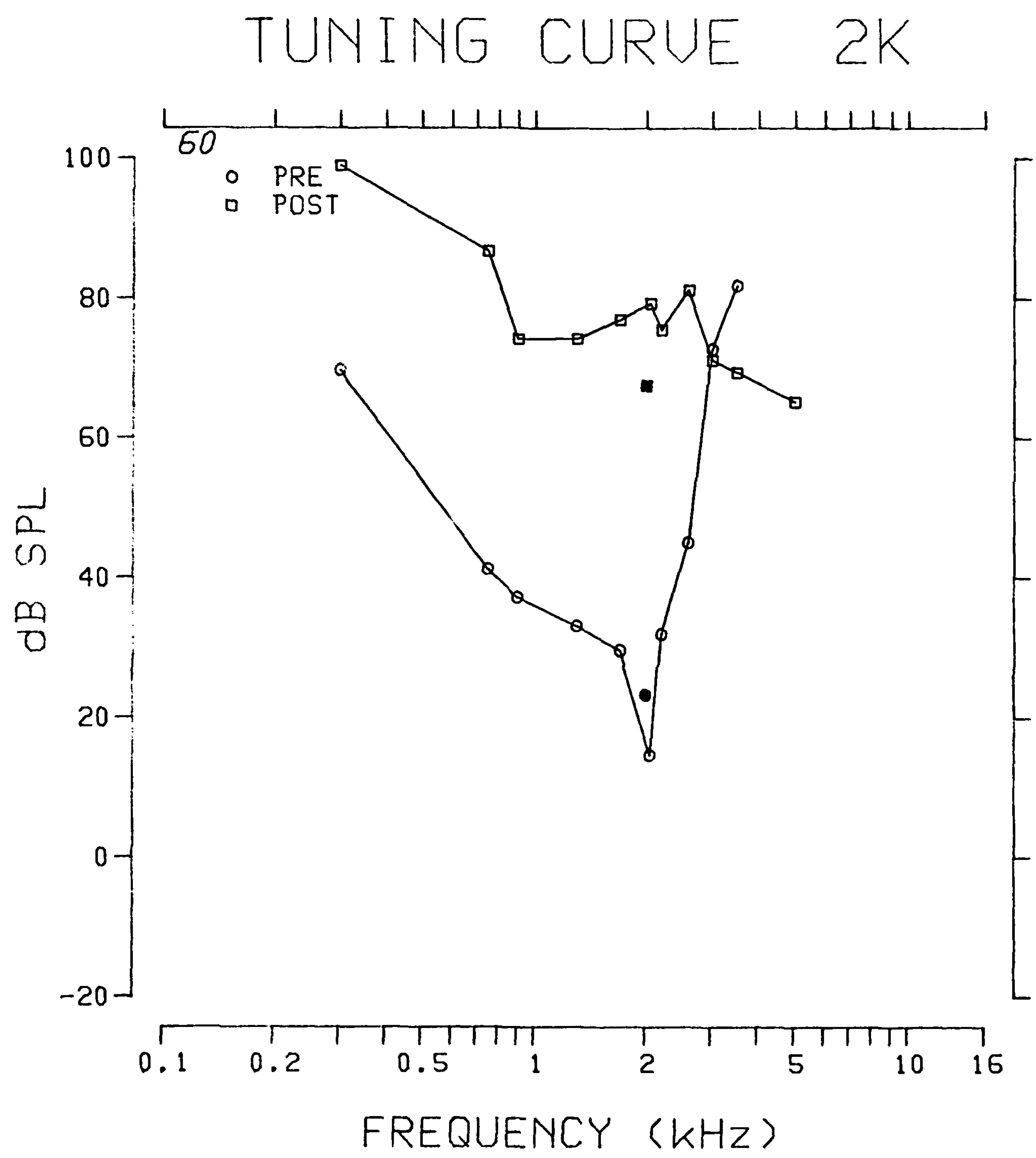


Fig. 3.3.11: Pre- and postexposure psychophysical tuning curves at 2.0 kHz of chinchilla 60.

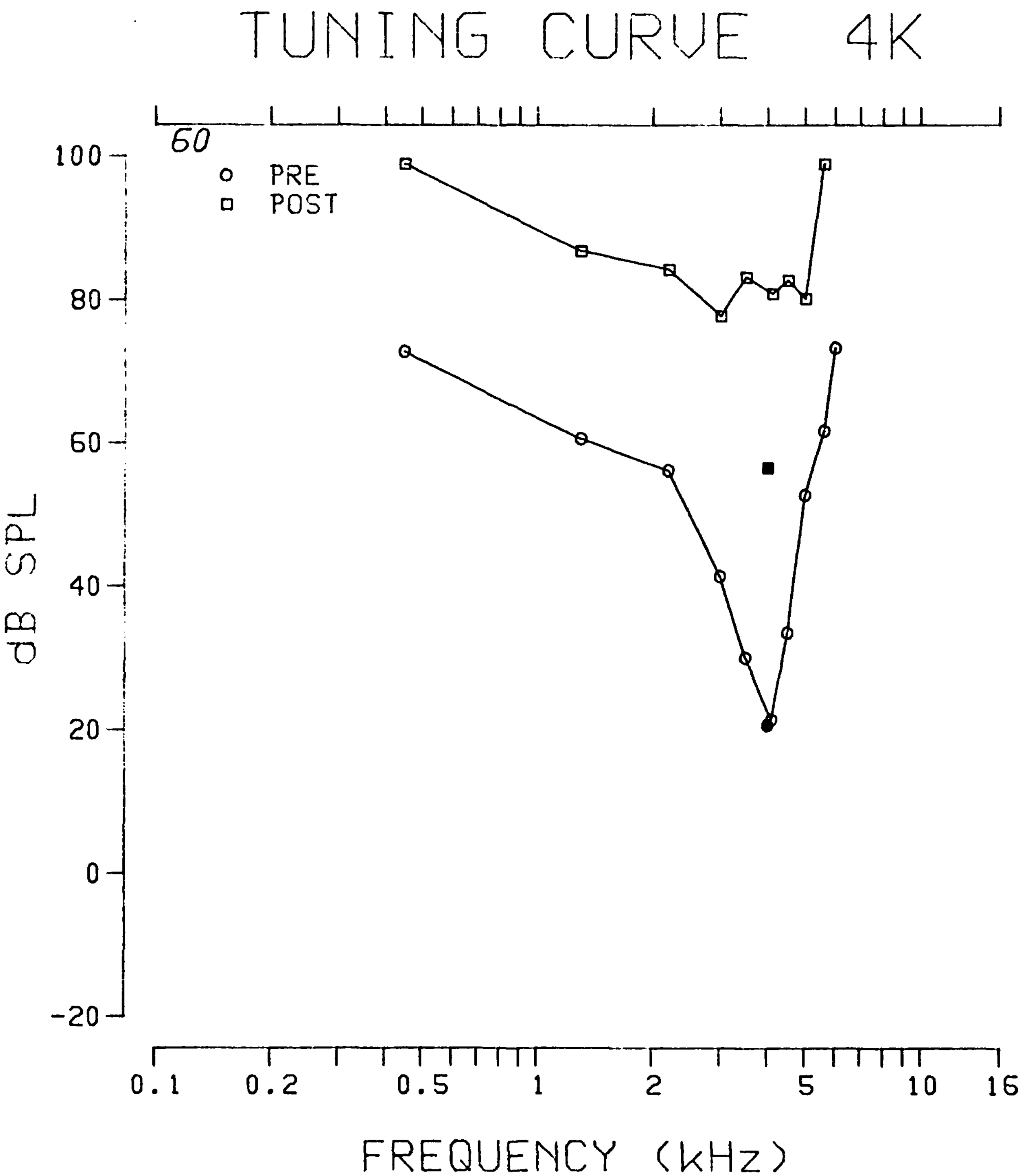


Fig. 3.3.12: Pre- and postexposure psychophysical tuning curves at 4.0 kHz of chinchilla 60.

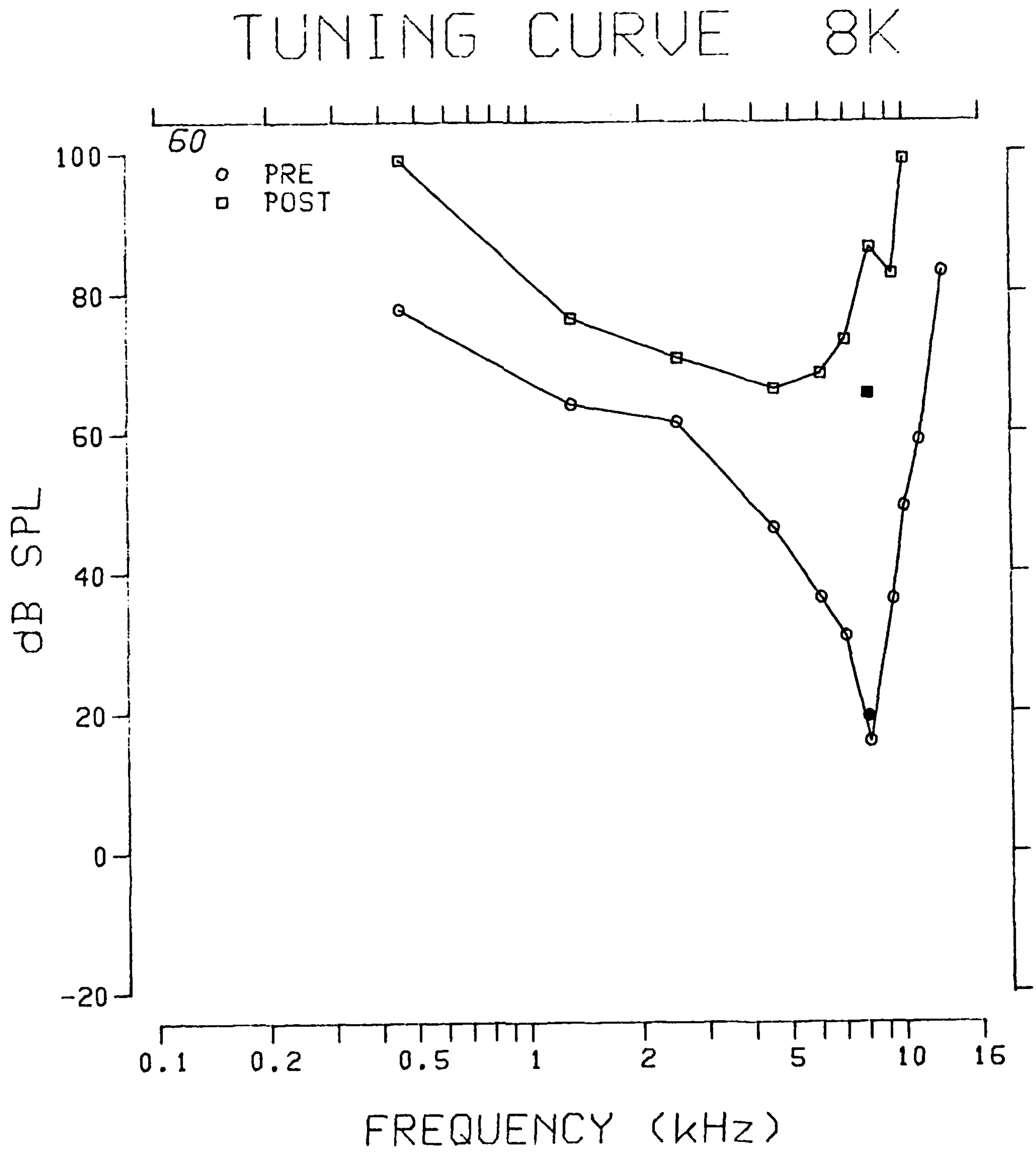


Fig. 3.3.13: Pre- and postexposure psychophysical tuning curves at 8.0 kHz of chinchilla 60.

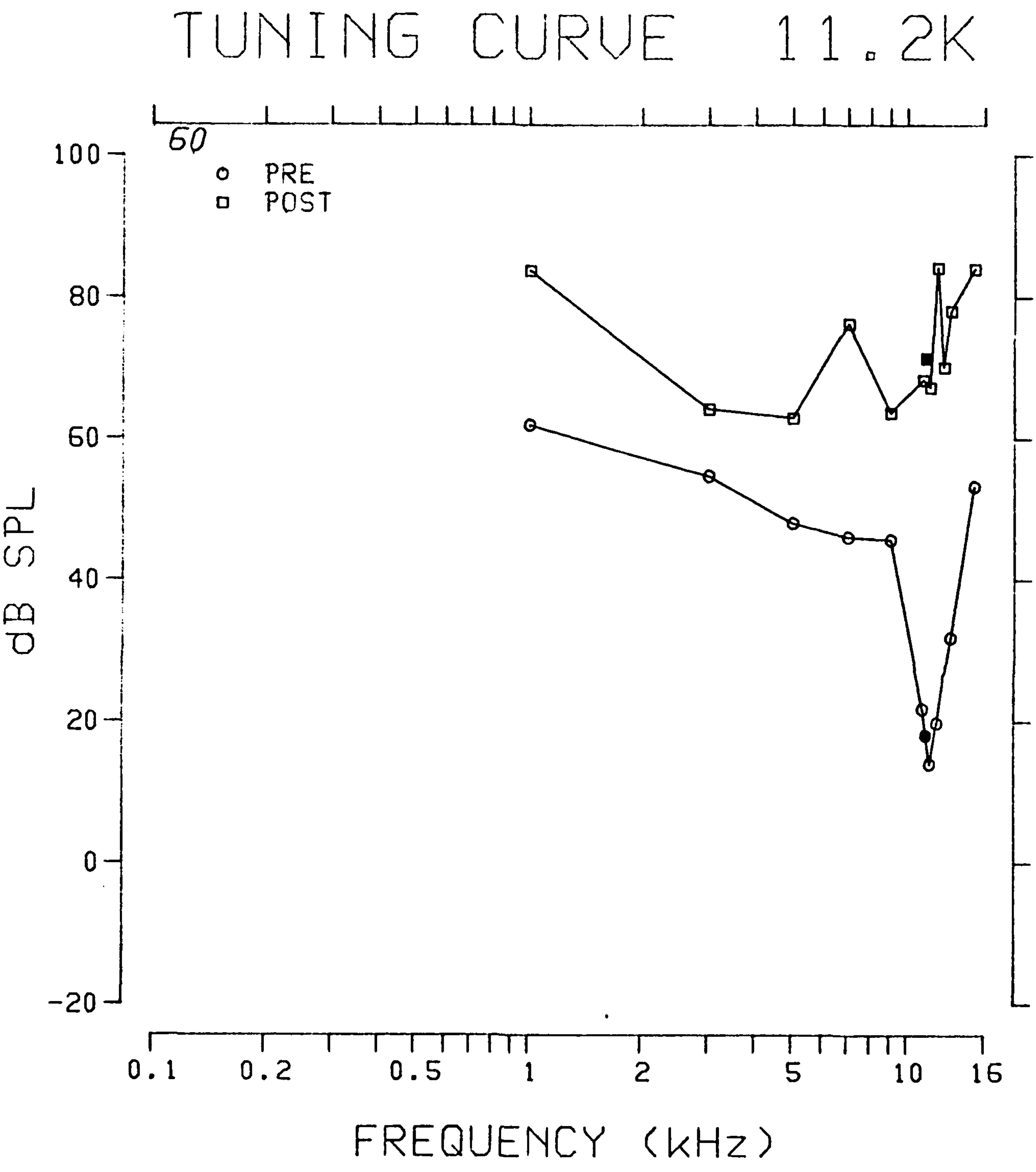


Fig. 3.3.14: Pre- and postexposure psychophysical tuning curves at 11.2 kHz of chinchilla 60.

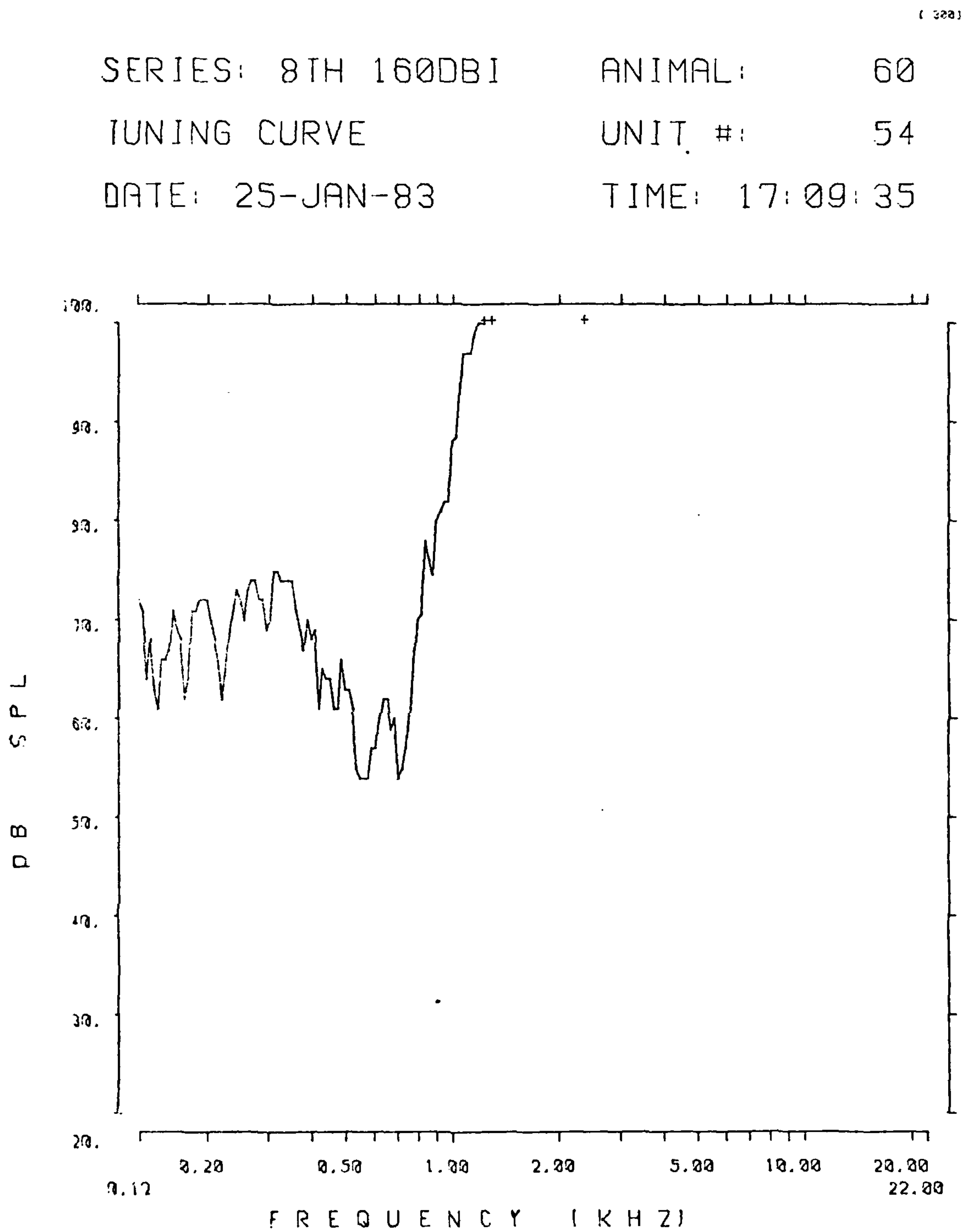


Fig. 3.3.15: Auditory nerve fiber tuning curve from chinchilla 60.

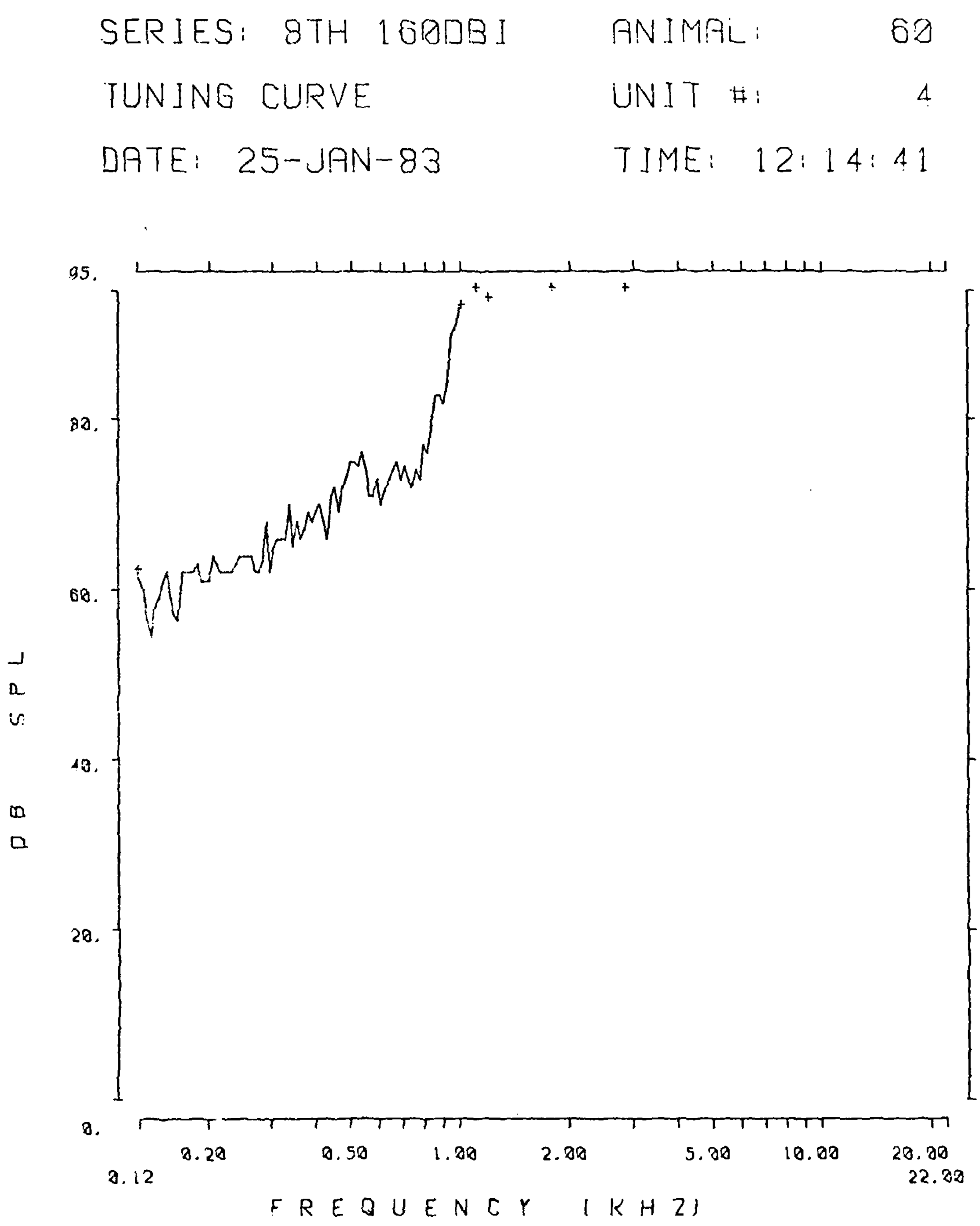


Fig. 3.3.16: Auditory nerve fiber tuning curve from chinchilla 60.

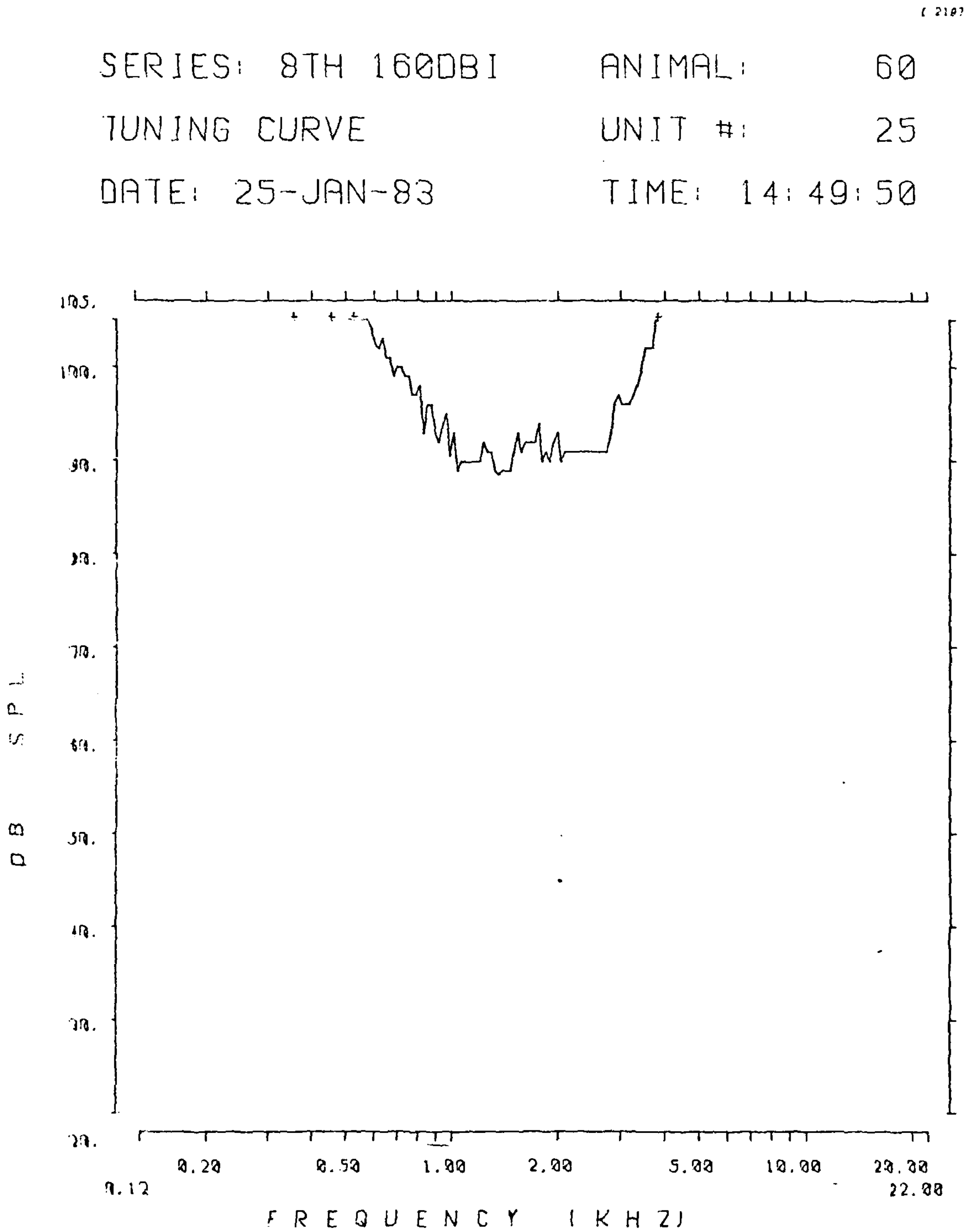


Fig. 3.3.17: Auditory nerve fiber tuning curve from chinchilla 60.

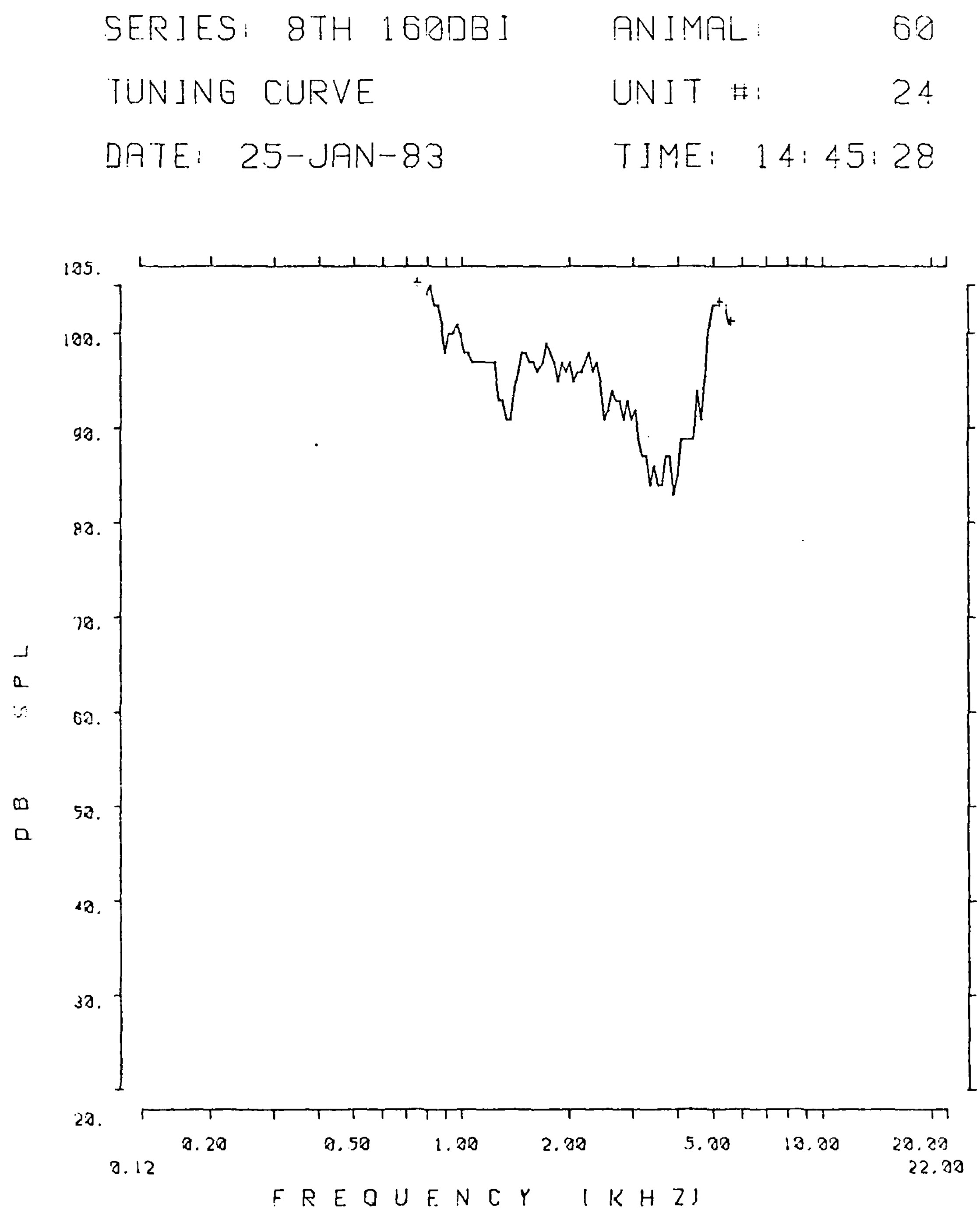


Fig. 3.3.18: Auditory nerve fiber tuning curve from chinchilla 60.

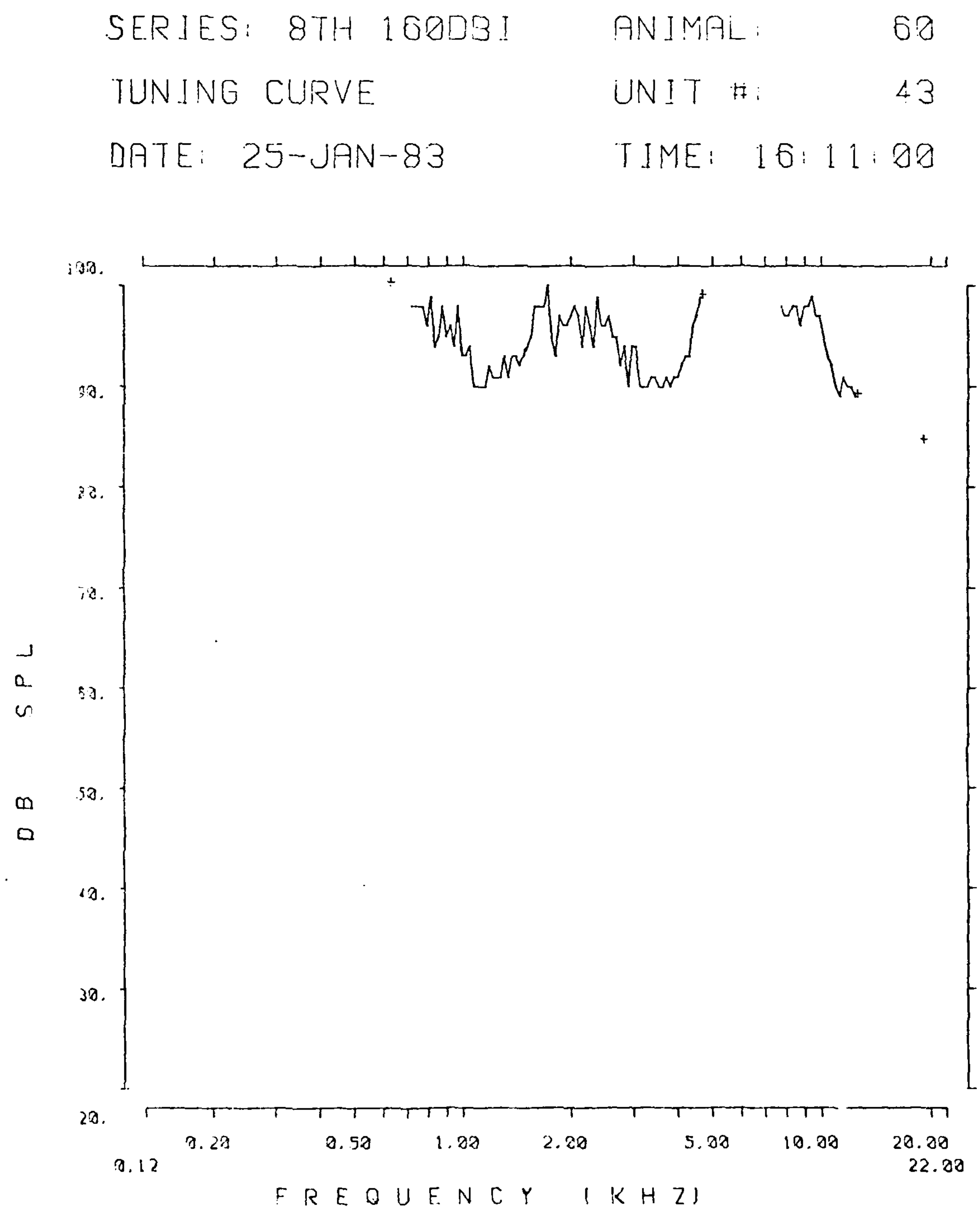


Fig. 3.3.19: Auditory nerve fiber tuning curve from chinchilla 60.

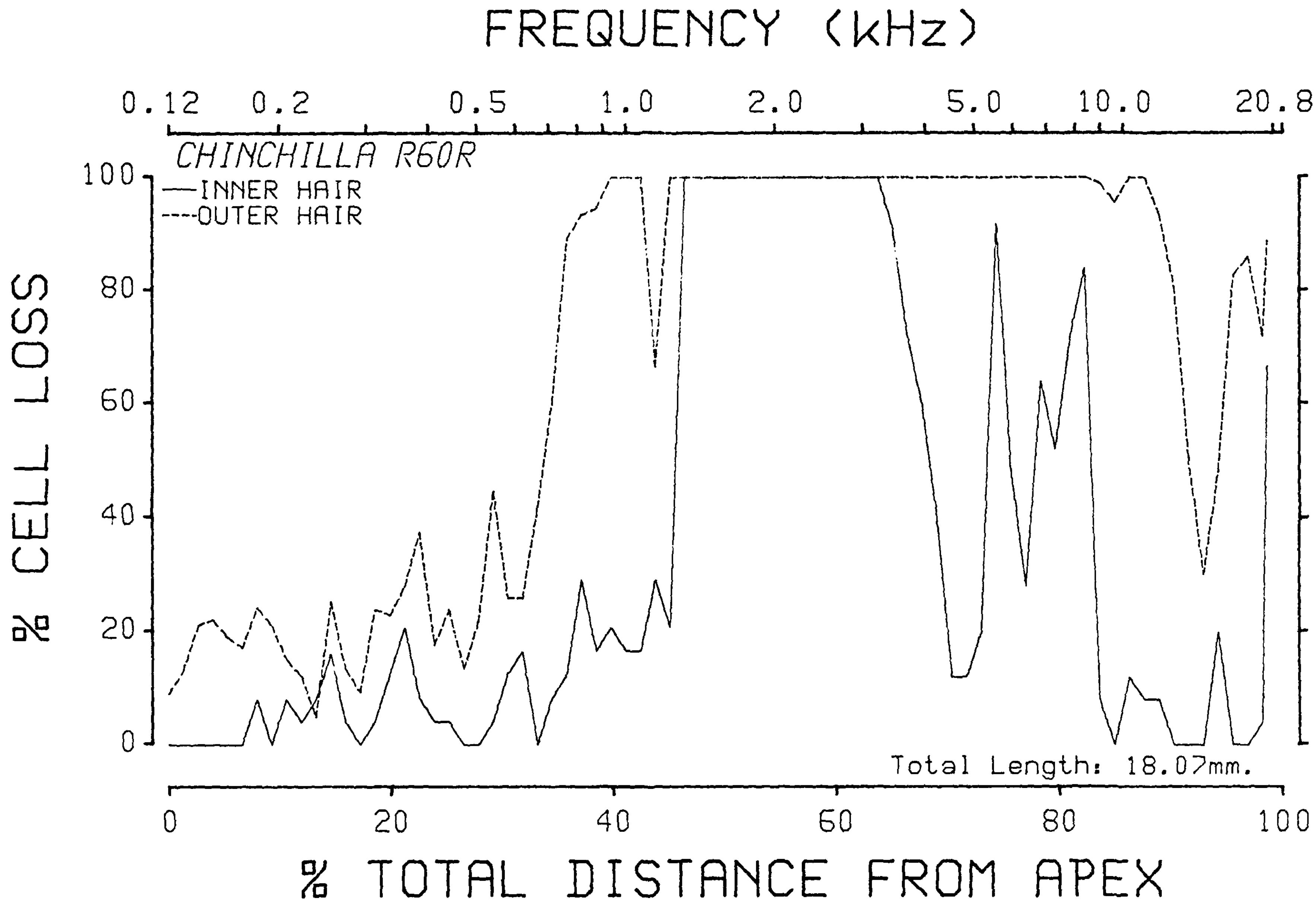


Fig. 3.3.20: Cochleogram of chinchilla 60.

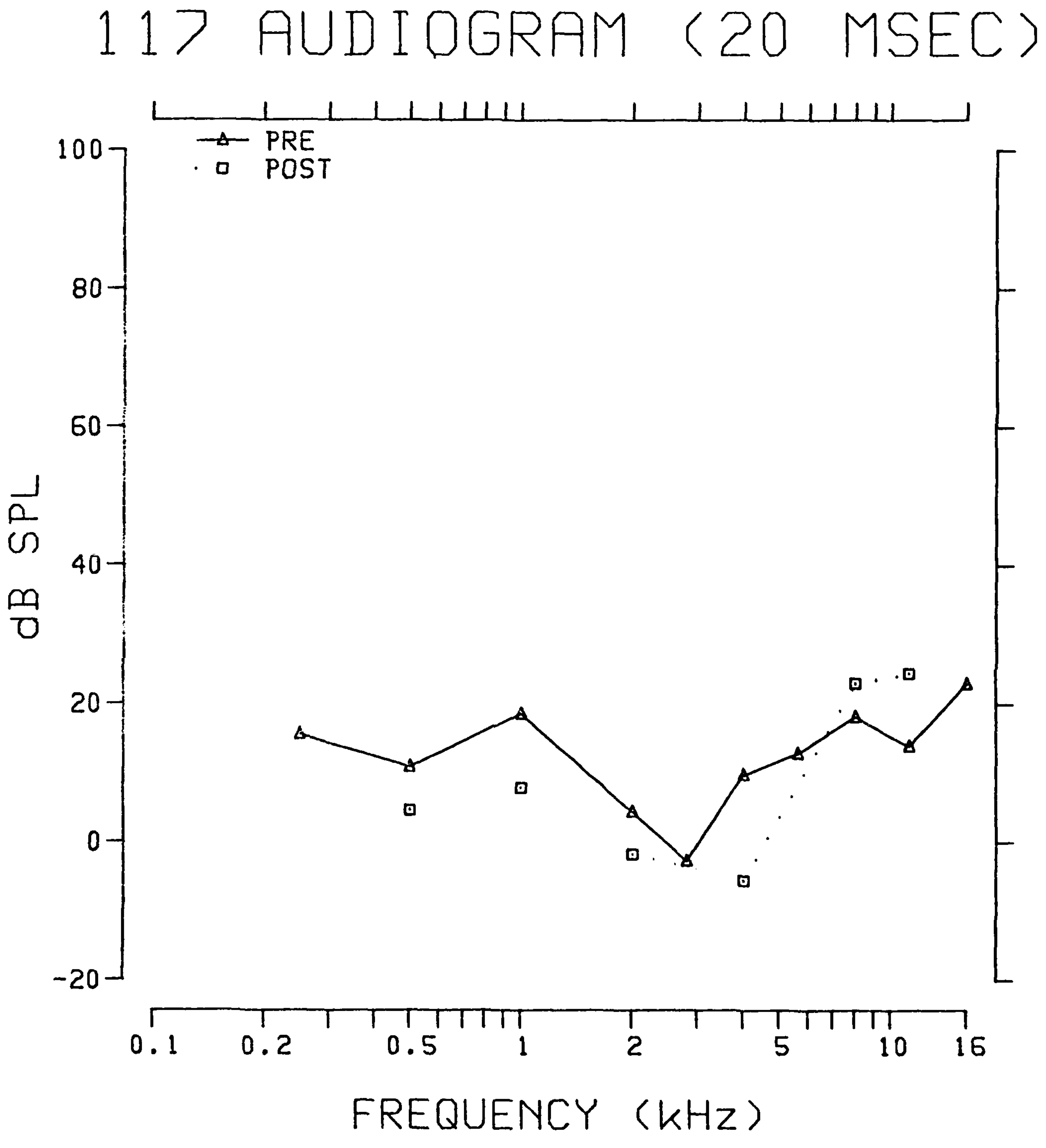


Fig. 3.3.21: Pre- and postexposure behavioral audiograms of chinchilla 117.

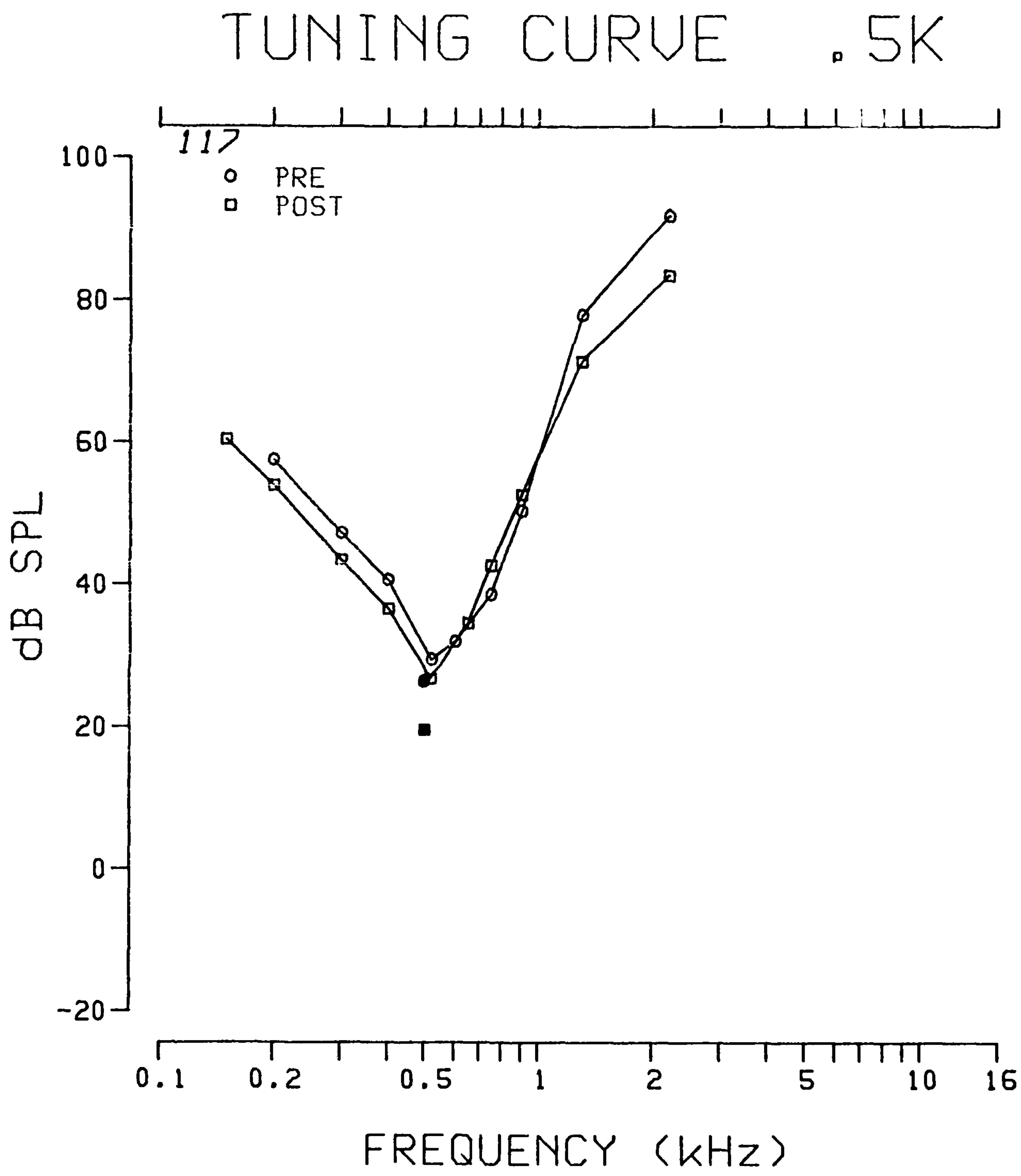


Fig. 3.3.22: Pre- and postexposure psychophysical tuning curve at 0.5 kHz of chinchilla 117.

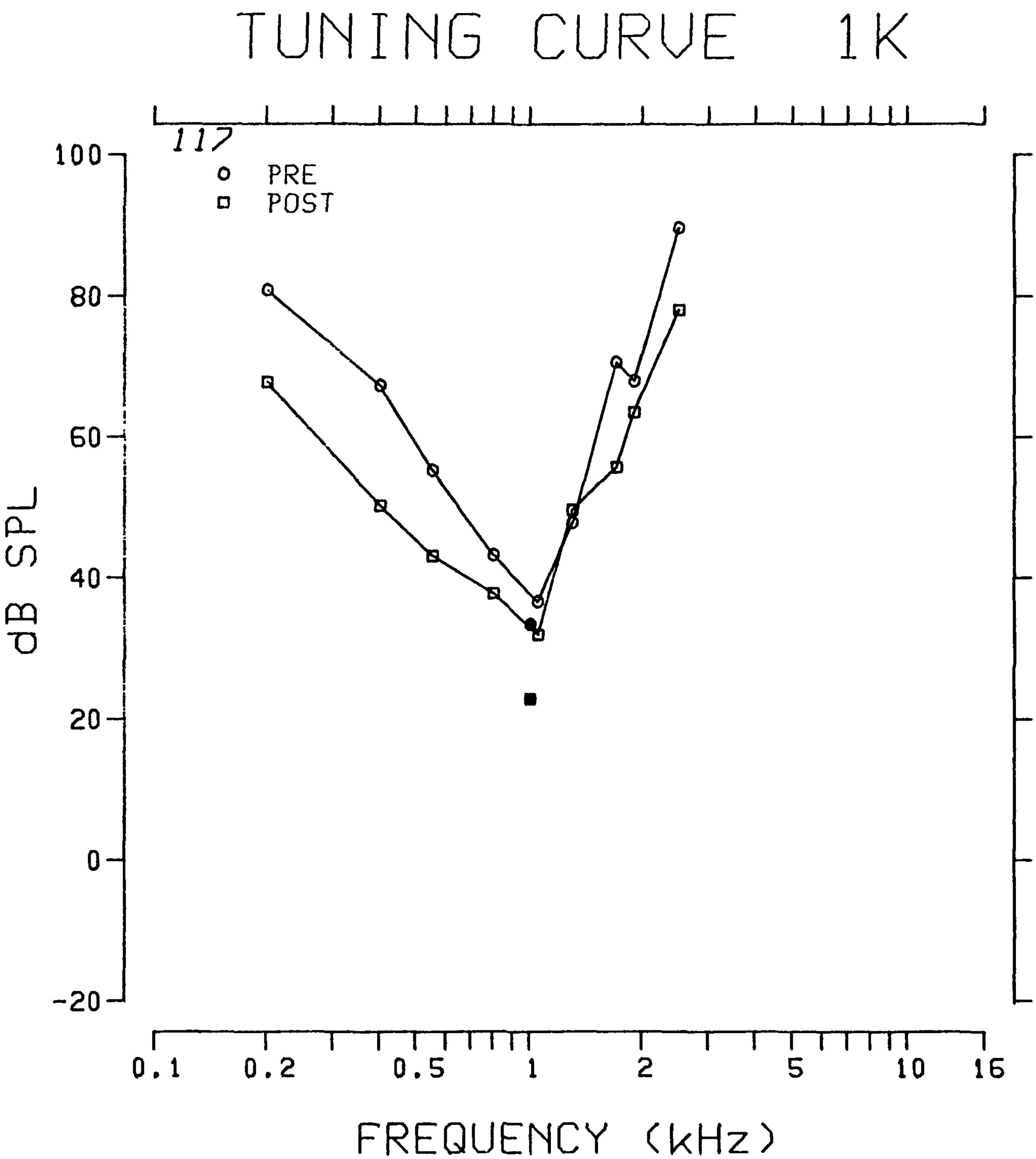


Fig. 3.3.23: Pre- and postexposure psychophysical tuning curve at 1.0 kHz of chinchilla 117.

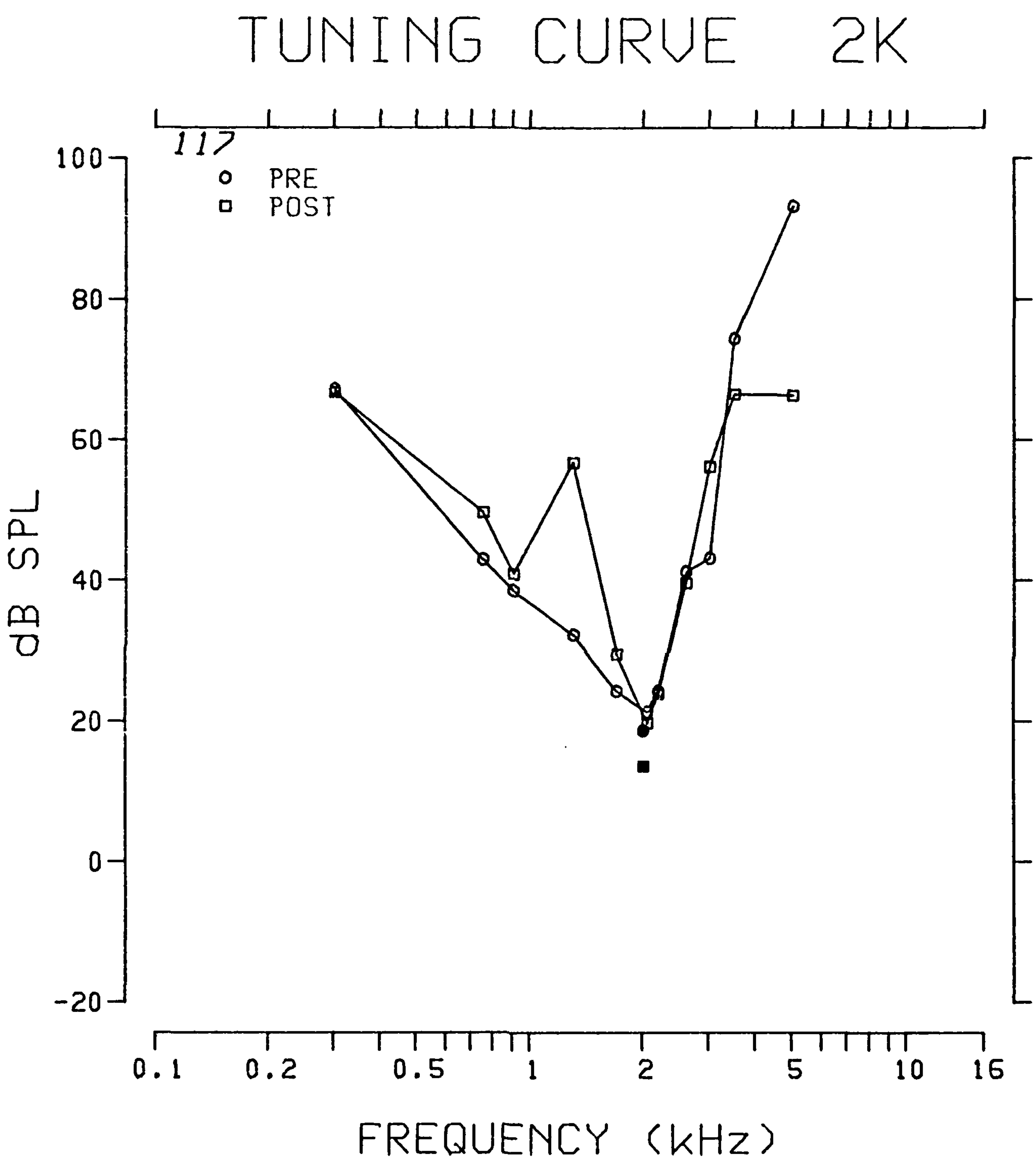


Fig. 3.3.24: Pre- and postexposure psychophysical tuning curve at 2.0 kHz of chinchilla 117.

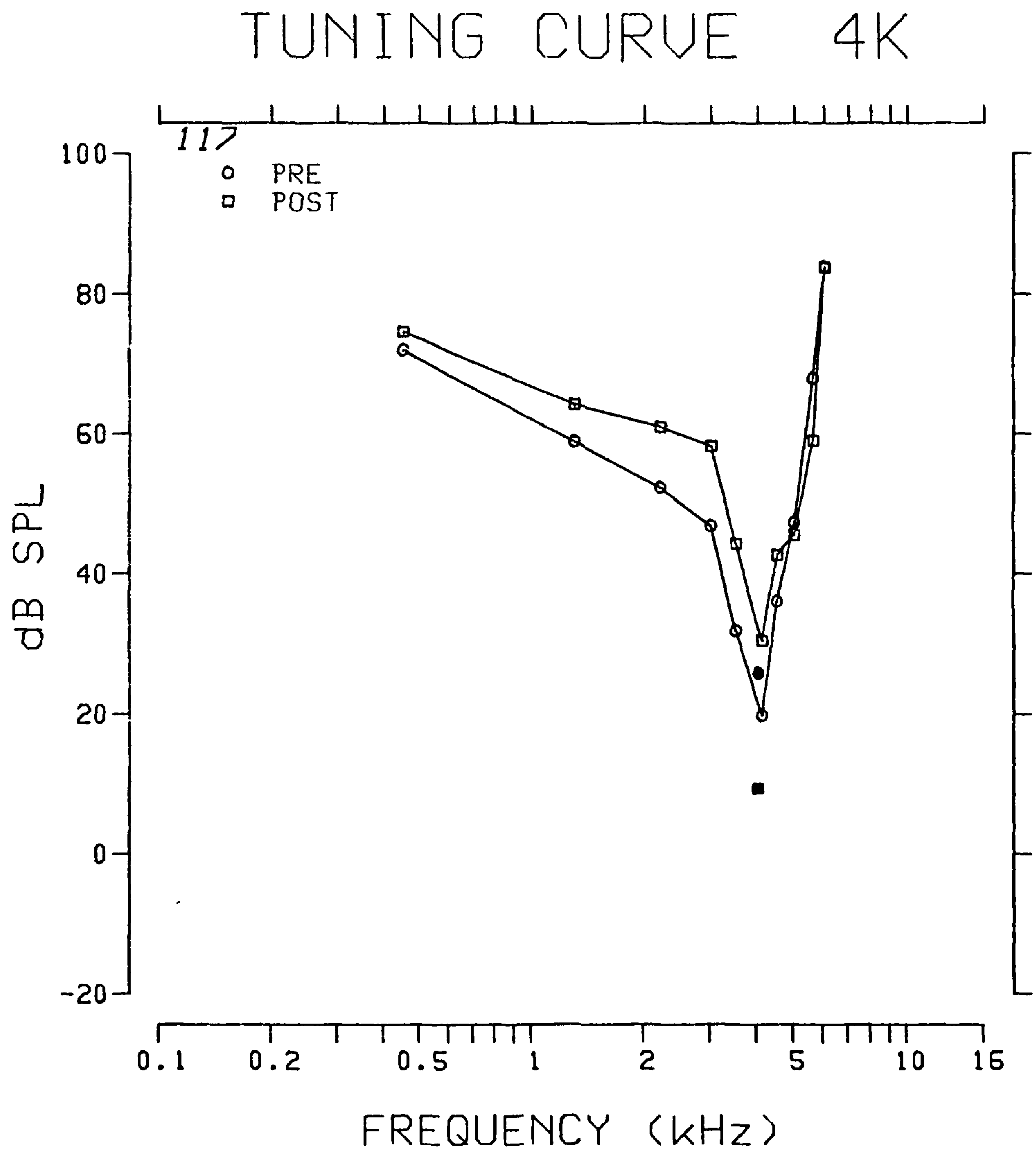


Fig. 3.3.25: Pre- and postexposure psychophysical tuning curve at 4.0 kHz of chinchilla 117.

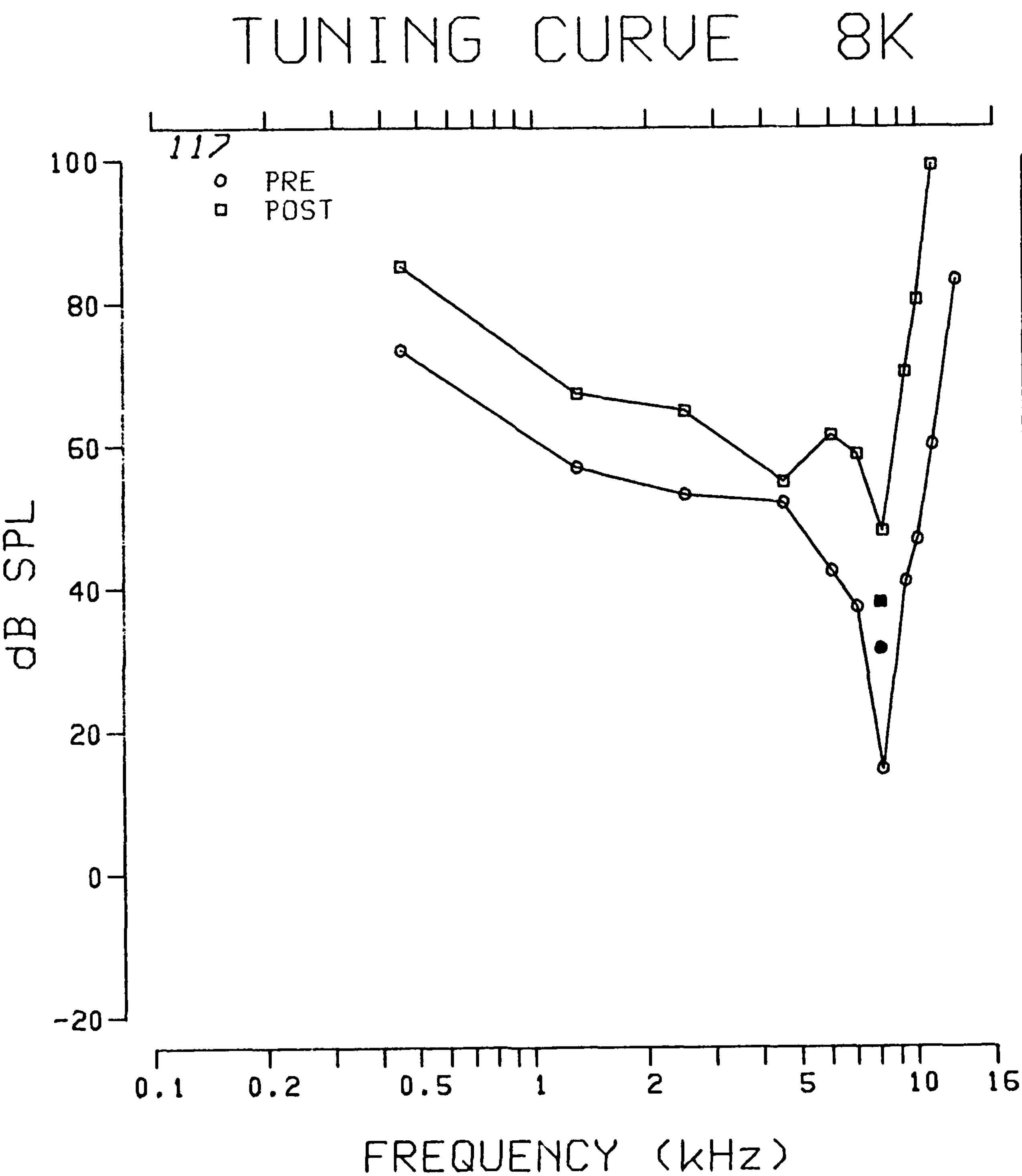


Fig. 3.3.26: Pre- and postexposure psychophysical tuning curve at 8.0 kHz of chinchilla 117.

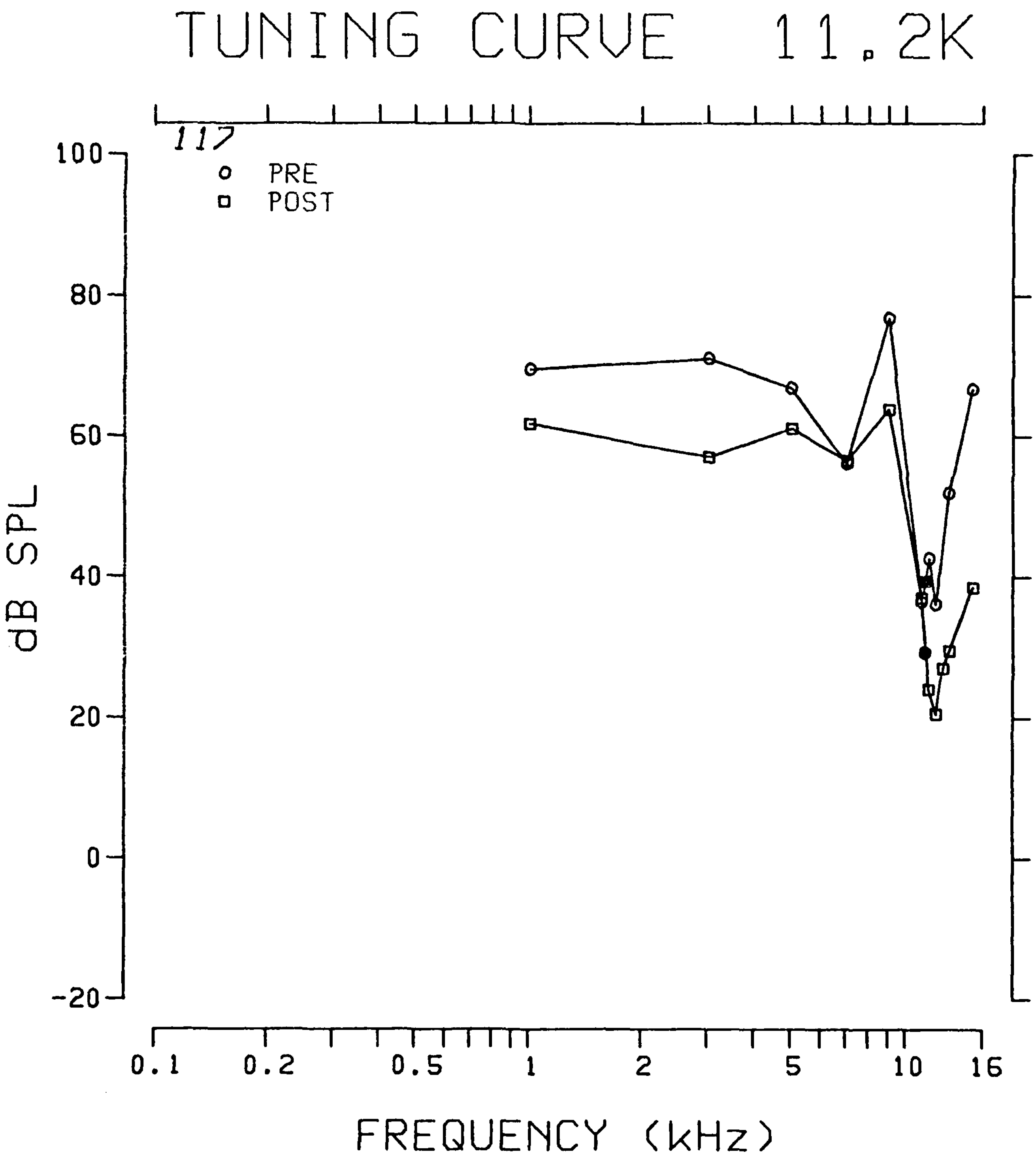


Fig. 3.3.27: Pre- and postexposure psychophysical tuning curve at 11.2 kHz of chinchilla 117.

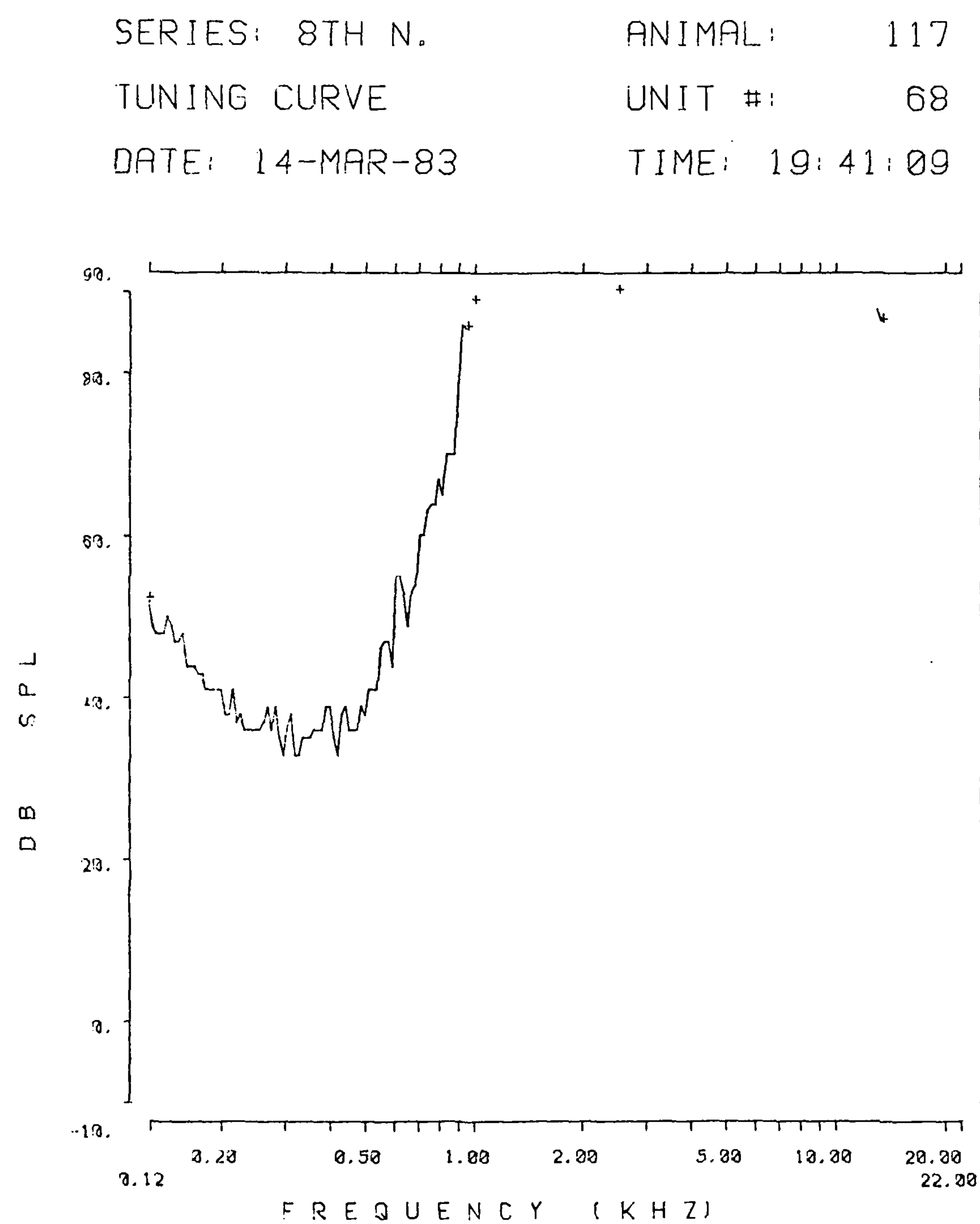


Fig. 3.3.28: Auditory nerve fiber tuning curve from chinchilla 117.

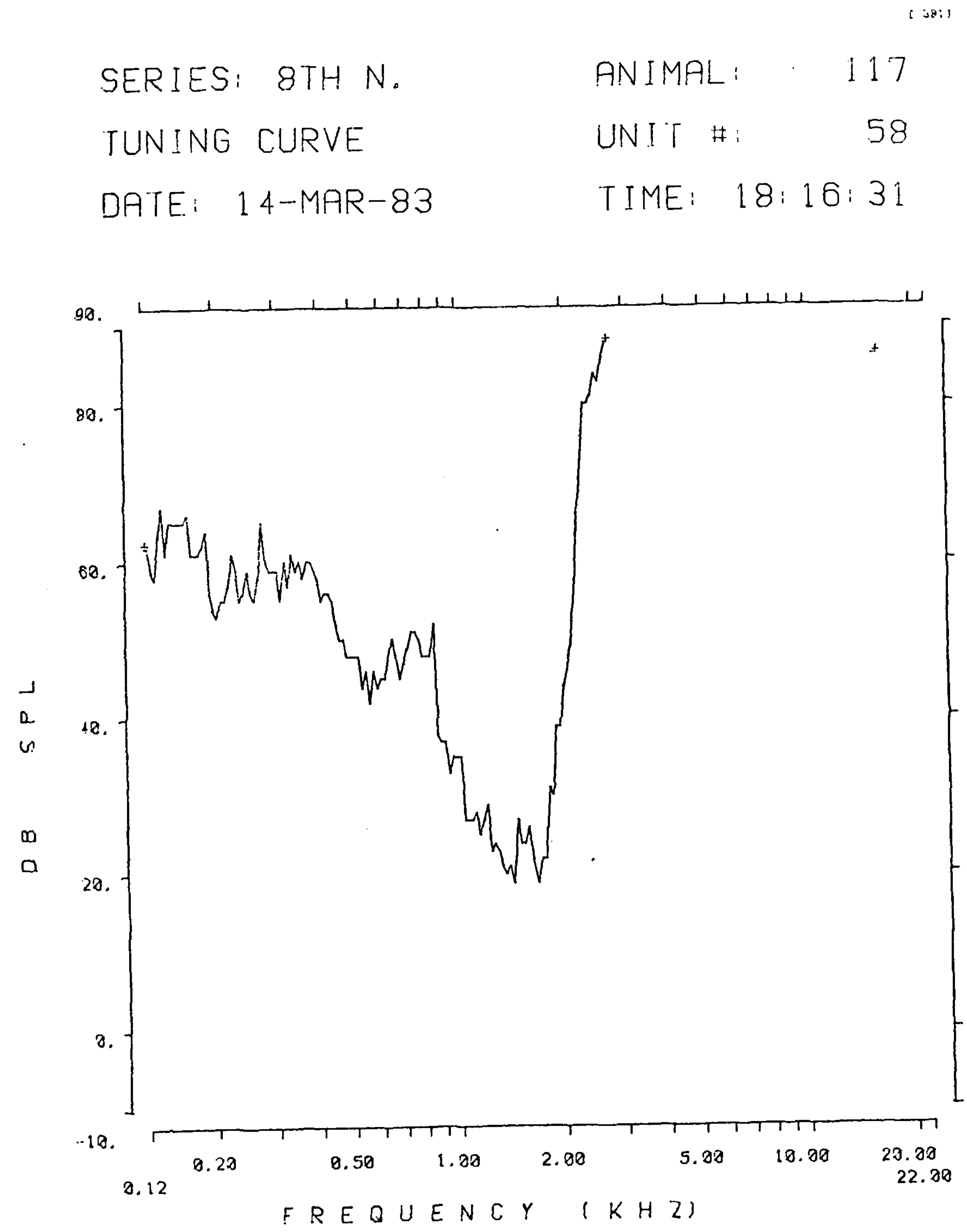


Fig. 3.3.29: Auditory nerve fiber tuning curve from chinchilla 117.

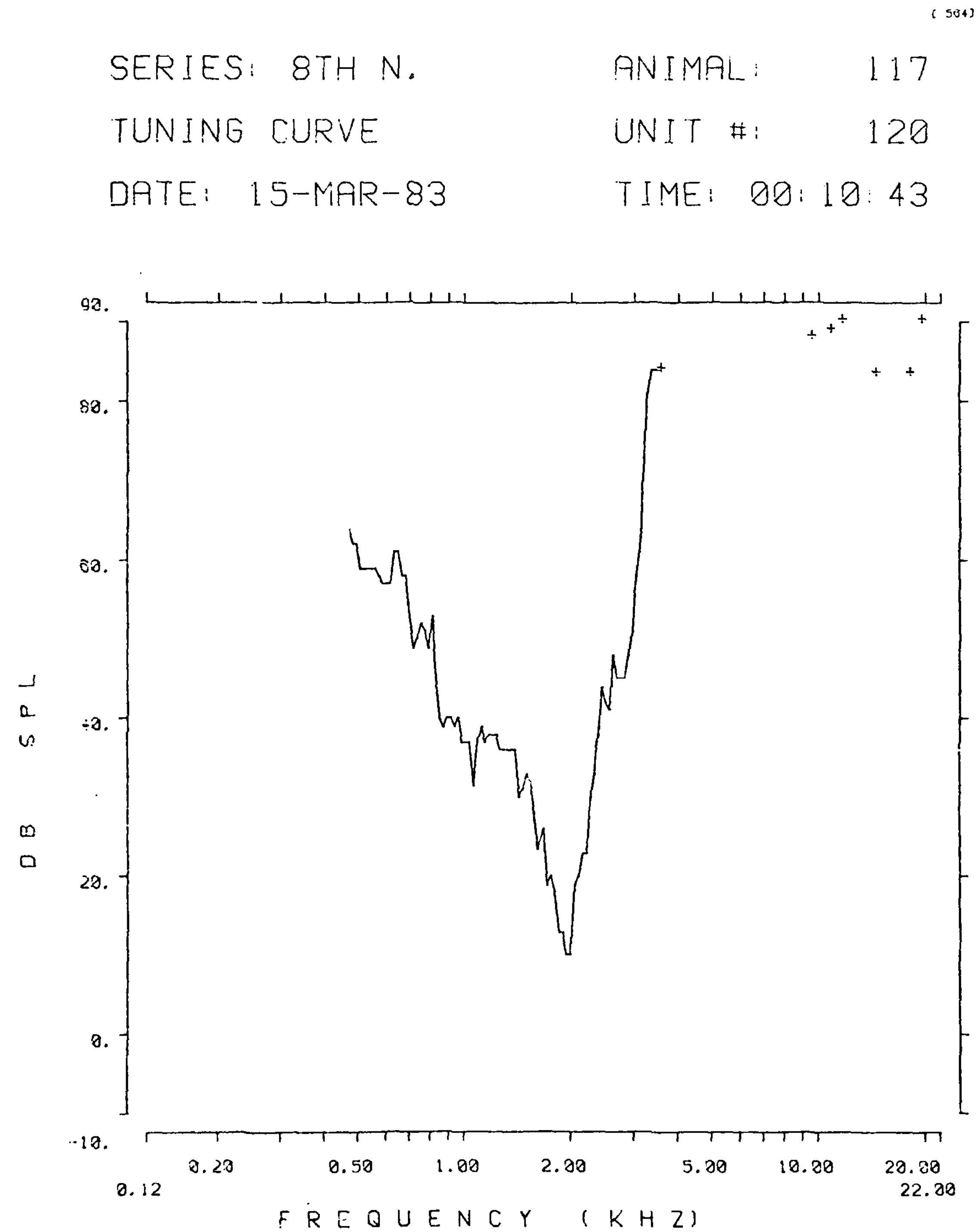


Fig. 3.3.30: Auditory nerve fiber tuning curve from chinchilla 117.

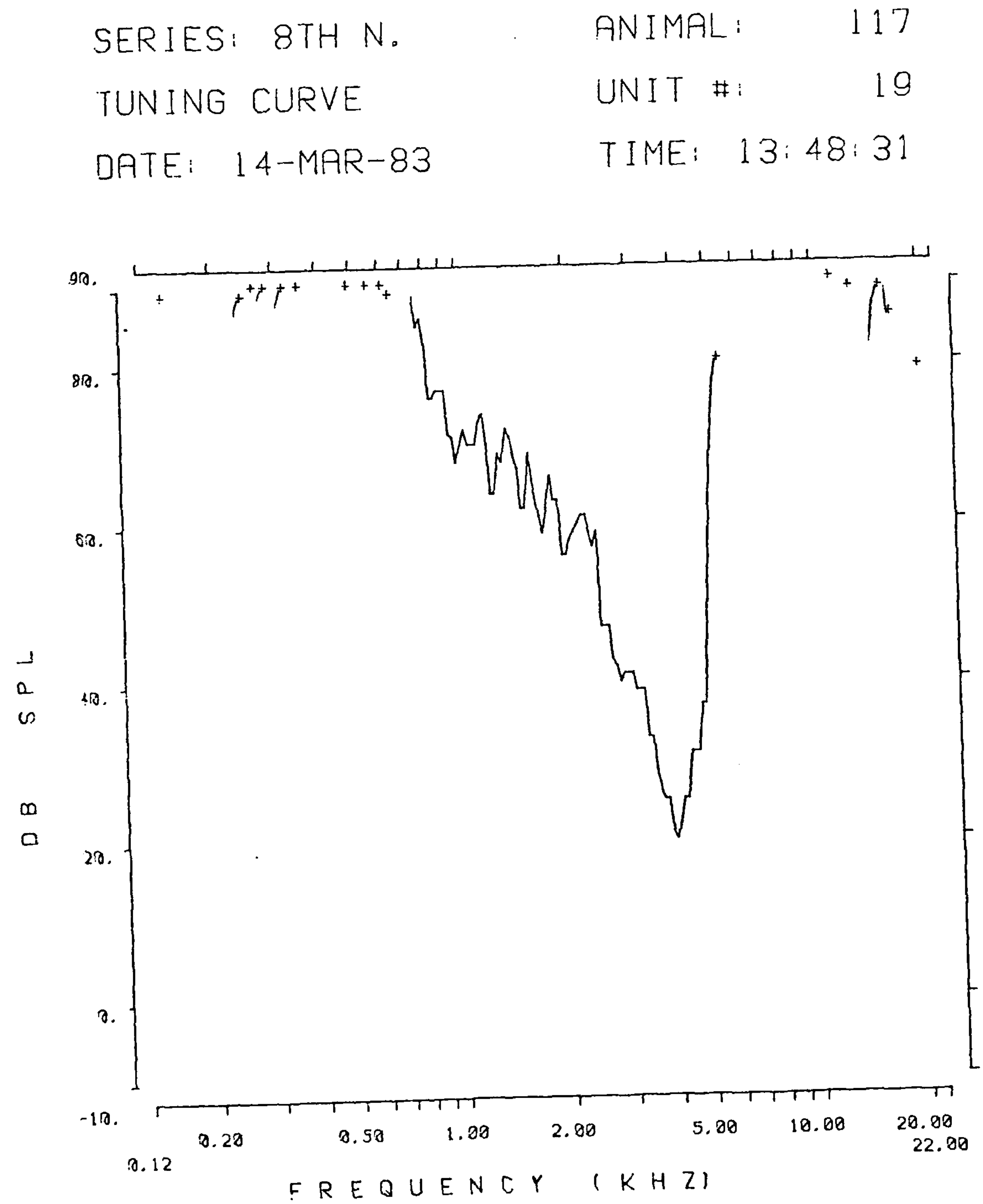


Fig. 3.3.31: Auditory nerve fiber tuning curve from chinchilla 117.

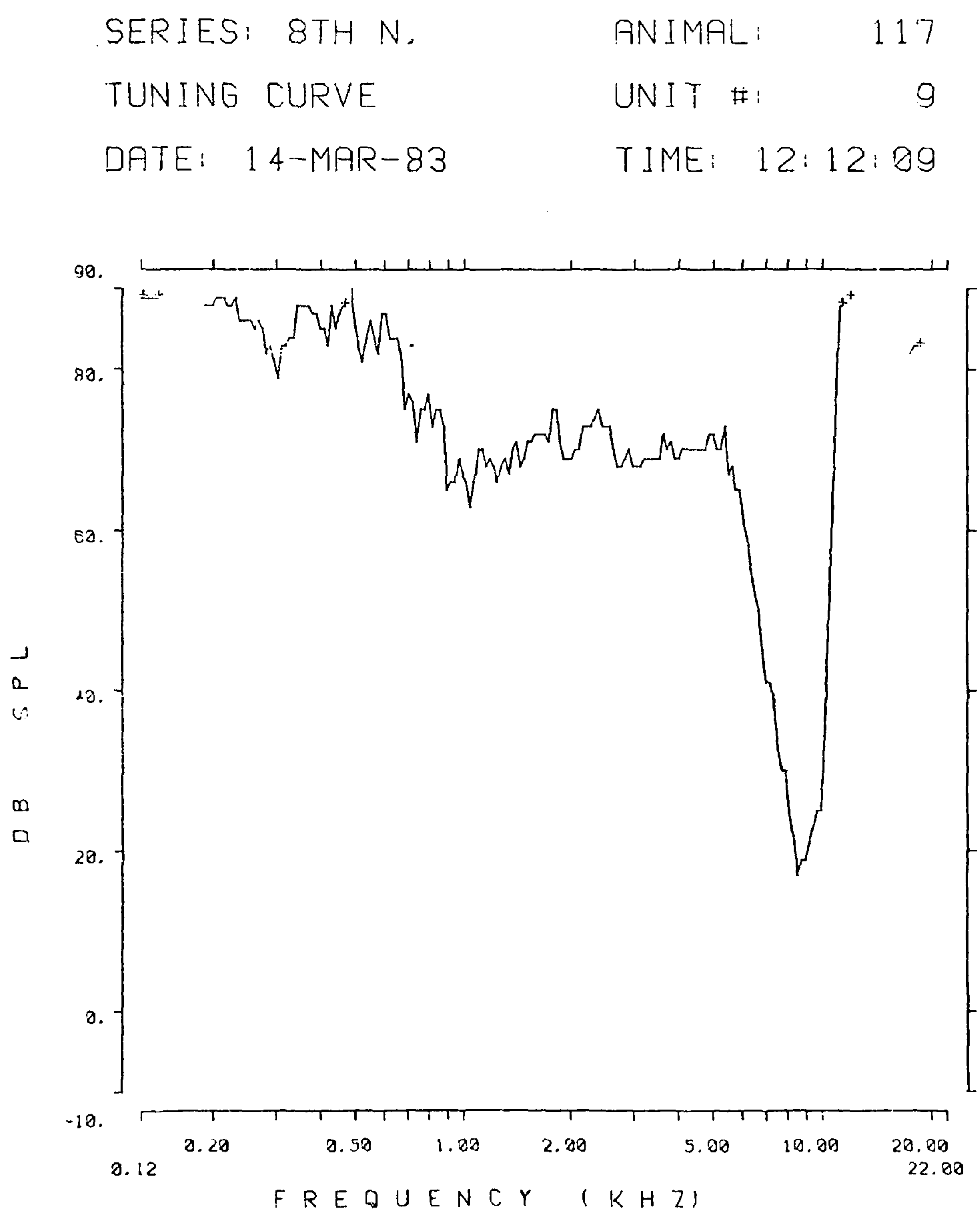


Fig. 3.3.32: Auditory nerve fiber tuning curve from chinchilla 117.

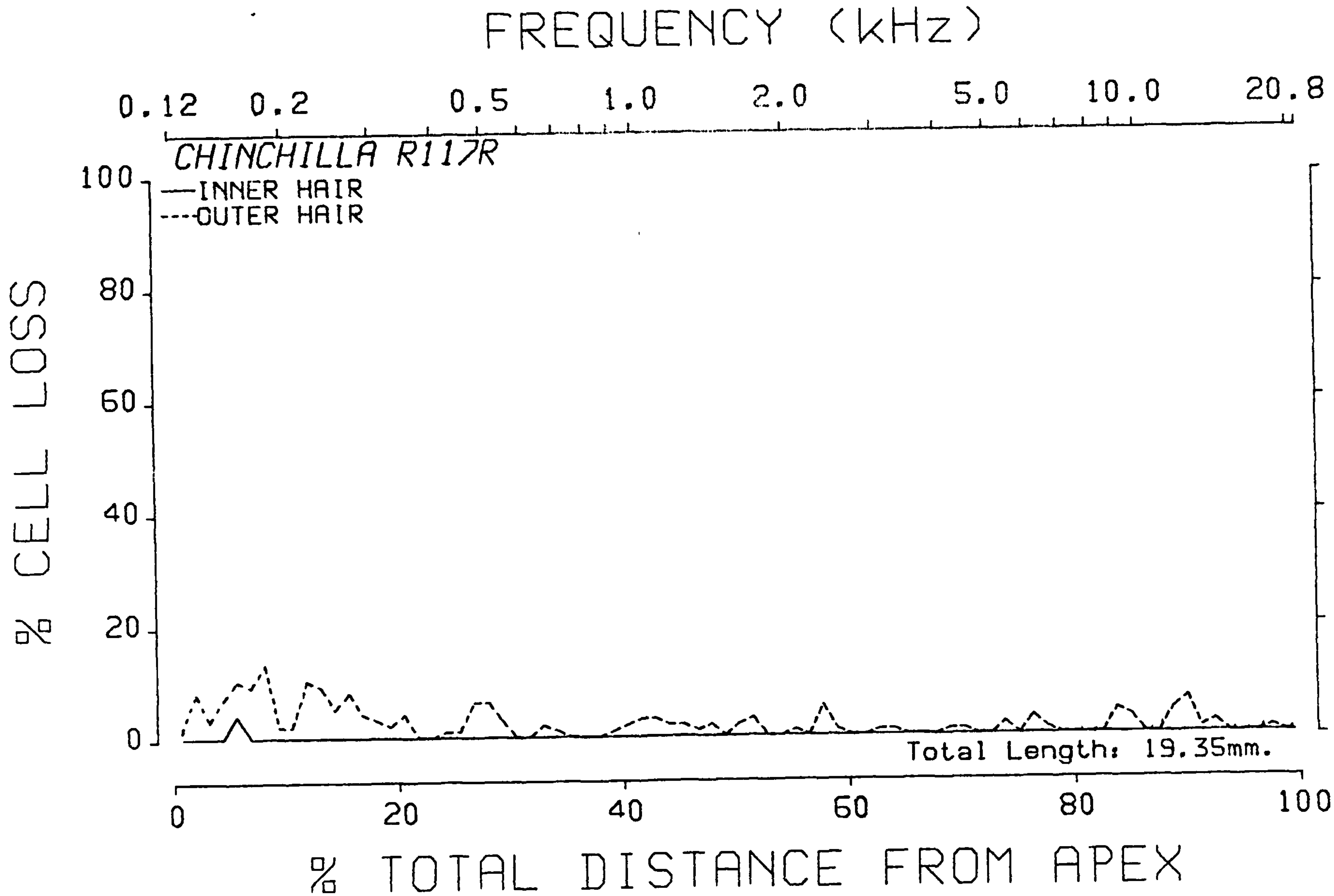


Fig. 3.3.33: Cochleogram from chinchilla 117.

AD-A172 467 BLAST TRAUMA THE EFFECT ON HEARING(U) TEXAS UNIV AT DALLAS CALLIER CENTER FOR COMMUNICATION DISORDERS R P HAMERNIK ET AL. JUL 83 DAMD17-80-C-0133 2/4

UNCLASSIFIED F/G 6/19 NL

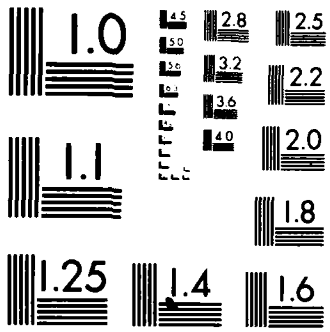


MICROCOPY RESOLUTION TEST CHART
NATIONAL BUREAU OF STANDARDS 1963-A

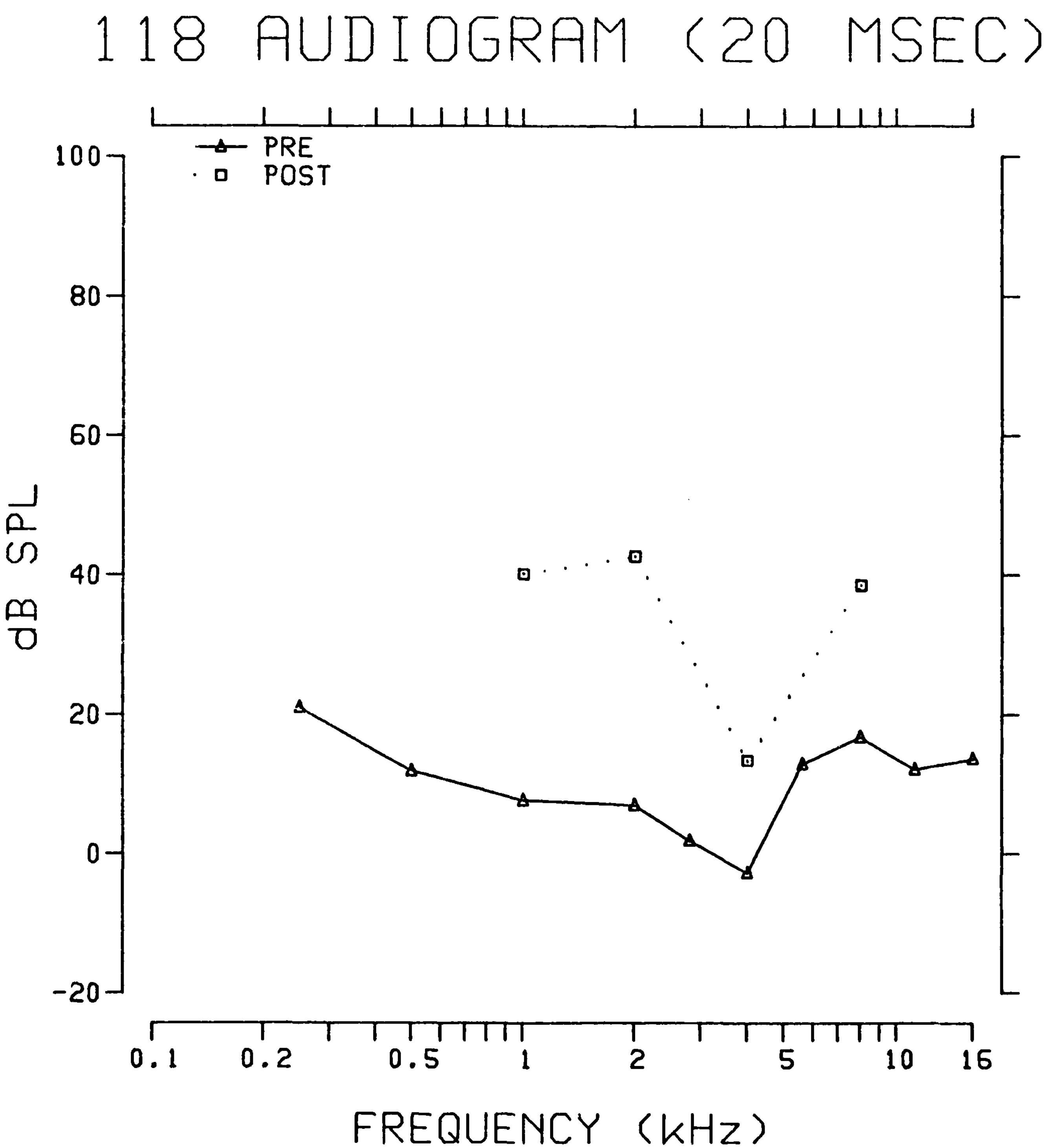


Fig. 3.3.34: Pre- and postexpore behavioral audiograms from chinchilla 118.

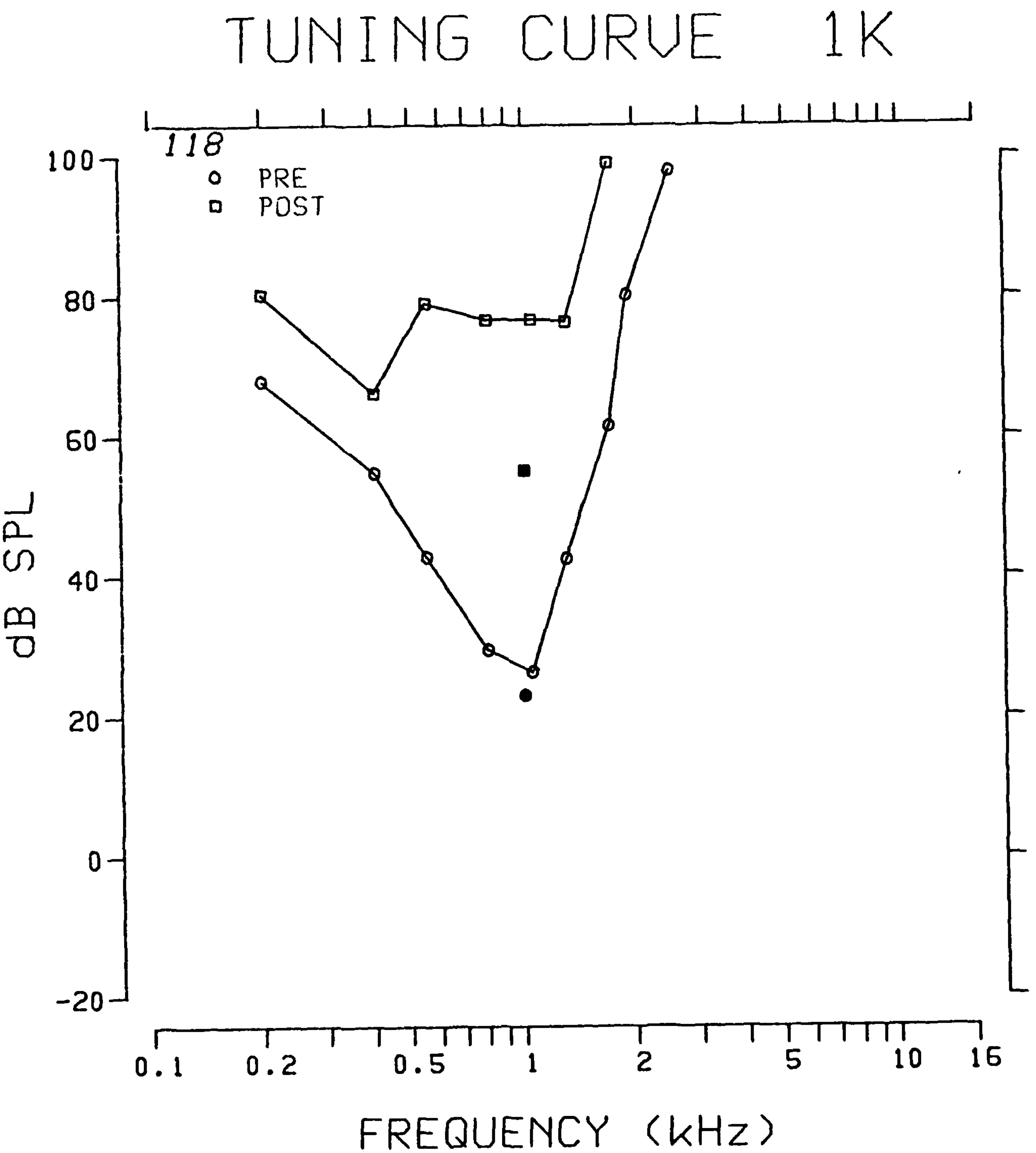


Fig. 3.3.35: Pre- and postexposure psychophysical tuning curves at 0.5 kHz from chinchilla 118.

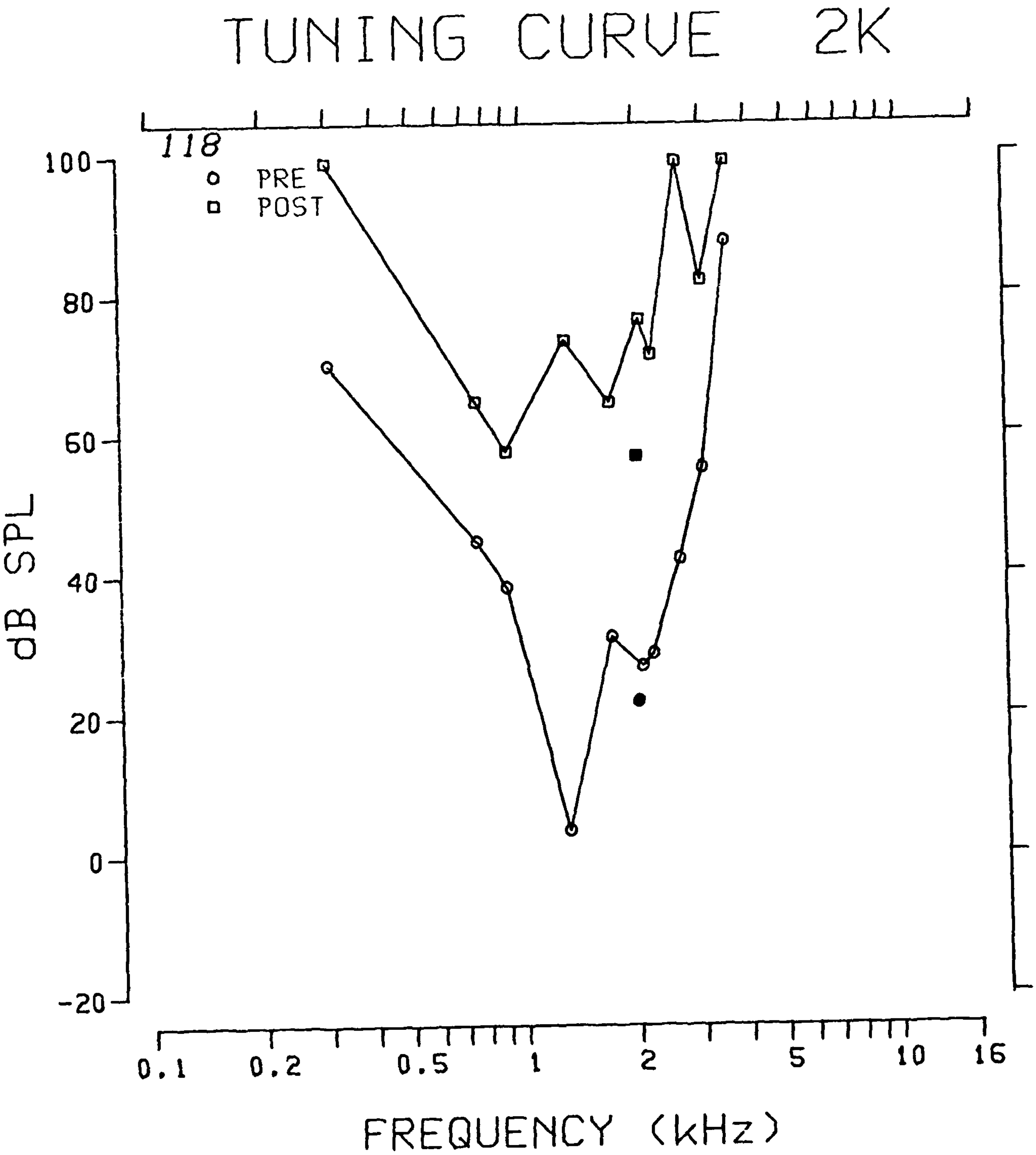


Fig. 3.3.36: Pre- and postexposure psychophysical tuning curves at 1.0 kHz from chinchilla 118.

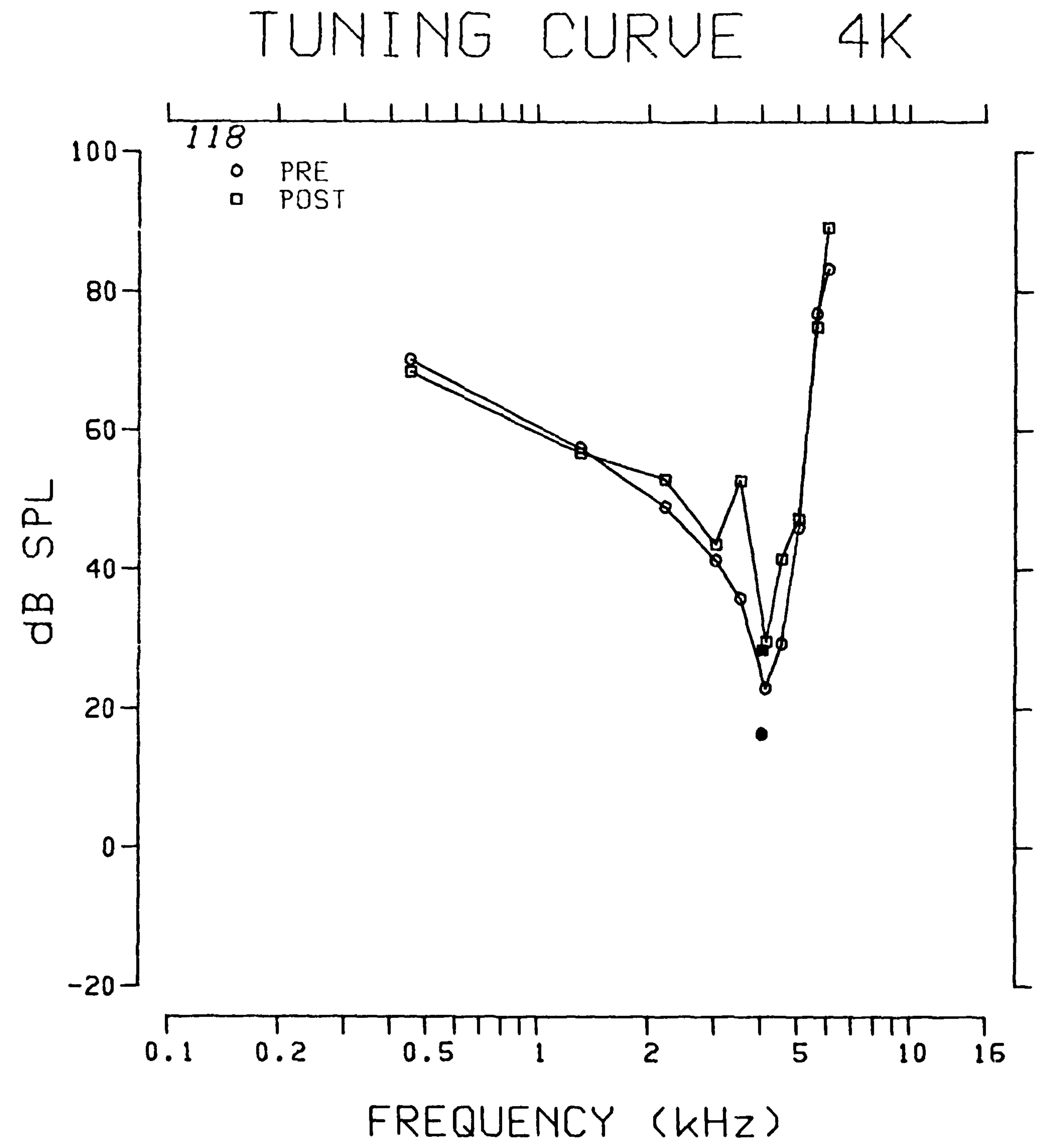


Fig. 3.3.37: Pre- and postexposure psychophysical tuning curves at 2.0 kHz from chinchilla 118.

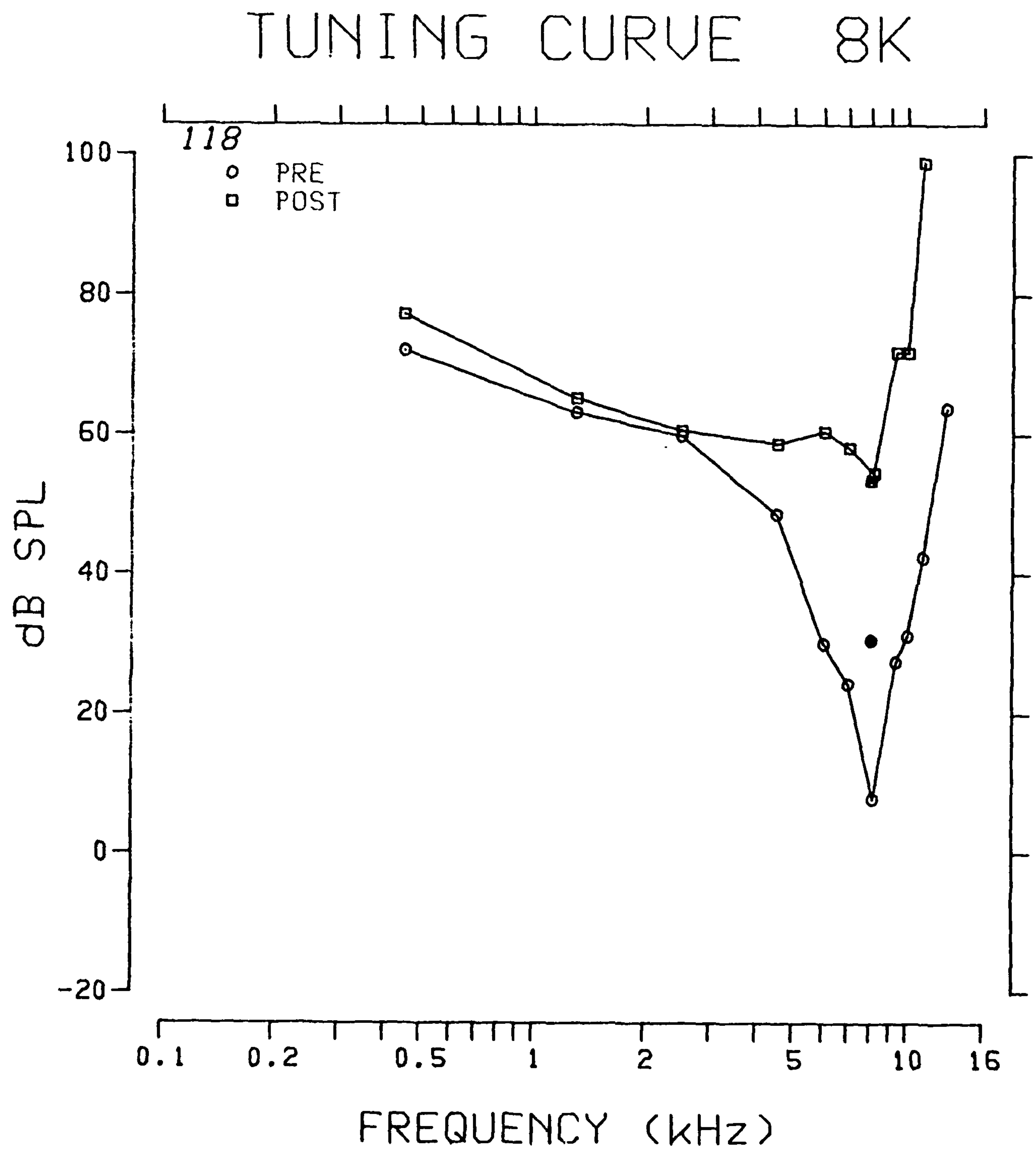


Fig. 3.3.38: Pre- and postexposure psychophysical tuning curves at 4.0 kHz from chinchilla 118.

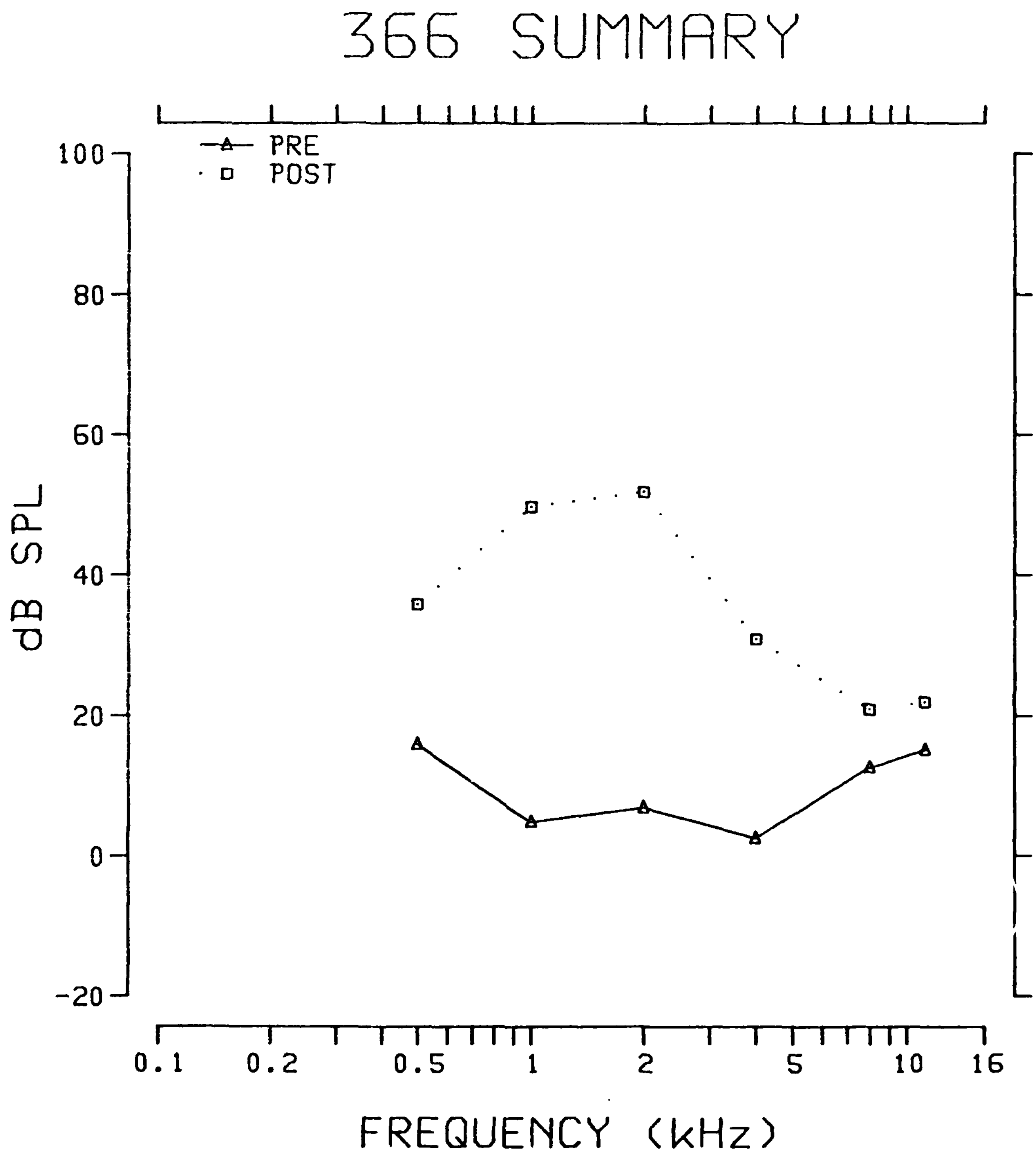


Fig. 3.3.39: Pre- and postexposure evoked response audiograms from chinchilla 366.

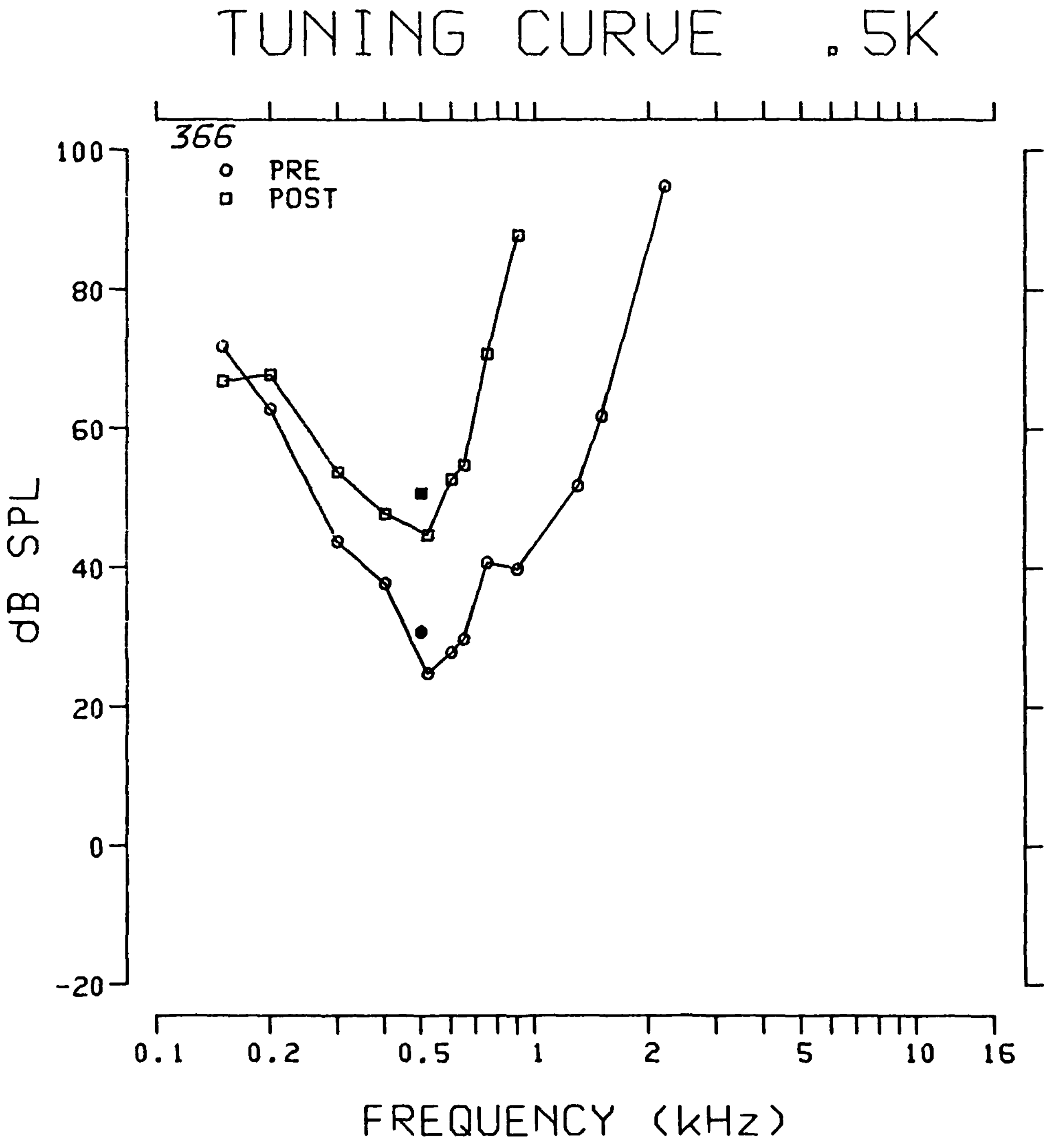


Fig. 3.3.40: Pre- and postexposure evoked response tuning curves at 0.5 kHz from chinchilla 366.

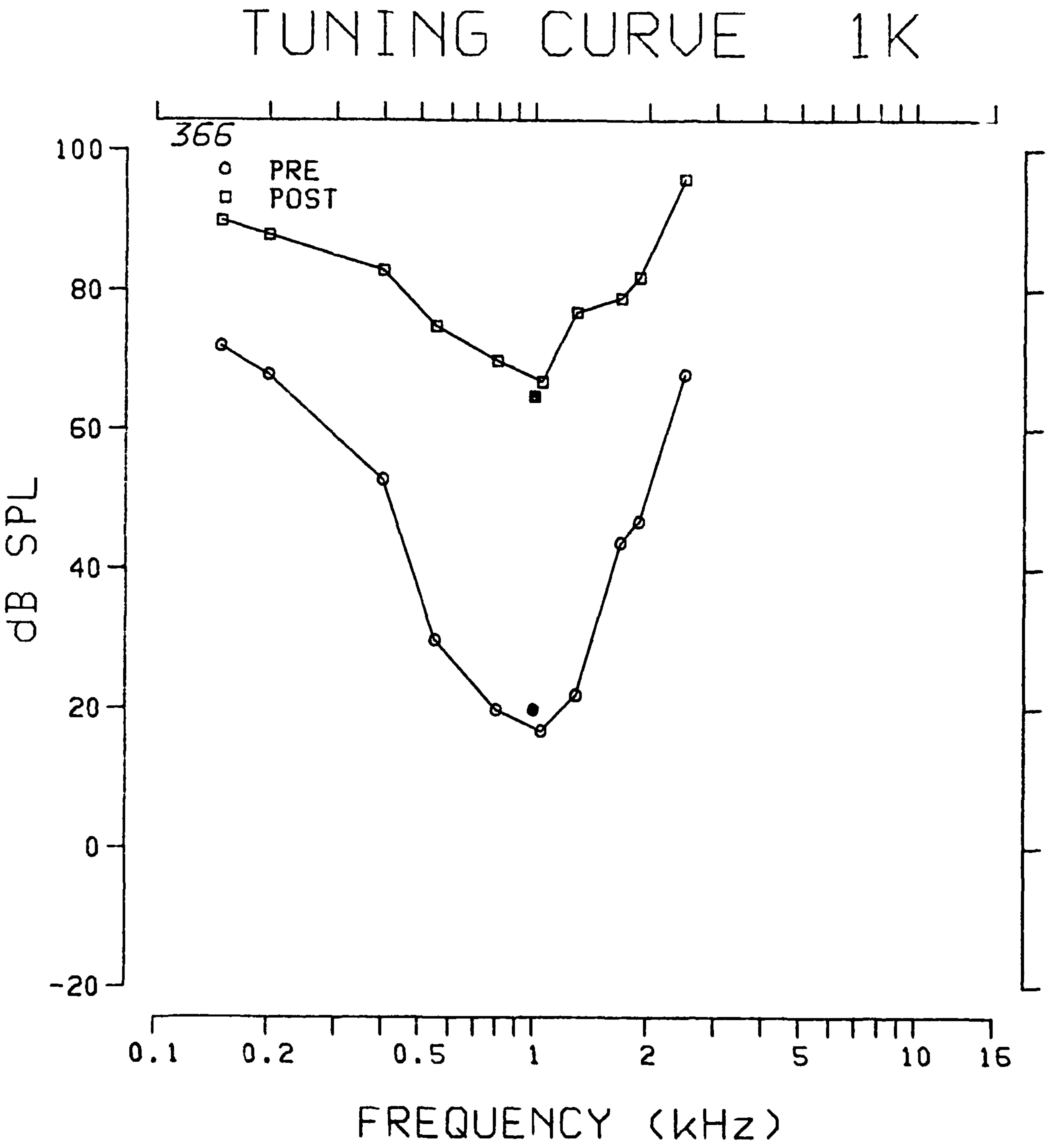


Fig. 3.3.41: Pre- and postexposure evoked response tuning curves at 1.0 kHz from chinchilla 366.

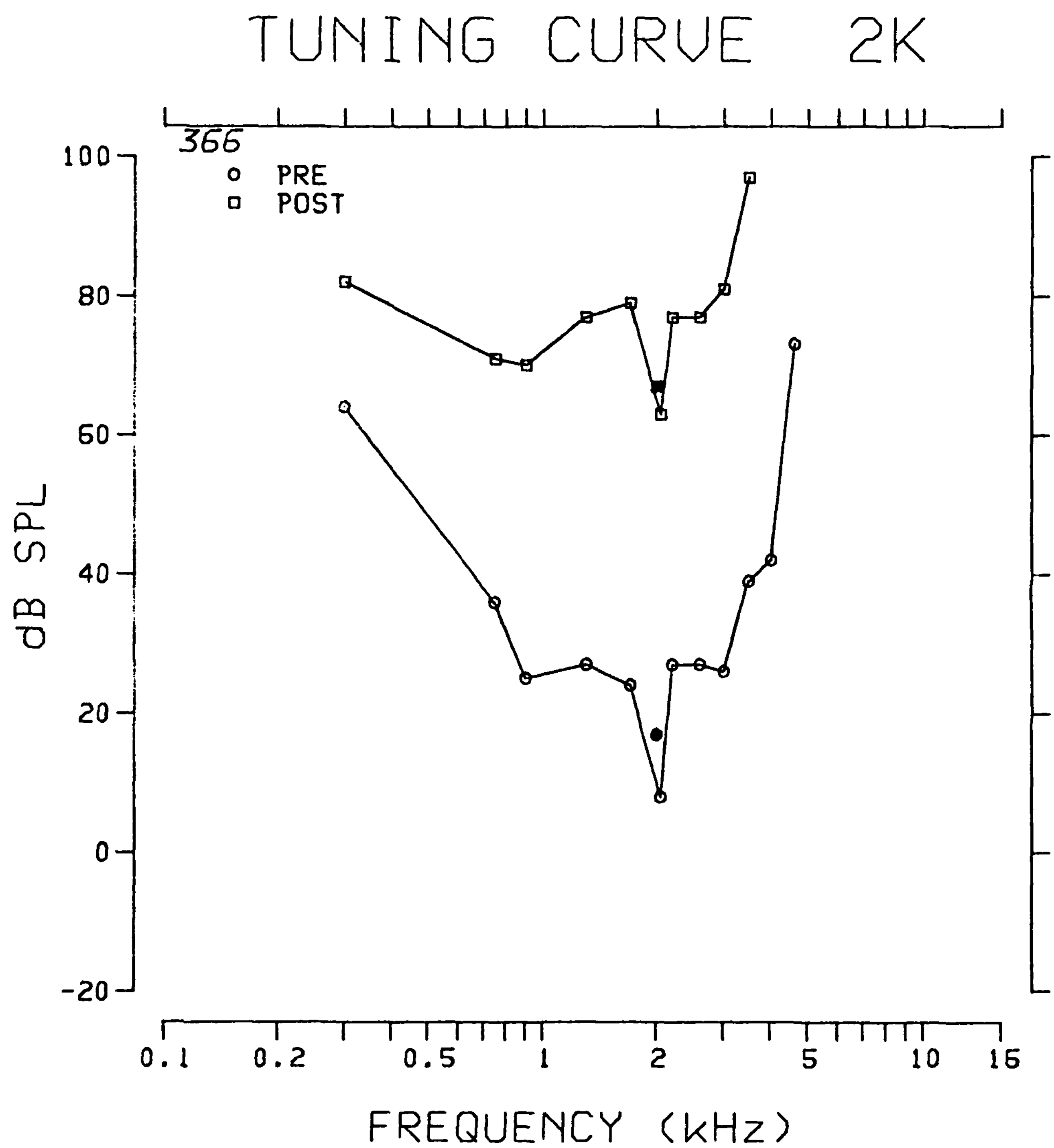


Fig. 3.3.42: Pre- and postexposure evoked response tuning curves at 2.0 kHz from chinchilla 366.

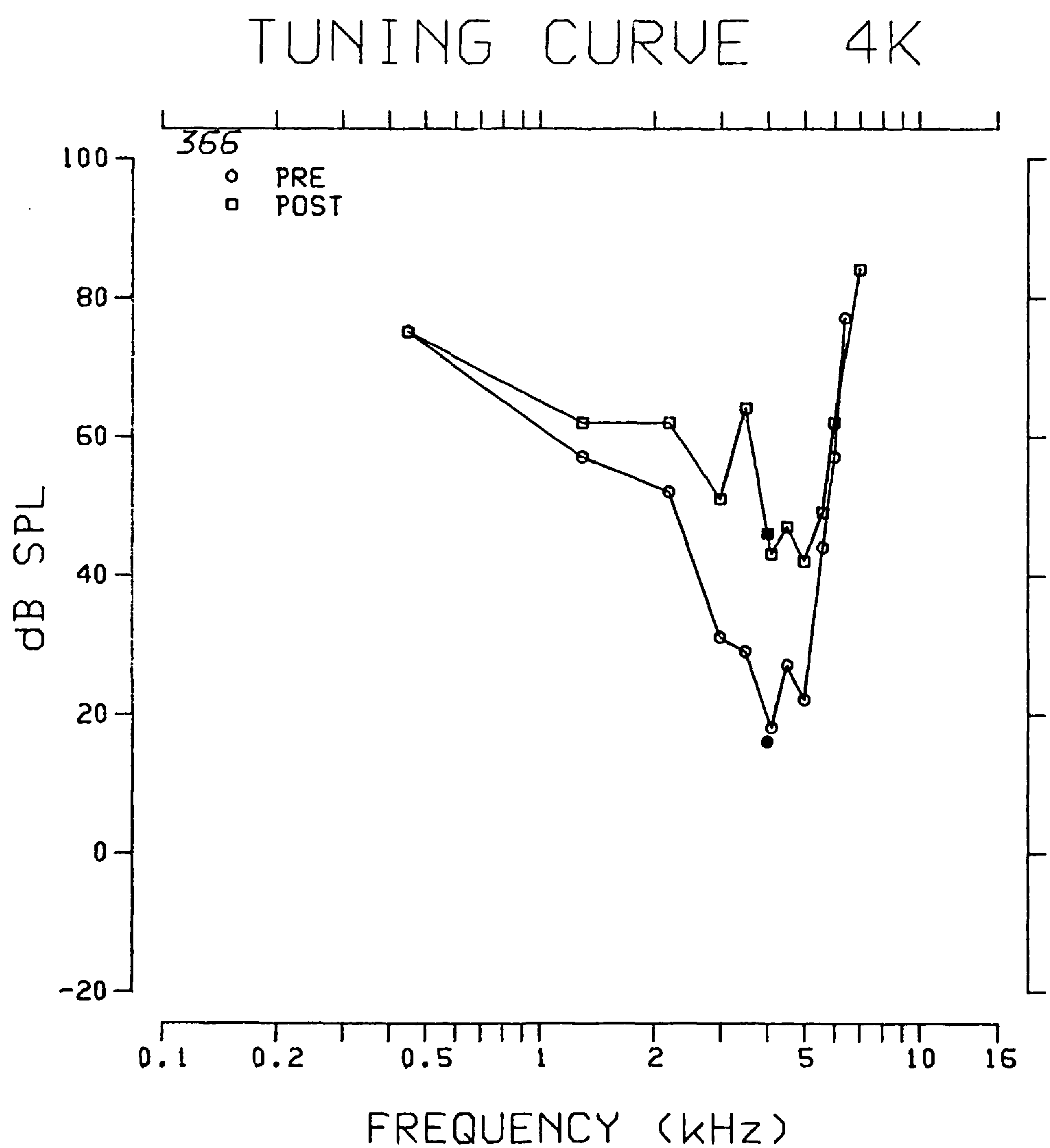


Fig. 3.3.43: Pre- and postexposure evoked response tuning curves at 4.0 kHz from chinchilla 366.

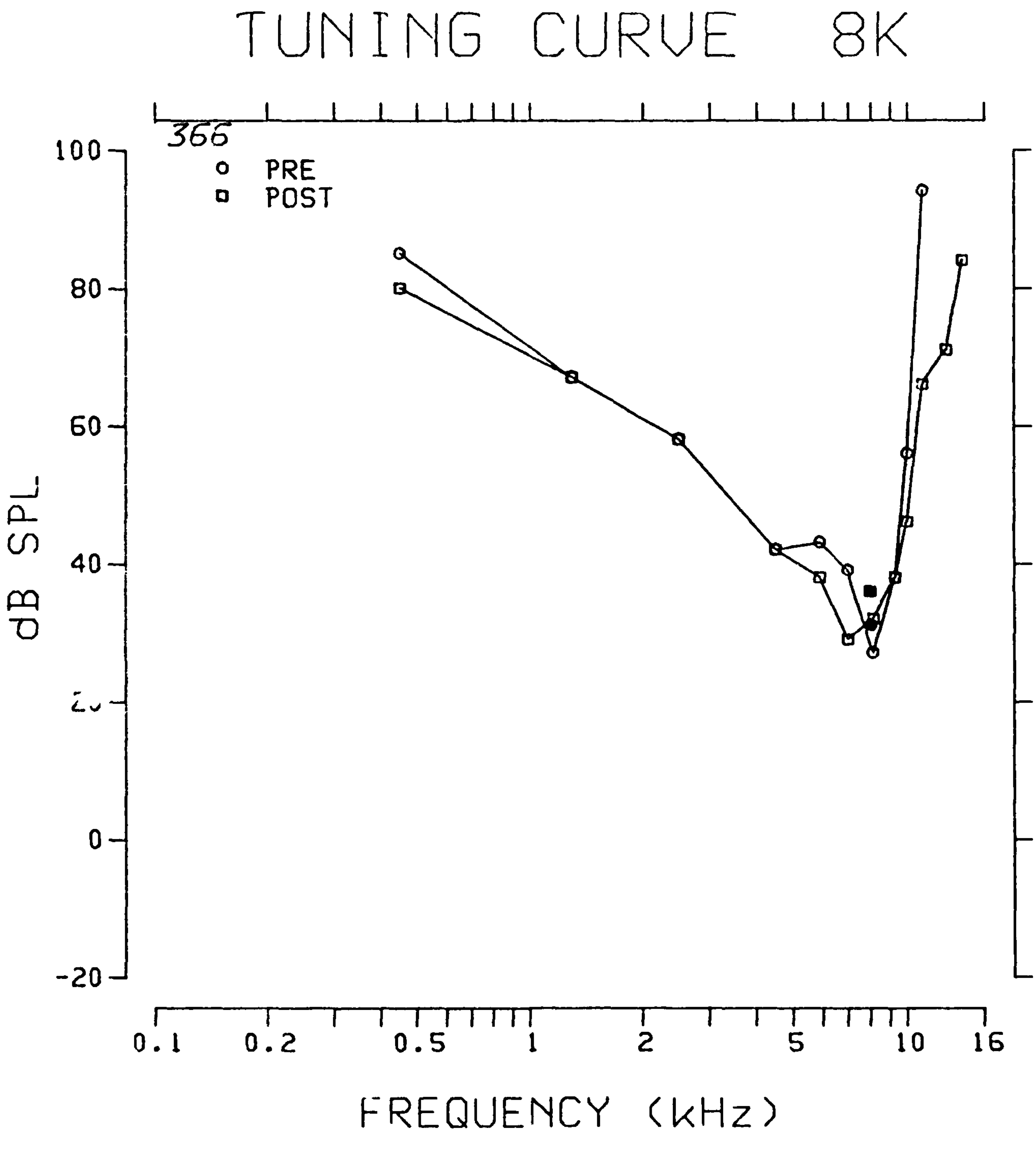


Fig. 3.3.44: Pre- and postexposure evoked response tuning curves at 8.0 kHz from chinchilla 366.

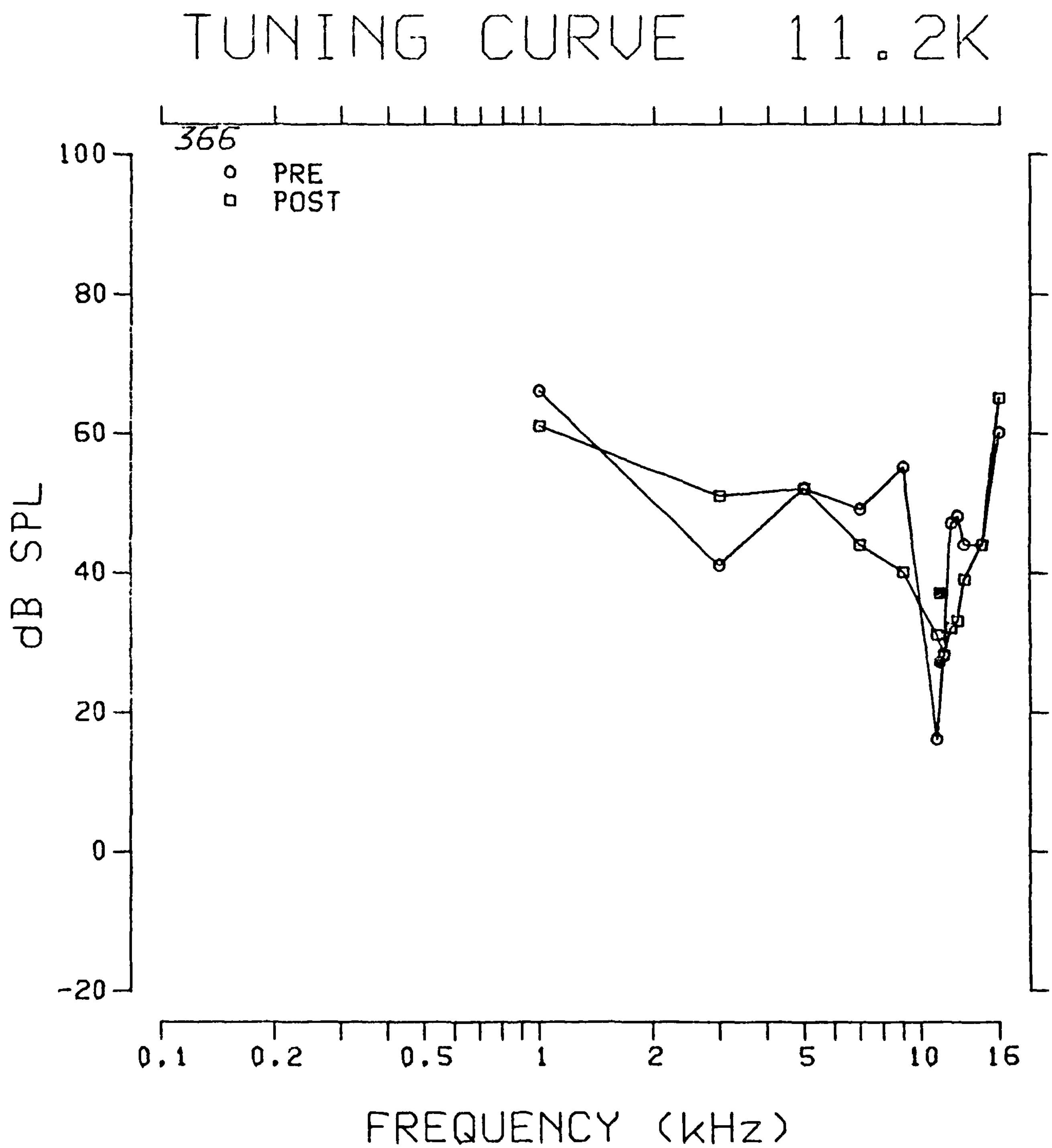


Fig. 3.3.45: Pre- and postexposure evoked response tuning curves at 11.2 kHz from chinchilla 366.

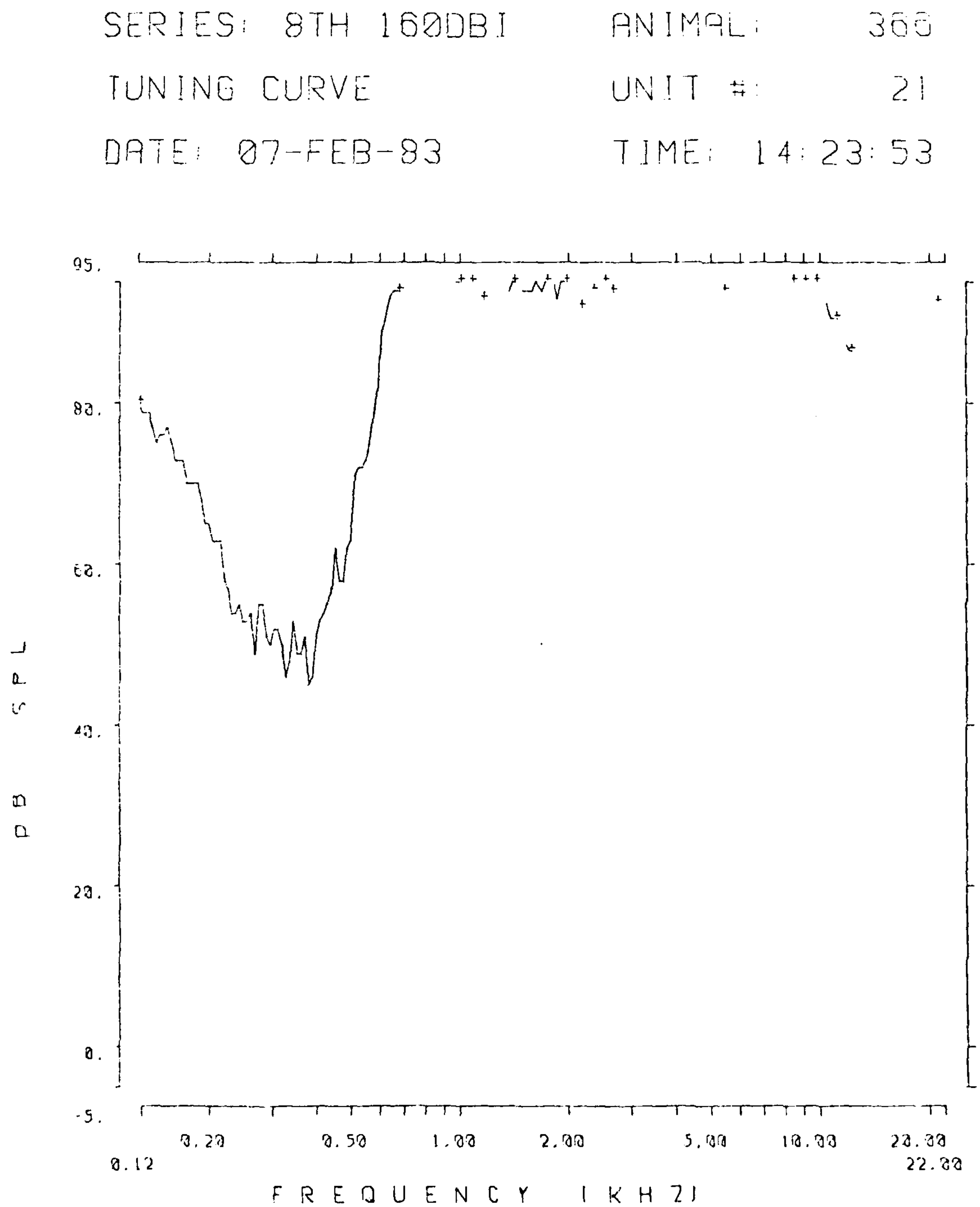


Fig. 3.3.46: Auditory nerve fiber tuning curve from chinchilla 366.

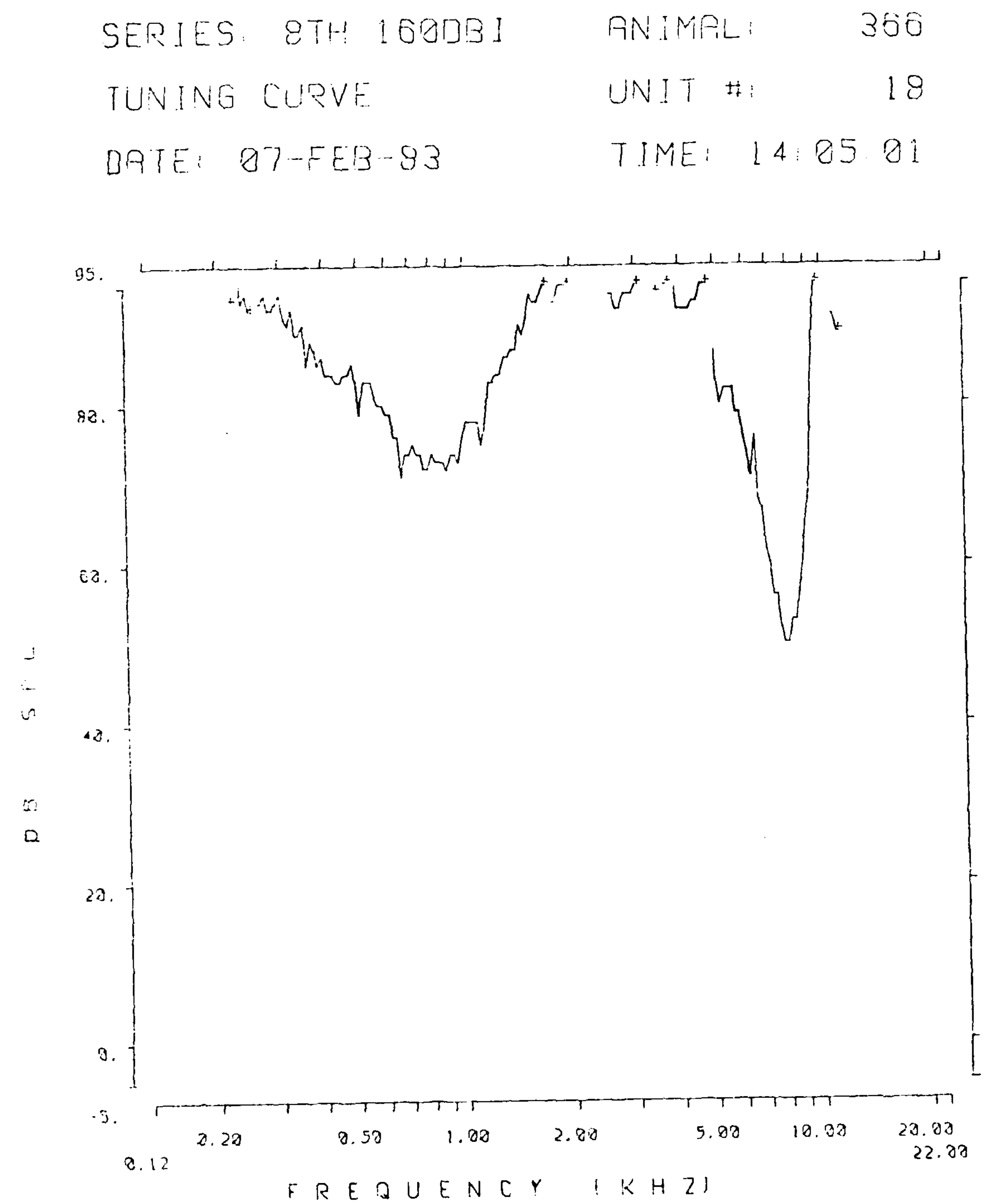


Fig. 3.3.47: Auditory nerve fiber tuning curve from chinchilla 366.

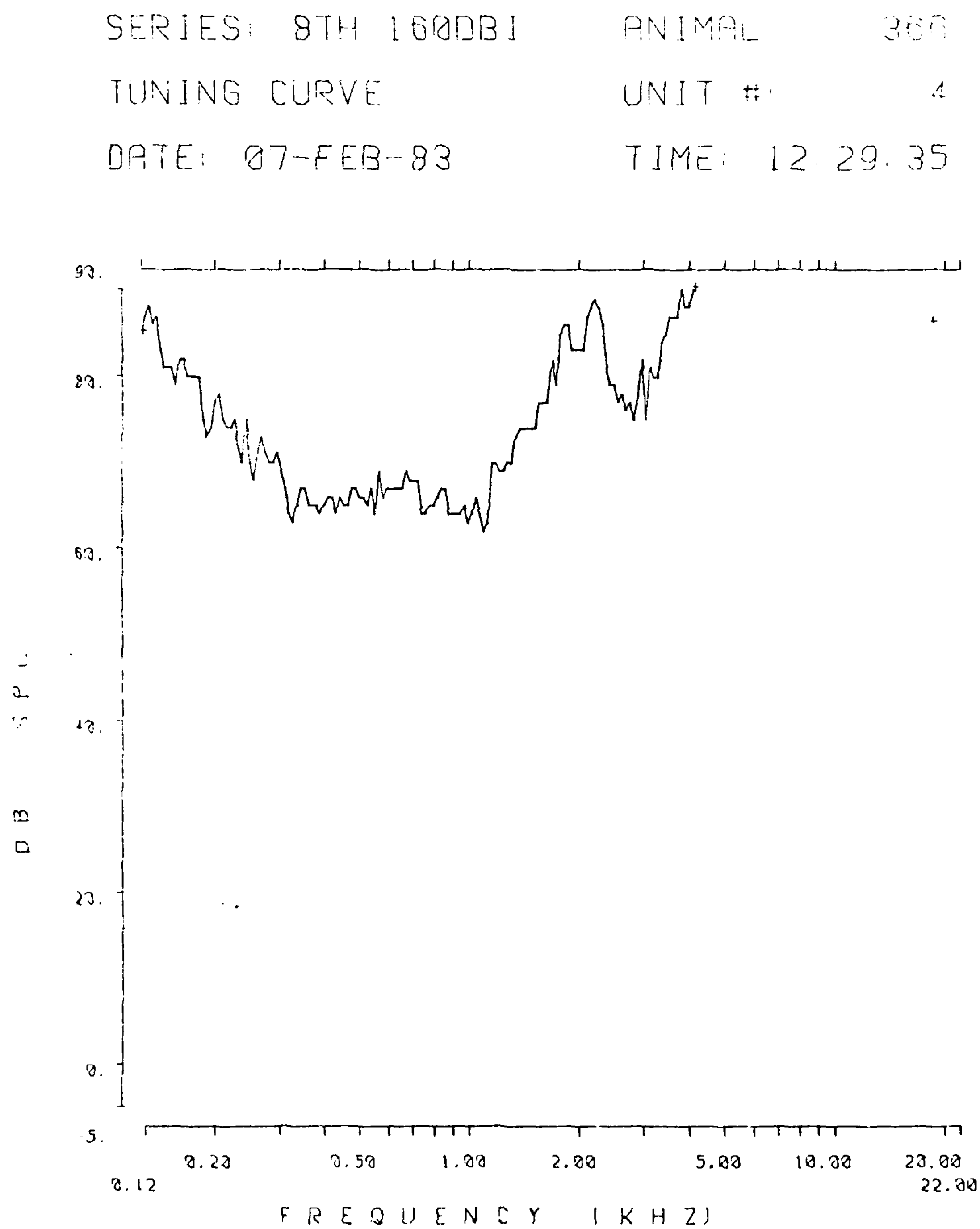


Fig. 3.3.48: Auditory nerve fiber tuning curve from chinchilla 366.

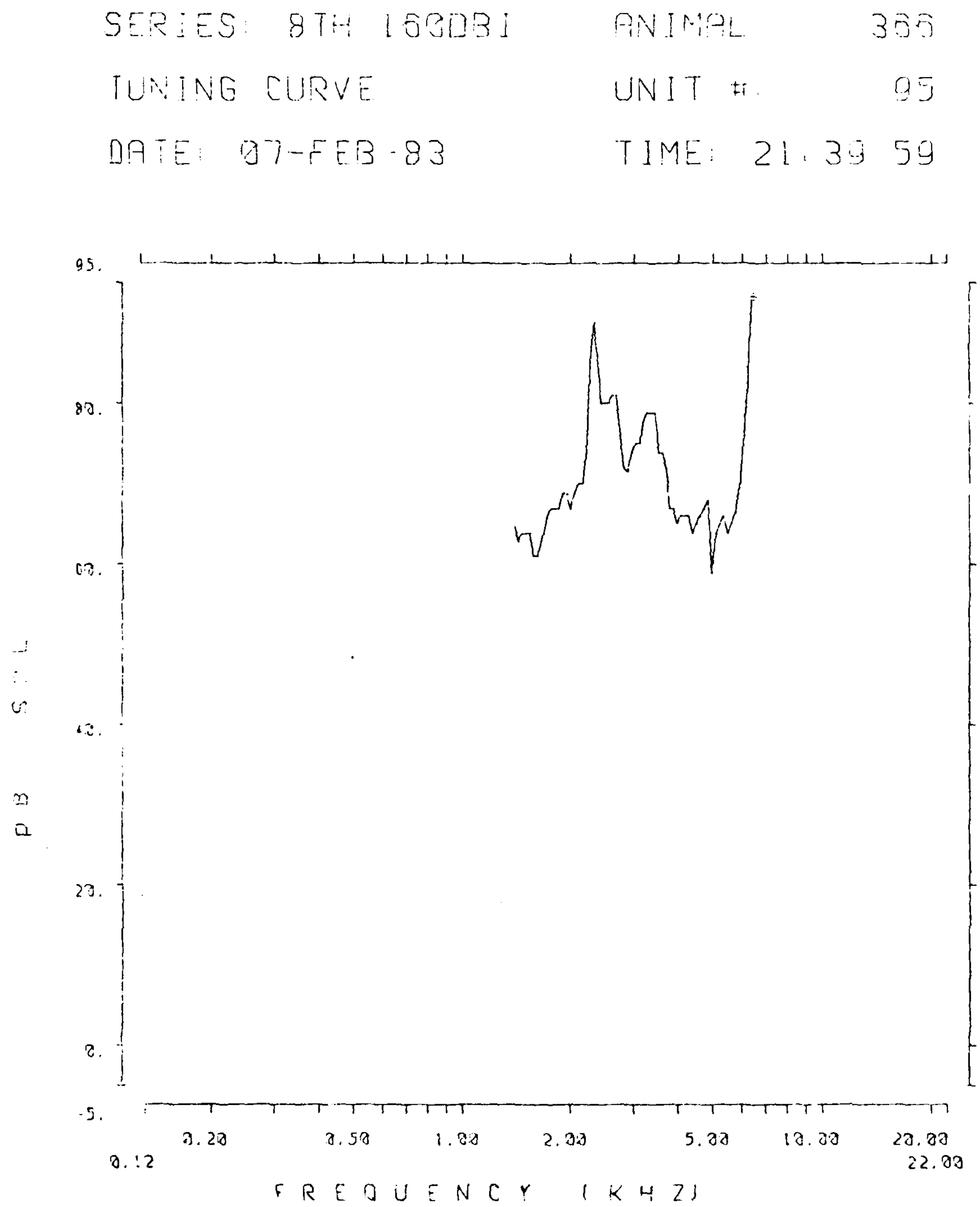


Fig. 3.3.49: Auditory nerve fiber tuning curve from chinchilla 366.

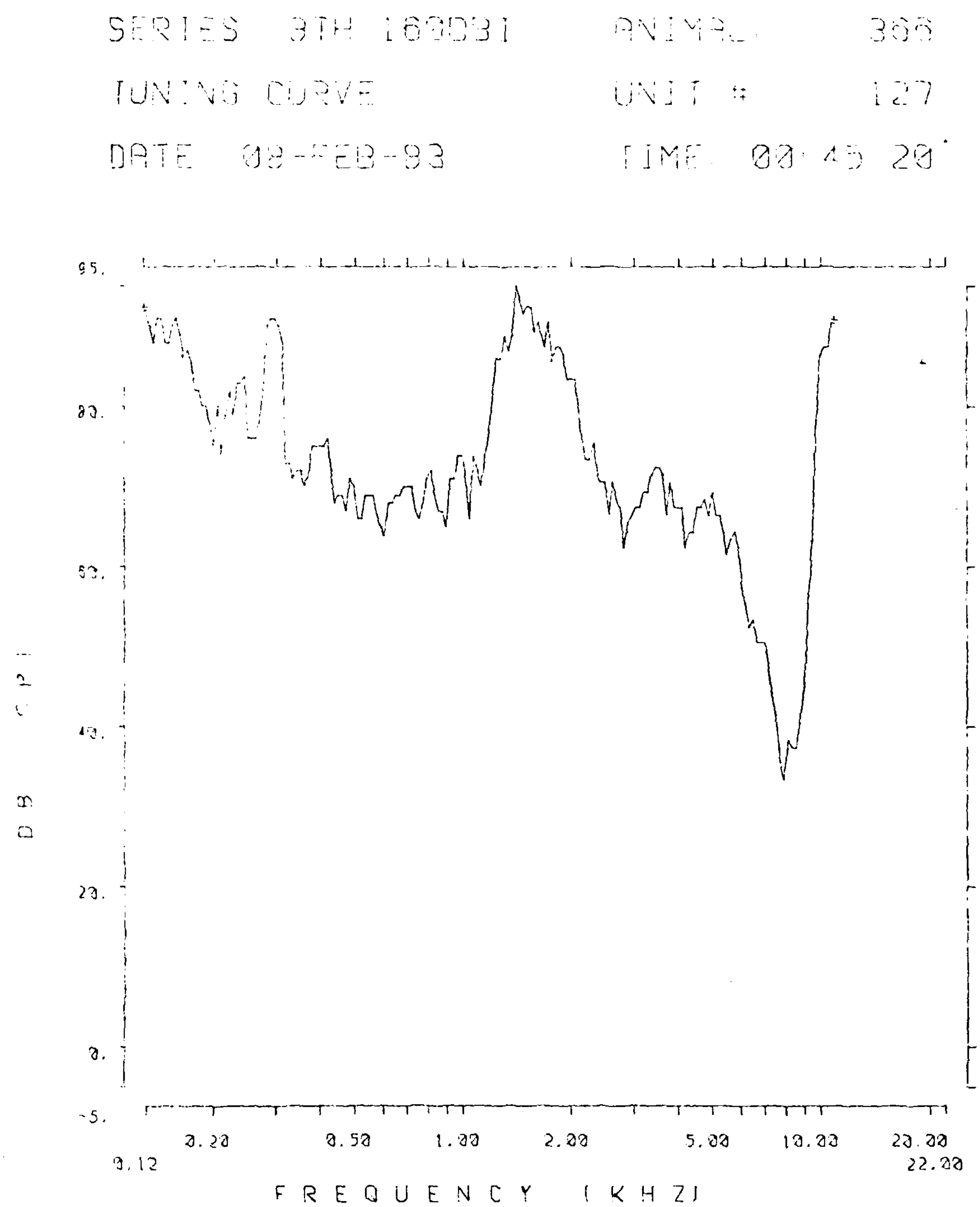


Fig. 3.3.50: Auditory nerve fiber tuning curve from chinchilla 336.

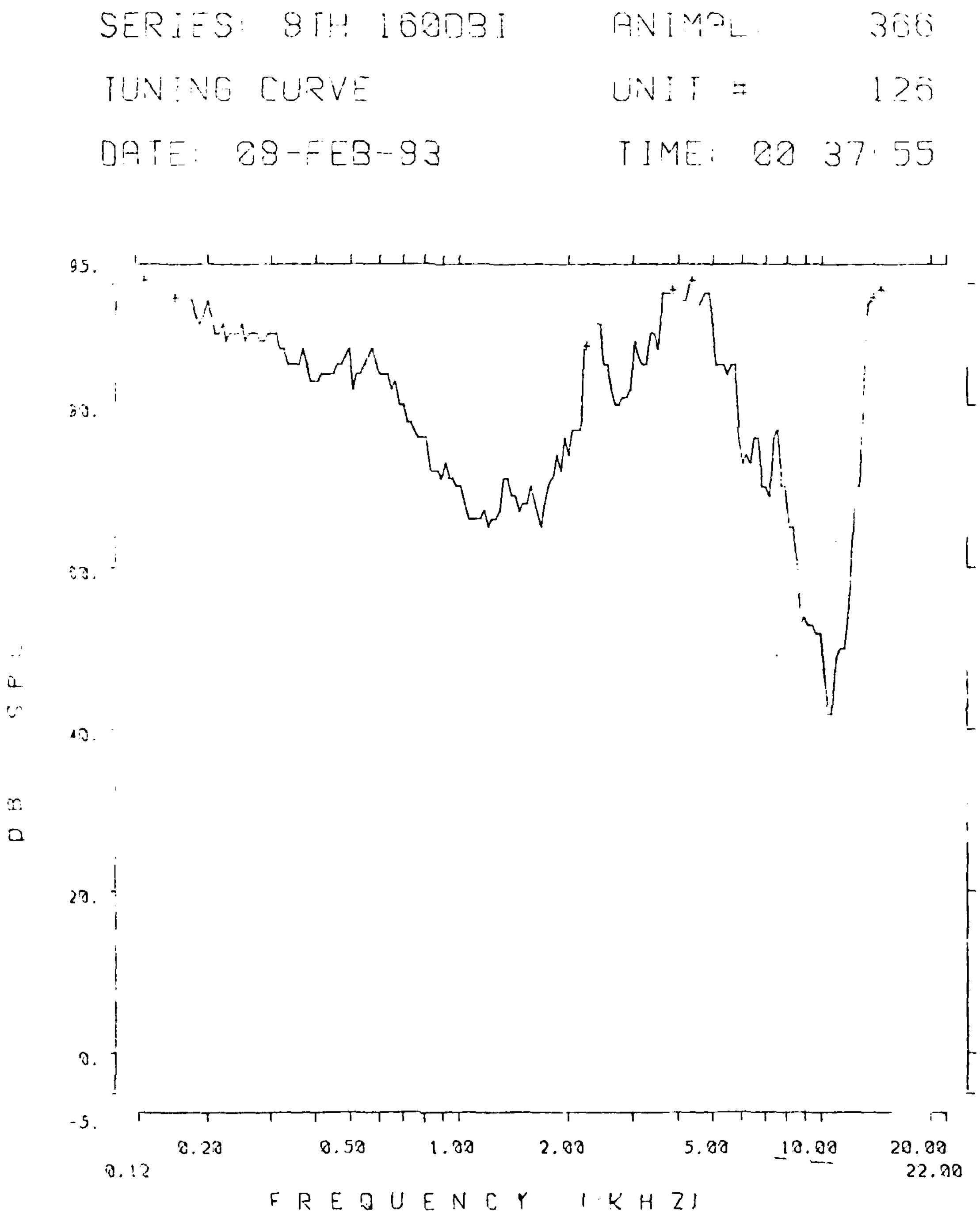


Fig. 3.3.51: Auditory nerve fiber tuning curve from chinchilla 366.

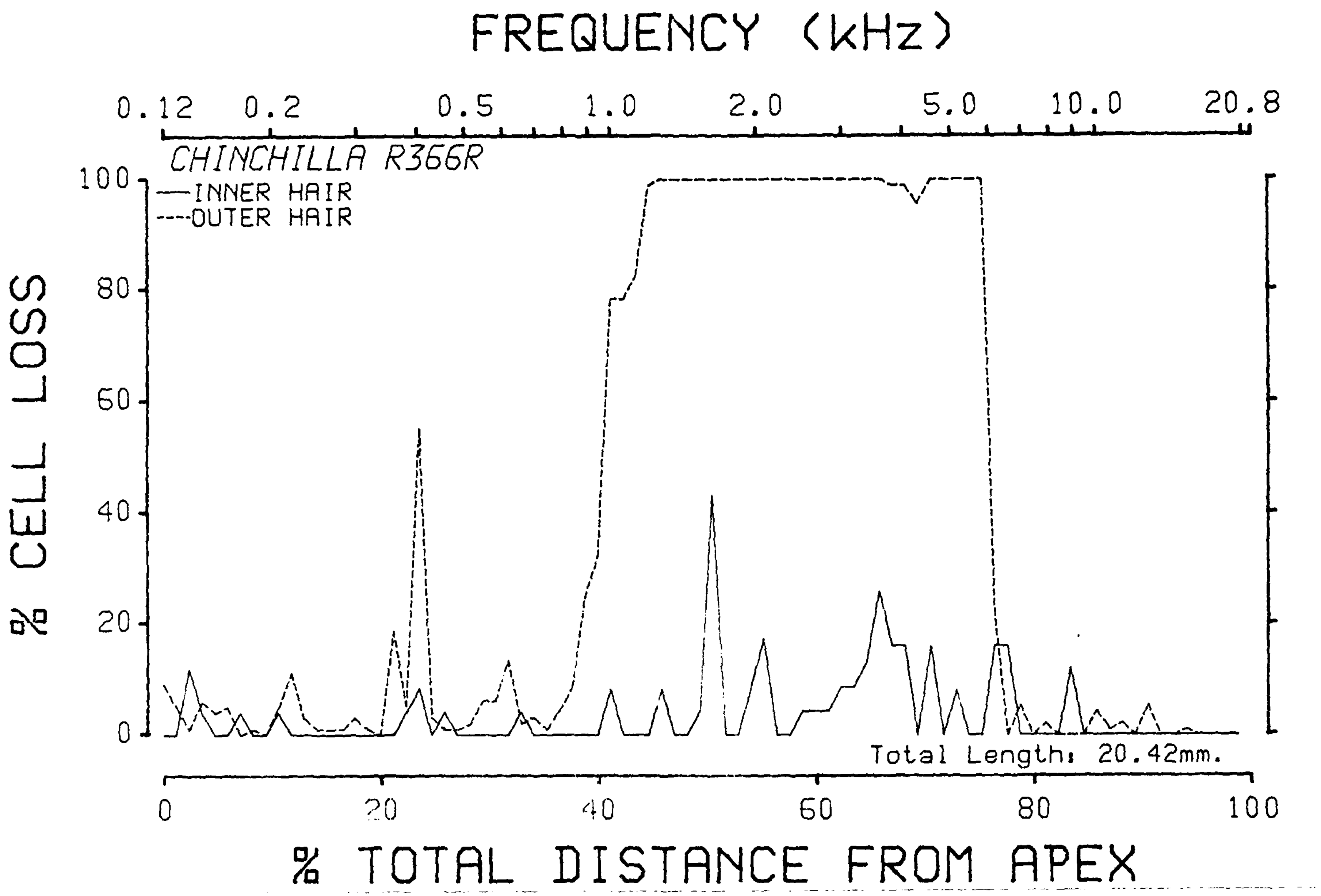


Fig. 3.3.52: Cochleogram from chinchilla 366.

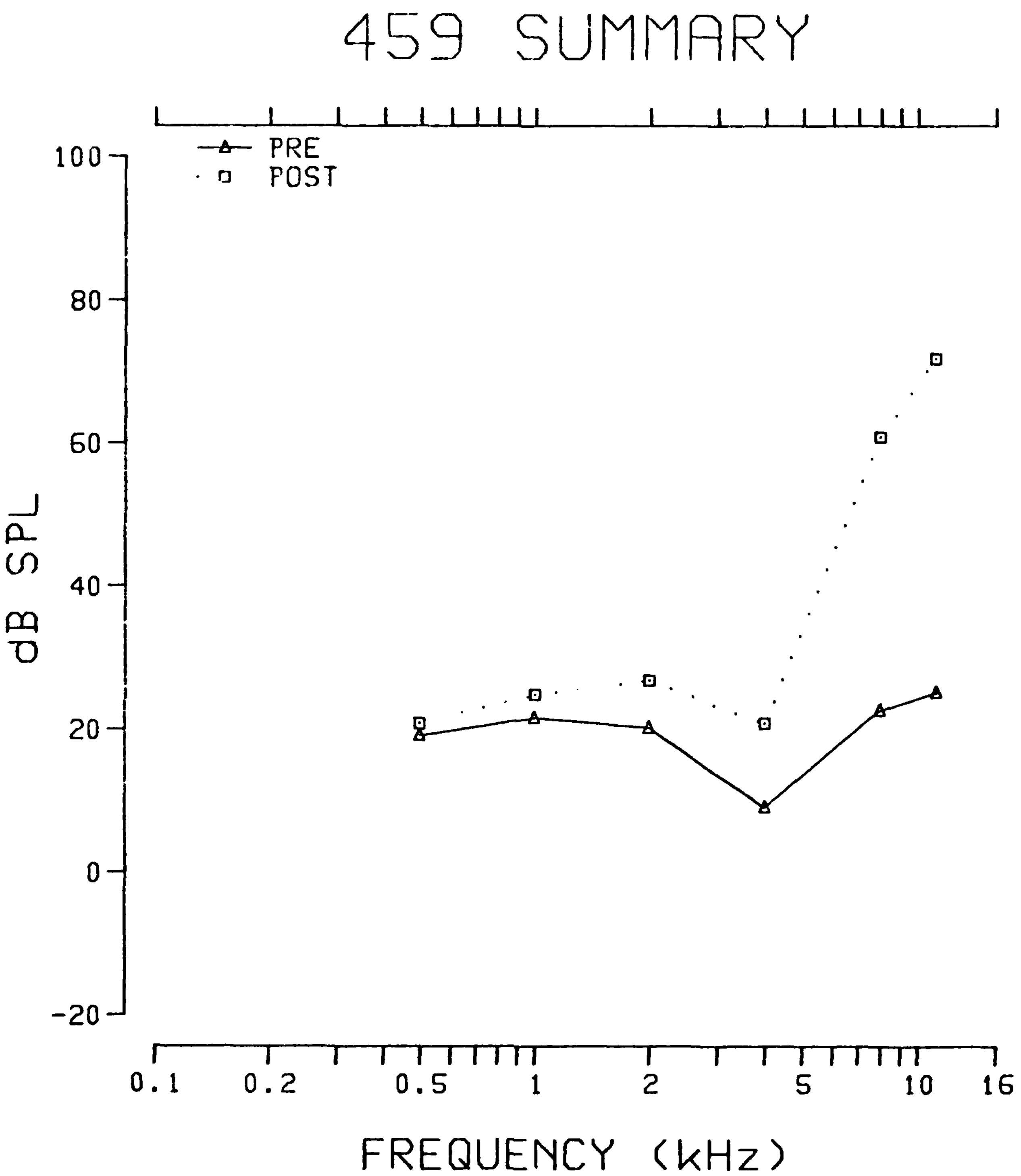


Fig. 3.3.53: Pre- and postexposure evoked response audiogram from chinchilla 459.

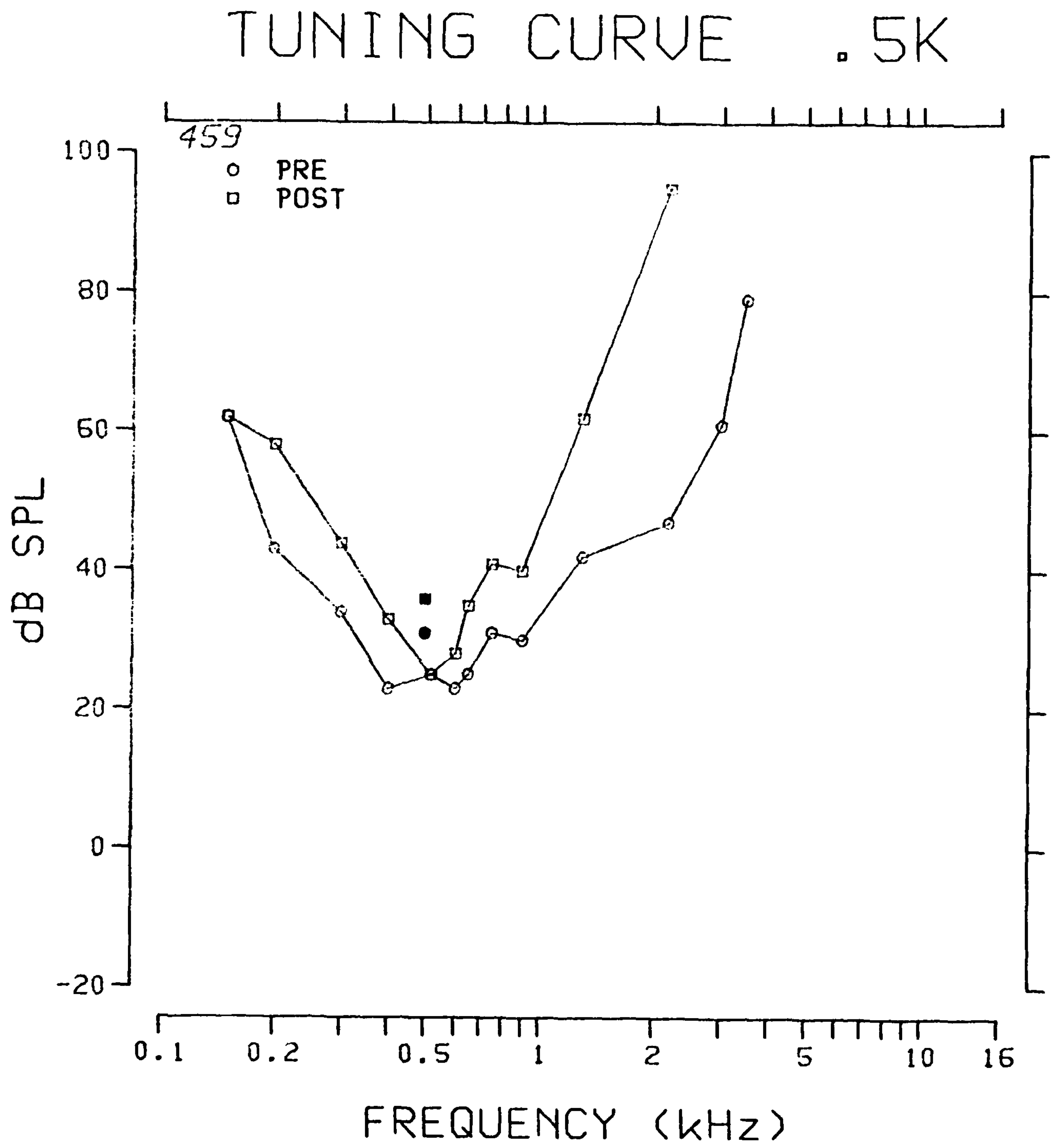


Fig. 3.3.54: Pre- and postexosure evoked response tuning curve at 0.5 kHz from chinchilla 459.

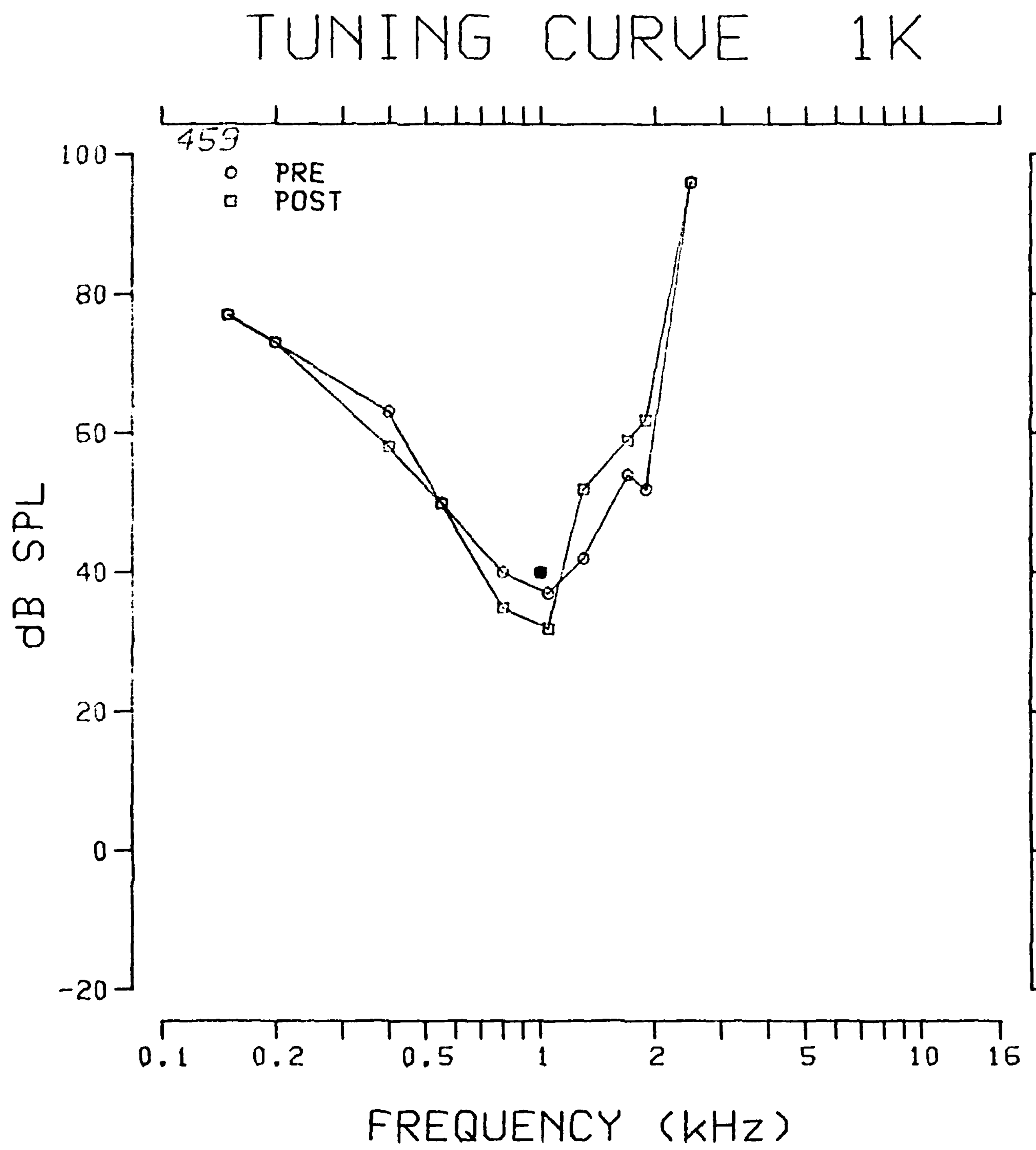


Fig. 3.3.55: Pre- and postexposure evoked response tuning curve at 1.0 kHz from chinchilla 459.

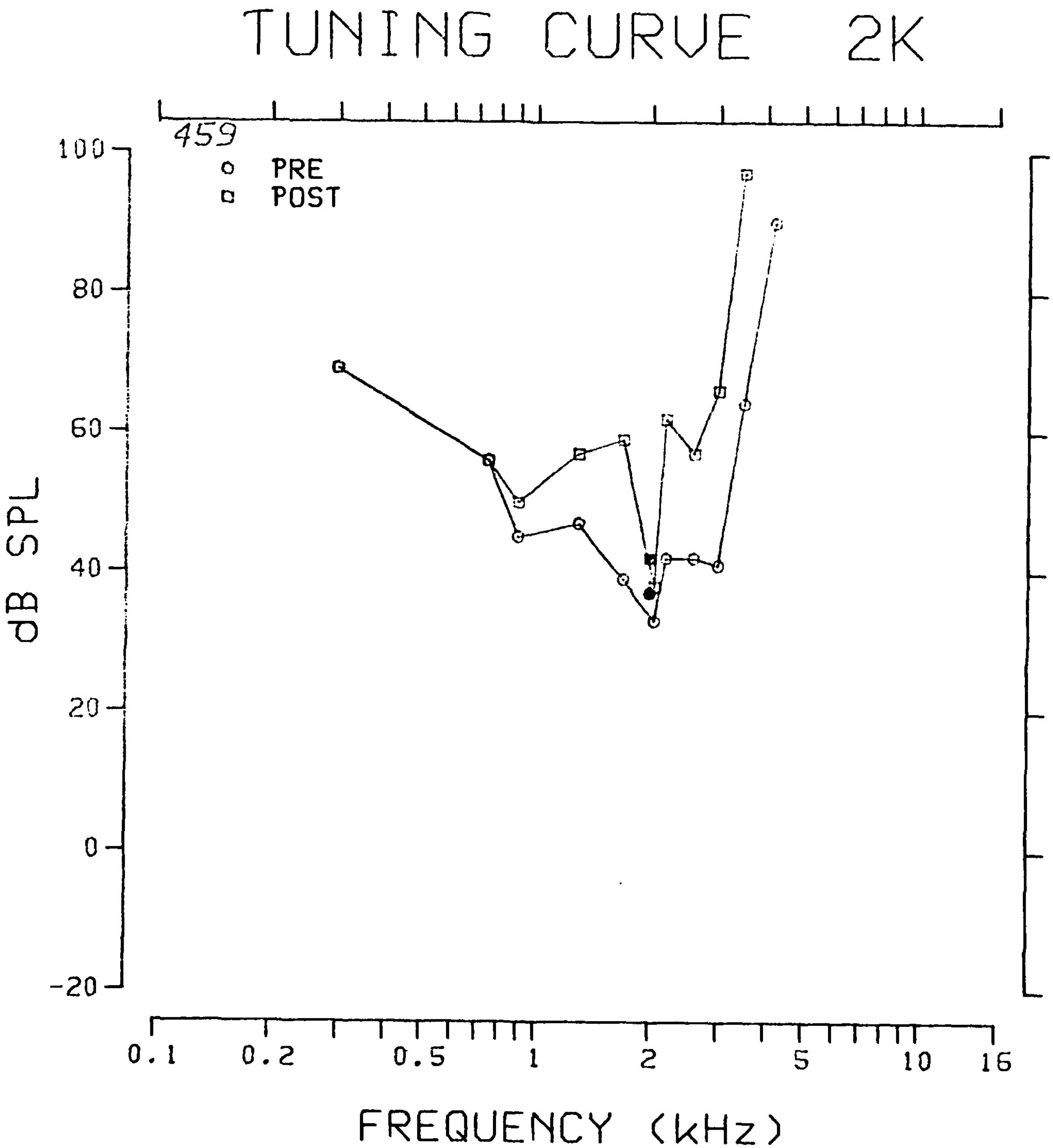


Fig. 3.3.56: Pre- and postexposure evoked response tuning curve at 2.0 kHz from chinchilla 459.

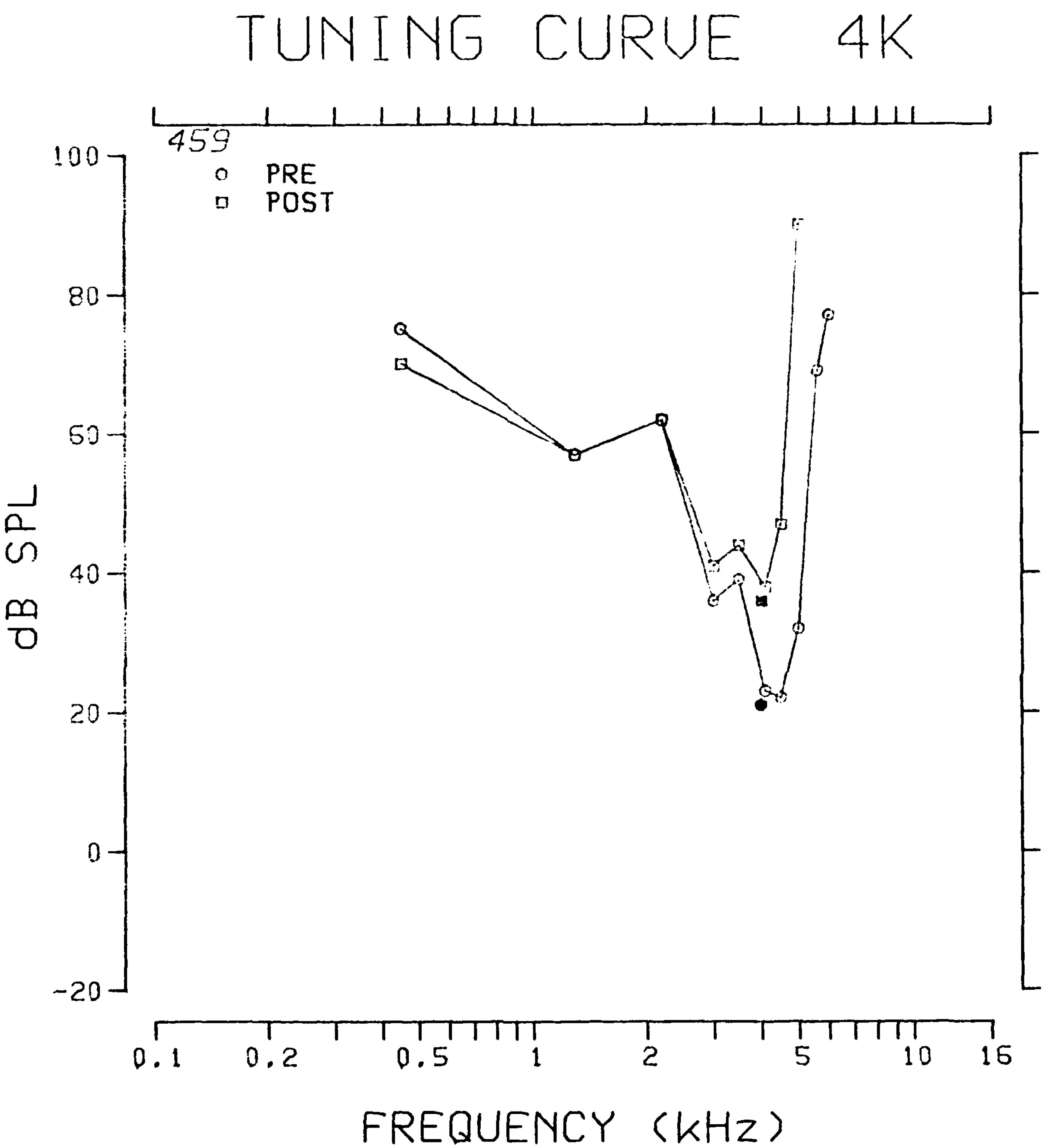


Fig. 3.3.57: Pre- and postexposure evoked response tuning curve at 4.0 kHz from chinchilla 459.

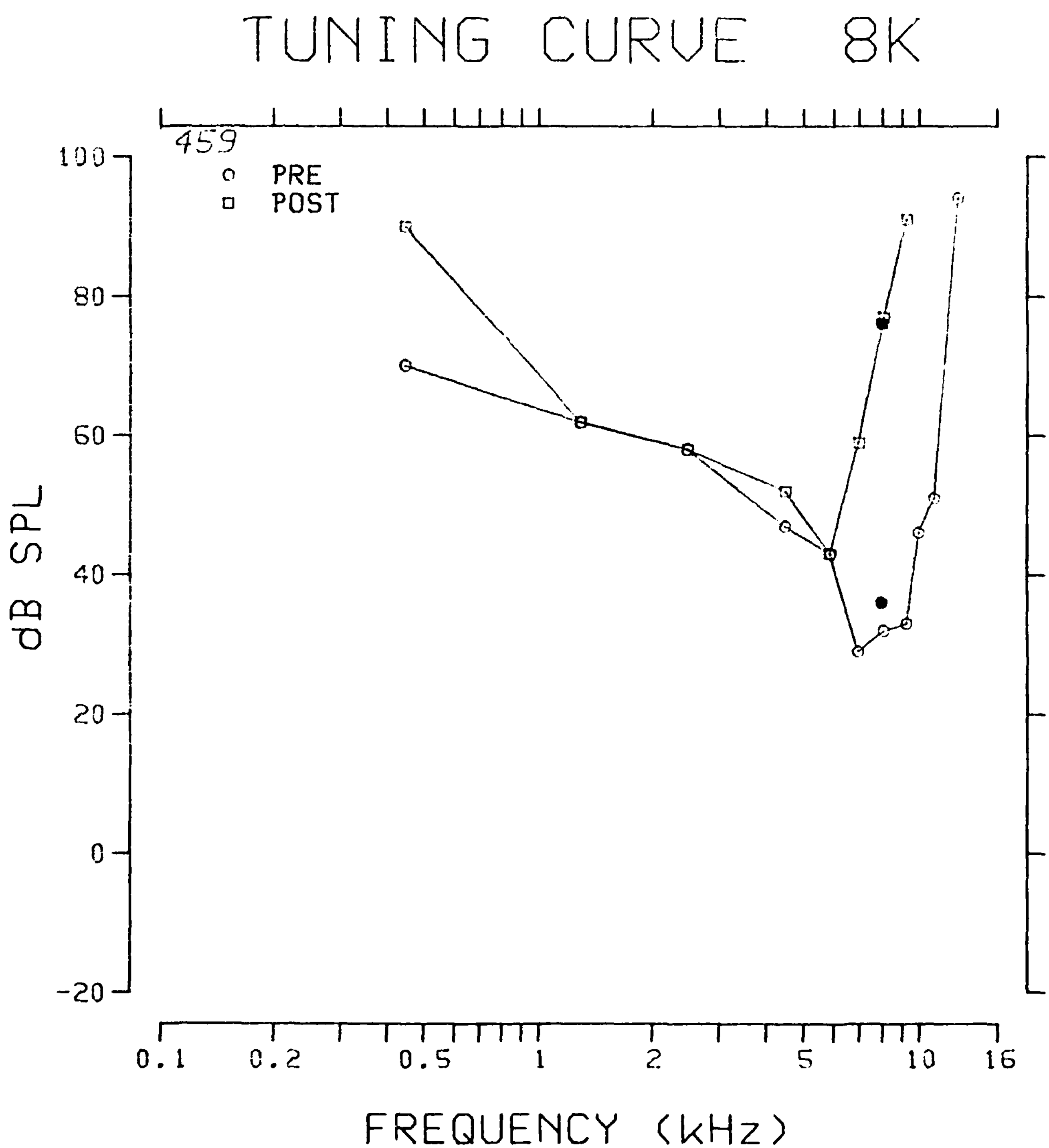


Fig. 3.3.58: Pre- and postexposure evoked response tuning curve at 8.0 kHz from chinchilla 459.

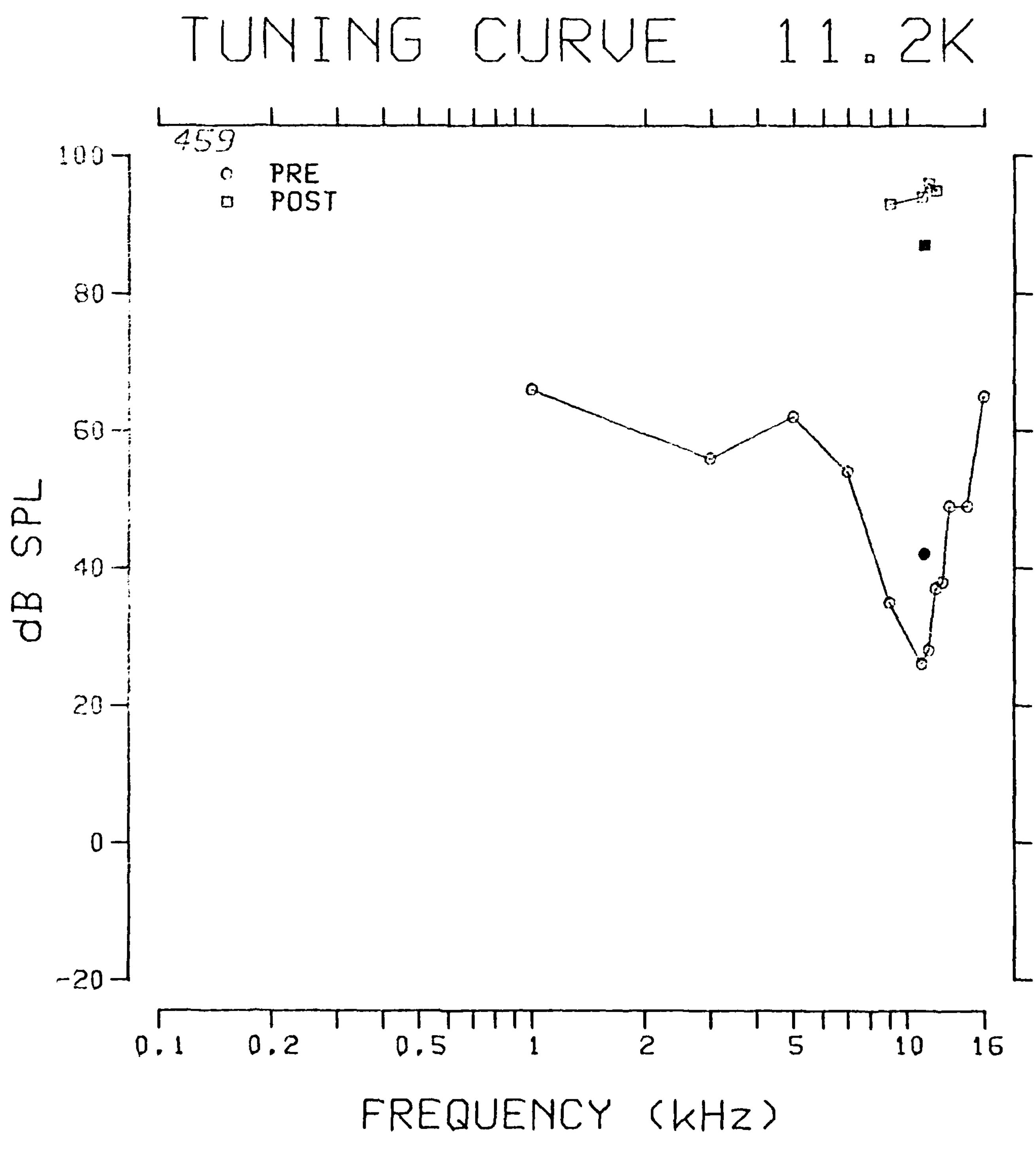


Fig. 3.3.59: Pre- and postexposure evoked response tuning curves at 11.2 kHz from chichilla 459.

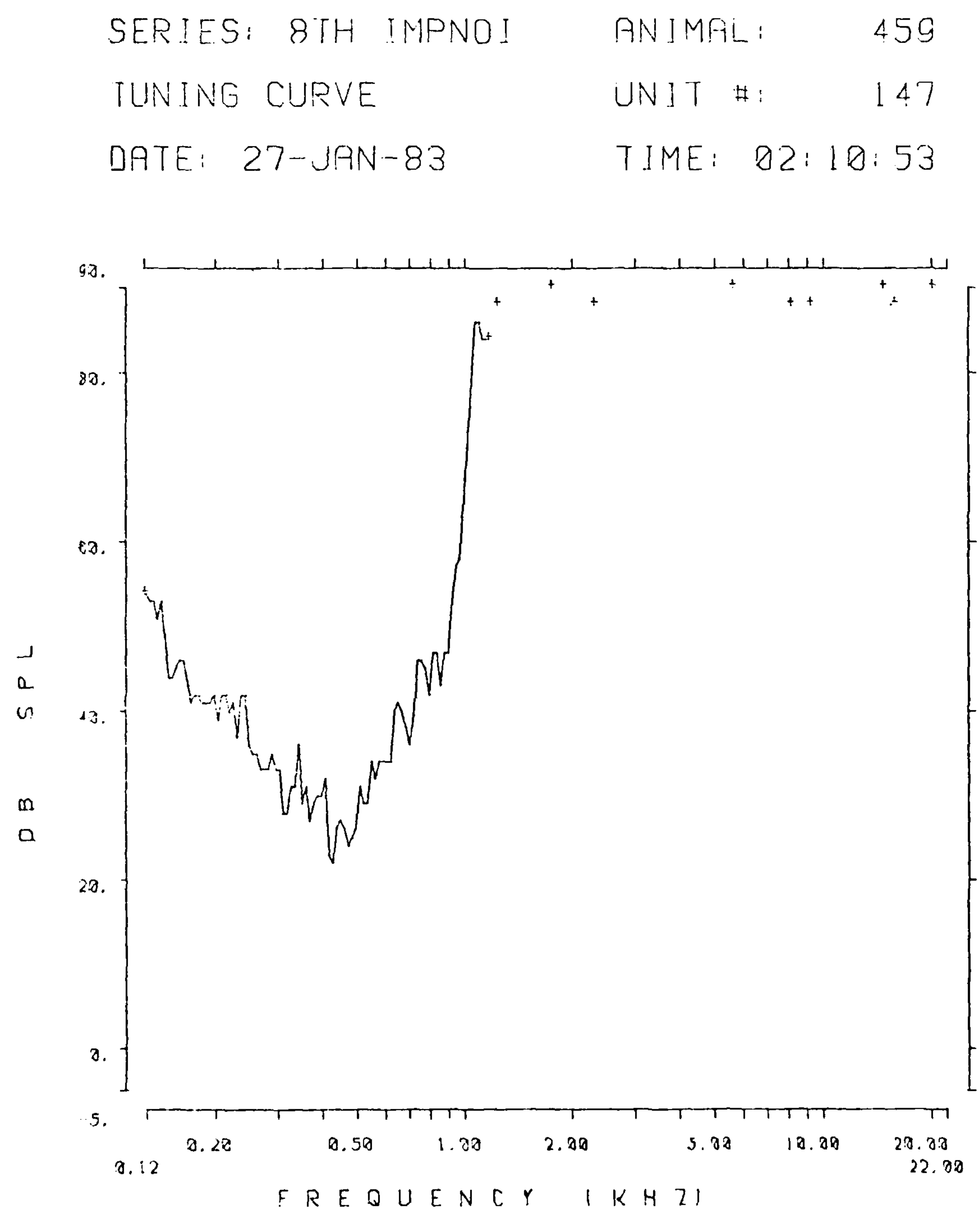


Fig. 3.3.60: Auditory nerve fiber tuning curve from chinchilla 459.

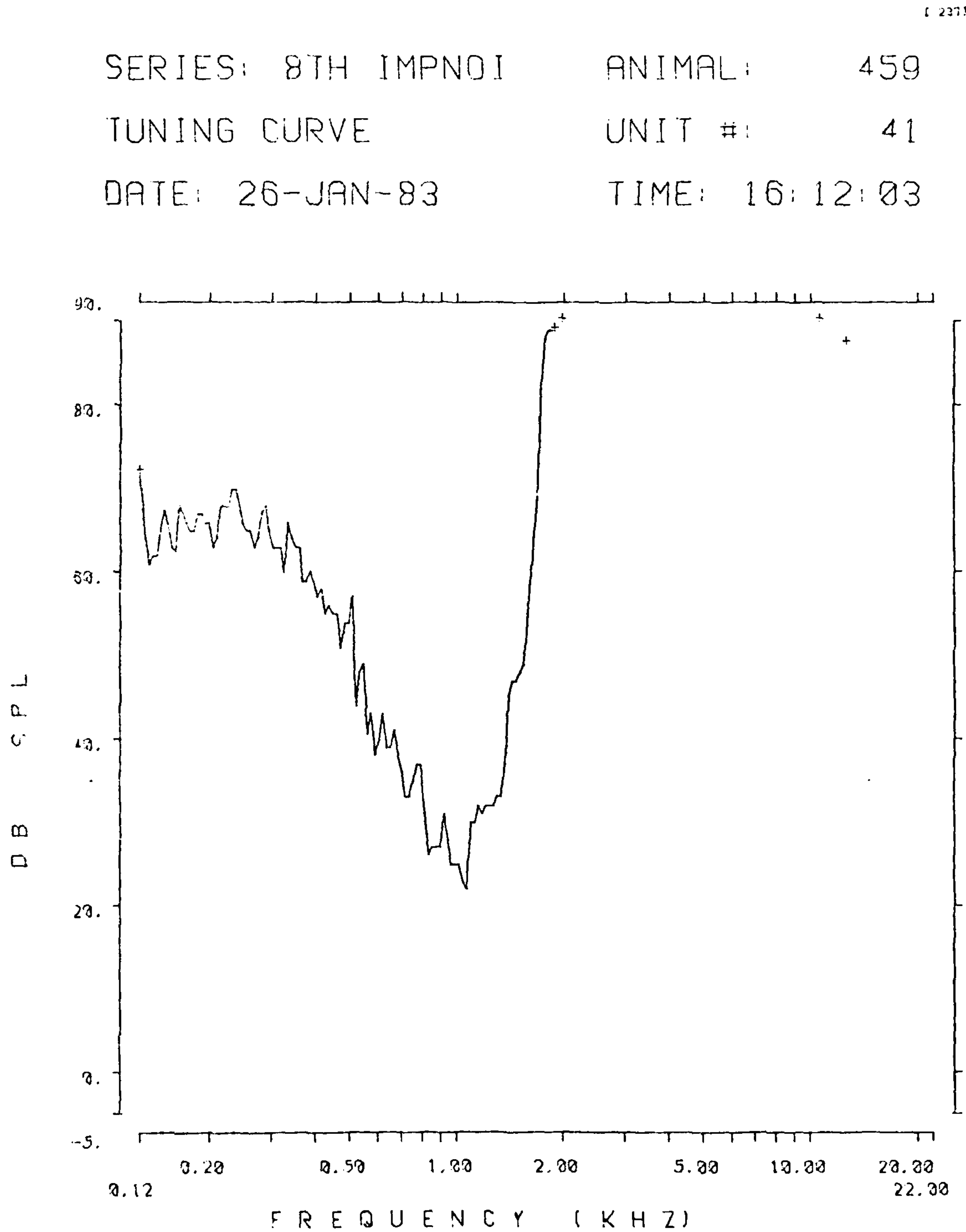


Fig. 3.3.61: Auditory nerve fiber tuning curve from chinchilla 459.

SERIES: 8TH IMPNOI ANIMAL: 459

TUNING CURVE UNIT #: 16

DATE: 26-JAN-83 TIME: 13:31:54

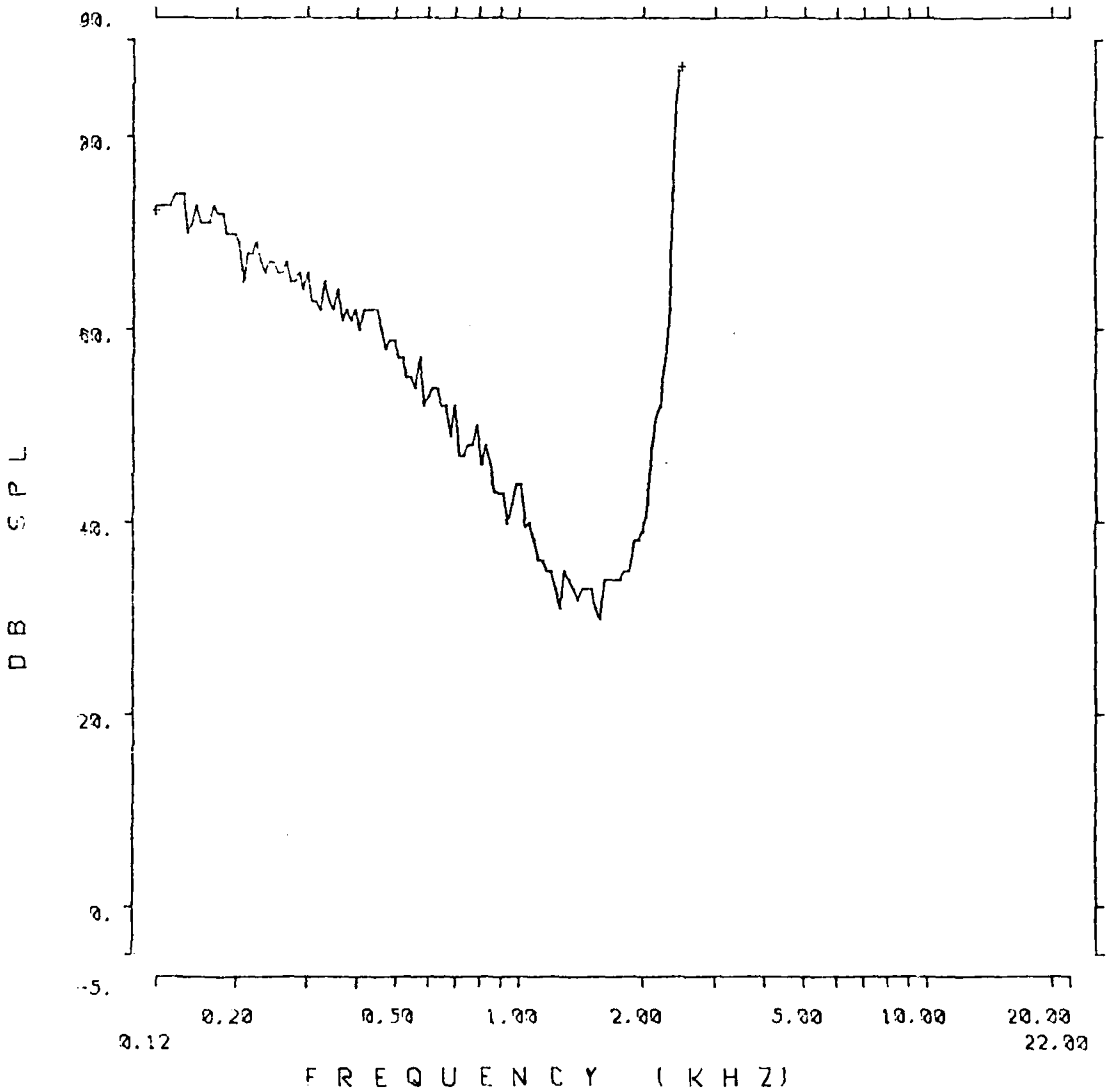


Fig. 3.3.62: Auditory nerve fiber tuning curve from chinchilla 459.

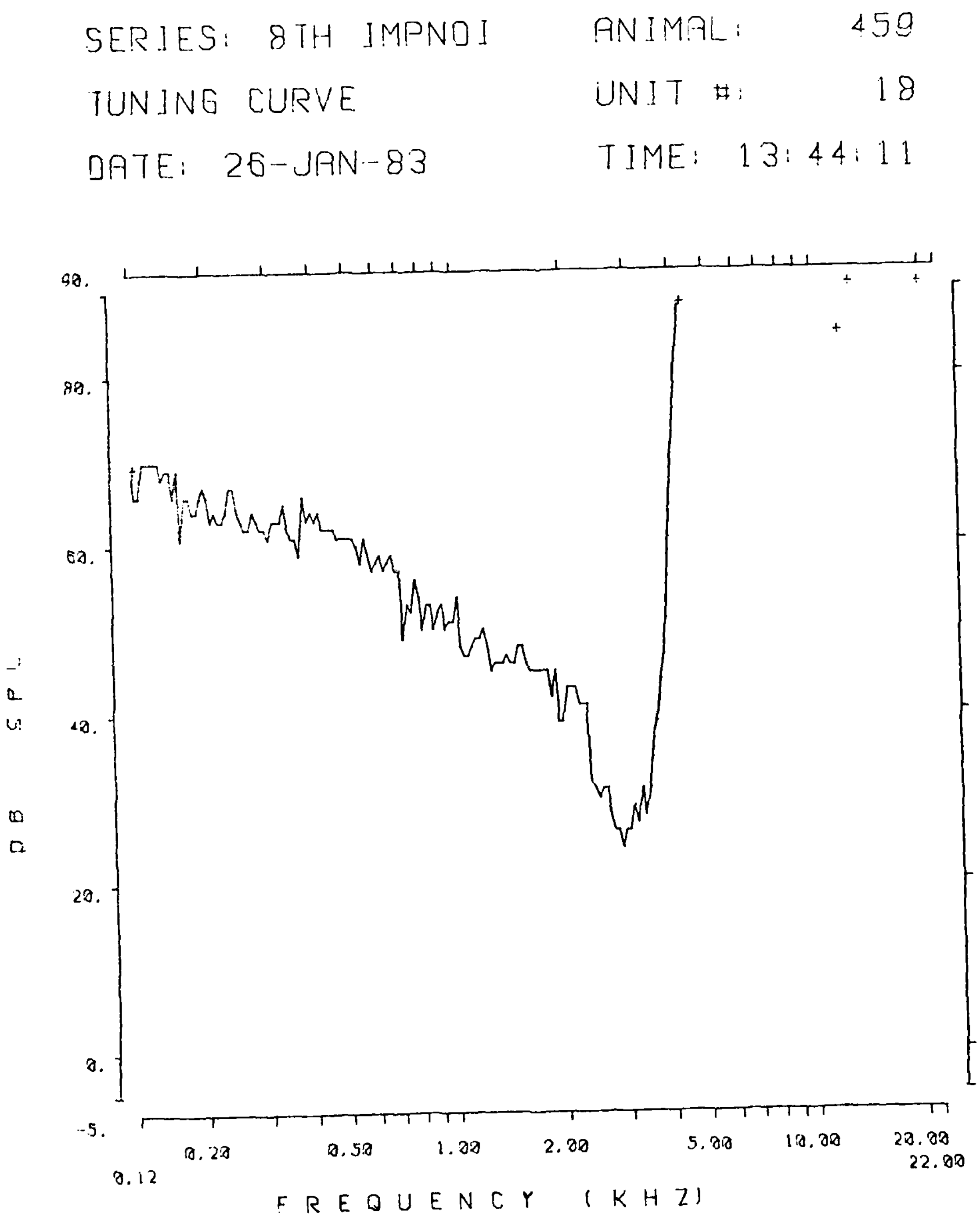


Fig. 3.3.63: Auditory nerve fiber tuning curve from chinchilla 459.

SERIES: 8TH IMPNOI ANIMAL: 459

TUNING CURVE UNIT #: 14

DATE: 26-JAN-83 TIME: 13:17:59

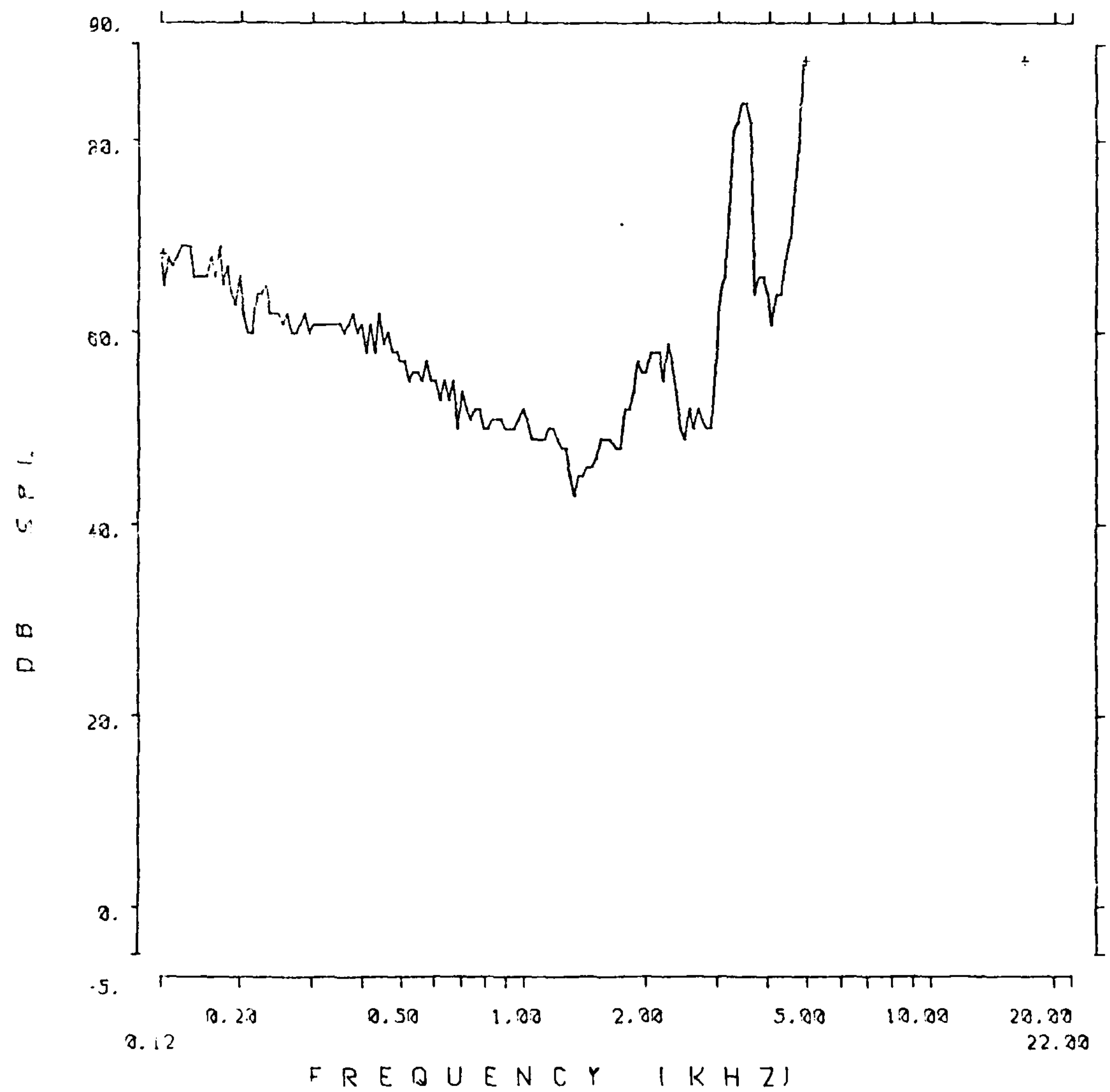


Fig. 3.3.64: Auditory nerve fiber tuning curve from chinchilla 459.

( 510 )

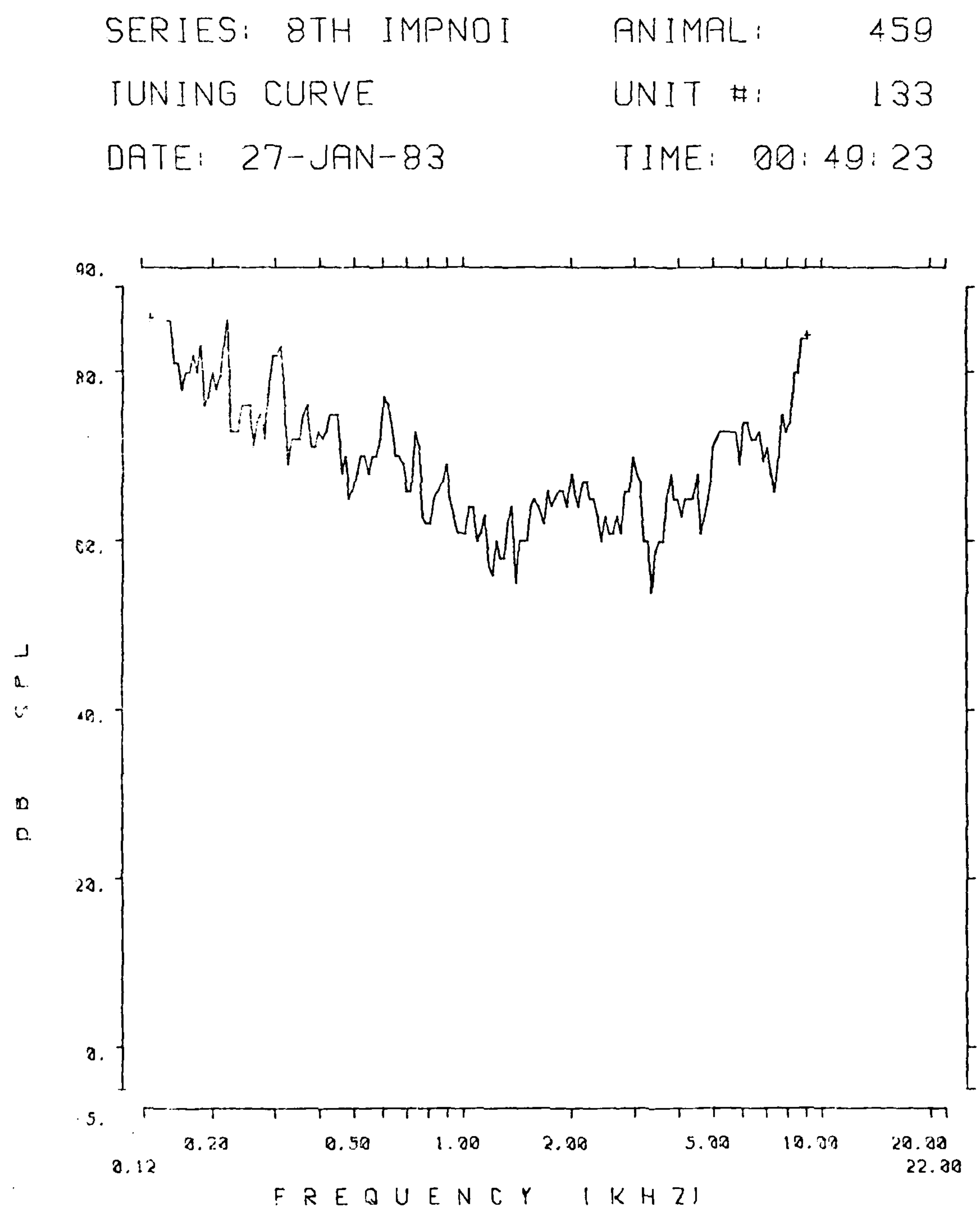


Fig. 3.3.65: Auditory nerve fiber tuning curve from chinchilla 459.

SERIES: 8TH IMPNOI ANIMAL: 459

TUNING CURVE UNIT #: 60

DATE: 26-JAN-83 TIME: 18:02:58

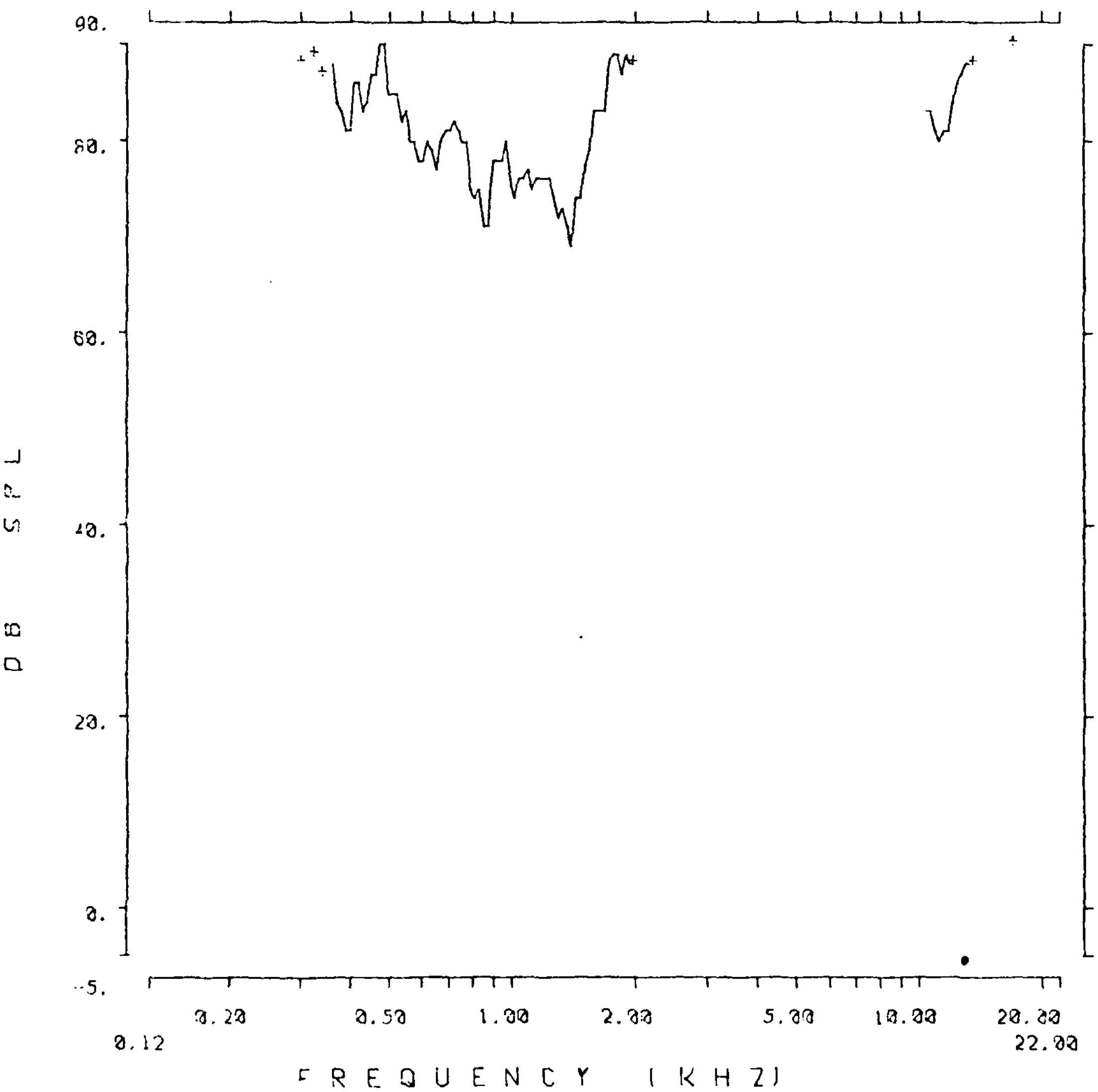


Fig. 3.3.66: Auditory nerve fiber tuning curve from chinchilla 459.

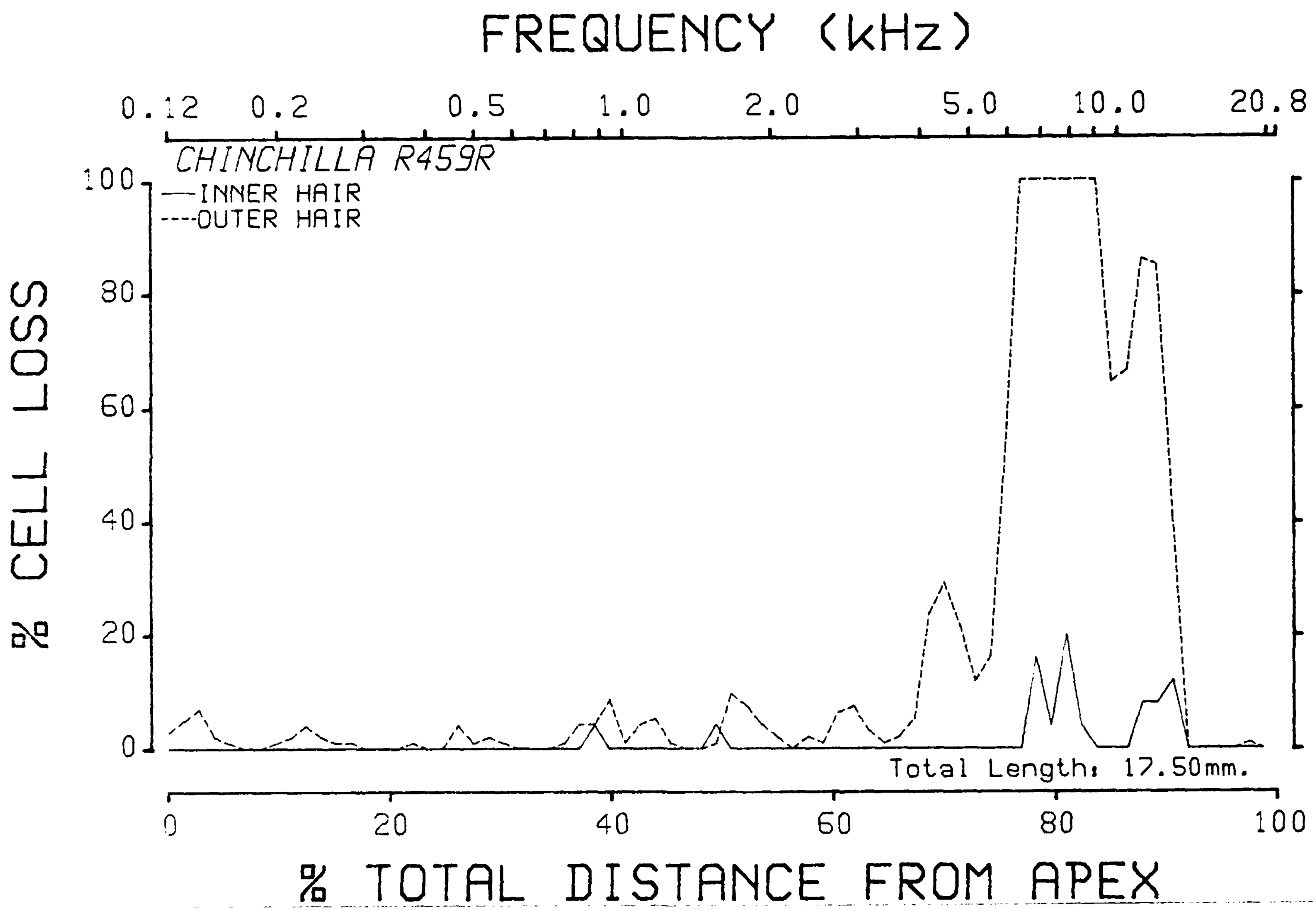


Fig. 3.3.67: Cochleogram from chinchilla 459.

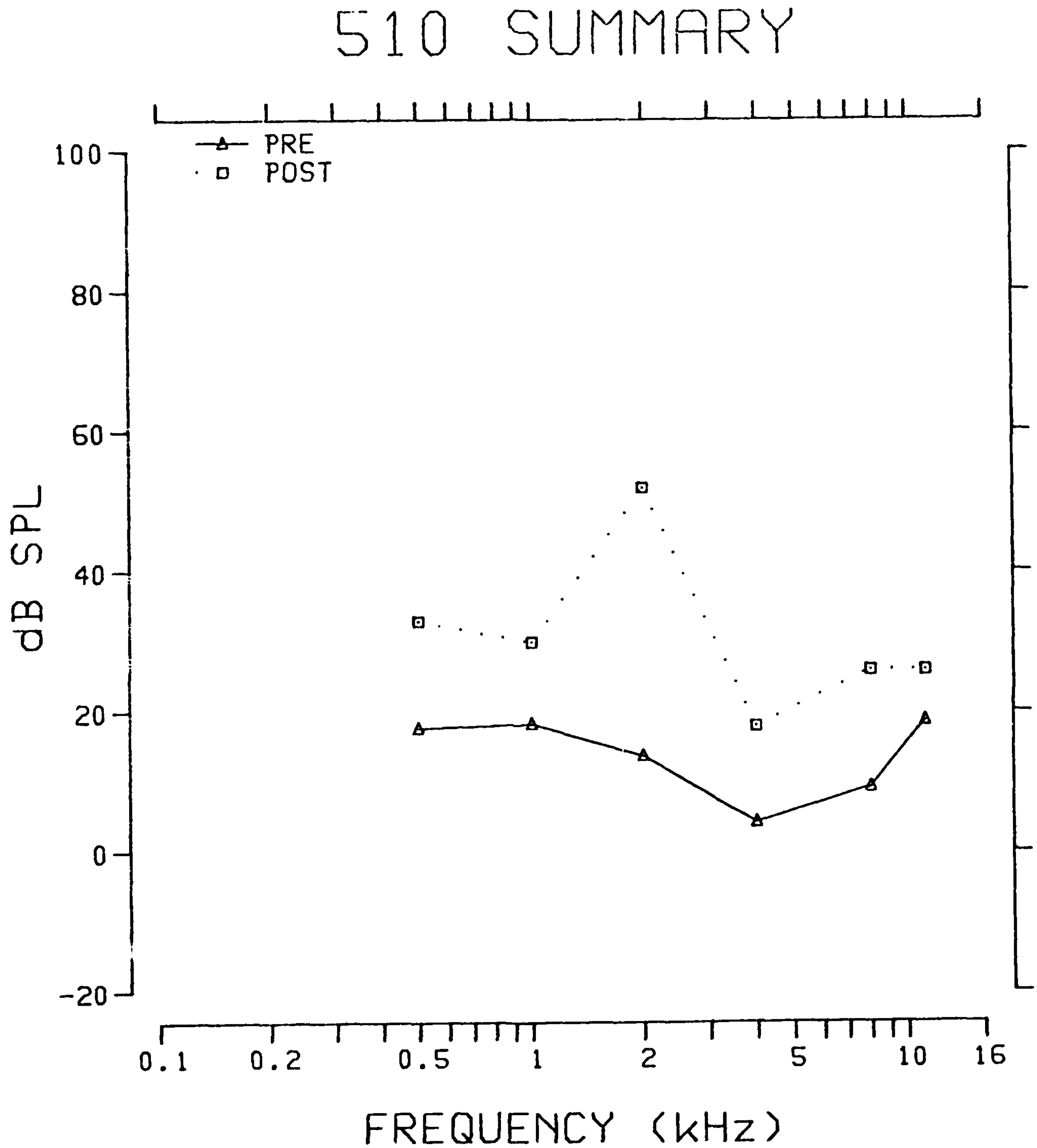


Fig. 3.3.68: Pre- and postexposure evoked response audiograms from chinchilla 510.

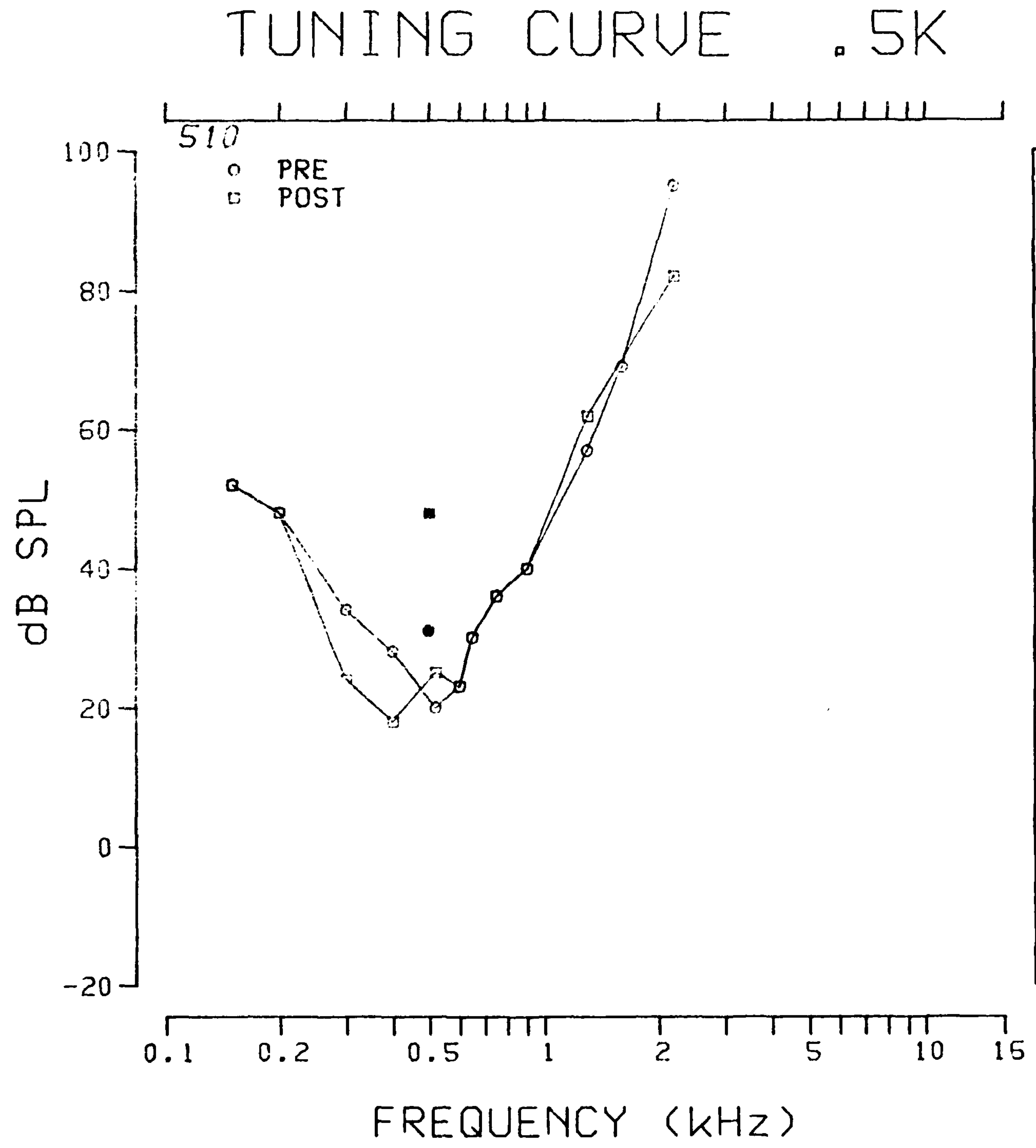


Fig. 3.3.69: Pre- and postexposure evoked response tuning curves at 0.5 kHz from chinchilla 510.

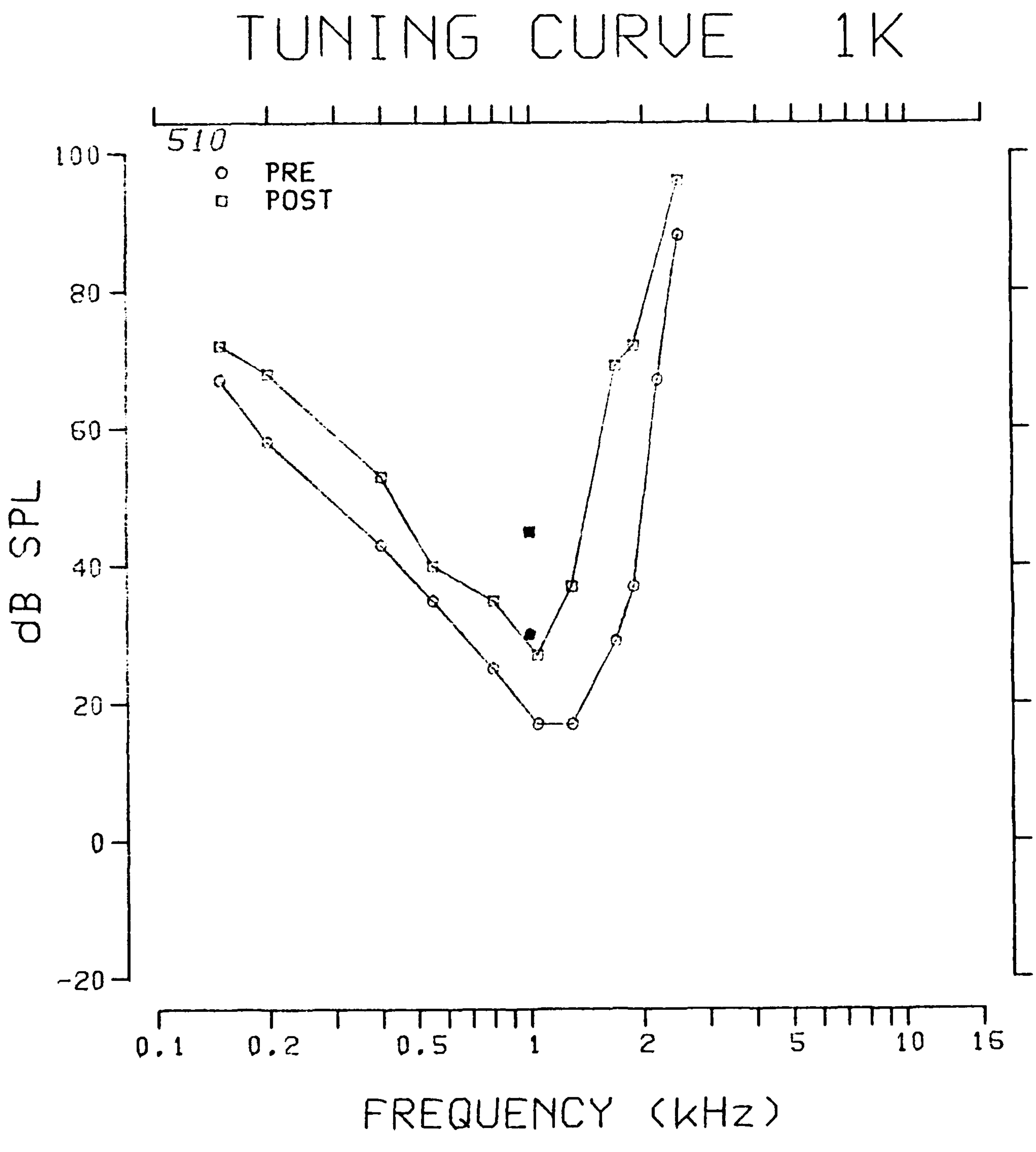


Fig. 3.3.70: Pre- and postexposure evoked response tuning curves at 1.0 kHz from chinchilla 510.

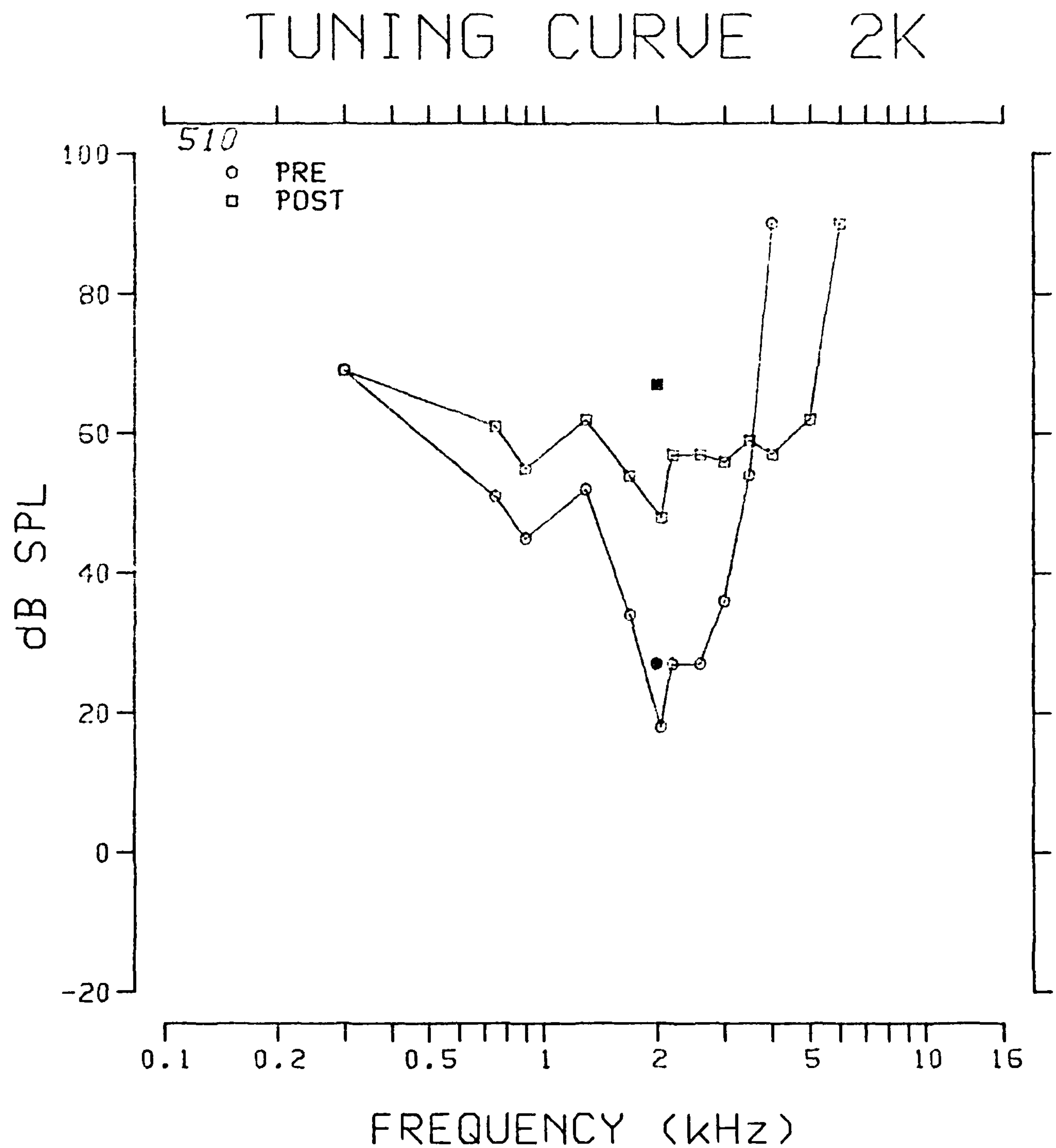


Fig. 3.3.71: Pre- and postexposure evoked response tuning curves at 2.0 kHz from chinchilla 510.

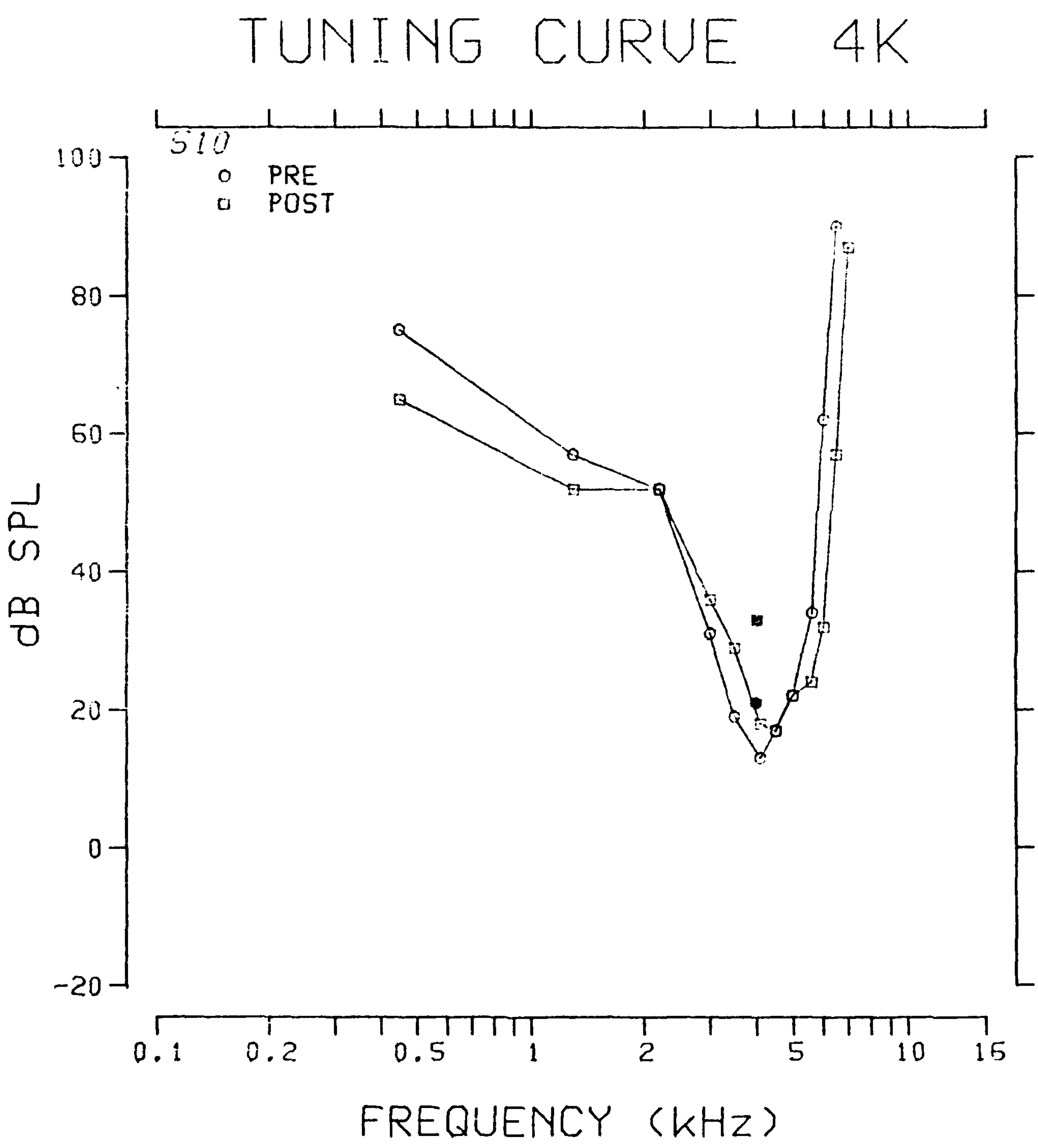


Fig. 3.3.72: Pre- and postexposure evoked response tuning curves at 4.0 kHz from chinchilla 510.

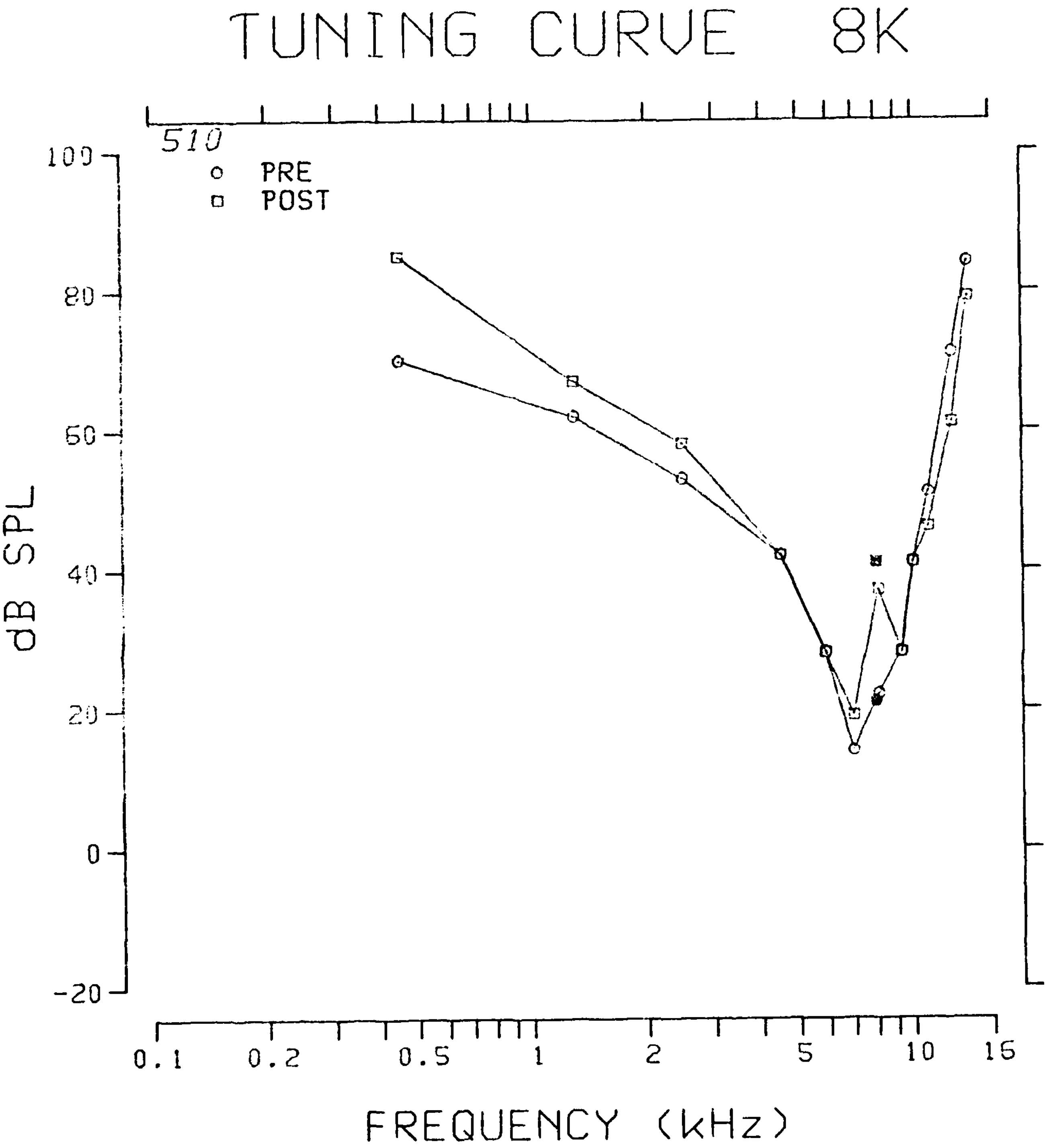


Fig. 3.3.73: Pre- and postexposure evoked response tuning curves at 8.0 kHz from chinchilla 510

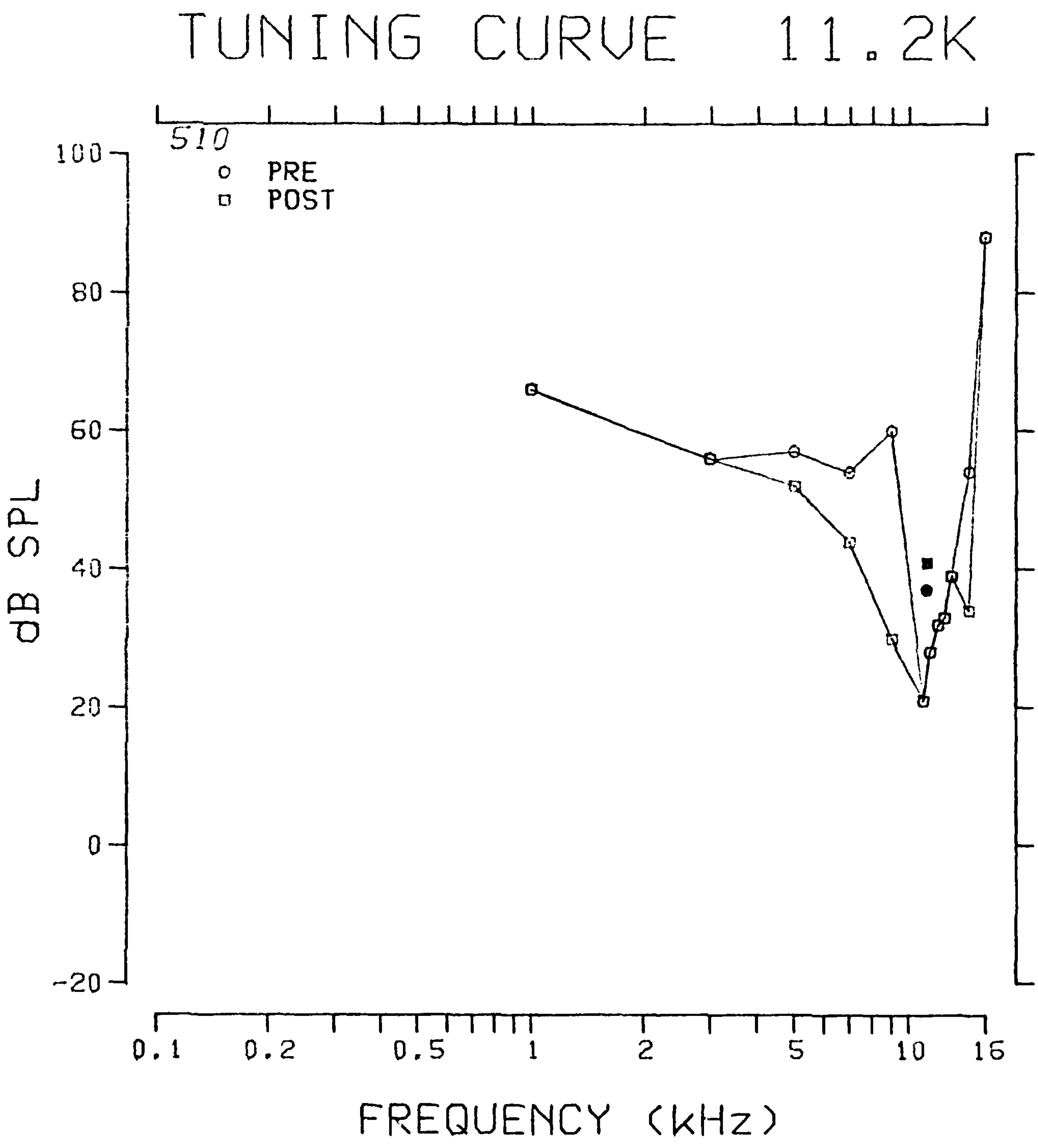


Fig. 3.3.74: Pre- and postexposure evoked response tuning curves at 11.2 kHz from chinchilla 510.

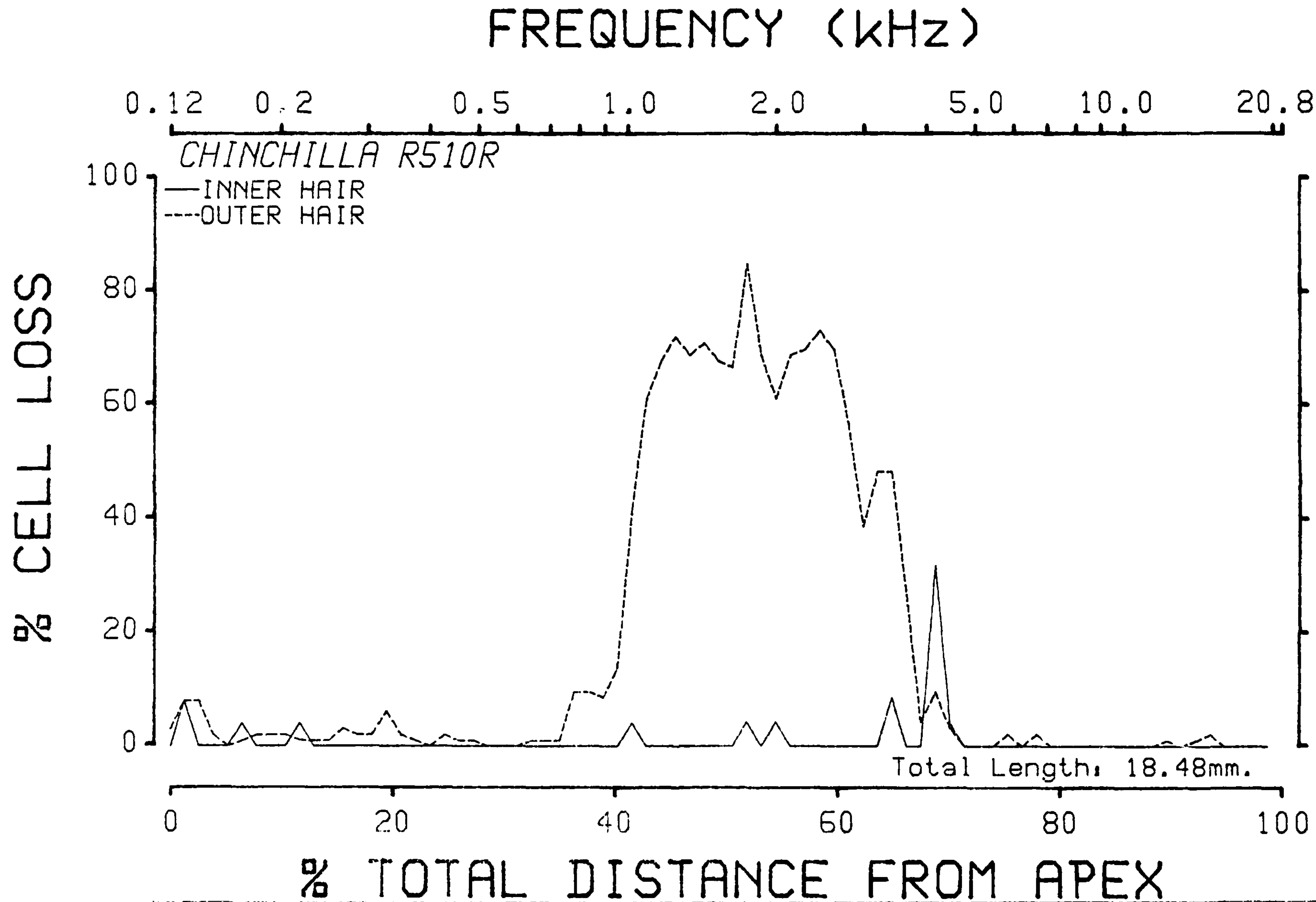


Fig. 3.3.75: Cochleogram from chinchilla 510.

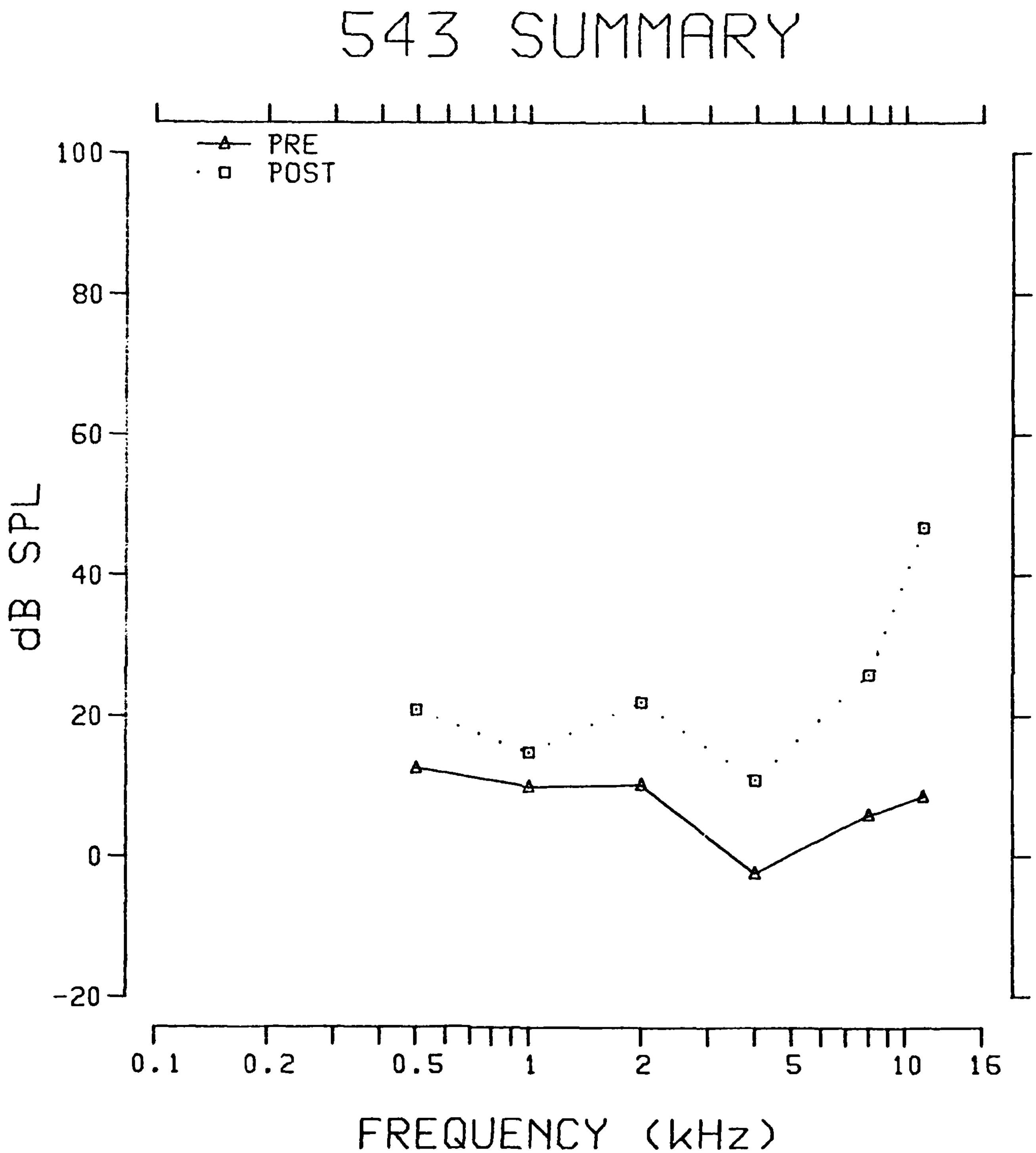


Fig. 3.3.76: Pre- and postexposure evoked response audiograms from chinchilla 543.

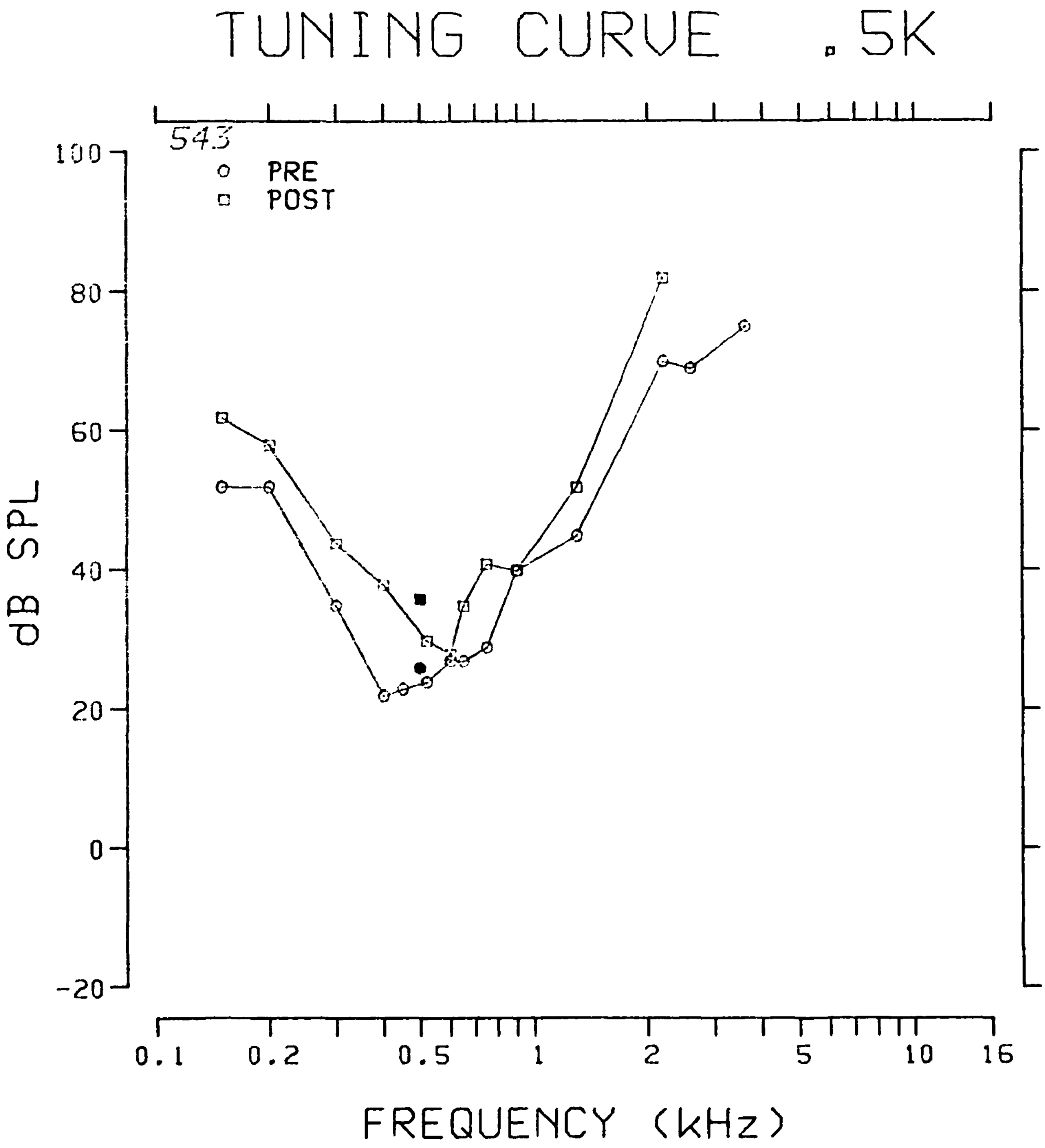


Fig. 3.3.77: Pre- and postexposure evoked response tuning curves at 0.5 kHz from chinchilla 543.

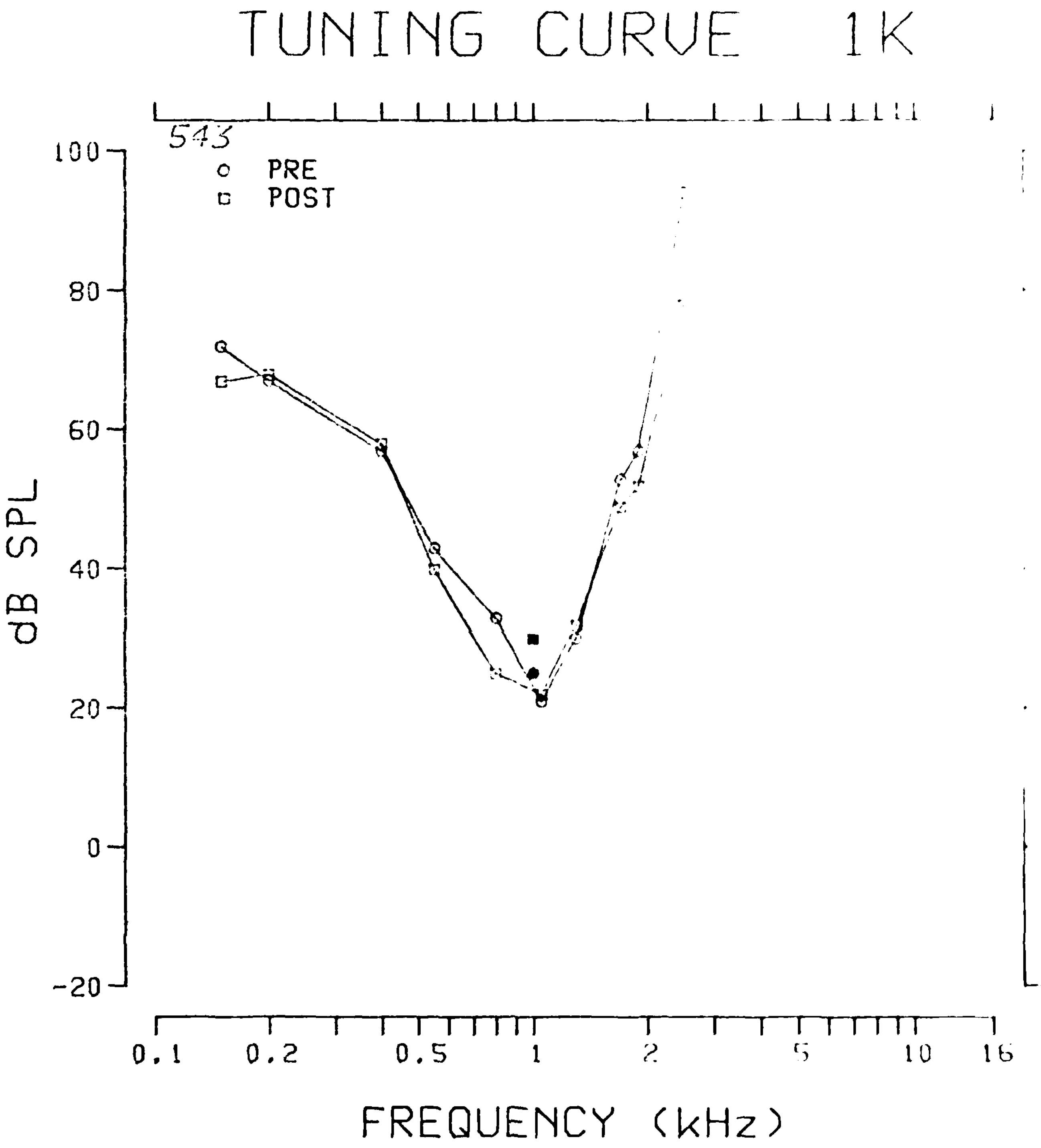


Fig. 3.3.78: Pre- and postexposure evoked response tuning curves at 1.0 kHz from chinchilla 543.

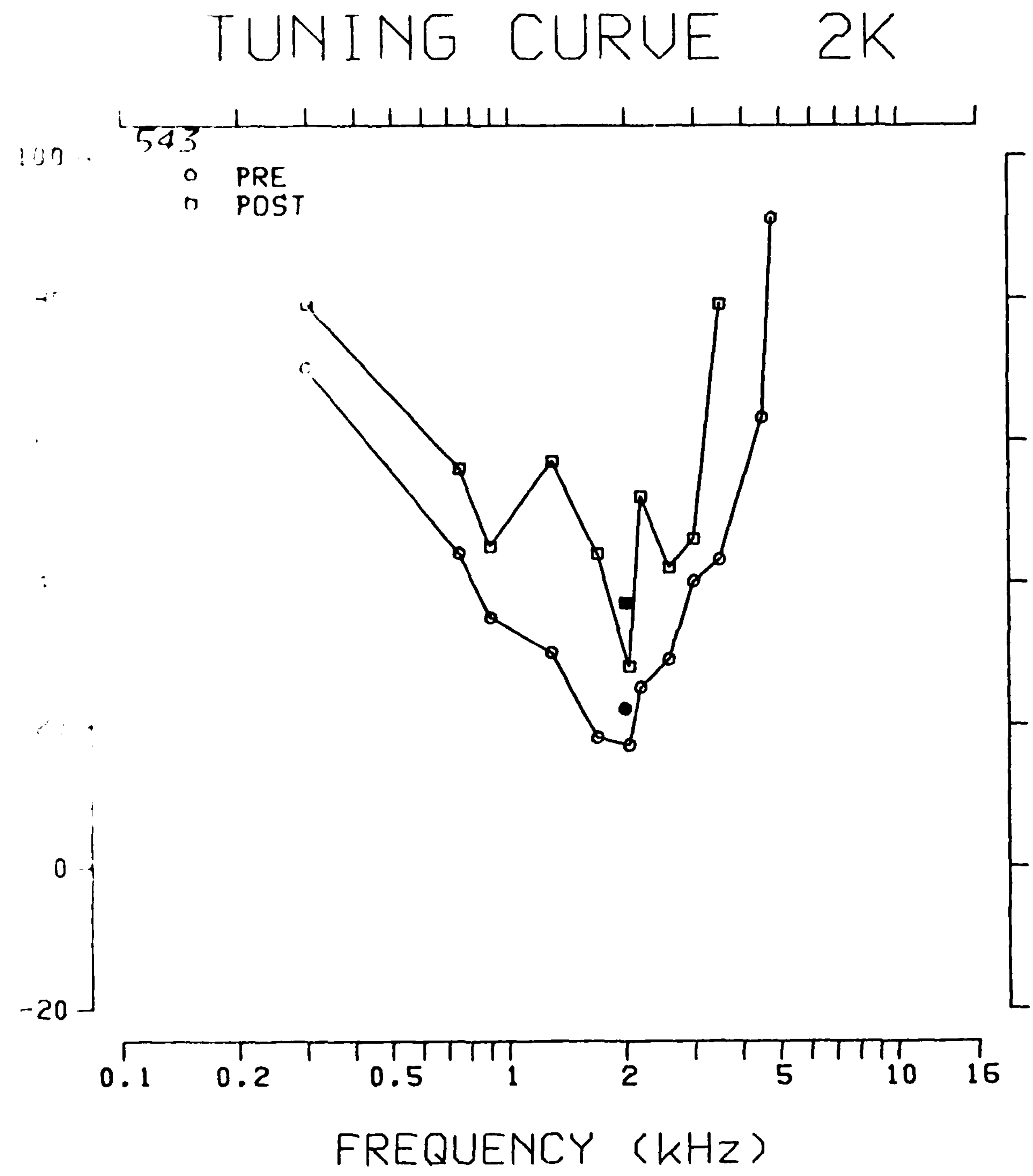


Fig. 3.3.79: Pre- and postexpousre evoked response tuning curves at 2.0 kHz from chinchilla 543.

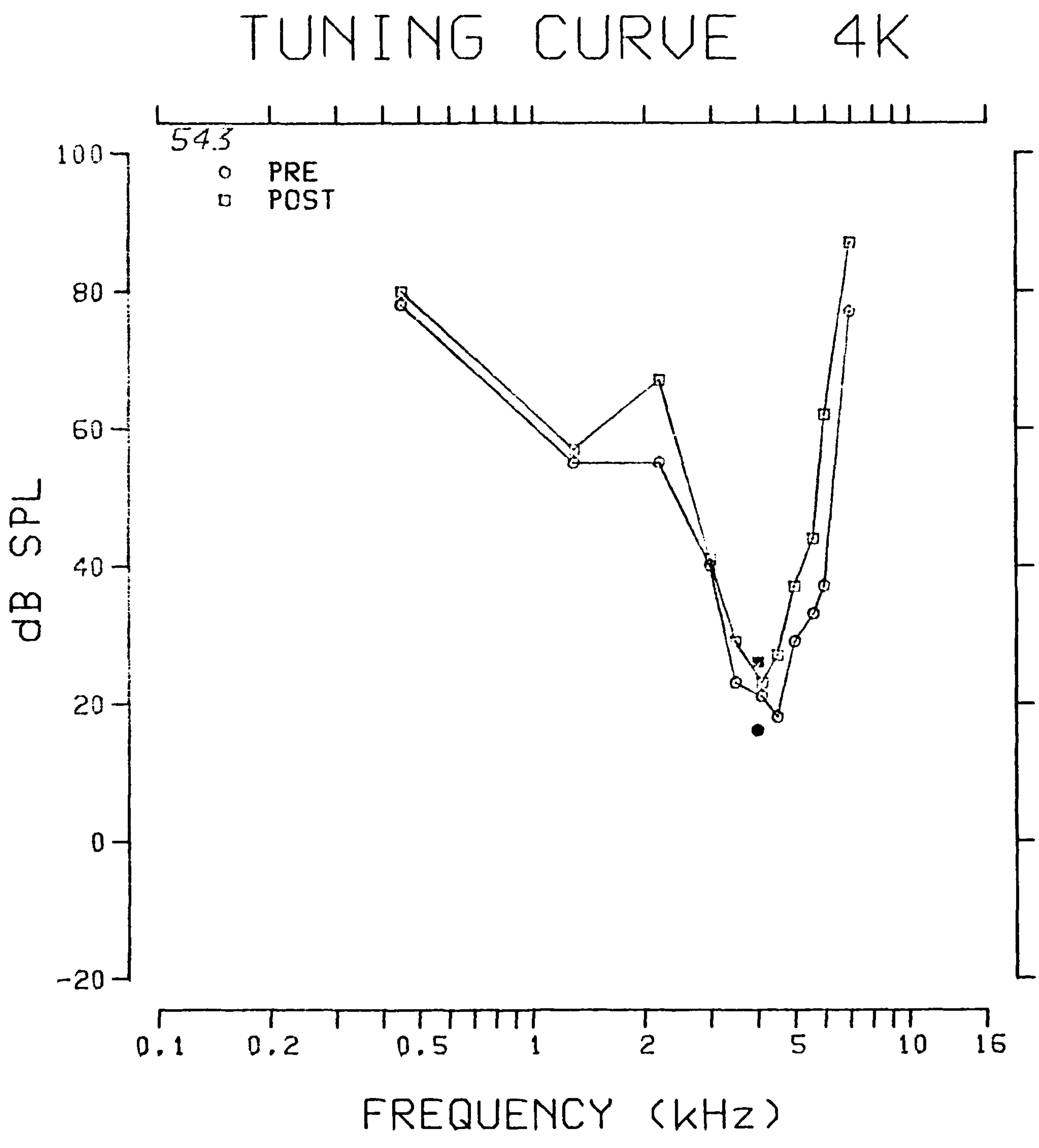


Fig. 3.3.80: Pre- and postexposure evoked response tuning curves at 4.0 kHz from chinchilla 543.

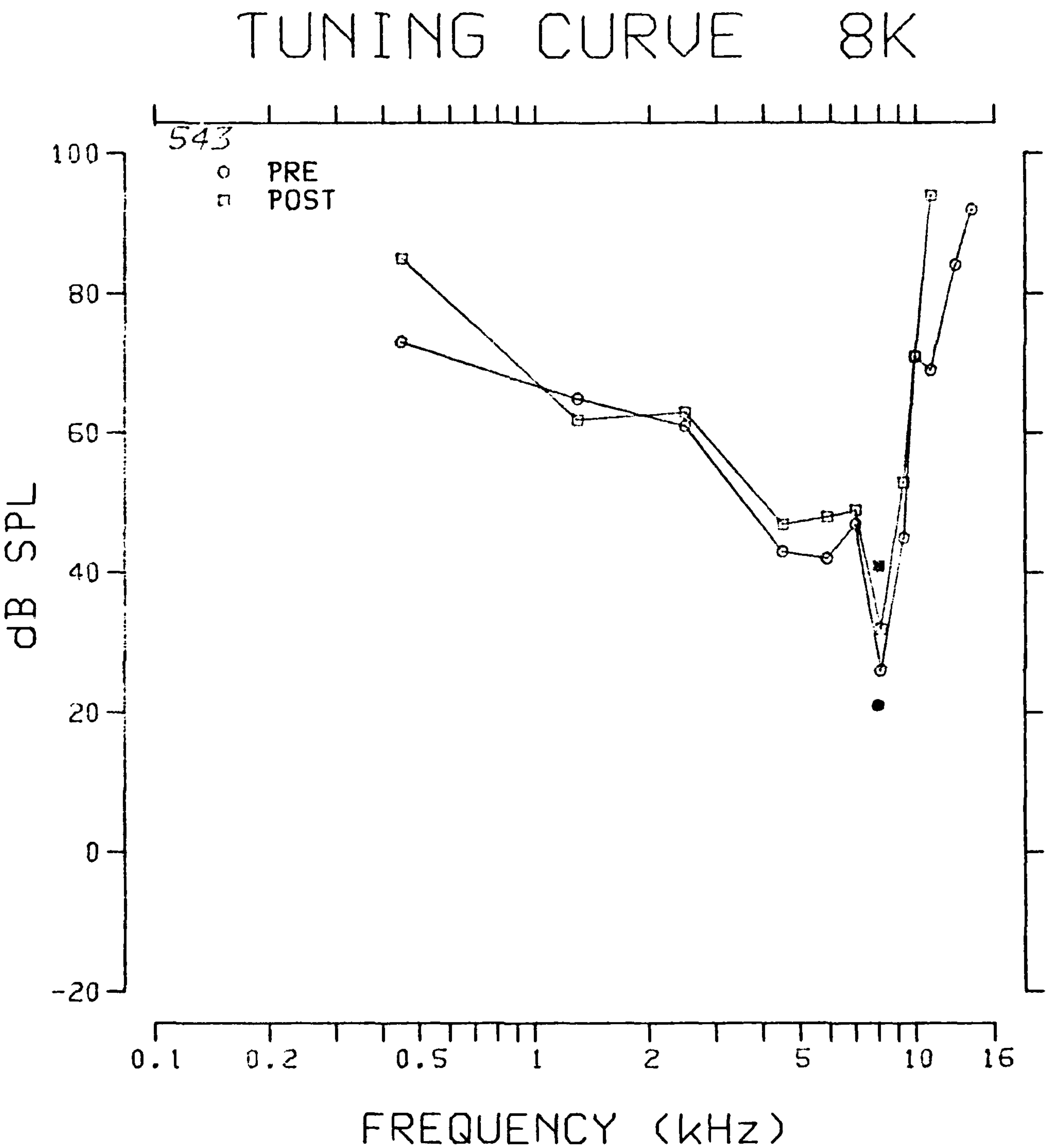


Fig. 3.3.81: Pre- and postexposure evoked response tuning curves at 8.0 kHz from chinchilla 543.

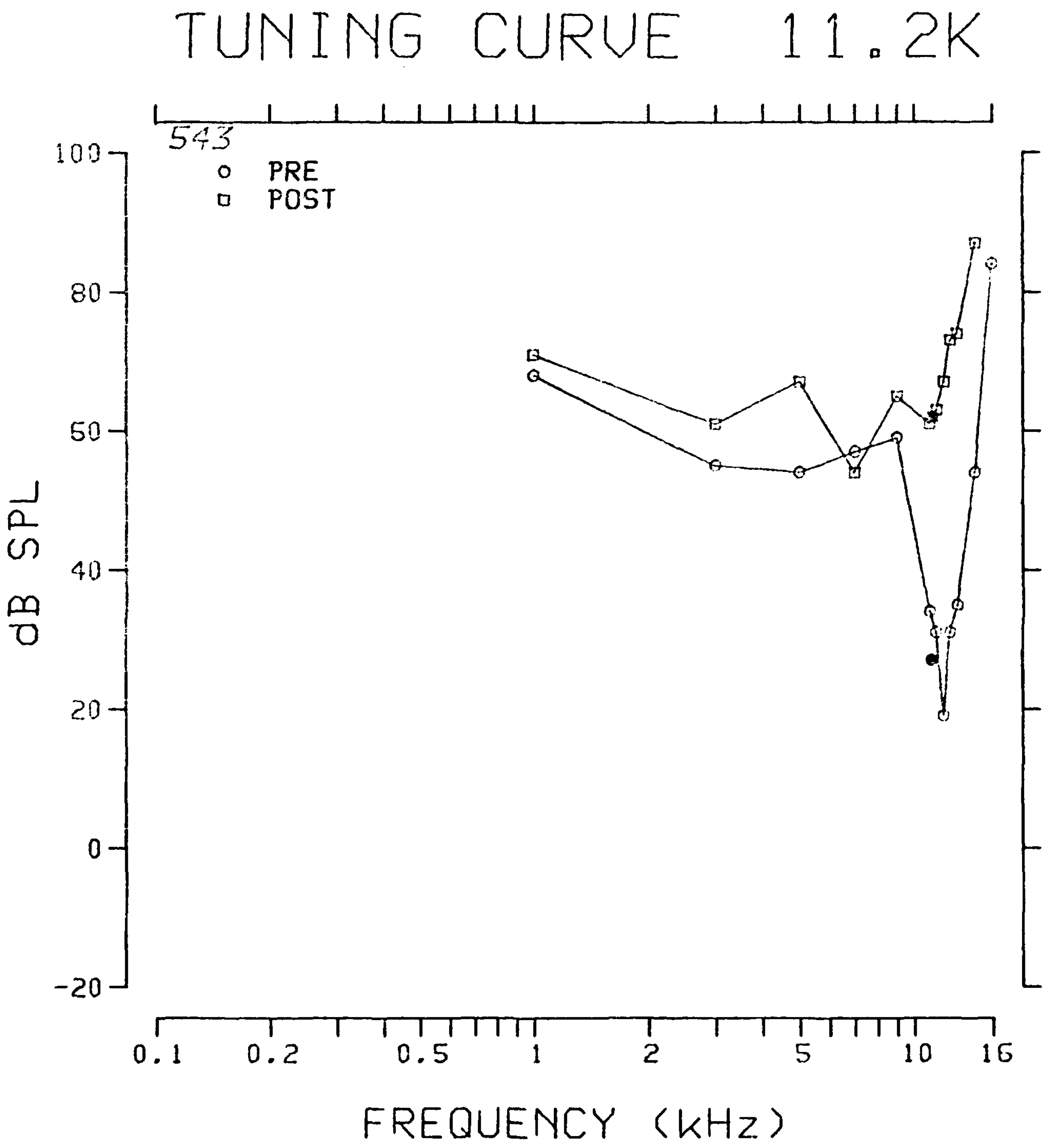


Fig. 3.3.82: Pre- and postexposure evoked response tuning curves at 11.2 kHz from chinchilla 543.

SERIES: 8TH-IMPULS ANIMAL: 543

TUNING CURVE UNIT #: 3

DATE: 31-JAN-83 TIME: 12:12:09

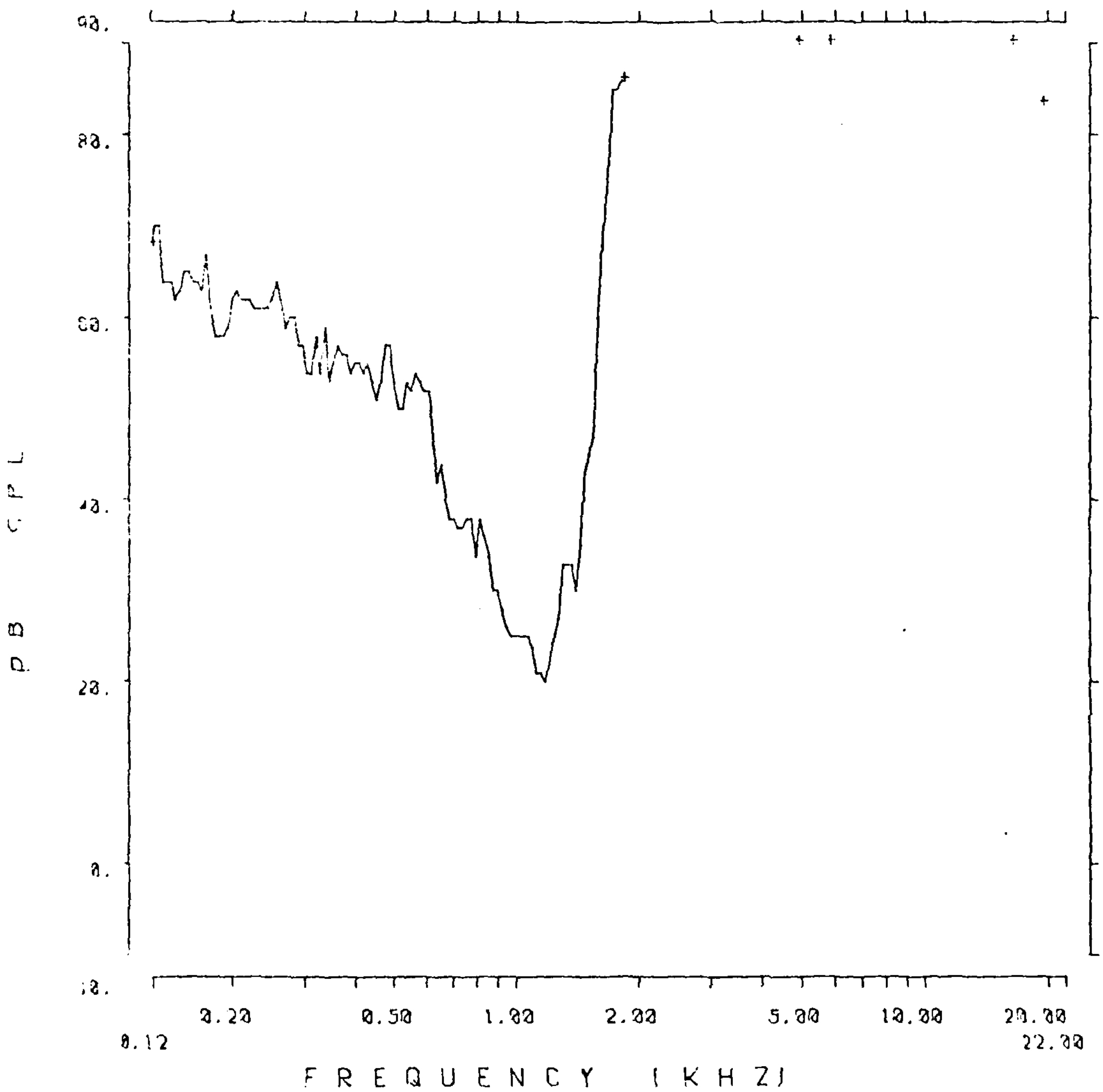


Fig. 3.3.83: Auditory nerve fiber tuning curve from chinchilla 543.

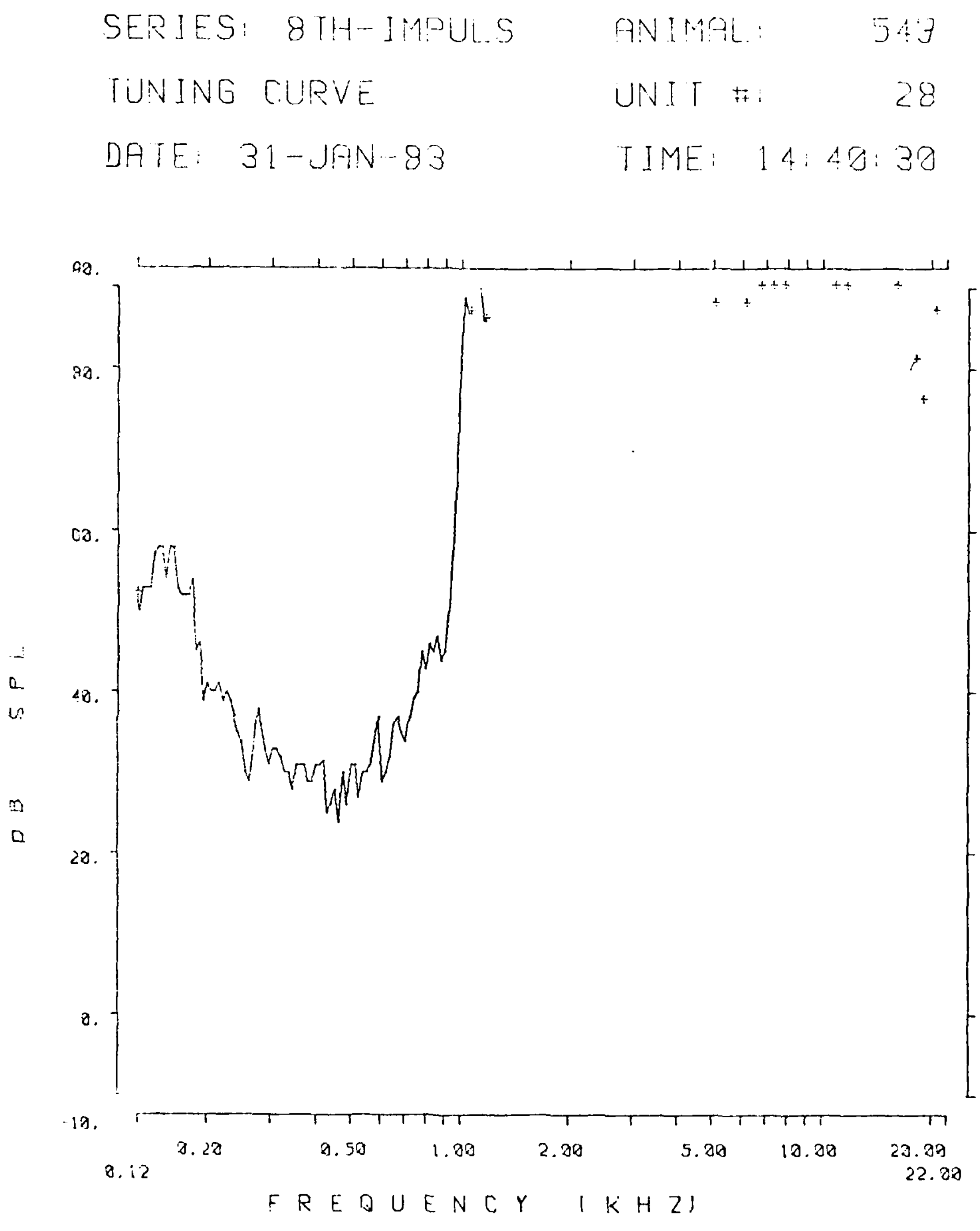


Fig. 3.3.84: Auditory nerve fiber tuning curve from chinchilla 543.

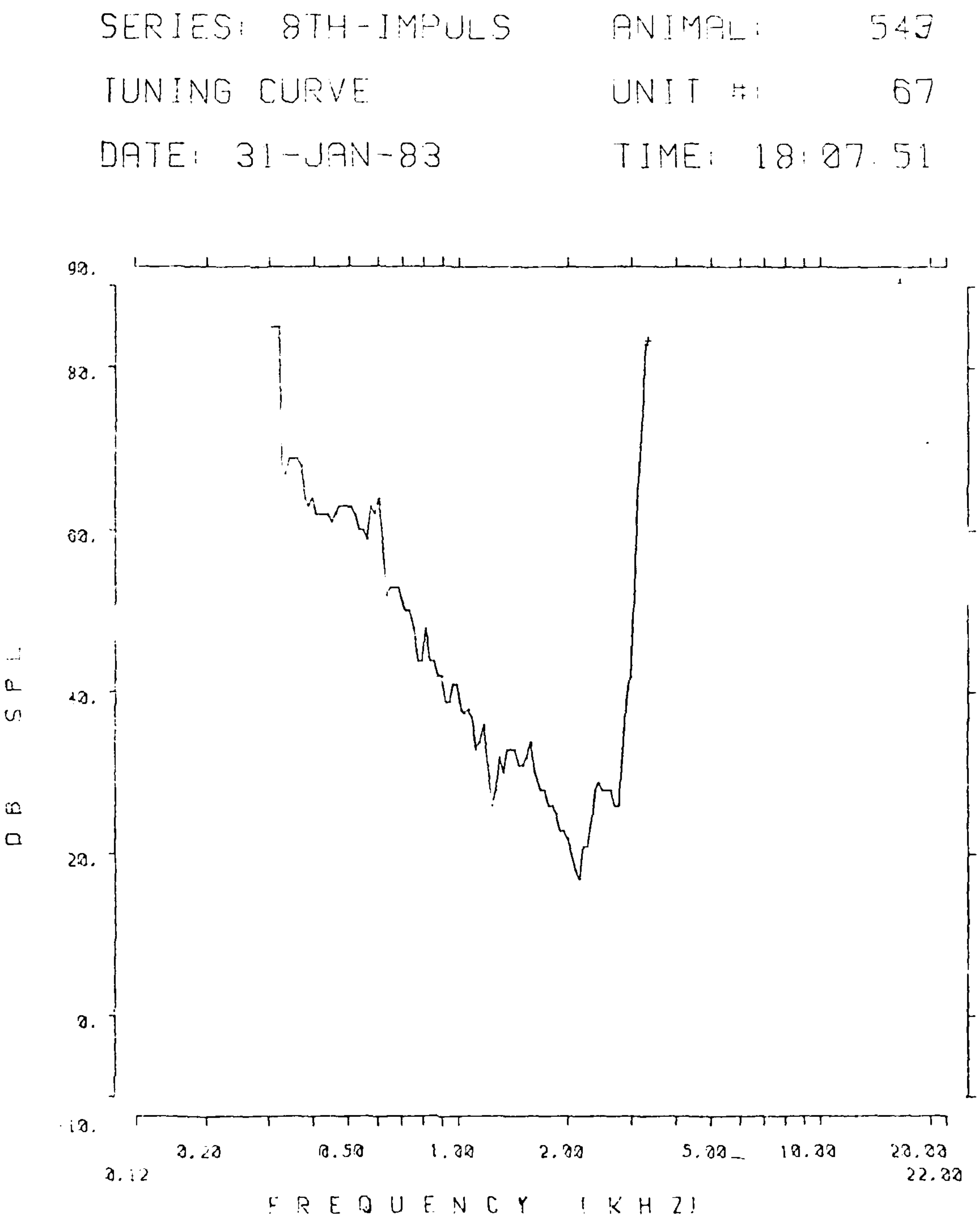


Fig. 3.3.85: Auditory nerve fiber tuning curve from chinchilla 543.

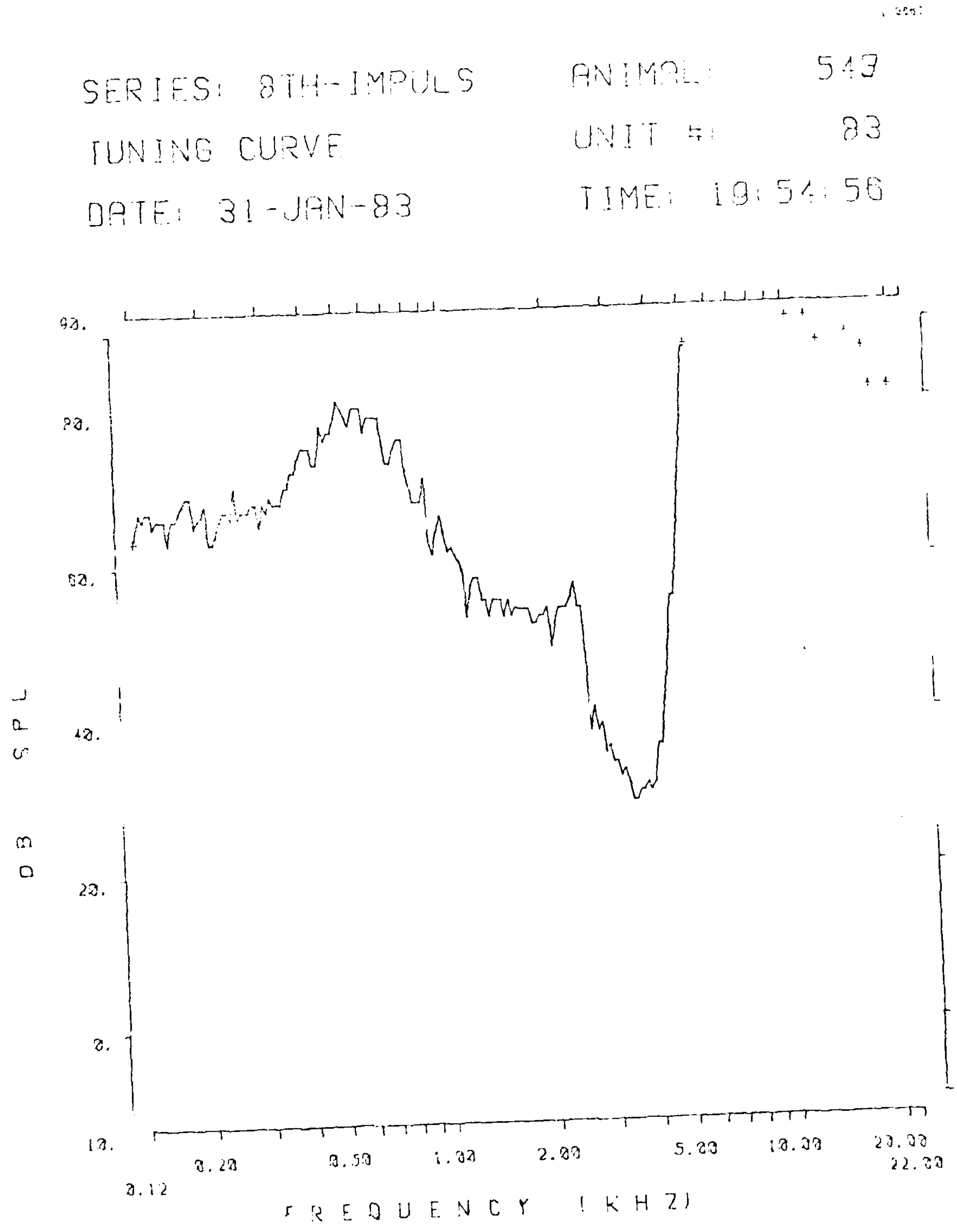


Fig. 3.3.86: Auditory nerve fiber tuning curve from chinchilla 543.

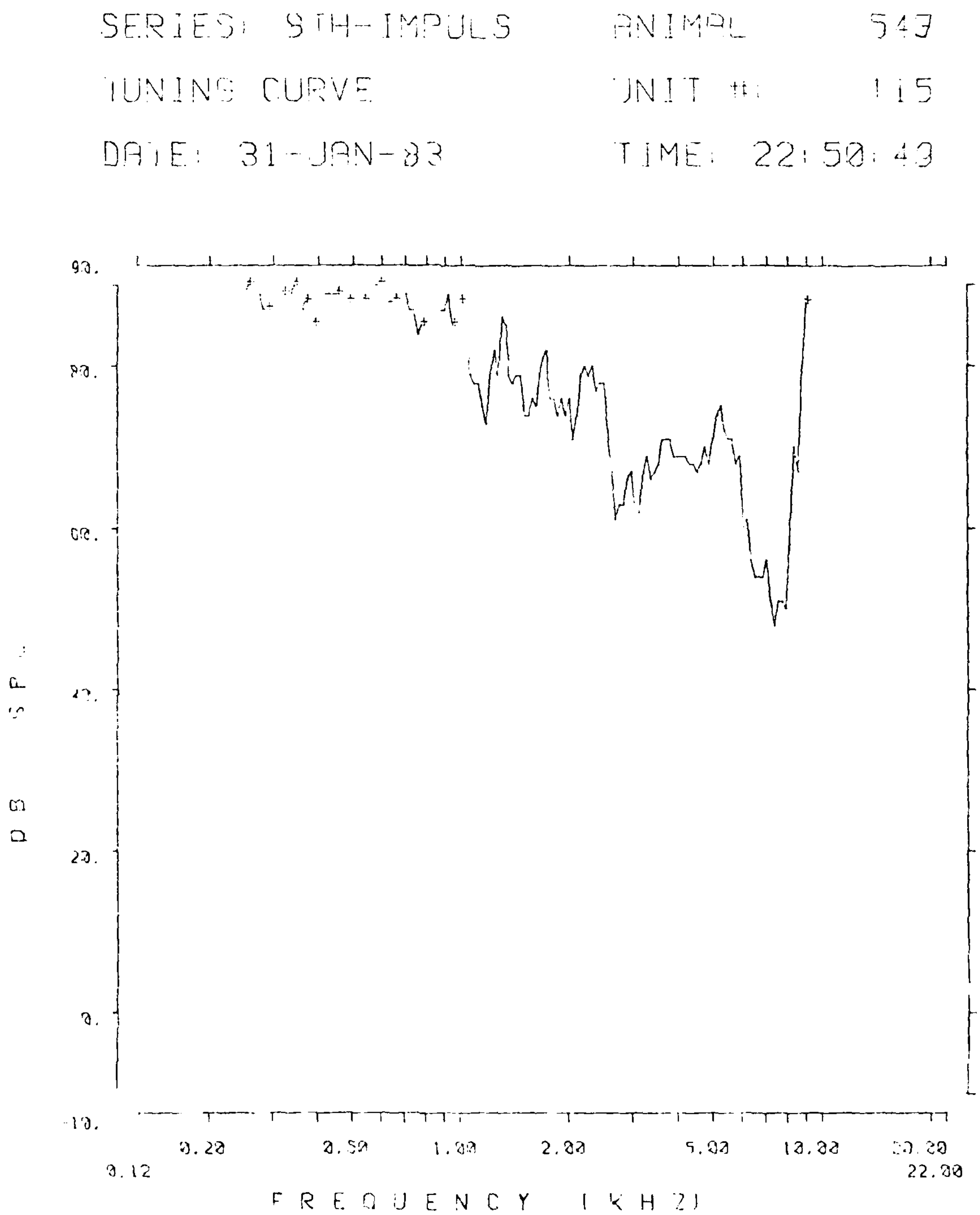


Fig. 3.3.87: Auditory nerve fiber tuning curve from chinchilla 543.

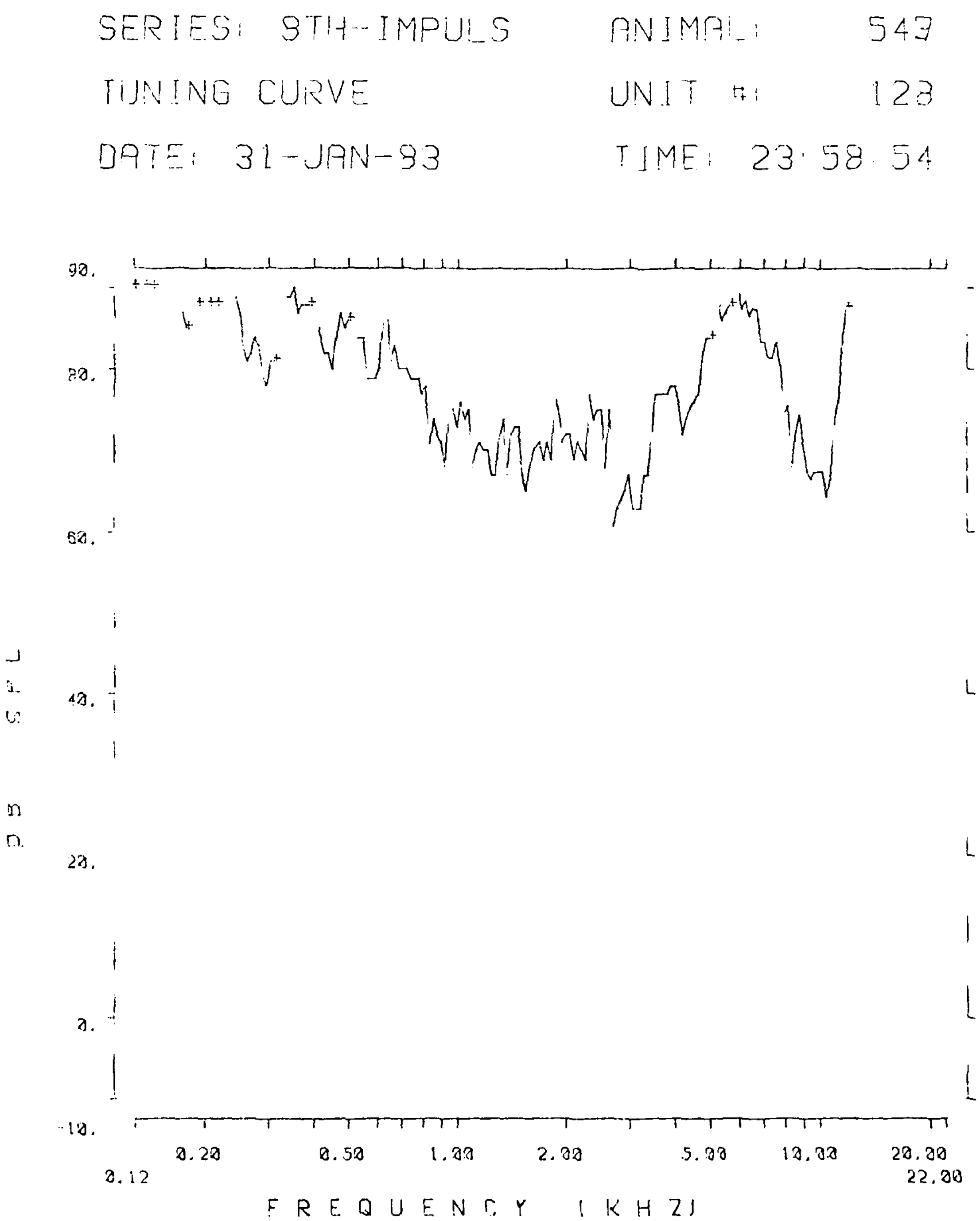


Fig. 3.3.88: Auditory nerve fiber tuning curve from chinchilla 543.

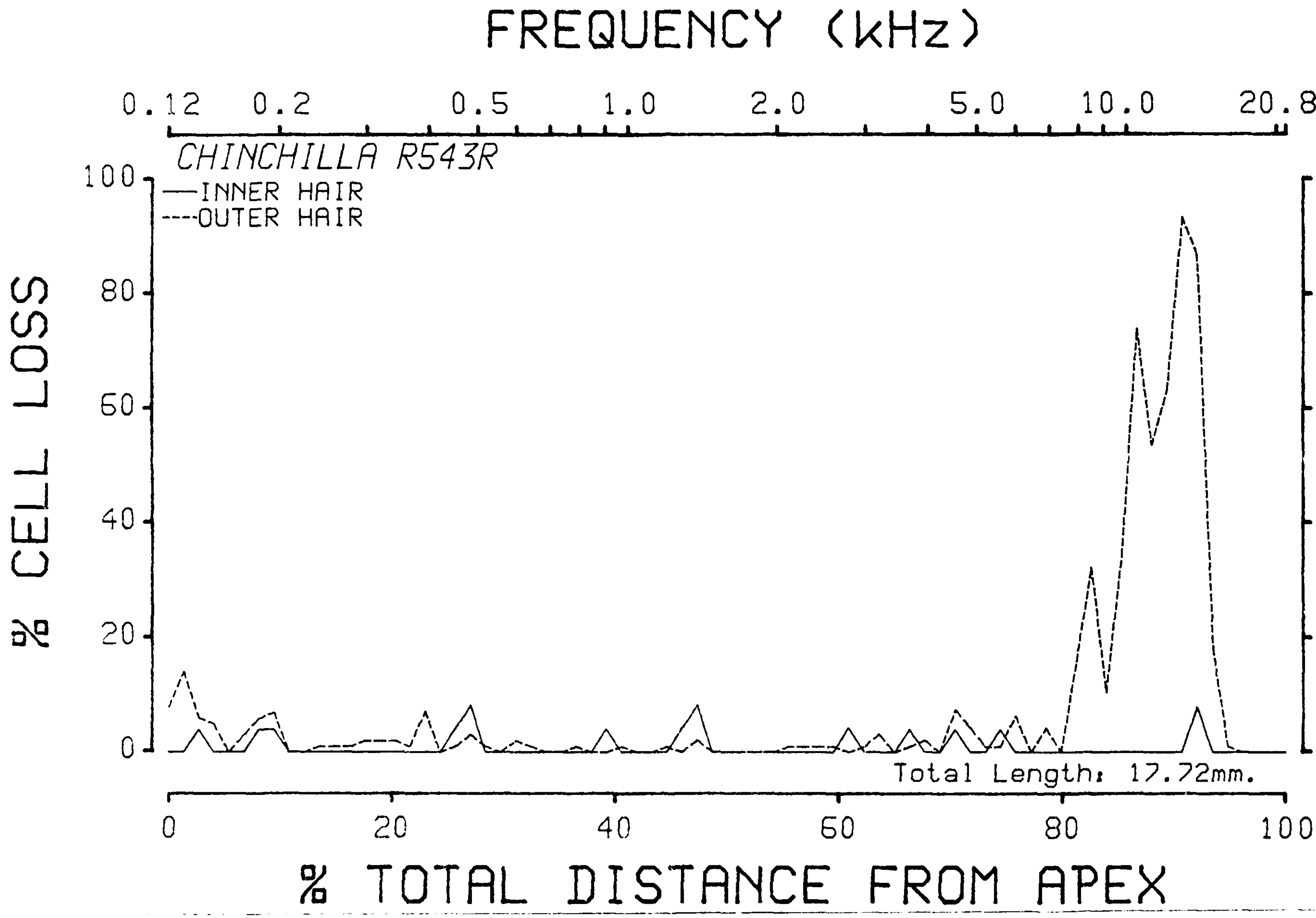


Fig. 3.3.89: Cochleogram from chinchilla 543.

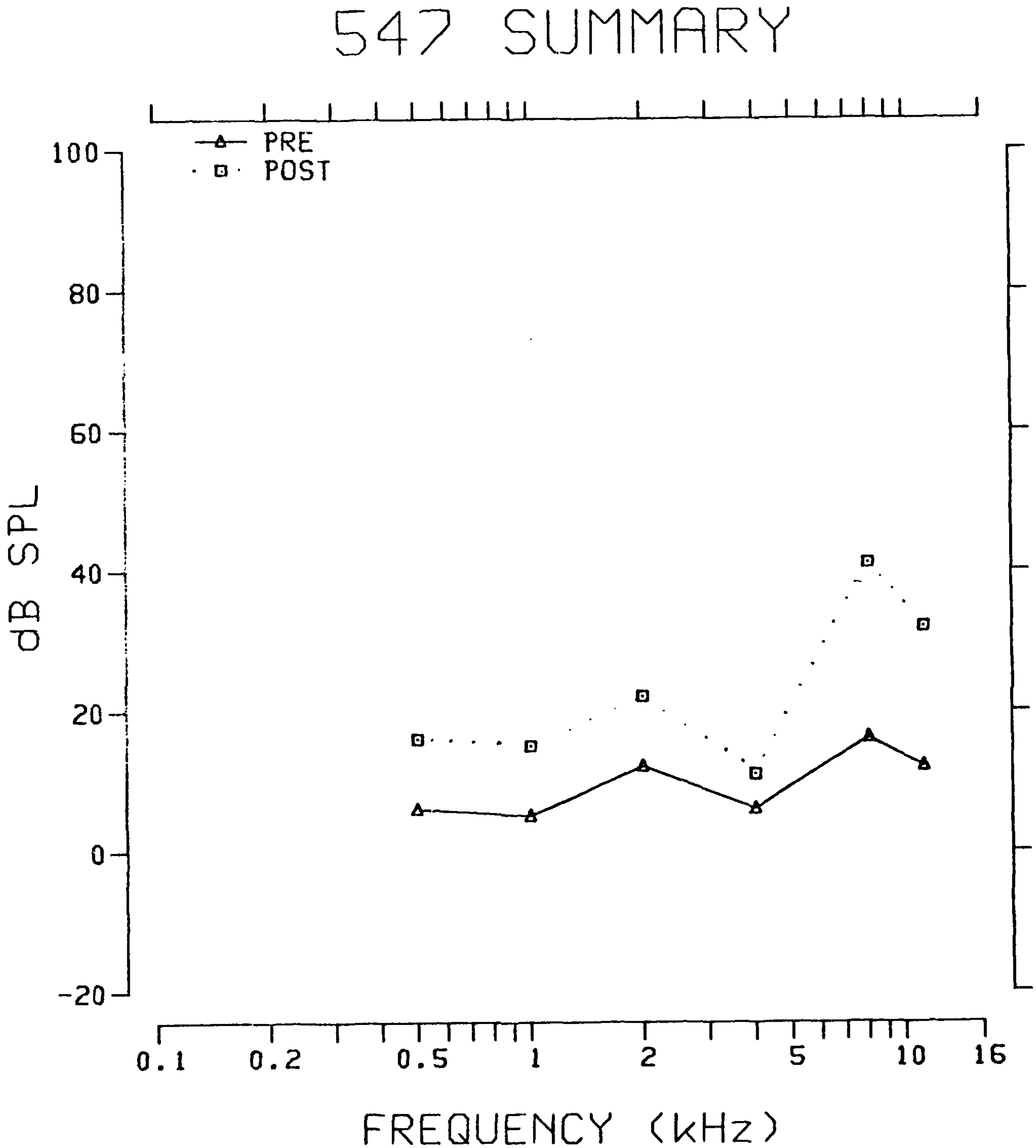


Fig. 3.3.90: Pre- and postexposure evoked response audiograms from chinchilla 547.

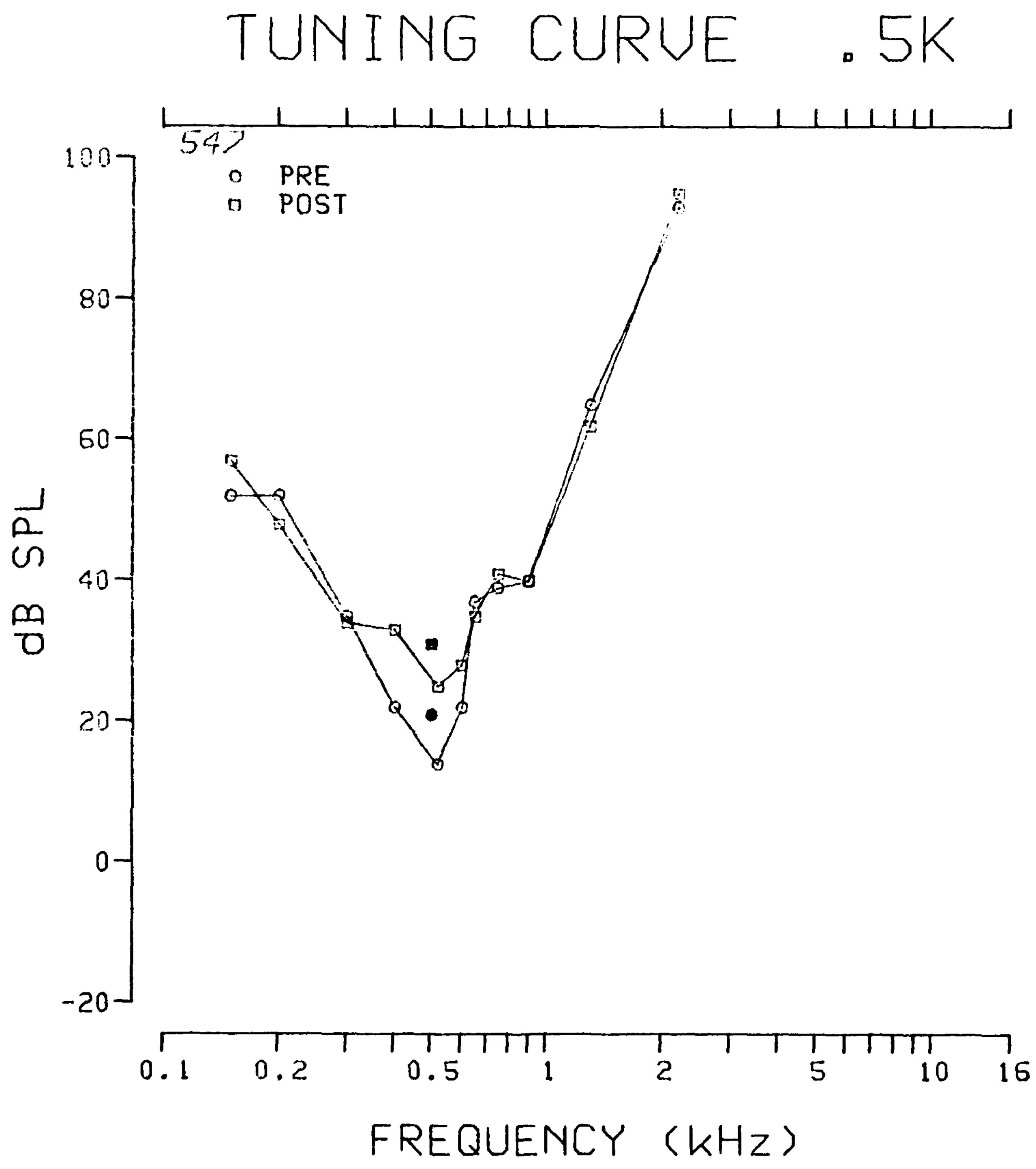


Fig. 3.3.91: Pre- and postexposure evoked response tuning curves at 0.5 kHz from chinchilla 547.

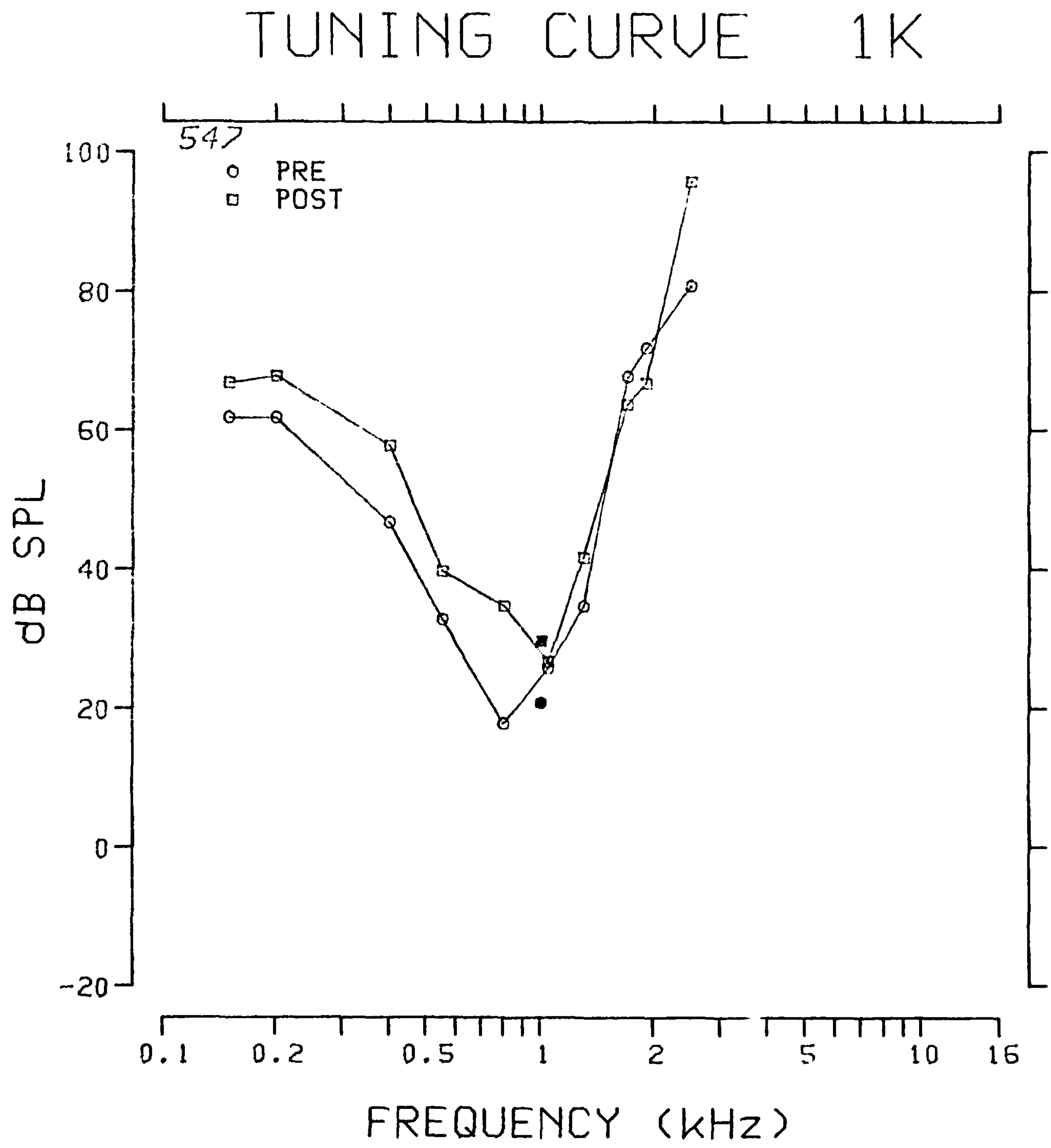


Fig. 3.3.92: Pre- and postexposure evoked response tuning curves at 1.0 kHz from chinchilla 547.

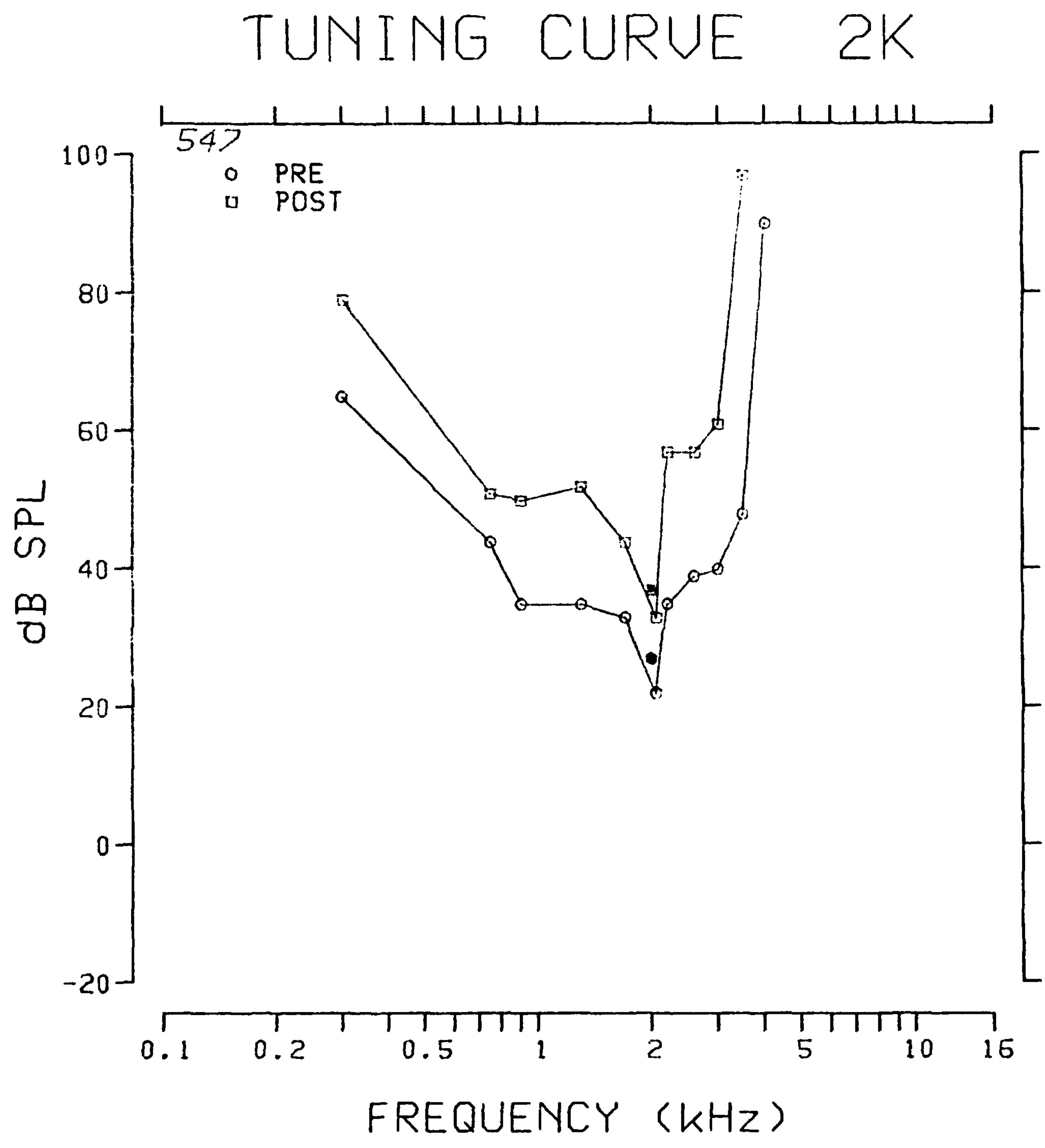


Fig. 3.3.93: Pre- and postexposure evoked response tuning curves at 2.0 kHz from chinchilla 547.

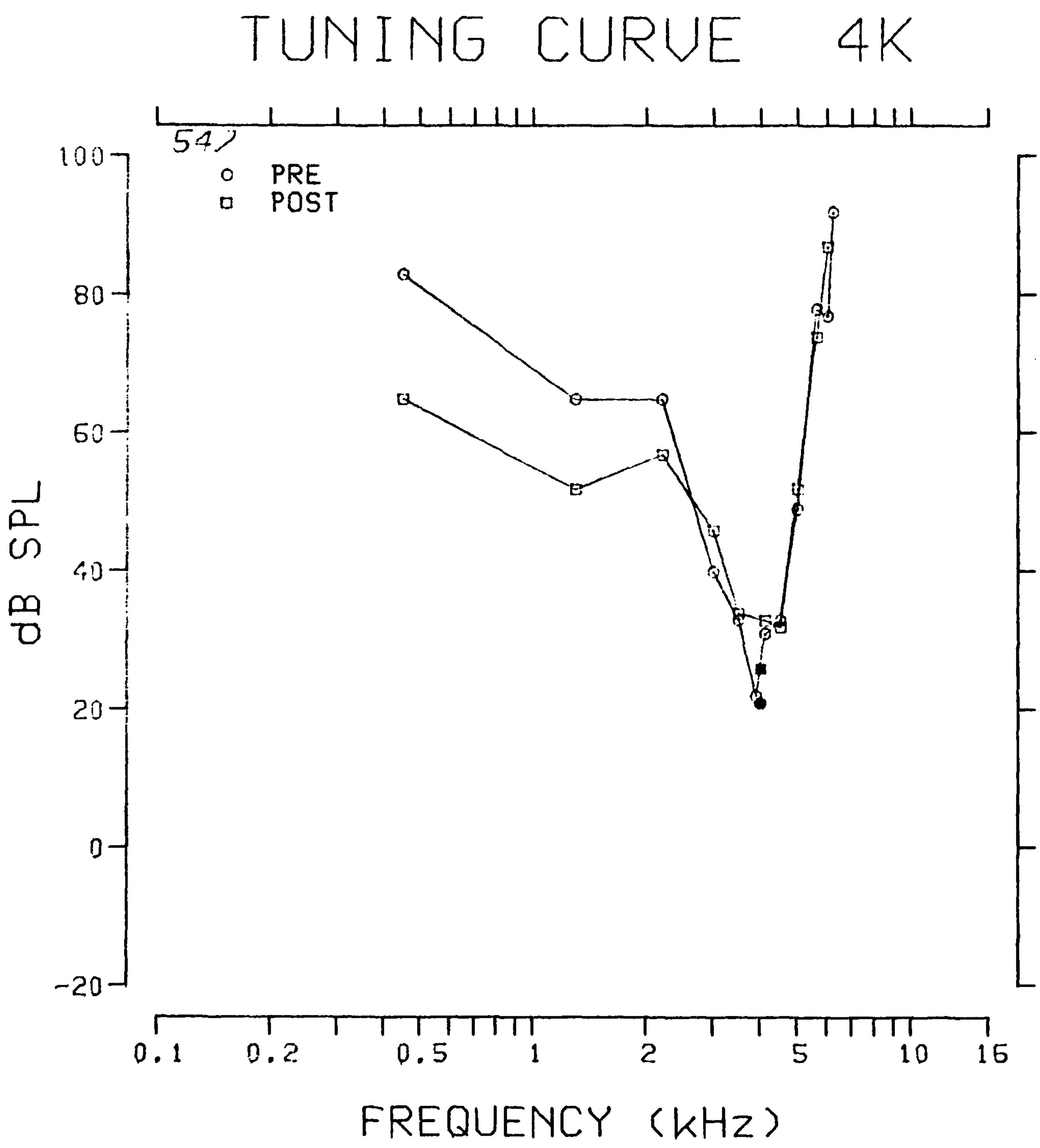


Fig. 3.3.94: Pre- and postexposure evoked response tuning curves at 4.0 kHz from chinchilla 547.

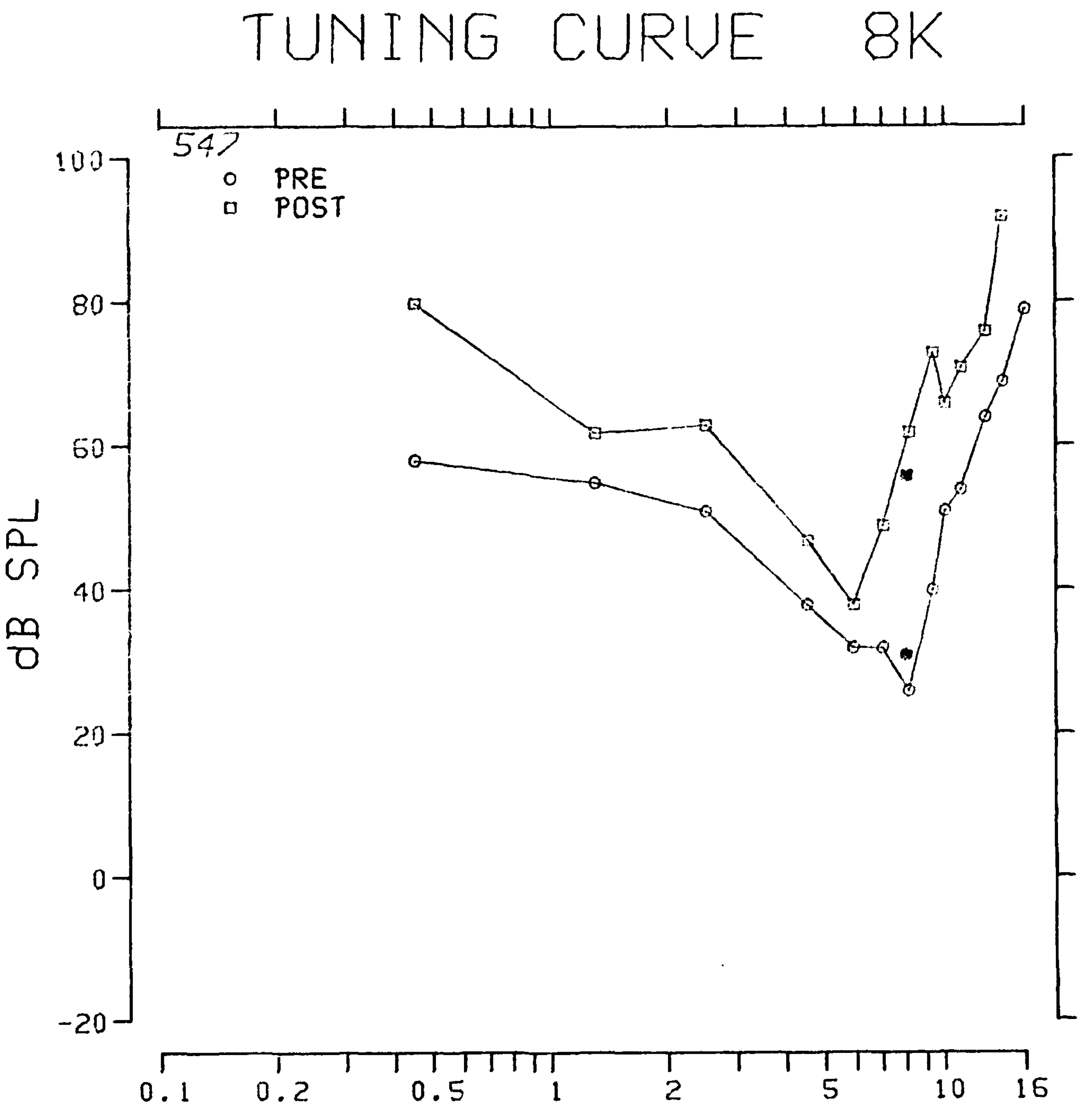


Fig. 3.3.95: Pre- and postexposure evoked response tuning curves at 8.0 kHz from chinchilla 547.

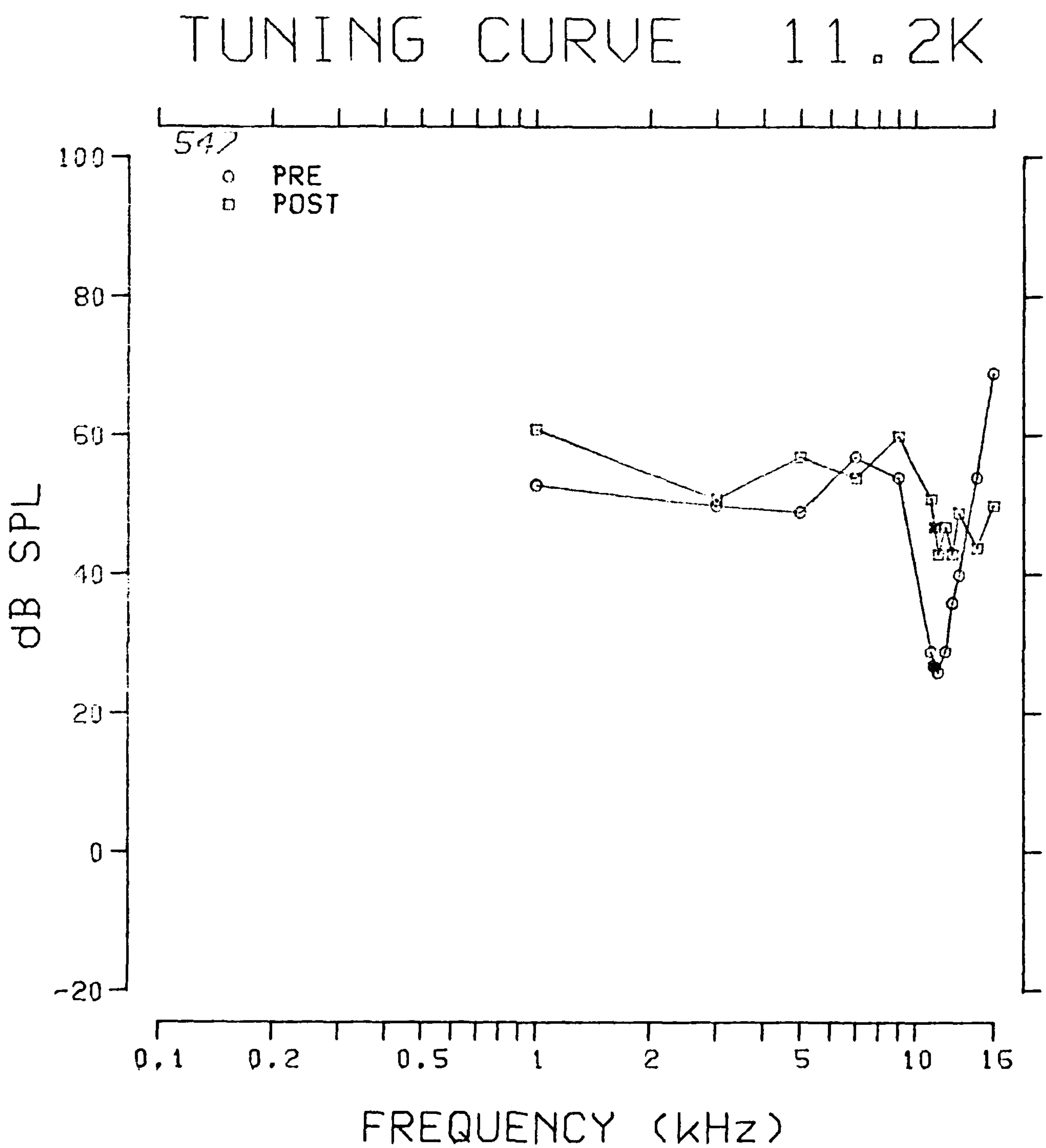


Fig. 3.3.96: Pre- and postexposure evoked response tuning curves at 11.2 kHz from chinchilla 547.

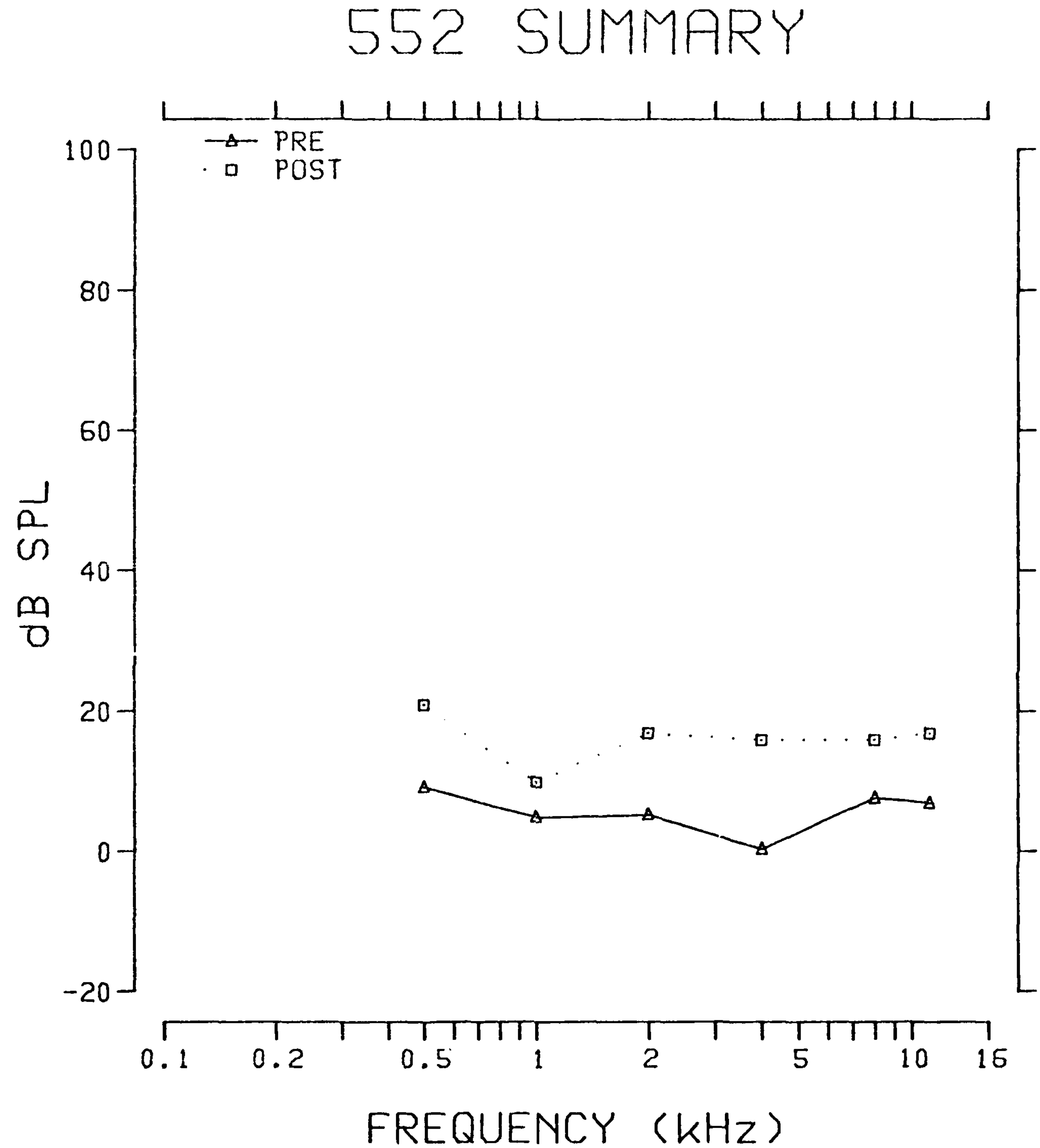


Fig. 3.3.97: Pre- and postexposure evoked response audiograms from chinchilia 552.

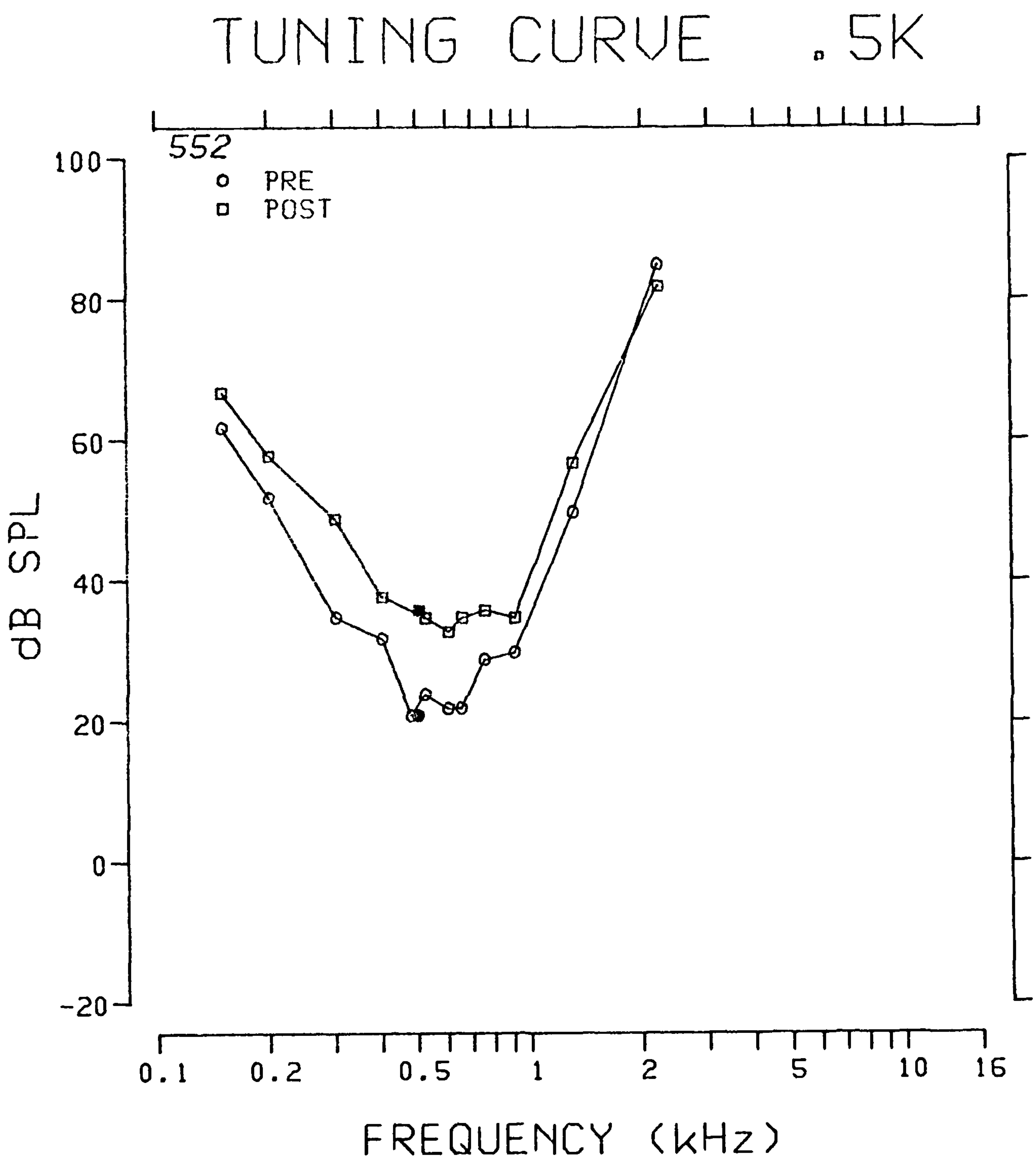


Fig. 3.3.98: Pre- and postexposure evoked response tuning curves at 0.5 kHz from chinchilla 552.

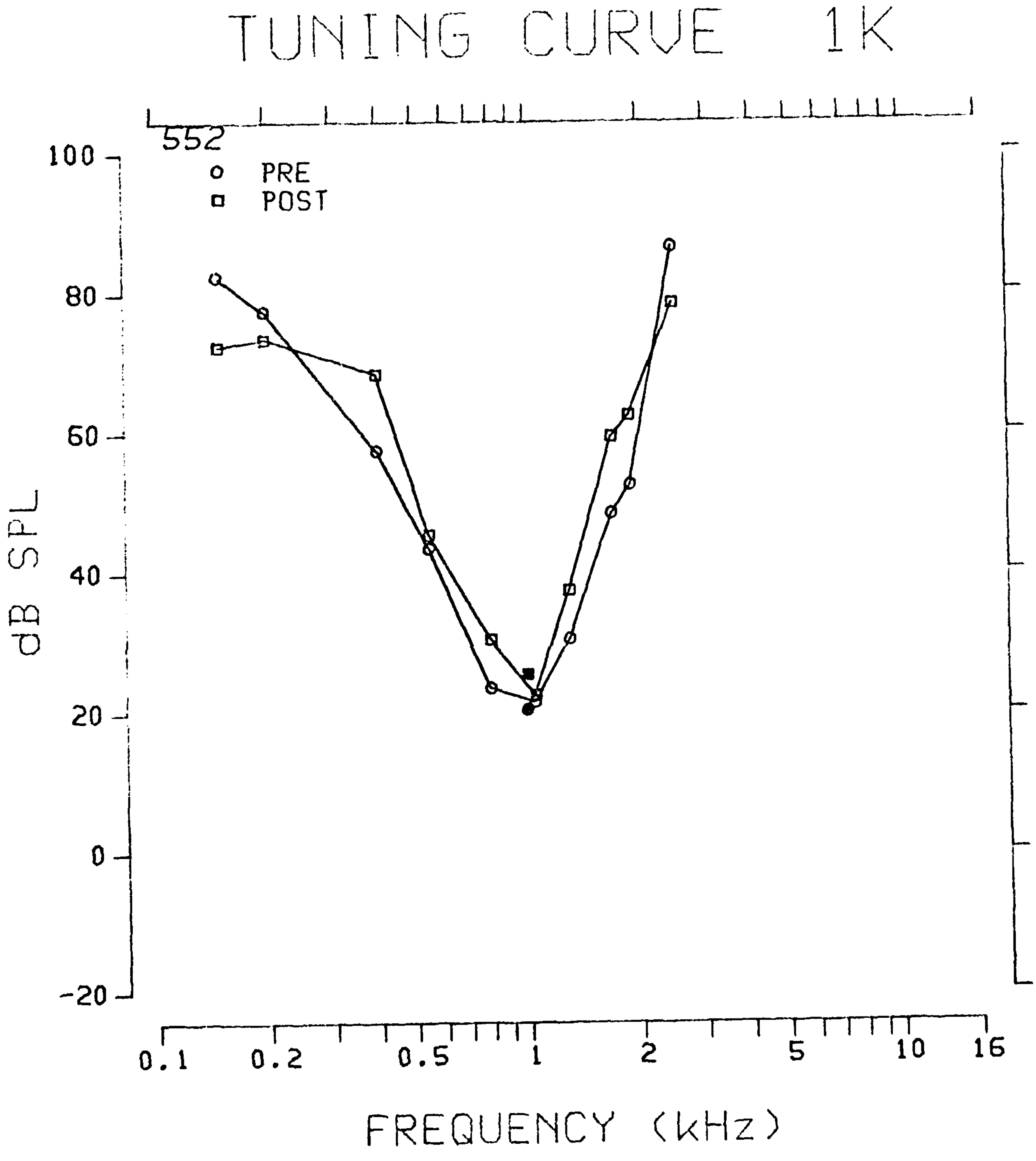


Fig. 3.3.99: Pre- and postexposure evoked response tuning curves at 1.0 kHz from chinchilla 552.

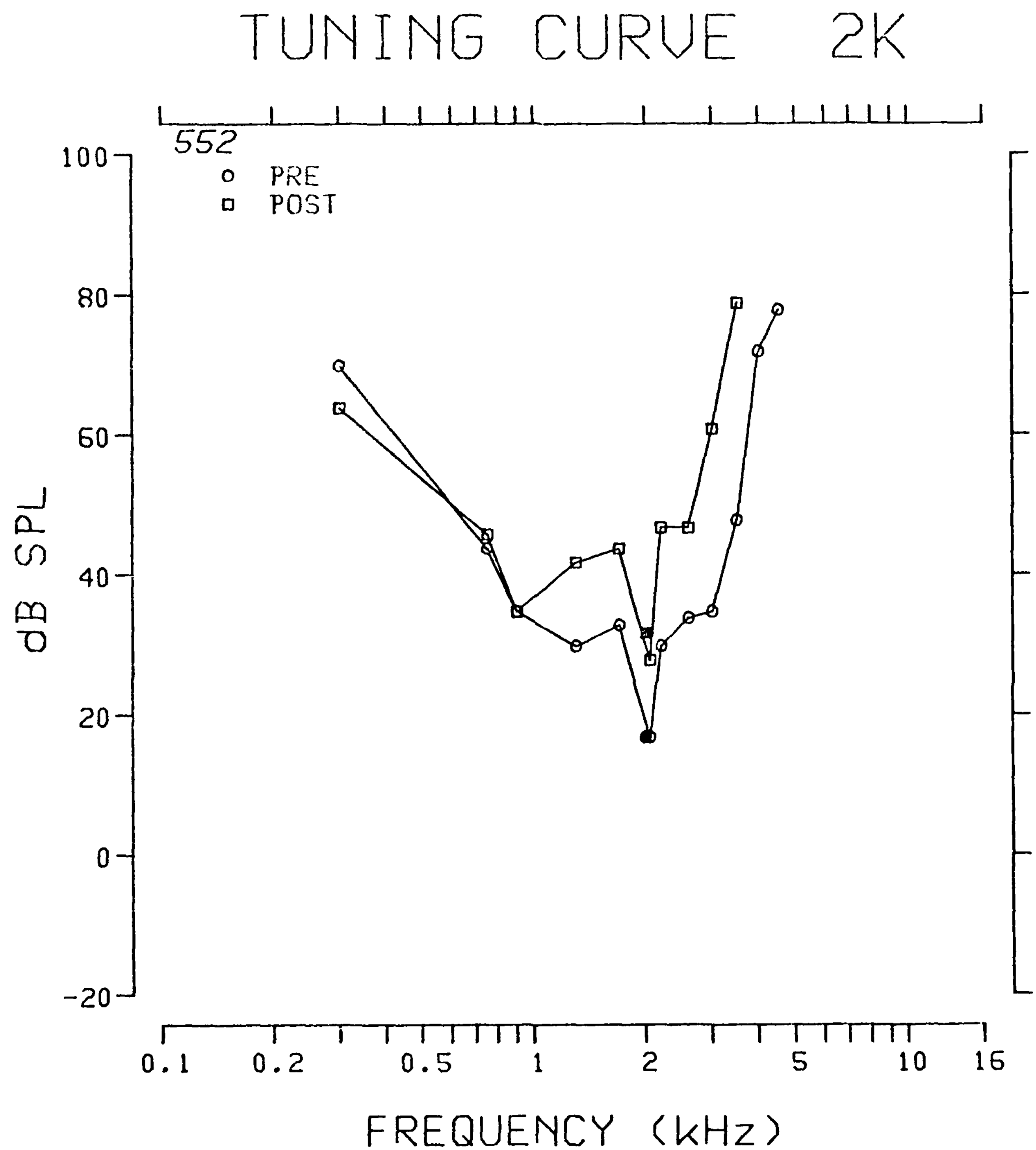


Fig. 3.3.100: Pre- and postexposure evoked response tuning curves at 2.0 kHz from chinchilla 552.

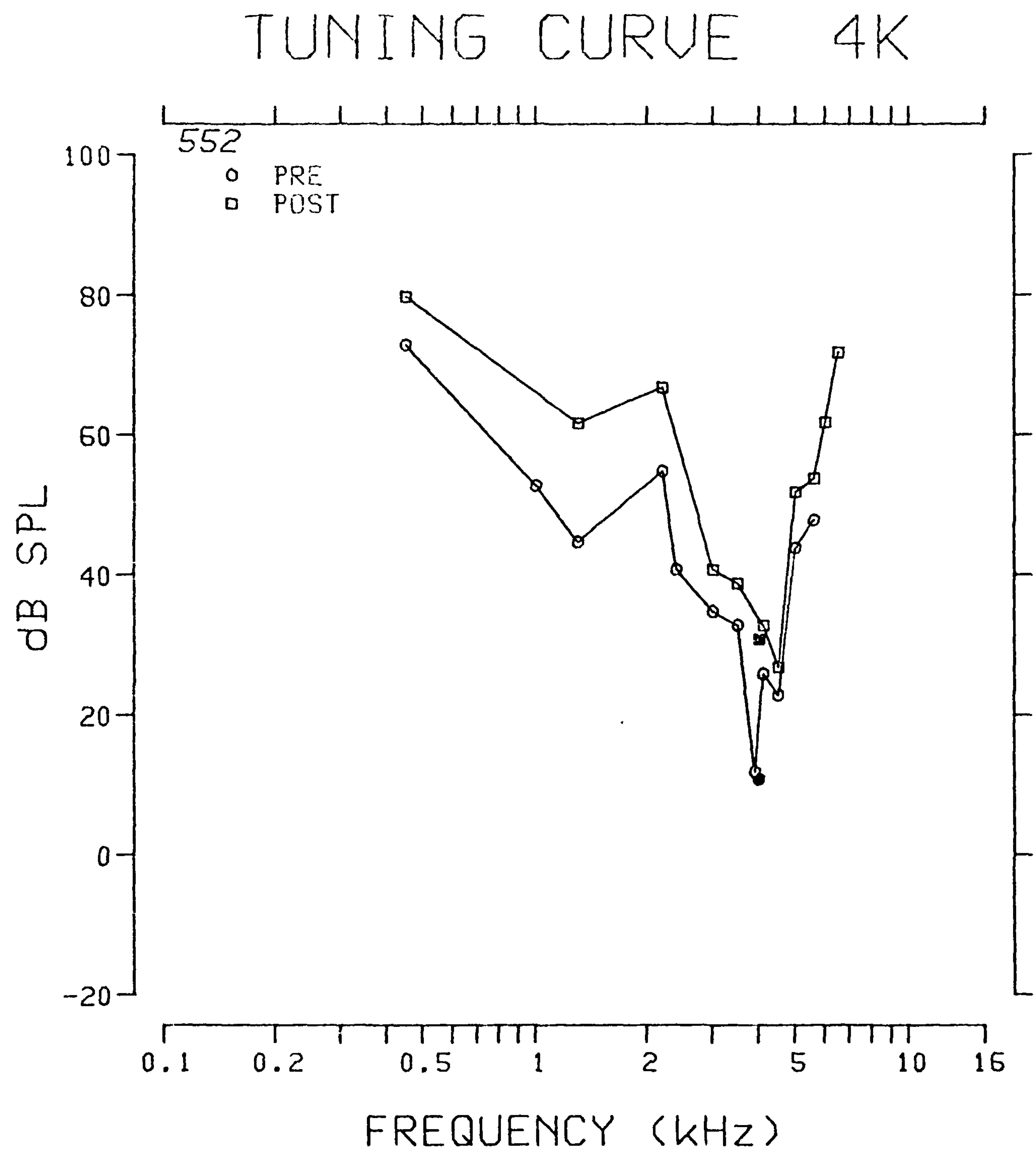


Fig. 3.3.101: Pre- and postexposure evoked response tuning curves at 4.0 kHz from chinchilla 552.

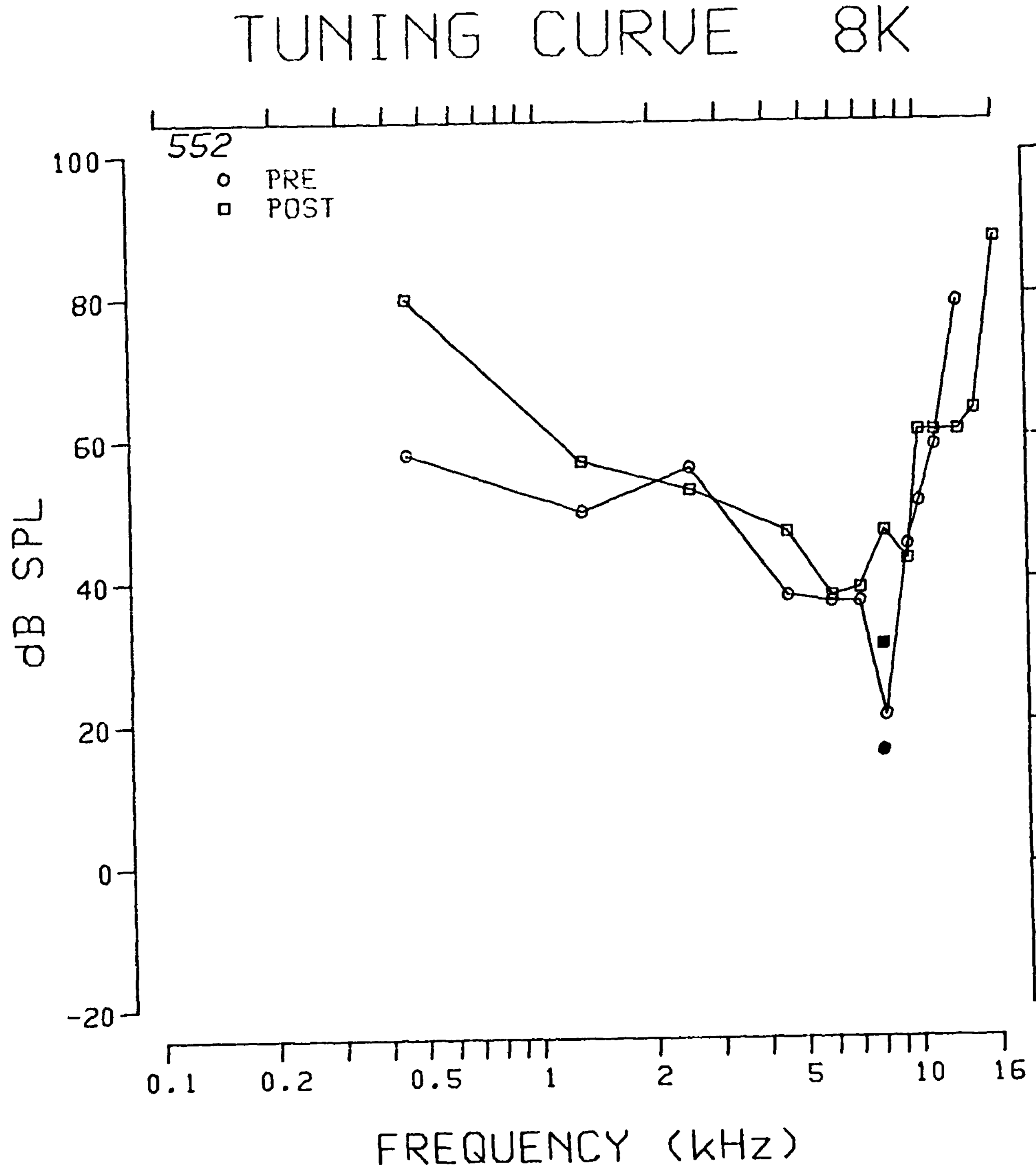


Fig. 3.3.102: Pre- and postexposure evoked response tuning curves at 8.0 kHz from chinchilla 552.

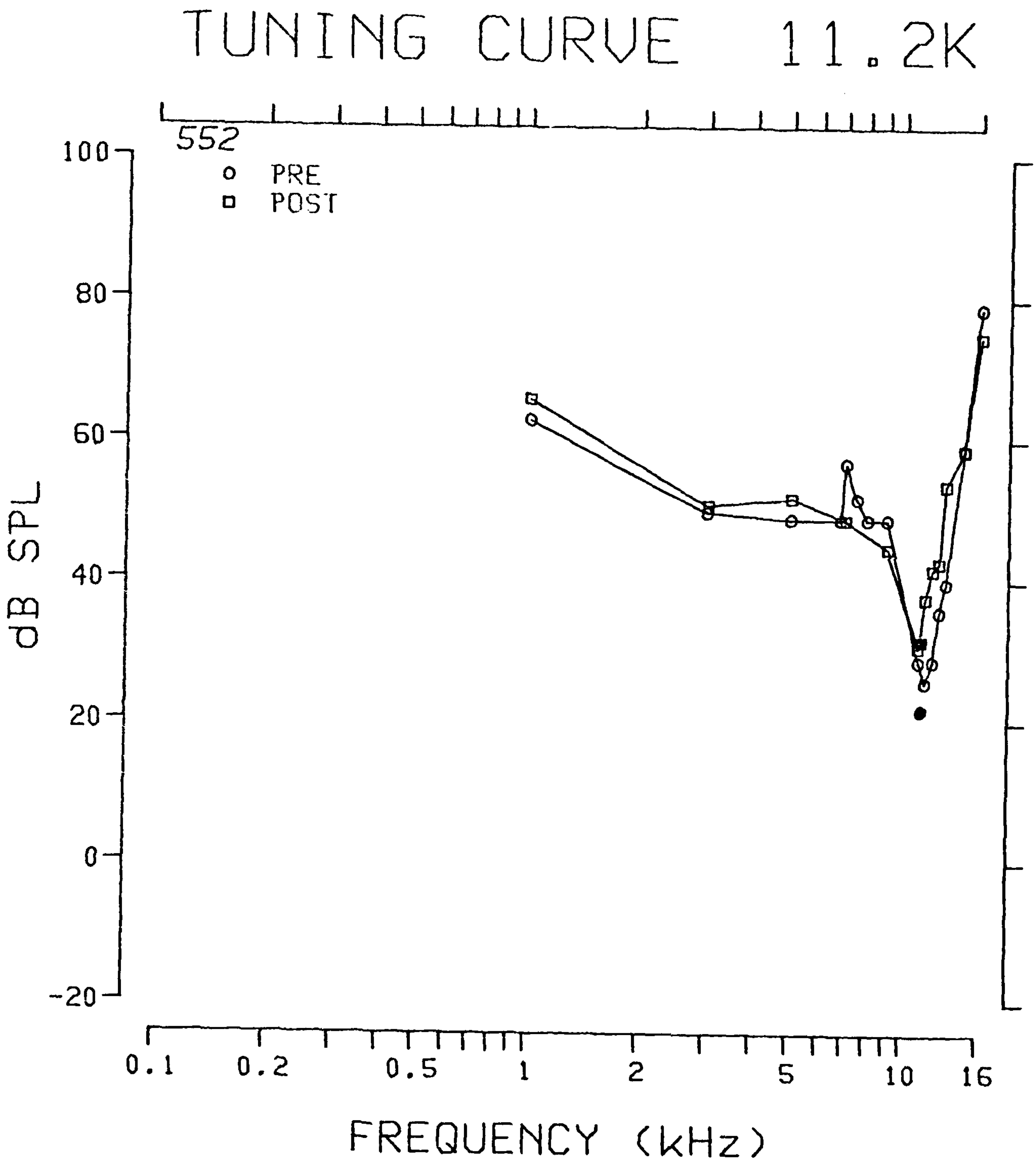


Fig. 3.3.103: Pre- and postexposure evoked response tuning curves at 11.2 kHz from chinchilla 552.

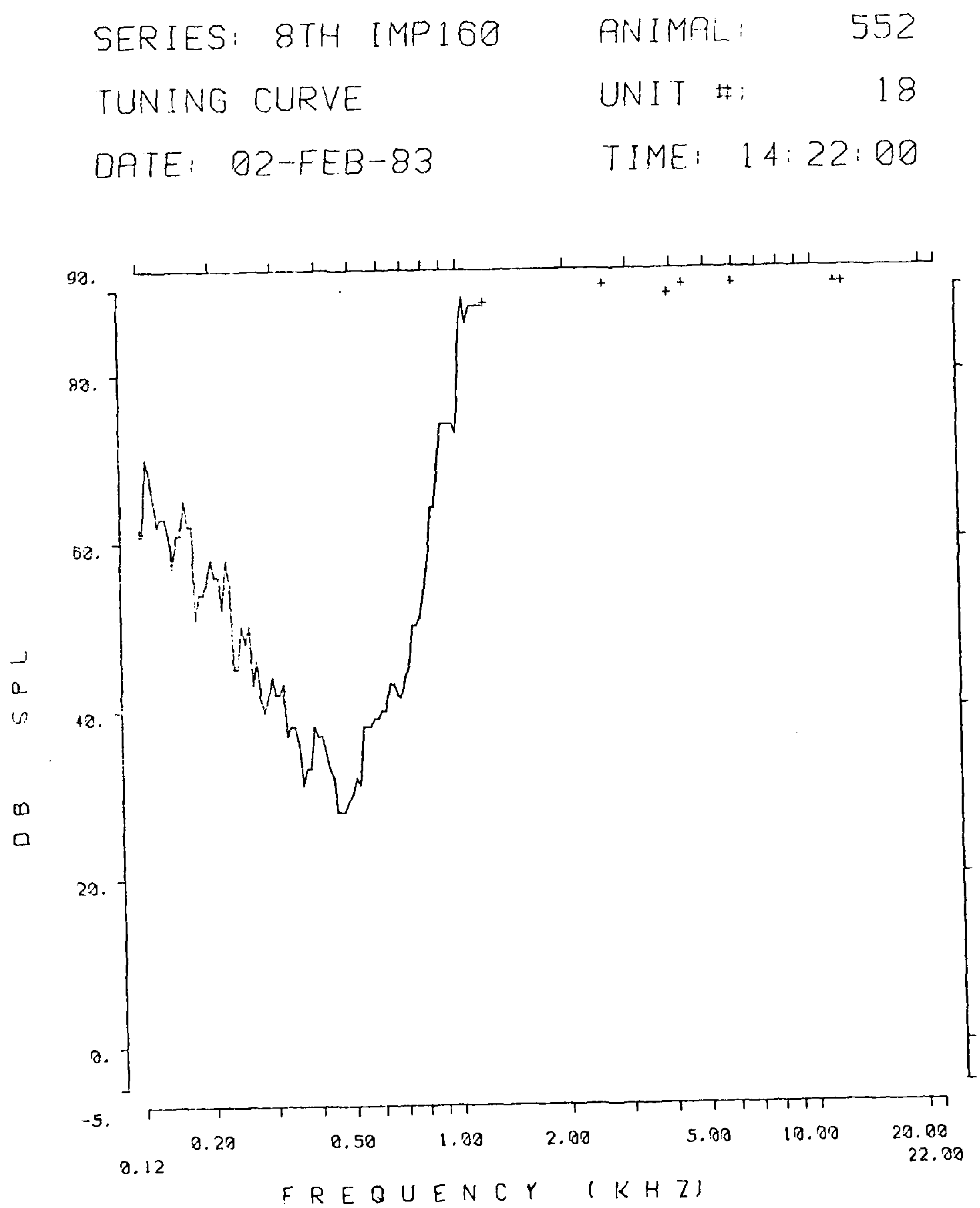


Fig. 3.3.104: Auditory nerve fiber tuning curve from chinchilla 552.

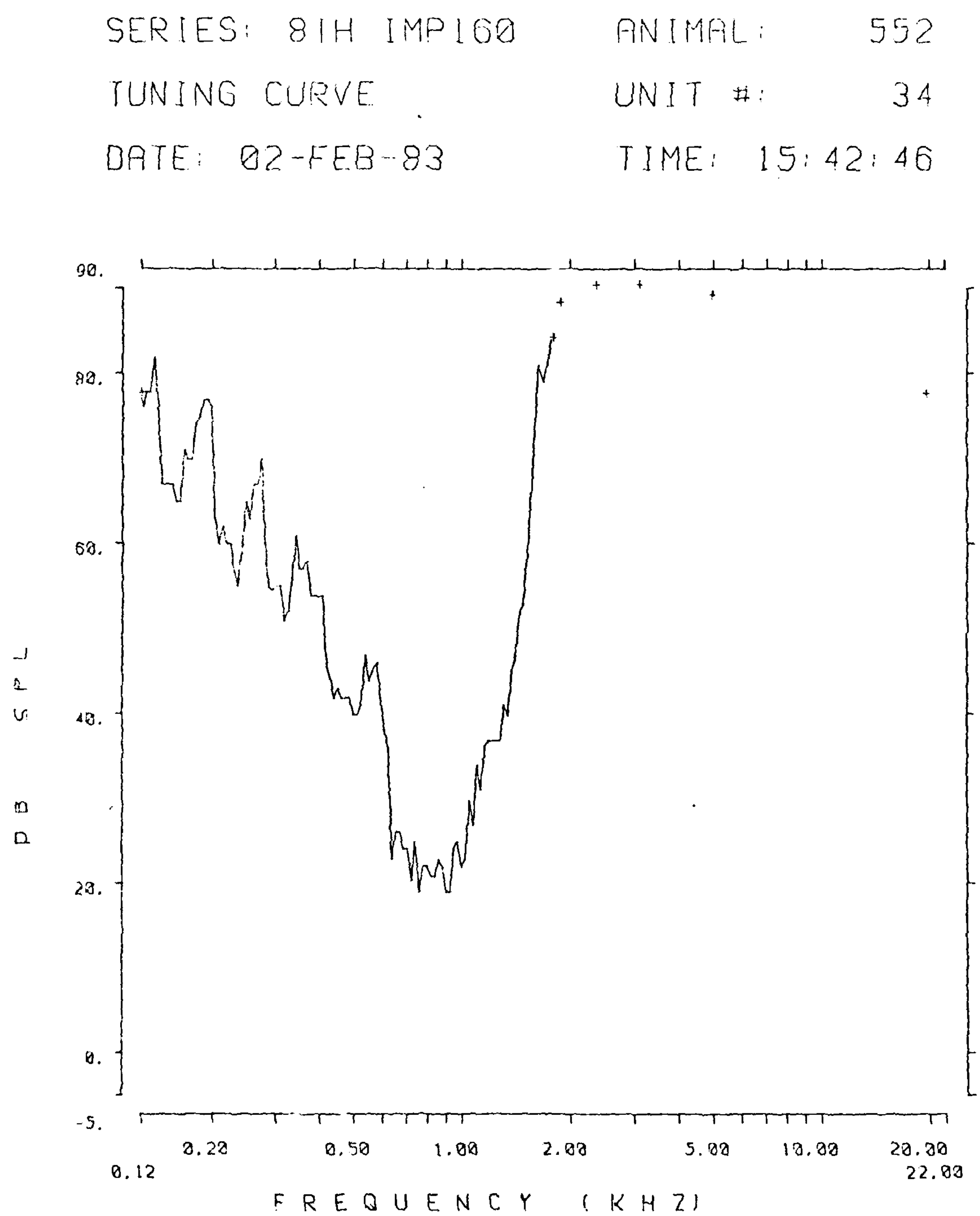


Fig. 3.3.105: Auditory nerve fiber tuning curve from chinchilla 552.

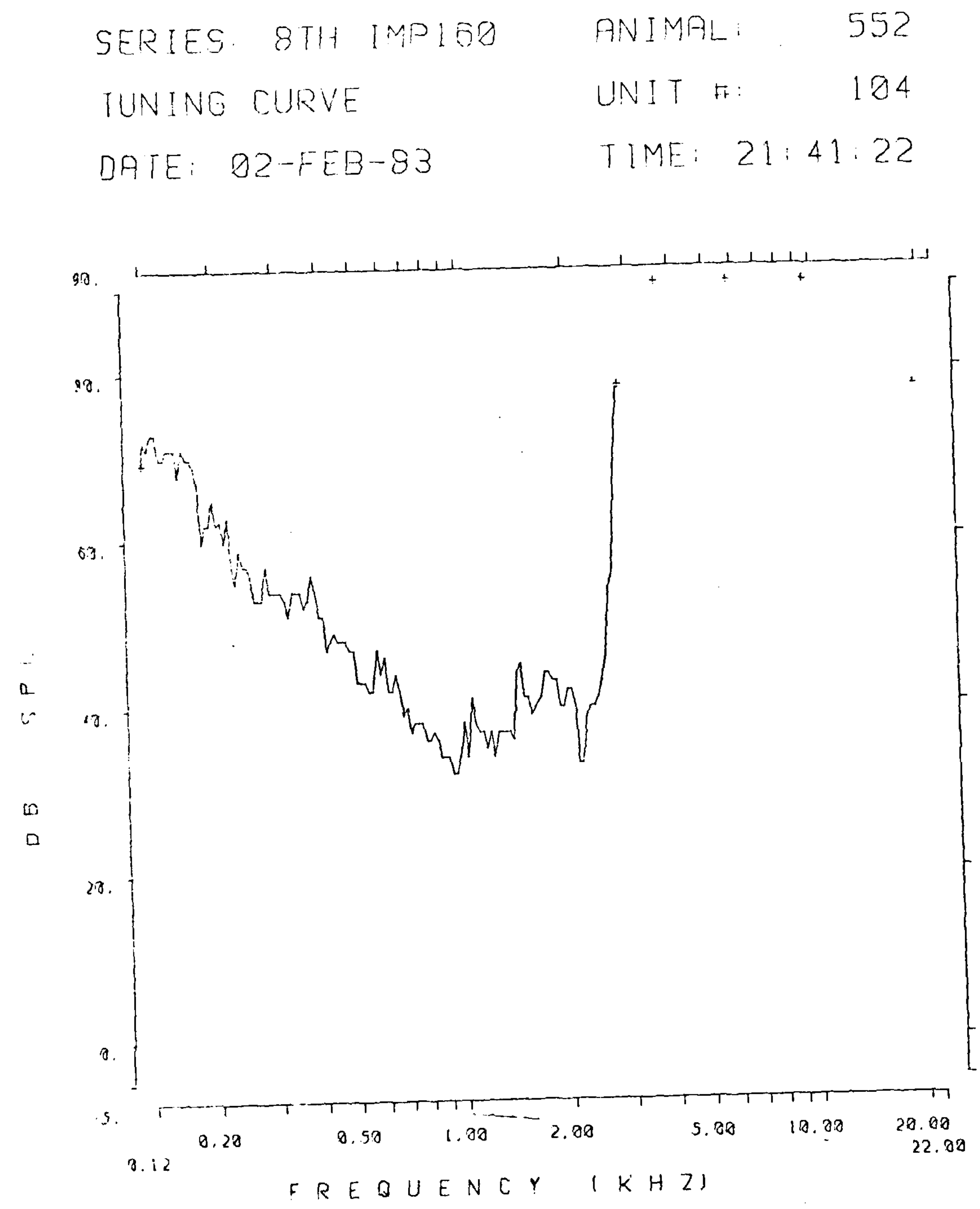


Fig. 3.3.106: Auditory nerve fiber tuning curve from chinchilla 552.

( 123)

SERIES: 8TH IMP160 ANIMAL: 552

TUNING CURVE UNIT #: 1

DATE: 02-FEB-83 TIME: 12:27:00

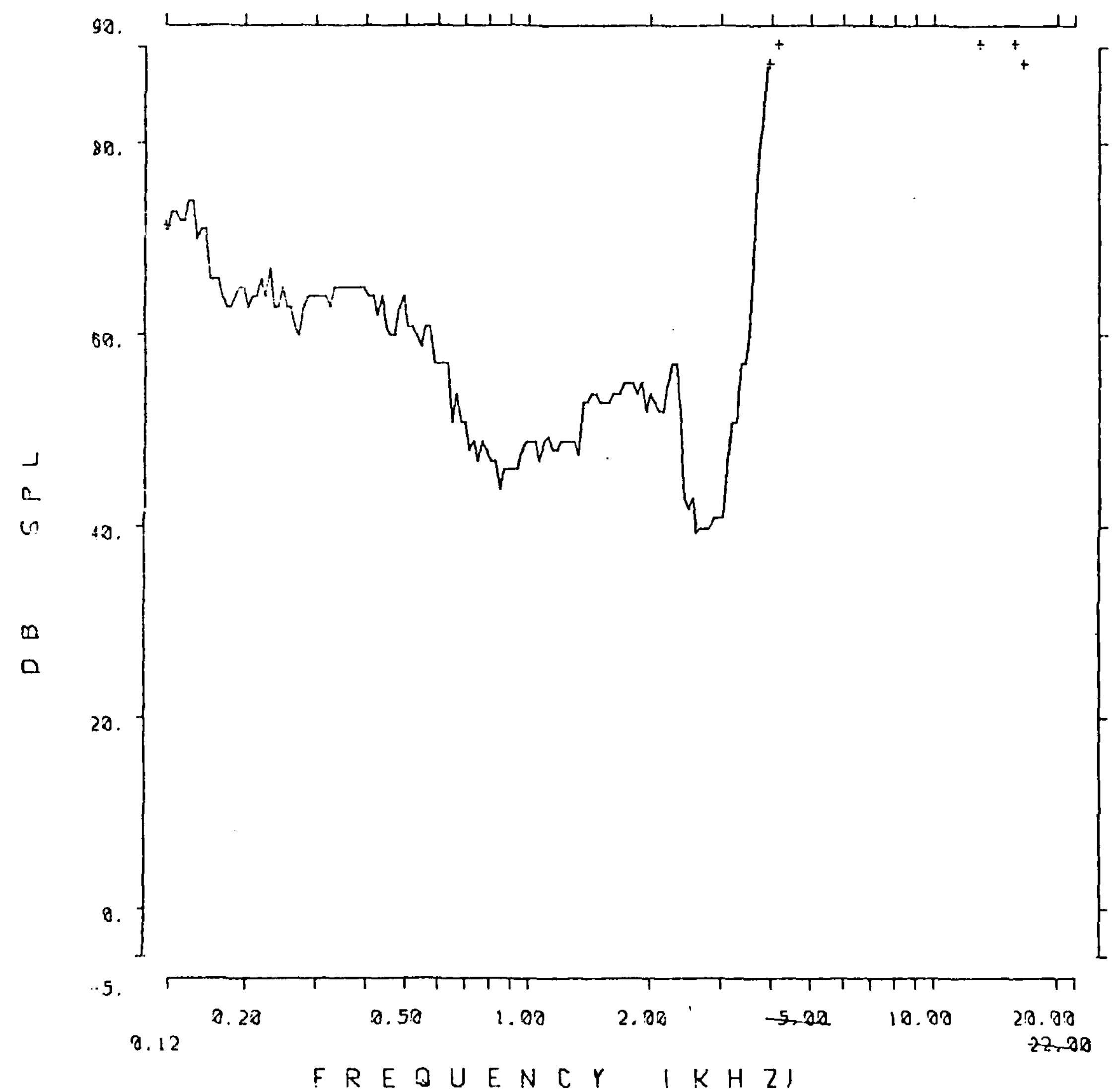


Fig. 3.3.107: Auditory nerve fiber tuning curve from chinchilla 552.

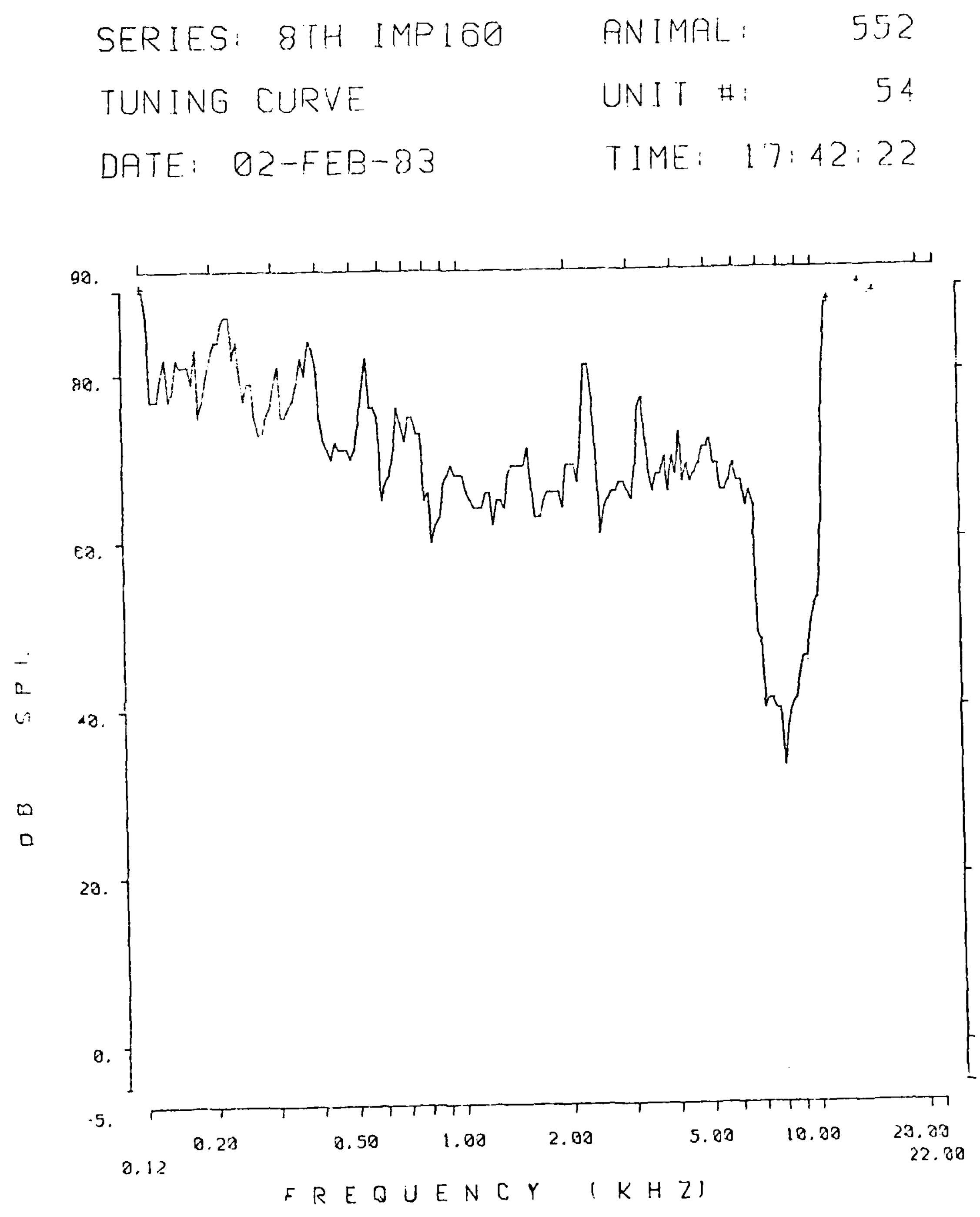


Fig. 3.3.108: Auditory nerve fiber tuning curve from chinchilla 552.

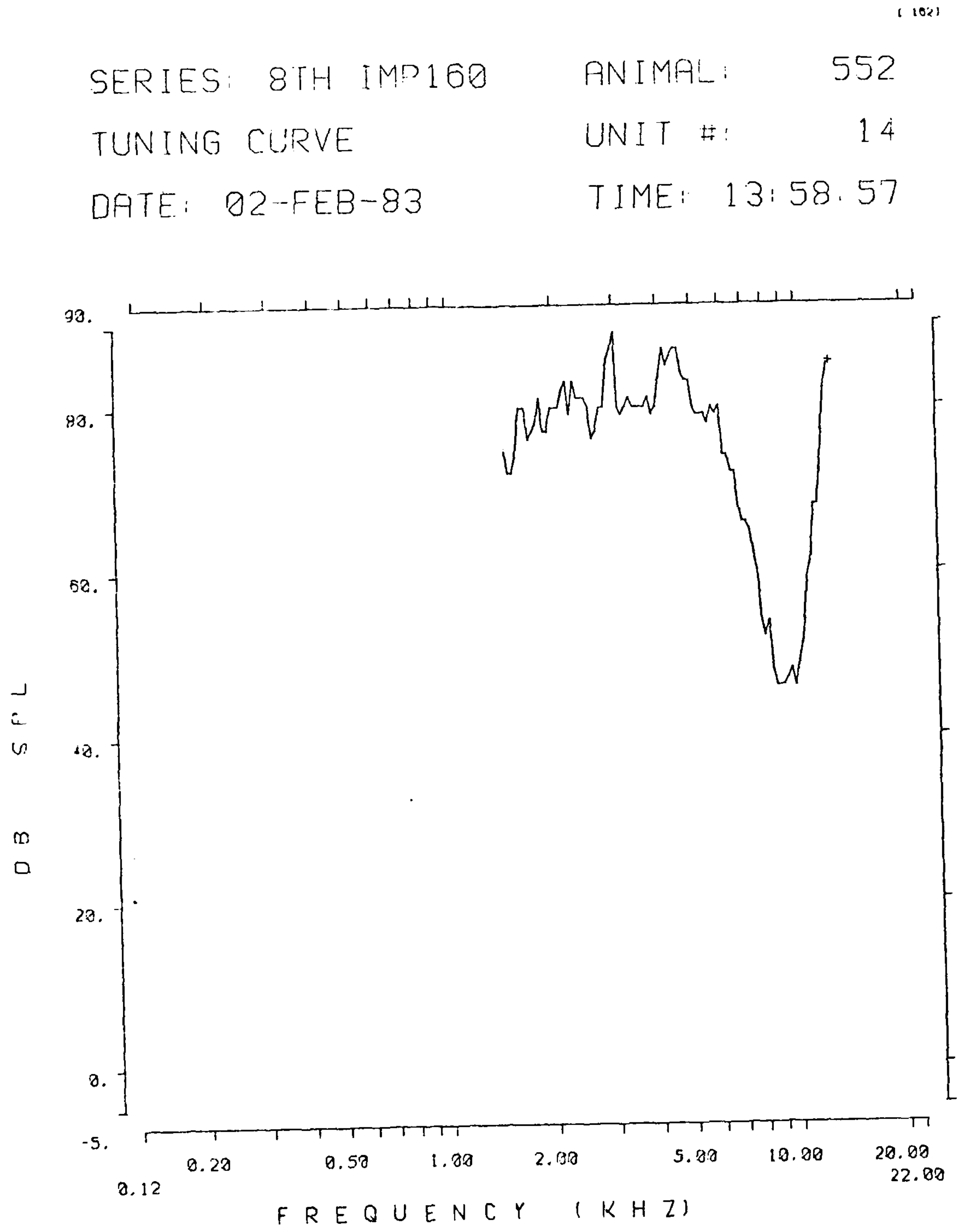


Fig. 3.3.109: Auditory nerve fiber tuning curve from chinchilla 552.

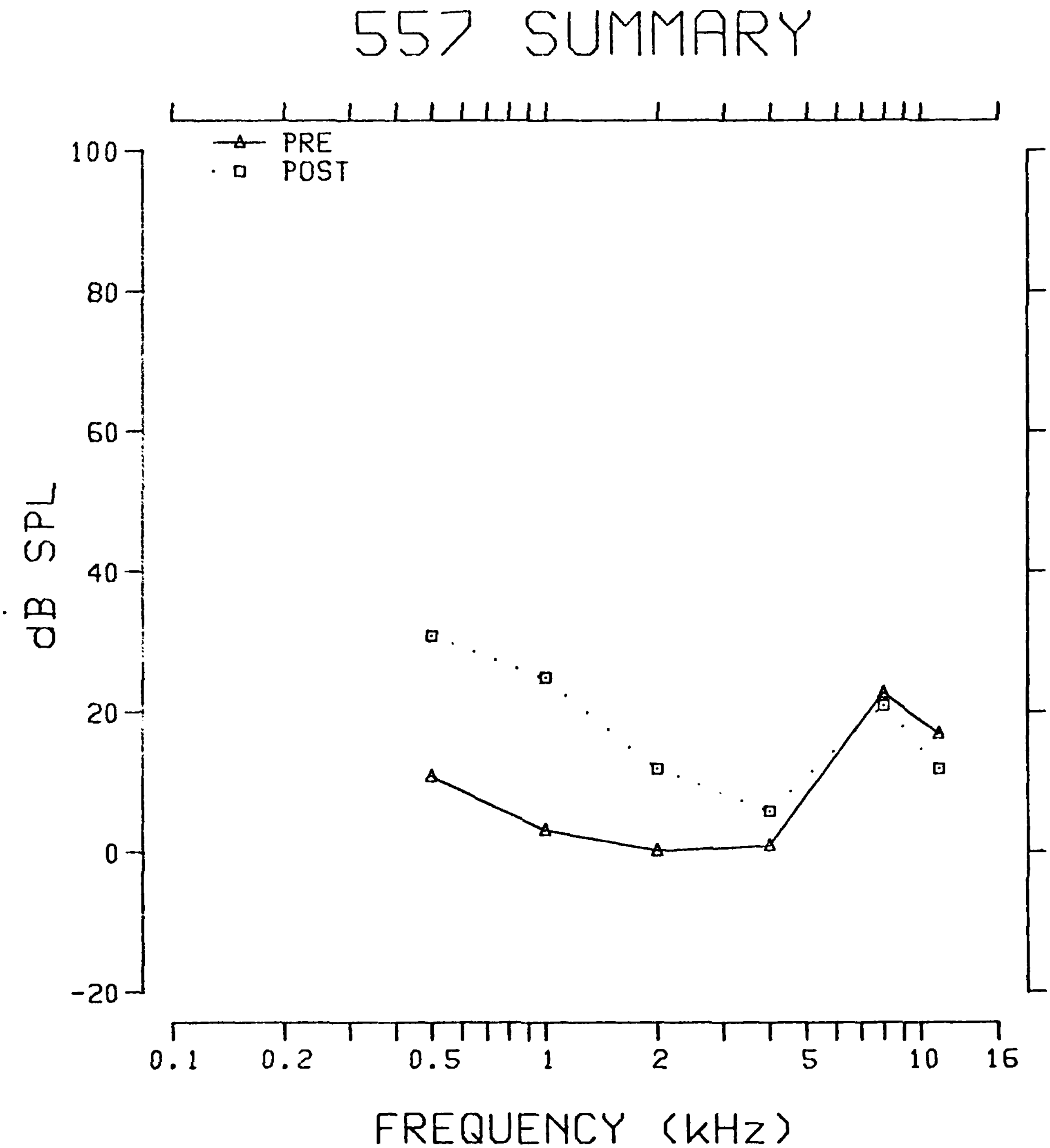


Fig. 3.3.110: Pre- and postexposure evoked response audiograms from chinchilla 557.

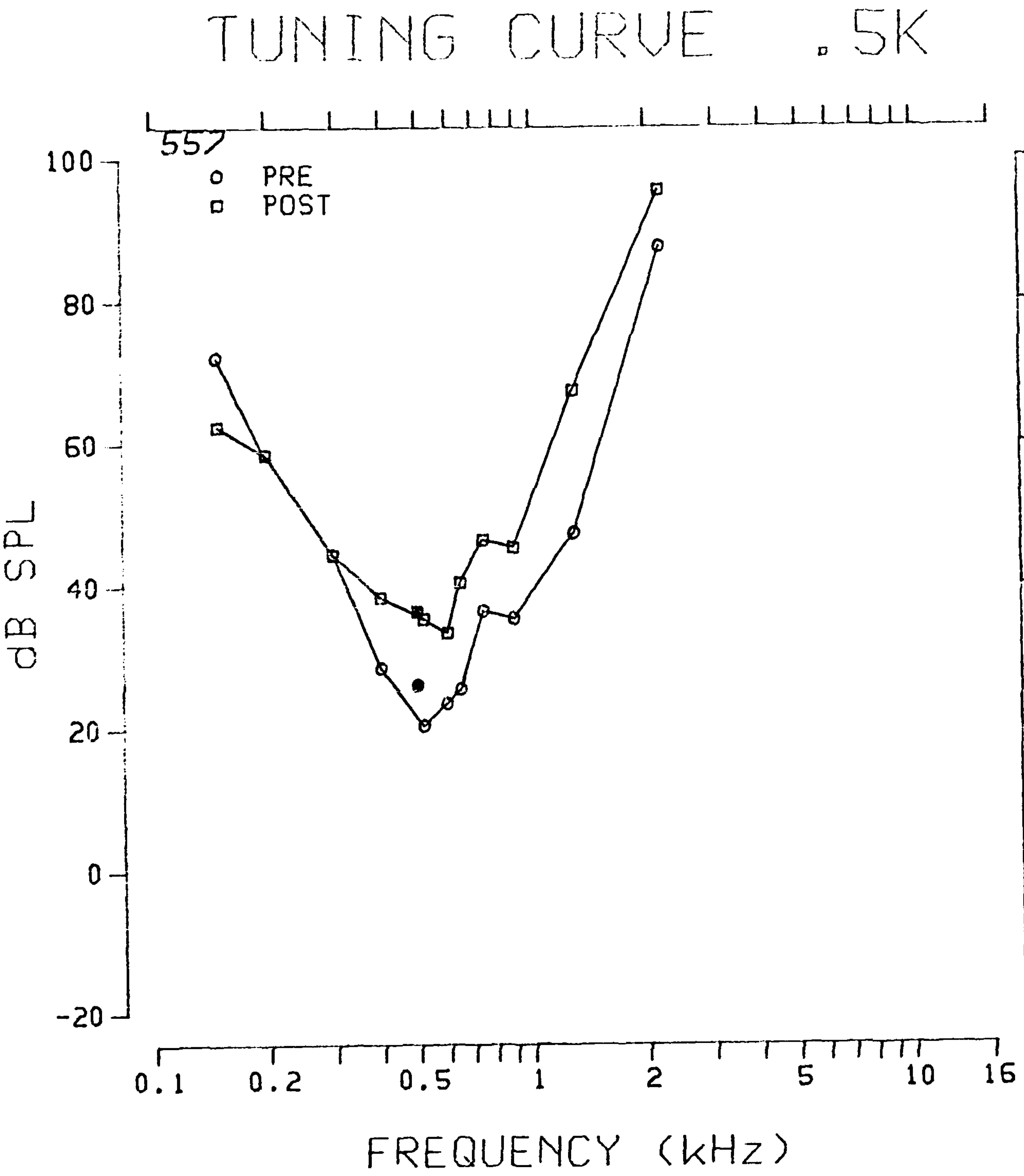


Fig. 3.3.111 Pre- and postexposure evoked response tuning curves at 0.5 kHz from chinchilla 557.

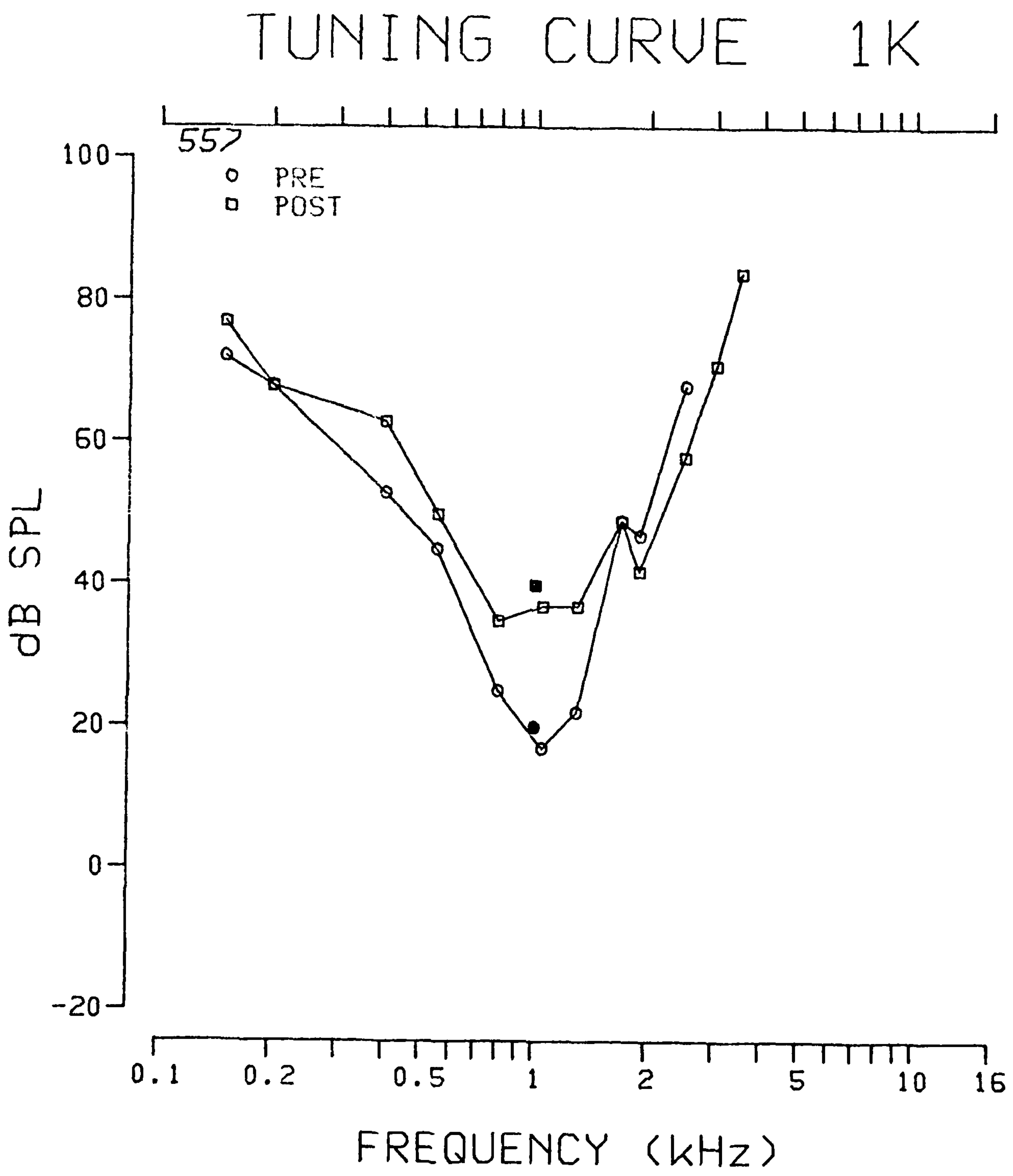


Fig. 3.3.112: Pre- and postexposure evoked response tuning curves at 1.0 kHz from chinchilla 557.

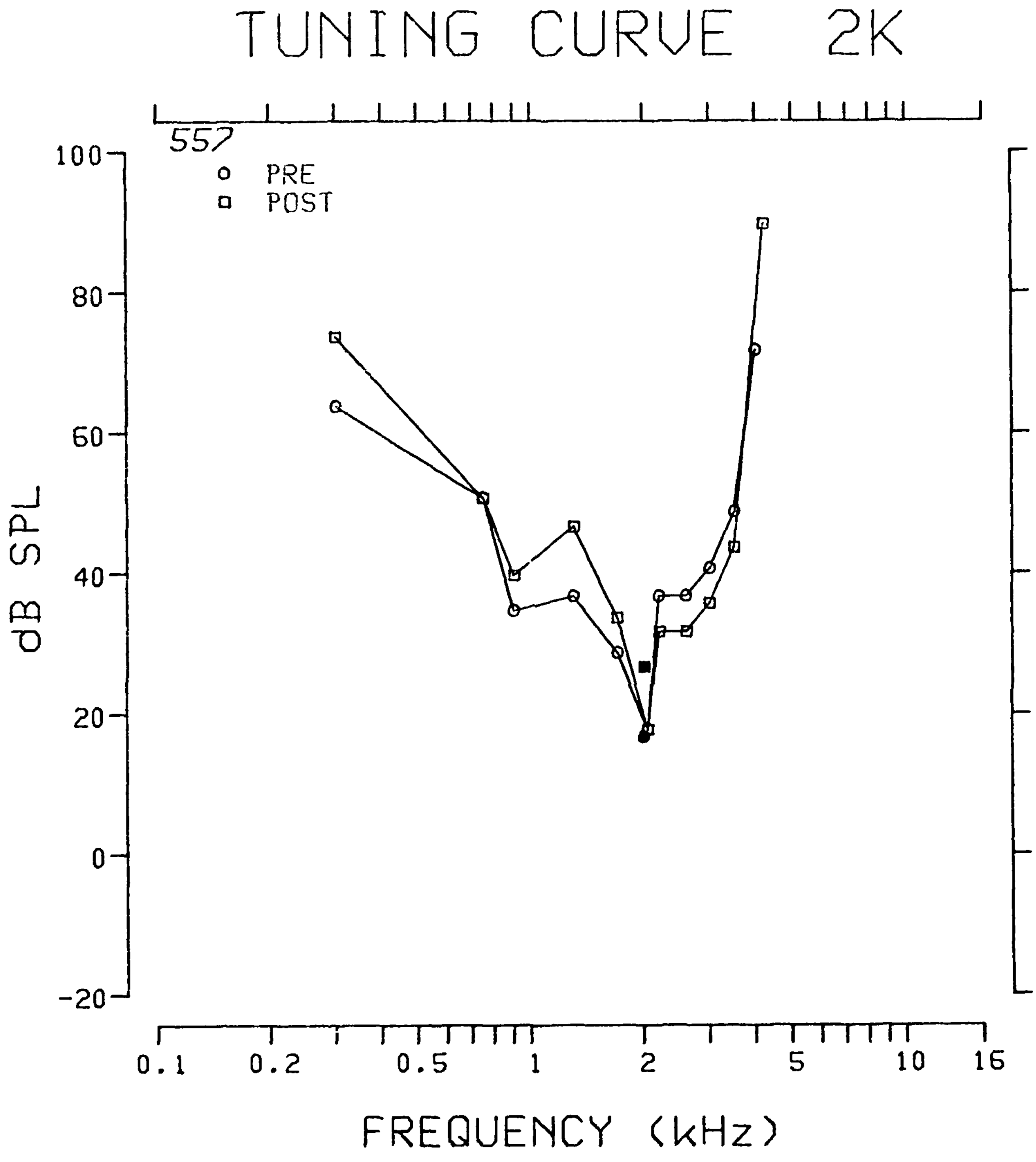


Fig. 3.3.113: Pre- and postexposure evoked response tuning curves at 2.0 kHz from chinchilla 557.

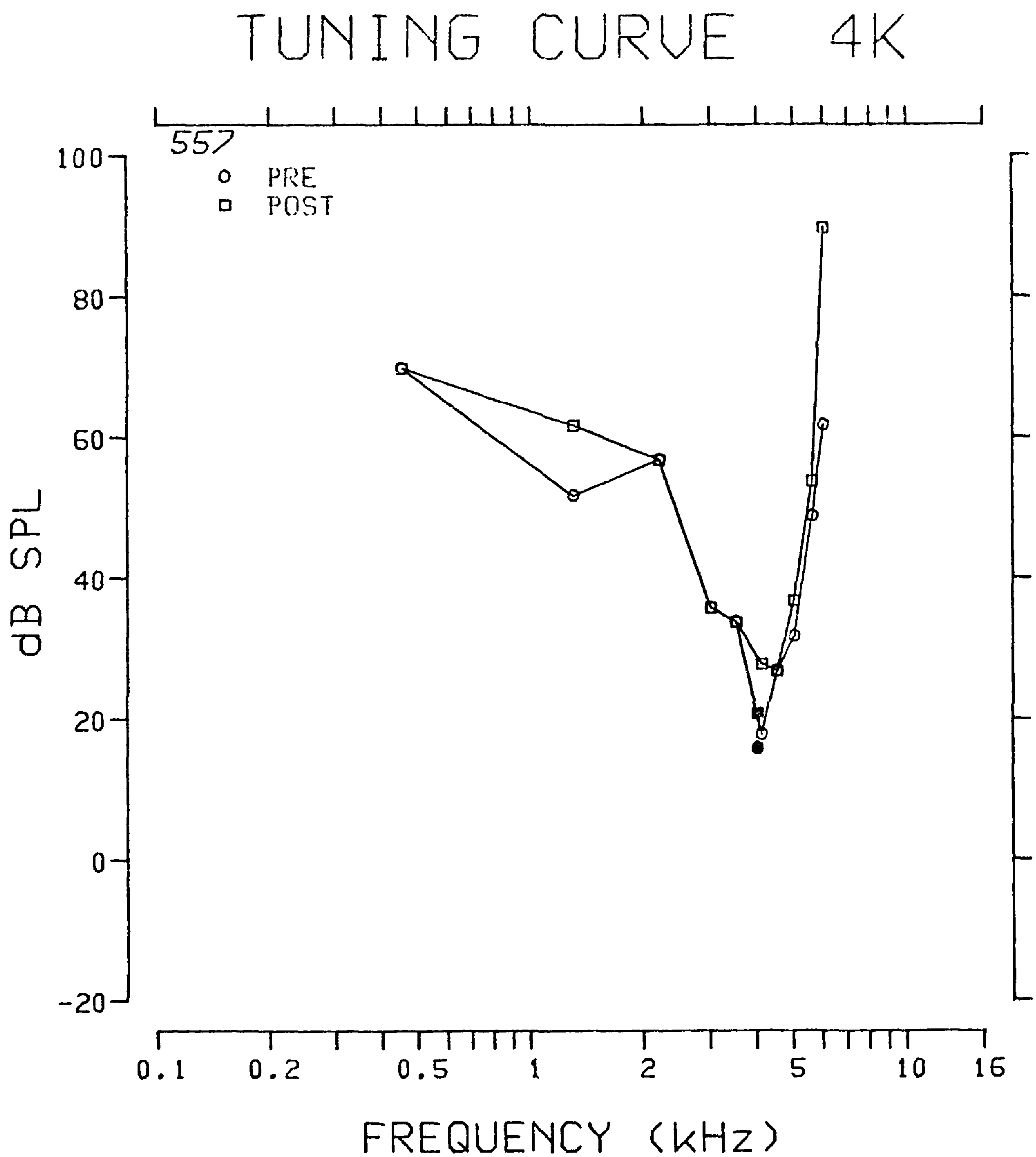


Fig. 3.3.114: Pre- and postexposure evoked response tuning curves at 4.0 kHz from chinchilla 557.

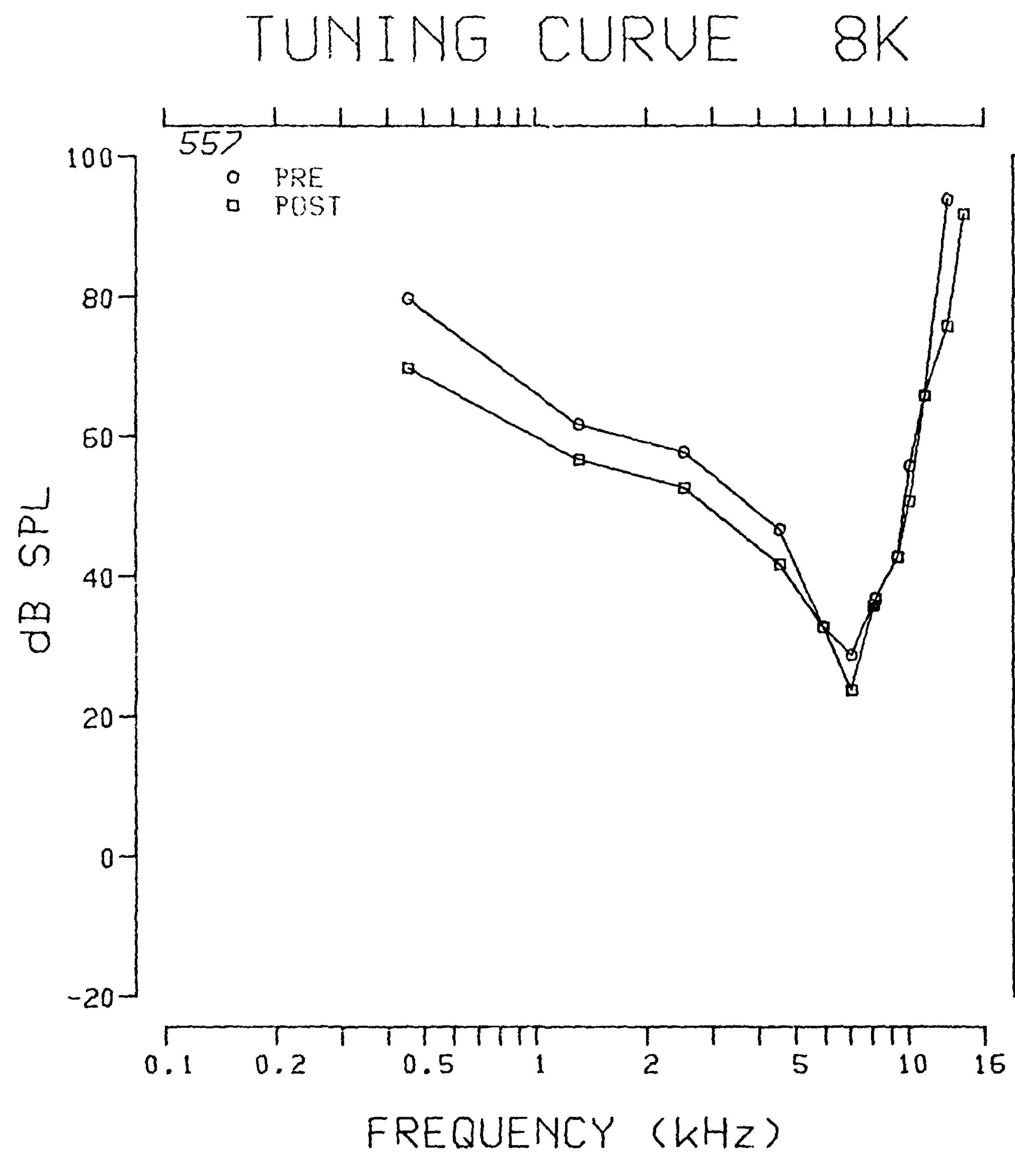


Fig. 3.3.115: Pre- and postexposure evoked response tuning curves at 8.0 kHz from chinchilla 557.

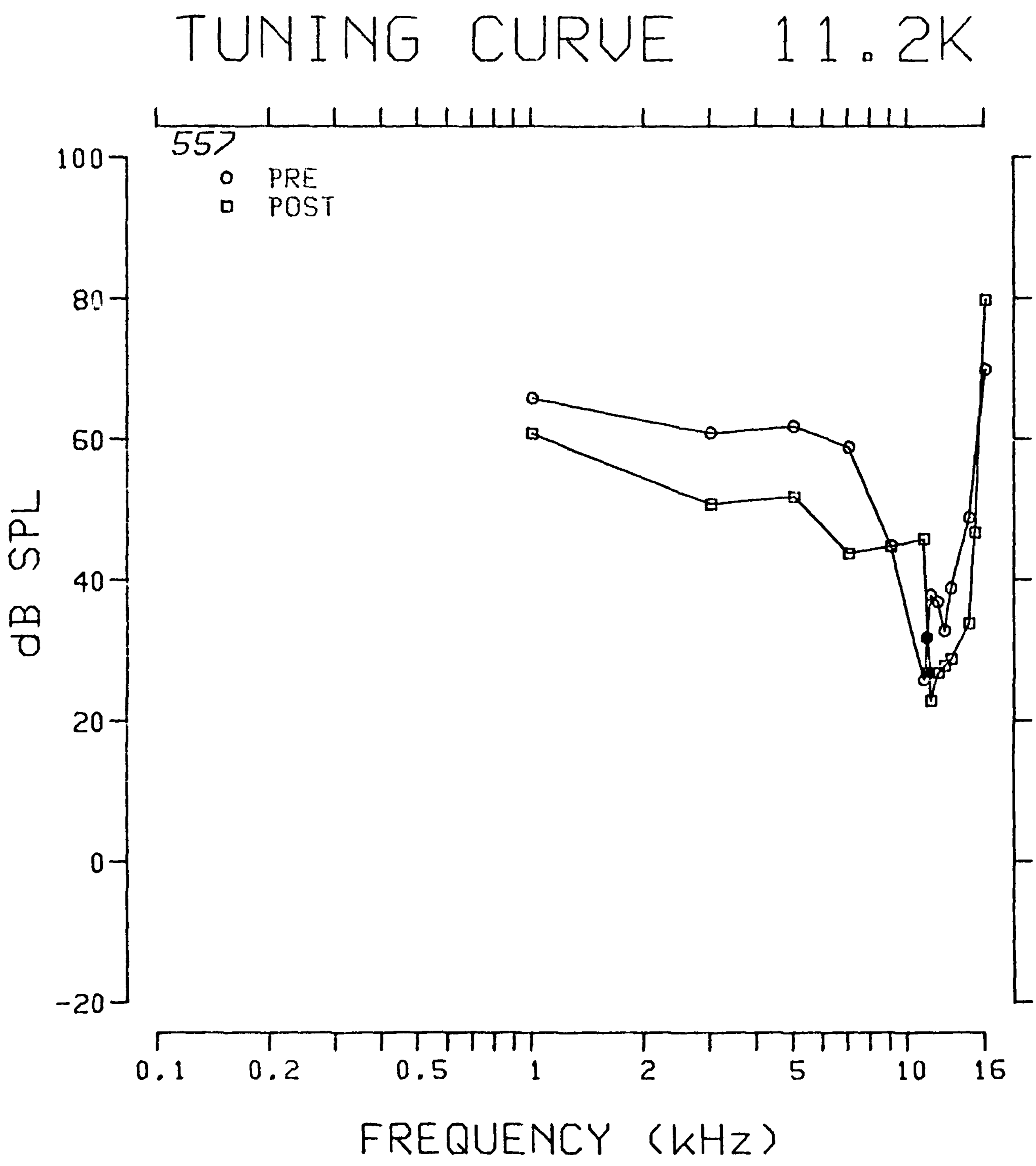


Fig. 3.3.116: Pre- and postexposure evoked response tuning curves at 11.2 kHz.

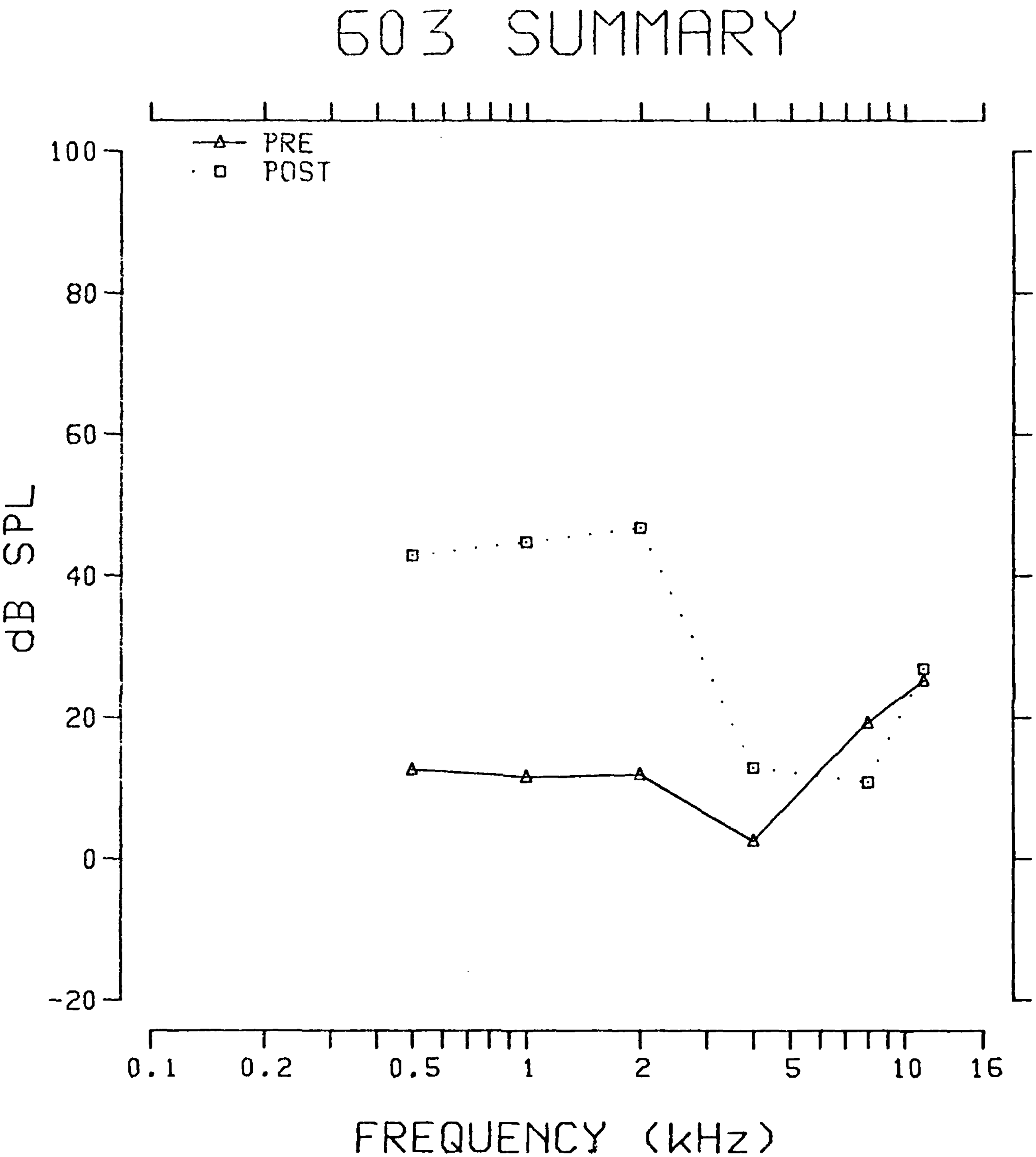


Fig. 3.3.117: Pre- and postexposure evoked response audiograms from chinchilla 603.

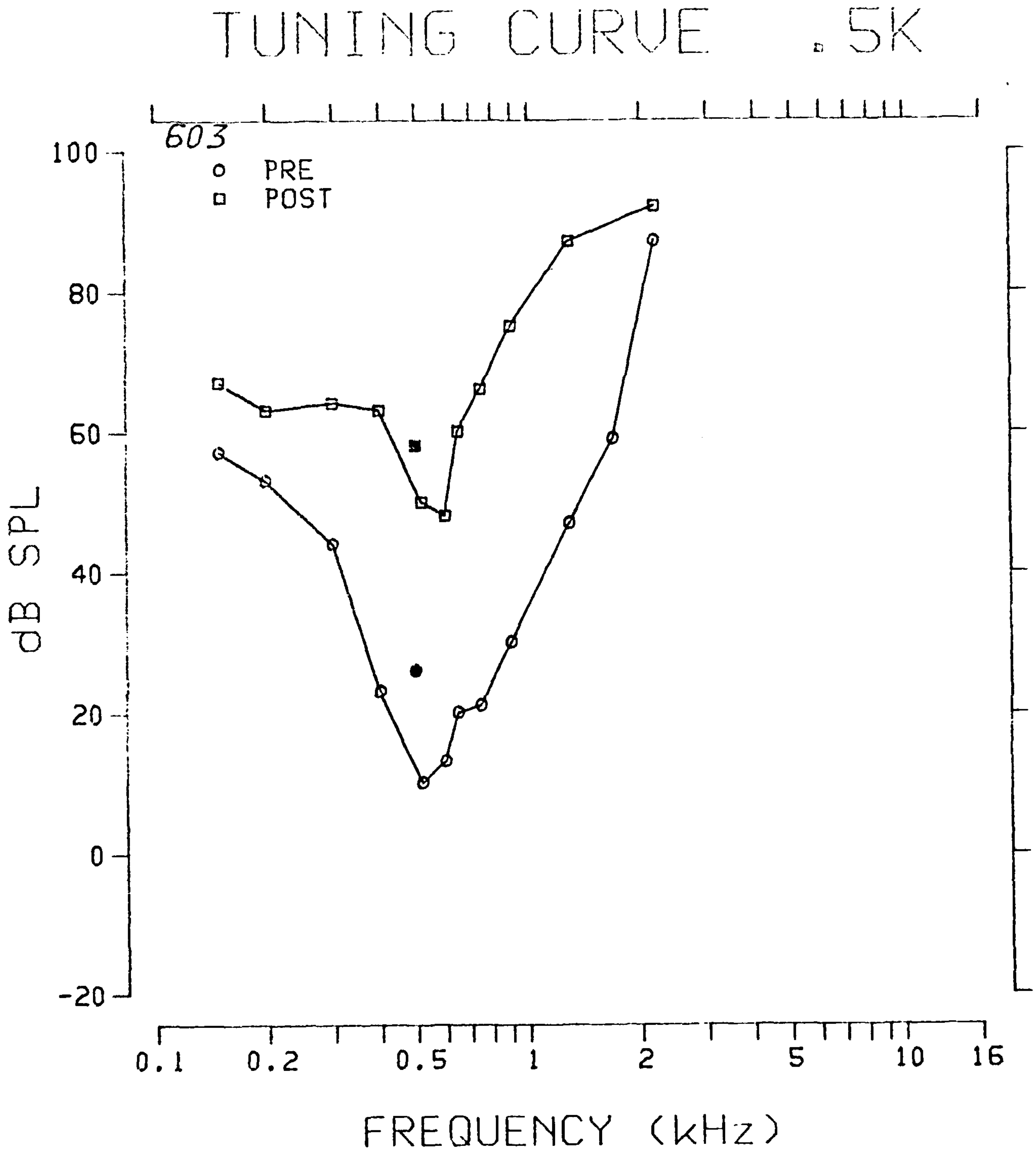


Fig. 3.3.118: Pre- and postexposure evoked response tuning curves at 0.5 kHz from chinchilla 603.

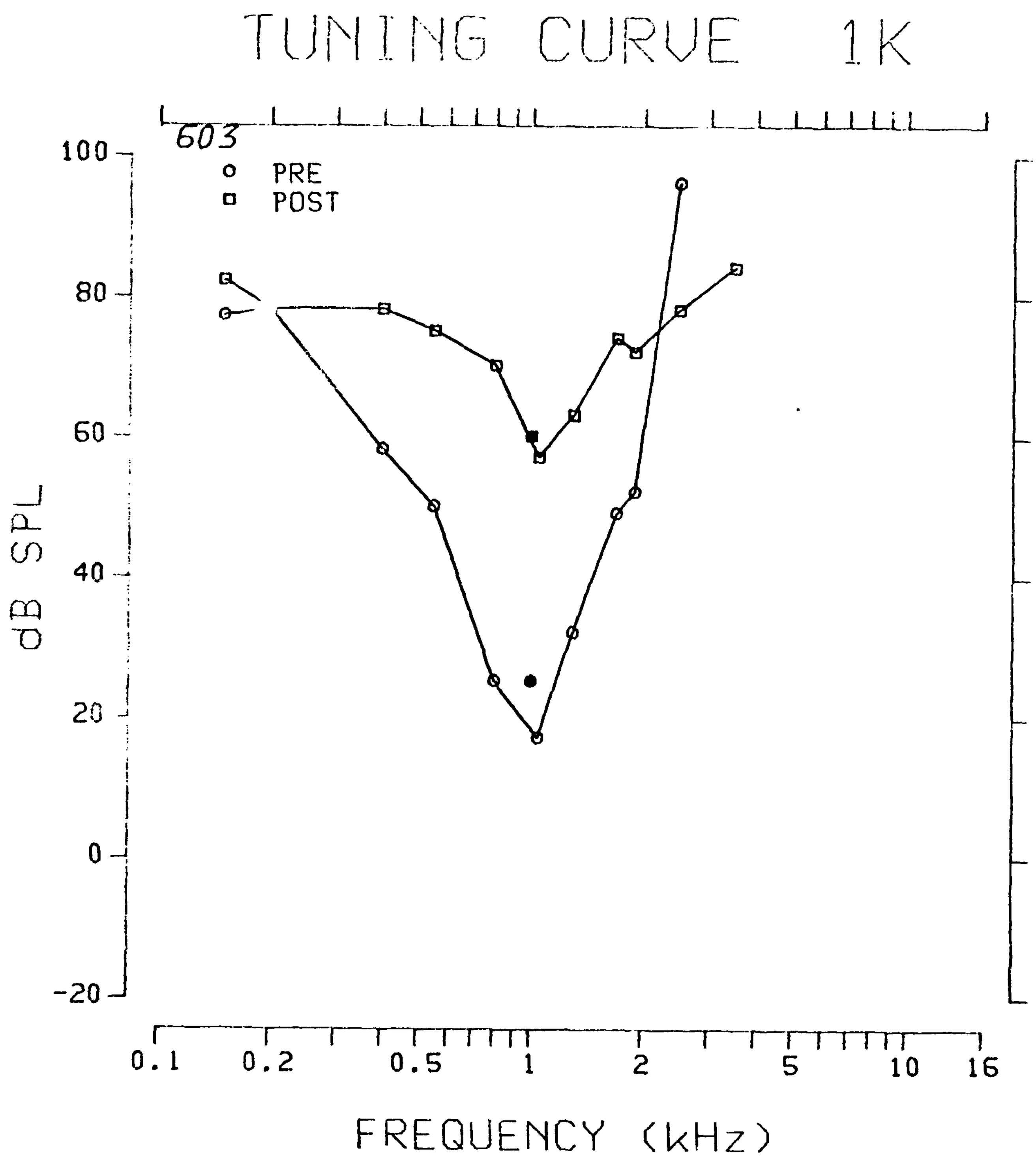


Fig. 3.3.119: Pre- and postexposure evoked response tuning curves at 1.0 kHz from chinchilla 603.

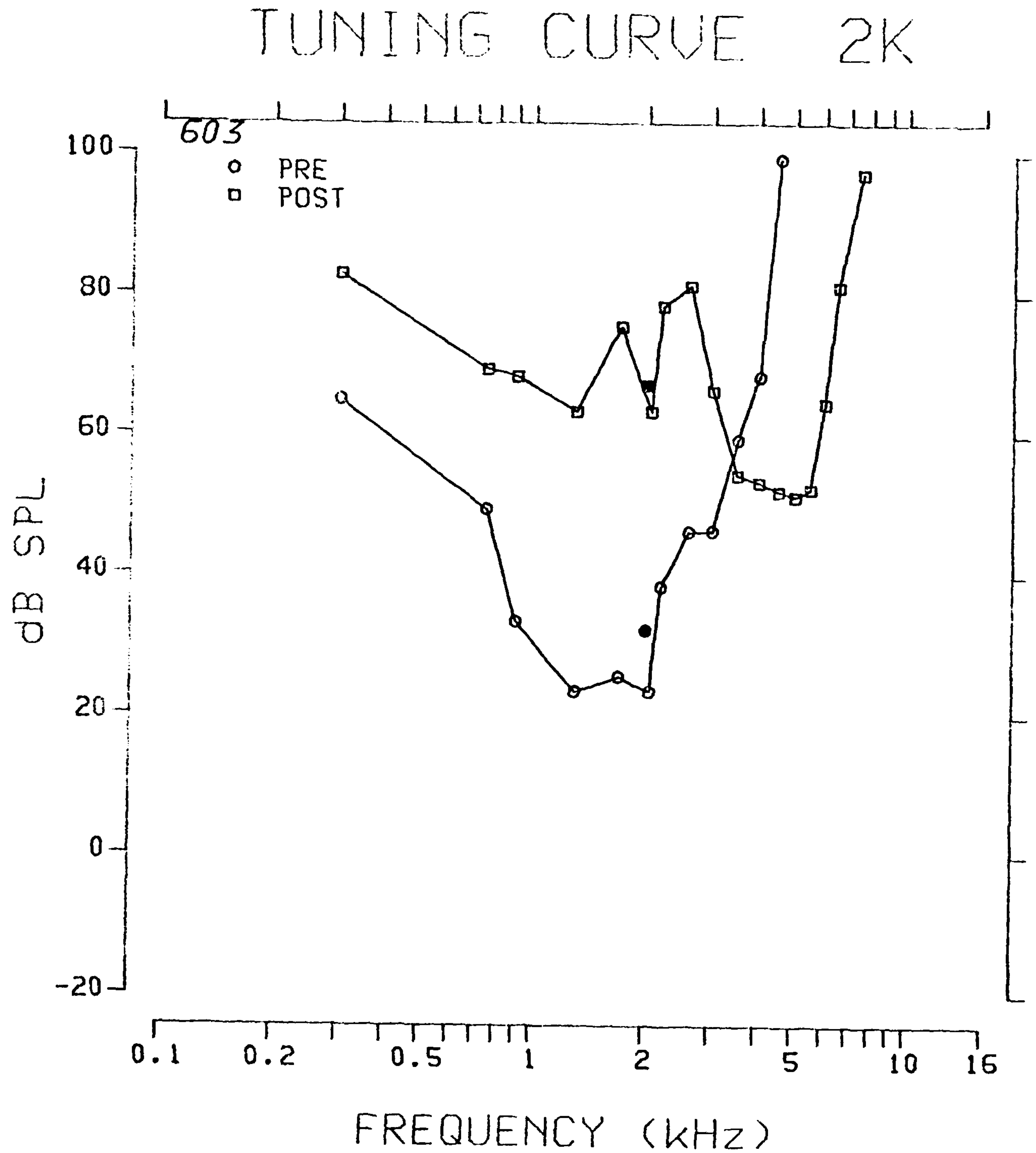


Fig. 3.3.120: Pre- and postexposure evoked response tuning curves at 2.0 kHz from chinchilla 603.

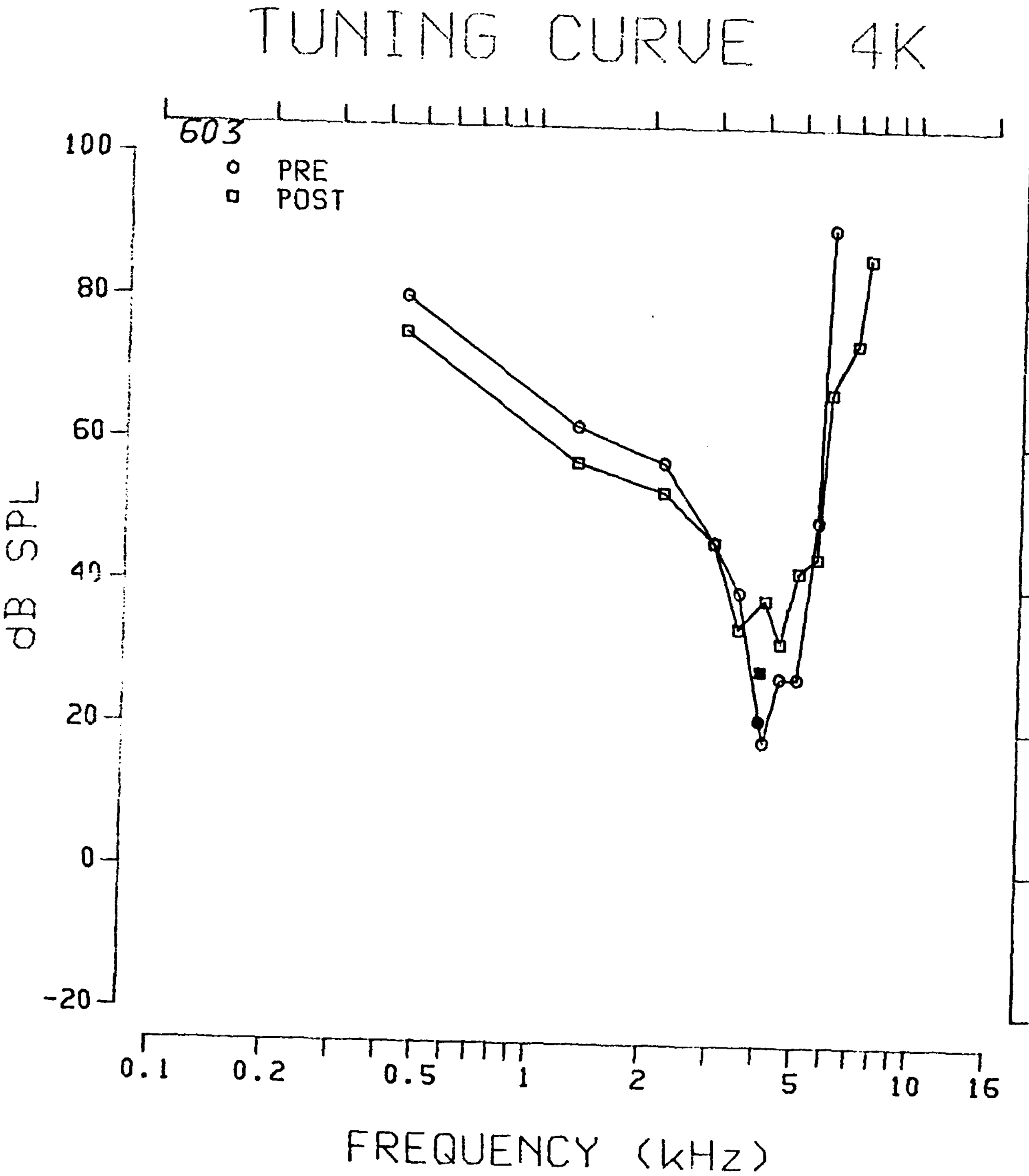


Fig. 3.3.121: Pre- and postexposure evoked response tuning curves at 4.0 kHz from chinchilla 603.

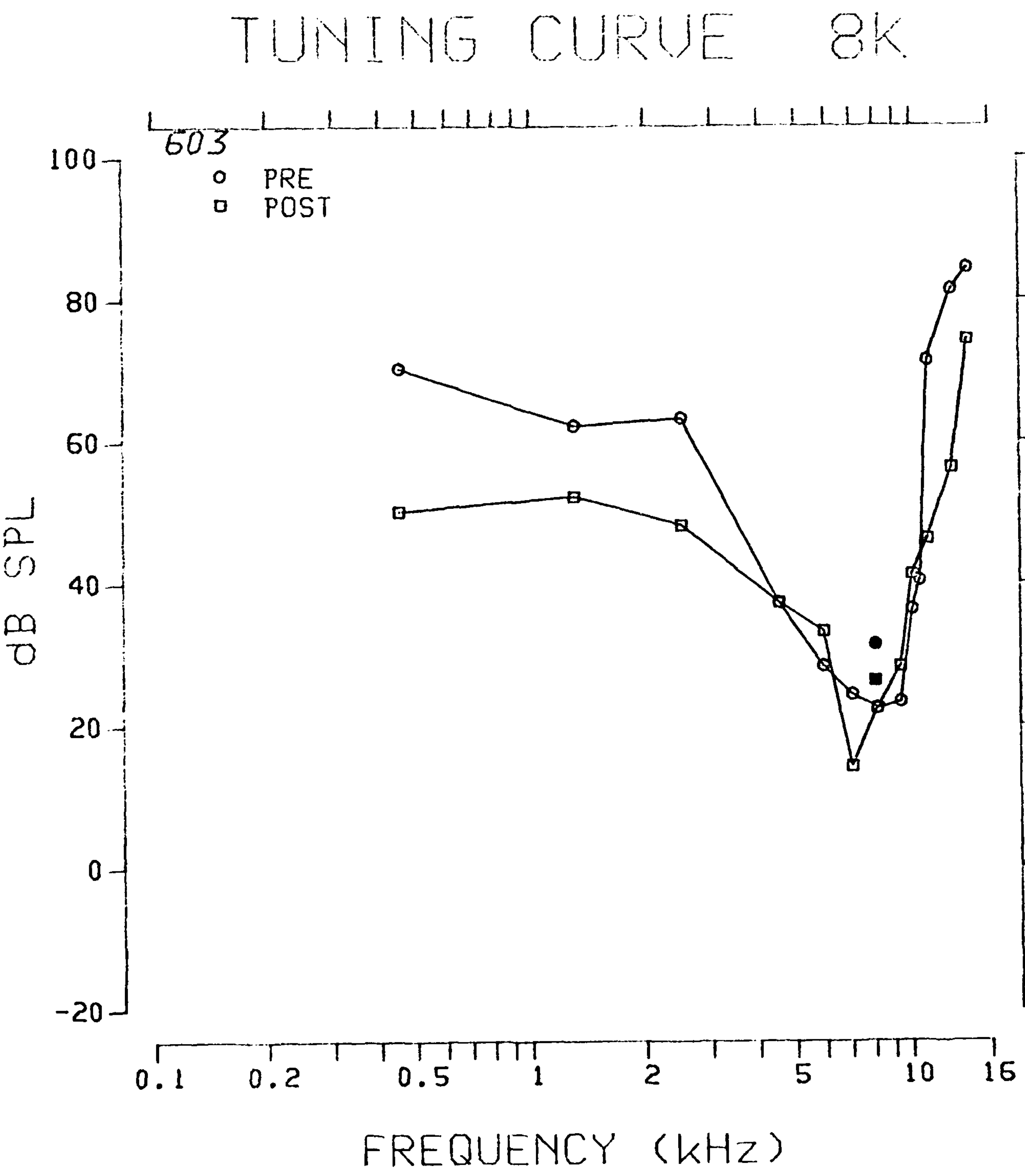


Fig. 3.3.122: Pre- and postexposure evoked response tuning curves at 8.0 kHz from chinchilla 603.

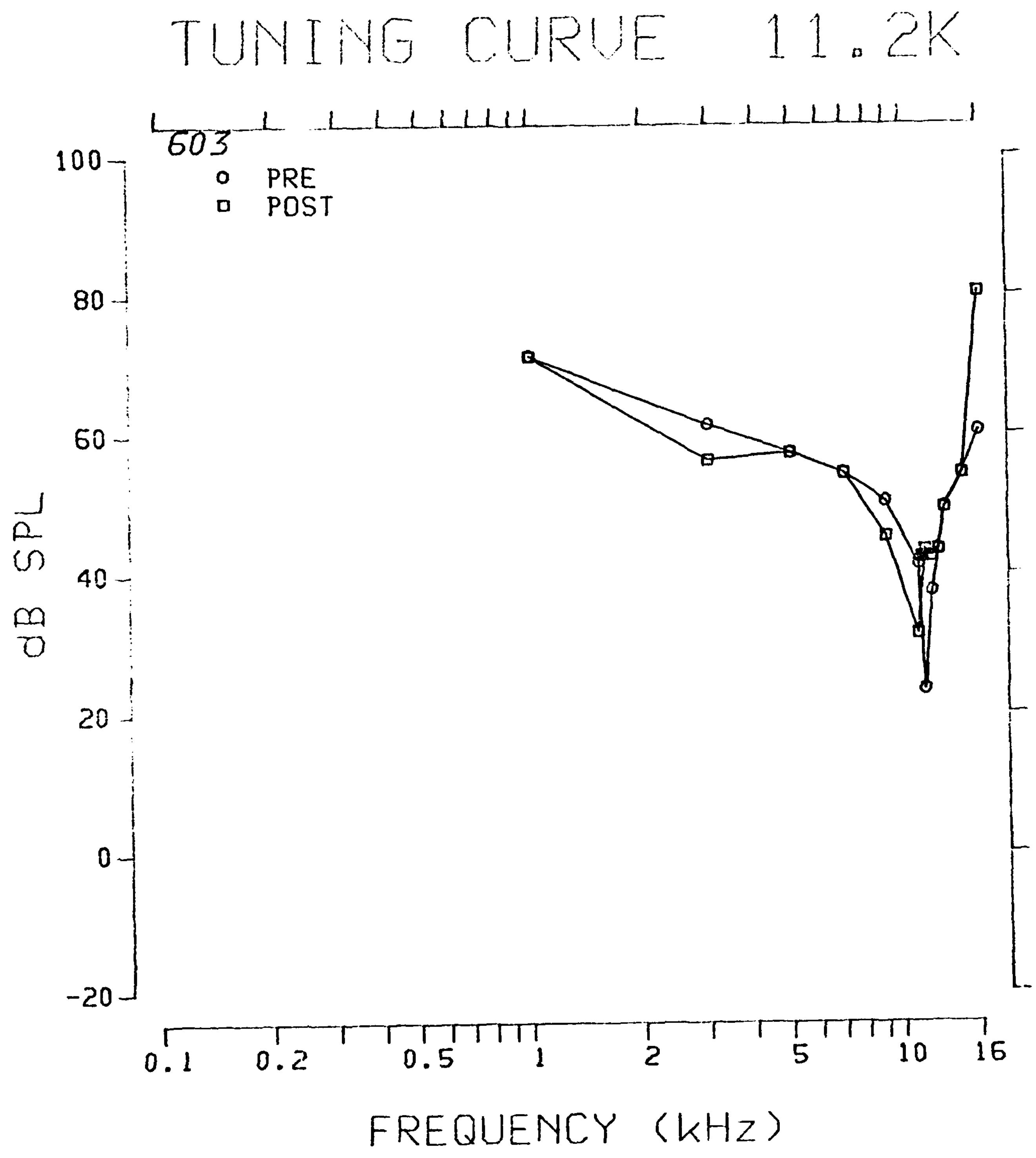


Fig. 3.3.123: Pre- and postexposure evoked response tuning curves at 11.2 kHz from chinchilla 603.

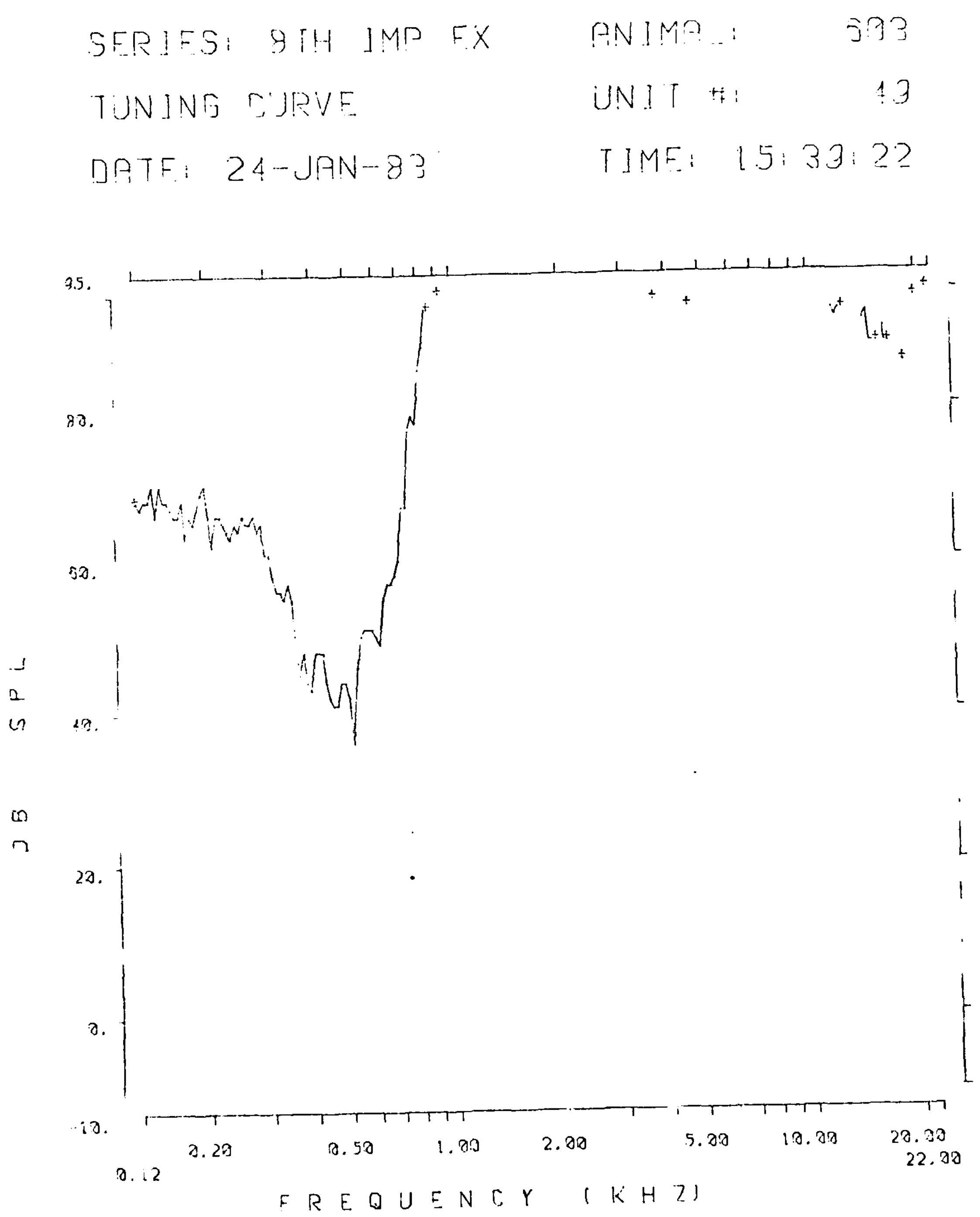


Fig. 3.3.124: Auditory nerve fiber tuning curve from chinchilla 603.

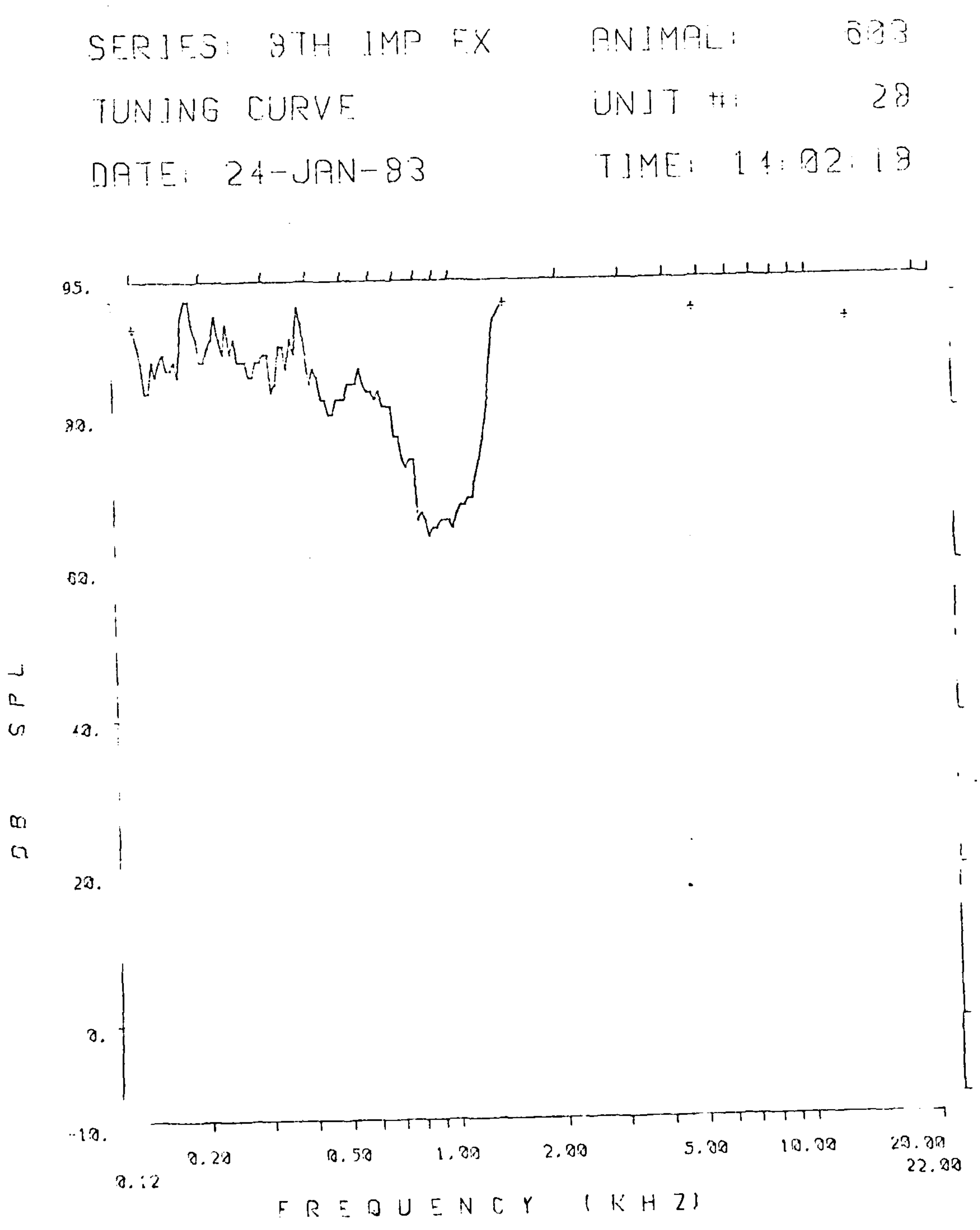


Fig. 3.3.125: Auditory nerve fiber tuning curve from chinchilla 603.

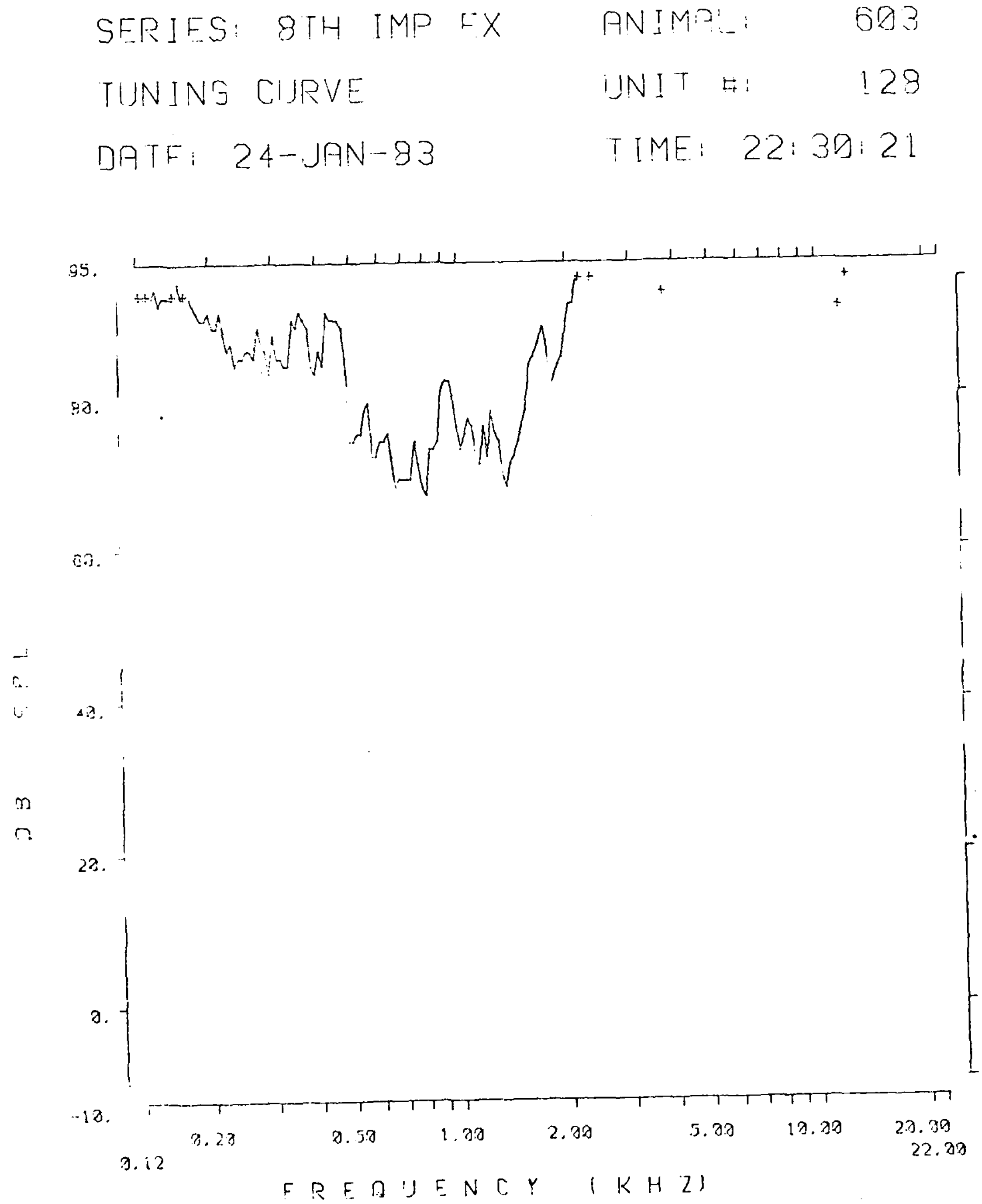


Fig. 3.3.126: Auditory nerve fiber tuning curve from chinchilla 603.

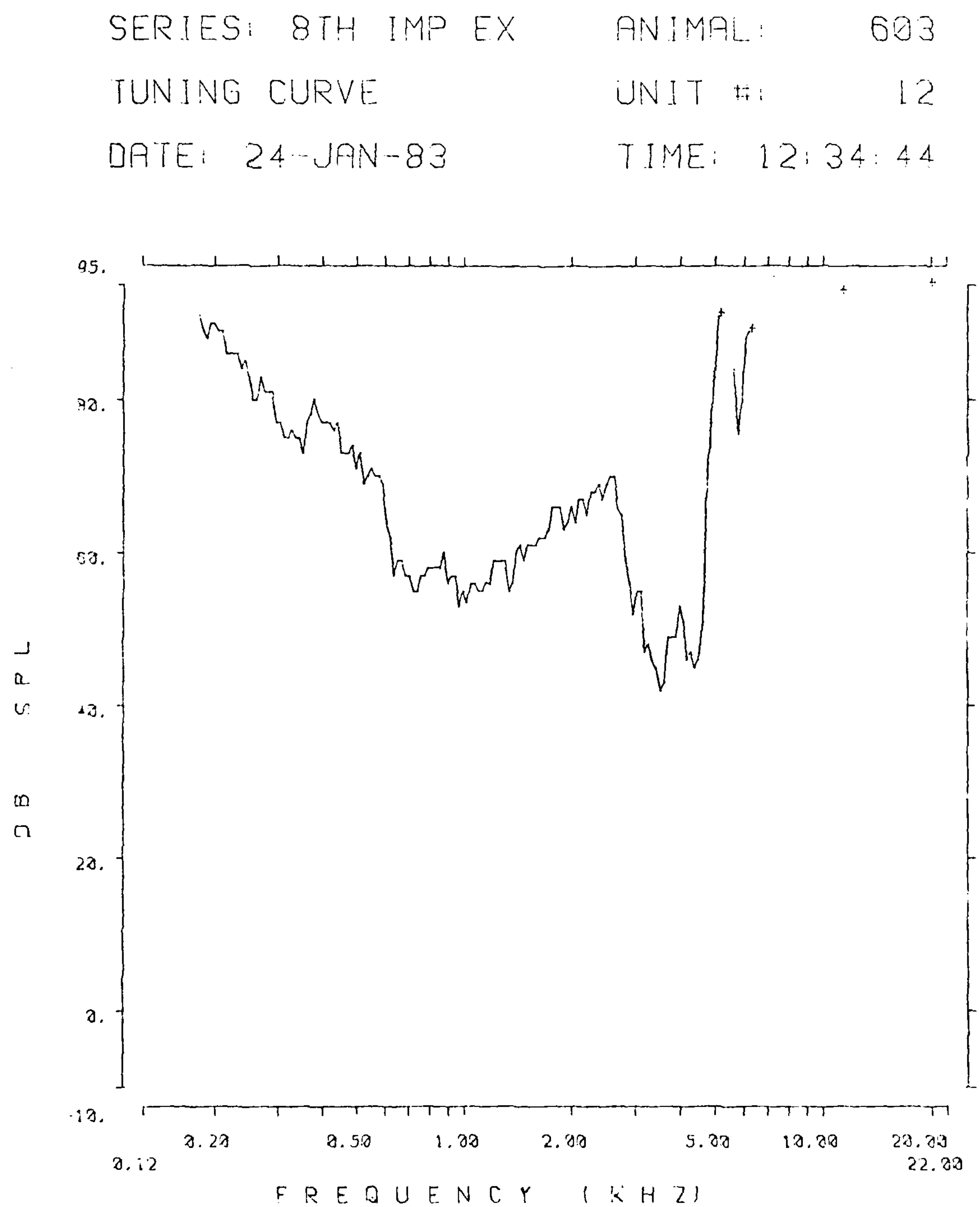


Fig. 3.3.127: Auditory nerve fiber tuning curve from chinchilla 603.

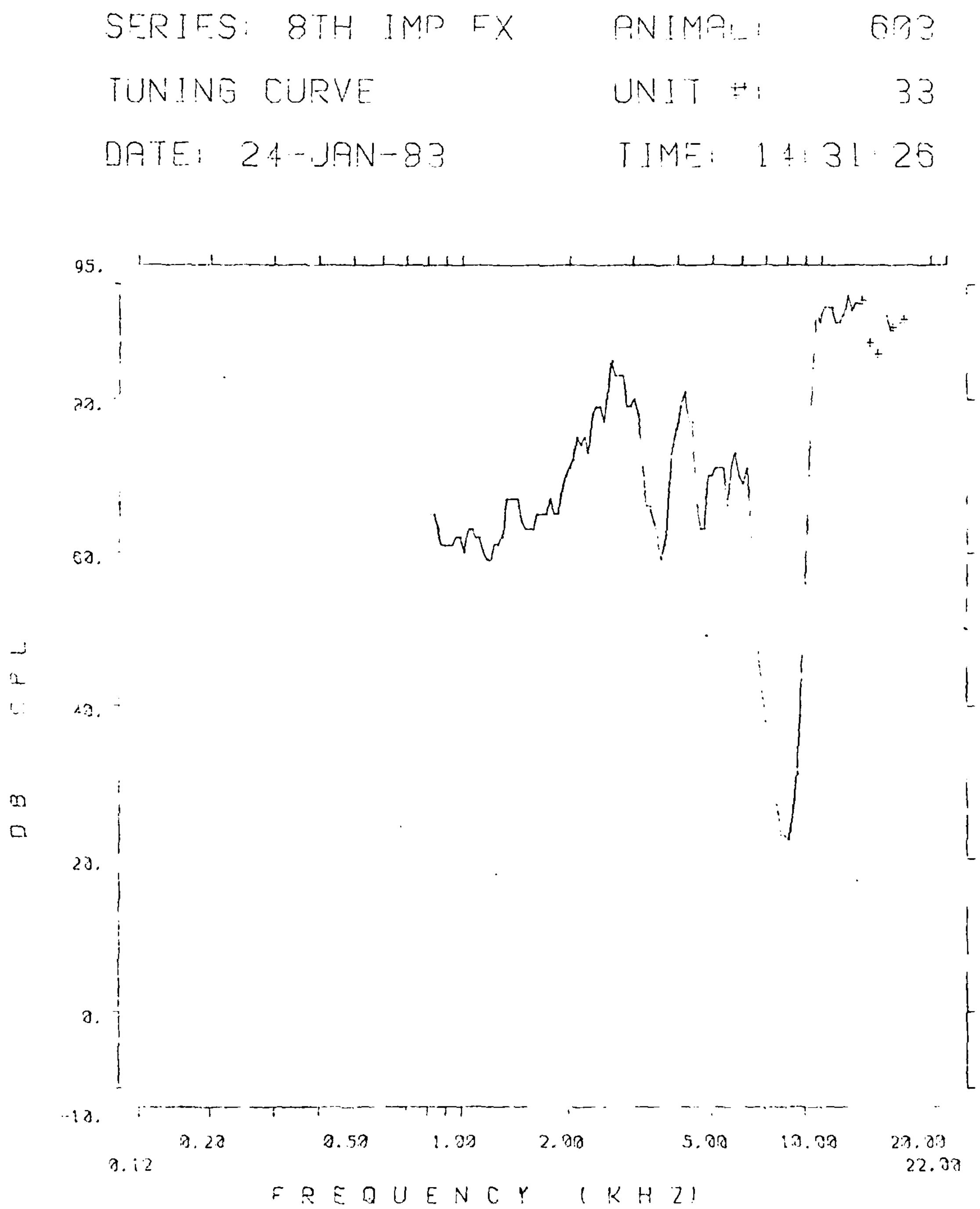


Fig. 3.3.128: Auditory nerve fiber tuning curve from chinchilla 603.

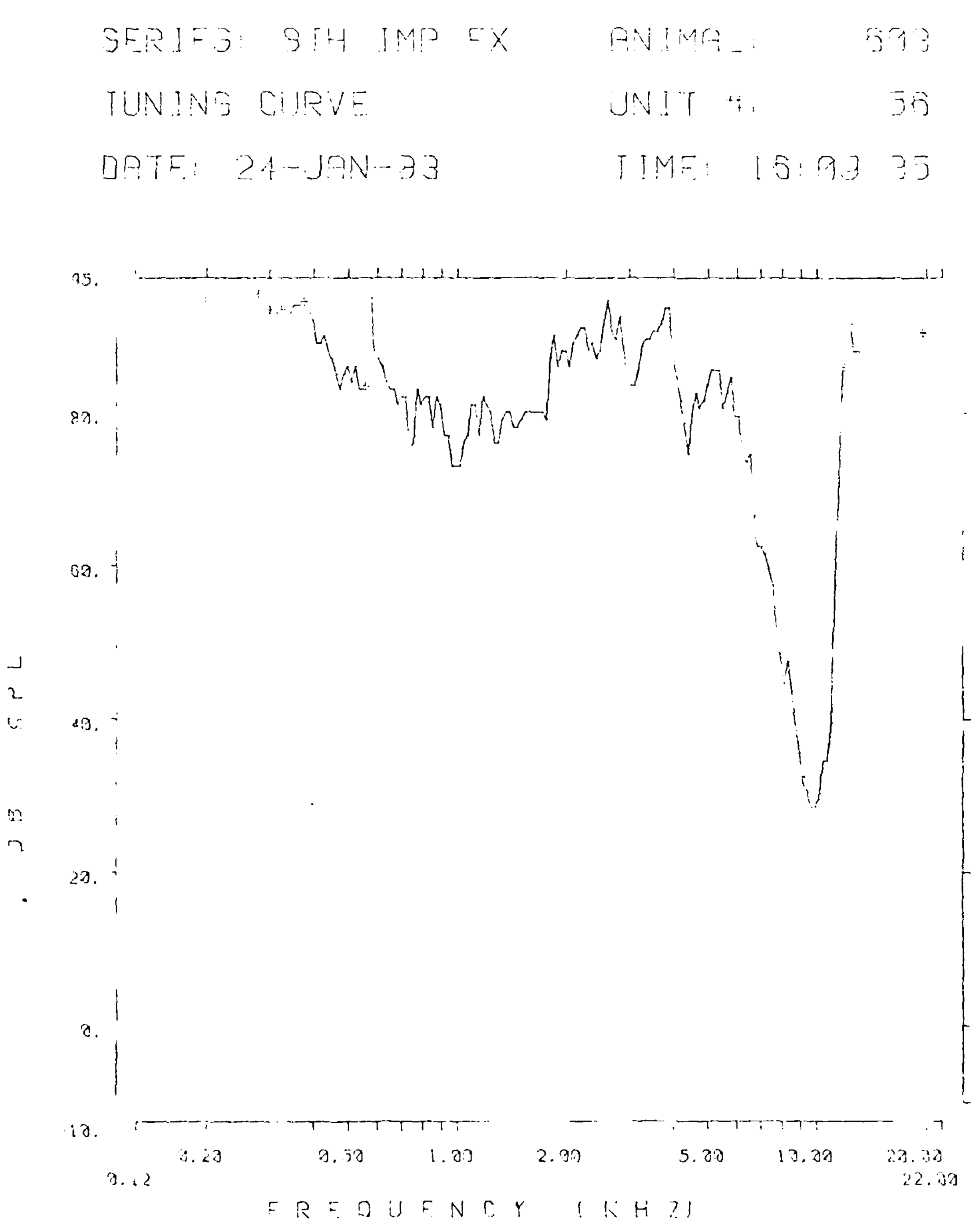


Fig. 3.3.129: Auditory nerve fiber tuning curve from chinchilla 603.

AD-A172 467 BLAST TRAUMA THE EFFECT ON HEARING(U) TEXAS UNIV AT DALLAS CALLIER CENTER FOR COMMUNICATION DISORDERS R P HAMERNIK ET AL. JUL 83 DAMD17-80-C-0133



UNCLASSIFIED F/G 6/19 NL

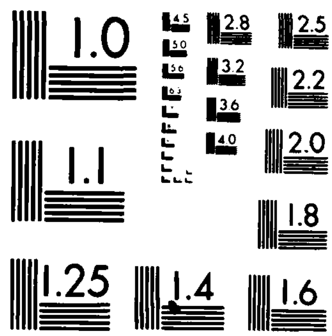


MICROCOPY RESOLUTION TEST CHART
NATIONAL BUREAU OF STANDARDS-1963-A

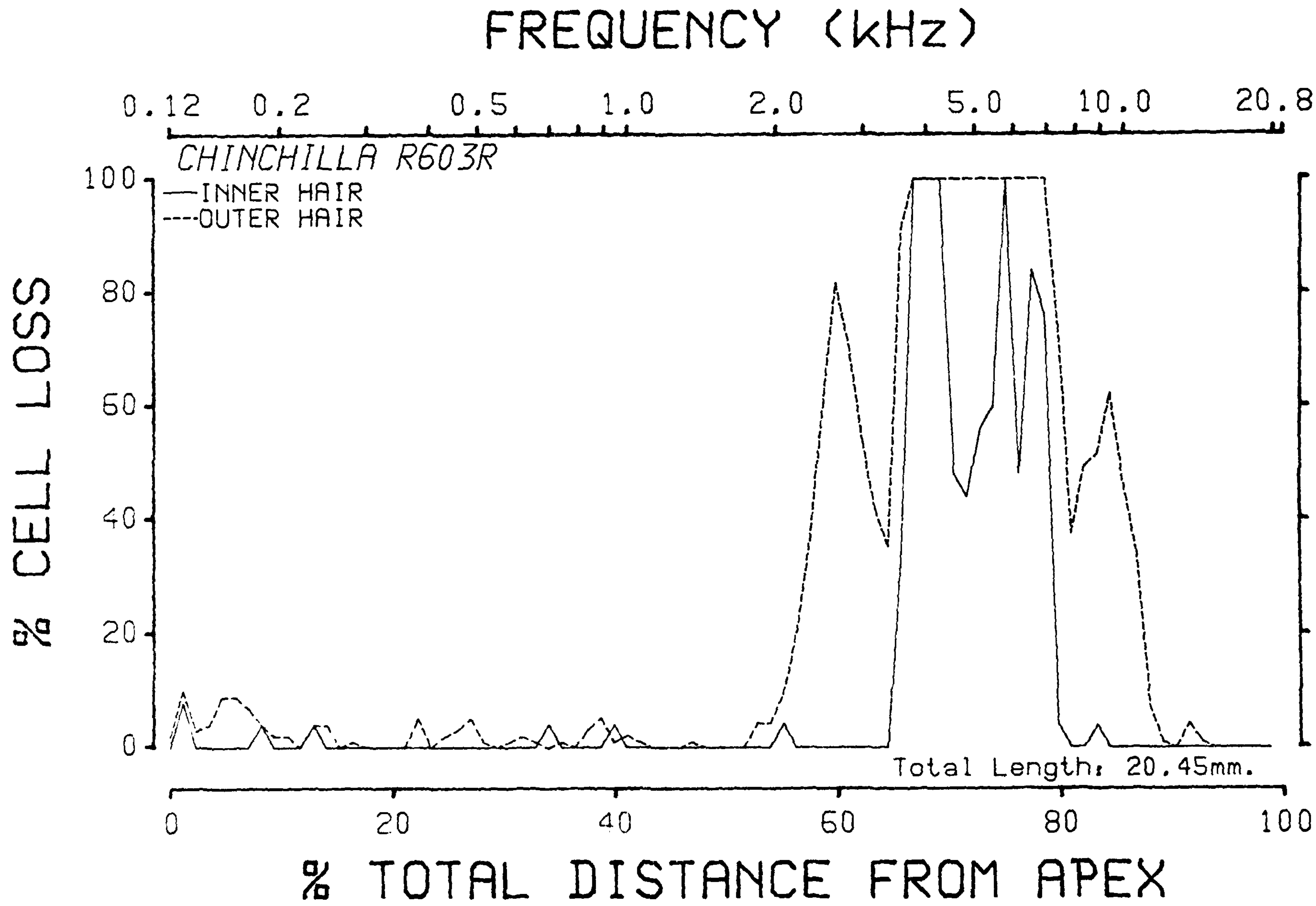


Fig. 3.3.130: Cochleogram of chinchilla 603

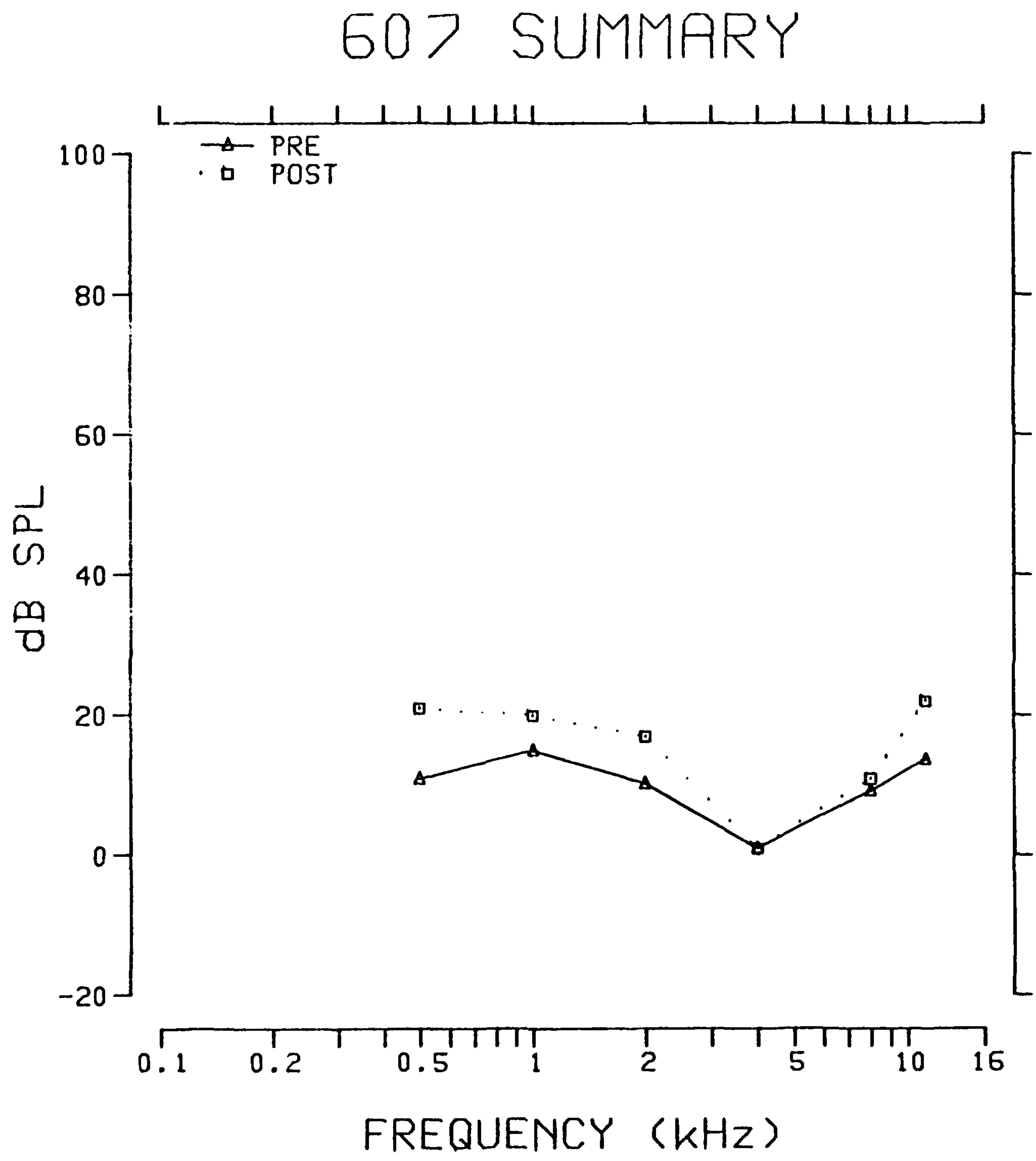


Fig. 3.3.131: Pre- and postexposure evoked response audiograms for chinchilla 607.

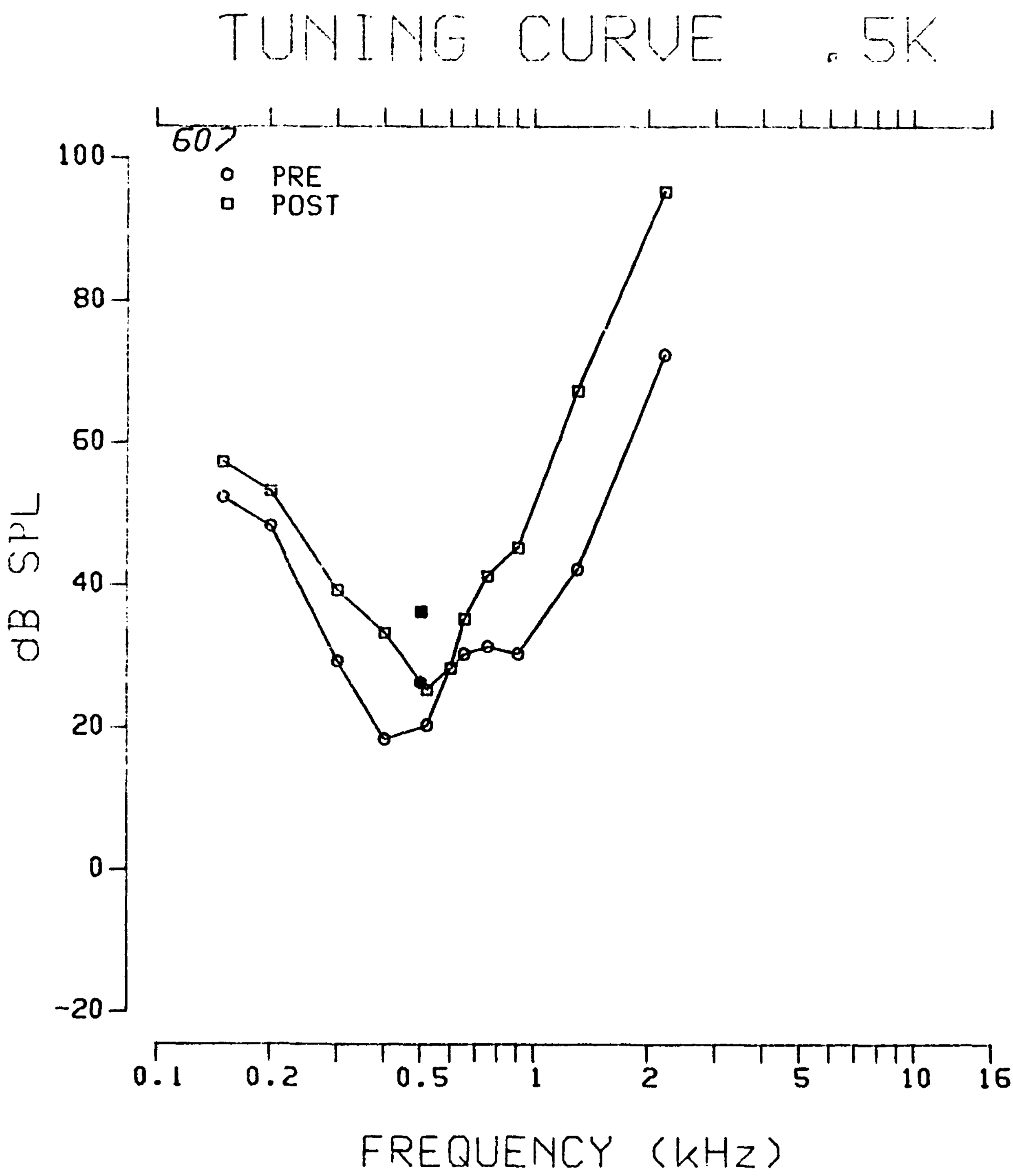


Fig. 3.3.132: Pre- and postexposure evoked response tuning curves at 0.5 kHz for chinchilla 607.

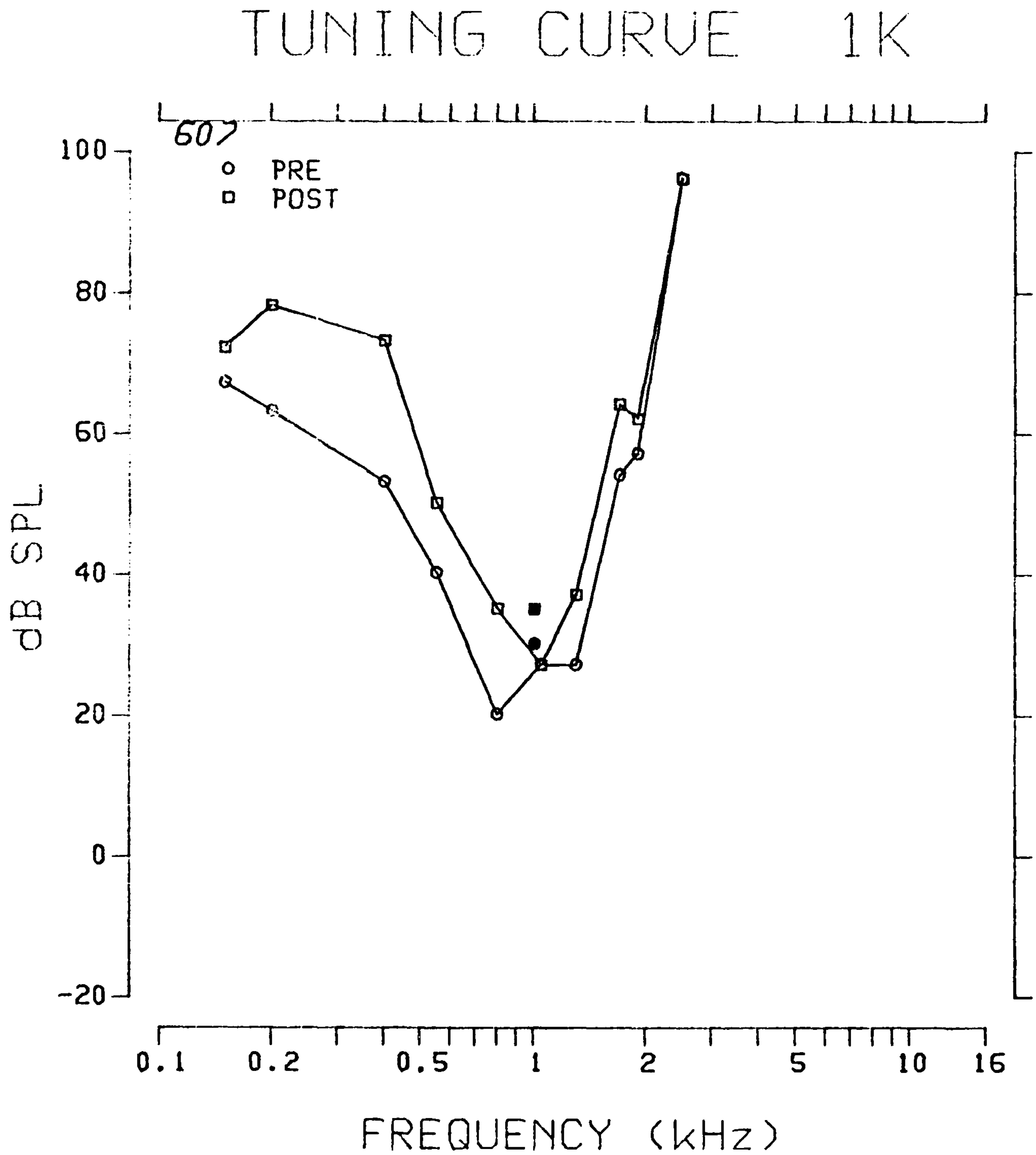


Fig. 3.3.133: Pre- and postexposure evoked response tuning curves at 1.0 kHz for chinchilla 607.

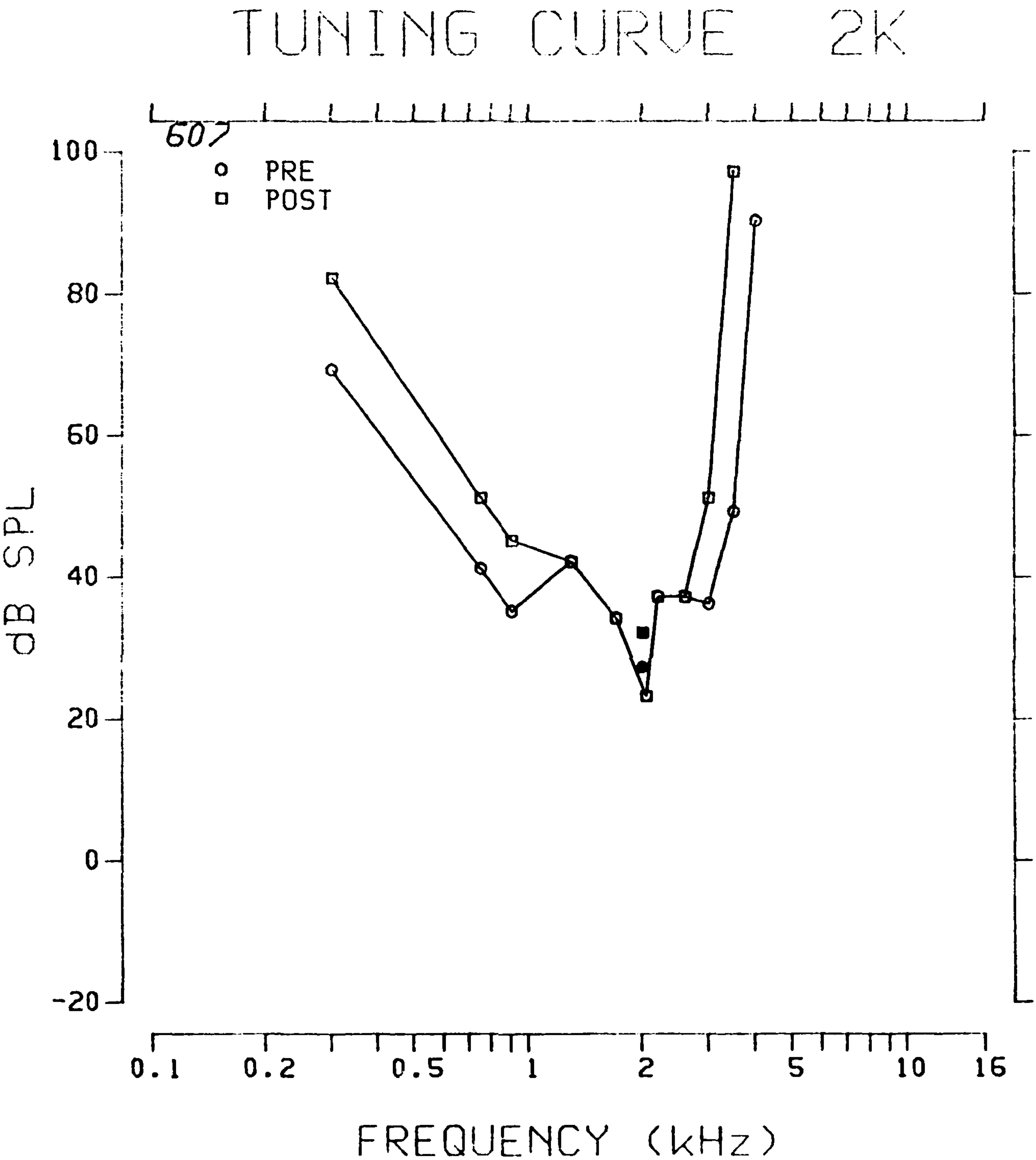


Fig. 3.3.134: Pre- and postexposure evoked response tuning curves at _.0 kHz for chinchilla 607.

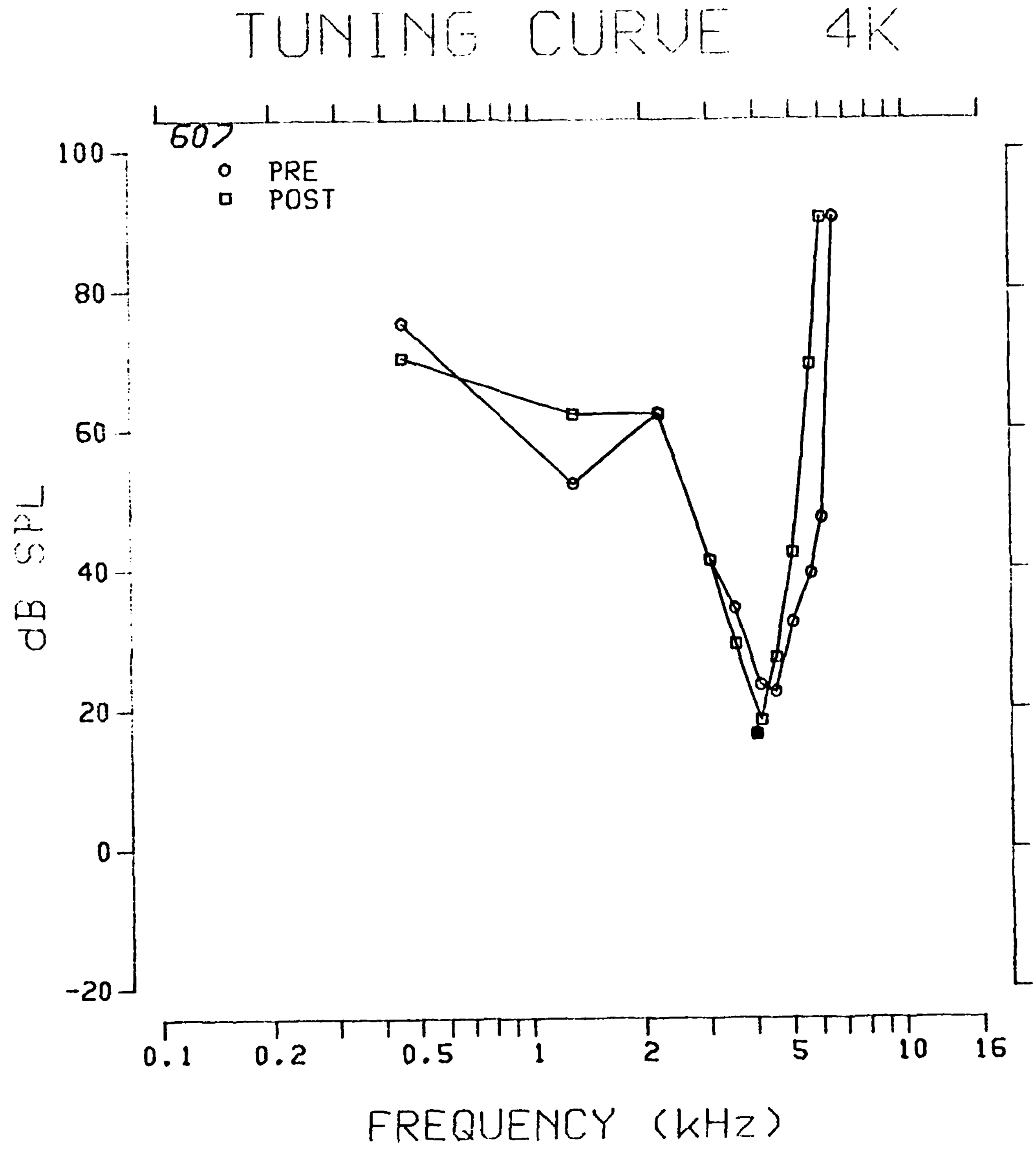


Fig. 3.3.135: Pre- and postexposure evoked response tuning curves at 4.0 kHz for chinchilla 607.

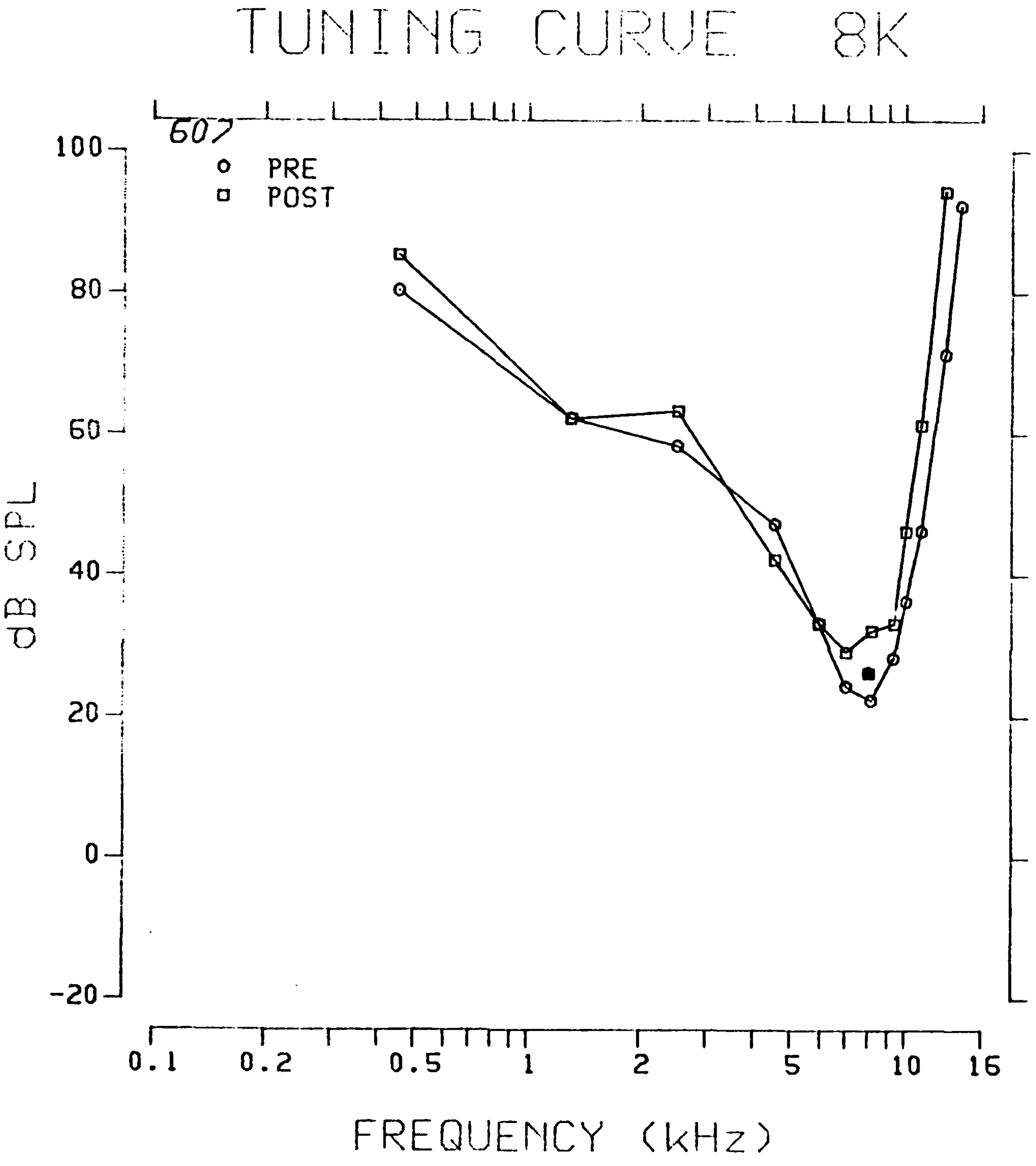


Fig. 3.3.136: Pre- and postexposure evoked response tuning curves at 8.0 kHz for chinchilla 607.

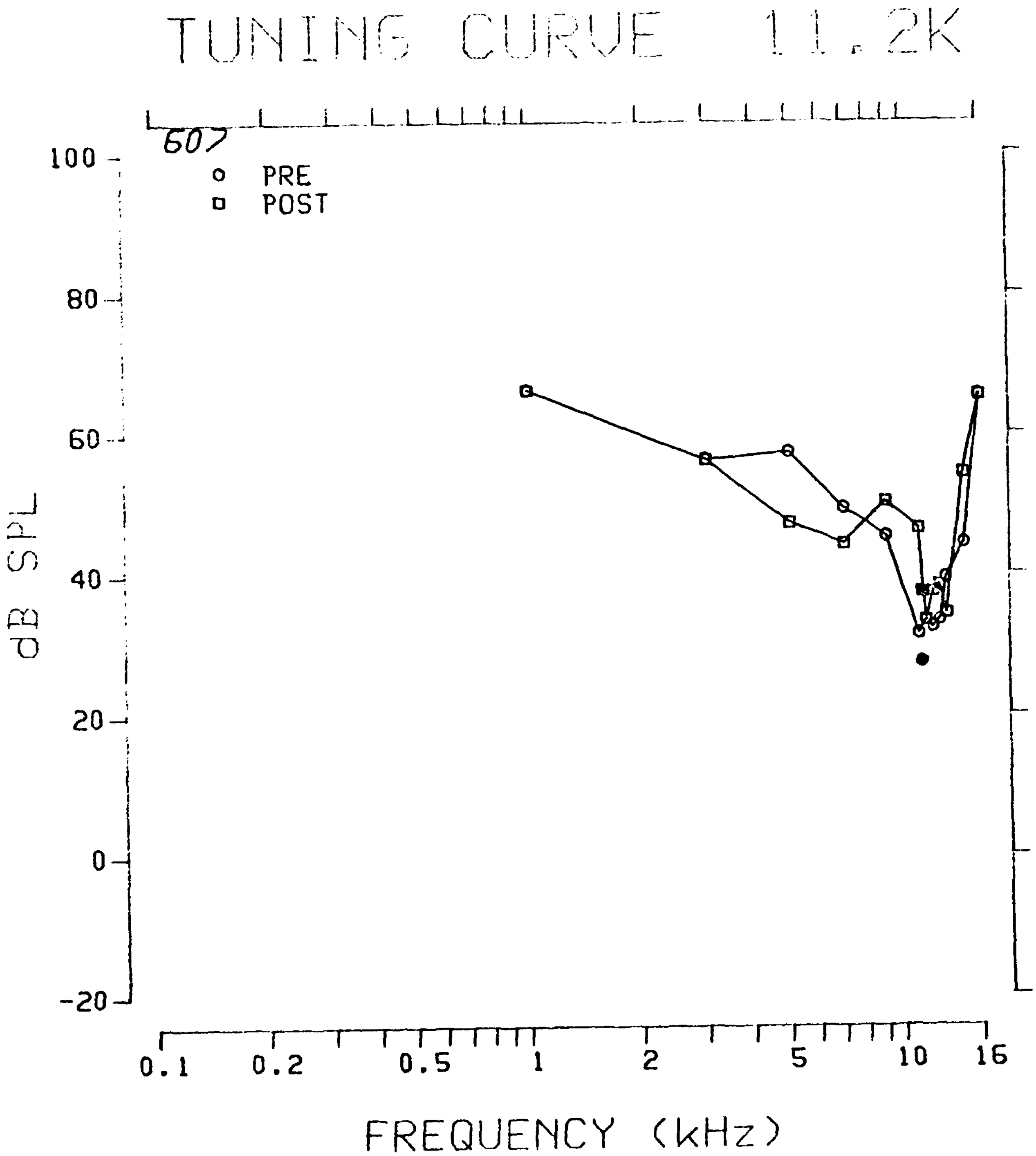


Fig. 3.3.137: Pre- and postexposure evoked response tuning curves at 11.2 kHz for chinchilla 607.

( 324 )

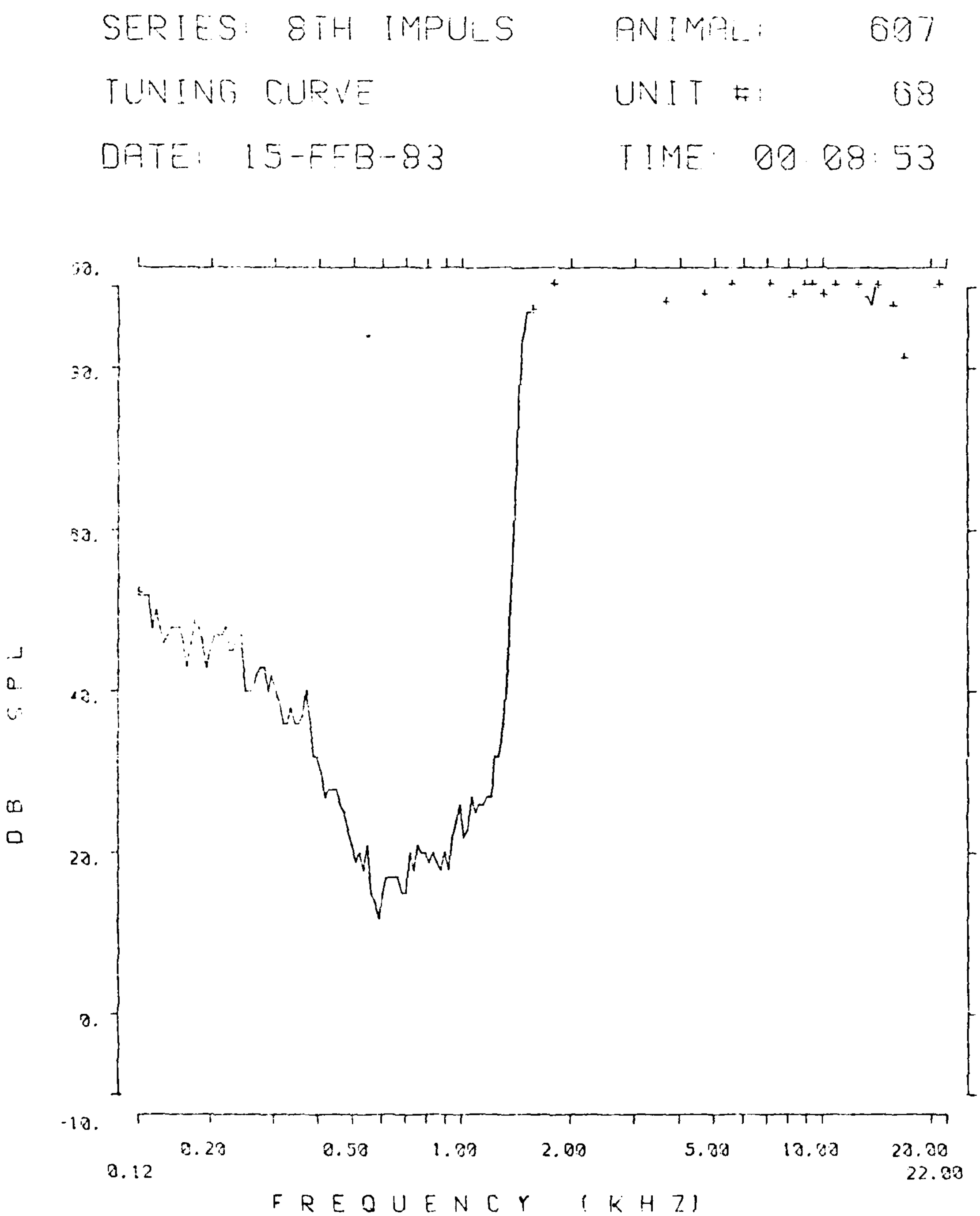


Fig. 3.3.138: Auditory nerve fiber tuning curve from chinchilla 607.

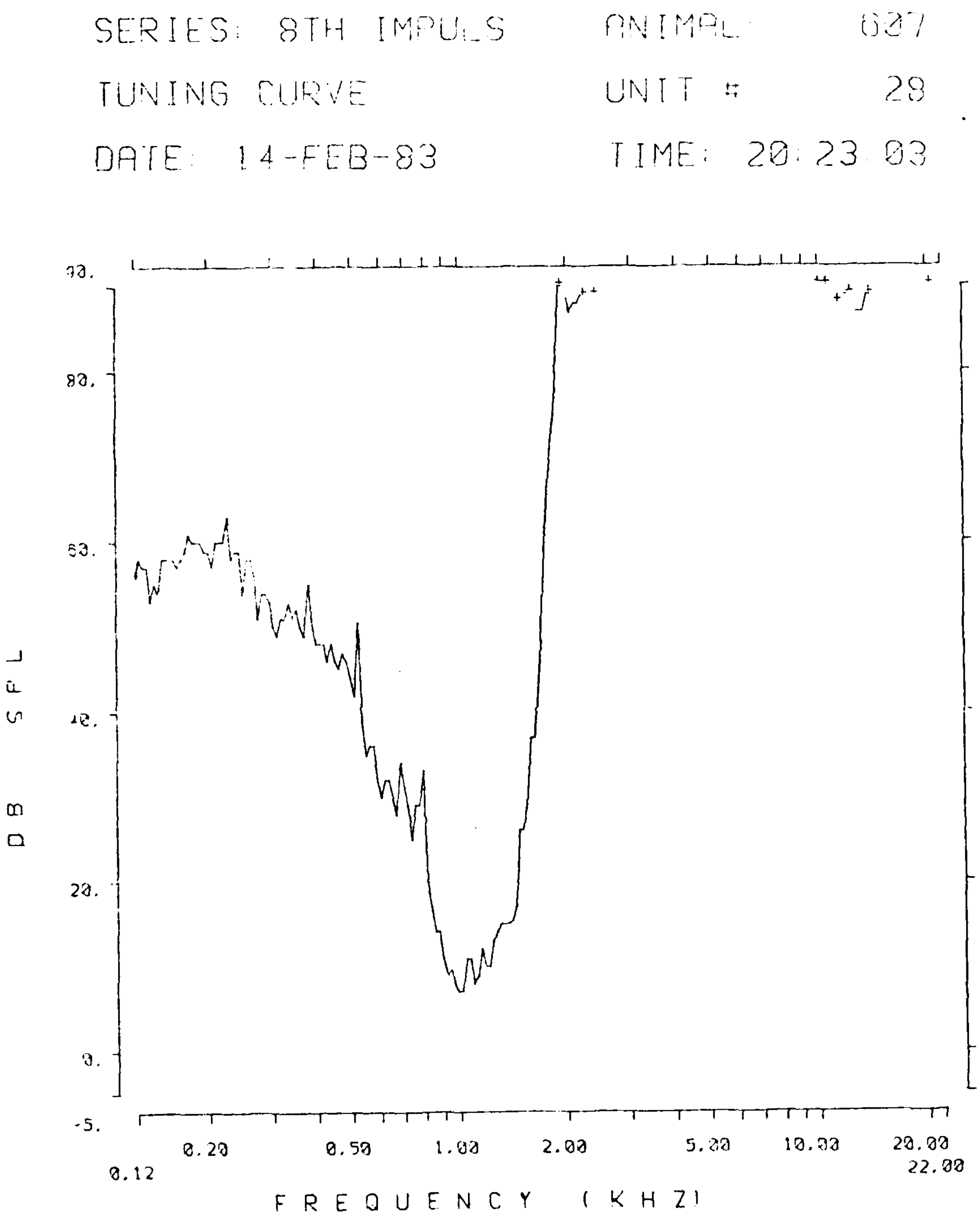


Fig. 3.3.139: Auditory nerve fiber tuning curve from chinchilla 607.

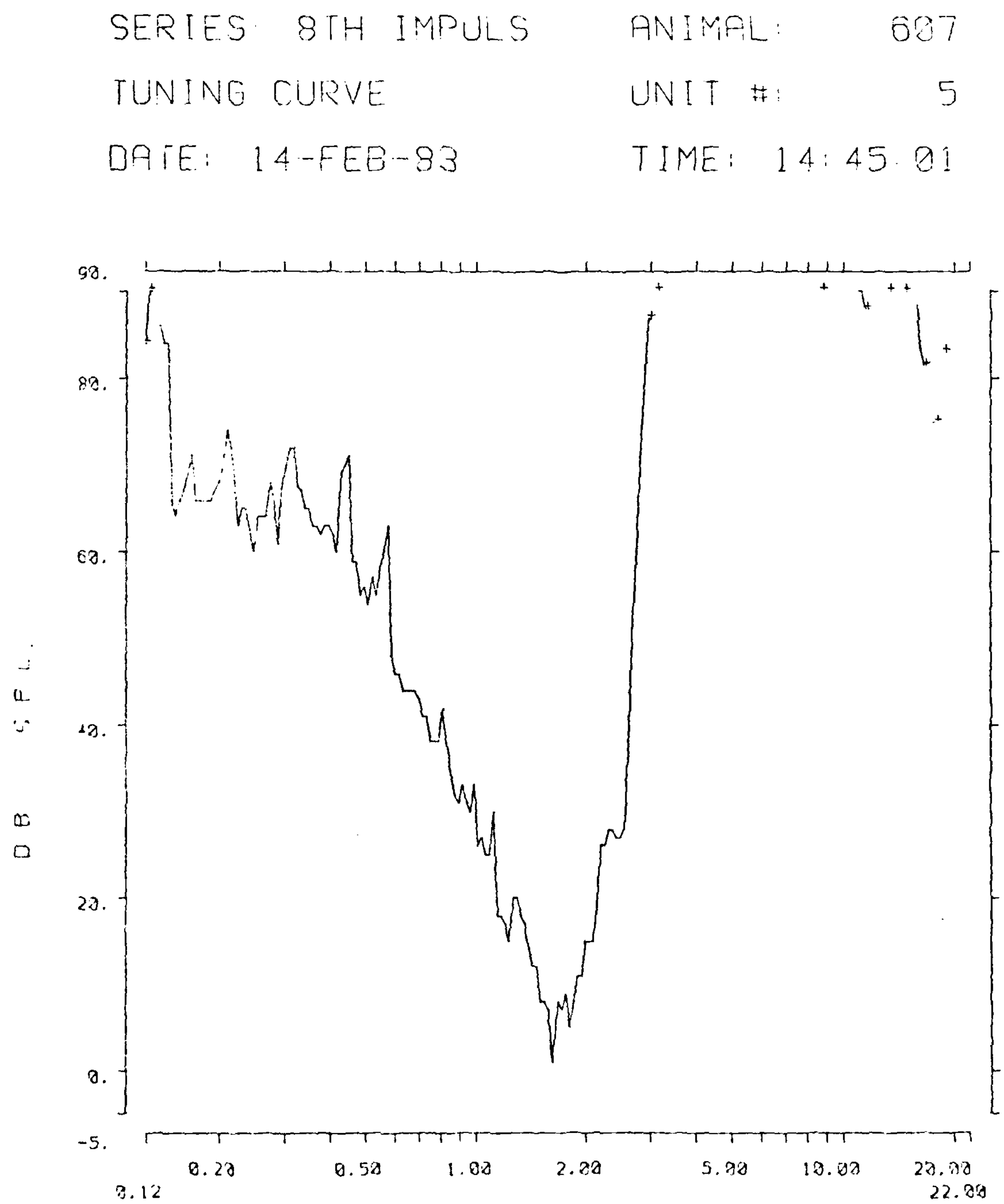


Fig. 3.3.140: Auditory nerve fiber tuning curve from chinchilla 607.

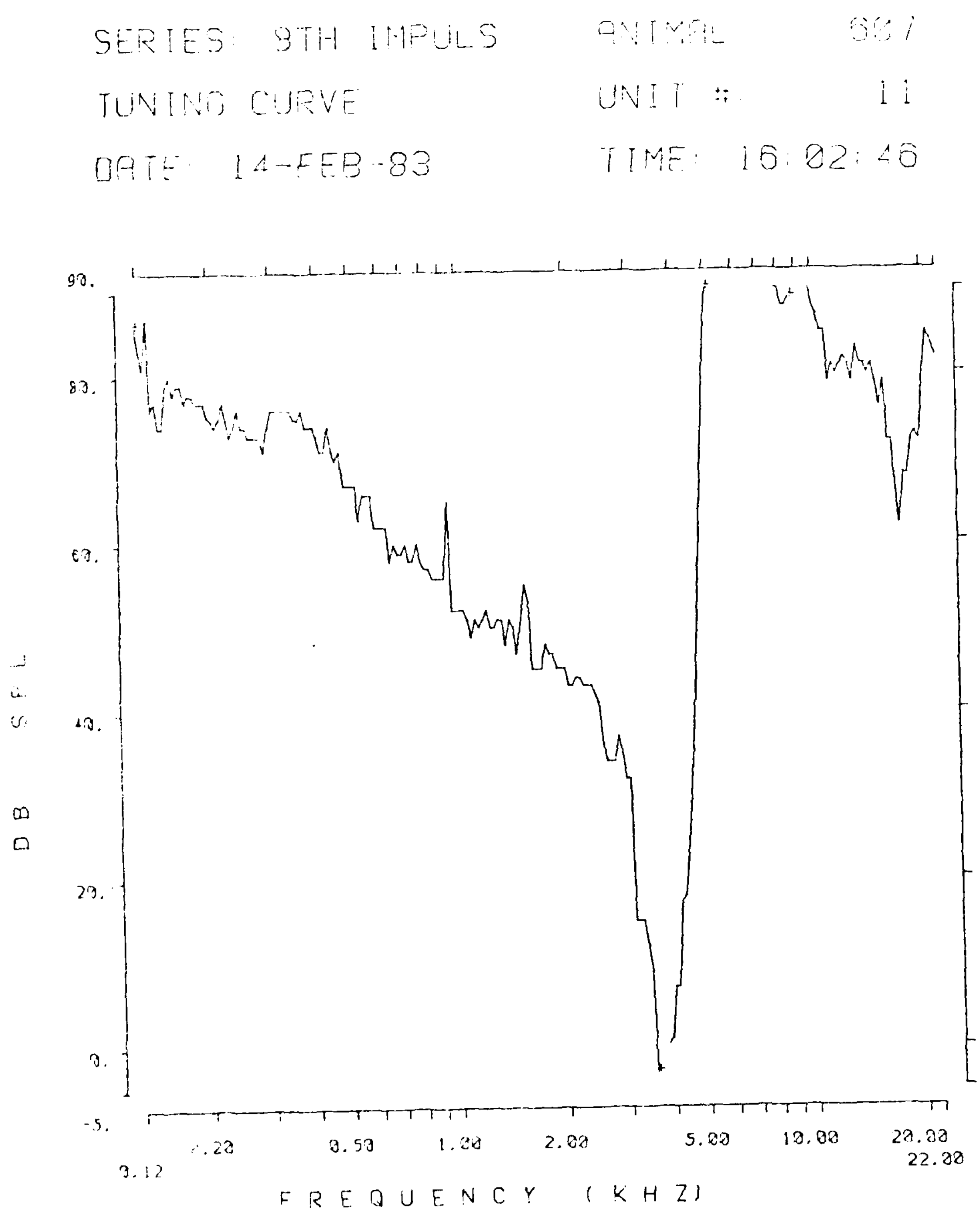


Fig. 3.3.141: Auditory nerve fiber tuning curve from chinchilla 607.

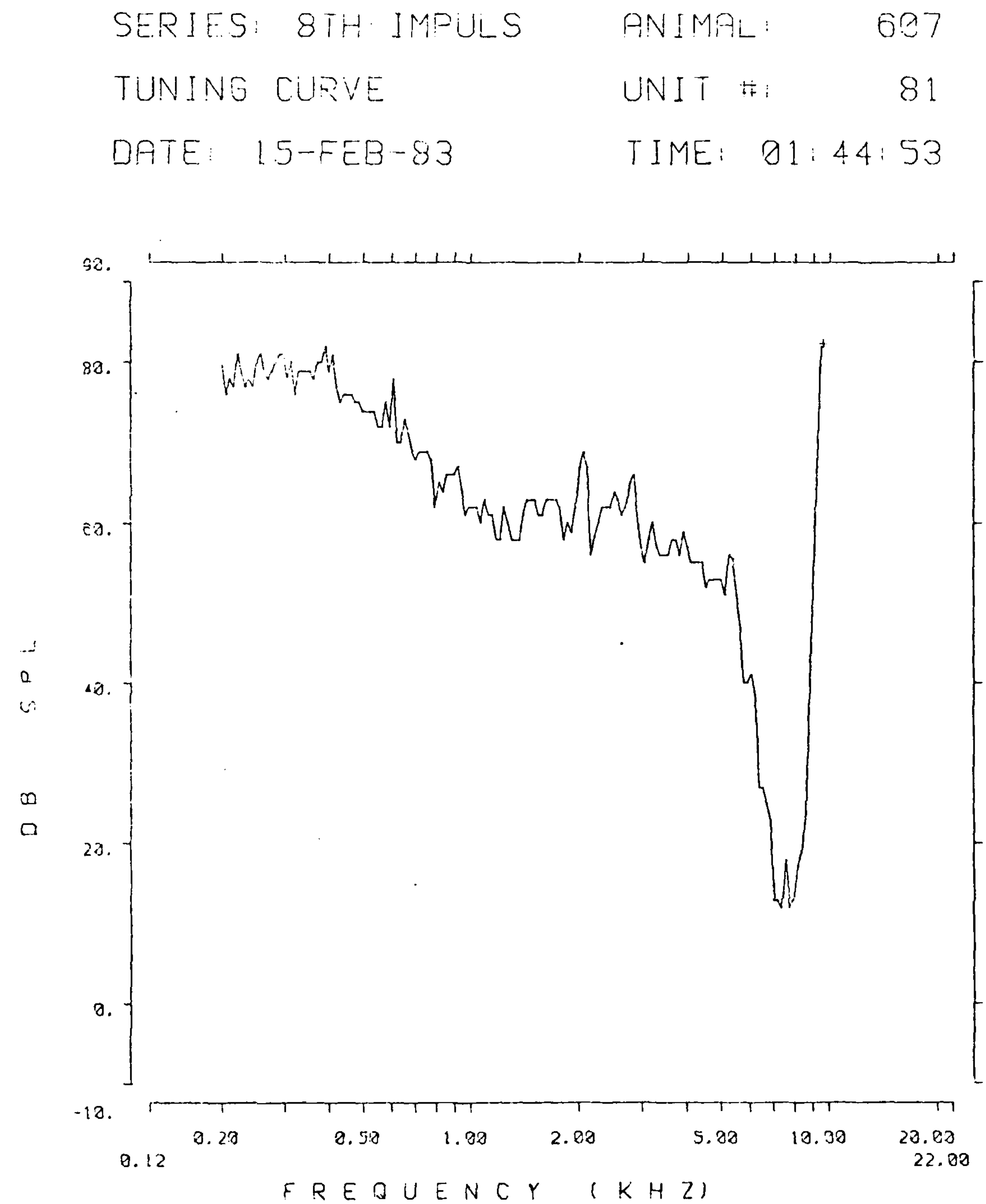


Fig. 3.3.142: Auditory nerve fiber tuning curve from chinchilla 607.

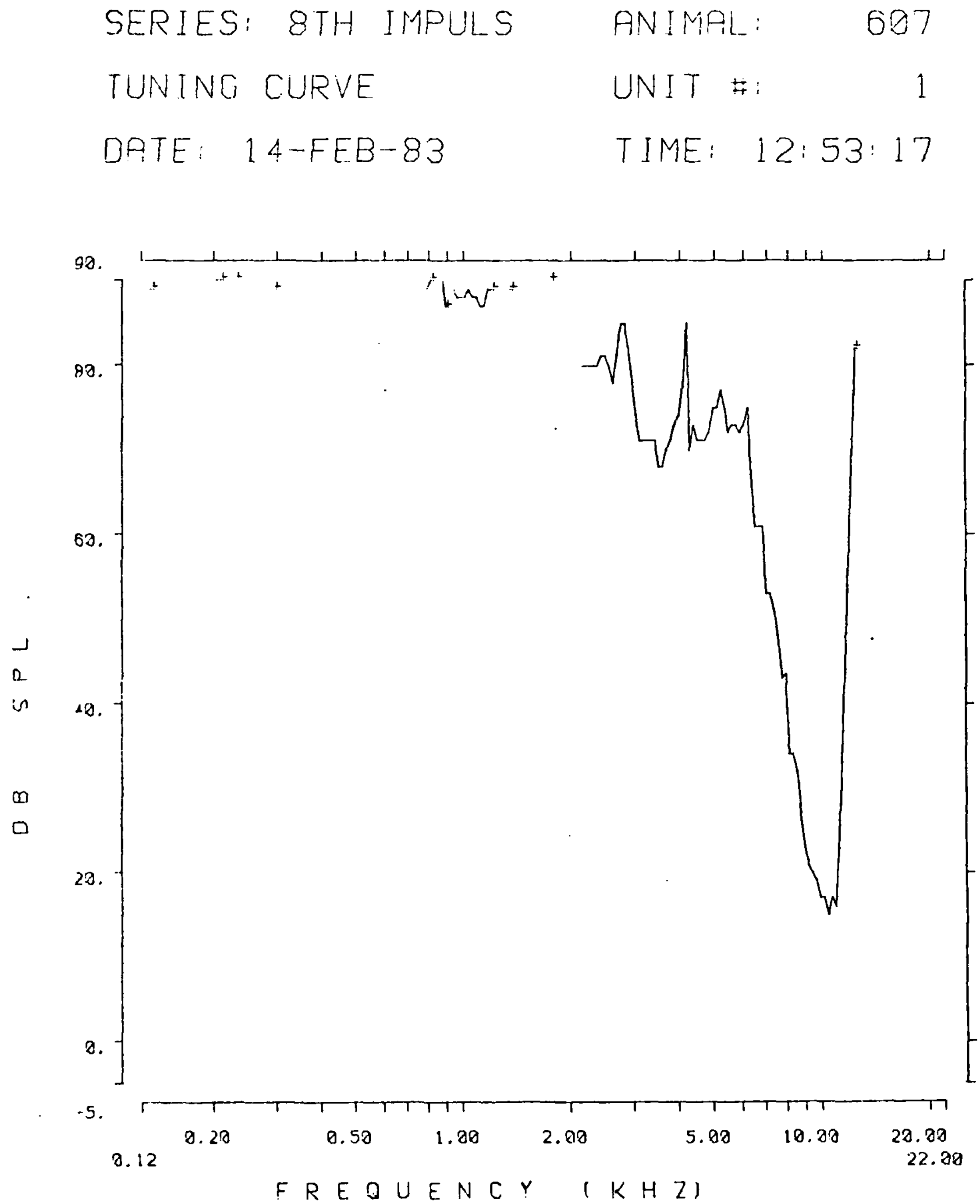


Fig. 3.3.143: Auditory nerve fiber tuning curve from chinchilla 607.

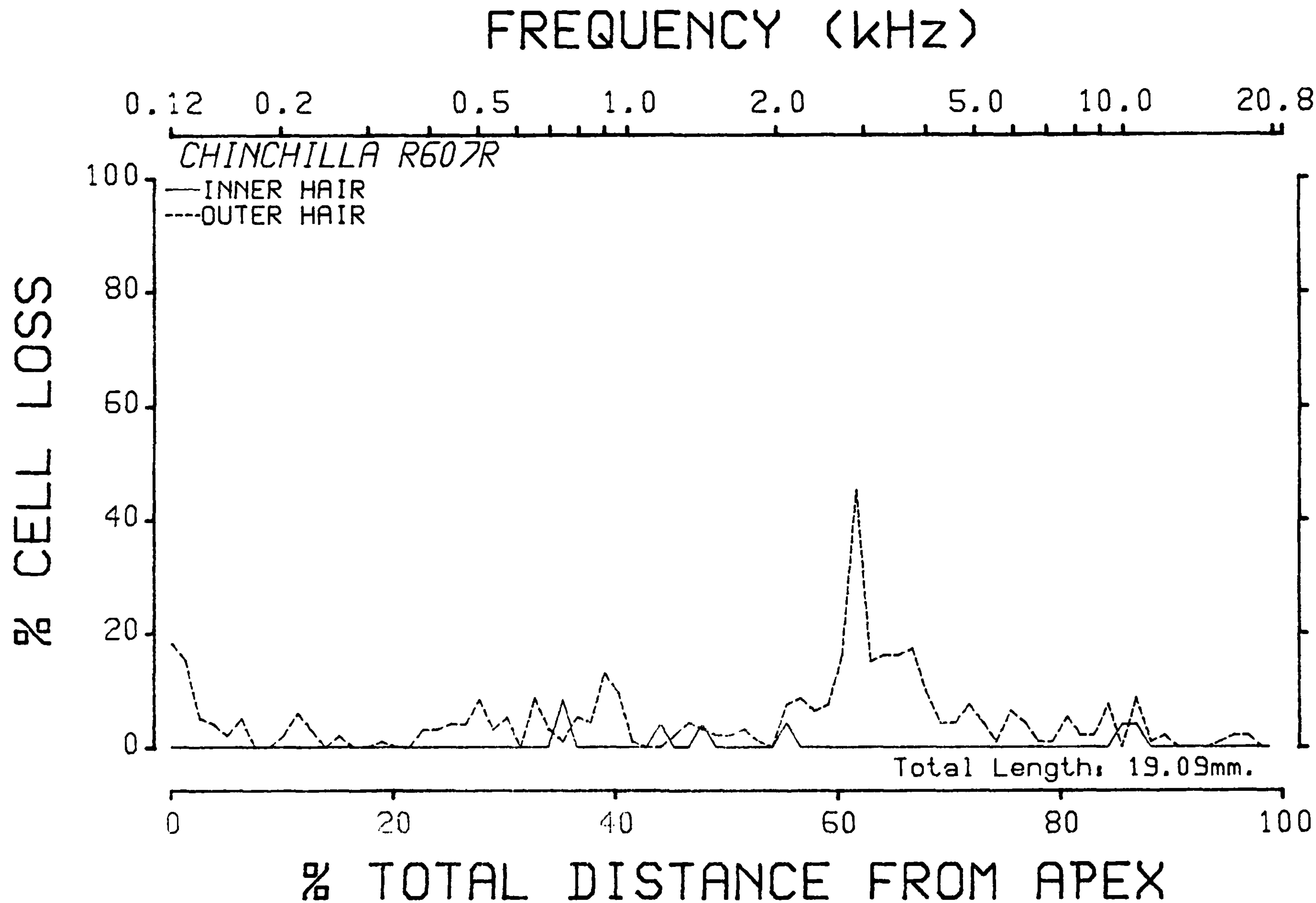


Fig. 3.3.144: Cochleogram from chinchilla 607.

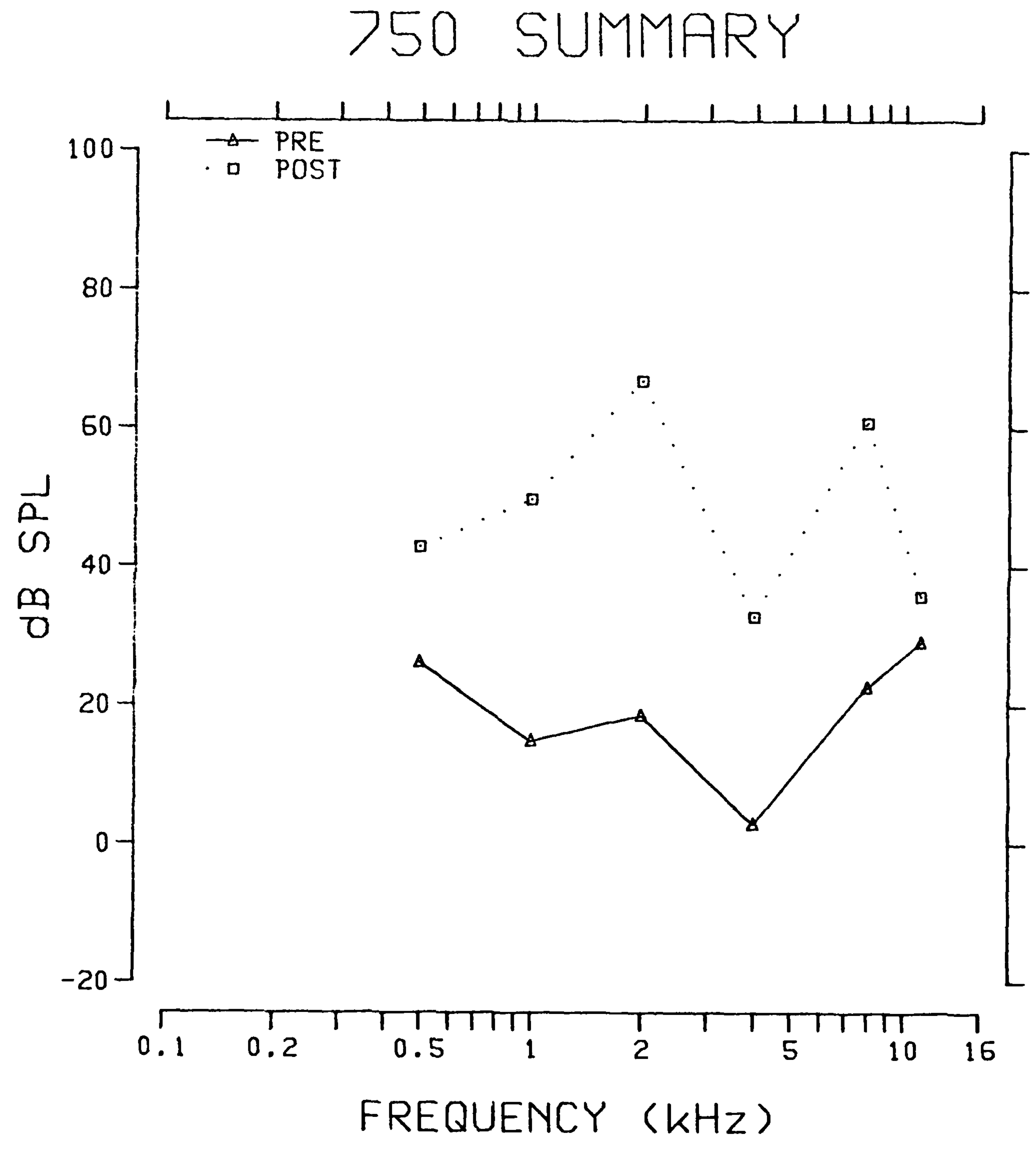


Fig. 3.3.145: Pre- and postexposure evoked response audiograms from chinchilla 750.

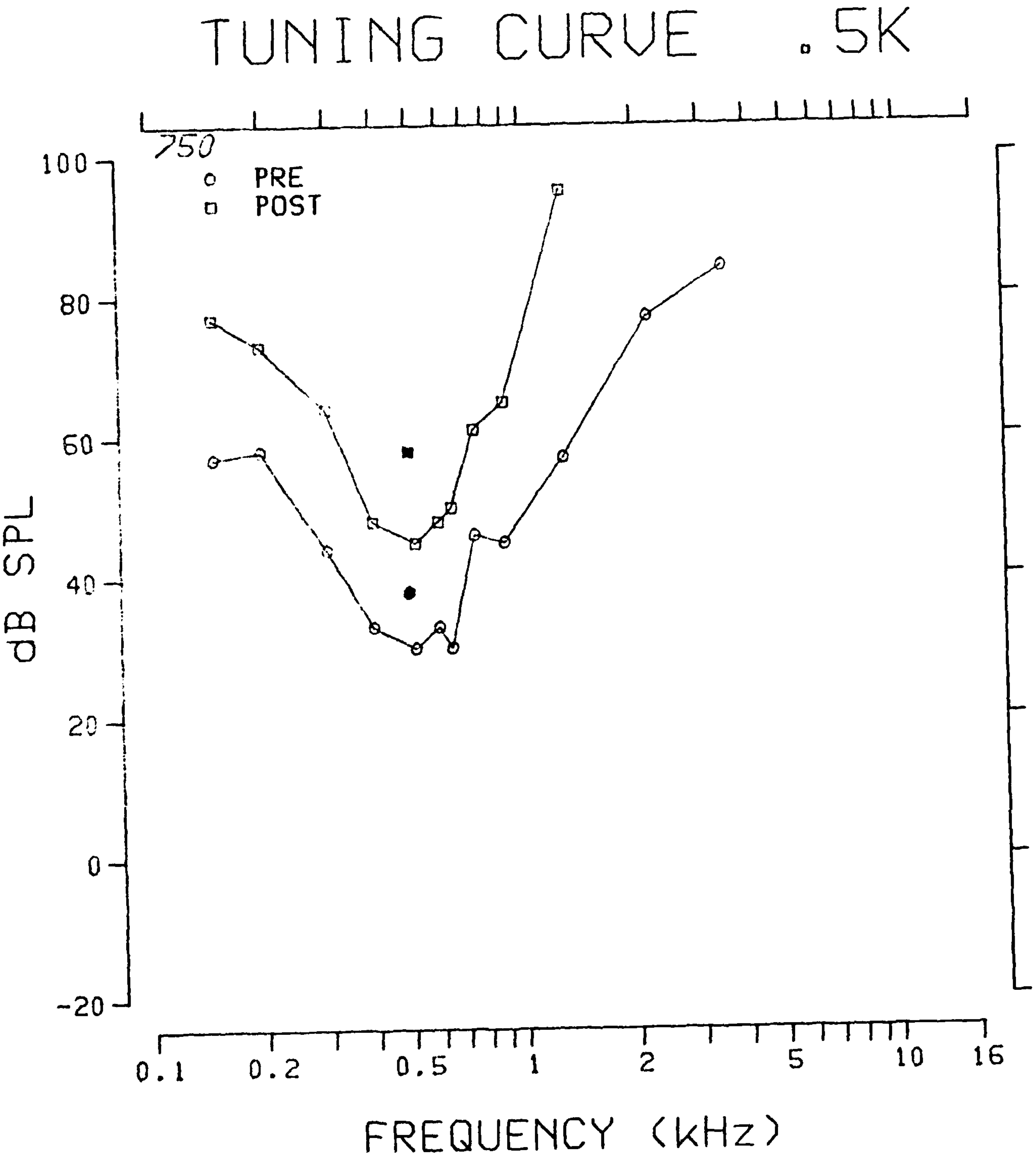


Fig. 3.3.146: Pre- and postexposure evoked response tuning curves at 0.5 kHz from chinchilla 750.

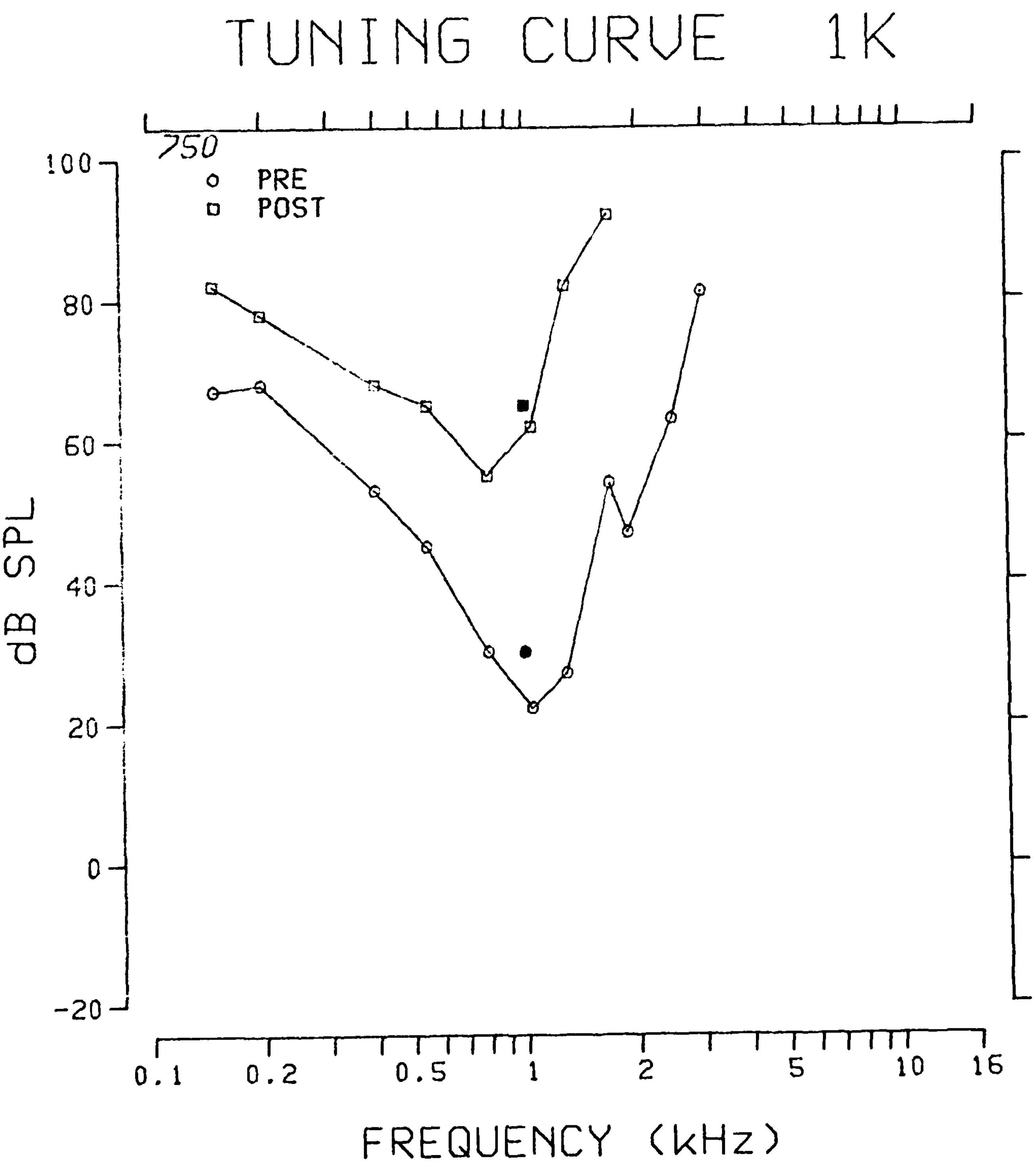


Fig. 3.3.147: Pre- and postexposure evoked response tuning curves at 1.0 kHz from chinchilla 750.

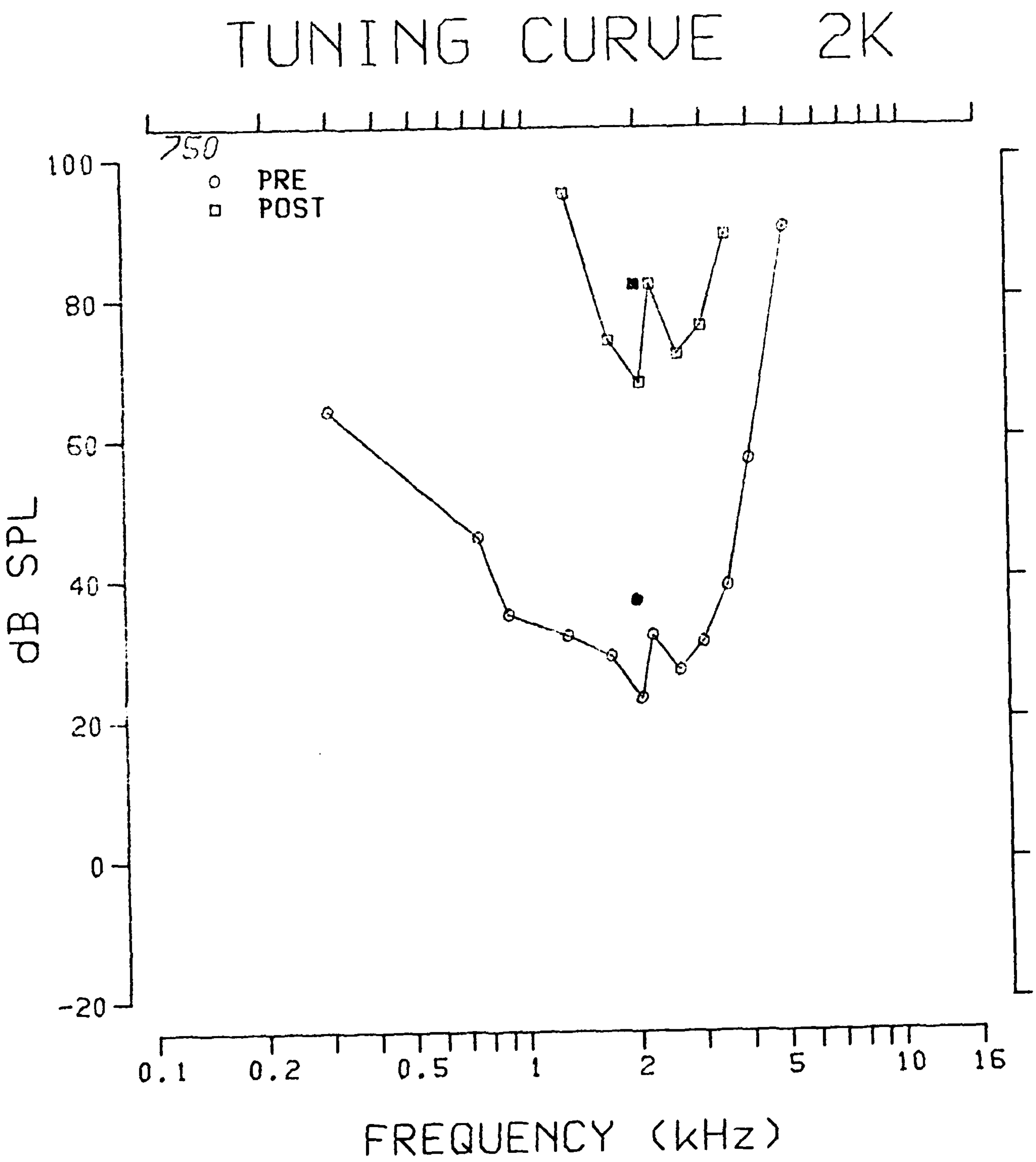


Fig. 3.3.148: Pre- and postexpsure evoked response tuning curves at 2.0 kHz from chinchilla 750.

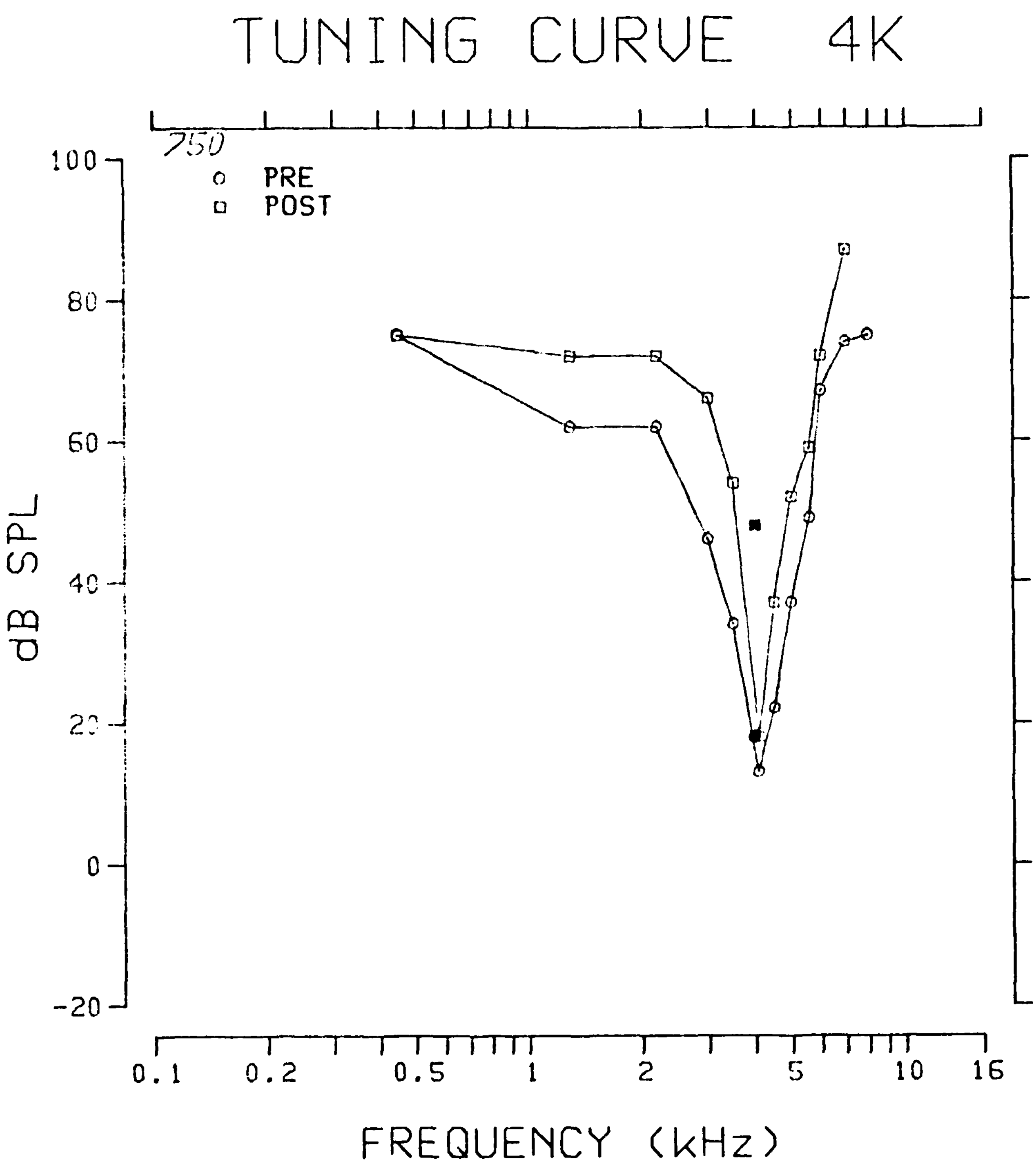


Fig. 3.3.149: Pre- and postexposure evoked response tuning curves at 4.0 kHz from chinchilla 750.

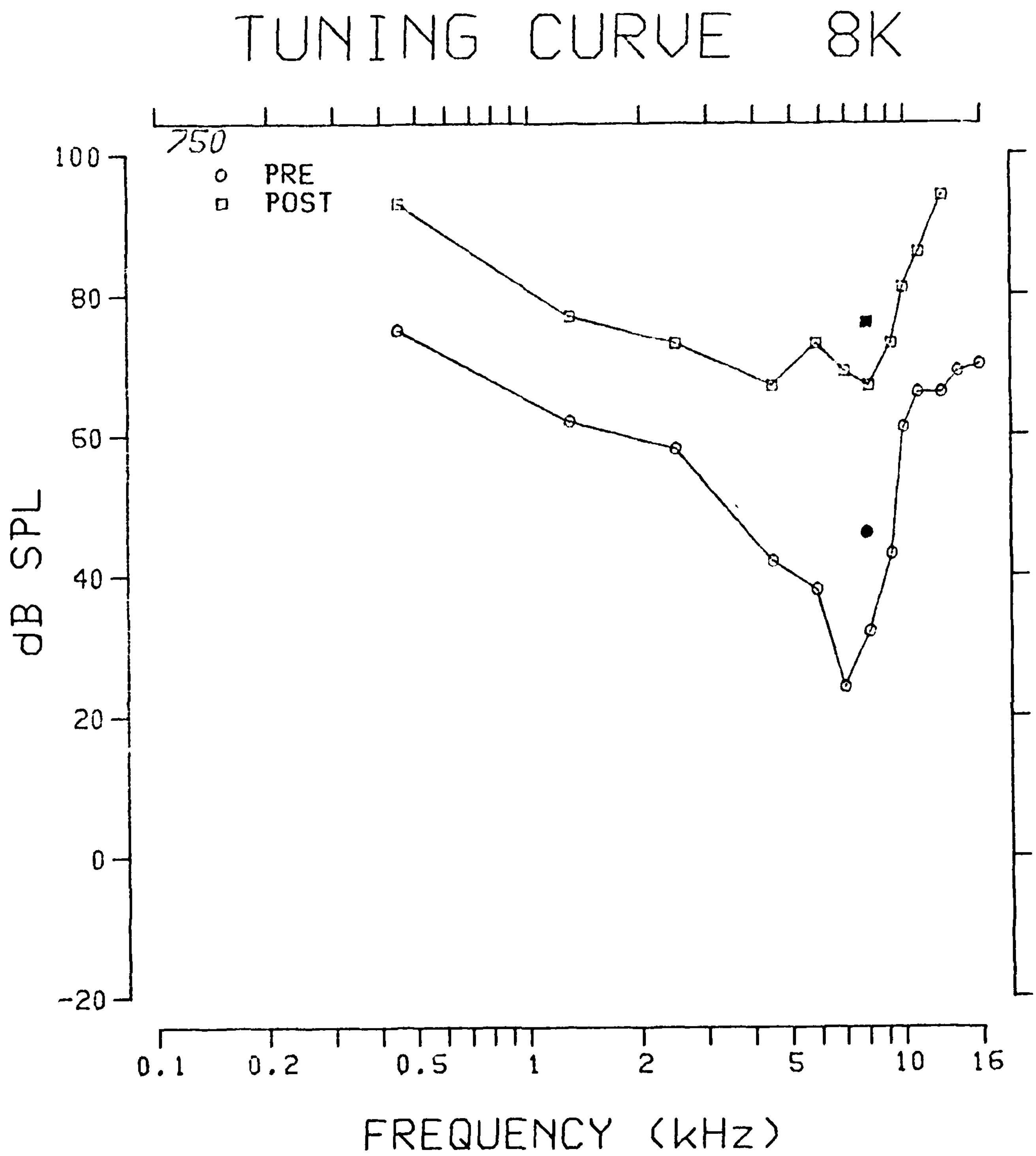


Fig. 3.3.150: Pre- and postexposure evoked response tuning curves at 8.0 kHz from chinchilla 750.

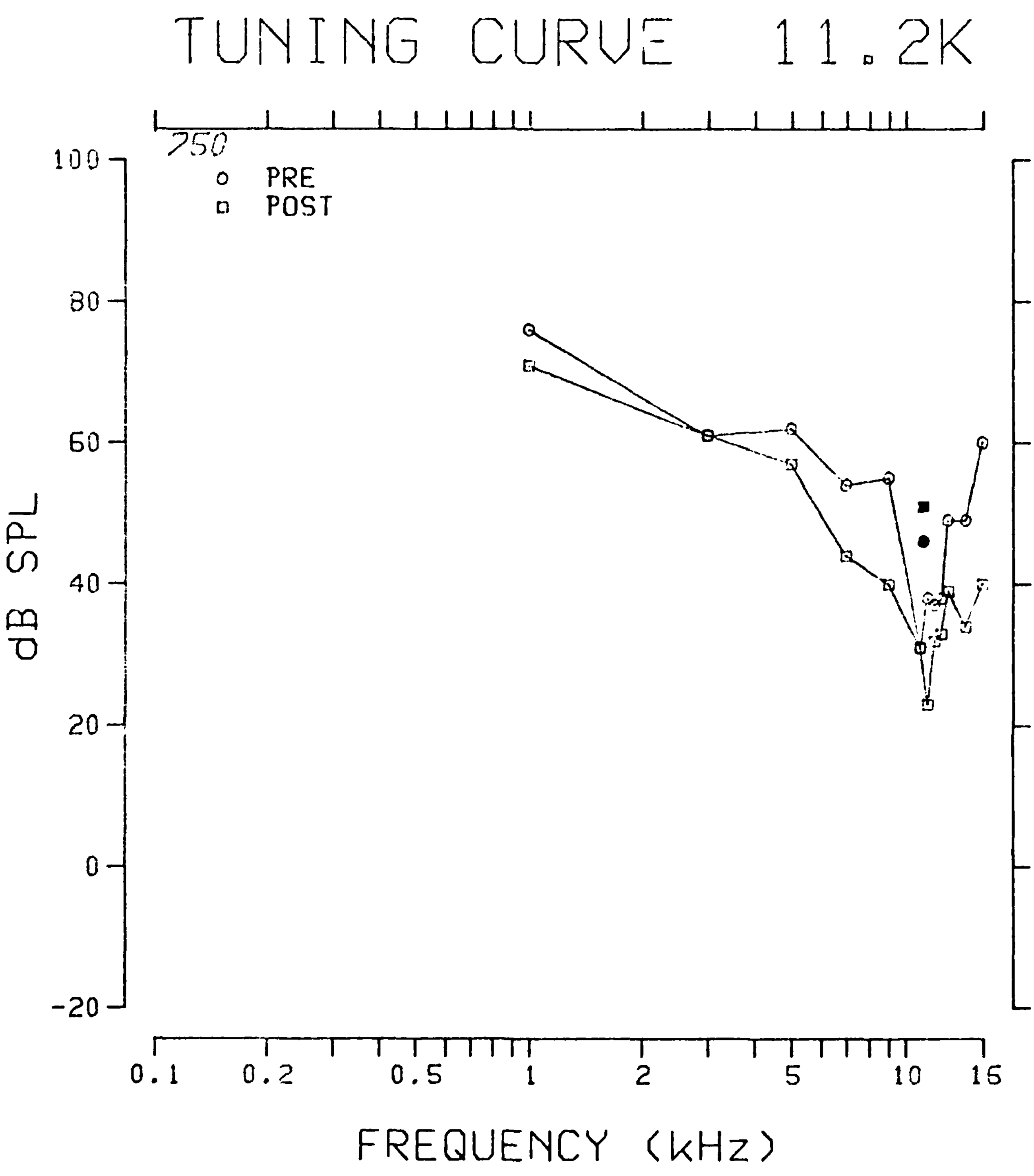


Fig. 3.3.151: Pre- and postexposure evoked response tuning curves at 11.2 kHz from chinchilla 750.

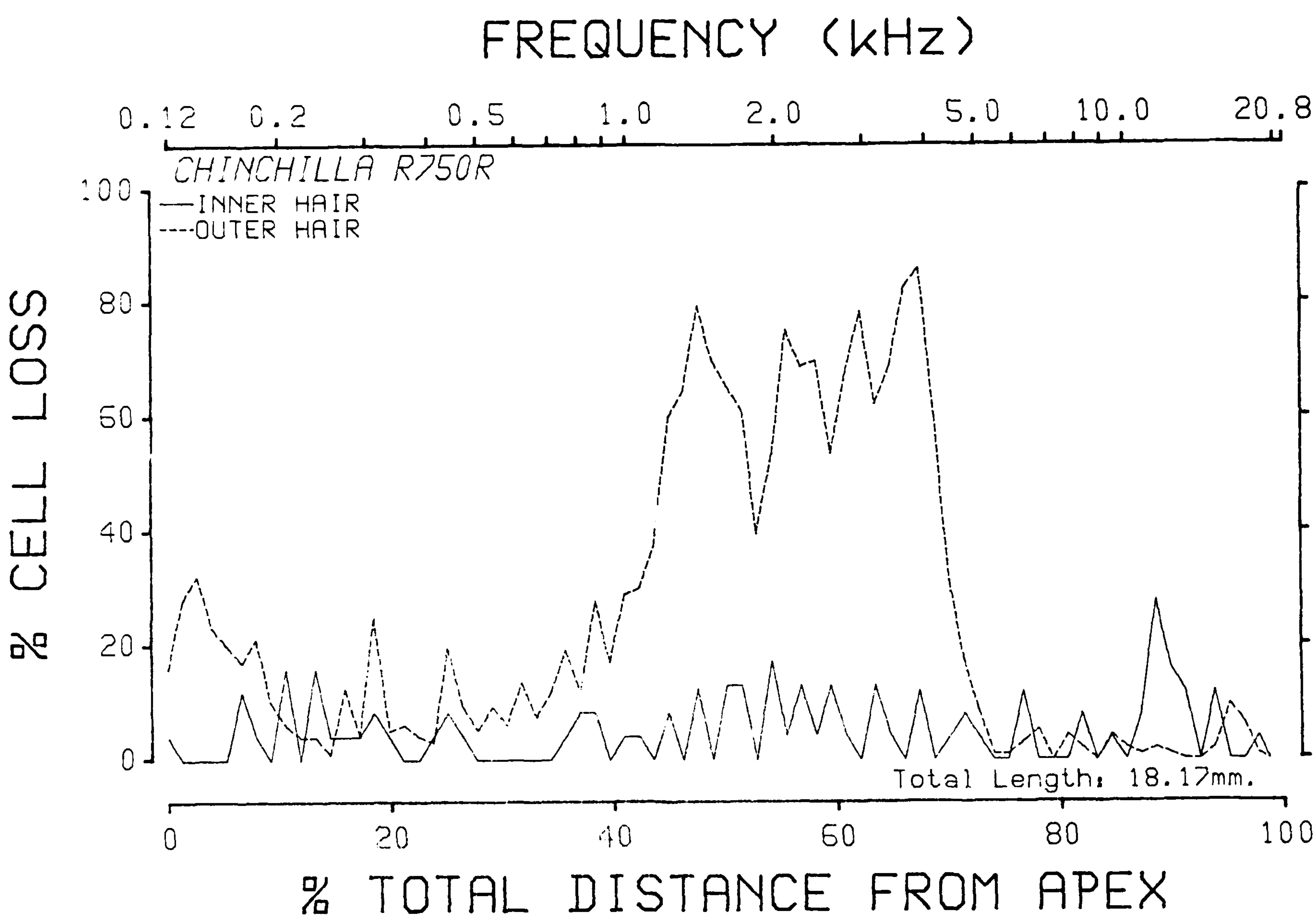


Fig. 3.3.152: Cochleogram from chinchilla 750.

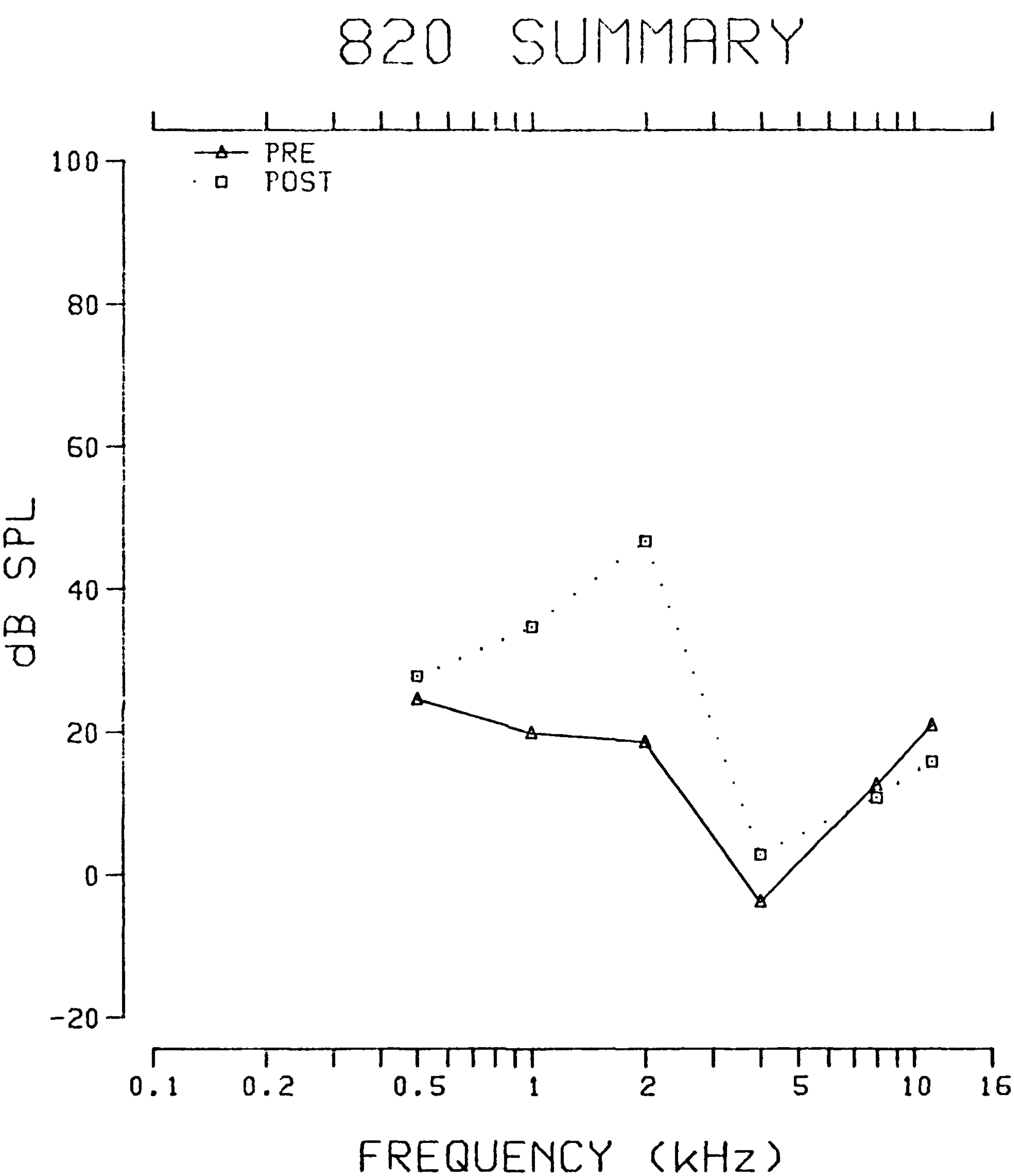


Fig. 3.3.153: Pre- and postexposure evoked response audiograms from chinchilla 820.

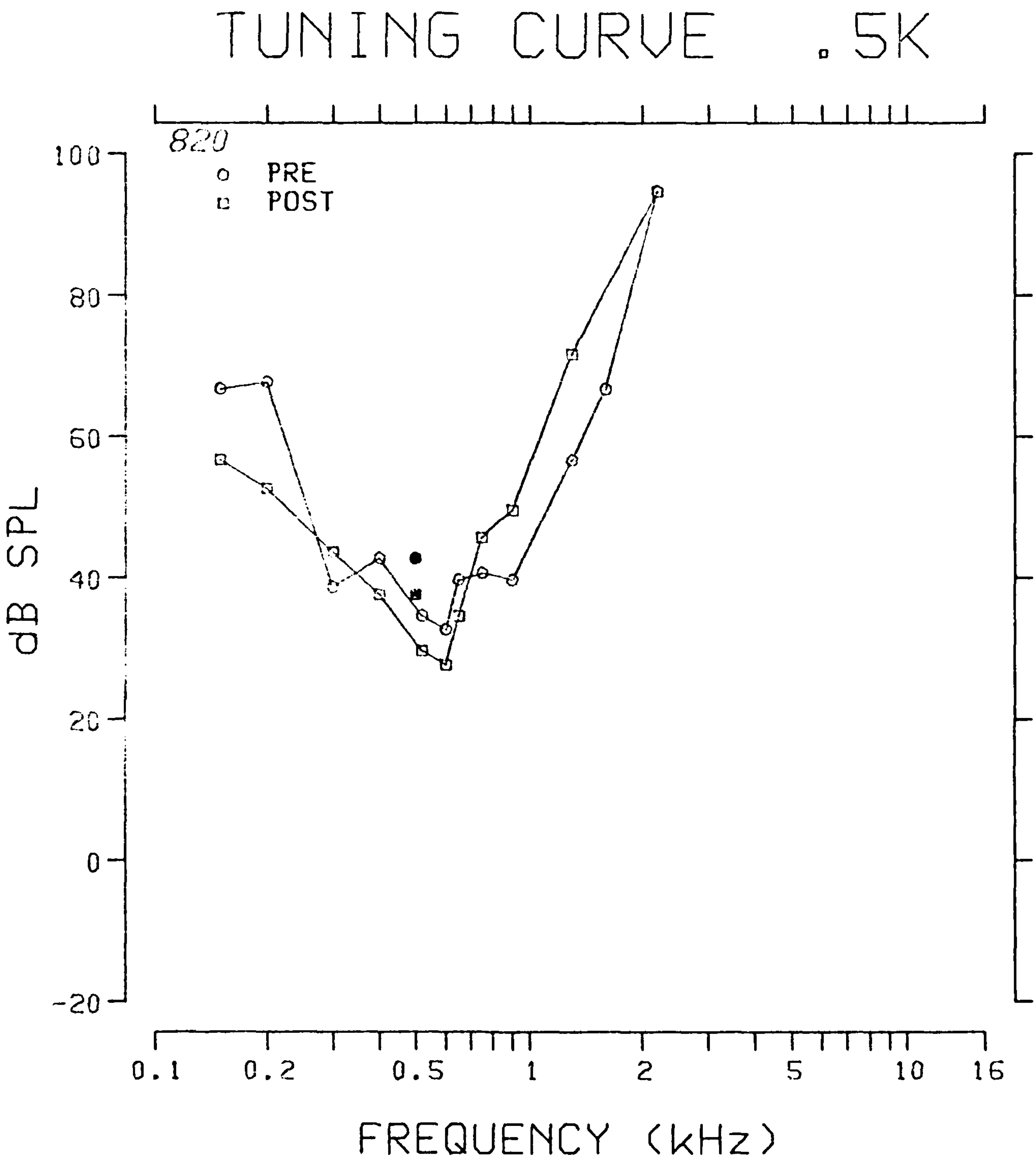


Fig. 3.3.154: Pre- and postexposure evoked response tuning curves at 0.5 kHz from chinchilla 820.

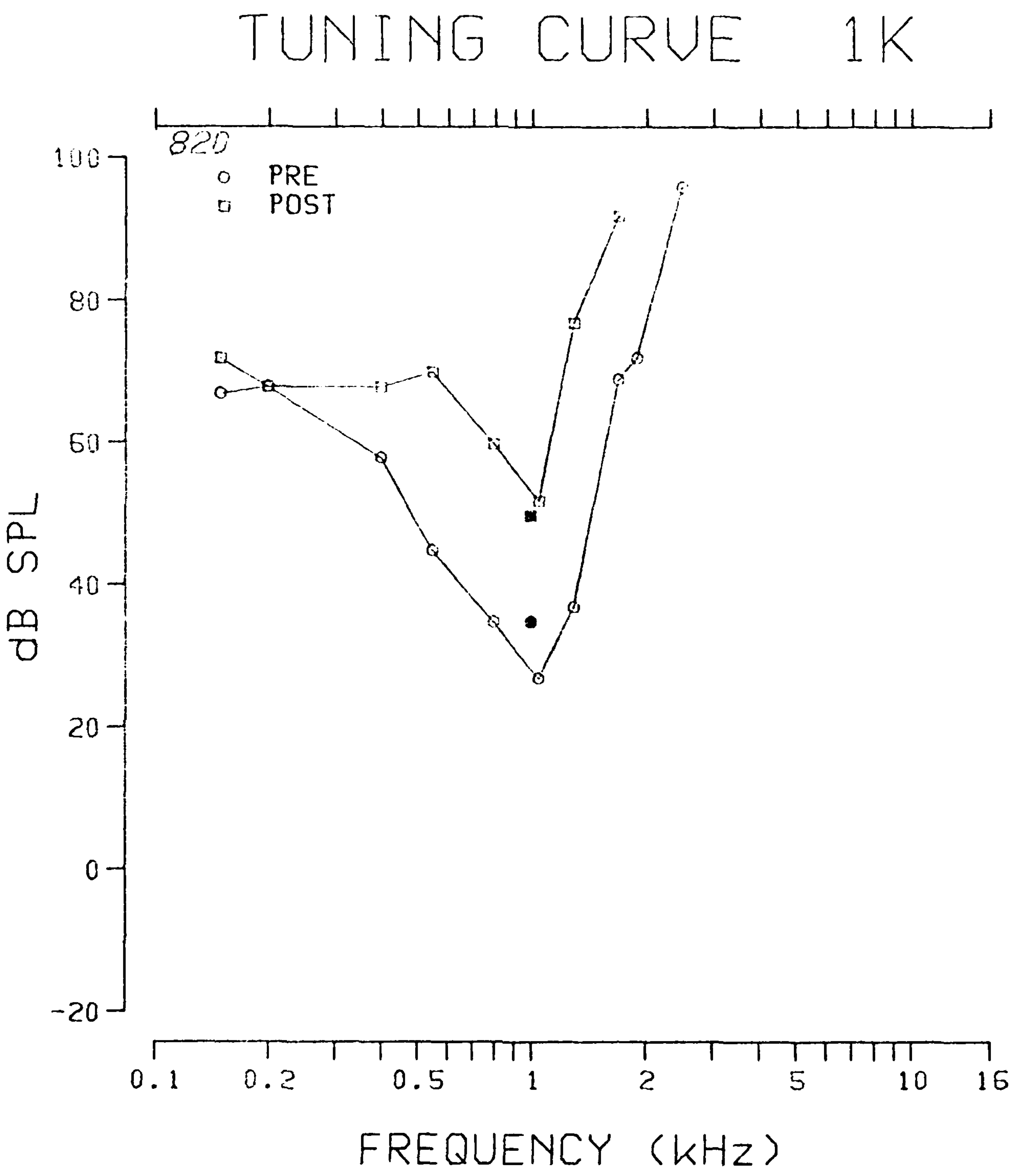


Fig. 3.3.155: Pre- and postexposure evoked response tuning curves at 1.0 kHz from chinchilla 820.

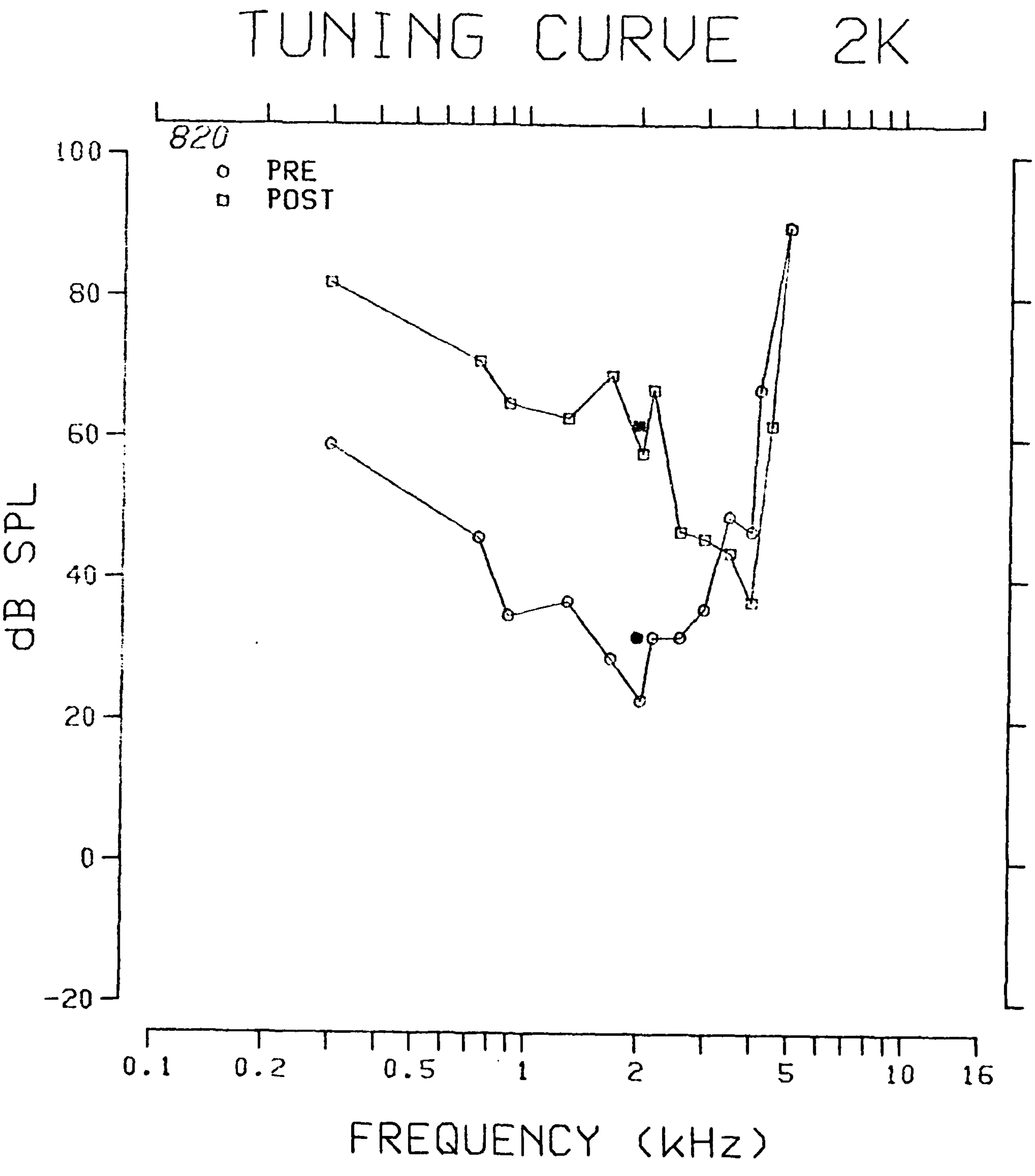


Fig. 3.3.156: Pre- and postexposure evoked response tuning curves at 2.0 kHz from chinchilla 820.

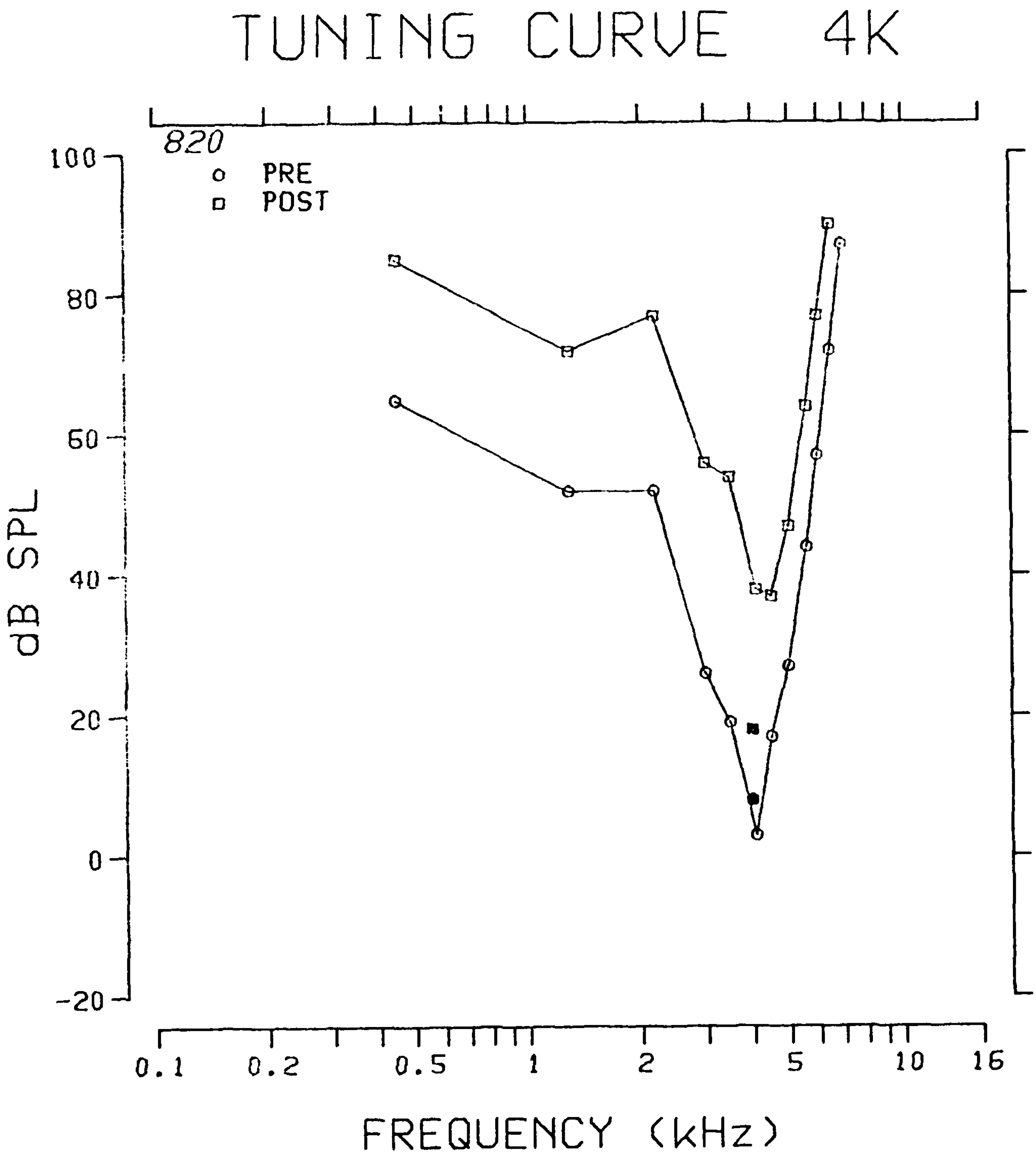


Fig. 3.3.157: Pre- and postexposure evoked response tuning curves at 4.0 kHz from chinchilla 820.

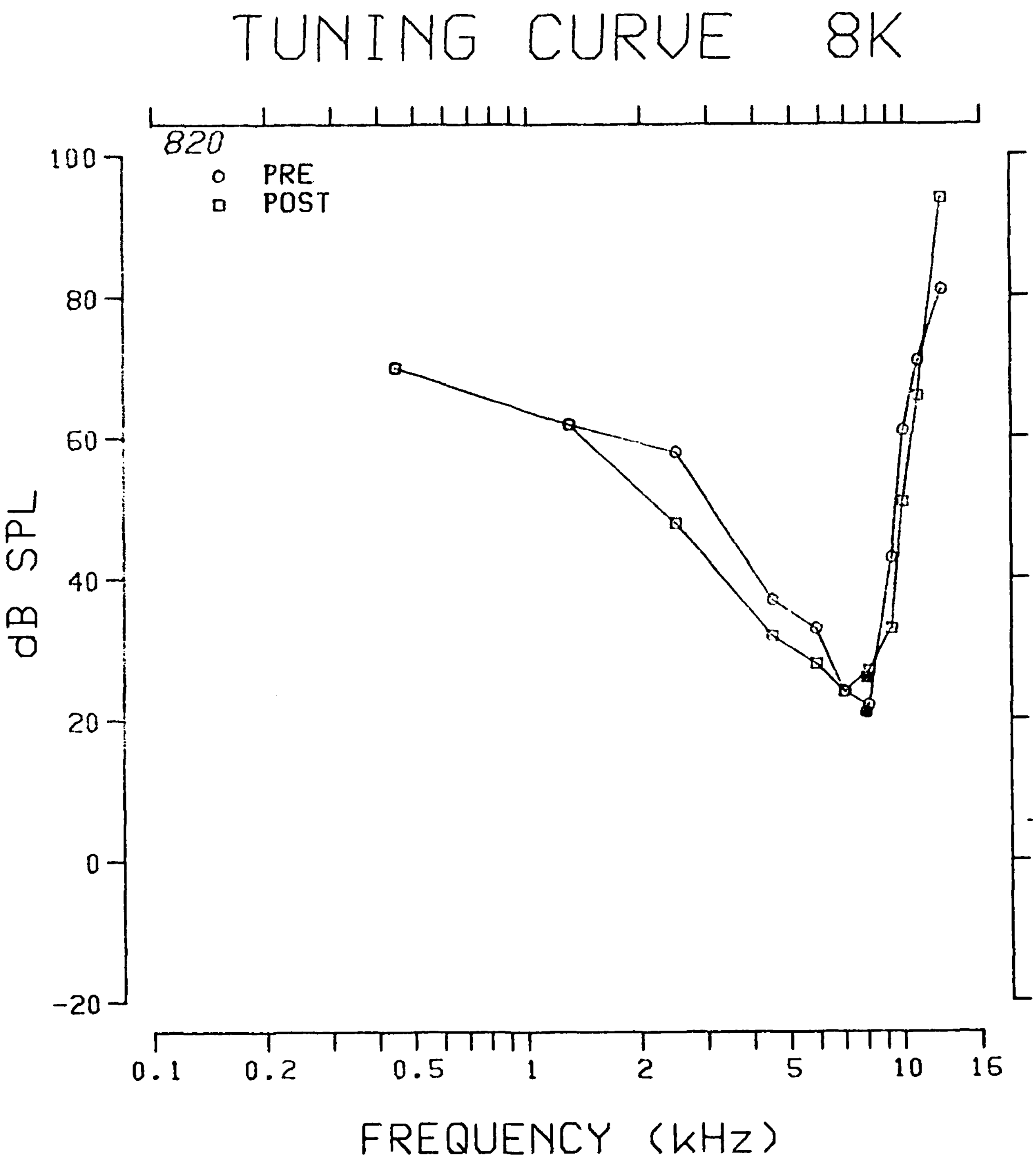


Fig. 3.3.158: Pre- and postexposure evoked response tuning curves at 8.0 kHz from chinchilla 820.

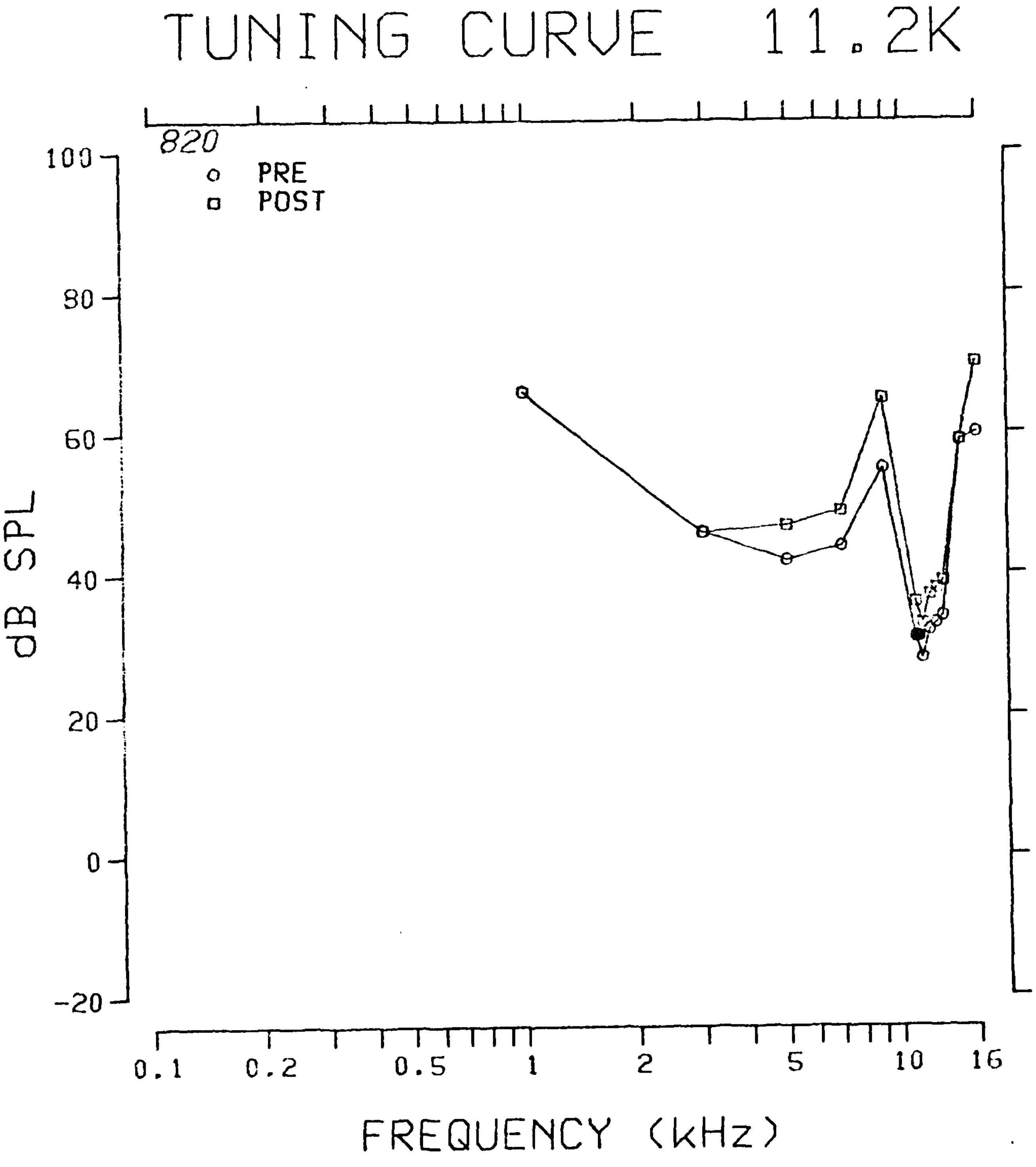


Fig. 3.3.159: Pre- and postexposure evoked response tuning curves at 11.2 kHz from chinchilla 820.

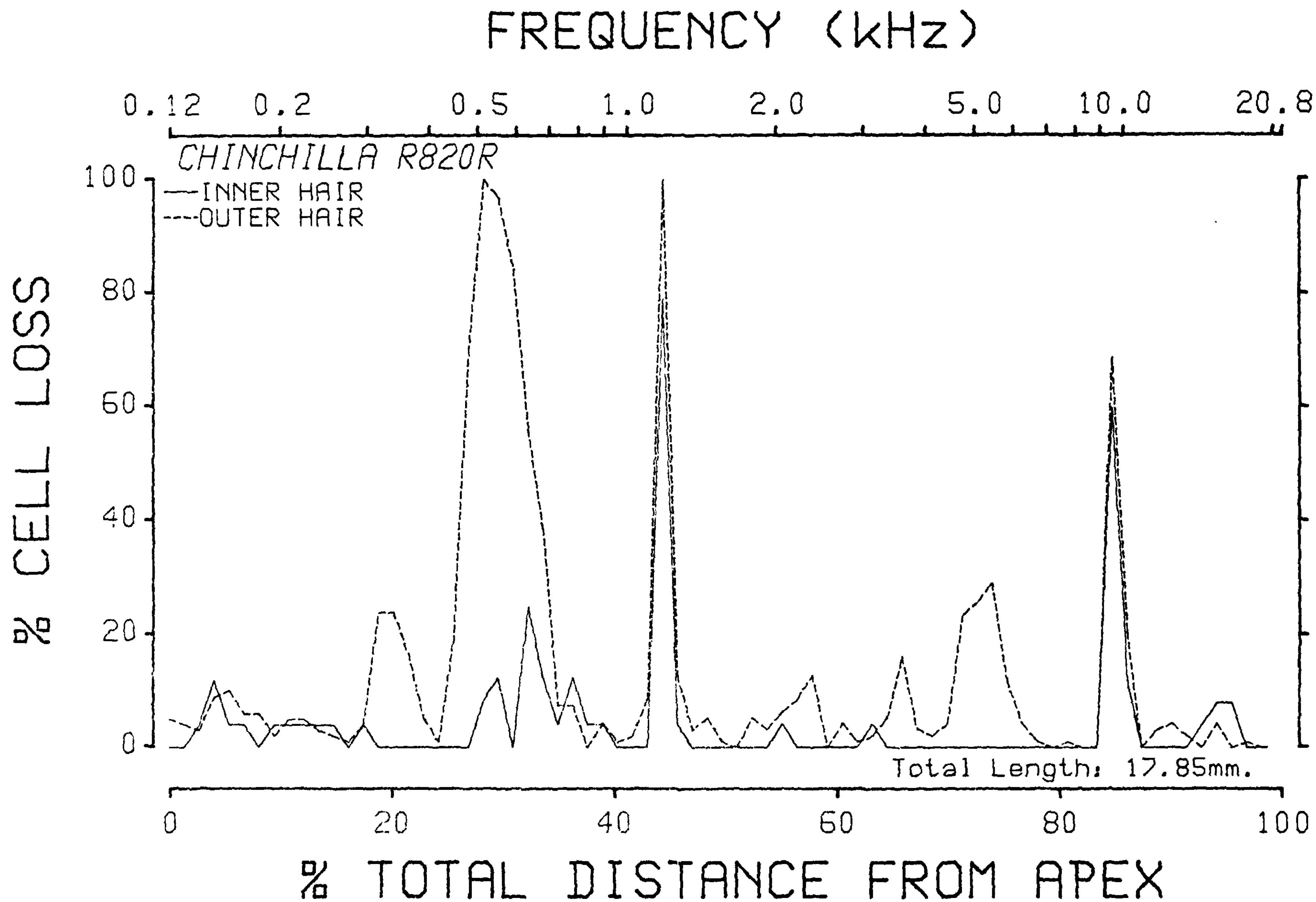


Fig. 3.3.160: Cochleogram from chinchilla 820:

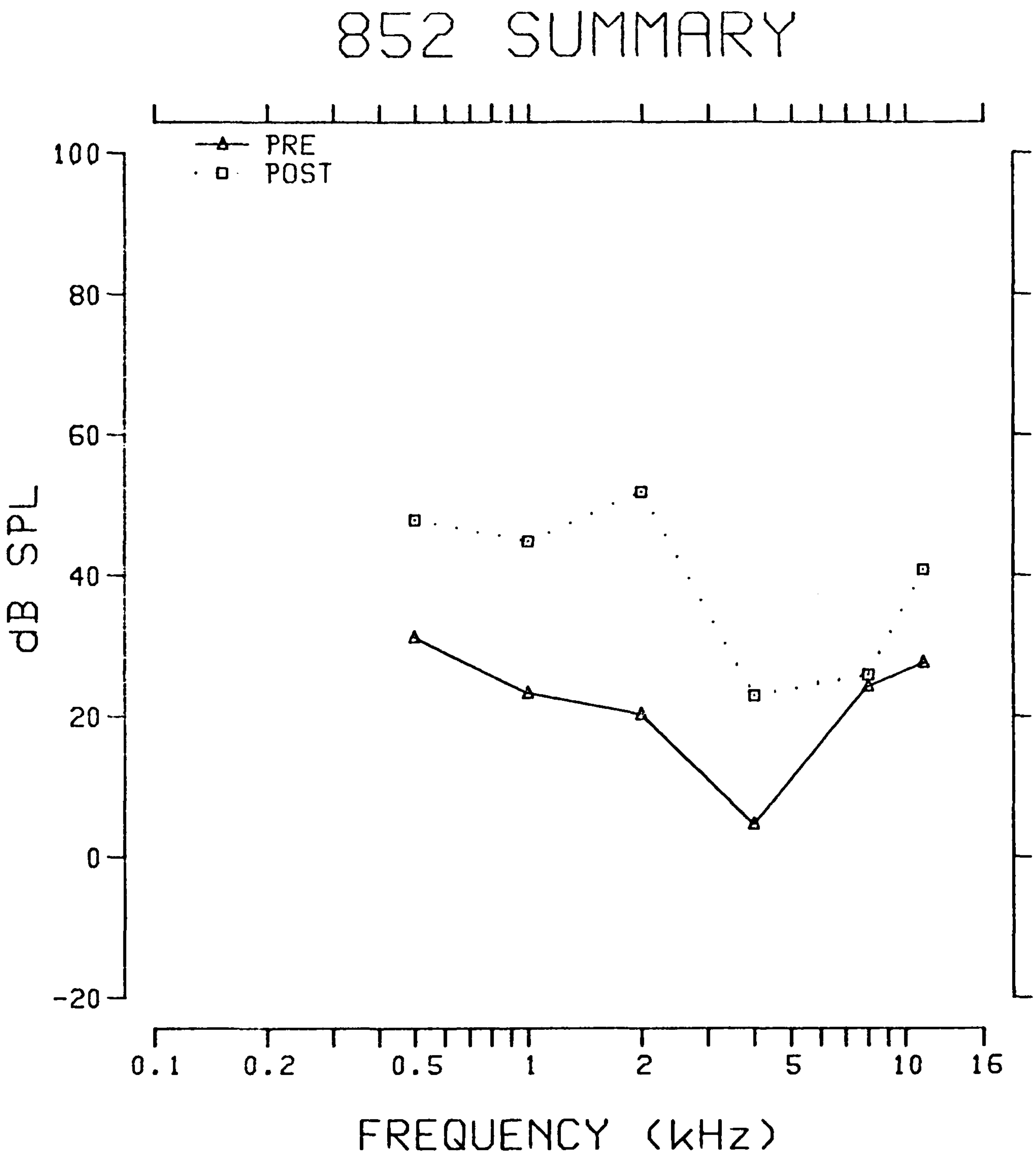


Fig. 3.3.161: Pre- and postexposure evoked response audiograms from chinchilla 852.

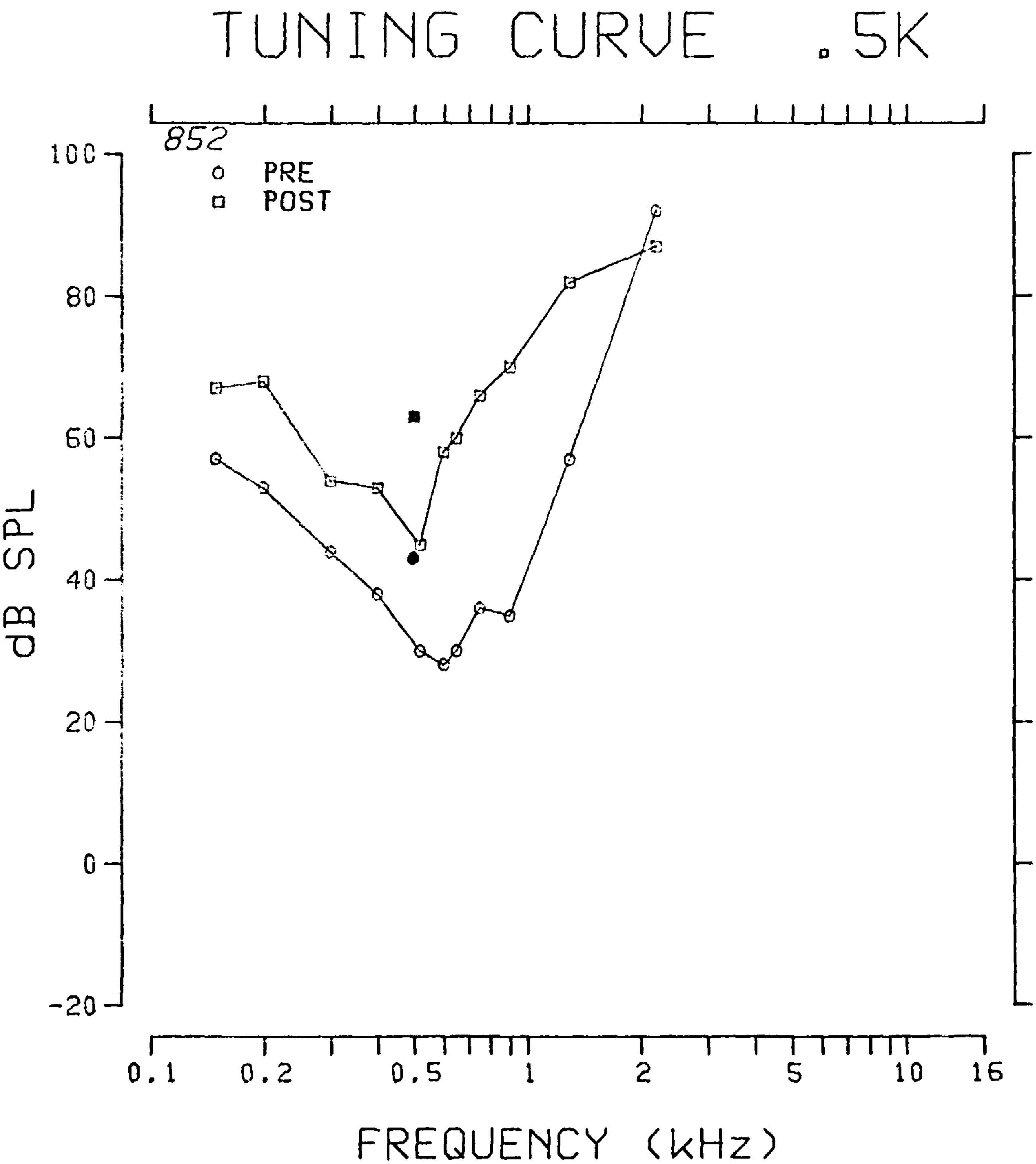


Fig. 3.3.162: Pre- and postexposure evoked response tuning curves at 0.5 kHz from chinchilla 852.

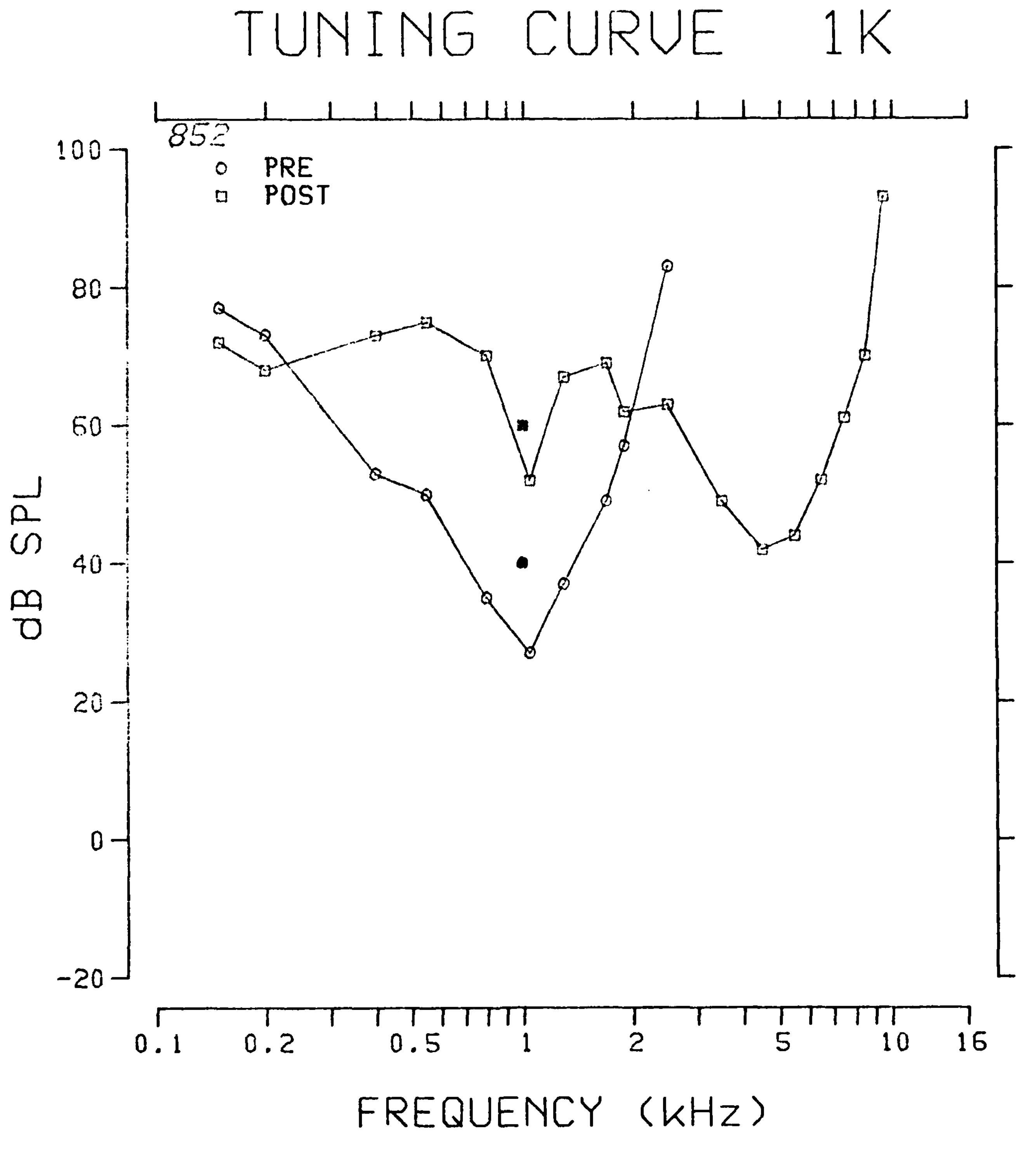


Fig. 3.3.163: Pre- and postexposure evoked response tuning curves at 1.0 kHz from chinchilla 852.

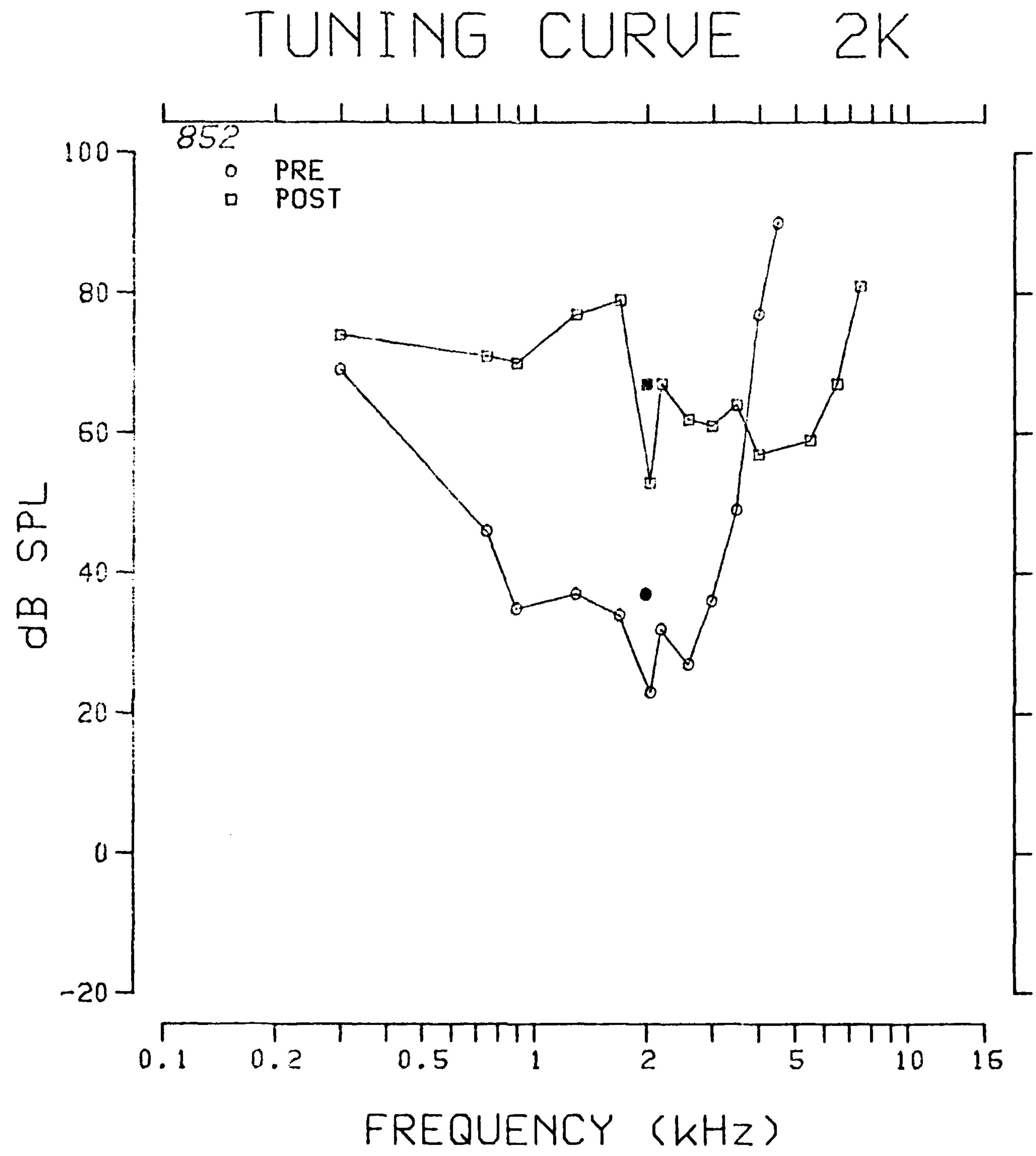


Fig. 3.3.164: Pre- and postexposure evoked response tuning curves at 2.0 kHz from chinchilla 852.

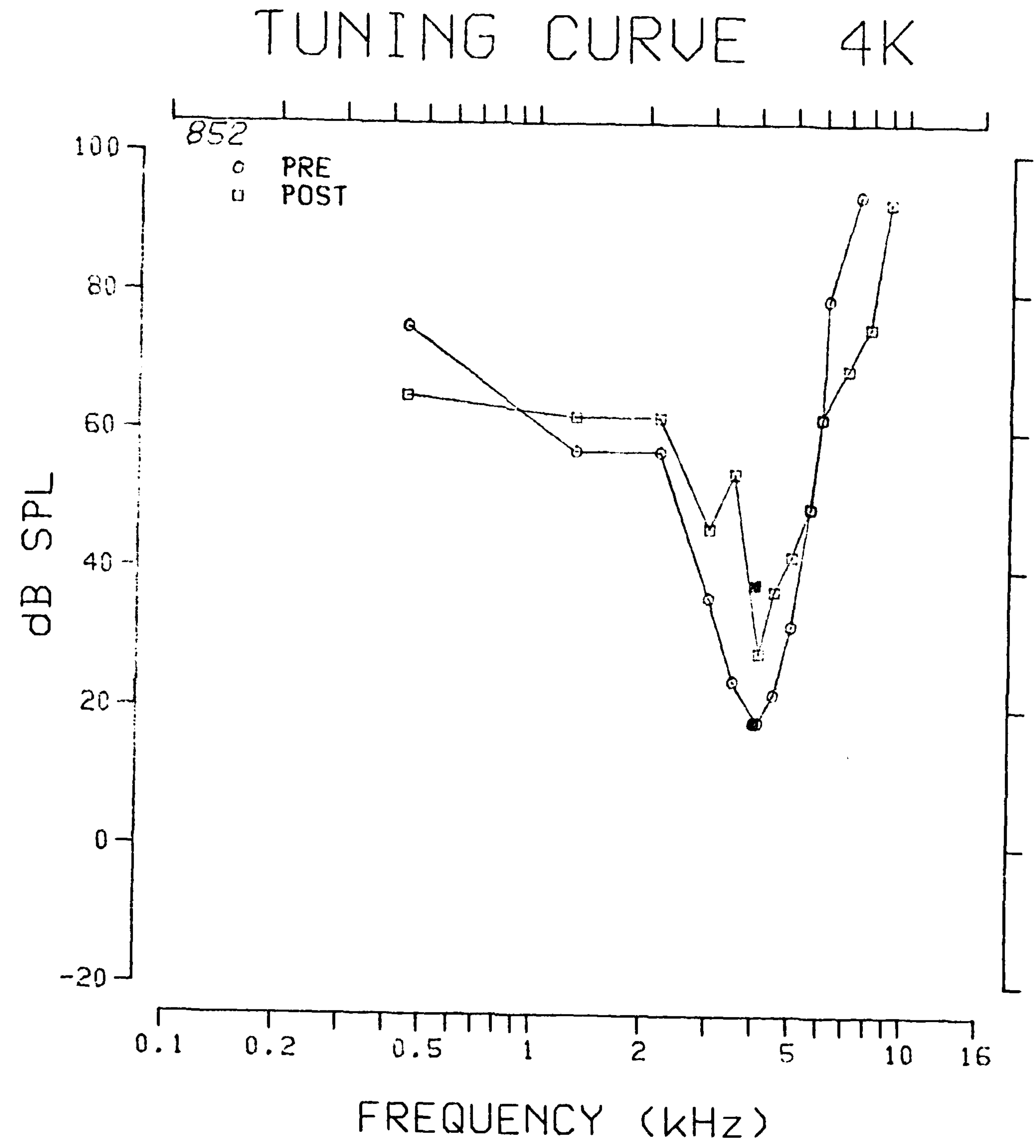


Fig. 3.3.165: Pre- and postexposure evoked response tuning curves at 4.0 kHz from chinchilla 852.

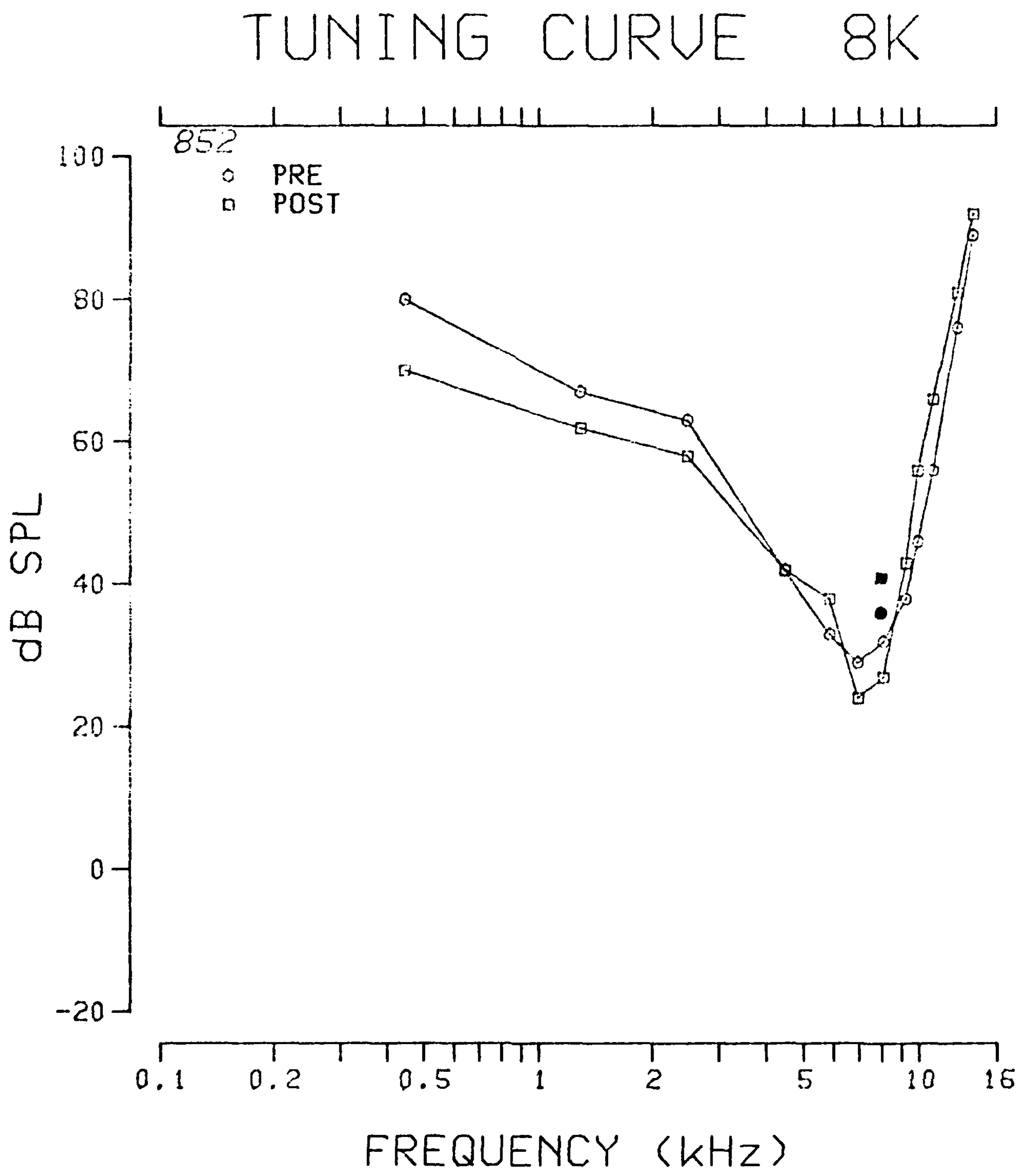


Fig. 3.3.166: Pre- and postexposure evoked response tuning curves at 8.0 kHz from chinchilla 852.

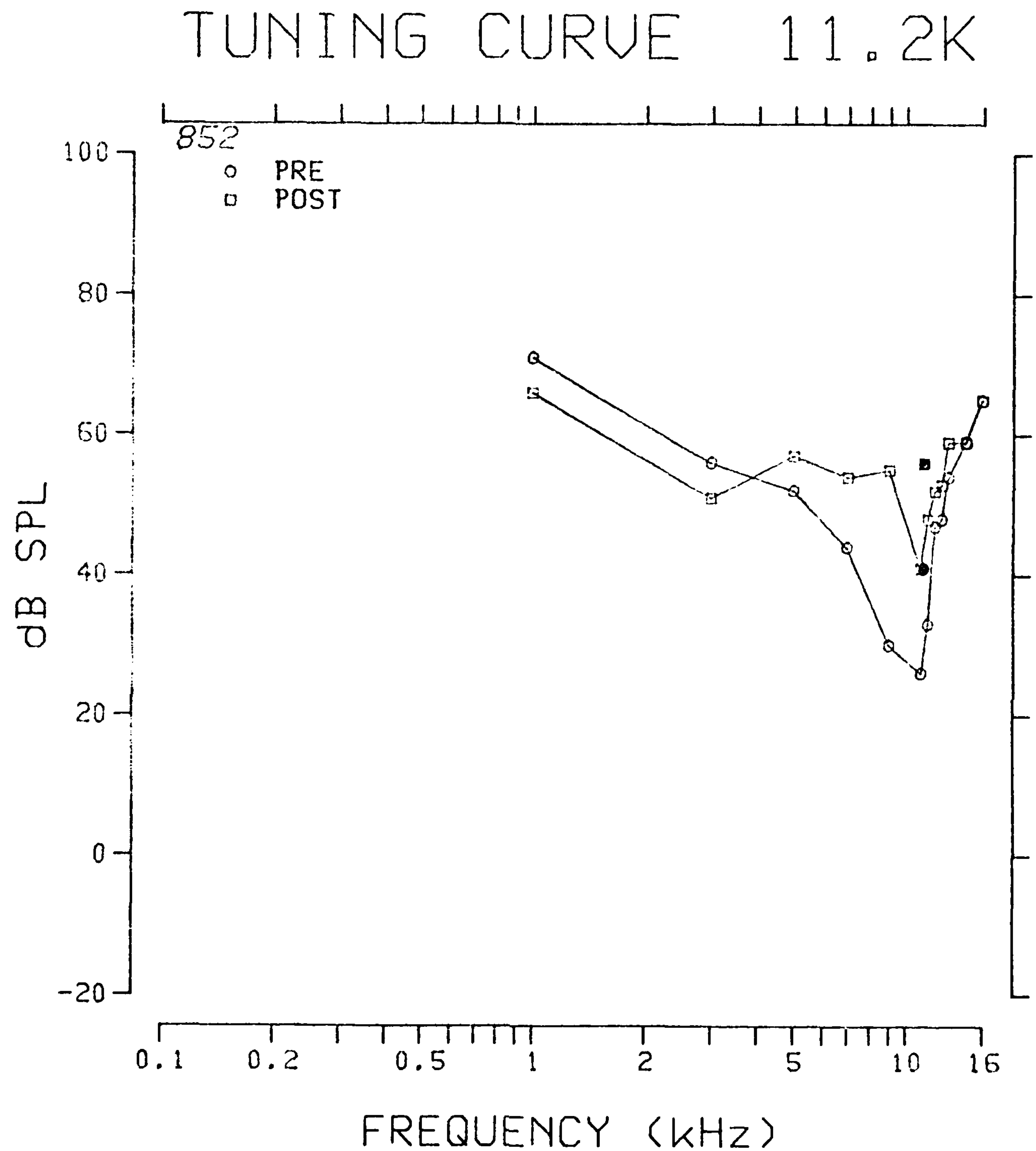


Fig. 3.3.167: Pre- and postexposure evoked response tuning curves at 11.2 kHz from chinchilla 852.

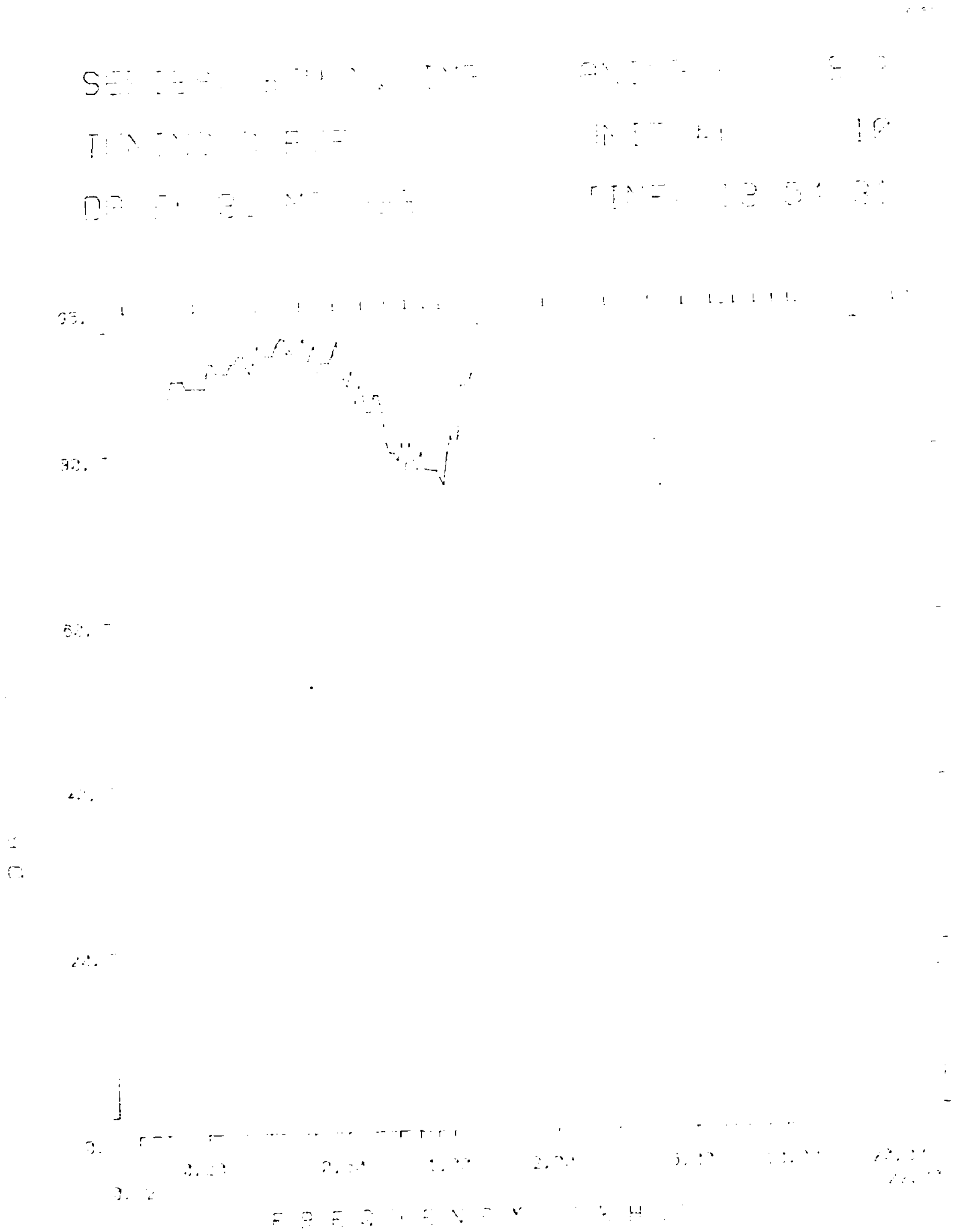

Fig. 3.3.168: Auditory nerve fiber tuning curve from chinchilla 852.

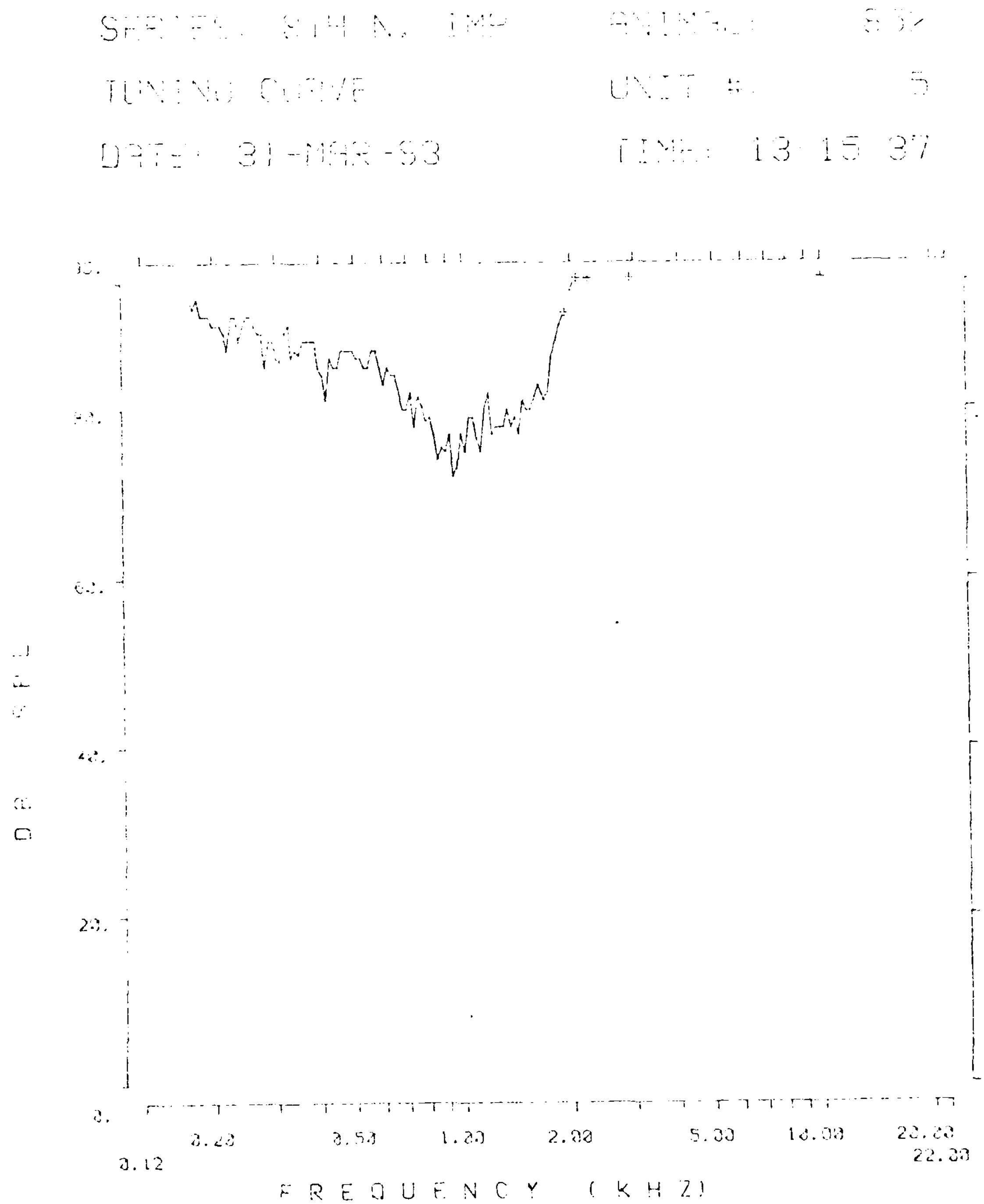


Fig. 3.3.169: Auditory nerve fiber tuning curve from chinchilla 852.

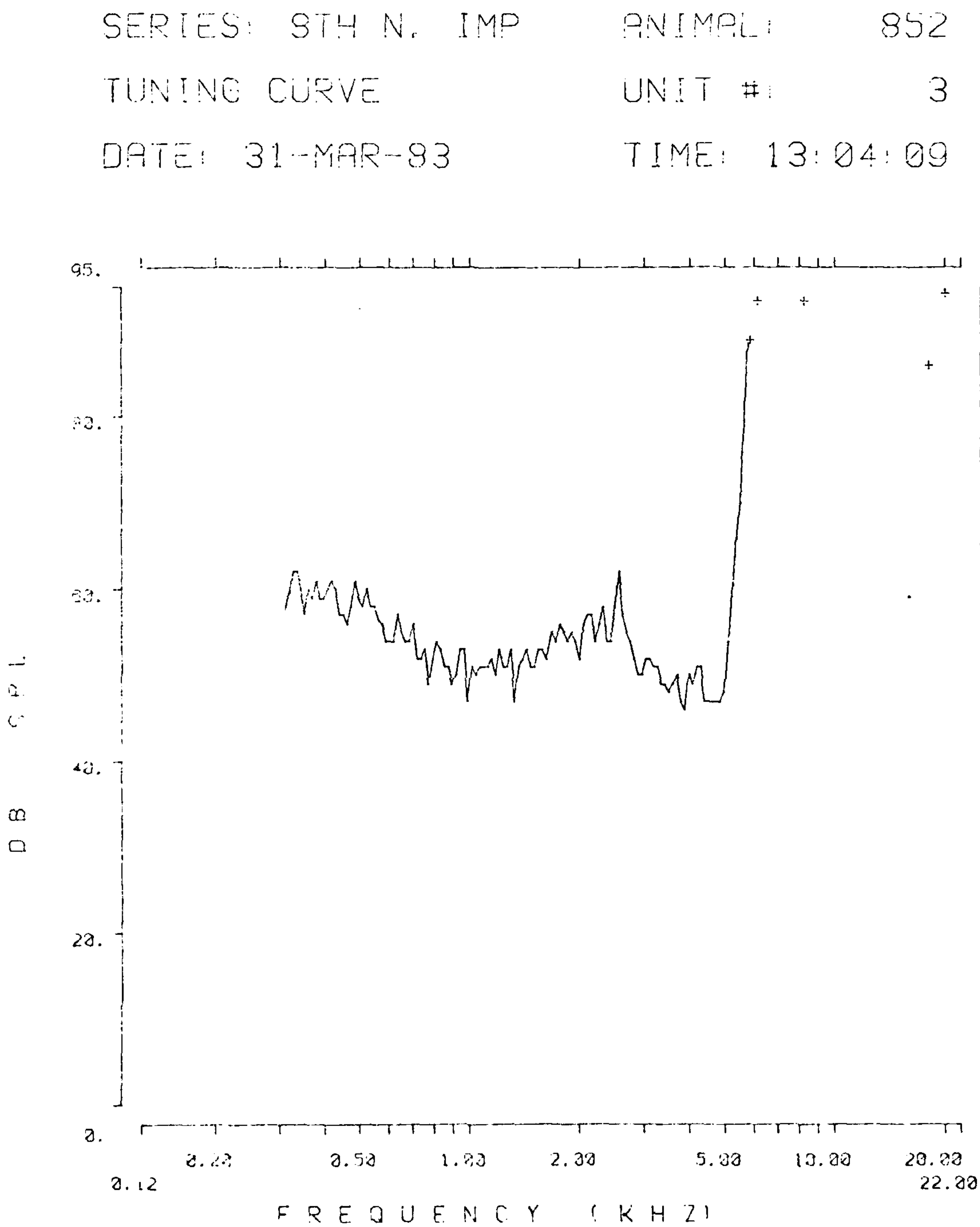


Fig. 3.3.170: Auditory nerve fiber tuning curve from chinchilla 852.

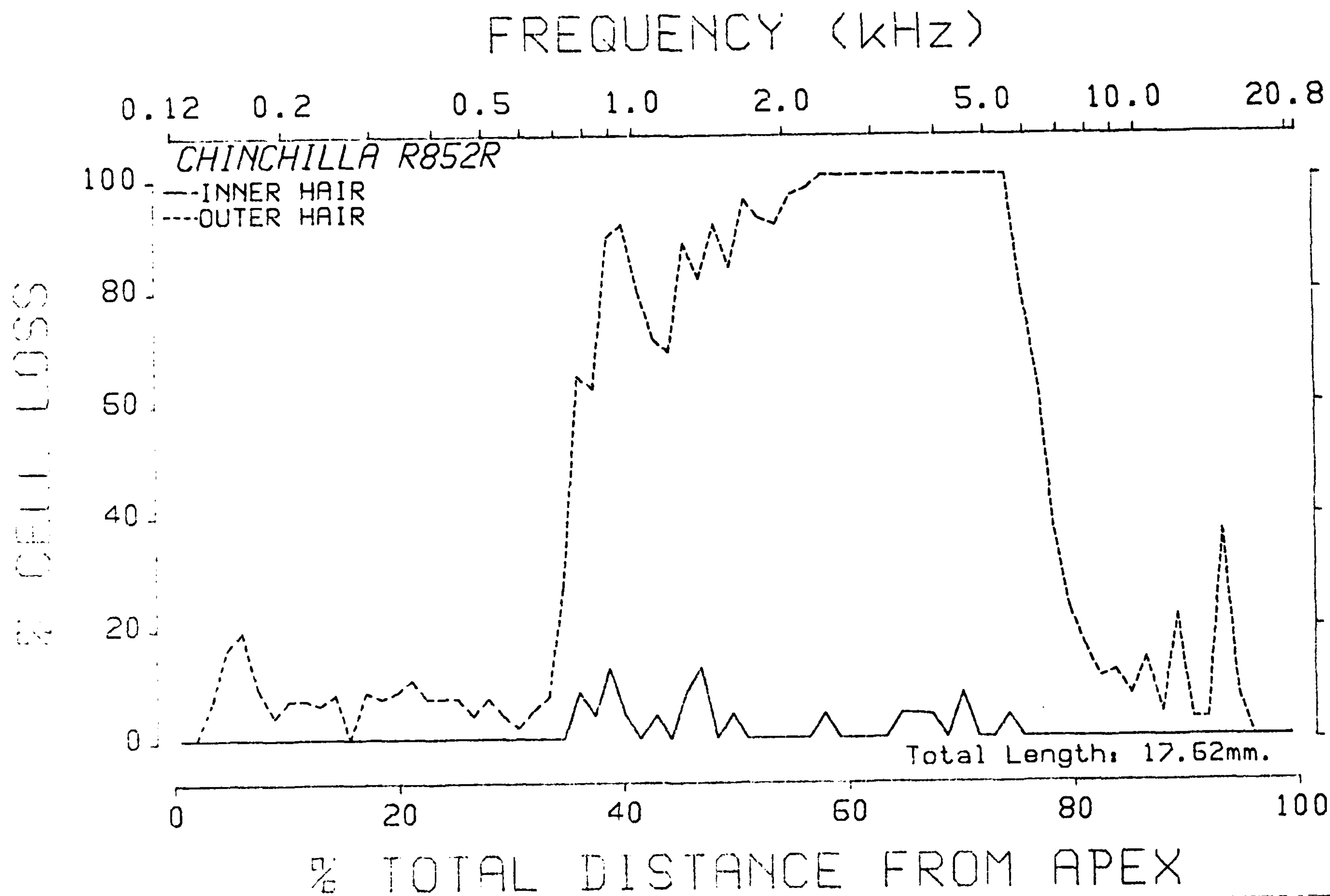


Fig. 3.3.171: Cochleogram from chinchilla 852.

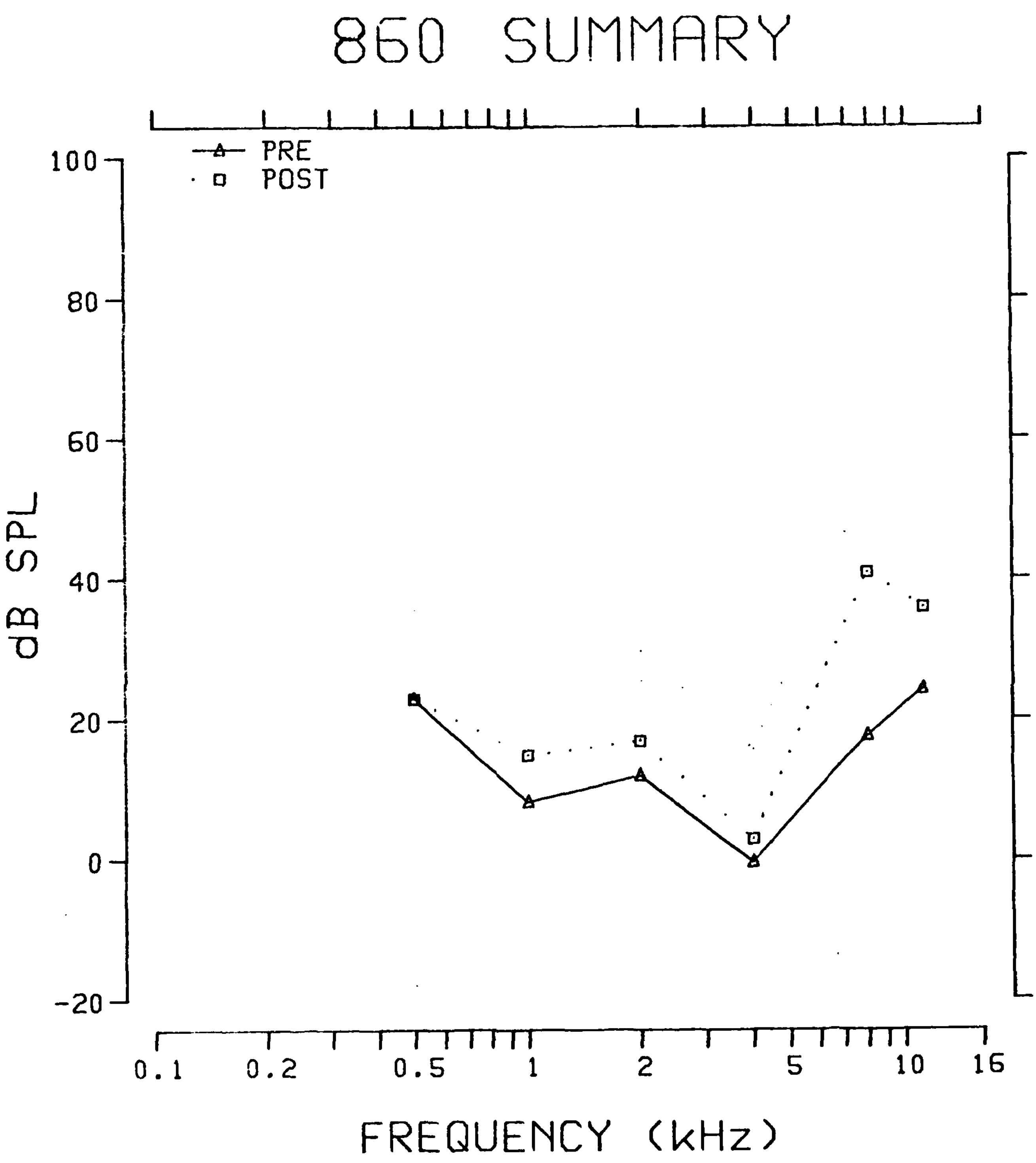


Fig. 3.3.172: Pre- and postexposure evoked response audiograms from chinchilla 860.

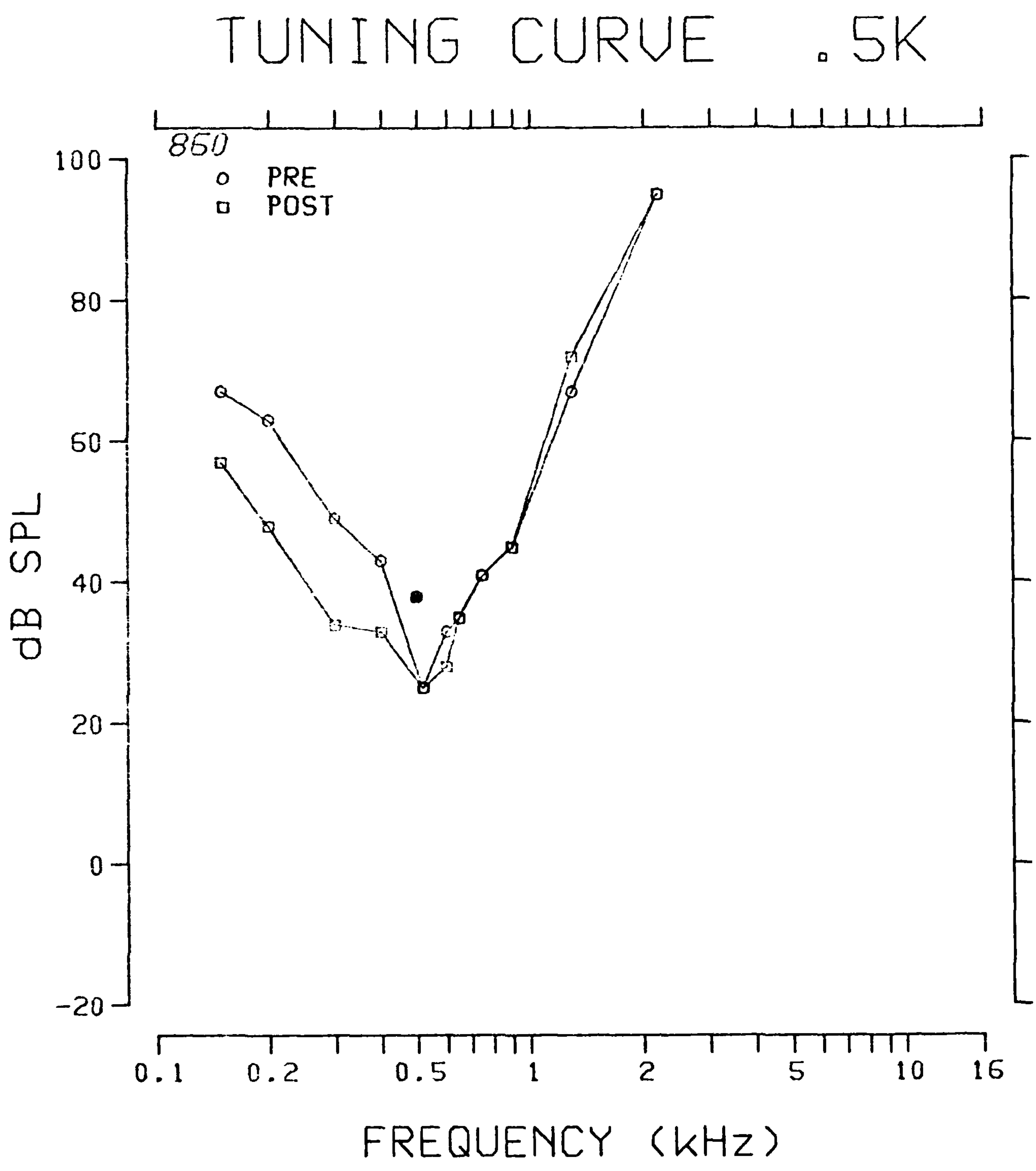


Fig. 3.3.173: Pre- and postexposure evoked response tuning curves at 0.5 kHz from chinchilla 860.

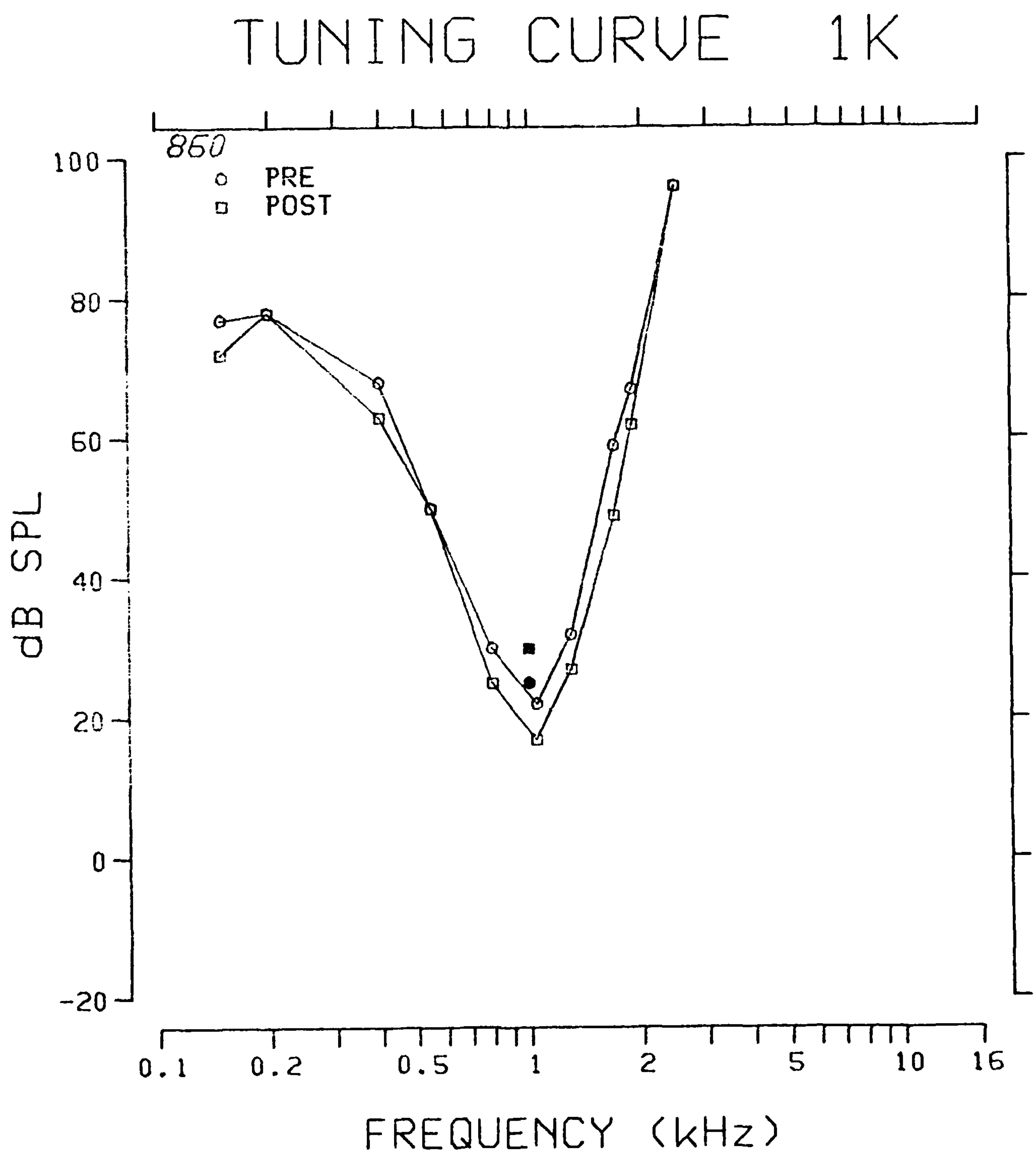


Fig. 3.3.174: Pre- and postexposure evoked response tuning curves at 1.0 kHz from chinchilla 860.

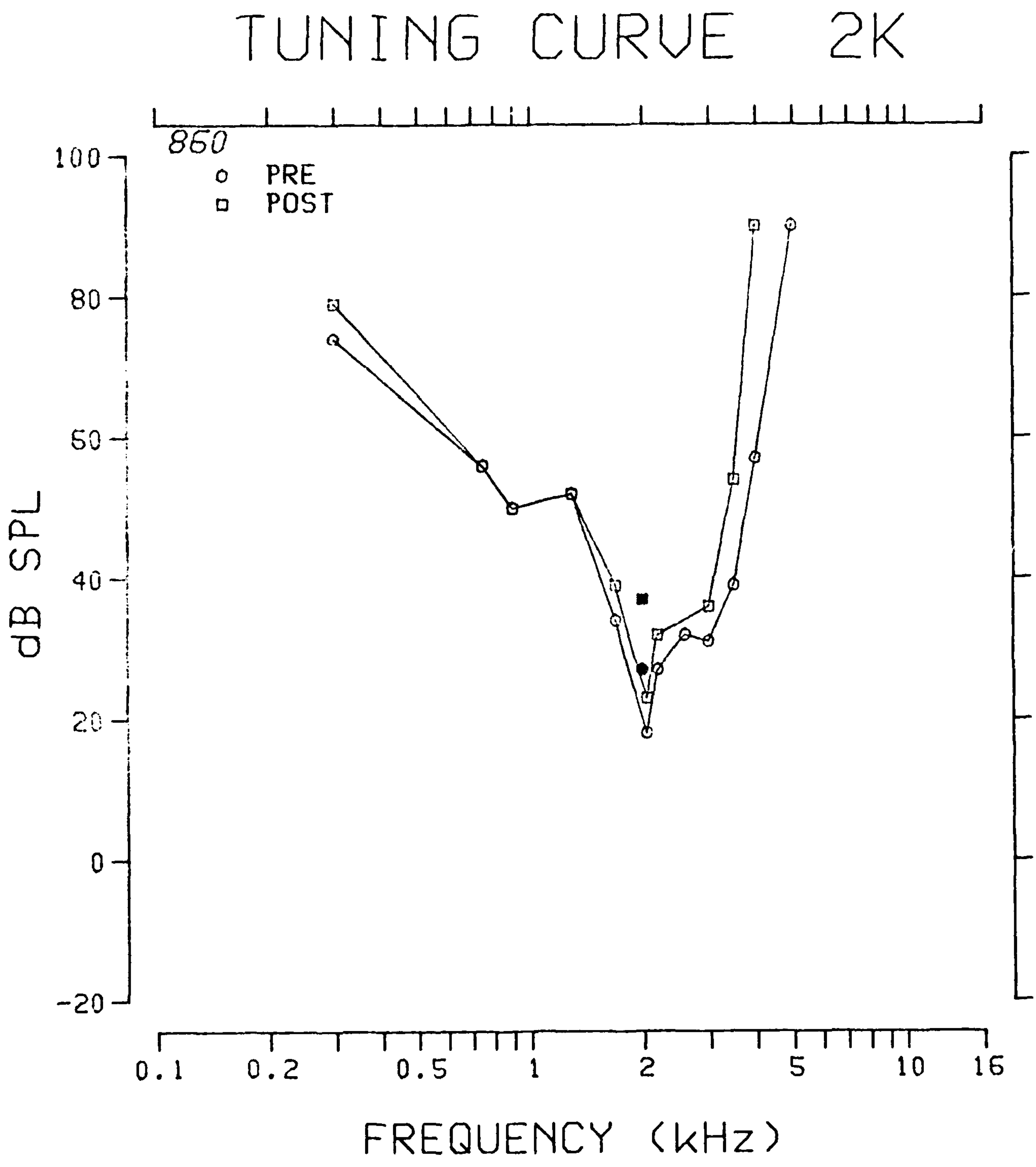


Fig. 3.3.175: Pre- and postexposure evoked response tuning curves at 2.0 kHz from chinchilla 860.

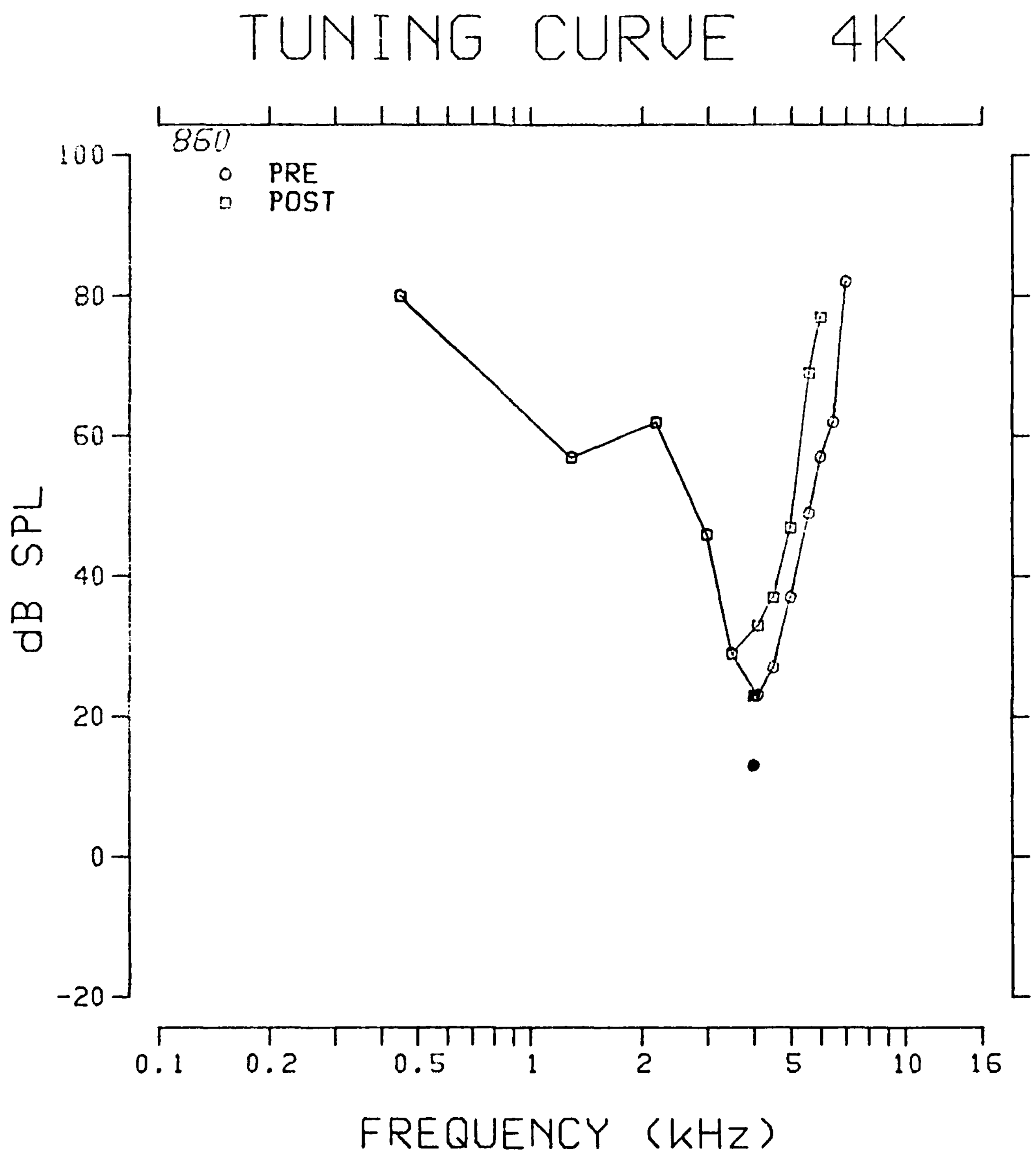


Fig. 3.3.176: Pre- and postexposure evoked response tuning curves at 4.0 kHz from chinchilla 860.

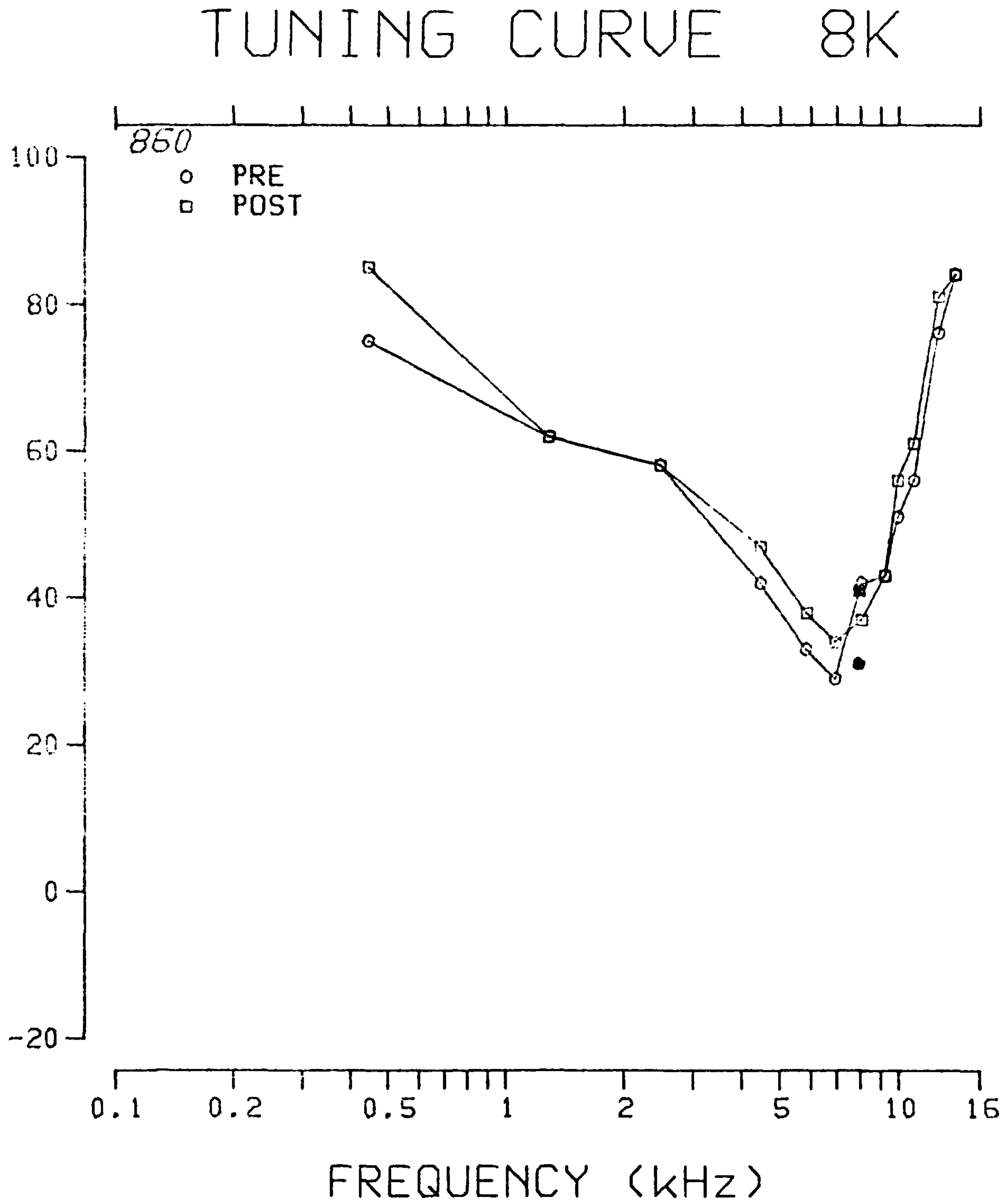


Fig. 3.3.177: Pre- and postexposure evoked response tuning curves at 8.0 kHz from chinchilla 860.

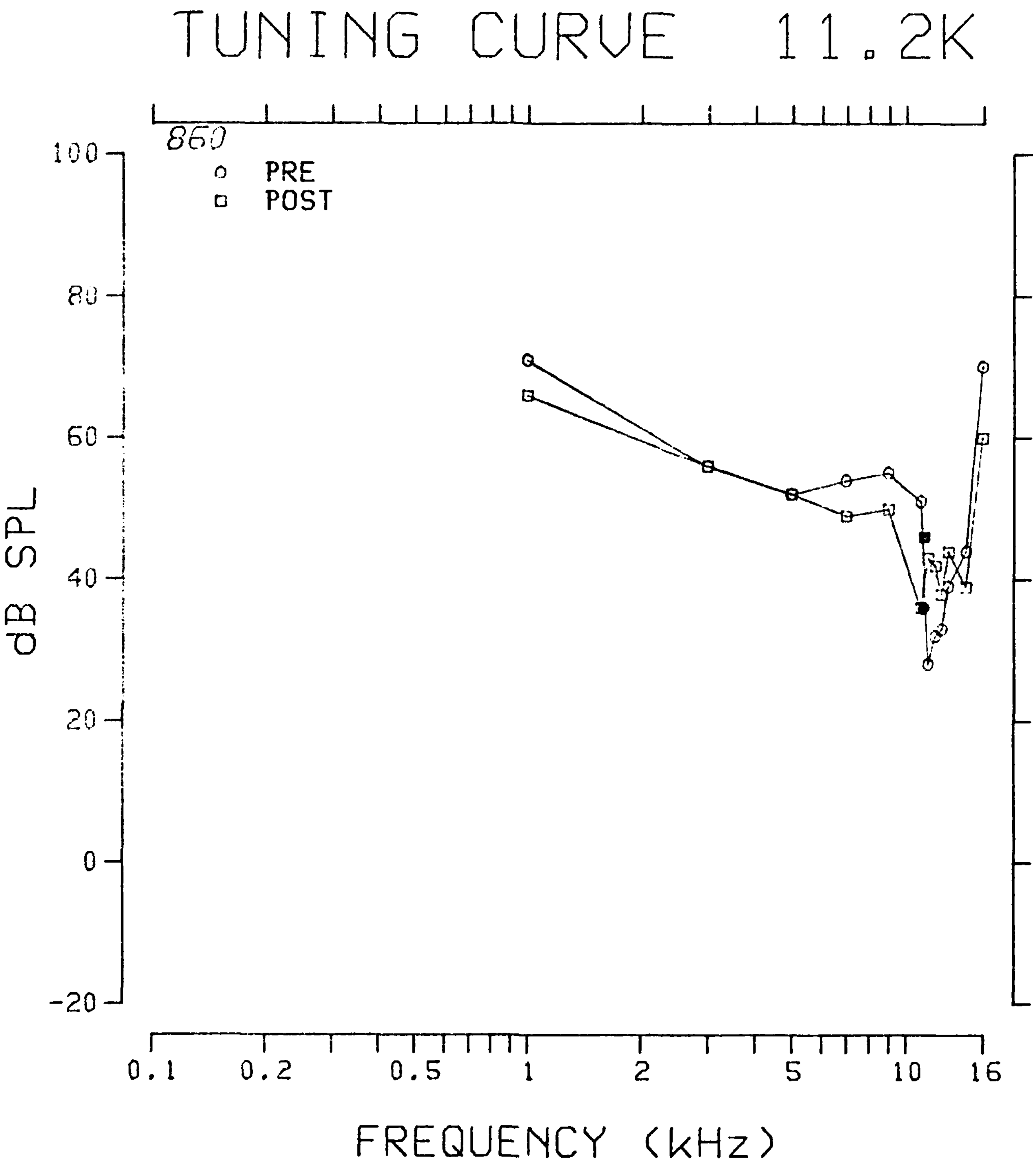


Fig. 3.3.178: Pre- and postexposure evoked response tuning curves at 11.2 kHz from chinchilla 860.

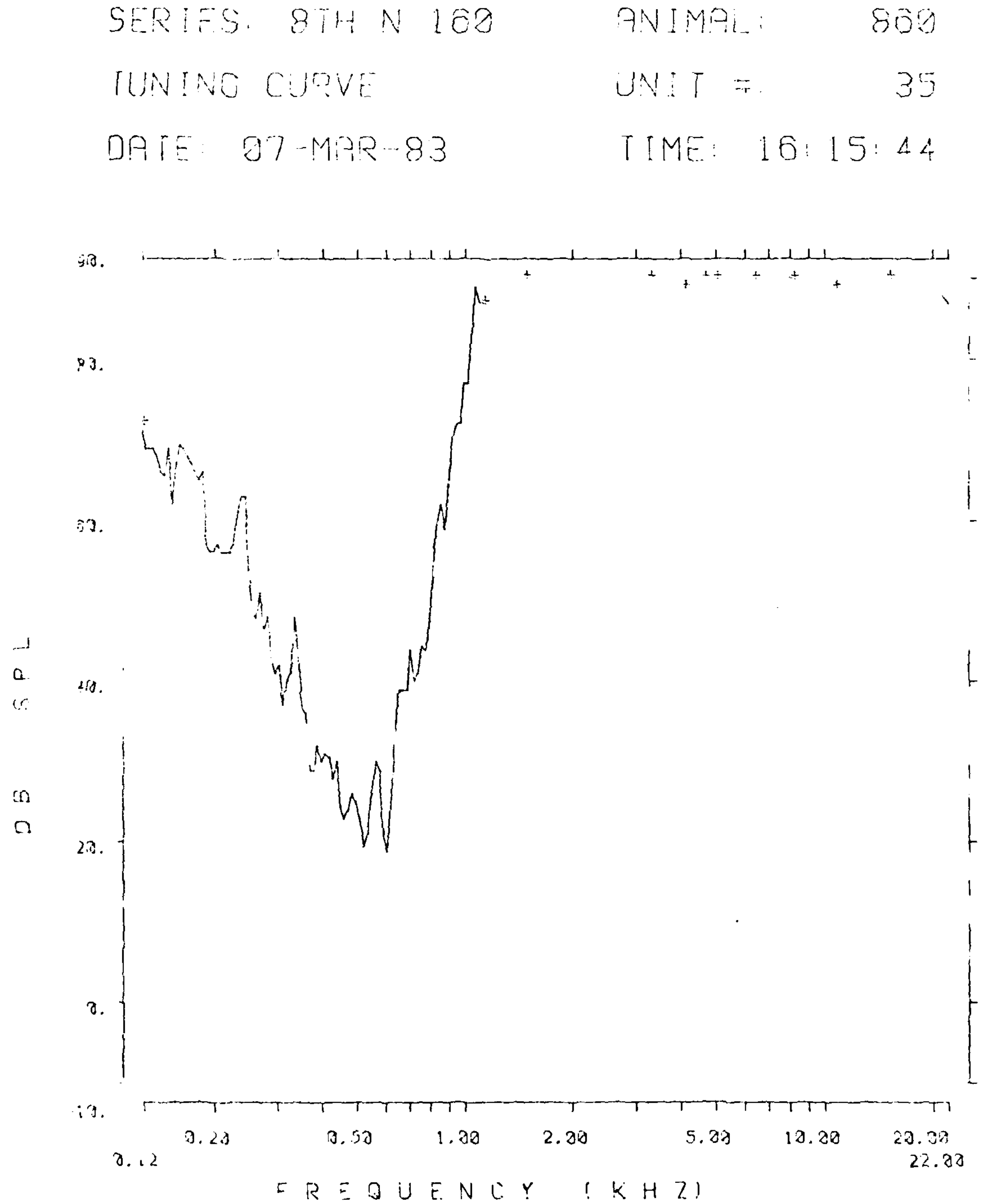


Fig. 3.3.179: Auditory nerve fiber tuning curve from chinchilla 860.

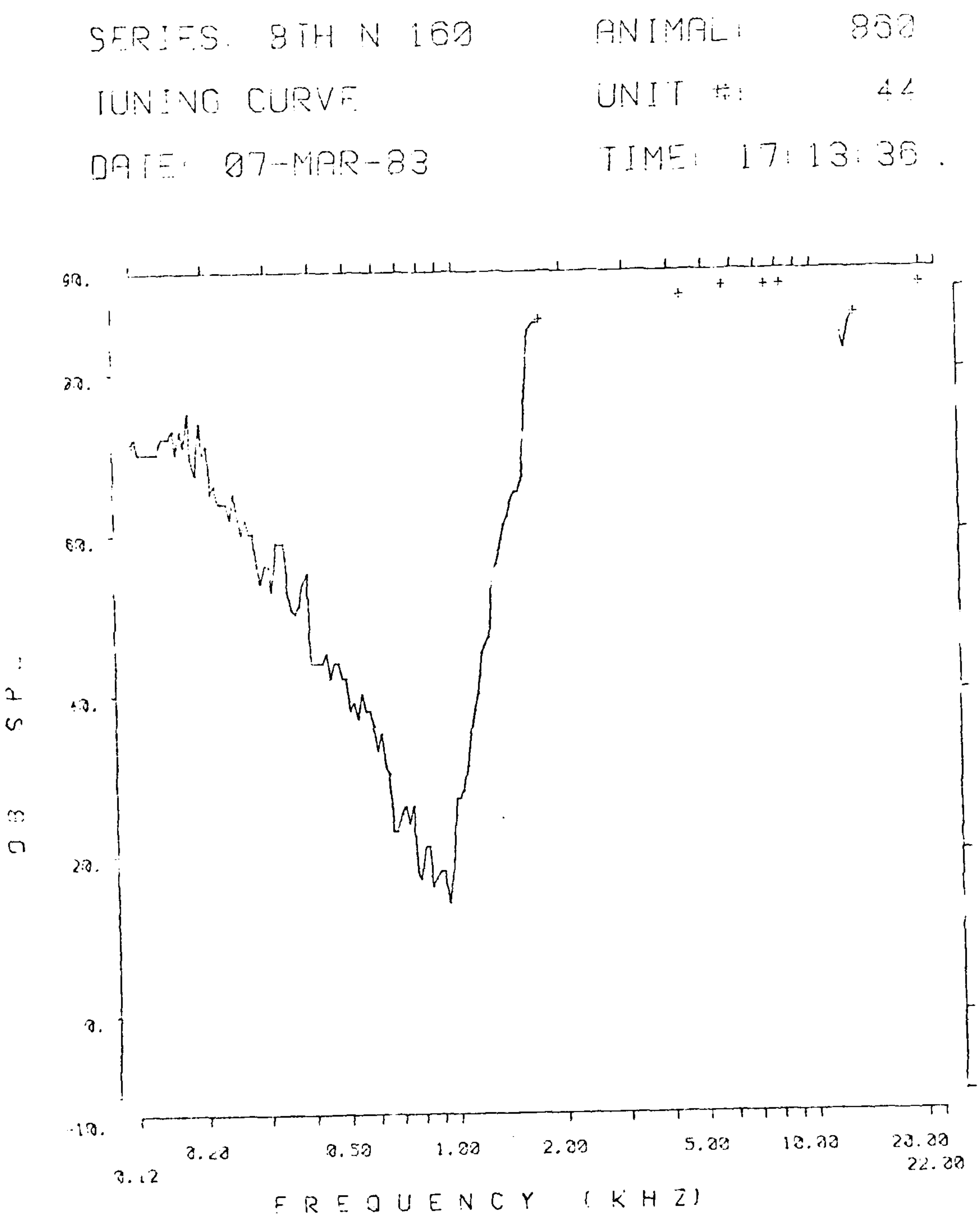


Fig. 3.3.180: Auditory nerve fiber tuning curve from chinchilla 860.

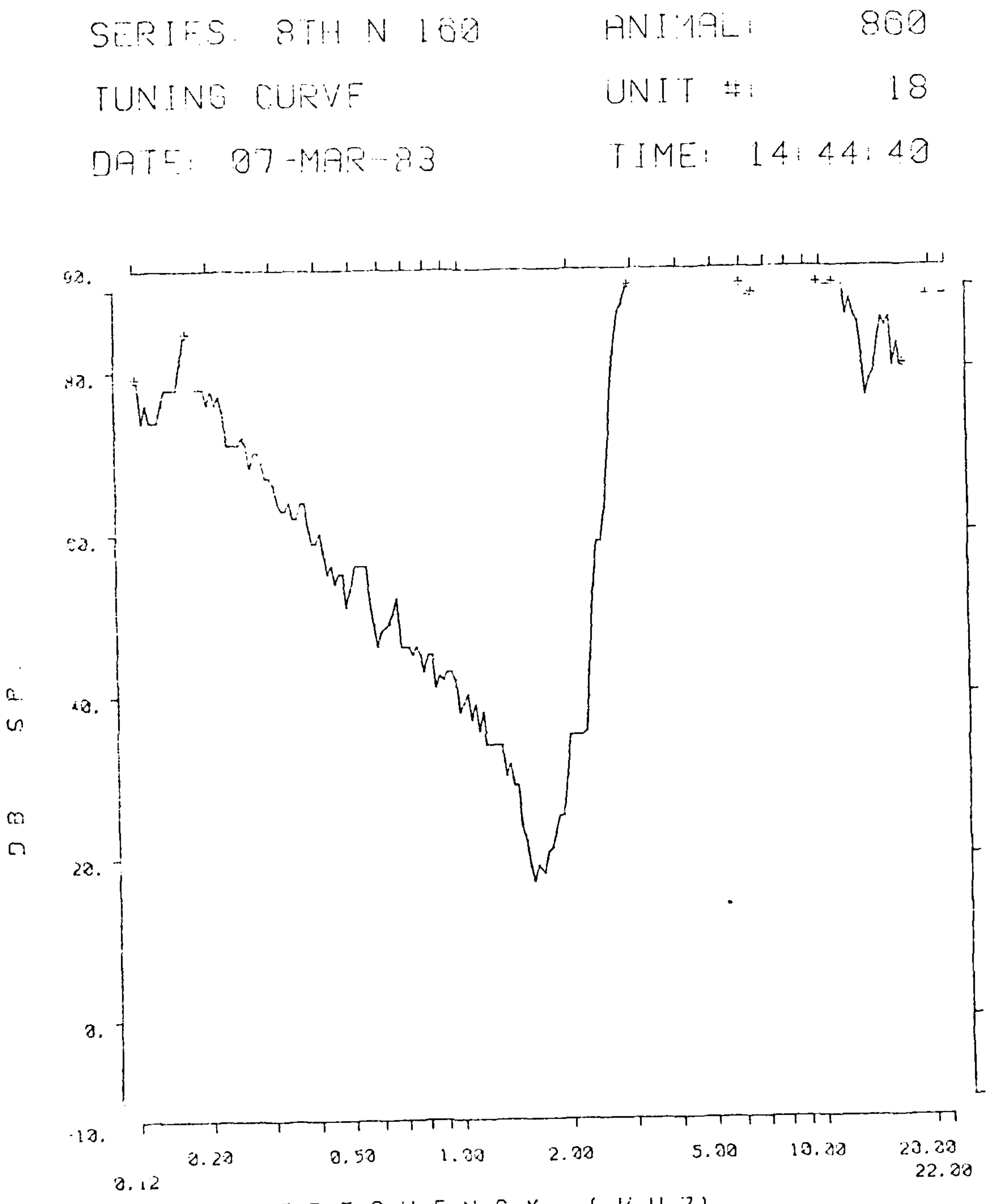


Fig. 3.3.181: Auditory nerve fiber tuning curve from chinchilla 860.

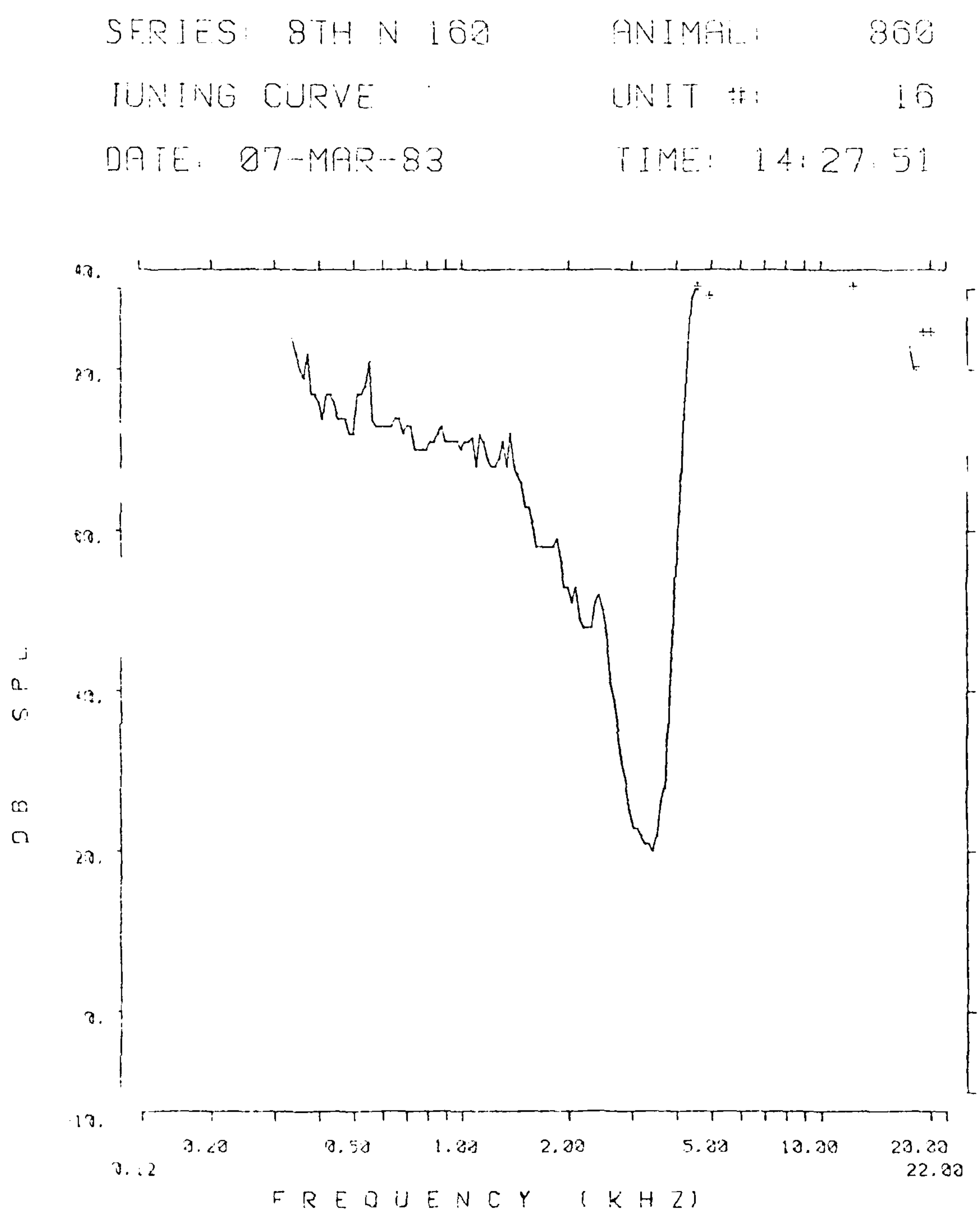


Fig. 3.3.182: Auditory nerve fiber tuning curve from chinchilla 860.

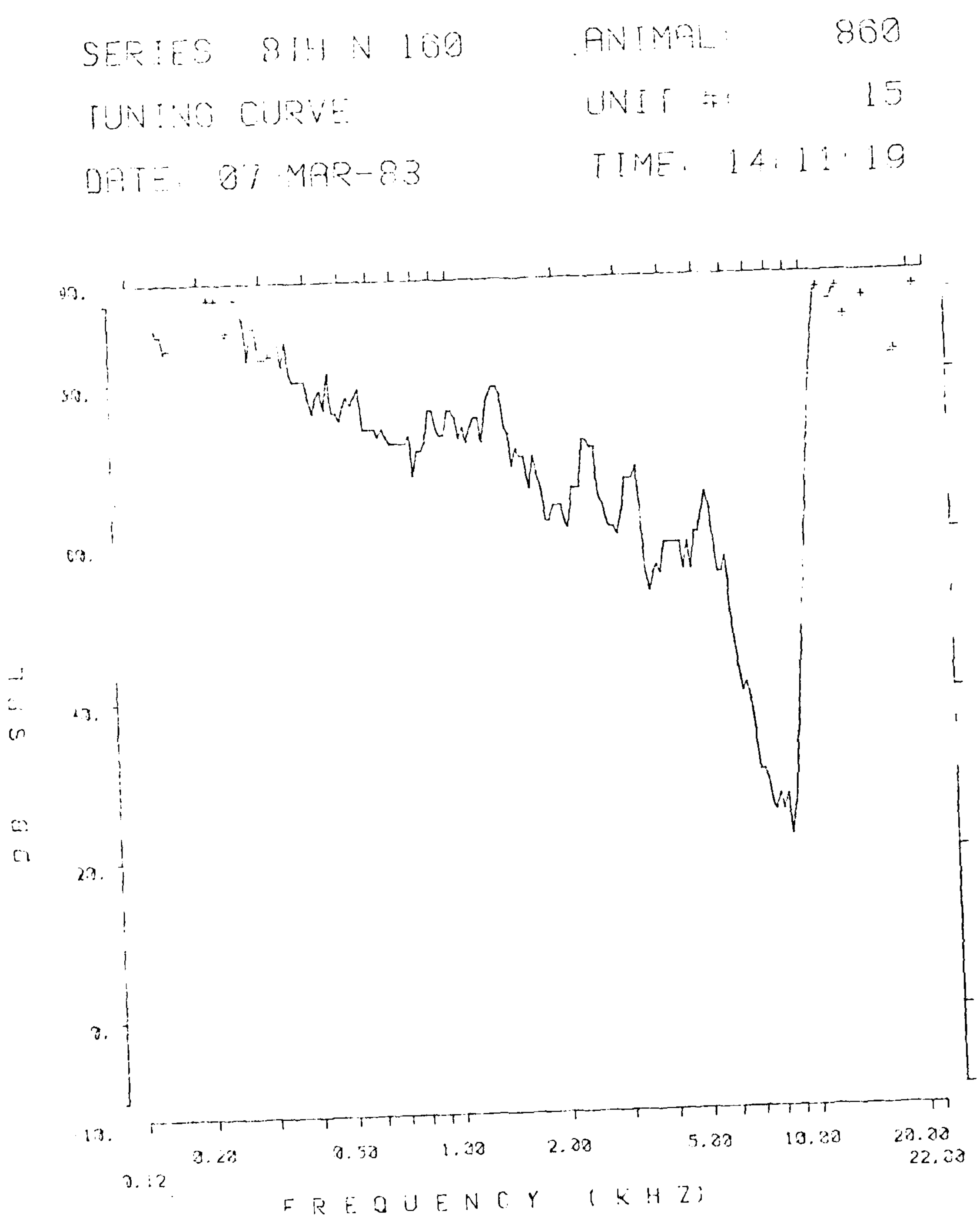


Fig. 3.3.183: Auditory nerve fiber tuning curve from chinchilla 860.

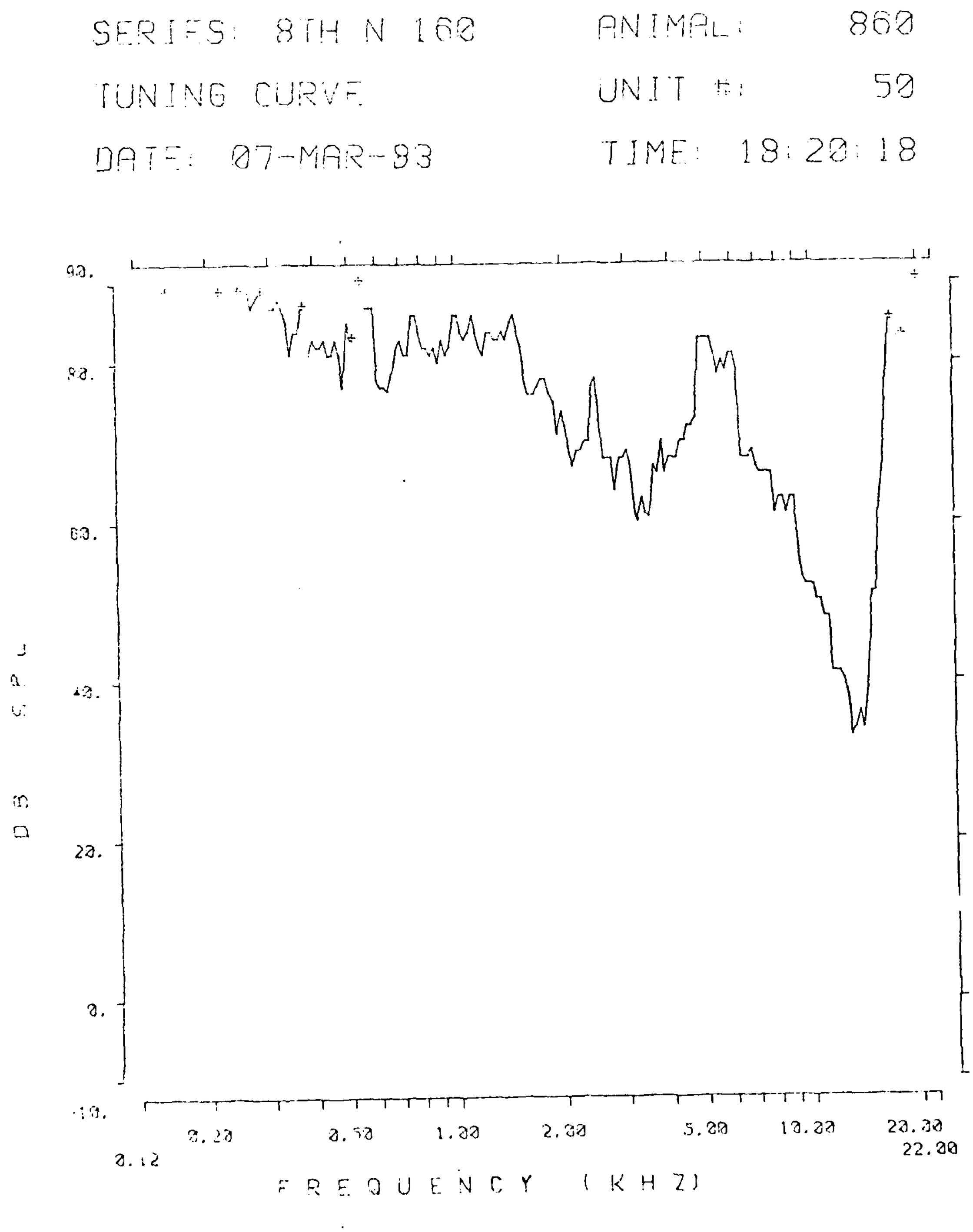


Fig. 3.3.184: Auditory nerve fiber tuning curve from chinchilla 860.

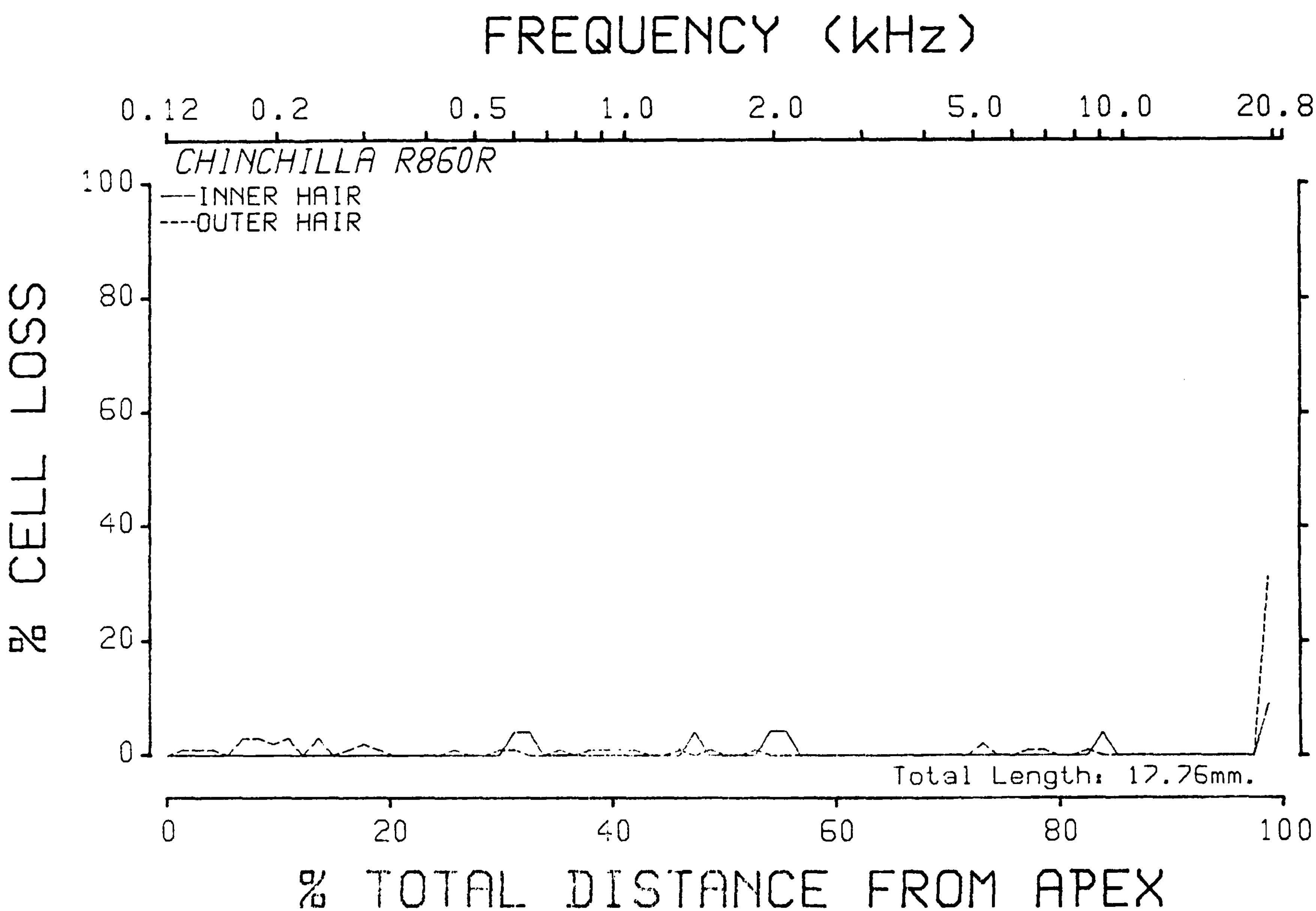


Fig. 3.3.185: Cochleogram from chinchilla 860.

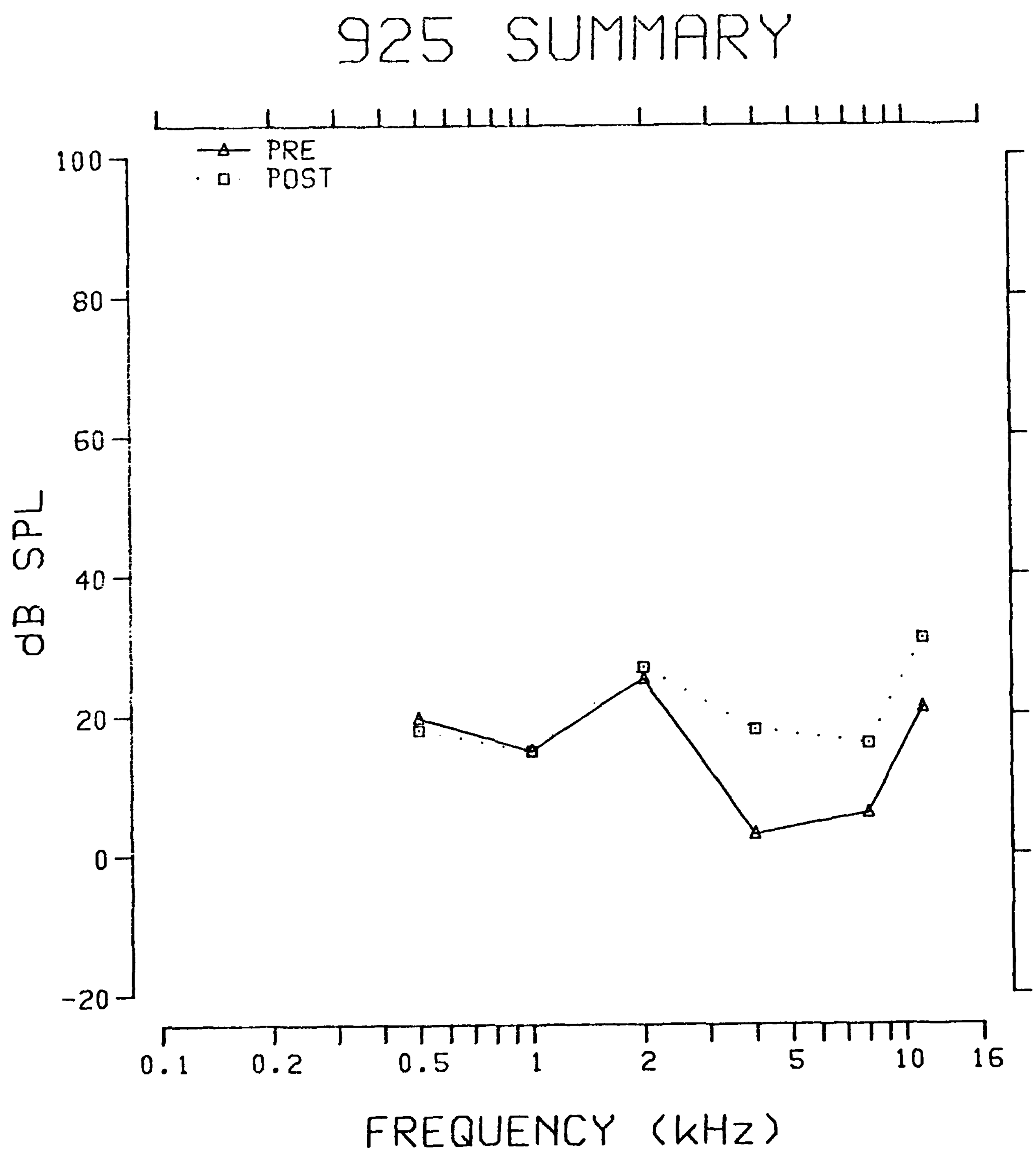


Fig. 3.3.186: Pre- and postexposure evoked response audiograms from chinchilla 925.

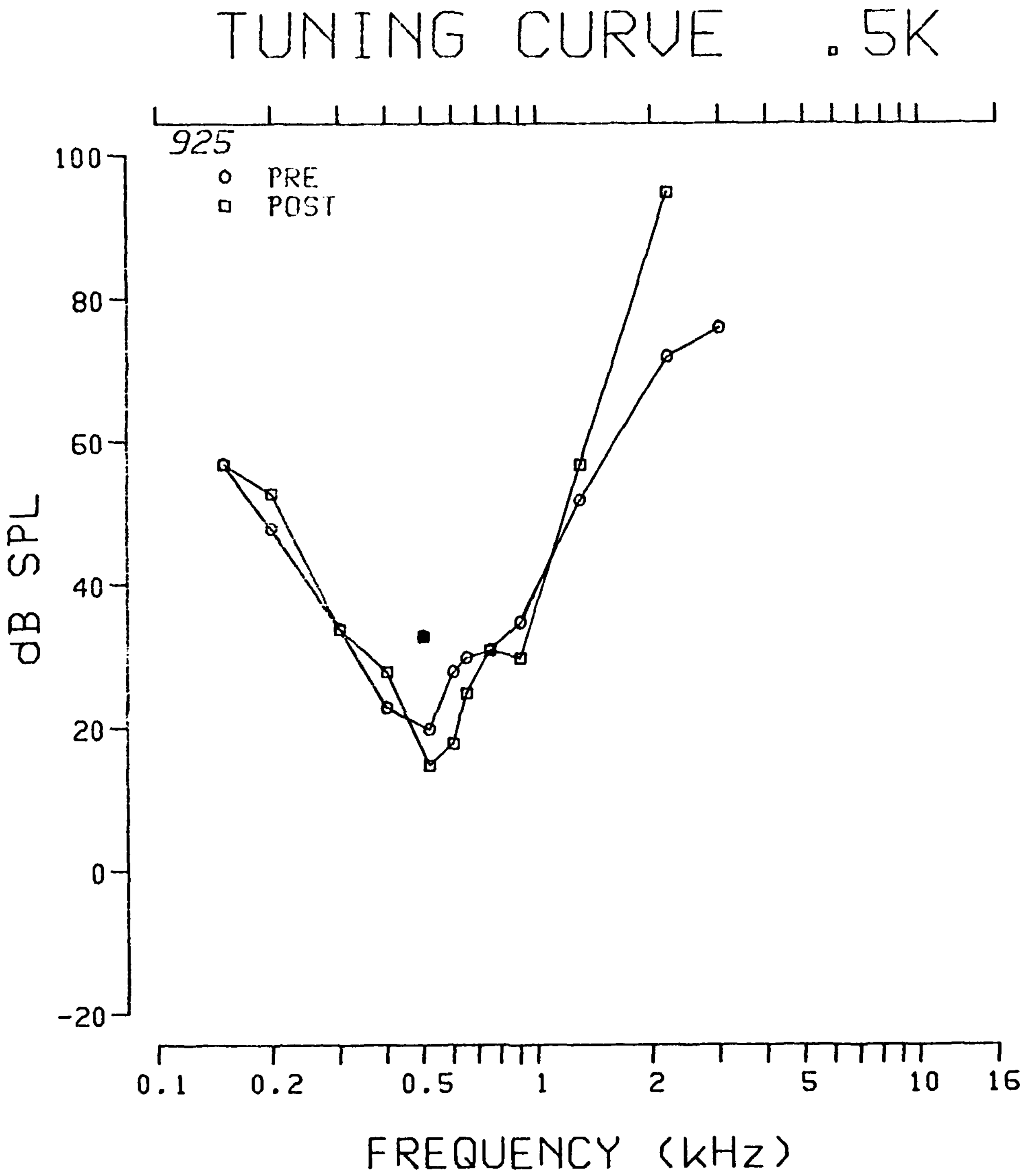


Fig. 3.3.187: Pre- and postexposure evoked response tuning curves at 0.5 kHz from chinchilla 925.

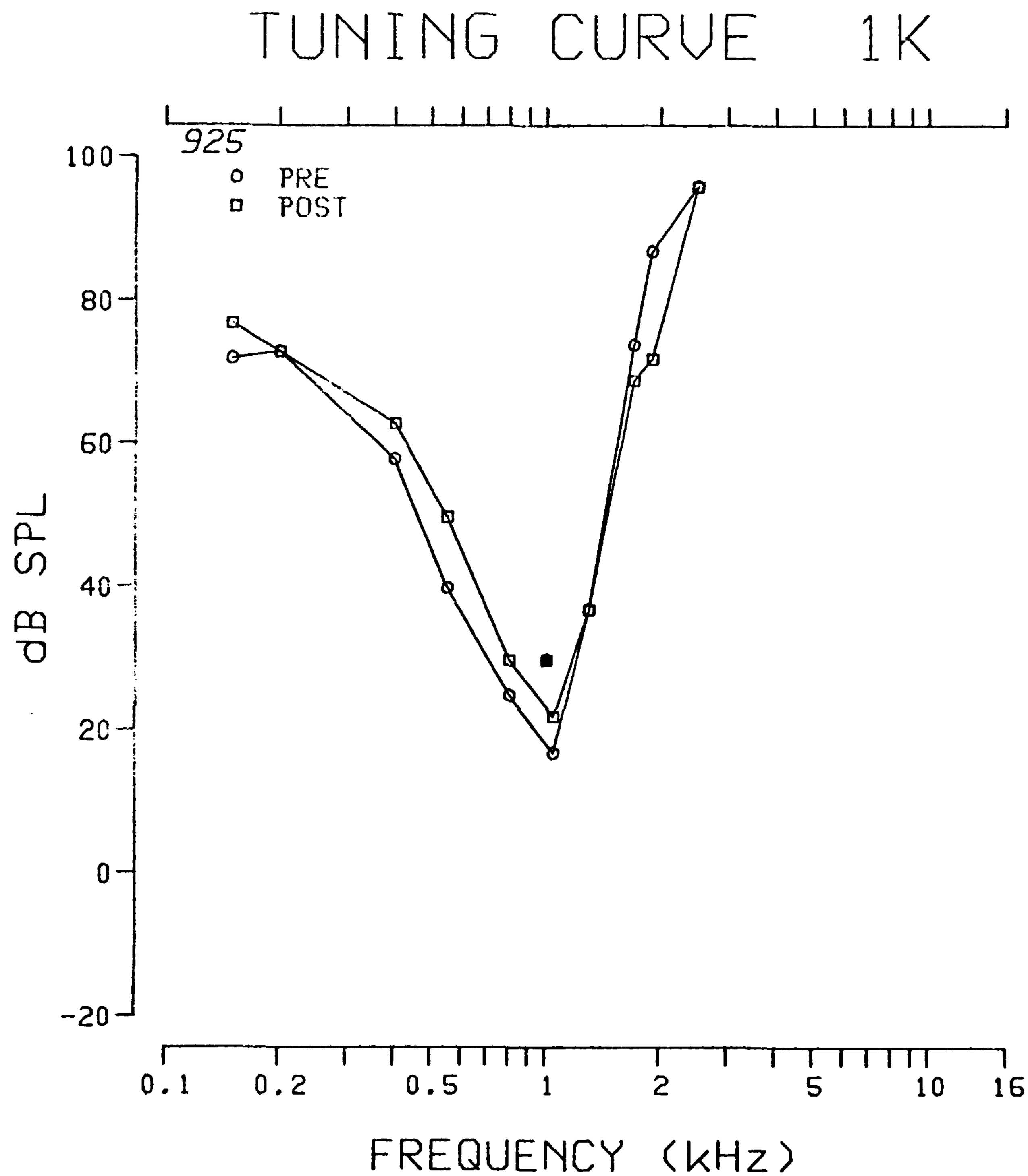


Fig. 3.3.188: Pre- and postexposure evoked response tuning curves at 1.0 kHz from chinchilla 925.

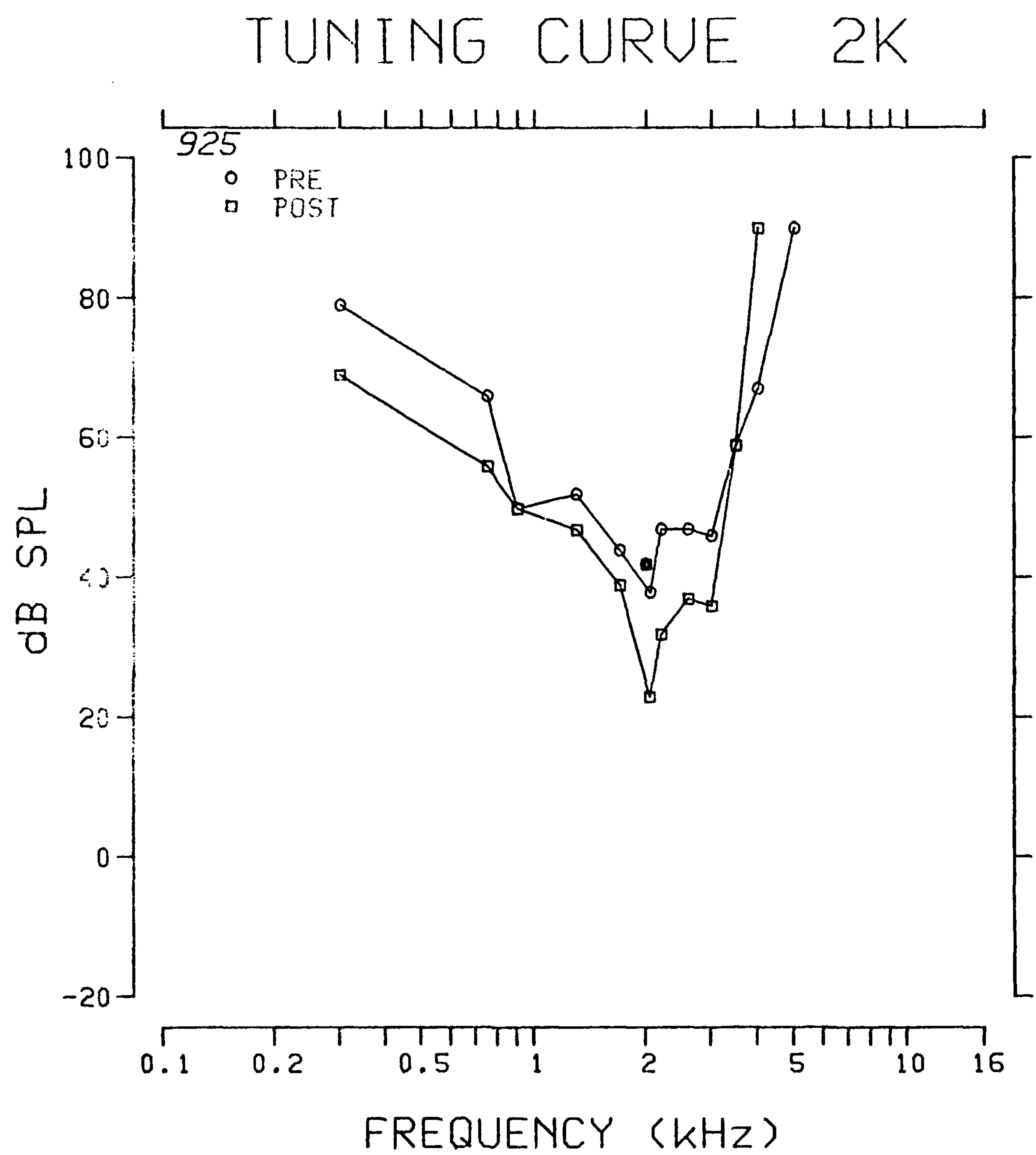


Fig. 3.3.189: Pre- and postexposure evoked response tuning curves at 2.0 kHz from chinchilla 925.

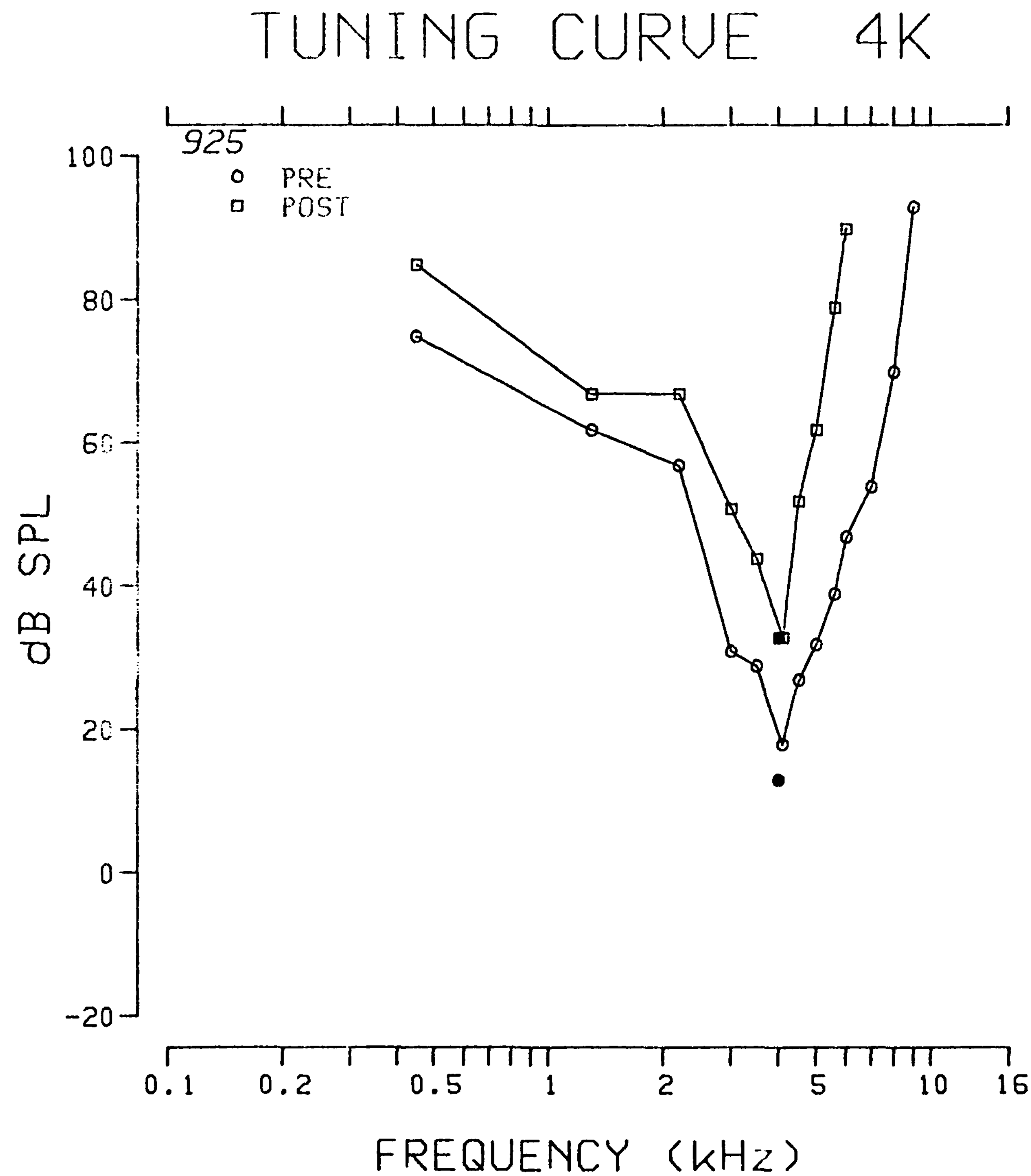


Fig. 3.3.190: Pre- and postexposure evoked response tuning curves at 4.0 kHz from chinchilla 925.

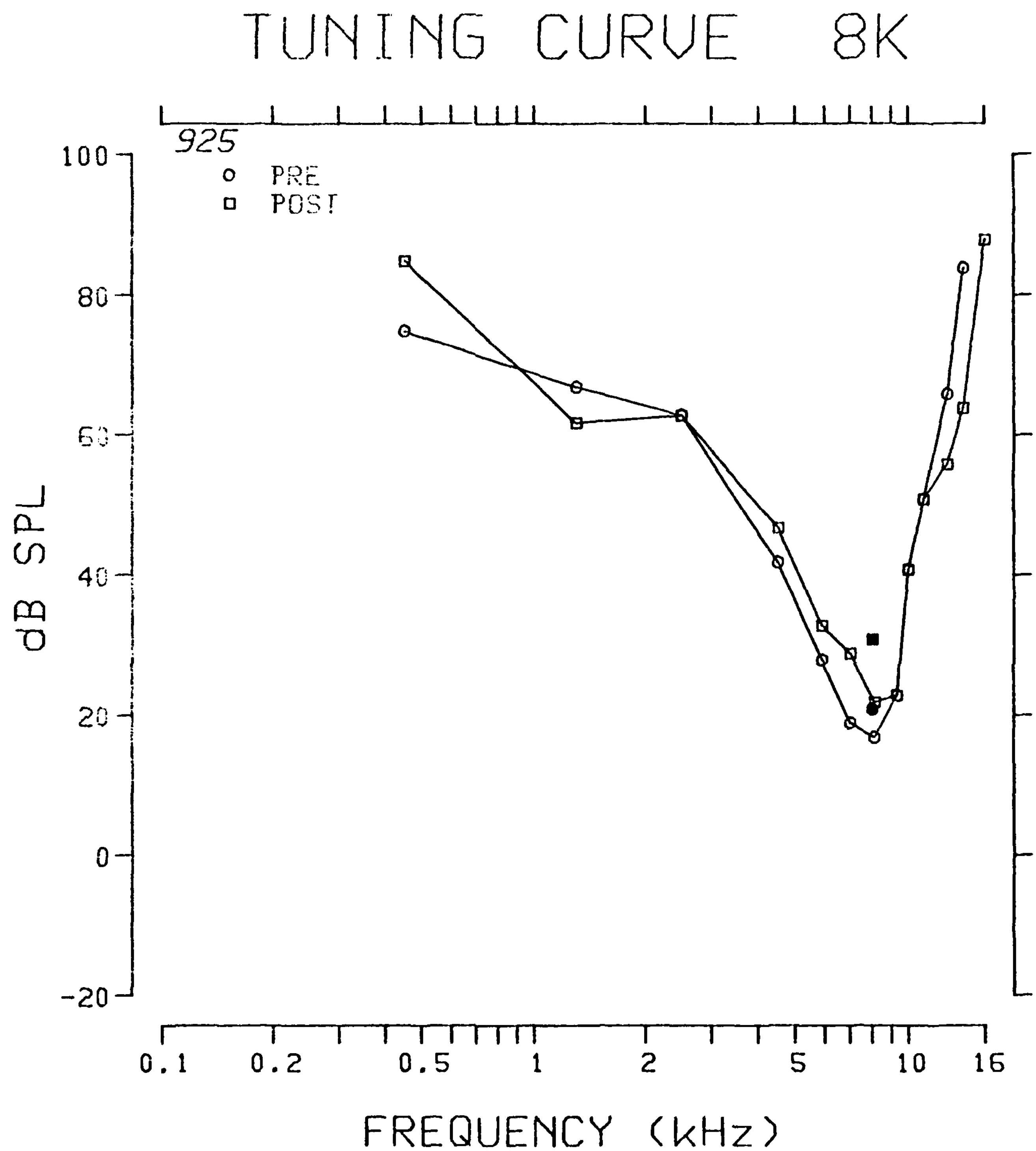


Fig. 3.3.191: Pre- and postexposure evoked response tuning curves at 8.0 kHz from chinchilla 925.

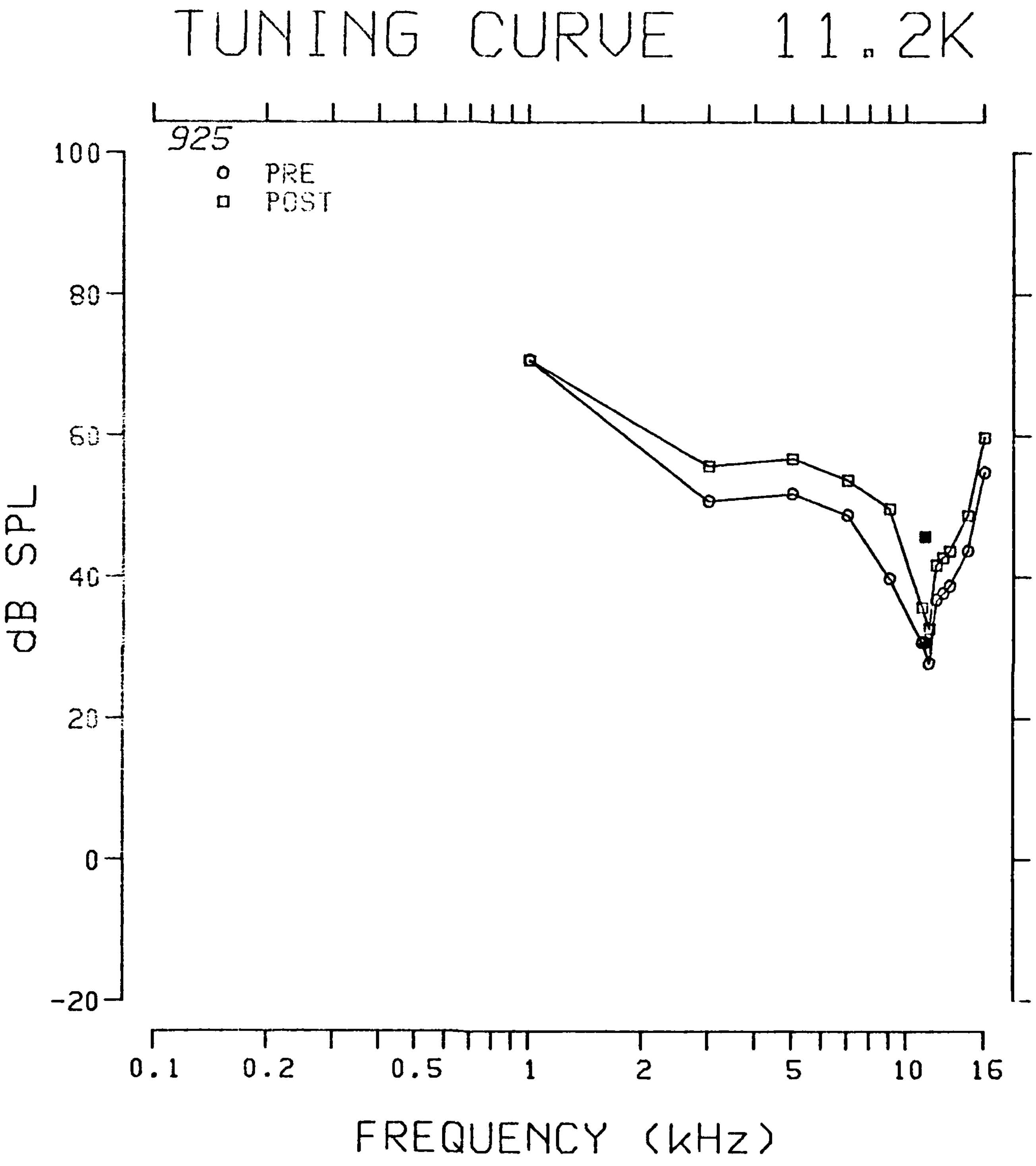


Fig. 3.3.192: Pre- and postexposure evoked response tuning curves at 11.2 kHz from chinchilla 925.

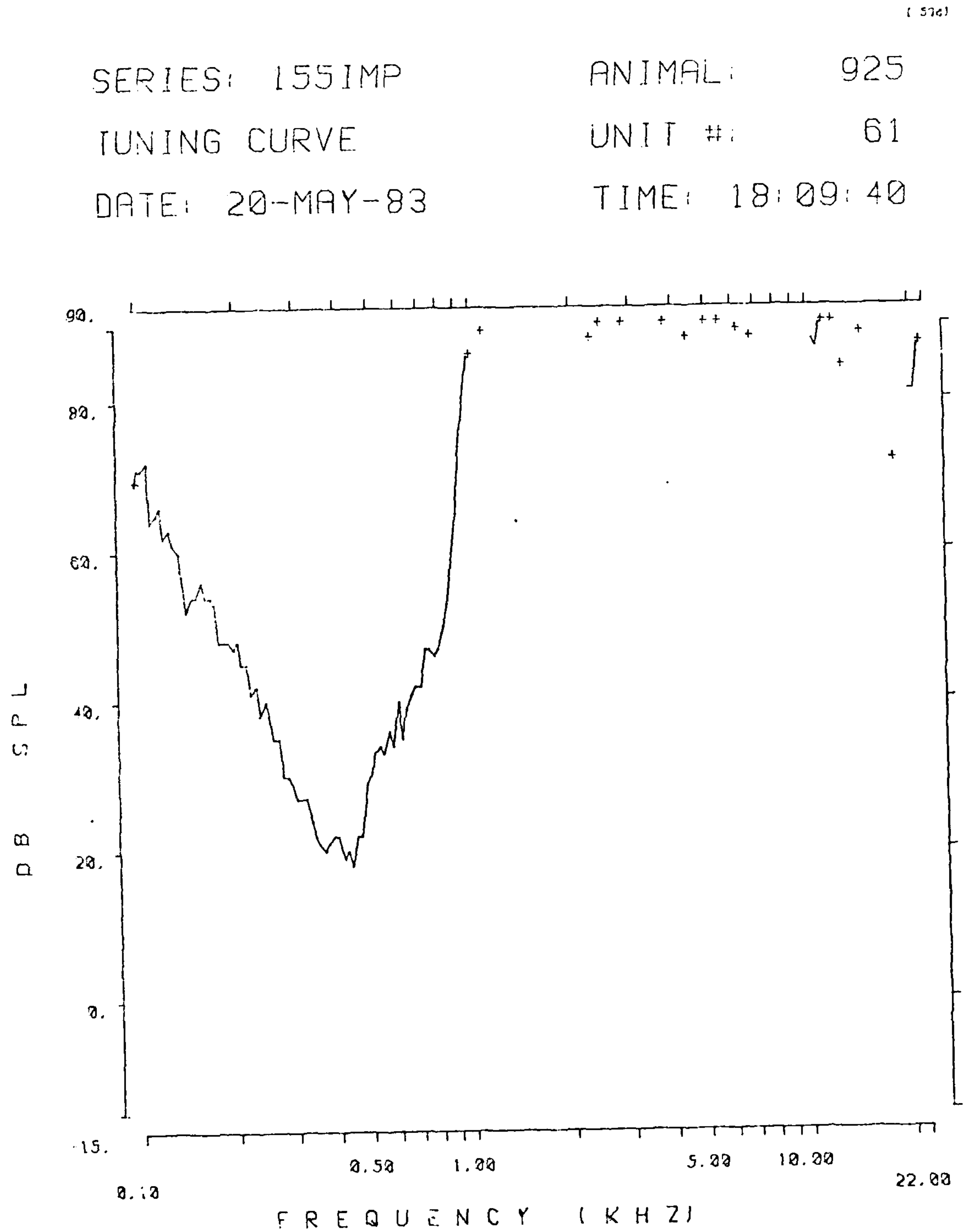


Fig. 3.3.193: Auditory nerve fiber tuning curve from chinchilla 925.

[544]

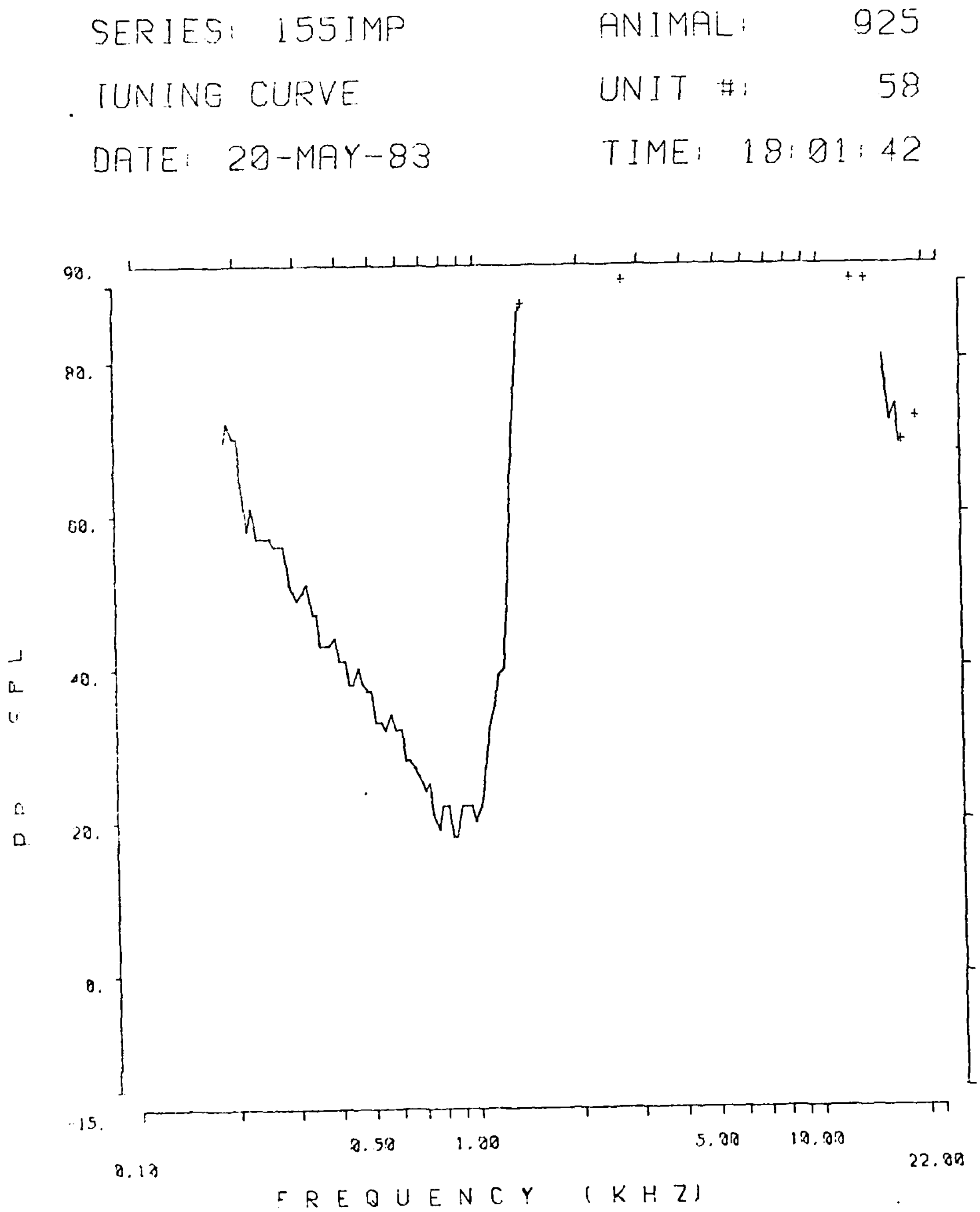


Fig. 3.3.194: Auditory nerve fiber tuning curve from chinchilla 925.

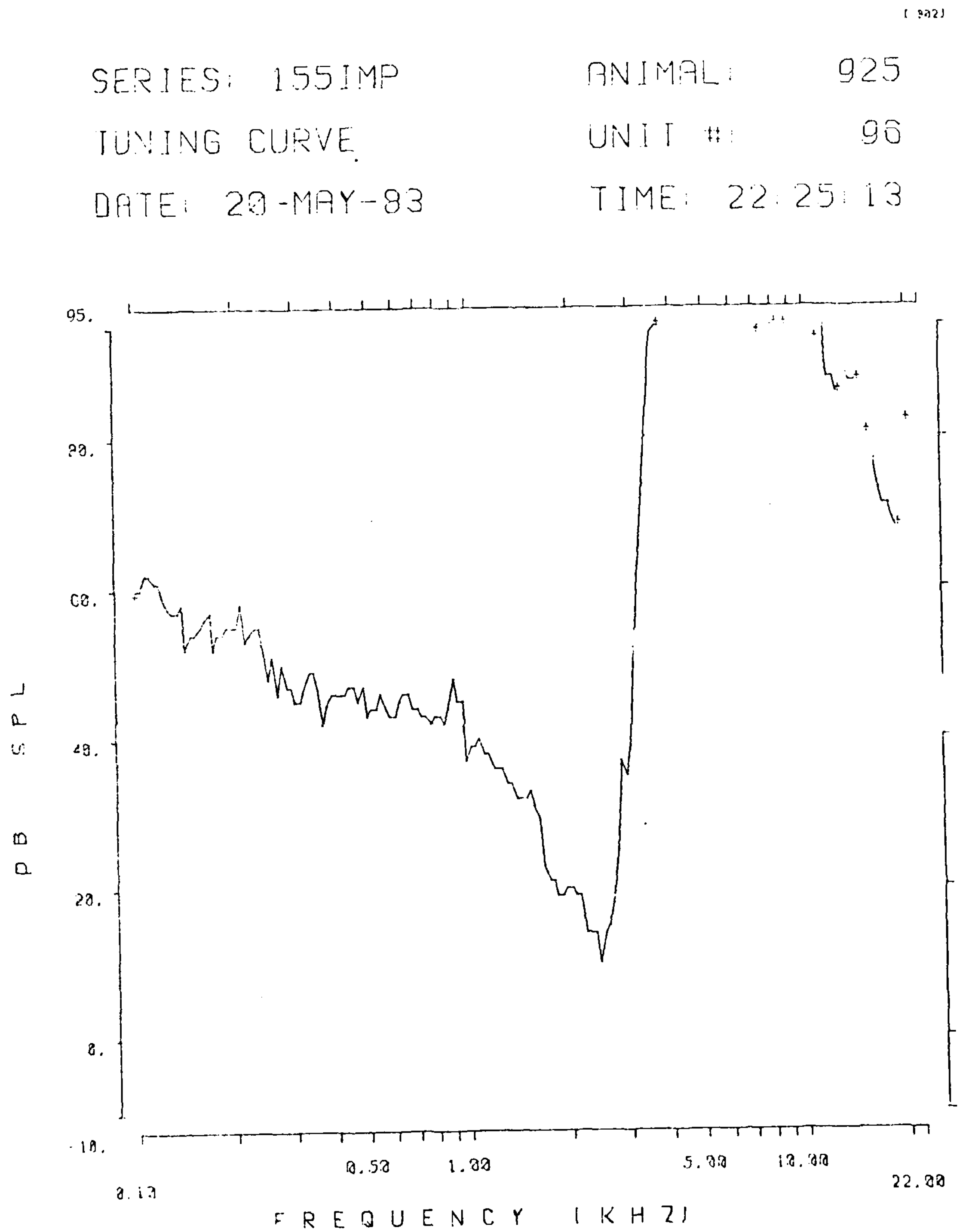


Fig. 3.3.195: Auditory nerve fiber tuning curve from chinchilla 925.

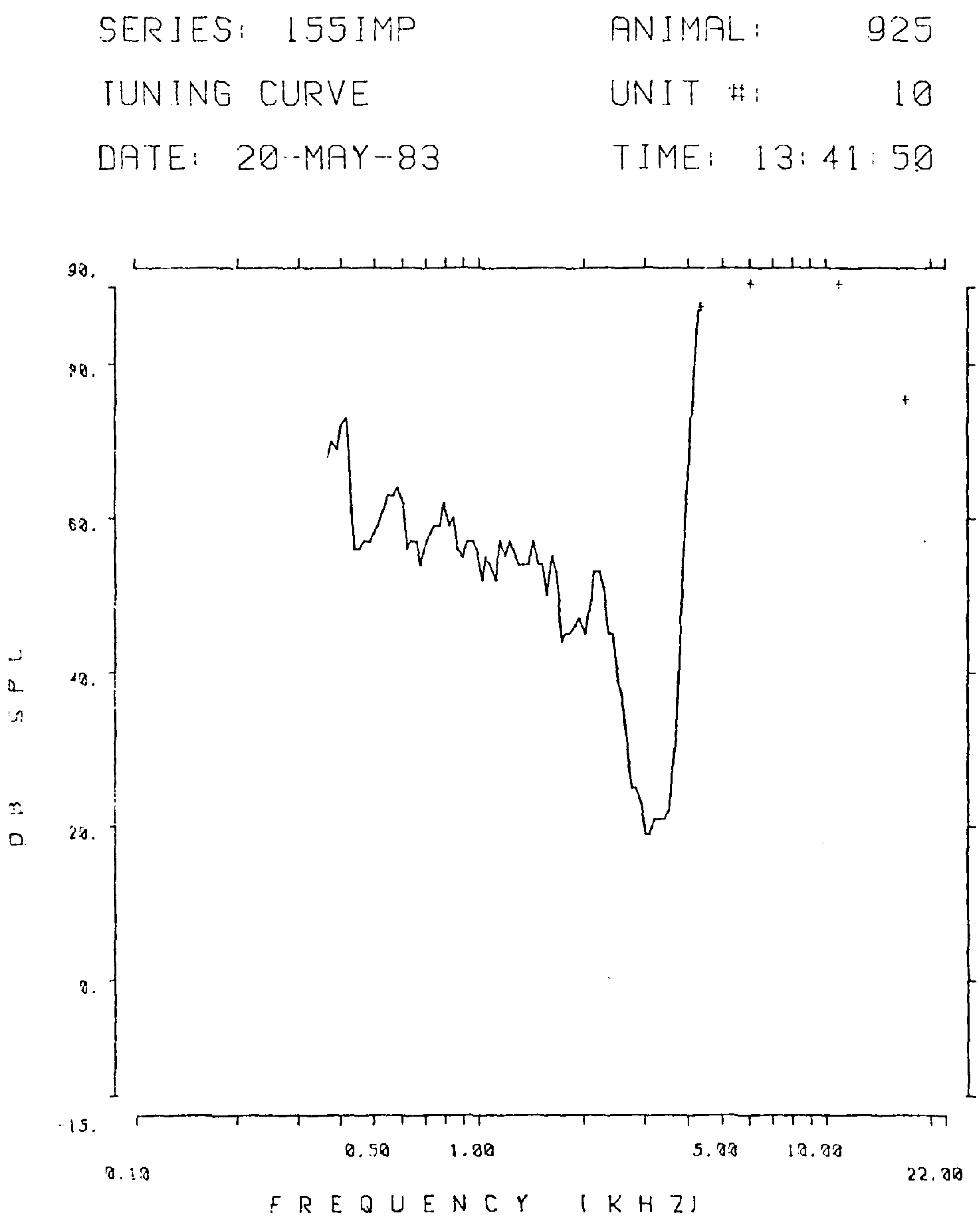


Fig. 3.3.196: Auditory nerve fiber tuning curve from chinchilla 925.

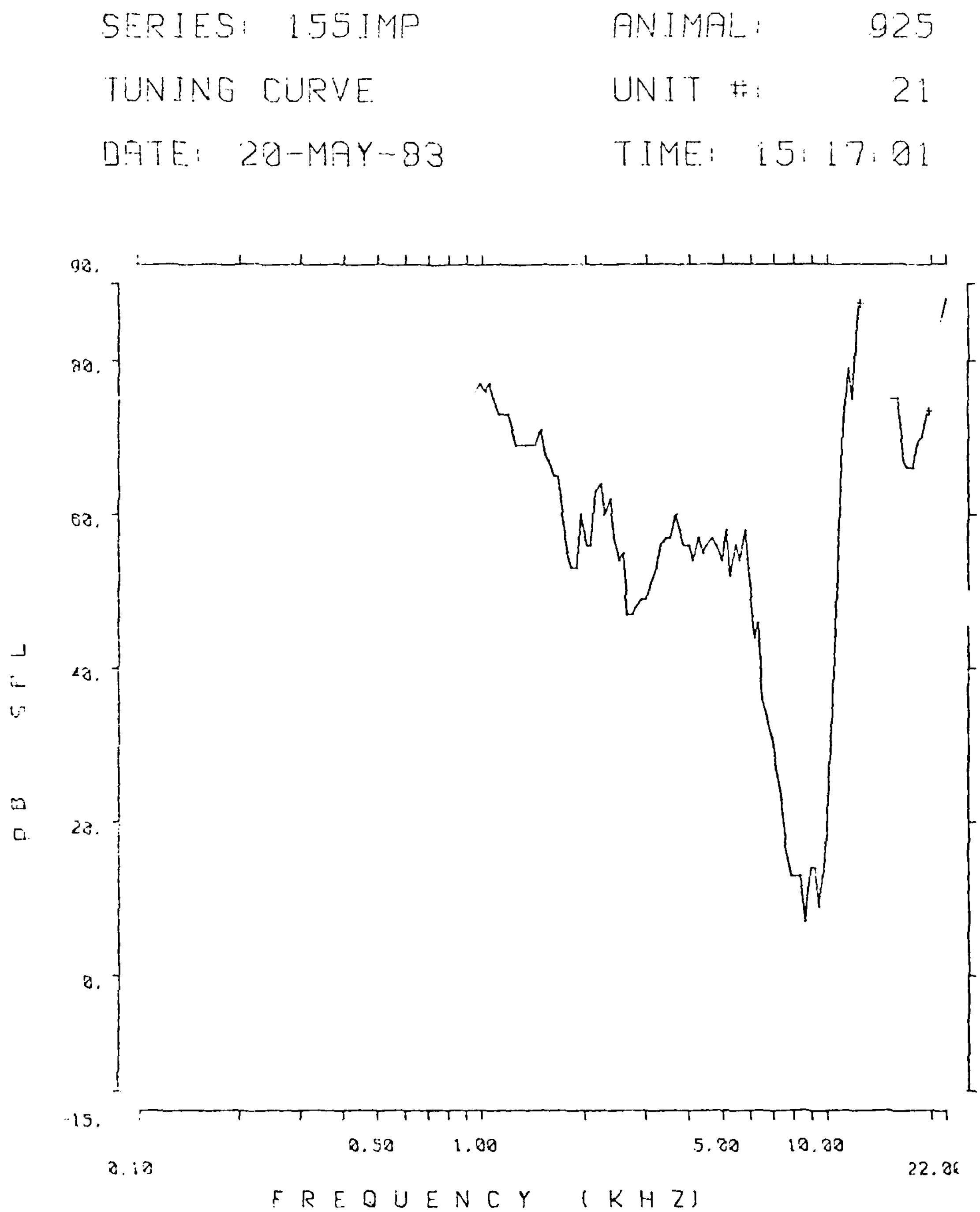


Fig. 3.3.197: Auditory nerve fiber tuning curve from chinchilla 925.

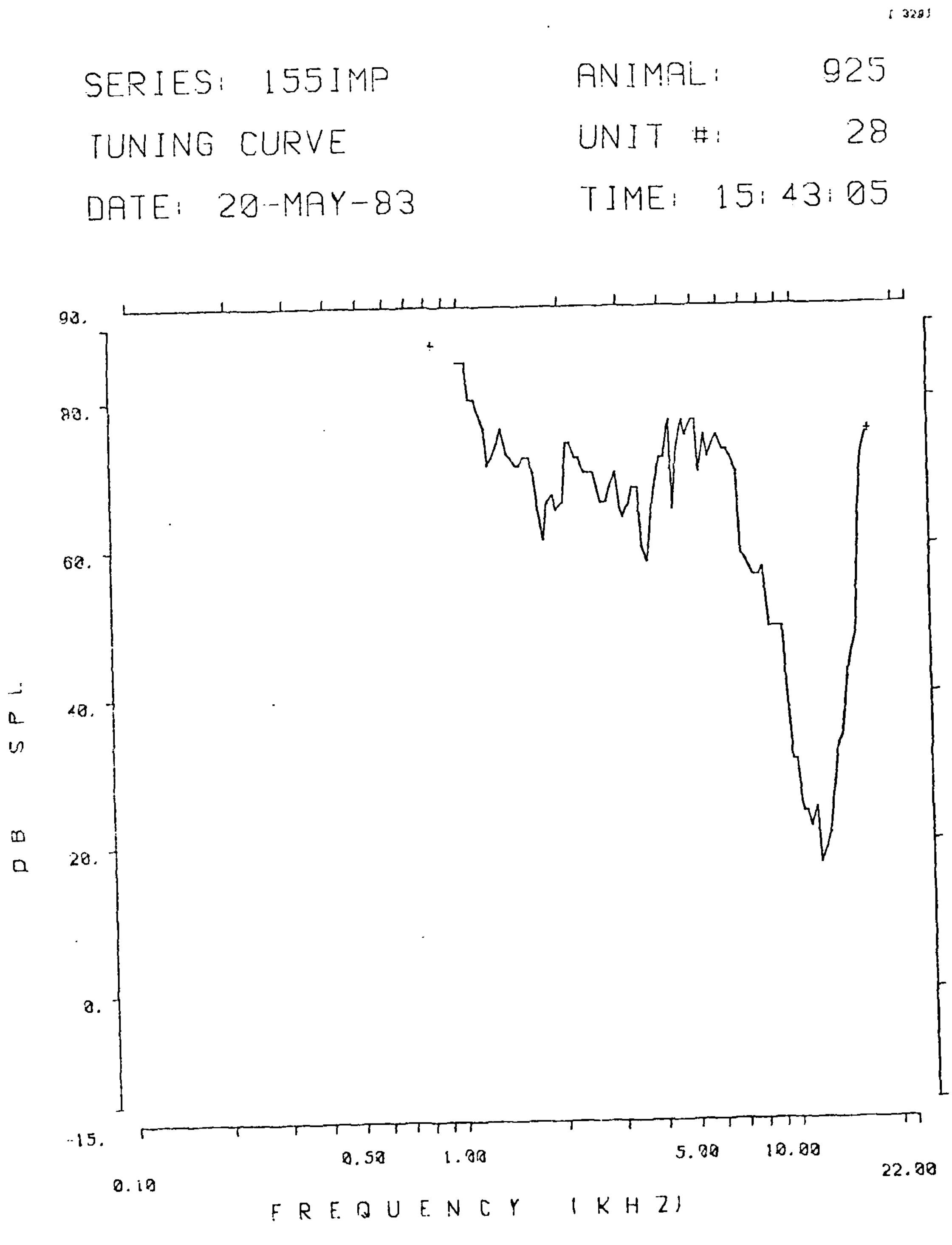


Fig. 3.3.198: Auditory nerve fiber tuning curve from chinchilla 925.

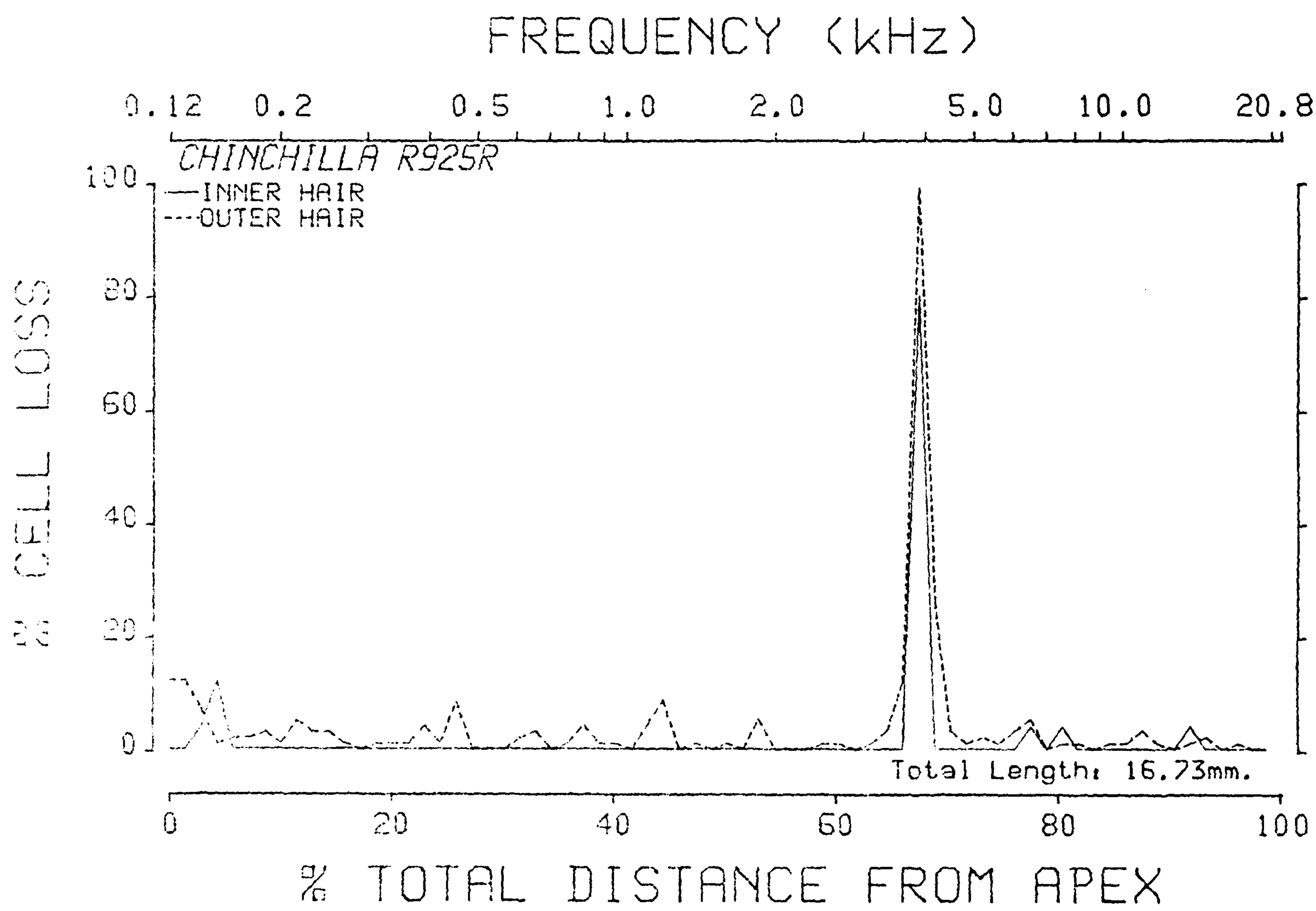


Fig. 3.3.199: Cochleogram from chinchilla 925.

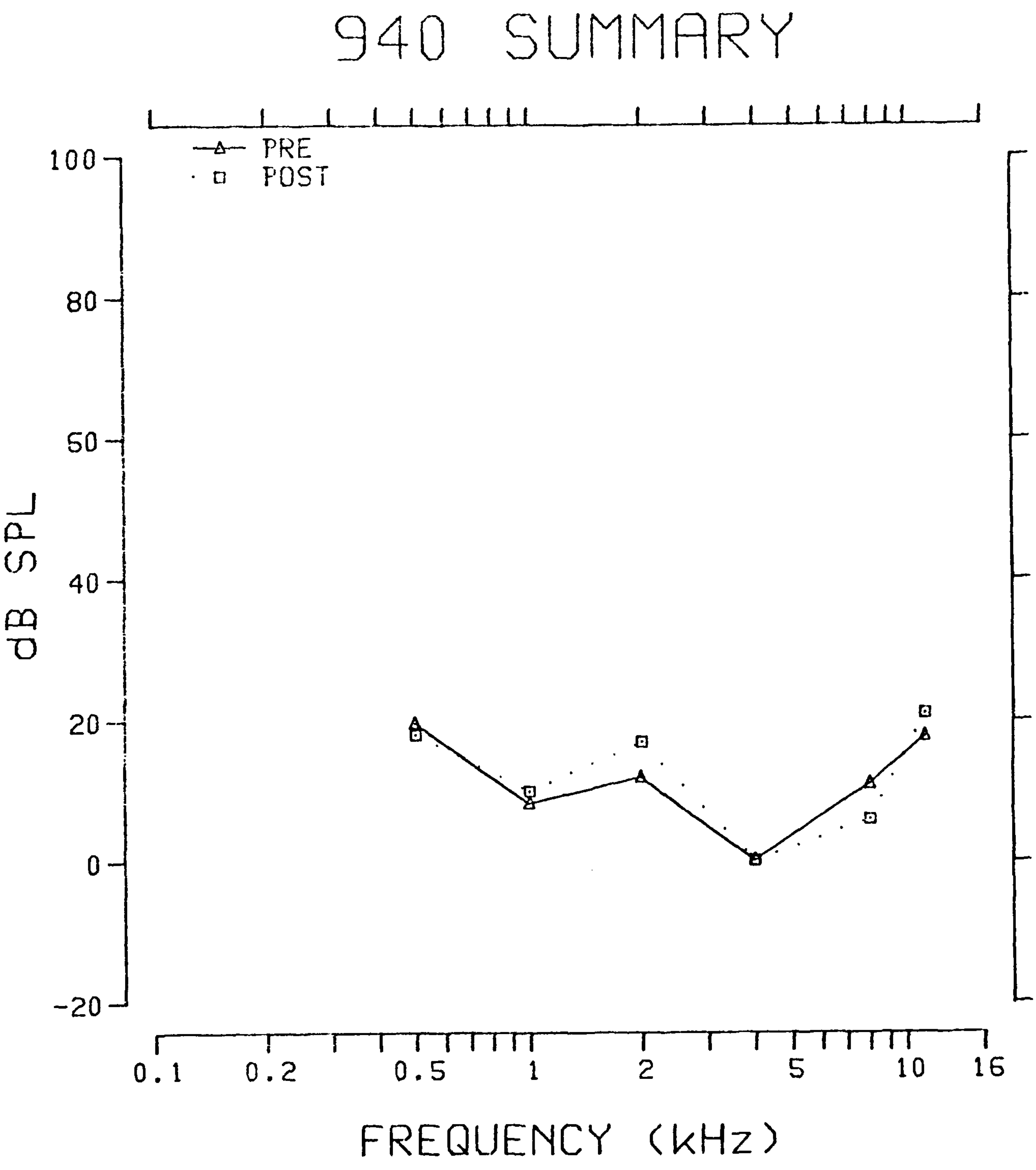


Fig. 3.3.200: Pre- and postexposure evoked response audiograms from chinchilla 940.

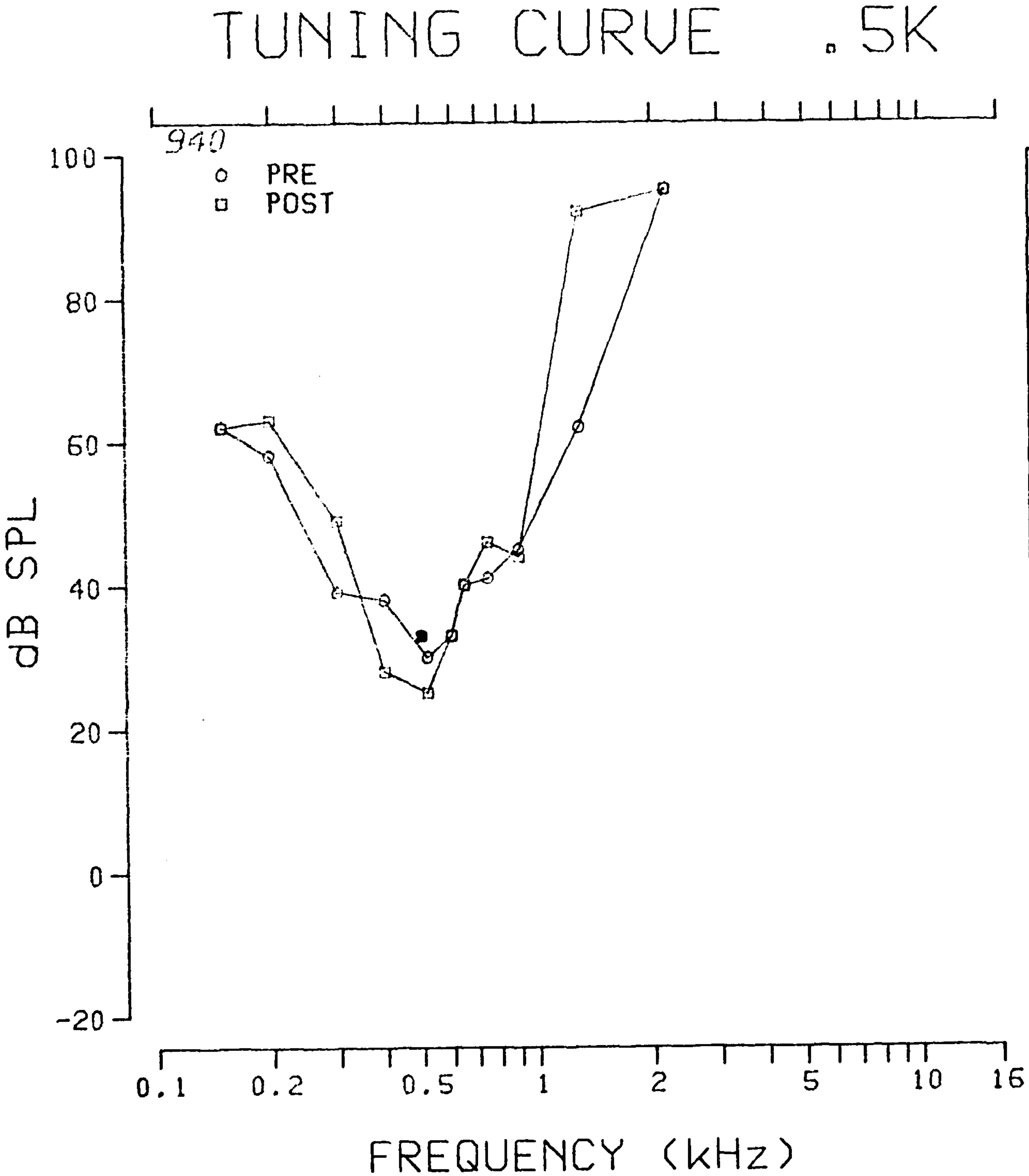


Fig. 3.3.201: Pre- and postexposure evoked response tuning curves at 0.5 kHz from chinchilla 940.

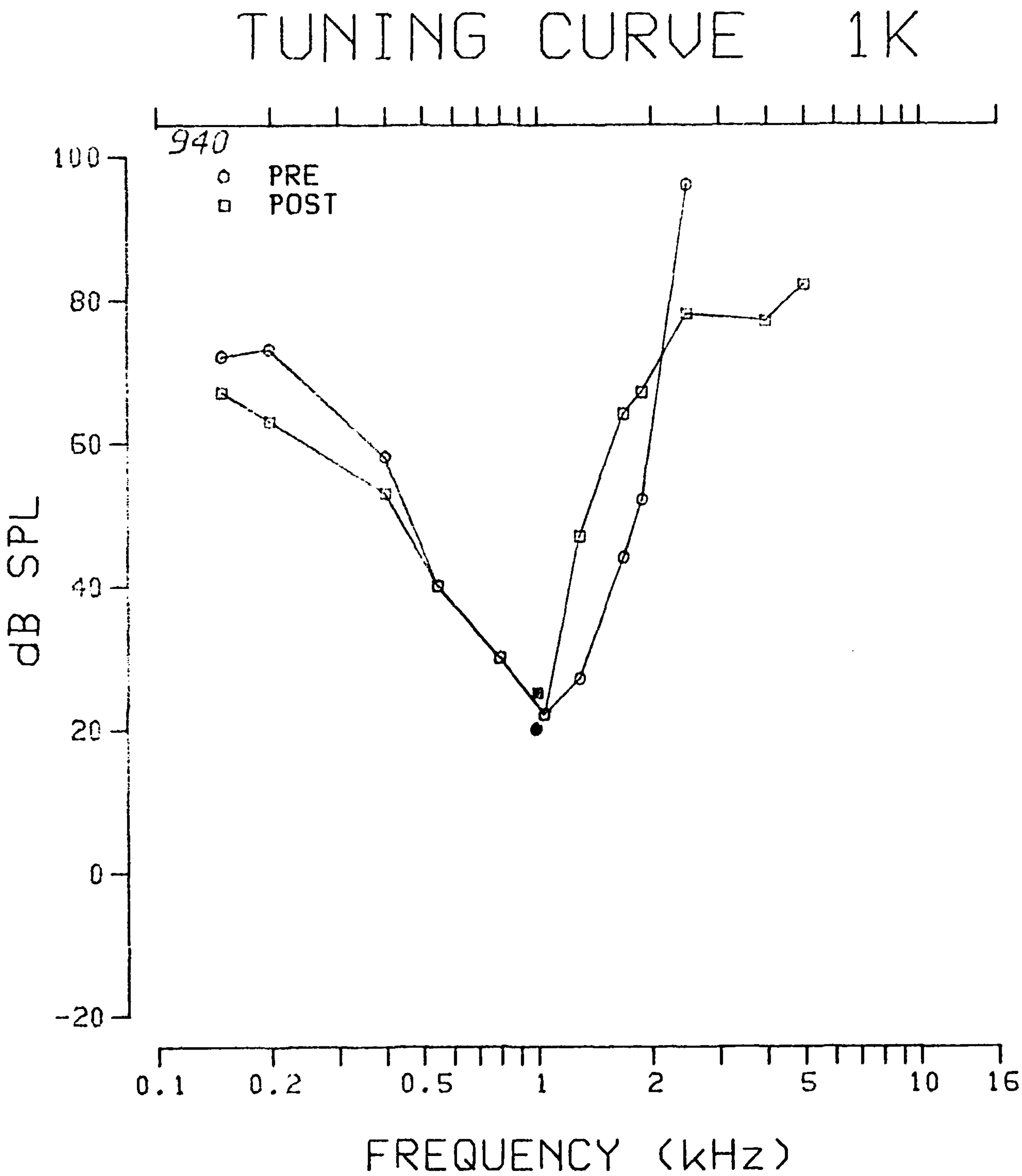


Fig. 3.3.202: Pre- and postexposure evoked response tuning curves at 1.0 kHz from chinchilla 940.

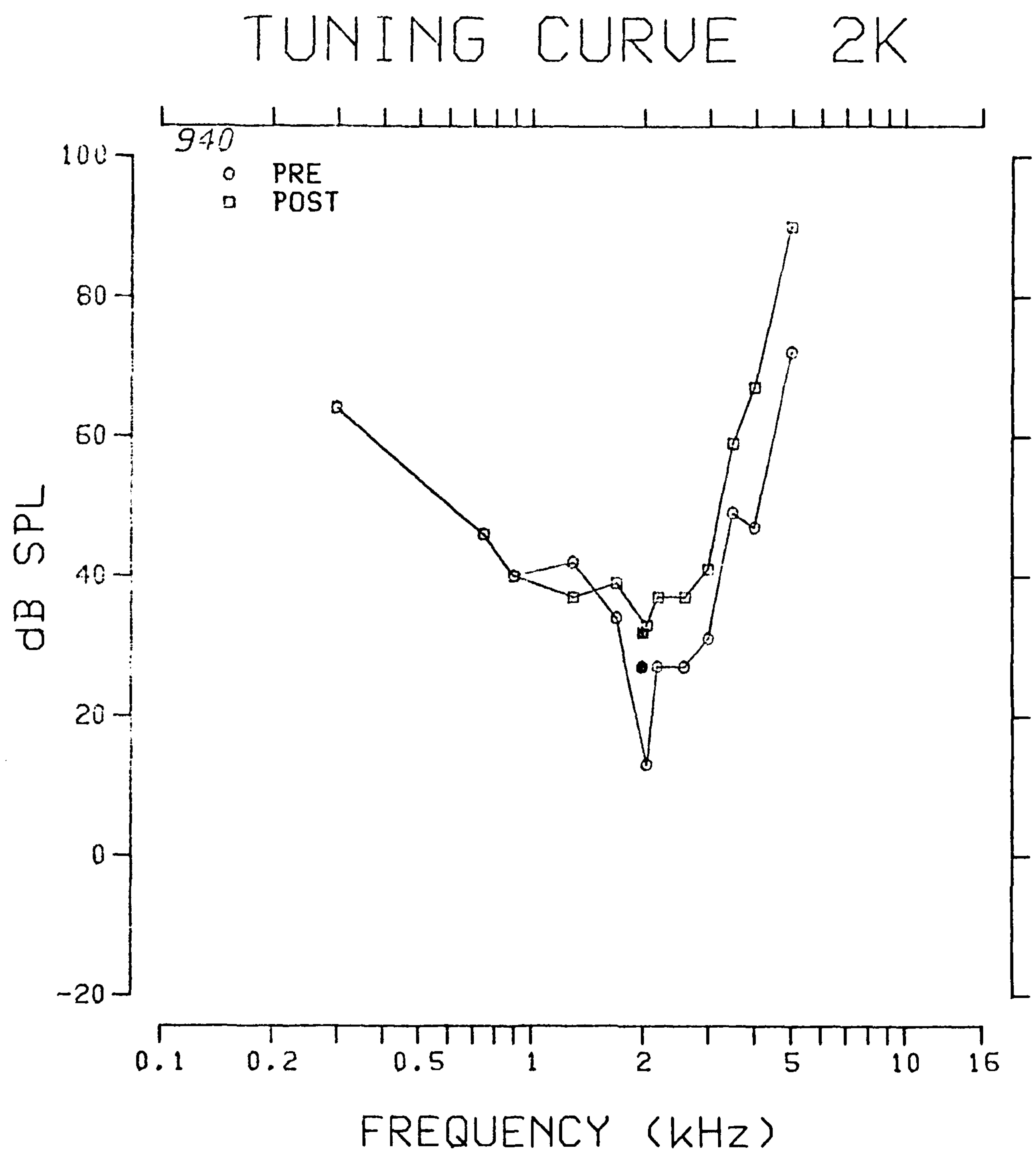


Fig. 3.3.203: Pre- and postexposure evoked response tuning curves at 2.0 kHz from chinchilla 940.

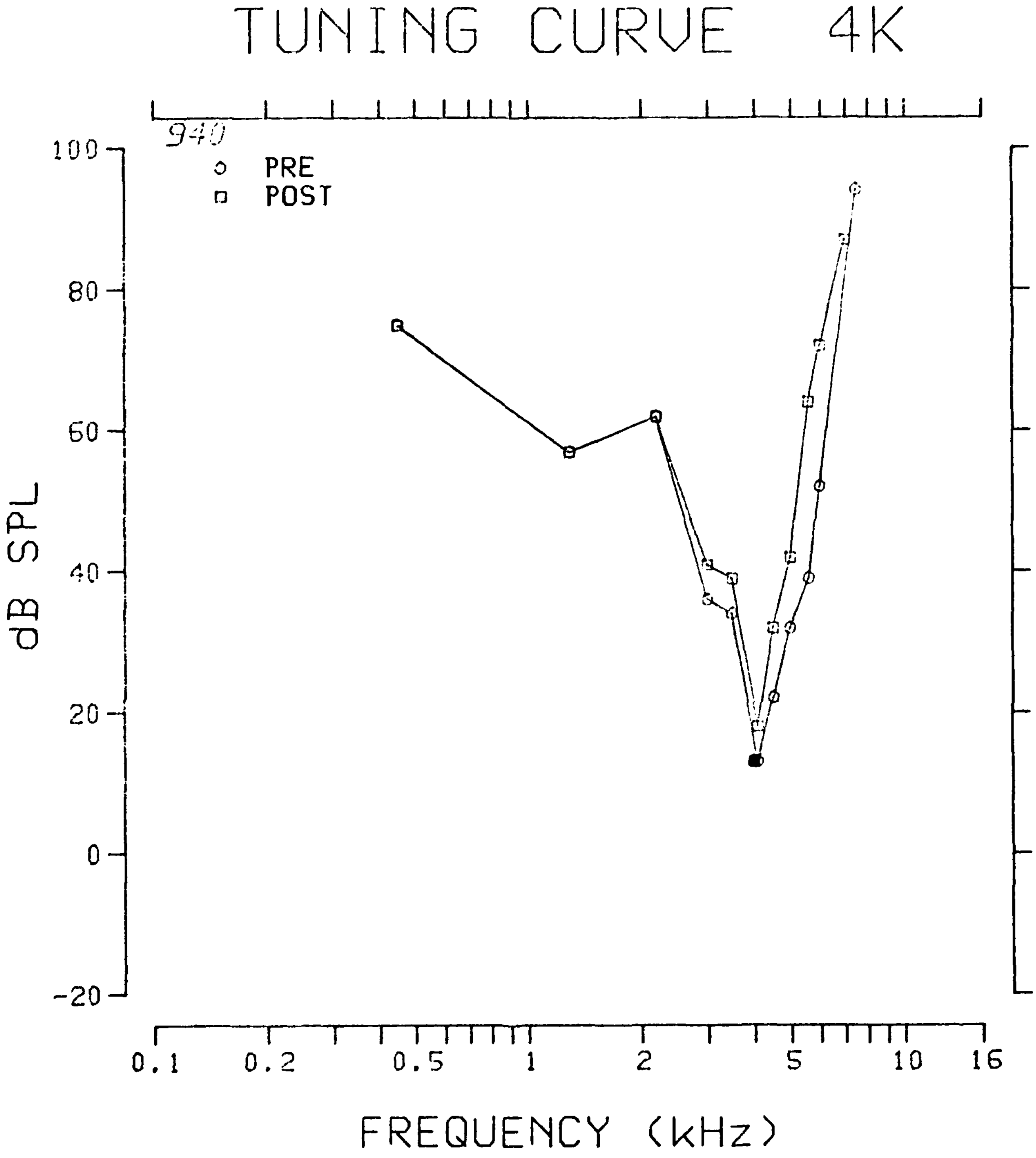


Fig. 3.3.204: Pre- and postexposure evoked response tuning curves at 4.0 kHz from chinchilla 940.

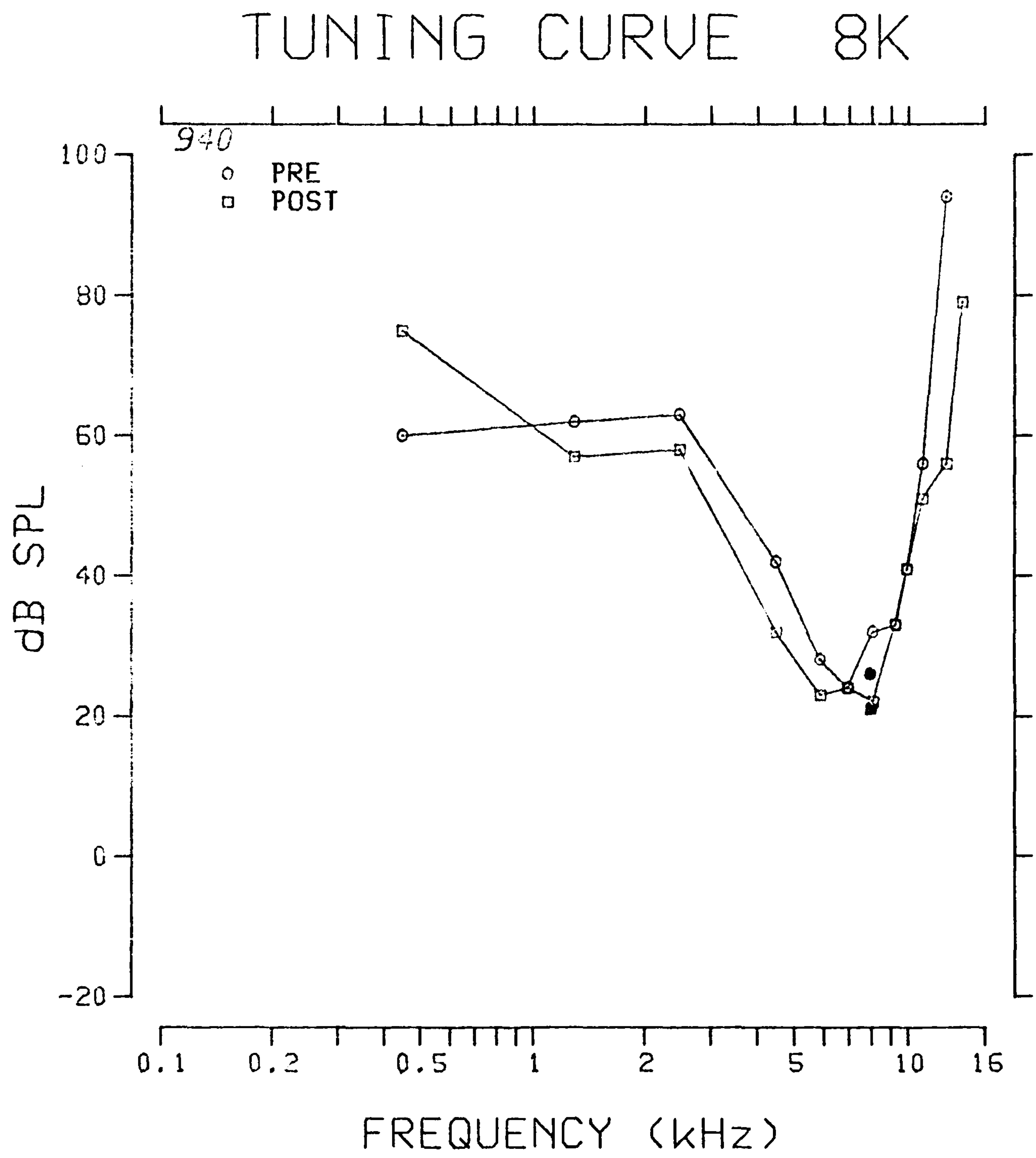


Fig. 3.3.205: Pre- and postexposure evoked response tuning curves at 8.0 kHz from chinchilla 940.

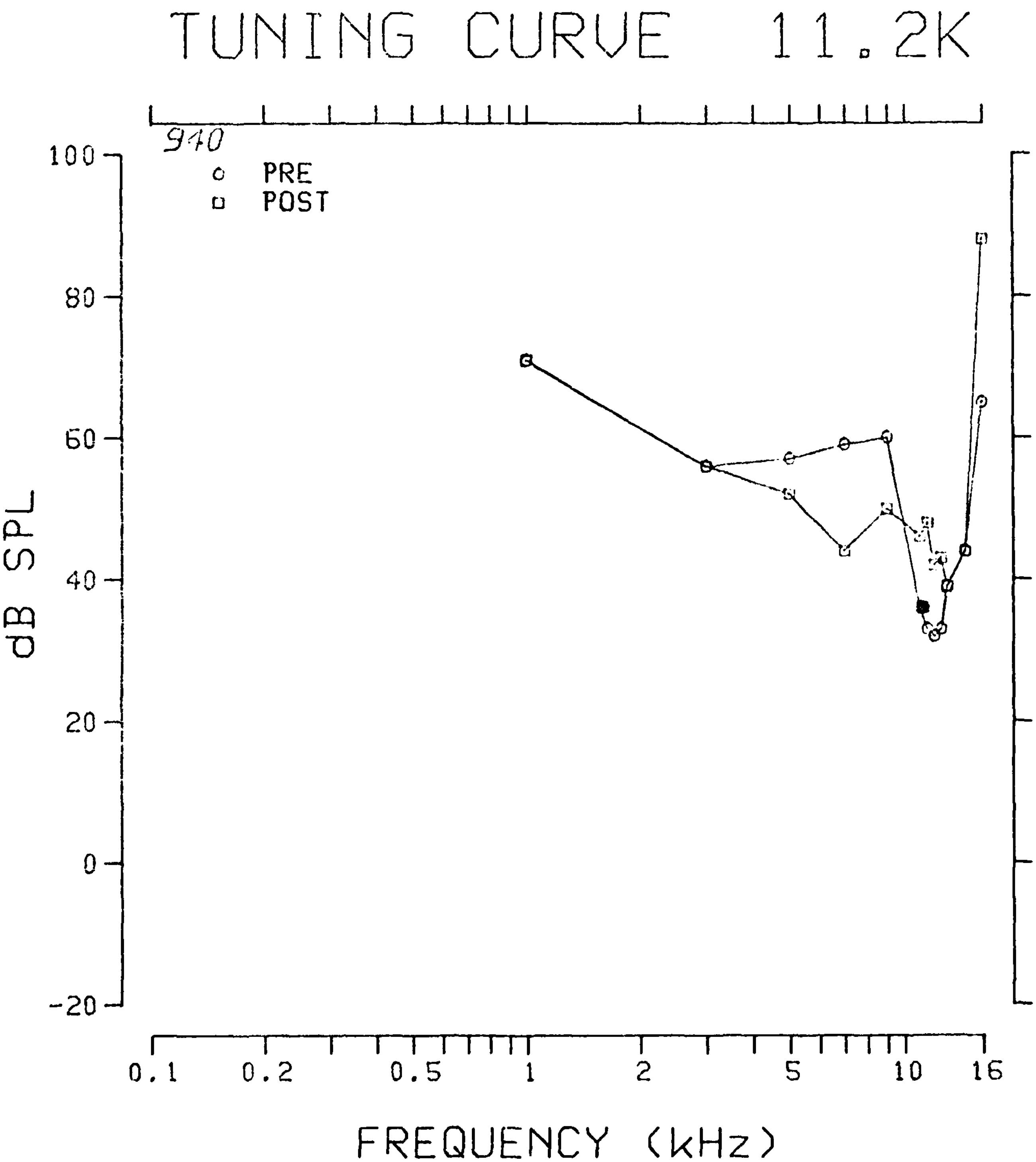


Fig. 3.3.206: Pre- and postexposure evoked response tuning curves at 11.2 kHz from chinchilla 940.

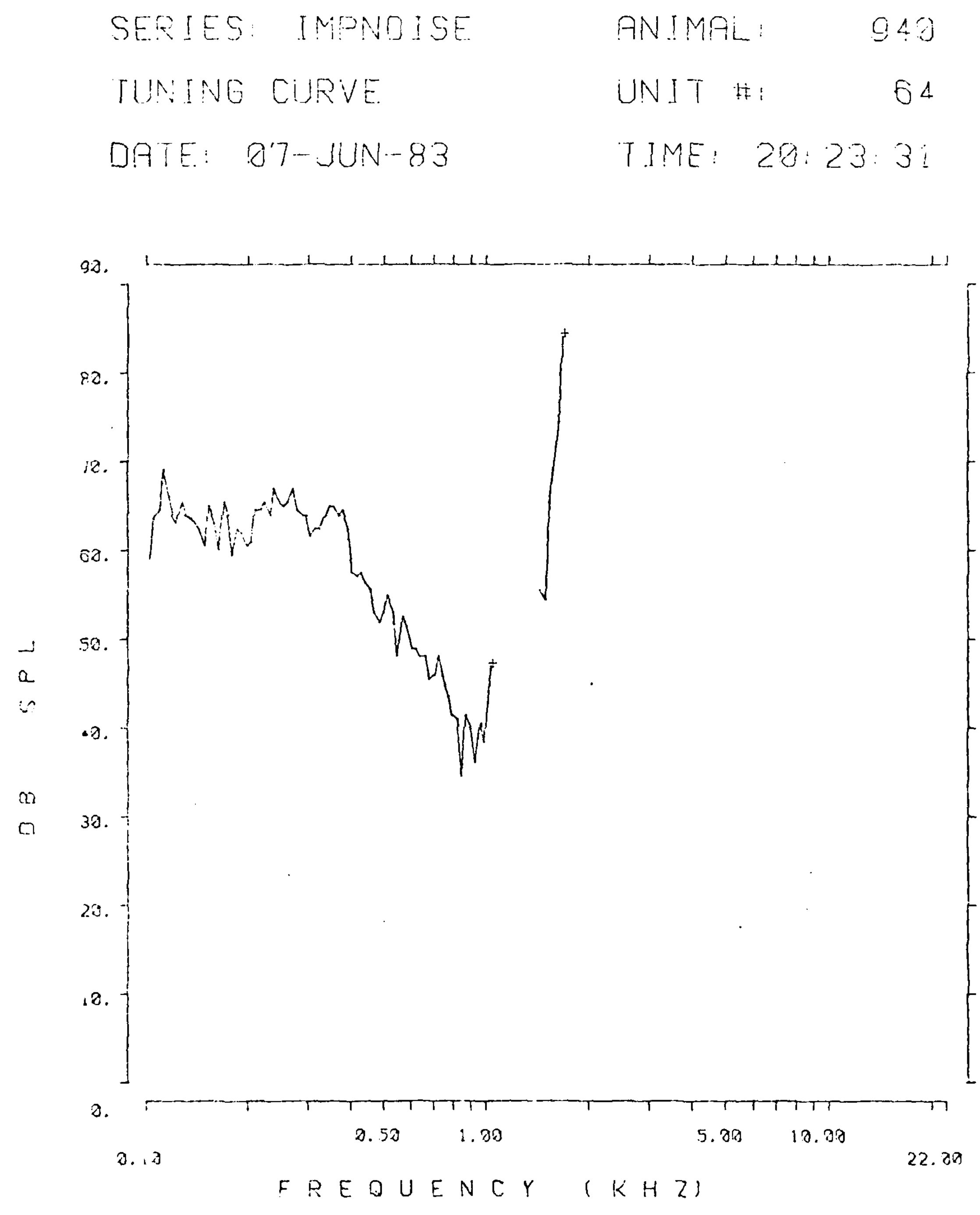


Fig. 3.3.207: Auditory nerve fiber tuning curve from chinchilla 940.

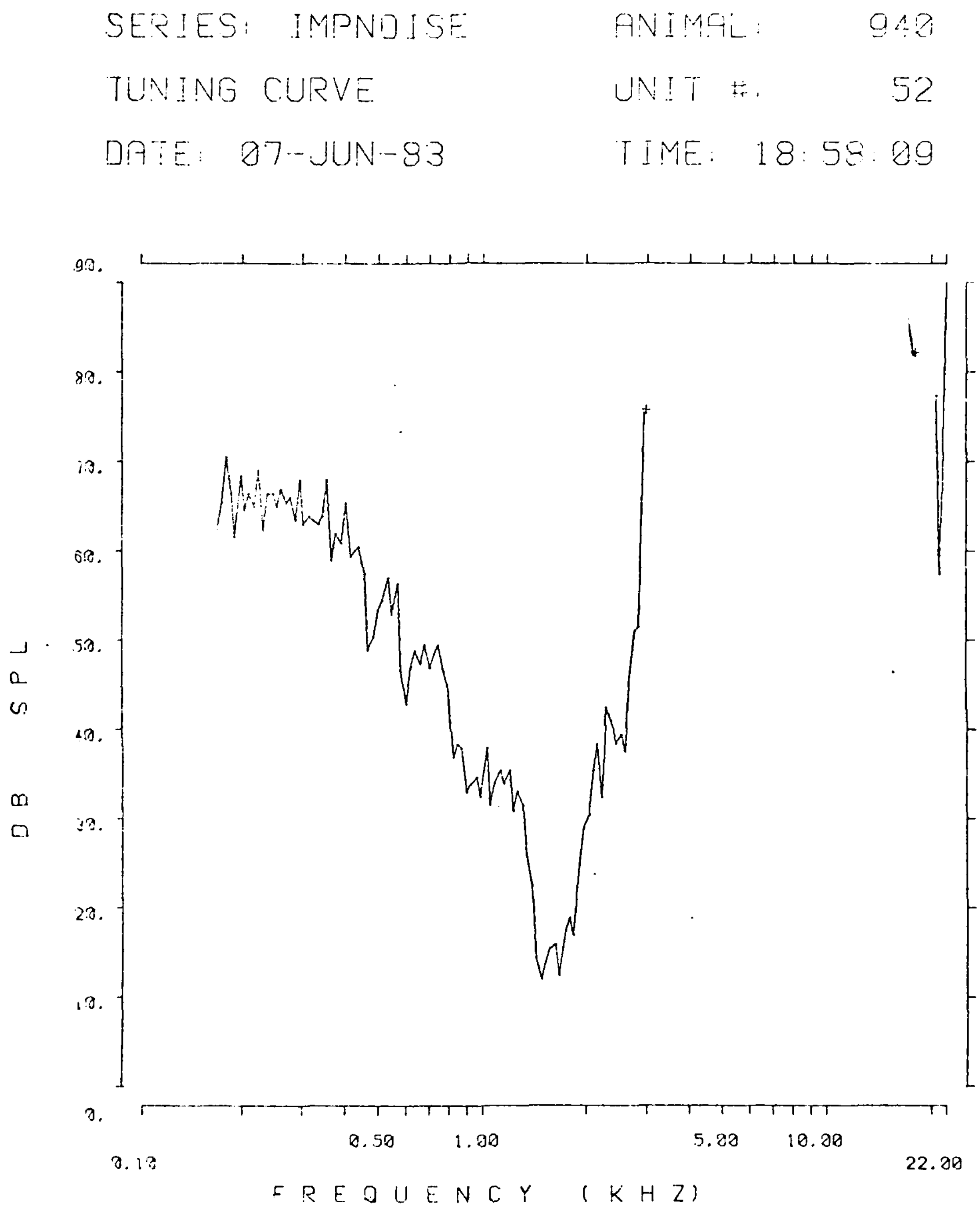


Fig. 3.3.208: Auditory nerve fiber tuning curve from chinchilla 940.

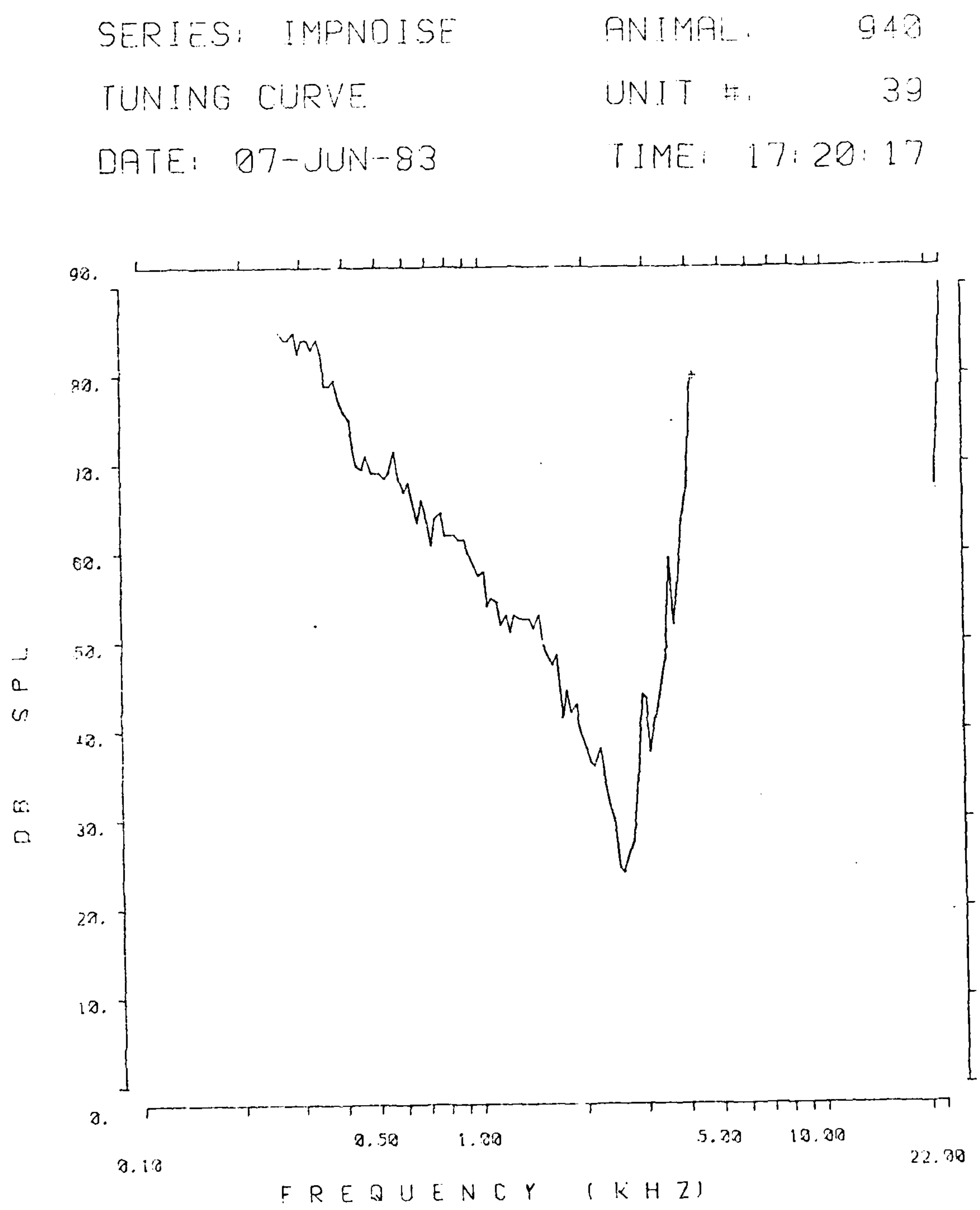


Fig. 3.3.209: Auditory nerve fiber tuning curve from chinchilla 940.

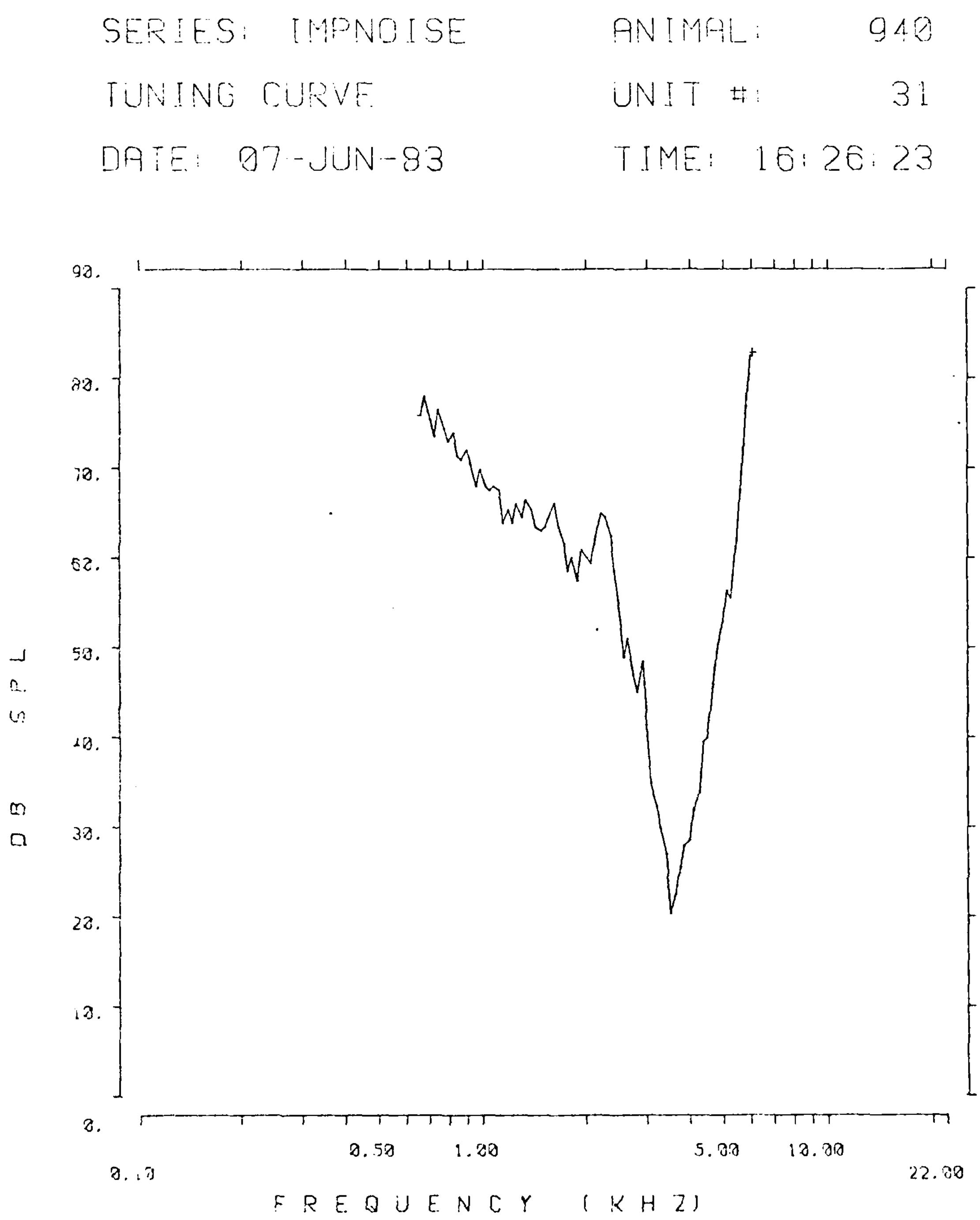


Fig. 3.3.210: Auditory nerve fiber tuning curve from chinchilla 940.

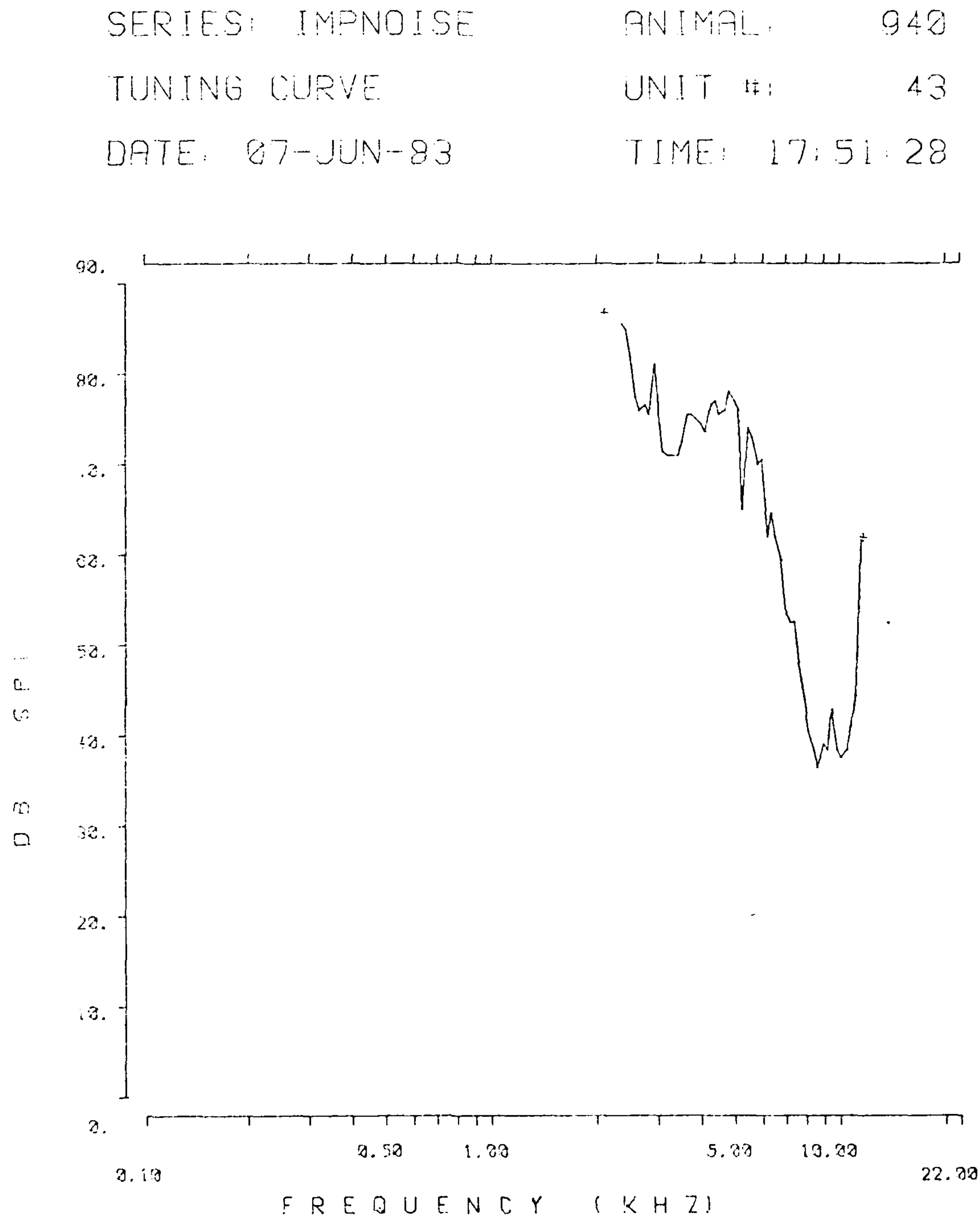


Fig. 3.3.211: Auditory nerve fiber tuning curve from chinchilla 940.

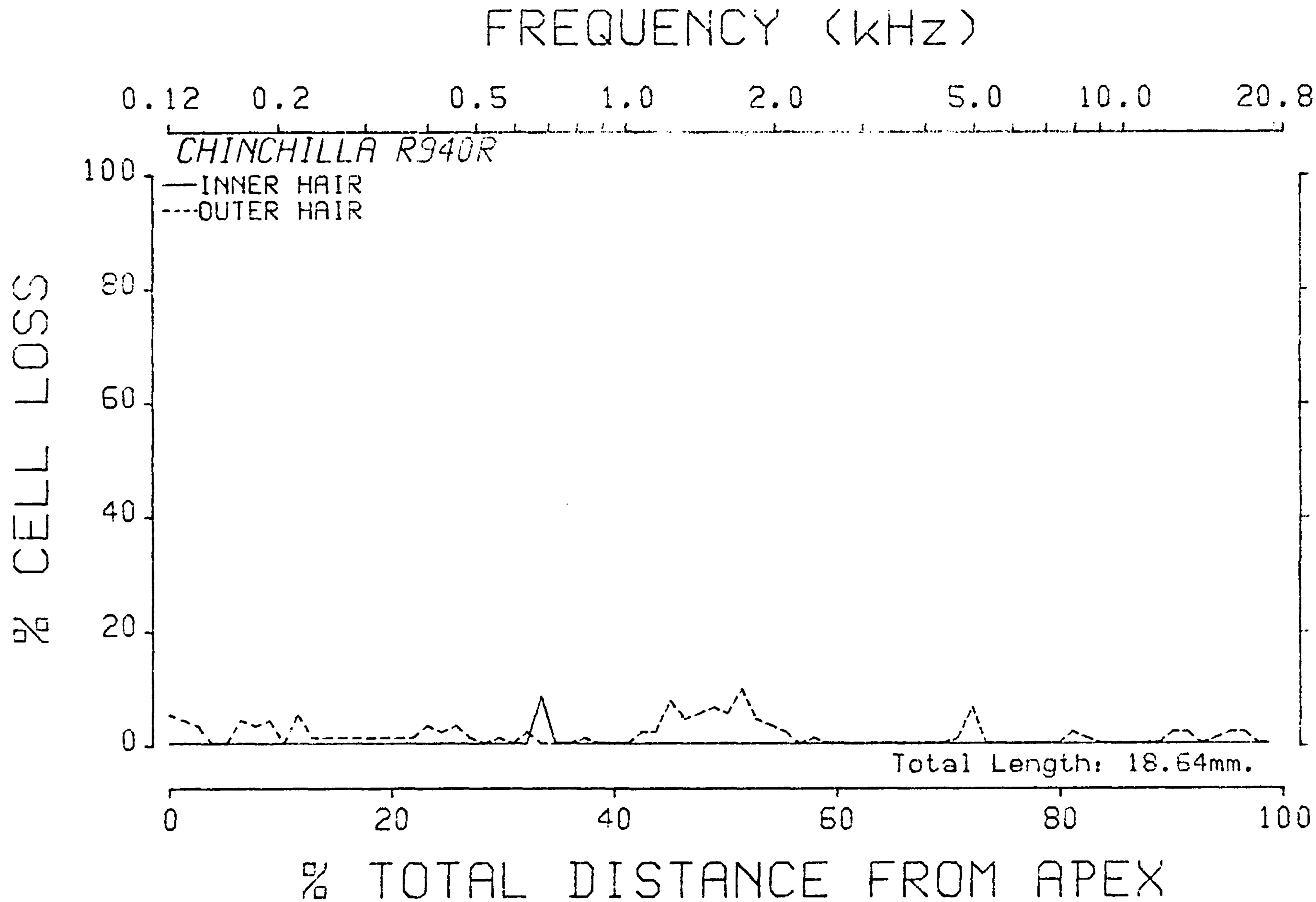


Fig. 3.3.212: Cochleogram from chinchilia 940.

Appendix 1

List of reprints related to the goals of the grant

1. Salvi, R. J., Ahroon, W. A., Perry, J. W., Gunnarson, A. D., and Henderson, D. (1982). "Comparison of psychophysical and evoked-potential tuning curves in the chinchilla." Am J. Otolaryngol. 3, 408-416.

2. Shaddock, L. C., Hamernik, R. P., Axelsson, A. (1983). "Vascular and sensory cell changes in the cochlea induced by elevated temperature and noise." Submitted to Hearing Res.

3. Shaddock, L. C., Hamernik, R. P., Axelsson, A. (1983). "The effect of high-intensity impulse noise on the vascular system of the chinchilla cochlea." Submitted to Ann. Oto. Rhin. Laryngol.

4. Hamernik, R. P., Turrentine, G., Salvi, R., Henderson, D., Roberto, M. (1983). "Scanning electron microscopic study of impulse noise induced mechanical damage in the cochlea." J. Acoust. Soc. Amer. 73; S81 (A).

Am J Otolaryngol
3:408-416, 1982

# Comparison of Psychophysical and Evoked-potential Tuning Curves in the Chinchilla

RICHARD J. SALVI, PH.D., WILLIAM A. AHROON, PH.D., JOHN W. PERRY, PH.D., ADELE D. GUNNARSON, M.S., AND DON HENDERSON, PH.D.

Frequency selectivity was examined in normal-hearing chinchillas using psychophysical and evoked-potential tuning curves. The acoustic conditions and masking procedures used for the evoked-potential and psychophysical studies were nearly identical. Frequency selectivities as measured by psychophysical and physiologic techniques were quite similar across different probe frequencies. The results suggest that the relatively *efficient evoked-potential procedure may be substituted for the time-consuming* psychophysical paradigm. Furthermore, the results are consistent with the view that tuning takes place primarily at the auditory periphery. (Key words: Evoked response; Frequency selectivity; Tuning curves.)

Brainstem electrical responses (BSER) have become popular metrics for estimating thresholds in both humans and animals. Generally, the responses have been measured with clicks or tone pips with fast rise–fall times, since these signals are the most suitable for synchronizing the underlying neural activity. Tone pips have the added advantage that thresholds may be assessed at different frequencies in order to obtain an "audiogram."[1-3]

One of the important issues surrounding the interpretation of the BSER data concerns the degree of frequency-specific information contained in the response. Frequency specificity is suggested by several properties of the response. The latency of the BSER decreases as stimulus frequency increases[4] in a manner consistent with the mechanics of the basilar membrane.[5] Furthermore, the "threshold" of the BSER varies with frequency in roughly the same manner as the behavioral threshold.[2]

From the Callier Center for Communication Disorders, University of Texas at Dallas, Dallas, Texas. Received May 14, 1982. Accepted for publication July 12, 1982.

Supported in part by grants from the National Institute of Health (1-R01-NS1676), the National Institute of Occupational Safety and Health (1-R01-OH-00364), and the U.S. Army Medical Research and Development Command (DAMD 17-80-C-0133).

Address correspondence and reprint requests to Dr. Salvi: Callier Center for Communication Disorders, 1966 Inwood Road, Dallas, Texas 75235.

More refined techniques have been used to demonstrate the frequency-specific nature of the BSER. Don and Eggermont[6] and Terkildsen et al.[7] used a masking paradigm to derive the frequency-dependent components of the BSER response. Both studies demonstrated that frequency-specific information is contained in the BSER; however, it is difficult to relate the set of frequency-dependent components of the BSER to psychophysical measures of frequency selectivity.

A more direct way of assessing the degree of frequency specificity of the BSER response is to measure tone-on-tone masking patterns or tuning curves (TCs). In psychophysical studies, the subject's task is to detect a low-level probe tone that is fixed in level and frequency. The assumption is that the low-level probe excites a limited number of neurons having best frequencies in the vicinity of the probe tone. A masking tone then is introduced and adjusted in level until it abolishes the response to the probe. The masking procedure is carried out over a range of frequencies around the probe. Masked thresholds are lowest in the vicinity of the probe and then increase with frequency separation between probe and masker.[8]

The same tone-on-tone masking paradigm has been employed in physiologic studies to obtain tuning curves for the compound action potential (AP) of cranial nerve VIII of man, guinea pig, and chinchilla[9-12] and Wave I and Wave V of the

0196-0709/82/1100/0408 $01.80 © W. B. Saunders Co.

BSERs from humans and guinea pigs.[12,13] These physiologic TCs are qualitatively similar to those obtained psychophysically; however, it is difficult to compare the results since many of the stimulus conditions used to obtain the psychophysical and physiologic data are different. For example, most psychophysical studies employ tones with relatively long rise–fall times in order to minimize spectral spread,[8,14-18] whereas physiologic studies use short-duration signals with rapid rise–fall times to maximize neural synchrony.[10,12,13] Comparing TCs from animals can also be difficult because the psychophysical measurements are frequently performed under free-field conditions[10] while the physiologic data are generally collected with a closed acoustic system and with the middle ear space vented.[11,12]

Recently, Klein and Mills[13] used identical stimulus conditions to collect both psychophysical and physiologic TCs (brainstem Wave I and Wave V) from humans. Although the TCs were qualitatively similar there were some important quantitative differences. For example, the bandwidth of the TC 10 dB above the tip was smallest for the Wave V TCs, followed by Wave I and the psychophysical TCs. However, when the TCs were compared at a fixed sound pressure level (SPL), 76 dB, the psychophysical bandwidths were smaller than the physiologic ones. While the results of Klein and Mills[13] show that the BSER can provide a reasonable estimate of frequency selectivity, the results are limited to one probe frequency. Since the shape of psychophysical tuning curves systematically changes with probe frequency,[16,18] it is important to assess the full range of neural tuning, particularly at low frequencies, where it is difficult to synchronize the onset response. In guinea pigs, Mitchell and Fowler[12] found a progressive broadening of the physiologic tuning curves with decreasing probe frequency. However, no behavioral measures were obtained, so it is unclear how well these physiologic tuning curves approximate the behavioral measures.

Psychophysical, AP, and single auditory nerve fiber tuning curves of the chinchilla have been measured,[11,14,19] but TCs from the brainstem have not yet been obtained. The dominant component of the brainstem potential in the chinchilla is a large positive wave which arises primarily from the inferior colliculus.[1] One practical reason for measuring the brainstem TCs is that the potentials can be easily and reliably recorded from awake chinchillas over many months using chronically implanted electrodes[2]; similar AP measurements are more difficult to obtain because of the possibility of middle ear infections. Furthermore, the time and effort required to collect the evoked-potential measures are considerably less than the time and effort involved in obtaining similar behavioral measures. Thus, if the evoked-potential tuning curves can be shown to approximate the behavioral tuning curves, one might consider substituting the evoked response for the psychophysical method when time and effort are important experimental variables. The objective of this study was to measure the brainstem TCs of the chinchilla over a broad range of probe tone frequencies. In order to compare the degrees of frequency specificity, the physiologic and psychological TCs were collected under similar acoustic conditions; however, the two sets of TCs were obtained from different animals because the behaviors required in the two procedures were mutually incompatible (i.e., jumping in the behavioral paradigm versus remaining stationary during evoked-potential testing).

## METHOD

### *Subjects*

Four chinchillas were used in the psychophysical experiment and another four were used in the physiologic study. The animals weighed between 400 and 800 g. Each animal was anesthetized and made monaural by surgical destruction of the left cochlea.[7] The probe tone was presented 15 dB above either the evoked response or the behavioral threshold; thus, the absolute SPLs of the probe varied a small amount from animal to animal and were slightly higher (approximately 5 to 15 dB) for the evoked potential than for the psychophysical conditions. It is important to note that both psychophysical and physiologic studies indicate that the shapes of the tuning curves are not substantially altered when the probe levels are varied over a 25- to 35-dB range above threshold.[10,16,17] By presenting the probe tone near threshold one reduces the effects of combination tones. Furthermore, the masker frequencies near the tip of the tuning curve were at least 20 Hz above or below the probe frequency to minimize the effects of beats.

### *Behavioral Testing*

Audiograms and psychophysical TCs were obtained using a shock-avoidance conditioning paradigm and a modified method of limits (for

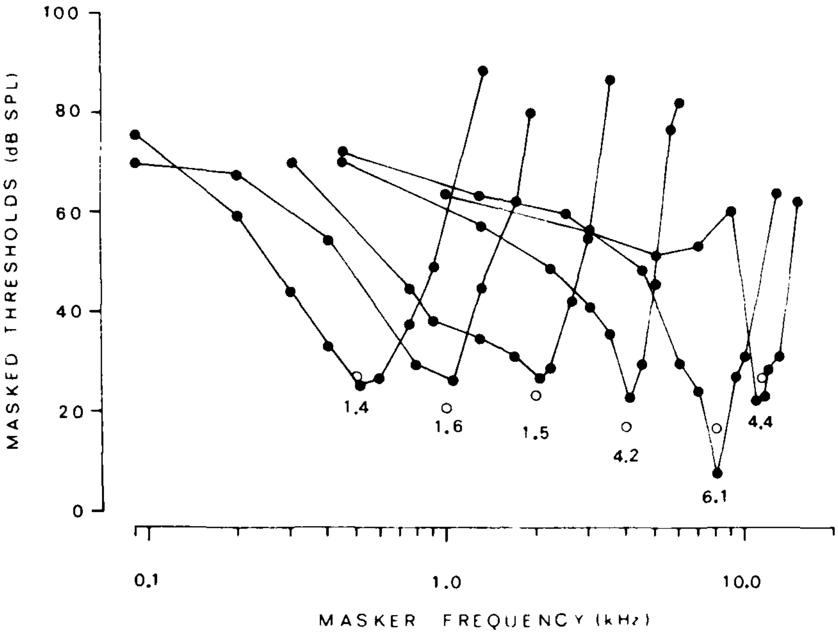


Figure 1. Psychophysical tuning curves obtained for one animal. The value of $Q_{10}$ dB is indicated below the tuning curve tip for each probe-tone frequency. Open circles indicate the probe tone level.

details, see references 19–21). The chinchilla was placed in a restraining yoke which fixed the orientation of its head in the sound field, but allowed a slight upward motion of the body so that the animal could register a response. A stimulus trial consisted of a train of eight tone bursts (20 ms duration between half-power points; 5 ms rise–fall time, 2 bursts/s). A response during bursts 1 to 4 was registered as a "hit" and was followed by the presentation of a safety light for 7.5 seconds. If the animal failed to respond by the onset of the fifth tone, mild pulsed shock was delivered to the animal's tail, except at near-threshold intensities. A response to tone bursts 5 through 8 or no response was scored as a "miss."

### Tone Threshold

Testing began at clearly audible levels. After each correct response, the signal was reduced in 10-dB steps until a "miss" occurred; then the signal was increased in 10-dB steps until a "hit" occurred. At that point, the step size was reduced to 5 dB and four additional threshold crossings were obtained. The data were accepted as valid if the threshold crossings differed by 10 dB or less. A total of 48 to 72 threshold crossings were used to estimate the threshold of the 20-ms probe tone.

### Psychophysical Tuning Curves

The procedures for obtaining psychophysical TCs are similar to those outlined earlier.[19] Tuning curves were obtained with the probe tone at a 15-dB sensation level (SL). A continuous tone then was introduced at a low level so that the probe, which was presented randomly, was clearly audible. The animal was trained to ignore the continuous masking tone and to respond to the probe.

The procedures for determining the level of the continuous tone necessary to mask the probe were similar to those used to estimate quiet threshold, except that masker level was varied. A total of at least 12 threshold crossings were used to compute each point on the psychophysical TCs.

### Evoked Response Testing

Chronic electrodes were implanted in the vicinity of the inferior colliculus in four chinchillas using procedures outlined in a previous report.[2] The animals were tested using the same restraining yoke and acoustic equipment employed in the behavioral experiments. The acoustic signals were identical to those in the behavioral experiments except that the probe tone was presented at the rate of 10/s throughout the averaging session. The electrical potential from the electrode was filtered (300 to 1,500 Hz), amplified (20,000 to 50,000 times) and led to a signal averager (Fabri-Tek 1070) with artifact-reject capability. The data were sampled at 25 kHz over 512 points to obtain a window of 20.48 ms. Normally, 512 samples were collected. However, if a clear evoked response was present with fewer samples, the averaging was terminated. No effort was made to measure the actual

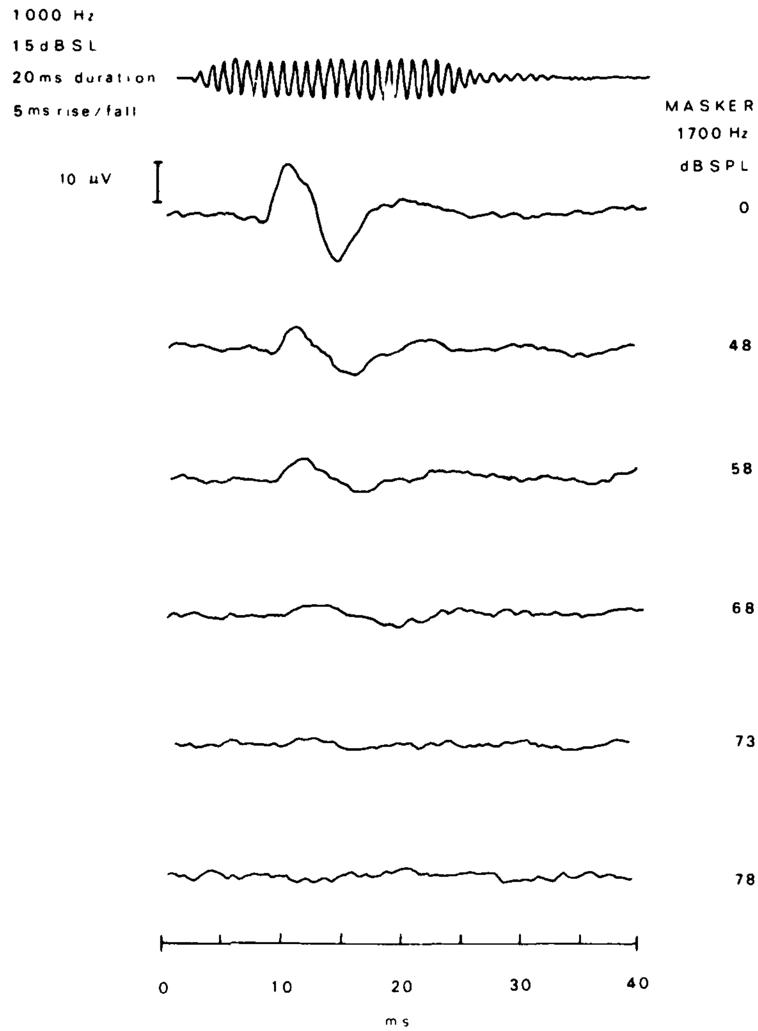


*Figure 2.* Examples of evoked responses from one chinchilla. The top trace represents the acoustic output of the speaker. The second trace is the evoked response to the 1-kHz probe tone at a level of 15 dB above the animal's threshold. Successive traces represent the evoked responses to the 1-kHz probe with a simultaneous 1.7-kHz masker increasing in intensity.

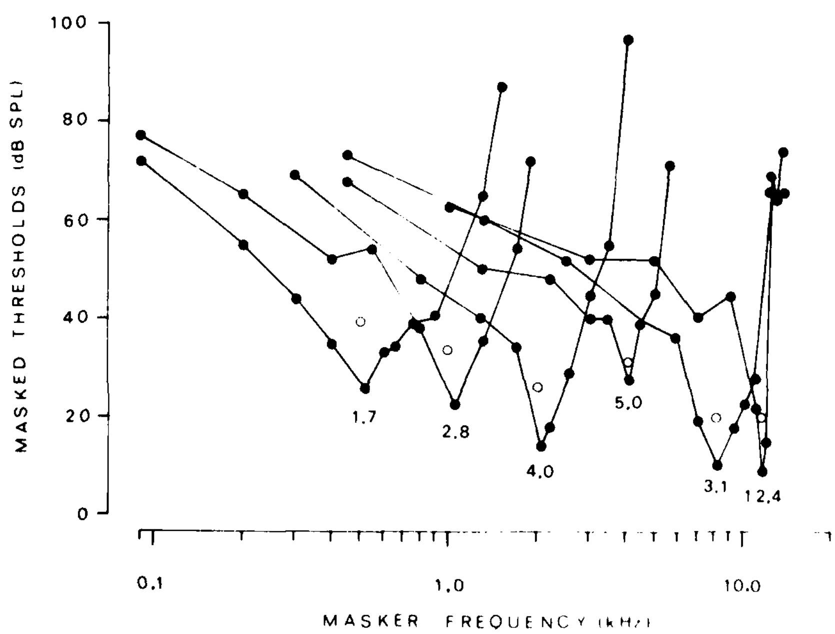


*Figure 3.* Evoked-response tuning curves obtained for one animal. The value of $Q_{10}$ dB is indicated below the tuning curve tip for each probe-tone frequency. Open circles indicate the level of the probe tone.

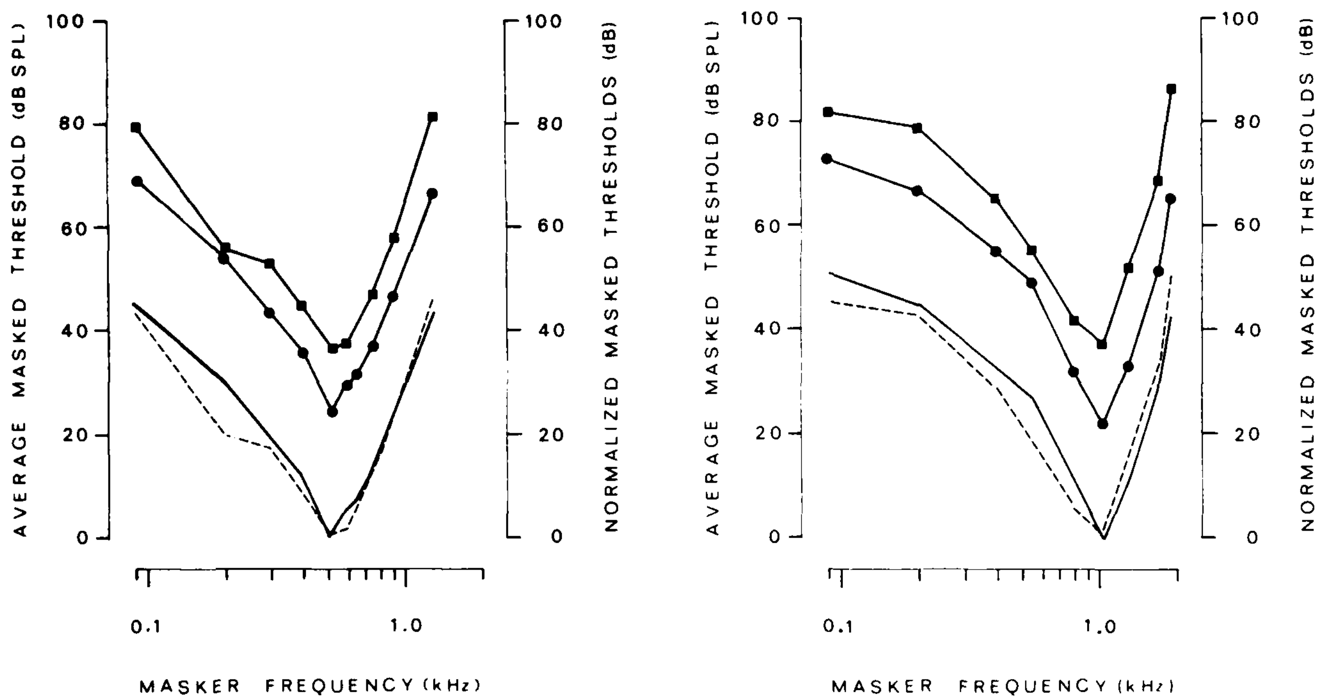


*Figure 4, A–F (above and facing page).* Comparison of average psychophysical and evoked-response tuning curves. Filled circles and filled squares are the average psychophysical and average physiologic tuning curves presented in dB SPL. The psychophysical (*solid line*) and physiologic (*dashed lines*) tuning curves have been normalized to 0 dB at their tips.

amplitude of the evoked response waveforms, since only the transition from the presence to the absence of the evoked response was used to make a judgement regarding the absolute and masked thresholds.

### Physiologic Threshold

Thresholds were determined with a 20-ms probe tone with random starting phase and 5 ms rise–fall times. Testing began at an intensity that produced a clear and unambiguous response. Then the signal level was reduced in 10-dB steps until the response was slightly above the background noise. At this point, the intensity step was reduced to 5 dB and additional samples were collected. Threshold was the point midway between the highest intensity where the response was absent and the lowest intensity where the response was present.

### Physiologic Tuning Curves

Immediately following the determination of a threshold, a tuning curve was collected for that frequency. The probe tone was presented at a level 15 dB above the evoked-potential threshold. A continuous masker then was introduced at a level low enough so that a clear evoked potential was obtained. Masker level was subsequently increased in 10-dB steps until the evoked response was nearly obliterated; then the step size was reduced to 5 dB and additional samples were collected. Masked threshold was the intensity midway between the lowest intensity where the response was present and the highest intensity where the response was absent. Masking was employed at frequencies above and below the probe tone in order to obtain a TC that could be compared with the psychophysical data.

## RESULTS

### Individual Psychophysical Tuning Curves

Figure 1 shows six psychophysical TCs obtained from one chinchilla at six probe frequencies from 0.5 to 11.2 kHz. At probe frequencies above 2 kHz, the psychophysical TCs tend to be asymmetrically shaped on a log-frequency plot, while those below 2 kHz are nearly symmetrical. In general, the psychophysical TCs are characterized by a low masked-threshold region near the probe sandwiched between a steep high-frequency slope and a somewhat shallower low-frequency slope. The "tail" segment of high-frequency psychophysical TCs refers to the region where the low-frequency slope becomes

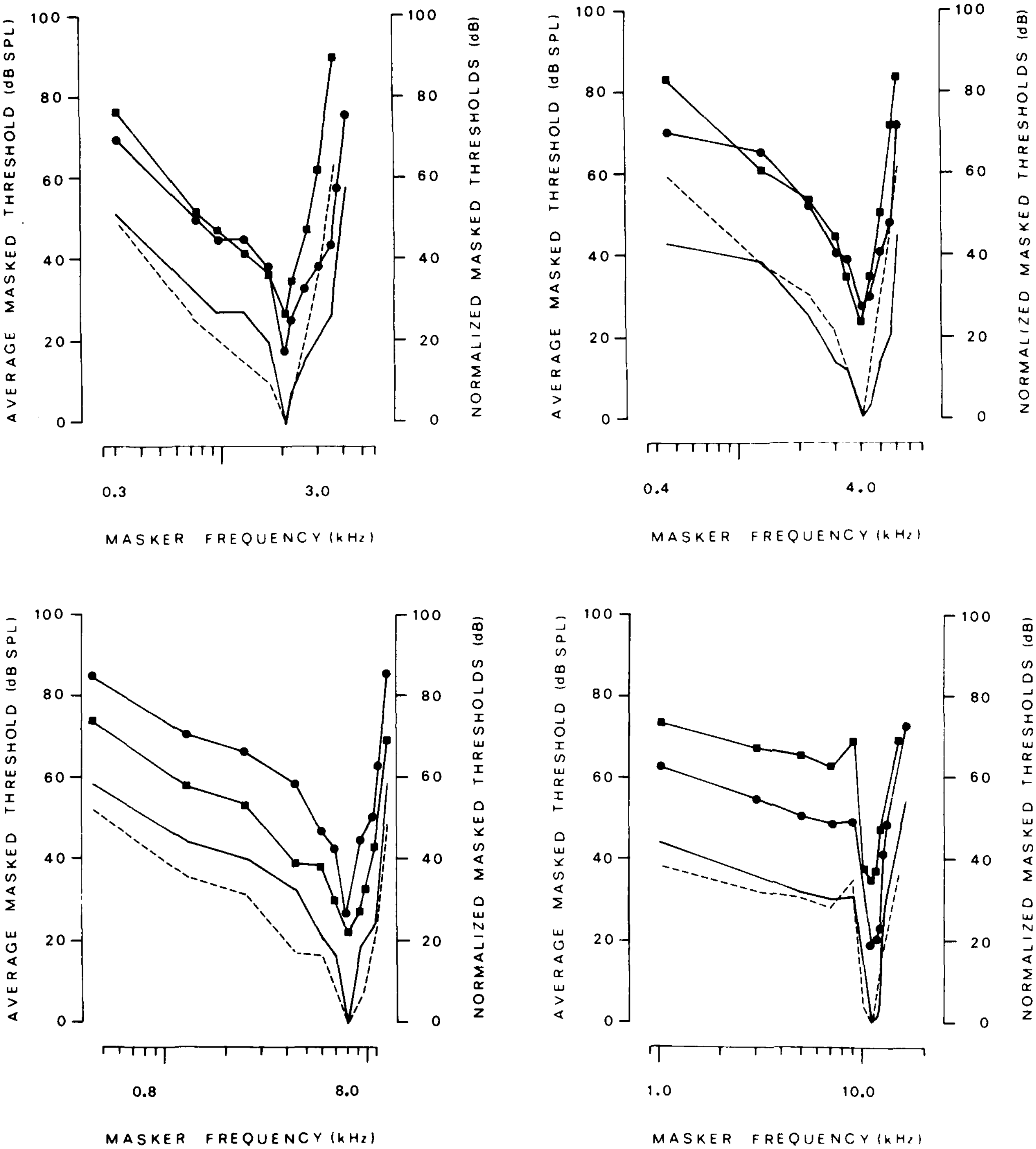


extremely shallow, usually 1–2 octaves below the probe. The transition to the tail segment can be easily identified in the 11.2-kHz psychophysical TC because of the high threshold notch at 9 kHz that separates the tip from the tail segment. The transition to the tail segment occurs much more gradually at lower probe frequencies.

A popular and useful measure of quantitatively assessing the frequency selectivity of tuning curves is to compute the $Q_{10}$ dB value, defined as the center frequency of the tuning curve divided by the bandwidth 10 dB above the minimum threshold. Generally, $Q_{10}$ dB values increase with probe frequency. A similar trend

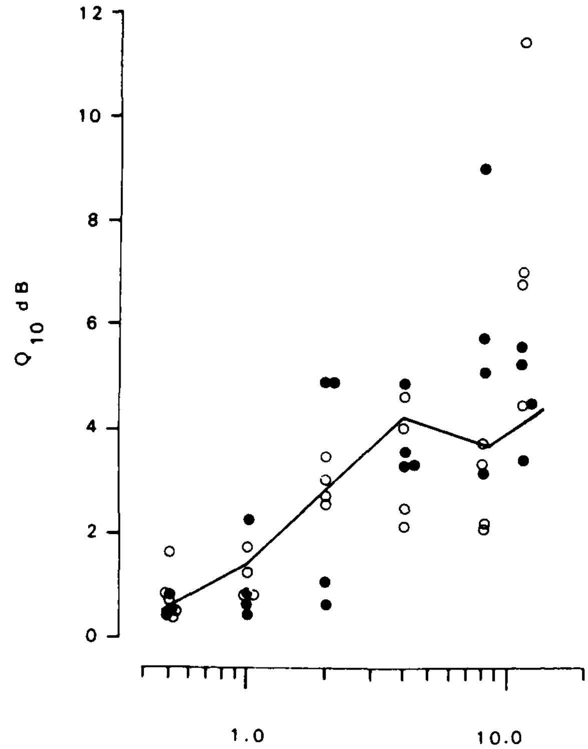


Figure 5. Values of $Q_{10}$ dB for psychophysical (*solid circles*) and evoked-response (*open circles*) tuning curves. The solid line represents $Q_{10}$ dB values for single auditory nerve fibers, from Salvi et al.[19]

occurs in Figure 1, where the $Q_{10}$ dB values range from 1.4 at a probe frequency of 0.5 kHz to 6.1 at a probe frequency of 8.0 kHz.

The psychophysical TCs shown in Figure 1 are representative of the four animals and are similar to psychophysical TCs reported in an earlier study.[19] However, the psychophysical TCs of our chinchillas did not appear to be quite as sharply tuned as those reported by McGee et al.[14]

### Individual Evoked-potential Tuning Curves

Before presenting the evoked-potential tuning curve data, it is important to identify the evoked-response waveforms obtained with the tone-on-tone masking paradigm. The top trace in Figure 2 shows the voltage–time waveform of the acoustic signal, while the second trace represents the evoked potential obtained with a 1-kHz tone pip at 15 dB above the evoked-response threshold. In the absence of the masker, the response consists of a large positive wave at approximately 11 ms, followed by a negative wave at 17 ms. Traces 3 through 7 illustrate how the evoked response is affected by a 1.7-kHz masker. As the masker intensity is increased, amplitude decreases and latency increases. There is a remnant of the positive wave with a masker of 68 dB SPL; however the evoked potential is completely obliterated at 78 dB SPL. Response waveforms similar to those were obtained at other frequency–intensity combinations of the probe and masker; the waveform closely resembles those obtained from microelectrodes in the inferior colliculus.[1]

Shown in Figure 3 are the six evoked-potential TCs from a single chinchilla. The evoked-potential TCs are remarkably similar to those obtained behaviorally. While the overall similarity is encouraging, a much more comprehensive assessment can be made by comparing the average behavioral TC and the average evoked-potential TC at each probe frequency.

### Psychophysical versus Evoked-potential Tuning Curves

The intersubject variability was quite small, generally less than 8 dB, so that it is reasonable to average the tuning curves from each condition. The average evoked-potential and the average psychophysical tuning curves are shown in Figure 4. In order to aid the comparison further, the tuning curves were normalized at their tips to compensate for differences in sensitivity and then plotted in the lower portion of each panel.

When the data are normalized, four of the six pairs of tuning curves (0.5, 1, 4, and 11.2 kHz) are essentially the same. The bandwidths are similar for the curves at 2 kHz, except that the evoked-potential TC has a steeper high-frequency skirt, while the psychophysical TC has a steeper low-frequency skirt. The 8-kHz evoked-potential TC is broader than the psychophysical TC; this difference is somewhat difficult to explain given the fact that the 4-kHz and 11.2-kHz evoked-potential TCs are essentially the same as their psychophysical counterparts.

A standard metric for comparing TCs is the $Q_{10}$ dB value. Figure 5 shows the individual $Q_{10}$ dB values plotted as a function of the center frequency of the probe for both the evoked-potential and the psychophysical measures. The median $Q_{10}$ dB values for single auditory nerve fibers in the chinchilla also are presented to aid the analysis.[19] It should be noted that the acoustic conditions for the single-unit data are different from those in the present experiment; however, this should not significantly influence the comparison, since the $Q_{10}$ dB values are computed over a relatively narrow range of frequencies. The $Q_{10}$ dB values are in good agreement up to 4 kHz, and still show considerable overlap at higher frequencies. At 8 kHz, the $Q_{10}$ dB values obtained with the evoked response tend to be somewhat smaller than the psychophysical data. Conversely, the evoked-potential $Q_{10}$ dB values tend to be larger than those obtained psychophysically at 11.2 kHz. Note that the median $Q_{10}$ dB values of single auditory nerve fibers (solid line) provide a reasonably good fit to the psychophysical and evoked-response data.

## DISCUSSION

Since masked thresholds increase rapidly with increasing separation between probe and masker, it seems reasonable to conclude that the evoked potential elicited by the probe tone synchronizes the response of a limited number of single units with best frequencies in the vicinity of the probe. Furthermore, the response appears to contain considerable frequency-specific information.

The present results also indicate that the evoked-potential TCs provide a reasonable approximation of the psychophysical TCs in the normal-hearing chinchilla over a broad range of probe frequencies; the only difference between the two is a 5–15-dB difference in sensitivity. The evoked-potential TCs can be obtained easily in a matter of a few weeks from awake chinchillas using the procedures outlined above, but months of training and testing are needed to obtain the psychophysical TCs. Consequently, when time and effort are critical experimental factors, it would be advantageous to use the evoked-potential TC as an estimate of tuning in normal chinchillas. While the evoked-potential TC appears to offer a promising technique for assessing frequency selectivity, its application to hearing-impaired subjects needs to be explored more fully before its use is justified completely.

One important issue in hearing concerns the origin(s) of tuning within the auditory pathway, i.e., which structures or processes set the limits of frequency selectivity of the final detector represented by the psychophysical TC. There is some evidence to suggest that tuning is primarily set at the level of the cochlea and that no further sharpening takes place centrally.[22,23] Other data, however, suggest that the central auditory pathway may provide additional frequency selectivity beyond that seen at the cochlea.[24–26] One way of evaluating this issue is to compare the $Q_{10}$ dB values at different levels of the auditory pathway with the psychophysical data. Figure 5 shows that the median $Q_{10}$ dB values of single auditory nerve fibers in the chinchilla correspond closely to the $Q_{10}$ dB values of the evoked potential that arises in the inferior colliculus. Thus, one might argue that the brainstem nuclei do not substantially alter the tuning properties established at the cochlea, but this interpretation should be made with caution, given that the acoustic conditions and testing procedures for the two conditions are somewhat different. However, at a more central level, one finds that the evoked-potential $Q_{10}$ dB values show considerable overlap with the psychophysical data, implying that little or no sharpening takes place beyond the colliculus. Recall that the acoustic conditions for this comparison are nearly identical. Thus, the present data provide support for the view that tuning originates primarily at the auditory periphery.

*Acknowledgments.* The authors thank Patricia L. Robinson and Harley Willet for technical assistance and G. and D. Clemmer, J. and O. Mooneyham, E. and K. Rockwood and N. and M. Sifford for their generous support.

*References*

1. Rothenberg S, Davis H: Auditory evoked response in chinchilla: application to animal audiometry. Percep Psychophys 2:443–447, 1967
2. Henderson D, Hamernik RP, Woodford C, et al: Evoked response audibility curve of the chinchilla. J Acoust Soc Am 54:1099–1101, 1973
3. Mitchell C, Clemis JD: Audiograms derived from the brainstem response. Laryngoscope 87:2016–2022, 1977
4. Klein AJ, Teas DC: Acoustically dependent latency shifts of BSER (Wave V) in man. J Acoust Soc Am 63:1887–1895, 1978
5. von Bekesy G: Experiments in Hearing. New York, McGraw-Hill, 1960.
6. Don M, Eggermont JJ: Analysis of the click evoked brainstem potentials in man using the high pass noise masking. J Acoust Soc Am 63:1084–1092, 1978
7. Terkildsen K, Osterhammel P, Huis in't Veld F: Far field electrocochleography: frequency specificity of the response. Scand Audiol 4:167–172, 1975
8. Chistovich LA: Frequency characteristics of masking effect. Biofizika 2:749–755, 1957
9. Eggermont JJ: Compound action potential tuning curves in normal and pathological human ears. J Acoust Soc Am 62:1247–1251, 1977
10. Dallos P, Cheatham MA: Compound action potential tuning curves. J Acoust Soc Am 59:591–597, 1976
11. Harris M: Action potential suppression, tuning curves and thresholds: comparison with single fiber data. Hearing Res 1:133–154, 1979
12. Mitchell C, Fowler C: Tuning curves of cochlear and brainstem responses of the guinea pig. J Acoust Soc Am 68:896–900, 1980
13. Klein AJ, Mills JH: Physiological (waves I and V) and psychophysical tuning curves in human subjects. J Acoust Soc Am 69:760–768, 1981

14. McGee T, Ryan A, Dallos P: Psychophysical tuning curves of chinchillas. J Acoust Soc Am 60:1146–1150, 1976
15. Small AM: Pure tone masking. J Acoust Soc Am 31:1619–1625, 1959
16. Vogten LLM: Pure tone masking: a new result from a new method, *in*: Zwicker E, Terhardt E (eds.): Facts and Models in Hearing. New York, Springer, 1974, pp 142–155
17. Wightman FL, McGee T, Kramer M: Factors influencing frequency selectivity in normal and hearing impaired listeners, *in*: Evans EF, Wilson JP (eds.): Psychophysics and Physiology of Hearing. London, Academic Press, 1977, pp 295–306
18. Zwicker E: On a psychoacoustic equivalent of tuning curves, *in*: Zwicker E, Terhandt E (eds.): Facts and Models in Hearing. New York, Springer, 1974, pp 132–141
19. Salvi R, Perry J, Hamernik RP, et al: Relationships between cochlear pathologies and auditory nerve and behavioral responses following acoustic trauma, *in*: Hamernik RP, Henderson D, Salvi RJ (eds.): New Perspectives on Noise-induced Hearing Loss. New York, Raven Press, 1982, pp 165–188
20. Blakeslee EA, Hyson K, Hamernik RP, et al: Asymptotic threshold shift in chinchillas exposed to impulse noise. J Acoust Soc Am 63:876–882, 1978
21. Salvi R, Hamernik RP, Henderson D: Discharge patterns in the cochlear nucleus of the chinchilla following noise induced asymptotic threshold shift. Exp Brain Res 32:301–320, 1978
22. Moller AR: Coding of sounds in lower levels of the auditory system. Q Rev Biophys 5:59–155, 1972
23. Pickles JO: Psychophysical frequency resolution in the cat as determined by simultaneous masking and its relation to auditory nerve resolution. J Acoust Soc Am 66:1725–1732, 1979
24. Dallos P, Harris D: Properties of auditory nerve responses in the absence of outer hair cells. J Neurophysiol 41:365–383, 1978
25. Dallos P, Ryan A, Harris D, et al: Cochlear frequency selectivity in the presence of hair cell damage, *in*: Evans EF, Wilson JP (eds.): Psychophysics and Physiology of Hearing. London, Academic Press, 1977, pp 249–261
26. Pickles JO: Role of centrifugal pathways to cochlear nucleus in determination of critical bandwidth. J Neurophysiol 39:344–400, 1976

Scanning electron microscopic study of impulse noise - induced mechanical damage in the cochlea. R.P. Hamernik, G. Turrentine, R. Salvi, D. Henderson, (Callier Center, University of Texas, 1966 Inwood Road, Dallas, Texas 75235), M. Roberto (Cattedra Di Bioacustica, Universita di Bari, Bari, Italy).

Binaural chinchillas were exposed at normal incidence to 160 dB peak SPL impulse noise at the rate of 2 impulses per minute for 50 minutes. Animals were sacrificed at post-exposure times varying from t = 0 through 30 days. The cochleas were prepared for SEM observation using a standard protocol. Immediately following exposure, a large ( 6 mm) area of the organ of Corti was separated from its attachments to the basilar membrane along a fracture line that follows the outer pillar cells. The separated portion of the organ of Corti is left floating in the scala media with both ends attached to viable portions of the remaining sensory epithelia. Surprisingly, in the denuded areas of the basilar membrane, the inner hair cell surface structure remains comparatively normal during the early post-exposure times while outer hair cells in the region bordering the main lesion show considerable changes in cilia structure and in the appearance of the reticular lamina - cuticular plate complex. Scar formation and the absorption/phagocytosis of the free-floating portions of the organ of Corti will be described, as well as the differing susceptibilities of inner and outer hair cell cilia to morphological changes.

[Work supported by U.S. Army Med R & D Command, DAMD 17-80-C-0133]

Technical Committee: Psychological and Physiological Acoustic---Psychological
Subject Classification Number: 43:66 Ed., 43,63 Rf
Telephone Number: (214) 783-3062
Send acceptance or rejection notice to R.P. Hamernik

THE EFFECT OF HIGH-INTENSITY IMPULSE NOISE ON THE VASCULAR SYSTEM OF THE CHINCHILLA COCHLEA

RUNNING HEAD: EFFECT OF NOISE ON VASCULATURE

LYNN CARLISLE SHADDOCK (1) ROGER P. HAMERNIK (1) ALF AXELSSON (2)

(1) CALLIER CENTER FOR COMMUNICATION DISORDERS, THE UNIVERSITY OF TEXAS AT DALLAS, 1966 INWOOD ROAD, DALLAS, TEXAS 75235

(2) DEPARTMENTS OF OTOLARYNGOLOGY AND AUDIOLOGY, UNIVERSITY OF GOTHENBURG, SAHLGREN'S HOSPITAL, S-413 45, GOTHENBURG, SWEDEN

This research was partially supported by the U.S. Army Medical Research and Development Command DAMD17-80-C-0133, The Department of Health Education and Welfare, National Institute for Occupational Safety and Health grant no. 1-R01-OH-00364 and The Swedish Work Environment Fund 81-0792.

Send reprint requests to:

Lynn Carlisle Shaddock

Callier Center for Communication Disorders

1966 Inwood Road

Dallas, Texas 75235

(ac)214-783-3062

(Correspondence and proofs to Ms. Shaddock)

# ABSTRACT

Forty-five days after impulse noise exposure of either 155 or 160 dB peak SPL, changes in the vasculature of the cochlea were quantitatively assessed. The condition of the vessels in the lateral wall and spiral lamina of each cochlea was evaluated in terms of 20 morphological parameters. Multivariate statistical analysis identified the parameters that were significantly affected by the noise exposure. An evaluation of these significant parameters indicates a net reduction in blood flow to the cochlea. All of the noise-exposed cochleas showed vascular changes when compared to controls, and the magnitude of these changes was related to the amount of hair cell loss. The vascular changes are presumed to be of a permanent nature.


key words: impulse noise, cochlear vasculature, inner and outer hair cells

AD-A172 467 BLAST TRAUMA THE EFFECT ON HEARING(U) TEXAS UNIV AT DALLAS CALLIER CENTER FOR COMMUNICATION DISORDERS R P HAMERNIK ET AL. JUL 83 DAMD17-80-C-0133

4/4

UNCLASSIFIED F/G 6/19 NL

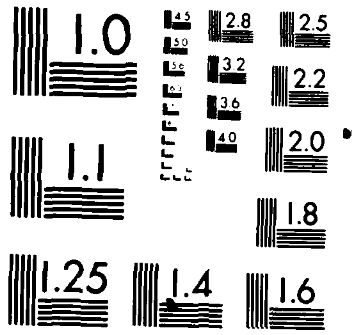

MICROCOPY RESOLUTION TEST CHART
NATIONAL BUREAU OF STANDARDS-1963-A

High levels of noise can adversely affect the normal functioning of the cochlea and result in significant hearing loss. Structural alterations of the cochlea due to noise exposure include sensory cell damage (1,2) as well as changes in the morphology of vascular elements in the external wall and the spiral lamina (3). Vascular changes are thought to be related to altered metabolism due to intense stimulation of the inner ear. Alterations in the cochlear vascular structure resulting from noise exposure have been reported by many authors, and a comprehensive review of this topic has recently been published (4). Perusal of the literature shows that the results of many of the early vascular studies are either contradictory or difficult to interpret. Nevertheless, there is a general consensus that noise does affect the function and morphology of the cochlear vasculature, but to date there is little agreement on precisely how. Since most studies have relied on qualitative assessment, there is a need for a quantitative approach to the analysis of the cochlear vasculature. A recently developed surface technique provides one means for a quantitative assessment of the vascular system of the cochlea (5,6,7). This method utilizes a rating scheme for evaluation of a variety of parameters describing morphology of the vessels of the external wall and spiral lamina. This method was used in the present study to determine the long-term effects of a high intensity impulse noise exposure on the vasculature of the chinchilla cochlea. Impulse noise was chosen as the traumatizing agent in order to cause serious mechanical and metabolic changes in the cochlea, thereby creating an environment in which vascular changes were likely to occur.

Method:

Subjects: Thirty binaural adult chinchillas were used. Of these, 5 animals served as controls, 13 were exposed to 155 dB impulse noise and 12 were exposed to 160 dB impulse noise.

Noise exposure: The impulses were generated by a modified shock tube (compressed air-driven source) coupled to an exponential horn. The impulse waveform was that of a typical blast wave (Friedlander wave) having a 1.5 msec initial over-pressure. The impulses were generated in semi-anechoic surroundings to minimize reflections. The pressure-time trace as well as frequency spectrum of the impulse are published elsewhere (8). The impulses were presented at a rate of 1 impulse per minute for fifty minutes, at intensities of 155 or 160 dB peak equivalent SPL (re $20 \times 10^{-6}$ Pa) to chinchillas whose heads were fixed so that the wave passed at a grazing angle of incidence, i.e., the long axis of the external meatus was parallel to the advancing wavefront.

Histology: Forty-five days after the noise exposure, all of the animals were decapitated without anesthetic using a guillotine. The temporal bones were removed and the cochleas were immediately fixed following one of two different protocols. Five cochleas from each noise-exposed group were processed according to standard surface preparation methods. This consisted of perilymphatic perfusion with 2.5% glutaraldehyde in Pipes (Piperazine N,N'-bis [2-ethane Sulfonic Acid]) buffer (pH 7.3), post-fixation with 1% $OsO_4$ in Pipes buffer, dehydration to 70% ethyl alcohol, microdissection of half turns of organ of Corti and spiral ligament, and mounting of the specimens in glycerol on glass slides for light microscopic evaluation. The remaining 50 cochleas were processed according to the "soft surface" technique (5,6,7). These cochleas were perfused with 2.0% glutaraldehyde in sodium cacodylate buffer (pH 7.4) and decalcified in 8% EDTA for a period of 7 days. After decalcification a mid-modiolar cut was made in each cochlea along the long axis and both halves were stained with 0.5% $OsO_4$, dehydrated and microdissected. Dissected specimens of the lateral wall and organ of Corti were mounted in glycerol on glass slides and evaluated by phase contrast microscopy.

Analysis: Evaluation of the hair cell damage and of the vascular changes was performed by two different observers, and each was blind as to group membership of the cochlea and to the other observer's results. Cochleograms from the control group and the two exposure groups were categorized according to the type of lesion that was found. The four categories were:

a) normal: cochleas with 2% or less outer hair cell (OHC) loss and less than 1% inner hair cell (IHC) loss were considered normal.

b) low-level scattered loss: a diffuse loss throughout the cochlea ranging from 3% to 17% loss of OHC and from 0% to 8% IHC loss. Most cochleas in this category showed 3% to 10% OHC loss and less than 1% IHC loss. Punctate lesions with the same percentage hair cell loss were also included in this category.

c) mid-cochlear focal lesion: cochleas with 100% loss of OHC in the 1 kHz to 5 kHz region of the cochlea and up to 10% IHC loss in same area.

d) severe: cochleas with a lesion beginning around the 1 kHz region and extending basalward with 100% loss of OHC and up to 20% loss of IHC in the same area.

Typical cochleograms from both experimental groups which define each category are shown in figures 1 - 4.

The vascular anatomy was evaluated in 49 of the 60 cochleas. Vascular data were not collected for five cochleas in each of the noise-exposed groups, and one cochlea was lost during processing. A subjective evaluation of the 20 parameters described in Table 1 was made for the regularly occurring vessels in each half turn of each cochlea. The vessels located in the lateral wall that were evaluated are illustrated in figure 5. They are radiating arterioles (RAL) and the vessel at the vestibular membrane (VSVM) in scala vestibuli, the strial vessels (SVS) and the vessel of the spiral prominence (VSSP) in scala media and collecting venules (CVL) in scala tympani. The vessel of the tympanic lip (VSTL) in the spiral lamina was also evaluated.

A computer-assisted statistical analysis was performed on the data collected. The statistics consisted of a stepwise discriminant analysis procedure (9) which was used to identify the parameters that differentiated between the control group and the two experimental groups. This statistical test is a multivariate technique that identifies variables that differ according to group membership. The results of the analysis consist of a hierarchical listing of the parameters that are significant ($p < 0.05$) predictors of group membership. The analysis was performed twice; first, the observations for each vessel were compared to identify vessel differences; second, observations for each half turn were compared to identify location differences. In addition, median values and ranges were computed for each parameter in each vessel and in each half turn for all cochleas in the control group.

Results:

Figure 6 shows the percentage of cochleas from the control group and the two impulse noise exposure groups that were classified into each of the four damage categories described in the methods section. Eighty percent of the control group cochleas were classified normal and the remaining 20% showed low level scattered hair cell loss. Fifteen percent of the cochleas from the 155 dB group and 26% from the 160 dB group were classified normal. A higher percentage of cochleograms showed low-level scattered loss in the 160 dB group (48%) than in the 155 dB group (35%). Mid-cochlear focal lesions were observed more often in the 155 dB group (46%) than in the 160 dB group (17%), while the percentage of cochleograms considered severely damaged was relatively low in both the 155 dB group (4%) and the 160 dB group (9%).

Median, range and histograms for the vascular variables were computed for the control group. There was a high degree of uniformity in the vasculature of the control cochleas. The experimental group results were then analyzed in relation to the control group. A stepwise discriminant analysis was computed for each vessel, regardless of turn, in order to identify those parameters that changed significantly as a result of noise exposure. Table 2 presents a listing of these parameters and also shows in which vessels each parameter was changed as well as the direction of change relative to the control group. Of the 20 parameters, 9 were found to be significantly changed by the noise exposure. In all cases with the exception of white blood cells (WBCs) in the strial vessels, there was no difference between the two noise-exposed groups. In the case of WBCs, there was an increase in the degree of change in the 160 dB group over the 155 dB group. In the second phase of the analysis, the stepwise discriminant analysis procedure was repeated; this time each half turn was evaluated with all vessels combined in order to identify location differences. The results are presented in table 3. No difference between the three groups was found in the two apical half-turns (T3.0 and T2.5). However, changes were seen from the upper middle turn (T2.0) through the basal end of the cochlea.

A "vasculogram" was generated for each cochlea to graphically represent the vascular changes seen in that particular cochlea. For each half turn, values for the parameters identified by the discriminant analysis procedure were compared to the median value from the control group for that parameter. The absolute value of the difference in rating between the experimental cochleas and the median value for that parameter from the control group was computed and a histogram was drawn which reflected parameters changed in each half turn and the magnitude of change for each parameter. These results were compared to the cochleogram for that cochlea. Typical vasculograms are shown in figures 1 -4.

Discussion:

The possibility that method of sacrifice may be an important factor when studying the microvasculature has been raised. Santi and Duvall (10) found that the effect of bumetanide treatment on the strial capillaries was related to method of sacrifice. However, no evidence is available that any particular method of sacrifice or fixation is superior to others for the evaluation of vascular morphology. Both the control and the noise-exposed animals in this study were sacrificed in an identical manner; therefore it was assumed that any artifact associated with method of sacrifice would not affect the statistical analysis of the data.

In terms of hair cell loss, the 155 dB group contained a higher percentage of badly damaged cochleas than the 160 dB group (see figure 6), and statistical tests (t test, $p < 0.05$) revealed a significant increase in OHC loss in the 155 dB group. These results agree with our previous study (11) in which 155 dB peak SPL exposures proved to be more hazardous to the hair cell population than higher intensity exposures. Whereas some aspects of the mechanism underlying this phenomenon remain obscure, failure of the conductive mechanism at higher intensities has been proposed (11), and recent evidence from our laboratory confirms that 160 dB peak SPL impulse noise causes rupture of the tympanic membrane approximately 50% of the time in the chinchilla.

All of the vessels examined except the strial vessels showed a decrease in plasma space between the RBCs and the vessel wall. This could be interpreted as the result of vessel constriction, of corpuscular rather than laminar blood flow or of a higher hematocrit. Since lumen irregularities and decreased columns of RBCs were found in 3 of the 6 vessels, vessel constriction is the most likely explanation for the decrease in plasma space. Constrictions and irregularities of the vessel lumen appear to be due to an increased activity of perivascular cells in two of the vessels, the vessel at the vestibular membrane and the collecting venules. Collectively these changes imply a net reduction in blood flow following noise.

The strial vessels showed changes that were quite different than the other vessels examined (see table 2). The only finding suggesting an influence on stria vascularis capillaries was a decrease in RBC columns. The increase in WBCs may related to the fact that damage due to the noise exposure may not be fully resolved at the time of sacrifice. Increased WBCs may indicate the presence of an inflammatory reaction in the stria vascularis. This may also explain the decreased occurrence of 'gaps' below the tight cell junctions of the marginal cells which could be caused by swelling of the strial cells.

The vasculograms revealed a tendency for vascular changes to be distributed throughout the length of the cochlea, with an increase in the degree of change in the middle and basal turns where the hair cell damage was greatest. Figures 1 - 4 show vasculograms from cochleas representing each of the four cochleogram categories. These figures suggest a tendency for vascular change to increase as degree of hair cell loss increases. However, statistical analysis of the vascular data using cochleogram category as the grouping variable identified no significant difference between groups on the basis of pattern or amount of hair cell loss. These results indicate that separate physiological mechanisms may have been responsible for the vascular changes and the hair cell damage.

Since most other studies of the cochlear vasculature were not quantitative, it is difficult to compare results directly. However, certain comparisons can be made. Changes in density of RBCs have been frequently reported following noise exposure (3,4, 12-17). In our study, several parameters related to RBC density such as a decrease in columns of

RBCs, an increase in variability in density of RBCs and a decrease in plasma space between RBC and vessel wall are signs that RBC flow was affected by noise. Other investigators have noted changes in vessel diameter following noise exposure (3,12,13,16). Several parameters reflecting aspects of vessel lumen, such as lumen irregularity, perivascular cells compressing the lumen and plasma space between RBC and vessel wall were altered in the present study. Changes in the cellular structure of the stria vascularis following noise exposure is another observation that has been made in the literature (3,12,16). This study identified several strial parameters that were influenced by noise. We observed an increase in pigment granules and pigment clumps in the cells of the stria vascularis as well as a decrease in 'gaps' below the tight cell junctions of the marginal cells after noise.

Changes in the morphology of the vascular system after noise exposure may be caused by a variety of factors. Among these are altered metabolic demands of the organ of Corti, altered endolymph composition due to mixing with perilymph as a result of mechanical damage or a combination of the two processes (18). The high intensity of both impulse noise levels used in this study can cause extreme mechanical damage to the organ of Corti leading to a mixing of endolymph and perilymph. Figure 7 shows the outer hair cells and supporting cells torn away from the basilar membrane in one severely damaged cochlea that was exposed to 160 dB peak SPL impulse noise. The vascular damage seen in such cochleas could be the result of a general poisoning of the vasculature caused by the inevitable mixing of perilymph and endolymph following rupture of the organ of Corti as illustrated in figure 7. It was somewhat surprising that severe strial degeneration was not seen in any of the most severely damaged cochleas in this study.

However, substantial vascular changes were seen in those noise-exposed cochleas categorized "normal" in terms of hair cell loss. The poisoning hypothesis cannot be used to explain these findings; it may be more reasonable to interpret these changes as secondary to overwhelming metabolic fatigue caused by the energy demands of the sensory cells during and following the exposure period.

The present method of data collection and analysis provides an increased sensitivity of analysis and an opportunity for standardization in an area of inner ear research that has suffered from a lack of consistency in methodology and of quantification in the past. If future studies can relate changes in vascular parameters as identified by this method to alteration in cochlear function, this method may provide a worthwhile analytical tool for the evaluation of inner ear pathology.

ACKNOWLEDGEMENTS

The authors wish to thank George Turrentine for the micrographs used in this paper and for his assistance in analyzing the hair cell data.

References:

1. Hunter-Duvar IM, Suzuki M, Mount RJ. Anatomical changes in the organ of Corti after acoustic stimulation. In: Hamernik RP, Henderson D, Salvi R, eds. New Perspectives on Noise-Induced Hearing Loss. New York: Raven Press, 1982:3-22.

2. Liberman MC, Mulroy MJ. Acute and chronic effects of acoustic trauma: cochlear pathology and auditory nerve pathophysiology. In: Hamernik RP, Henderson D, Salvi R, eds. New Perspectives on Noise-Induced Hearing Loss. New York: Raven Press, 1982:105-135.

3. Hawkins JE Jr. The role of vasoconstriction in noise-induced hearing loss. Ann Otol Rhinol Laryngol 1971; 80:903-914.

4. Axelsson A, Vertes D. Histological findings in cochlear vessels after noise. In: Hamernik RP, Henderson D, Salvi R, eds. New Perspectives on Noise-Induced Hearing Loss. New York: Raven Press, 1982:49-68.

5. Axelsson A, Vertes D. Methodological aspects for the study of cochlear blood vessels. JASA 1977; Suppl 1: 34.

6. Axelsson A, Vertes D. Vascular histology of the guinea pig cochlea. Acta Otolaryngol (Stockh) 1978; 85:198-212.

7. Vertes D, Axelsson A. Methodological aspects of some inner ear vascular techniques. Acta Otolarygol (Stockh) 1979; 88:328-334.

8. Hamernik RP, Henderson D, Coling D, Slepecky N. The interaction of whole body vibration and impulse noise. JASA 1980; 67(3): 928-934.

9. Cooley WW, Lohnes PR. Discriminant Analysis. In: Multivariate Data Analysis. New York: John Wiley and Sons, 1971: 243-261.

10. Santi PA, Duvall III AJ. Morphological alteration of the stria vascularis after administration of the diuretic bumetanide. Acta Otolarynol (Stockh) 1979; 88:1-12.

11. Hamernik RP, Henderson D. Impulse noise trauma: a study of histological susceptibility. Arch Otolaryngol 1974; 99:118-121.

12. Ruedi L. Some animal experimental findings on the functions of the inner ear. Scientific Papers of the Am. Otolog. Soc. 1951; 88: 993-1023.

13. Kellerhals B. Pathogenesis of inner ear lesions in acute acoustic trauma. Acta Otolaryngol.(Stockh) 1972; 73: 249-253.

14. Lawrence M, Gonzales G, Hawkins JE Jr. Some physiological factors in noise-induced hearing loss. Am. Ind. Hyg. Assoc. J., 1967; 28:425-430.

15. Vertes D, Axelsson A, Miller J, Liden G. Cochlear vascular and electrophysiological effects in the guinea pig to 4 kHz pure tones of different durations and intensities. Acta Otolaryngol (Stockh)1981; 92: 15-24.

16. Lawrence M, Yantis PS. Individual differences in functional recovery and structural repair following overstimulation of the guinea pig ear. Ann Otol Rhinol Laryngol 1957; 66: 595-621.

17. Ward WD, Duvall AJ. Behavioral and ultrastructural correlates of acoustic trauma. Ann Otol Rhinol Laryngol 1971; 80: 881-896.

18. Bohne BA. Mechanisms of noise damage in the inner ear. In: Henderson D, Hamernik RP, Dosanjh DS, Mills JH, eds. Effects of Noise on Hearing. New York: Raven Press, 1976: 41-68.

## TABLE 1: VASCULAR PARAMETERS

### Red Blood Corpuscles (RBCs)

DENS: density; frequency and spacing of RBCs in vessel lumen

COL: columns; number of rows of RBCs in vessel lumen

AGGREG: aggregations and plasma gaps; collections of RBCs and interspaced sections with plasma but without RBCs

ORIENT: orientation; manner and plane of RBCs in vessel lumen

VAR: variability; in density of RBCs

PLAS: plasma space; between RBC and vessel wall

### Vessel Lumen

LM IRRG: luman irregularity; local narrowing and widening of vessel lumen

PV LUM: perivascular cell compressing lumen; occurrence of narrow vessel lumen caused by endothelial cell nuclei and/or pericytes

DIAM: lumen diameter; width of vessel lumen

PVS: perivascular spaces; spaces surrounding vessel lumen

### Stria Vascularis

GRAN: granules; pigment formed of fine granulations

PIGM: pigment clumps; clusters or collections of granules

VAC: vacuoles in strial surface structure

GAPS: 'gaps' between cells; spaces occurring between strial marginal cells below the tight cell junctions

### Additional Vascular Parameters

AVC: avascular channels

WBC: white blood cells

EMB: emboli in vessel; bound, clear spaces within vessel lumen

DEP: deposits; osmiophilic materials surrounding vessels

MEL: melanocytes

SPH: precapillary sphincter; narrowing of vessel by perivascular elements

TABLE 2. SIGNIFICANT PARAMETERS BY VESSEL

| VESSEL / PARAMETER | RAL | VSVM | SVS | VSSP | CVL | VSTL |
|---|---|---|---|---|---|---|
| PLAS | ⇩ | ⇩ | | ⇩ | ⇩ | ⇩ |
| LM IRRG | | ⇧ | | | ⇧ | ⇧ |
| COL | ⇩ | | ⇩ | | ⇩ | |
| PV LUM | | ⇧ | | | ⇧ | |
| VAR | | | | ⇧ | | |
| PIGM | | | ⇧ | | | |
| GRAN | | | ⇧ | | | |
| GAPS | | | ⇩ | | | |
| WBC | | | ⇧ | | | |

TABLE 3.
SIGNIFICANT PARAMETERS BY TURN

| TURN / PARAMETER | 3.0 | 2.5 | 2.0 | 1.5 | 1.0 | 0.5 |
|---|---|---|---|---|---|---|
| PLAS | | | | ⇩ | ⇩ | |
| LM IRRG | | | ⇧ | ⇧ | ⇧ | ⇧ |

# FIGURES

1.-4. (these 4 figures should appear together) Examples of cochleograms from noise-exposed animals classified normal (1), low level scattered loss (2), mid-cochlear focal (3) and severe (4) are shown in the top of each figure. The bottom of each figure shows vasculograms for these 4 cochleas. See table 1 for definitions of the vascular parameters.

5. The vessels of the lateral wall that were evaluated for vascular changes. SV = scala vestibuli, VM = vestibular membrane, SM = scala media, BM = basilar membrane, ST = scala tympani. The vessel of the tympanic lip in the spiral lamina was also evaluated but is not shown.

6. Percentage of cochleas from the control group and the two noise-exposed groups placed in each category according to hair cell loss.

7. Scanning electron micrographs of the basal turn of the cochlea from an animal exposed to 150 dB impulse noise and sacrificed immediately after the exposure. (A) shows a 3 mm. section of third row outer hair cells and supporting cells that have been ripped off of the basilar membrane by the force of the impulse. (B) shows the fracture line at the basal end of the lesion, and (C) shows the region of separation of the sensory epithelium from the basilar membrane at the basal end of the lesion.

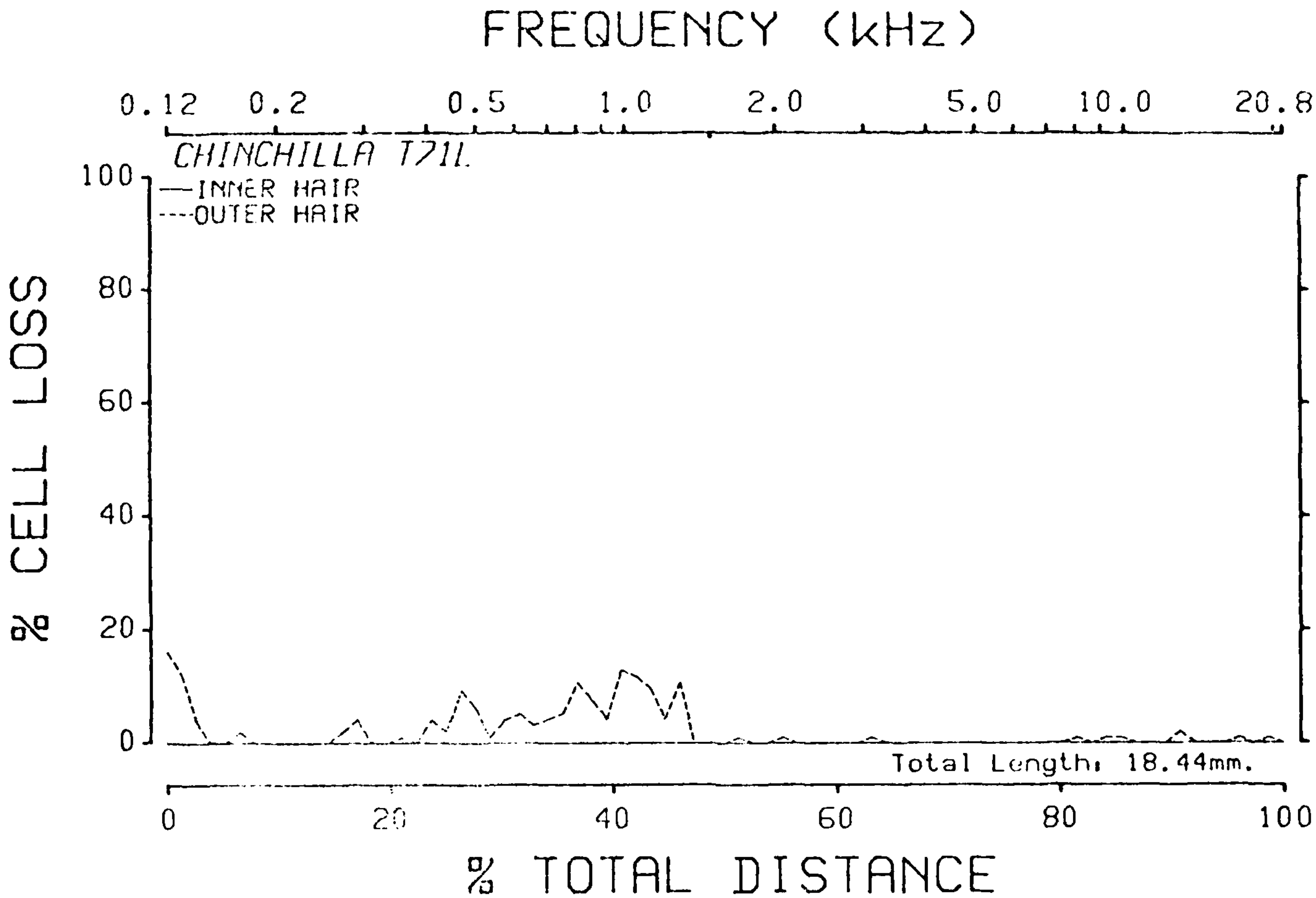
FREQUENCY (kHz)
0.12 0.2 0.5 1.0 2.0 5.0 10.0 20.8
CHINCHILLA T71L
—INNER HAIR
----OUTER HAIR
% CELL LOSS
100
80
60
40
20
0
Total Length: 18.44mm.
0 20 40 60 80 100
% TOTAL DISTANCE

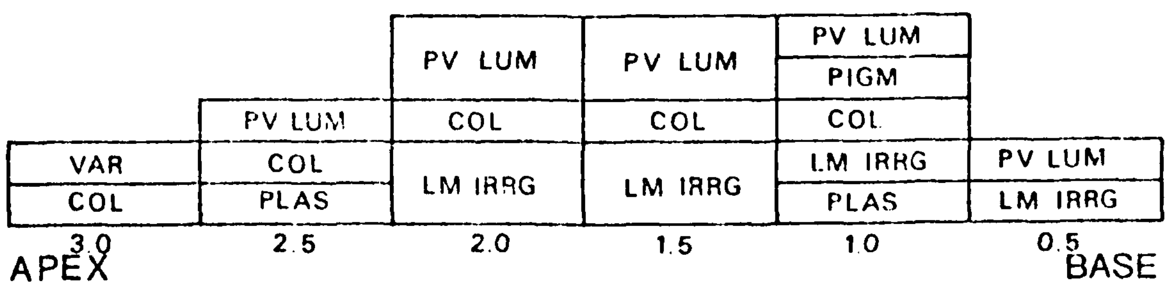
PV LUM
PV LUM
PV LUM
PIGM
PV LUM
COL
COL
COL
VAR
COL
LM IRRG
LM IRRG
LM IRRG
PV LUM
COL
PLAS
PLAS
LM IRRG
3.0
2.5
2.0
1.5
1.0
0.5
APEX
BASE

Figure 1

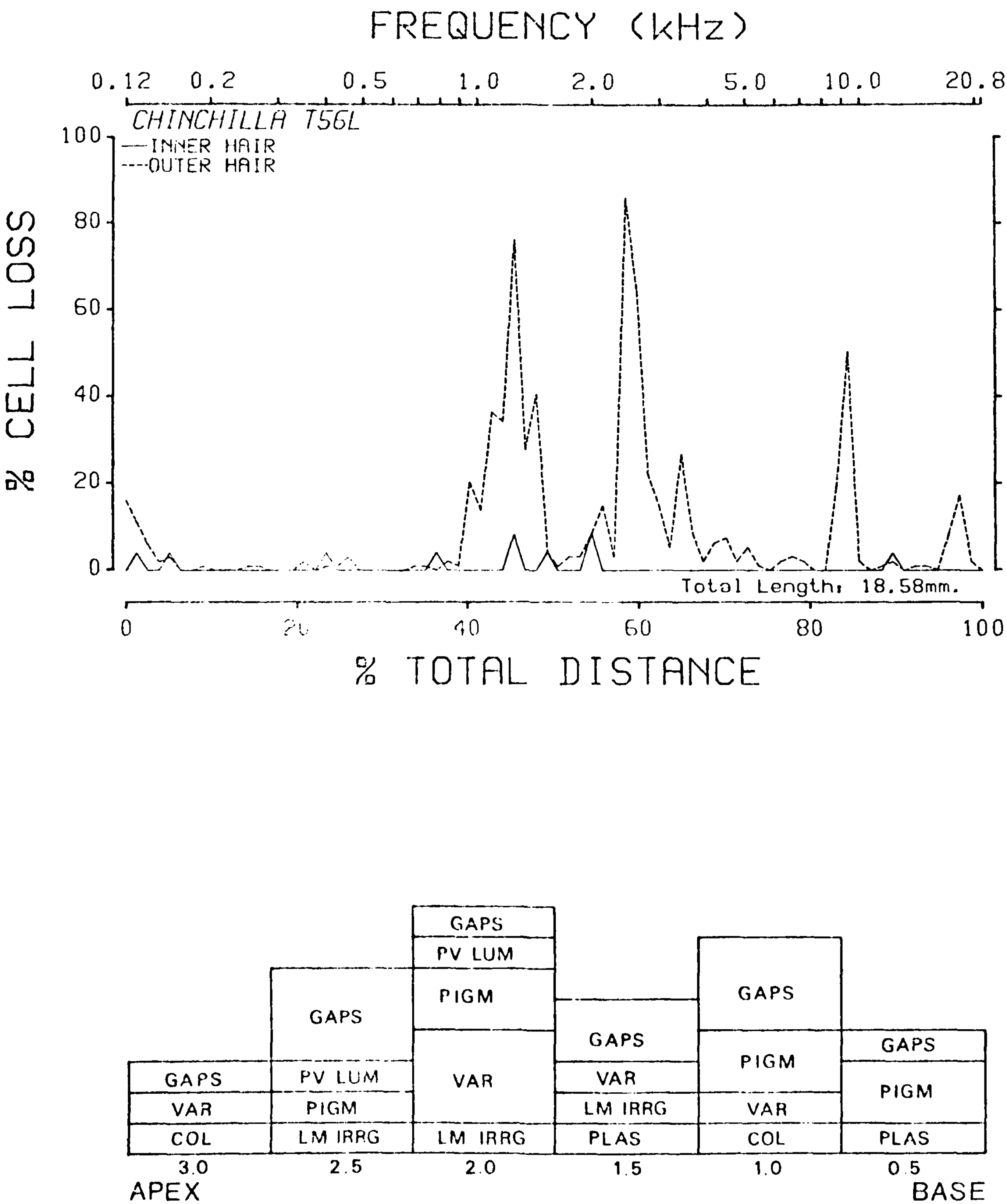
FREQUENCY (kHz)
0.12
0.2
0.5
1.0
2.0
5.0
10.0
20.8
CHINCHILLA T56L
—INNER HAIR
---OUTER HAIR
% CELL LOSS
100
80
60
40
20
0
Total Length: 18.58mm.
0
40
60
80
100
% TOTAL DISTANCE
GAPS
PV LUM
PIGM
GAPS
GAPS
GAPS
GAPS
PV LUM
VAR
VAR
PIGM
GAPS
VAR
PIGM
LM IRRG
VAR
PIGM
COL
LM IRRG
LM IRRG
PLAS
COL
PLAS
3.0
2.5
2.0
1.5
1.0
0.5
APEX
BASE

Figure 2

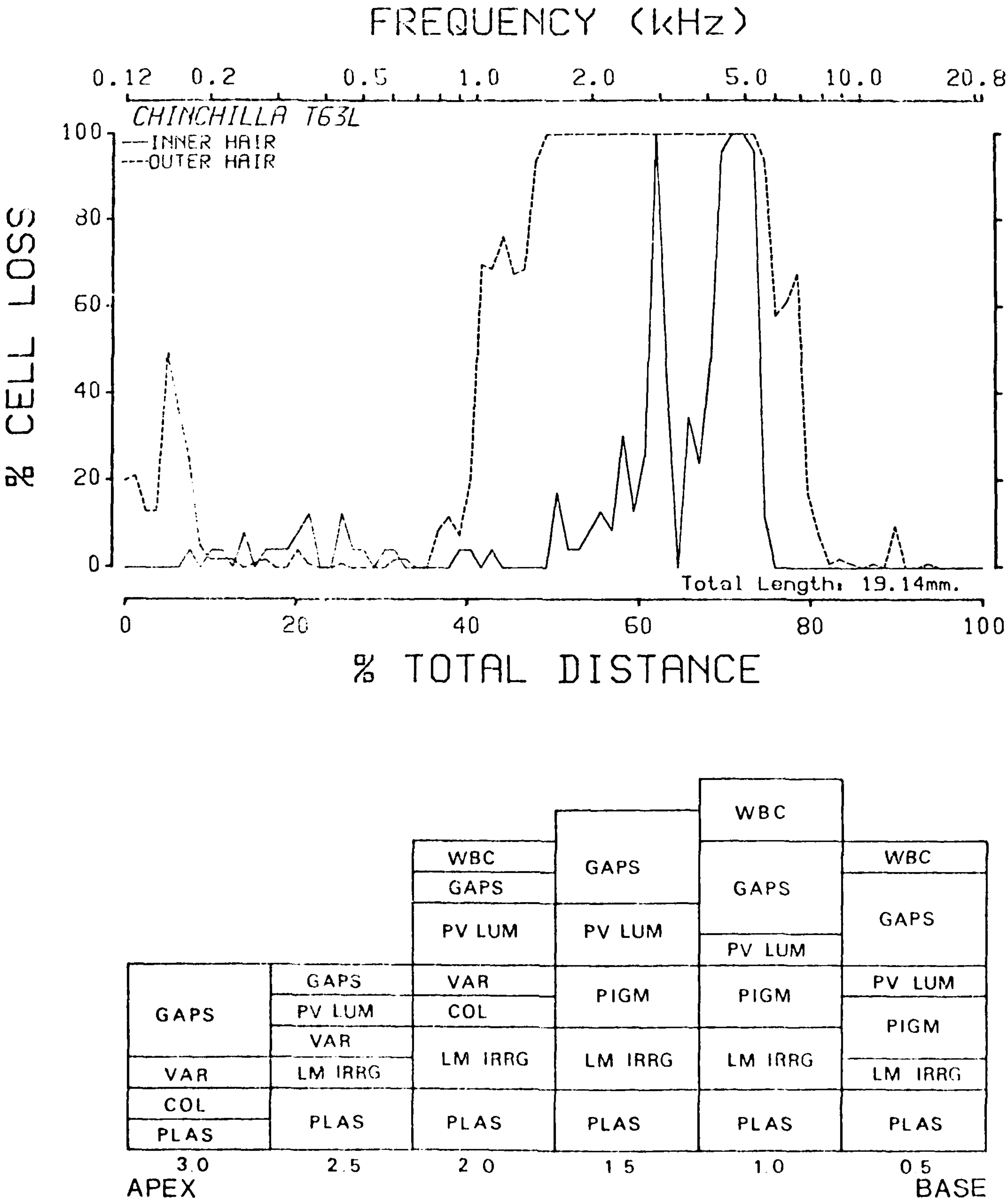
FREQUENCY (kHz)
0.12 0.2 0.5 1.0 2.0 5.0 10.0 20.8
CHINCHILLA T63L
—INNER HAIR
---OUTER HAIR
% CELL LOSS
100 80 60 40 20 0
Total Length: 19.14mm.
0 20 40 60 80 100
% TOTAL DISTANCE
GAPS
VAR
COL
PLAS
GAPS
PV LUM
VAR
LM IRRG
PLAS
WBC
GAPS
PV LUM
VAR
COL
LM IRRG
PLAS
GAPS
PV LUM
PIGM
LM IRRG
PLAS
WBC
GAPS
PV LUM
PIGM
LM IRRG
PLAS
WBC
GAPS
PV LUM
PIGM
LM IRRG
PLAS
3.0
2.5
2.0
1.5
1.0
0.5
APEX
BASE

Figure 3

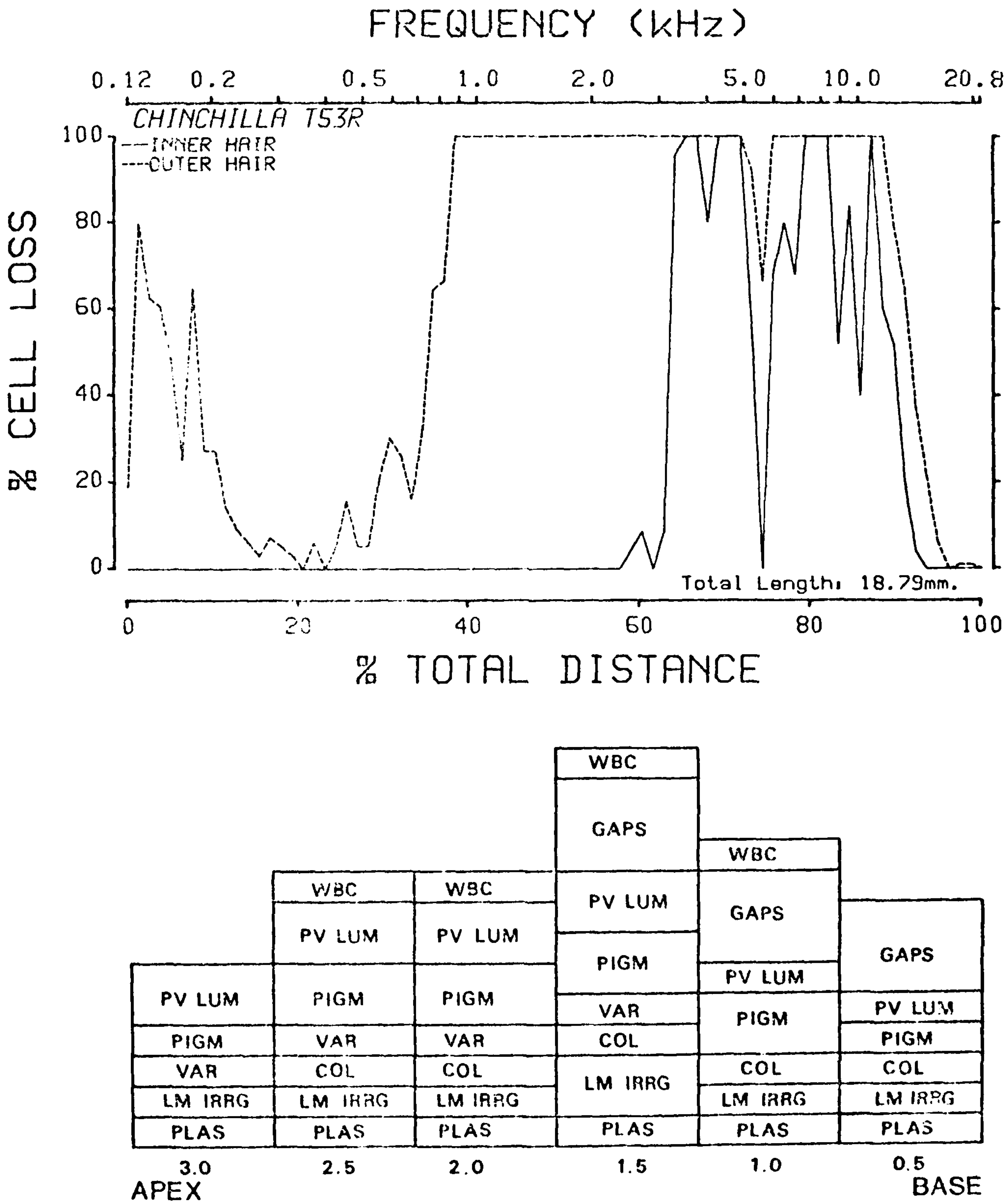

FREQUENCY (kHz)
0.12
0.2
0.5
1.0
2.0
5.0
10.0
20.8
CHINCHILLA T53R
—INNER HAIR
---OUTER HAIR
% CELL LOSS
100
80
60
40
20
0
Total Length: 18.79mm.
0
20
40
60
80
100
% TOTAL DISTANCE
WBC
GAPS
PV LUM
PIGM
VAR
COL
LM IRRG
PLAS
3.0
APEX
2.5
2.0
1.5
1.0
0.5
BASE


Figure 4

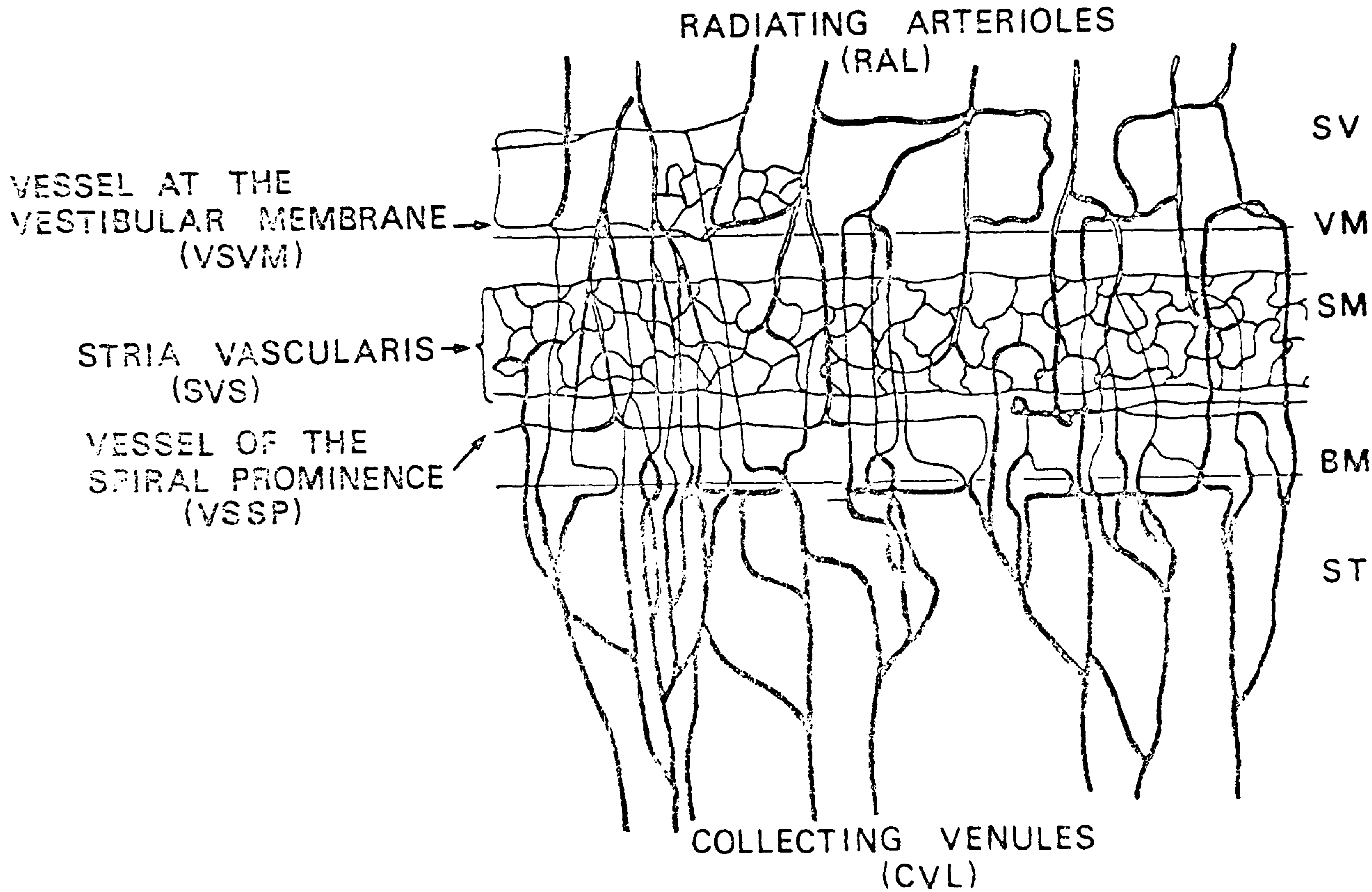
RADIATING ARTERIOLES
(RAL)
SV
VM
SM
BM
ST
VESSEL AT THE
VESTIBULAR MEMBRANE
(VSVM)
STRIA VASCULARIS
(SVS)
VESSEL OF THE
SPIRAL PROMINENCE
(VSSP)
COLLECTING VENULES
(CVL)

Figure 5

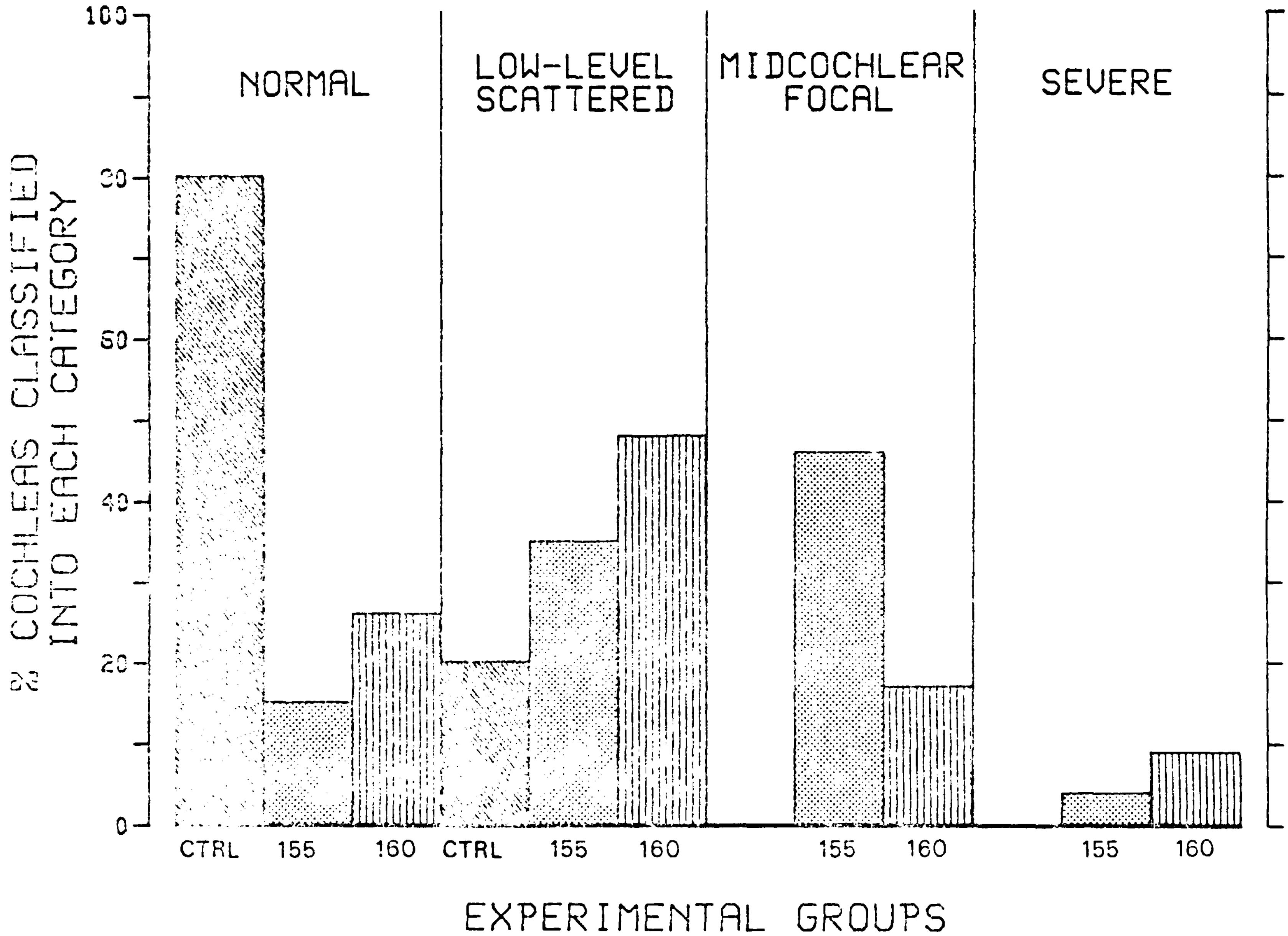

% COCHLEAS CLASSIFIED INTO EACH CATEGORY
100
80
60
40
20
0
NORMAL
LOW-LEVEL SCATTERED
MIDCOCHLEAR FOCAL
SEVERE
CTRL
155
160
CTRL
155
160
155
160
155
160
EXPERIMENTAL GROUPS


Figure 6

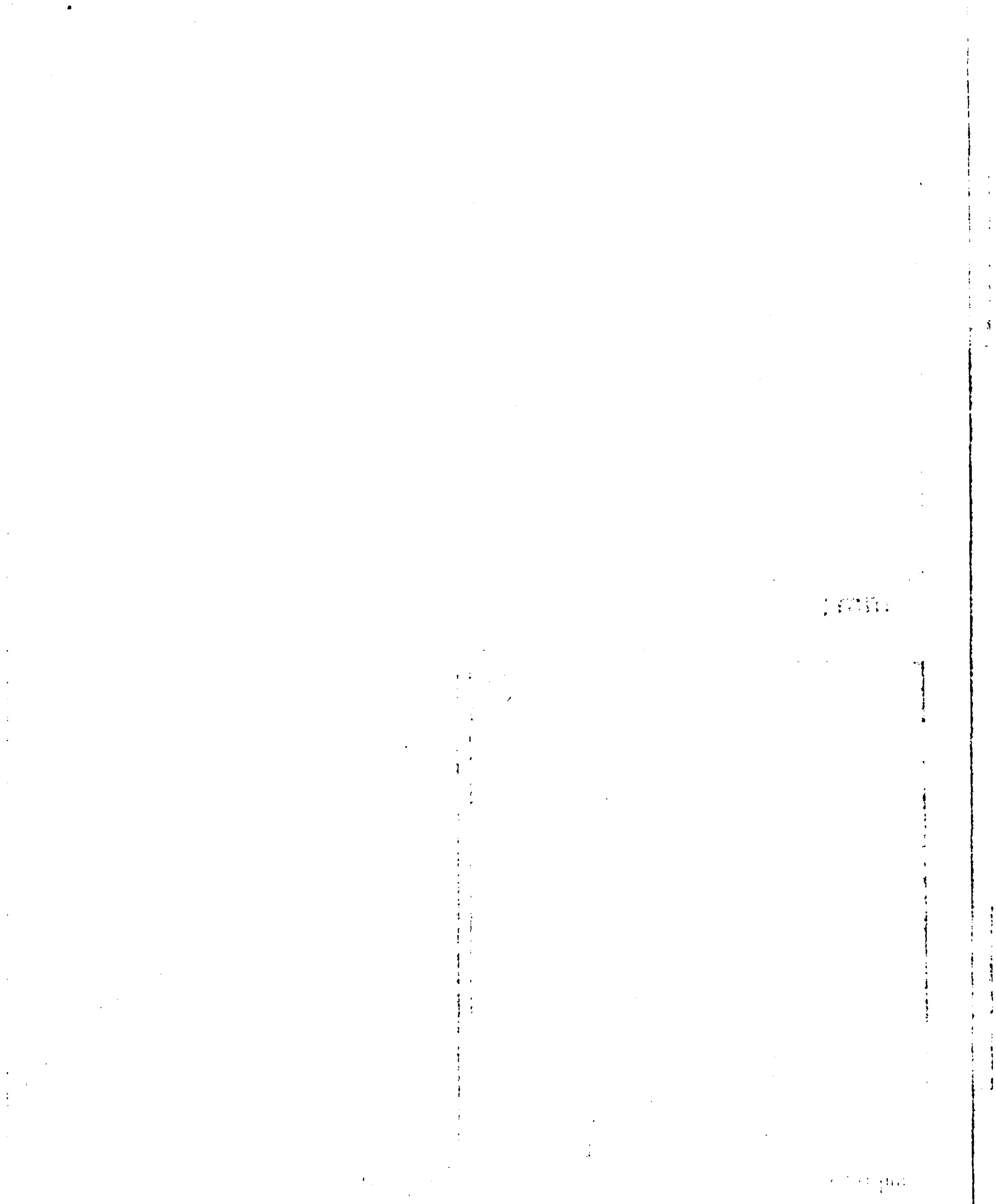

Figure 7

Vascular and Sensory Cell Changes in the Cochlea

Induced by Elevated Temperature and Noise

Lynn Carlisle Shaddock (1), Roger P. Hamernik (1) and Alf Axelsson (2)

(1) Callier Center for Communication Disorders, University of Texas at Dallas, 1966 Inwood Road, Dallas, Texas, 75235

(2) Departments of Otolaryngology and Audiology, University of Goteburg, Sahlgren's Hospital, S-413 45 Goteburg, Sweden

send correspondence to:

Lynn Carlisle Shaddock

Callier Center for Communication Disorders

University of Texas at Dallas

1966 Inwood Road

Dallas, Texas 75235

This research was partially supported by U. S. Army Medical Research and Development Command DAMD17-80-C-0133 and The Swedish Work Environment Fund.

## SUMMARY

The vascular anatomy of the chinchilla cochlea was quantitatively analyzed and compared in animals exposed to 155 or 160 dB impulse noise at normal (37°C) or elevated (40°C) body temperature. Vascular changes were found to persist 45 days after exposure in all experimental animals. Six parameters were shown to be most susceptible to change in one or more of the vessels studied. These were irregularities in vessel lumen, plasma spaces between red blood cells (RBCs) and vessel wall, columns of RBCs, variability in density of RBCs, pigment clumps in stria vascularis and perivascular cells compressing vessel lumen. These vascular changes, which are indicative of a permanent reduction in blood flow, were present throughout the length of the cochlea with a tendency toward maximum change in areas of maximum hair cell loss. There was no evidence to support the idea of an interaction between noise and increased body temperature in the vascular results. However, the cochleograms from these animals indicate that at the 160 dB exposure level the noise and high temperature did interact to increase hair cell loss.

key words: impulse noise, temperature elevation, cochlear vasculature, inner and outer hair cells

## Introduction

One hypothesized mechanism for damage to the organ of Corti is that in the presence of high level noise the metabolic demands made by the sensory cells in the cochlea are so great that they are eventually depleted of their energy reserves and cease to function. If the noise exposure persists, rupture of the cell membrane and degeneration of the sensory cell may follow (2). In studies of the effects of noise exposure on the cochlear vascular system, several authors (6-8,11) have noted constriction of the cochlear vessels and other changes consistent with a reduced blood flow following the exposure. When exposure to noise is coupled with high body temperature which also increases metabolic rate, a situation exists in which blood flow to the cochlea may be diminished while metabolic demands on the cochlea are increased due to the concomitant presence of noise and high temperature. We might expect such an exposure to produce considerably more vascular changes and to be potentially more damaging to the sensory cells of the cochlea than exposure to noise at normal body temperature.

Physiological indication that an interaction effect between noise and high temperature might exist is available. Drescher (5) studied the effect of body temperature on the cochlear microphonic response (CM) in the chinchilla. His results showed that the time required to reach asymptotic threshold shift (ATS) due to a continuous noise was dramatically reduced when body temperature was elevated to 39°C. In a study examining the effect of ambient room temperature on the degree of temporary threshold shift (TTS) in human subjects, Dengerink et al (4) found a significant (5 dB) increase in TTS measured at 4 kHz among non-smoking subjects who were exposed to 110 dB white noise at 38°C as compared to non-smokers exposed to the same noise at 4.5°C.

The purpose of this study was to investigate the possibility that high body temperature could increase the amount of damage to the sensory cell population and the vascular system of the cochlea following exposure to high intensity noise. The results of such a study may provide some insight into the role of the vascular system in cochlear trauma and could affect the development of damage risk criteria as well. In the work environment, damaging levels of noise are often accompanied by heat and other stressors which may interact with noise and increase the worker's risk for hearing loss; thus an interaction of noise and high temperature could make these groups high risk populations for noise induced hearing loss.

Methods

A total of 45 adult binaural chinchillas were used in the study. Each animal was assigned to one of six experimental conditions. Five animals served as histological controls, 5 animals had their body temperature elevated to 40°C but were not exposed to noise, 13 animals were exposed to 155 dB peak SPL impulse noise, 5 animals were exposed to 155 dB peak SPL impulse noise while their body temperature was elevated to 40°C, 12 animals were exposed to 160 dB peak SPL impulse noise, and 5 animals were exposed to 160 dB peak SPL impulse noise while their body temperature was elevated to 40°C.

Temperature elevation: The chinchillas were awake and restrained during the temperature elevation procedure. A thermostatically-controlled heating pad was used to raise body temperature. Two thermistor probes were inserted into the animal rectally; one was used to regulate the heating pad and the other measured core temperature. At the beginning of each exposure, the animal's normal temperature was recorded. All animals had normal temperatures between 36.5 and 37.5°C. To elevate temperature, the thermostat setting was gradually increased in one degree steps until 40°C was reached; a process which took from 15 to 30 minutes. Then body temperature was maintained at 40°C for one hour. At the end of the hour, the heating pad was turned off and the animal's temperature was monitored until it returned to normal, which generally took about 45 minutes.

Noise exposure: The impulses were presented at a rate of 1 impulse per minute at either 155 or 160 dB peak SPL (re 20 x $10^{-6}$ Pa). The impulses were generated by a modified shock tube coupled to an exponential horn and were discharged into a semi-anechoic chamber. Each animal was restrained in a yoke-type apparatus that prevented movement of the head and was positioned at grazing incidence to the advancing wavefront approximately 45 cm. from the exit of the acoustic horn.

Histology: Post-exposure survival time for the experiment was 45 days. All of the chinchillas were decapitated without anesthetic using a guillotine. The cochleas were divided into two groups for histological processing. Immediately after decapitation, the temporal bones from the chinchillas in the first group (n = 25) were removed and the cochleas were fixed via perilymphatic perfusion with 2.5% buffered glutaraldehyde (7.3 pH). The cochleas were stored overnight in glutaraldehyde, then post-fixed with 1% $OsO_4$ in the same buffer (Piperazine N, N'-bis[2 ethane Sulfonic Acid]) and dehydrated through a series of graded alcohols. The cochleas were stored in 70% alcohol until microdissected.

The remaining 65 cochleas were processed according to the "soft surface technique" of Vertes and Axelsson (10). Decapitation was followed by immediate removal of the temporal bones and perilymphatic perfusion of the cochleas with 2.0% glutaraldehyde in sodium cacodylate buffer (pH 7.4). After 24 hours in the fixative, the cochleas were decalcified in 8% EDTA for 7 days. A mid-modiolar section was made through each decalcified cochlea, then both halves were stained with 0.5% $OsO_4$ in Millonig buffer and dehydrated to 70% alcohol. The same microdissection technique was used for both groups. In each cochlea, half turns of organ of Corti and spiral ligament were removed and mounted in glycerol on glass slides for light microscopic evaluation.

Analysis: Cochleograms were generated for each cochlea. Cochleograms were classified into 1 of 4 categories based on type and extent of hair cell lesion. Cochleas exhibiting no more than 2% outer hair cell (OHC) loss scattered throughout the cochlea and less than 1% inner hair cell (IHC) loss were placed in the normal category. Cochleas with between 3% and 17% OHC loss and less than 8% IHC loss that was diffusely spread throughout the cochlea or cochleas with narrow focal lesions were placed in the low-level scattered category. Cochleas which had up to 100% loss of OHC in the 1 - 5 kHz region of the cochlea and up to 10% loss of IHC in the same region were classified mid-cochlear focal lesion, and those cochleas that showed 100% loss of OHC throughout the lower half of the cochlea and up to 20% loss of IHC were placed in the severe category. Examples of cochleograms from each category are presented in figures 1-4.

The method and parameters described by Axelsson and Vertes (1) were used to evaluate the vascular anatomy of the 64 cochleas in group 2 (one cochlea was lost in processing). Vascular data were not collected on the 25 cochleas in group 1. The vessels that were examined for vascular changes are illustrated schematically in figure 5. They are radiating arterioles (RAL) and the vessel at the vestibular membrane (VSVM) in scala vestibuli, the strial vessels (SVS) and the vessel of the spiral prominence (VSSP) in scala media, and collecting venules (CVL) in scala tympani. The vessel of the tympanic lip (VSTL) in the spiral lamina was also evaluated for vascular change. Each of these vessels was evaluated in each half turn of each cochlea. A subjective rating was assigned for each of the 20 parameters which are listed in table 1, and stepwise discriminant analysis (SDA) was performed on the data (3). This multivariate technique is used to identify those variables that are good predictors of group membership. The results consist of a hierarchical listing of the significant variables. The SDA procedure was performed three times. The first SDA compared the control group to the temperature-elevation-only group to see which of the 20 parameters were changed as a result of temperature elevation. The second SDA compared the control group with the two groups involving only noise exposure to identify parameters changed after noise exposure. The third SDA compared the control group with all five experimental groups, in order to detect those variables that showed a temperature/noise interaction.

Vascular changes in individual cochleas were quantified by generating vasculograms. For each half turn, values for the parameters identified by the stepwise discriminant analysis procedure were compared to the median value from the control group for that parameter. The absolute value of the difference in rating between the experimental ears and the median value for the parameter from the control group was computed and a histogram was drawn which reflected the parameters changed, location of the change and magnitude of the change.

## Results

Cochleograms: The results of the cochleogram classification for all 90 cochleas are summarized in figure 6. Eighty percent of the cochleas from the control group and 90% of the cochleas from the temperature-elevation-only group were classified normal. The other 20% of the control group cochleas and 10% of the temperature-elevation-only group cochleas fell into the low-level scattered loss category.

There were more cochleas classified normal in the 155 dB impulse noise + heat group (50%) than in the 155 dB impulse noise group (15%), while more cochleas were classified into the mid-cochlear category (46%) and the severe category (4%) in the 155 dB group than in the 155 dB + heat group (30% and 0% respectively). Therefore, for the 155 dB noise exposure a greater percentage of badly damaged cochleas were seen in the group exposed at normal body temperature than in the group exposed at elevated body temperature.

Twenty-six percent of the cochleas in the 160 dB impulse noise group were classified normal and 48% were classified low-level scattered loss, while none of the 160 dB impulse noise + heat group were classified normal and only 10% fell into the low-level scattered loss category. Sixty percent of the 160 dB + heat group showed severe damage and 30% had mid-cochlear lesions as compared to 9% severe and 17% mid-cochlear lesions in the 160 dB impulse noise group. Therefore at 160 dB the group exposed at elevated body temperature contained a much greater proportion of badly damaged cochleas than the group exposed at normal body temperature.

Table 2 shows the mean and standard error of the mean (SEM) for each group for both inner hair cell loss and outer hair cell loss. A one-way analysis of variance test was performed to compare the amount of hair cell loss across the six groups. A significant difference was found between group means for both inner hair cell loss ($F(5,82)=3.78, p < 0.005$) and outer hair cell loss ($F(5,82)=8.59$, $p < 0.001$). Dunnett's test of multiple comparisons (12) was used to determine which group means differed from the control group mean. This test revealed that group 3, the 155 dB impulse noise group, and group 6, the 160 dB impulse noise + heat group had significantly more outer hair cell loss than the control group and that only in group 6 was there a significant increase in inner hair cell loss over the control group.

Vasculograms: Vasculograms were drawn for cochleas from the control group and from each of the five experimental groups (see figures 1-4). All cochleas in the five experimental groups showed vascular changes which were present from the apex to the base with a slight tendency towards increased vascular changes in the middle and lower turns. In the 4 groups that were exposed to noise, there was a tendency for the degree of vascular change to be proportional to the amount of hair cell loss. In other words, cochleas classified into the normal and low-level scattered loss categories for hair cell loss showed fewer vascular changes than cochleas classified into the mid-cochlear and severe categories.

Vascular analysis: Table 3 summarizes the results from the three stepwise discriminant analysis procedures. All parameters that were found to be significant by the SDA procedures are listed along the left hand margin of the table. The arrows indicate direction of change (i.e. increase or decrease) in the parameter in the experimental groups relative to the control group. Of the 20 parameters entered into the analysis, 13 were significant in at least one case. These 13 variables are listed in descending order according to the number of times that they were significant predictors.

An examination of all the parameters that were significant in the SDA including all six groups revealed no effects attributable to an interaction between elevated body temperature and impulse noise. In each case the pattern of change was such that there was an effect of heat and an even greater effect of noise; however, there was no increase in vascular change in the impulse noise groups exposed at elevated body temperature as compared to the impulse noise groups exposed at normal body temperature which we would have expected if an interaction of noise and heat were present.

There were 7 instances in which we found an effect of temperature and an effect of noise, indicated by 'BOTH' in table 3. Since these parameters were significant in all three SDA procedures, they represent those vessel/parameter combinations that are most vulnerable to cochlear insult from our experimental manipulations. This pattern was found for: the parameter plasma spaces between RBCs and vessel wall in radiating arterioles, the vessel of the spiral prominence and collecting venules; the parameter lumen irregularities in the vessel at the vestibular membrane and collecting venules; the parameter columns of RBCs in the strial vessels; and the parameter describing variability in density of RBCs in the vessel of the spiral prominence.

We considered an effect to be 'robust' if a parameter was significant in the SDA including all six groups and in the control vs. heat SDA or the control vs. noise SDA but not both. There was only one instance of a robust effect of temperature elevation, indicated by 'HEAT' in the table. This was for the parameter pigment clumps in the spiral prominence. There were seven instances of robust effects of noise, indicated by 'NOISE' in the table: for the parameter plasma spaces in the vessel at the vestibular membrane and the vessel of the tympanic lip; for the variable lumen irregularities in the vessel of the tympanic lip; for the parameter columns of RBCs in radiating arterioles and collecting venules; for the parameter pigment clumps in the strial vessels and for the parameter perivascular cell compressing lumen in the vessel at the vestibular membrane.

There were five instances of temperature effects, indicated by 'heat' in the table: for the vessel at the vestibular membrane the parameters describing avascular channels and density of RBCs; for the strial vessels the parameter lumen irregularities; for collecting venules perivascular spaces surrounding the vessel lumen; and for the vessel of the tympanic lip the parameter perivascular cell compressing lumen.

In five instances there were noise effects, indicated by 'noise' in the table: in the strial vessels, granules in the cytoplasm of the strial marginal cells, gaps between strial marginal cells and occurrence of white blood cells; around the vessel of the spiral prominence the parameter melanocytes; and perivascular cells compressing vessel lumen in the collecting venules.

One issue concerning the cochlear vascular system has been the relationship between the location of vascular damage and damage to the organ of Corti. Axelsson and Vertes (1) cited a number of studies in which no regular correlation was found between site of vascular change and site of hair cell loss, as well as other studies in which a predictable relationship between the two factors was found. A stepwise discriminant analysis was performed for each half turn of each cochlea to see if the vascular changes found in this study were located in the same cochlear region where hair cell loss occurred. The results showed no difference between groups in the apical turn. Lumen irregularities was identified as a significant variable in the middle and basal turns. Plasma spaces between RBCs and vessel wall was also a significant variable in the lower middle and upper basal turns. Figure 7 displays these results, and indicates that the location of maximum vascular change does seem to correspond to the area where greatest hair cell loss was seen in the mid-cochlear and severe lesion cochleograms. However, some vasculograms from the temperature-elevation-only group showed the same tendency toward increased vascular changes in the lower middle and upper basal turn. This may indicate that the configuration is related to some factor other than the noise exposure, perhaps a greater susceptibility to vascular change in general in the lower half of the cochlea.

Discussion

Our decision to use impulse noise was dictated by a desire to maximize trauma to the organ of Corti. We hoped to enhance the chances of seeing interaction effects of noise and temperature and to produce vascular changes as a result of this insult. The significant increase in outer and inner hair cell loss in the 160 dB impulse noise + heat group may be attributable to a synergistic interaction of impulse noise and elevated body temperature. However, no such interaction was seen in the 155 dB impulse noise + heat group. In fact, this group showed the highest percentage of "normal" cochleas of any of the 4 groups involving noise exposure. The only other group which differed statistically from the control group was the group exposed to 155 dB impulse noise at normal temperature, which showed an increase in outer hair cell loss. These results are not what we would predict if a synergistic effect existed between elevated temperature and noise. Any clear effect was certainly obscured by the extreme variability encountered in all four of the groups involving noise exposure. This variability is common for impulse noise exposures, and may be attributable either to small sample size, individual susceptibility or possible tympanic membrane rupture in some animals due to the impulse. Our results indicate that temperature elevation alone does not cause hair cell damage. Nine of the 10 cochleas taken from the animals which only had their body temperature elevated had normal sensory cell populations and showed only occasional missing hair cells, and the tenth cochlea showed low-level scattered hair cell loss which may be attributable to pre-existing conditions.

The results of the vascular analysis are less variable than the hair cell data. All cochleas that were analyzed for vascular changes in the five experimental groups showed vascular changes throughout their length. Since the evaluation of the vessels was performed without knowledge of group membership of the cochlea being evaluated, the fact that the data collected on the control cochleas clearly separated out from the experimental groups provides verification that the vascular changes seen in the experimentally manipulated cochleas are the result of that manipulation.

The results of the statistical analysis of the vasculature identified 25 vessel/parameter combinations that showed significant change after temperature elevation, noise exposure or both. In general, all vessels seemed more susceptible to change due to noise exposure than temperature. Of the 25 entries in table 3, 19 included an effect of noise while only 13 included an effect of temperature. In those cases where both an effect of noise and an effect of temperature was seen, the vascular change was always greater in the group where noise was a factor. There was no indication that either noise or temperature elevation was more important in any particular vessel; temperature effects and noise effects were seen in all six vessels studied. Likewise, all parameters that appear in more than one vessel were significant sometimes in the temperature analysis and sometimes in the noise analysis.

Both a decrease in plasma space and an increase in lumen irregularities imply a reduced blood flow. Such a reduction is further indicated by the decrease in columns of RBCs found in the strial vessels as well as the radiating arterioles supplying them and the collecting venules draining them. An impairment of blood flow may also account for the increased variability in density of RBCs and the decreased density of RBCs in the vessel at the spiral prominence. All these vascular changes considered together indicate a decreased blood supply to the cochlea. This decrease in cochlear blood supply may be due to different mechanisms in the heat and noise conditions. The decrease in columns of RBCs seen in radiating arterioles and collecting venules after noise may reflect a vasoconstrictive effect. Since decreased columns of RBCs were not found after heat, perhaps another explanation, such as a slowing of cochlear blood flow, may be more defensible in explaining the results of the heat condition.

Another prominent feature in the results of the vascular analysis was the increased occurrence of pigment in the form of clusters of pigment granules and pigment clumps free in the cytoplasm of the strial cells, and melanocytes surrounding the vessel of the spiral prominence. These findings may suggest an inflammatory reaction in the stria vascularis. A description of pigment granules in the marginal and transitional cells of the stria and the cells of the spiral ligament can be found in Spoendlin (9), who raised the possibility that these structures may be related to thermoregulation in the cochlea. In our study, increases in pigment were not always related to temperature effects, but were seen in some vessels where their increase was attributed to an effect of noise. Ward and Duvall (11) reported dark inclusion bodies in the stria vascularis after noise exposure. Whatever the cause, our results do provide evidence for an increase in pigment in the stria vascularis following cochlear insult.

In this study, substantial changes in the cochlear vasculature were seen in all experimental animals, including those which had their body temperature elevated but were not exposed to noise. The same vascular parameters were affected in the temperature-elevation-only group as in the other experimental groups. This suggests that the inner ear is susceptible to long term changes in vascular morphology as a result of limited exposure to elevated body temperature. The addition of other stressors, in this case impulse noise, did not substantially increase the amount of vascular change. This argues against any sort of synergistic interaction of noise and elevated body temperature on the vasculature, and may indeed be indicative of a generalized reaction to stress regardless of the source. The fact that changes in vasculature morphology were seen in noise-exposed cochleas that showed no sensory cell damage may indicate that the vascular system of the cochlea is initially more susceptible to cochlear trauma than the sensory elements. Permanent changes in the cochlear vasculature may have an impact on the cochlea, especially in situations that are metabolically demanding.

References

1. Axelsson, A. and Vertes, D. (1982): Histological findings in cochlear vessels after noise. In: New Perspectives on Noise-Induced Hearing Loss. pp.49-68. Editors: R.P. Hamernik, D. Henderson, R. Salvi. Raven Press, New York.

2. Bohne, B.A. (1976): Mechanisms of noise damage in the inner ear. In: Effects of Noise on Hearing. pp.41-68. Editors: D. Henderson, R.P. Hamernik, D. Dosanjh and J. Mills. Raven Press, New York.

3 . Cooley, W.W. and Lohnes, P.R. (1971): Discriminant Analysis. In: Multivariate Data Analysis. pp. 243-361. John Wiley & Sons, New York.

4. Dengerink, H.A., Trueblood, G.W. and Dengerink, J.E. (1981): The effects of ambient air temperature and cigarette smoking on noise-induced temporary auditory threshold shifts. Presented at the American Speech and Hearing Association.

5. Drescher, D.G. (1976): Effect of temperature on cochlear responses during and after exposure to noise. JASA 59(2), 401-407.

6. Hawkins, J.E. Jr.(1971): The role of vasoconstriction in noise-induced hearing loss. Ann Otol Rhinol Laryngol 80, 903-914.

7. Lim, D. and Melnick, W. (1975): Mode of cochlear damage by excessive noise. In: Effects of Long Duration Noise Exposure on Hearing and Health, Editor: M.A. Whitcomb AGARD Conference Proceedings No. 171, C1-1-6.

8. Lipscomb, D.M. and Roettger, R. (1973): Capillary constriction in cochlear and vestibular tissues during intense noise stimulation. Laryngoscope 83, 259-263.

9. Spoendlin, H. (1967): Vascular stria. In: Submicroscopic Structure of the Inner Ear. Editor: S. Iurato. pp. 131-149. Pergamon Press, Oxford.

10. Vertes, D. and Axelsson, A. (1979): Methodological aspects of some inner ear vascular techniques. Acta Otolaryngol (Stockh) 88, 328-334.

11. Ward, W.D. and Duvall, A.J. (1971): Behavioral and ultrastructrual correlates of acoustic trauma. Ann Otol Rhinol Laryngol 80, 881-896.

12. Zar, J. (1974): Biostatistical Analysis. Prentice-Hall, New Jersey.

## FIGURES

1. Cochleogram (top) and vasculogram (bottom) from the left cochlea of a chinchilla which had it's body temperature elevated but was not exposed to noise. Even though this cochlea was classified normal in terms of hair cell loss (see text), substantial vascular changes were found throughout the length of the cochlea.

2. Cochleogram (top) and vasculogram (bottom) from the left cochlea of a chinchilla exposed to 160 dB impulse noise at elevated body temperature. The cochlea was classified in the low-level scattered loss category in terms of hair cell loss (see text) and the vascular changes are greatest in the area of the external wall corresponding to the region of the organ of Corti containing the narrow focal lesion.

3. Cochleogram (top) and vasculogram (bottom) from the left cochlea of a chinchilla exposed to 155 dB impulse noise at normal body temperature. This cochlea shows a mid-cochlear focal lesion (see text) and vascular changes which are evenly distributed throughout the length of the cochlea.

4. Cochleogram (top) and vasculogram (bottom) from the left cochlea of a chinchilla exposed to 155 dB impulse noise at normal body temperature. This cochlea showed severe hair cell loss (see text) and substantial vascular changes which are greatest in the area of the external wall corresponding to the maximal hair cell loss.

5. Schematic illustration of the vessels evaluated for vascular changes. The vessel of the tympanic lip in the osseous spiral lamina was also evaluated. SV = scala vestibuli, VM = vestibular membrane, SM = scala media, BM = basilar membrane, and ST = scala tympani.

6. Percentage of cochleas classified into each of the four categories in terms of hair cell loss. Group 1 = control, group 2 = temperature-elevation-only, group 3 = 155 dB impulse noise, group 4 = 155 dB impulse noise at elevated body temperature, group 5 = 160 dB impulse noise and group 6 = 160 dB impulse noise at elevated body temperature.

7. Composite vasculogram showing results of stepwise discriminant analysis by half cochlear turn including all six vessels. No difference was found between groups in the apical turn (3.0 and 2.5) but significant changes were found in the lower middle (1.5) and upper basal (1.0) turns.

TABLE I. VASCULAR PARAMETERS

| | |
|---|---|
| | RED BLOOD CORPUSCLES (RBCS) |
| DENS: | density; frequency and spacing of RBCs in vessel lumen |
| COL: | columns; number of rows of RBCs in vessel lumen |
| AGGREG: | aggregations and plasma gaps; collections of RBCs and interspaced sections with plasma but without RBCs |
| ORIENT: | orientation; manner and plane of RBCs in vessel lumen |
| VAR: | variability; in density of RBCs |
| PLAS: | plasma space; between RBC and vessel wall |
| | VESSEL LUMEN |
| LM IRRG: | lumen irregularity; local narrowing and widening of vessel lumen |
| PV LUM: | perivascular cell compressing lumen; occurrence of narrow vessel lumen caused by endothelial cell nuclei and/or pericytes |
| DIAM: | lumen diameter; width of vessel lumen |
| PVS: | perivascular spaces; spaces surrounding vessel lumen |
| | STRIA VASCULARIS |
| GRAN: | granules; pigment formed of fine granulations |
| PIGM: | pigment clumps; clusters or collections of granules |
| VAC: | vacuoles in strial surface structure |
| GAPS: | gaps between cells; spaces occurring between strial surface cells |
| | ADDITIONAL VASCULAR PARAMETERS |
| AVC: | avascular channels |
| WBC: | white blood cells |
| EMB: | emboli in vessel; bound, clear spaces within vessel lumen |
| DEP: | deposits; osmiophilic materials surrounding vessels |
| MEL: | melanocytes |
| SPH: | precapillary sphincter; narrowing of vessel by perivascular elements |

TABLE II. RESULTS OF HAIR CELL ANALYSIS

INNER HAIR CELL LOSS

| GROUP # | 1 | 2 | 3 | 4 | 5 | 6 |
|---|---|---|---|---|---|---|
| MEAN | 6 | 10 | 42 | 27 | 41 | 102* |
| SEM | 2 | 6 | 10 | 11 | 12 | 34 |

OUTER HAIR CELL LOSS

| GROUP # | 1 | 2 | 3 | 4 | 5 | 6 |
|---|---|---|---|---|---|---|
| MEAN | 205 | 110 | 932* | 416 | 546 | 2120* |
| SEM | 65 | 47 | 138 | 127 | 136 | 595 |

Results of one-way analysis of variance for inner and outer hair cell loss. Group 1 = control, group 2 = temperature-elevation-only, group 3 = 155 dB impulse noise, group 4 = 155 dB impulse noise + temperature elevation, group 5 = 160 dB impulse noise and group 6 = 160 dB impulse noise and temperature elevation. *denotes significant difference from control group.

TABLE III. RESULTS OF VASCULAR ANALYSIS

| | | VESSELS | | | | | |
|---|---|---|---|---|---|---|---|
| PARAMETERS | | RAL | VSVM | SVS | VSSP | CVL | VSTL |
| PLAS | ↓ | BOTH | NOISE | | BOTH | BOTH | NOISE |
| LM IRRG | ↑ | | BOTH | heat | | BOTH | NOISE |
| COL | ↓ | NOISE | | BOTH | | NOISE | |
| VAR | ↑ | | | | BOTH | | |
| PV LUM | ↑ | | NOISE | | | noise | heat |
| PIGM | ↑ | | | NOISE | HEAT | | |
| AVC | ↑ | | heat | | | | |
| DENS | ↓ | | heat | | | | |
| PVS | ↑ | | | | | heat | |
| GRAN | ↑ | | | noise | | | |
| GAPS | ↓ | | | noise | | | |
| WBC | ↑ | | | noise | | | |
| MEL | ↑ | | | | noise | | |

BOTH = statistically significant in all three stepwise discriminant analysis (SDA) procedures.

HEAT = significant in control vs. heat SDA and SDA including all six groups.

NOISE = significant in control vs. noise SDA and SDA including all six groups.

heat = significant in control vs. heat SDA.

noise = significant in control vs. noise SDA.

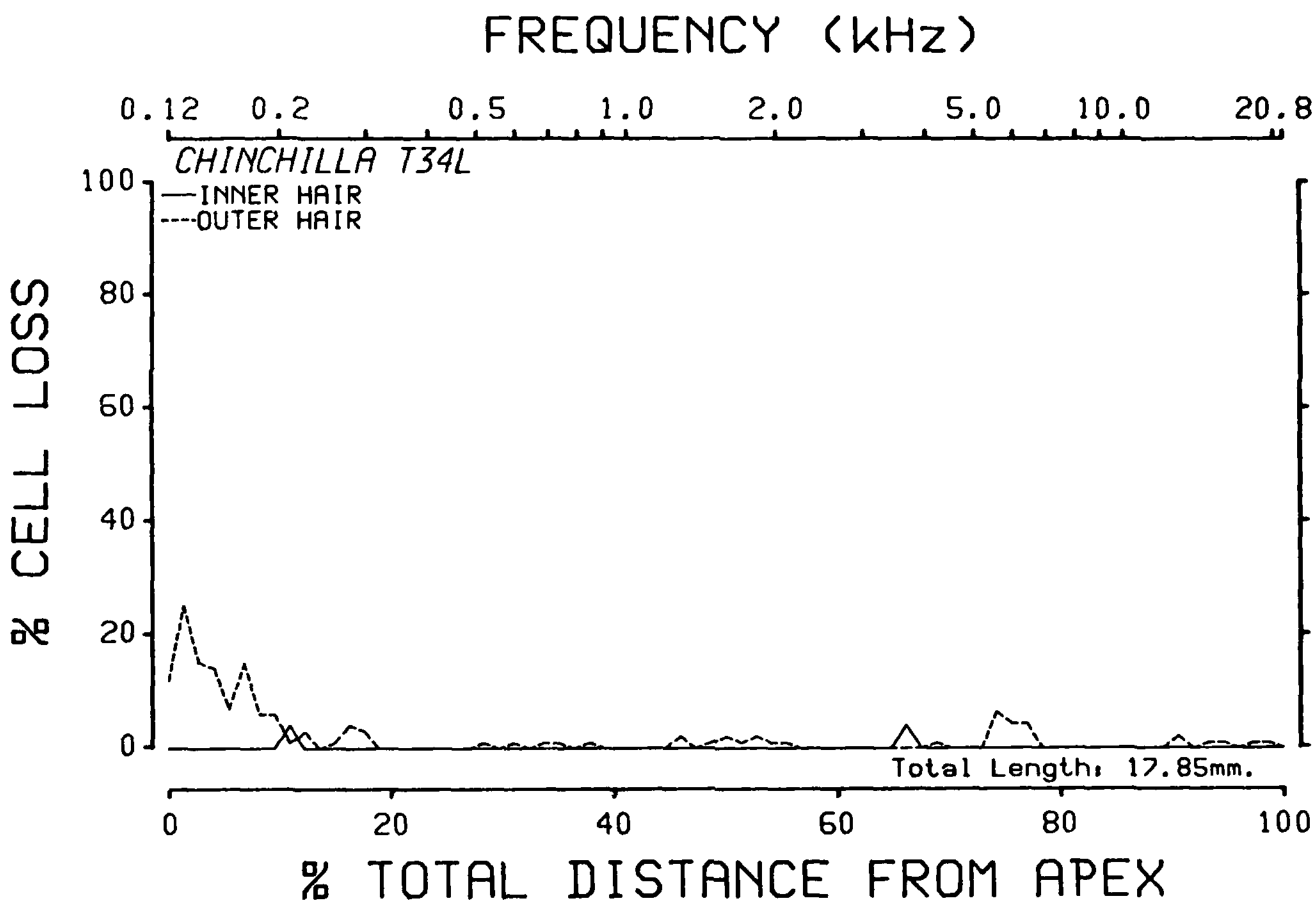
FREQUENCY (kHz)
0.12 0.2 0.5 1.0 2.0 5.0 10.0 20.8
CHINCHILLA T34L
—INNER HAIR
----OUTER HAIR
% CELL LOSS
100 80 60 40 20 0
Total Length: 17.85mm.
0 20 40 60 80 100
% TOTAL DISTANCE FROM APEX

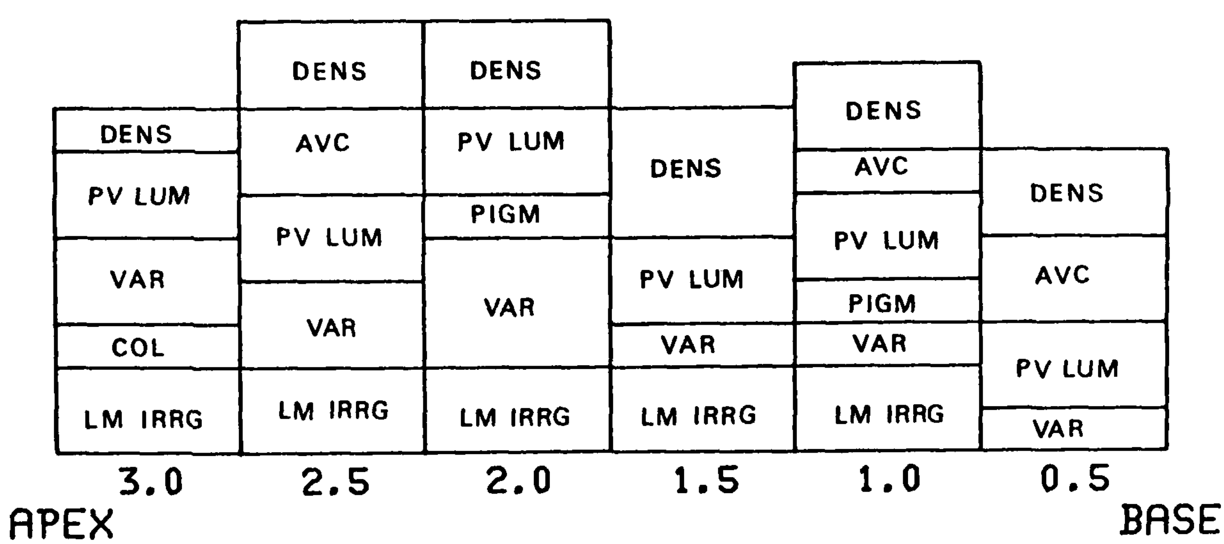
DENS
PV LUM
VAR
COL
LM IRRG
DENS
AVC
PV LUM
VAR
LM IRRG
DENS
PV LUM
PIGM
VAR
LM IRRG
DENS
PV LUM
VAR
LM IRRG
DENS
AVC
PV LUM
PIGM
VAR
LM IRRG
DENS
AVC
PV LUM
VAR
3.0 2.5 2.0 1.5 1.0 0.5
APEX
BASE

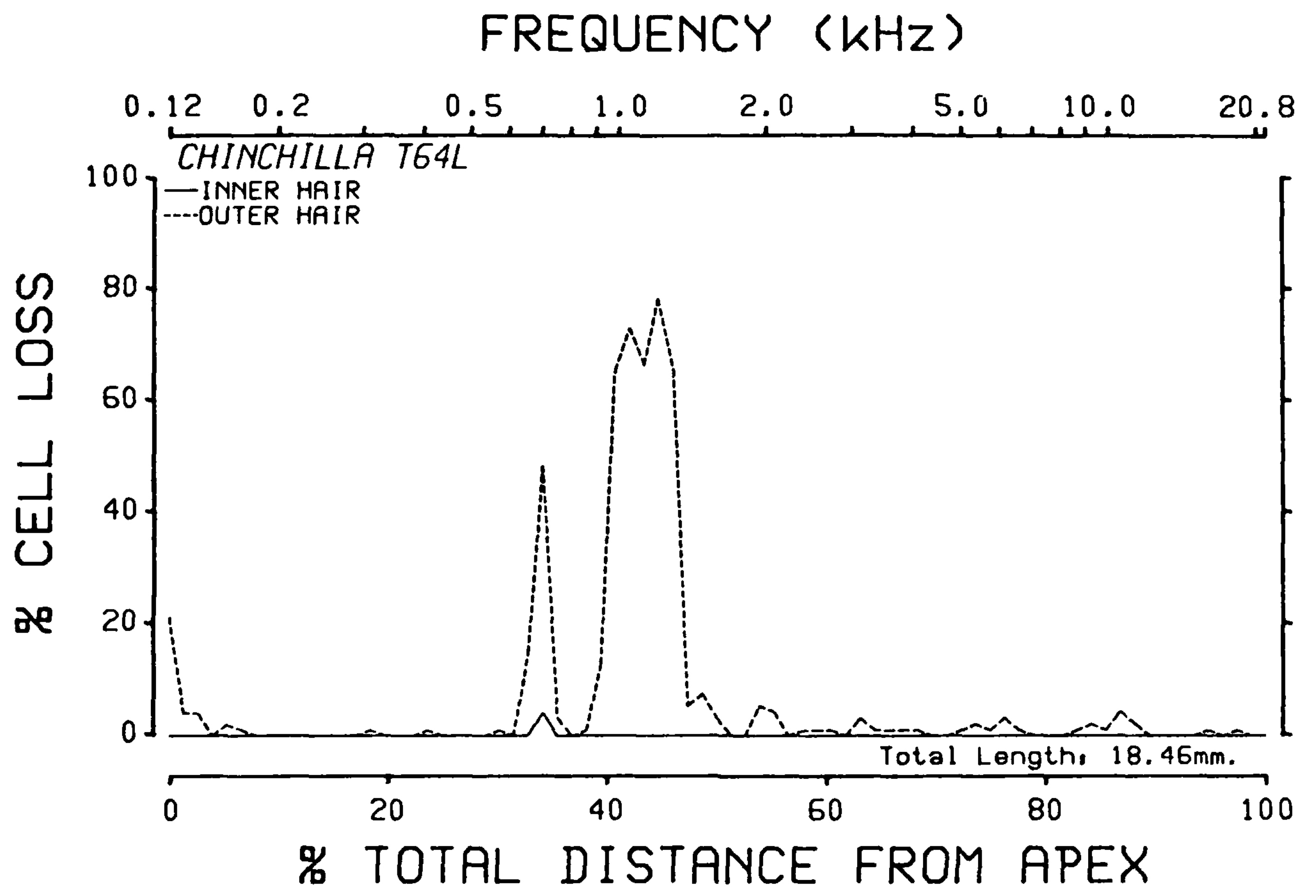
FREQUENCY (kHz)
0.12 0.2 0.5 1.0 2.0 5.0 10.0 20.8
CHINCHILLA T64L
—INNER HAIR
----OUTER HAIR
% CELL LOSS
100 80 60 40 20 0
Total Length: 18.46mm.
0 20 40 60 80 100
% TOTAL DISTANCE FROM APEX

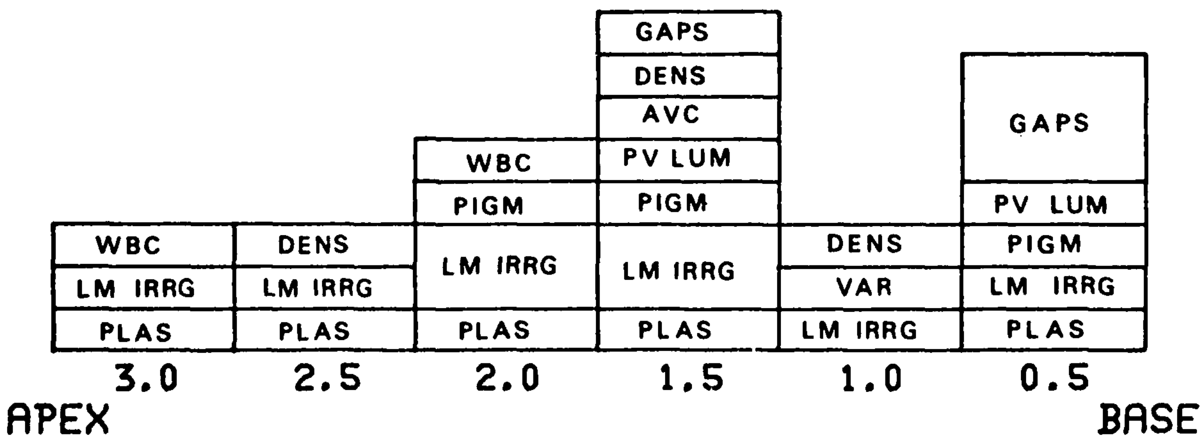
GAPS
DENS
AVC
WBC
PV LUM
PIGM
PIGM
GAPS
PV LUM
WBC
DENS
LM IRRG
LM IRRG
DENS
PIGM
LM IRRG
LM IRRG
LM IRRG
VAR
LM IRRG
PLAS
PLAS
PLAS
PLAS
LM IRRG
PLAS
3.0 2.5 2.0 1.5 1.0 0.5
APEX
BASE

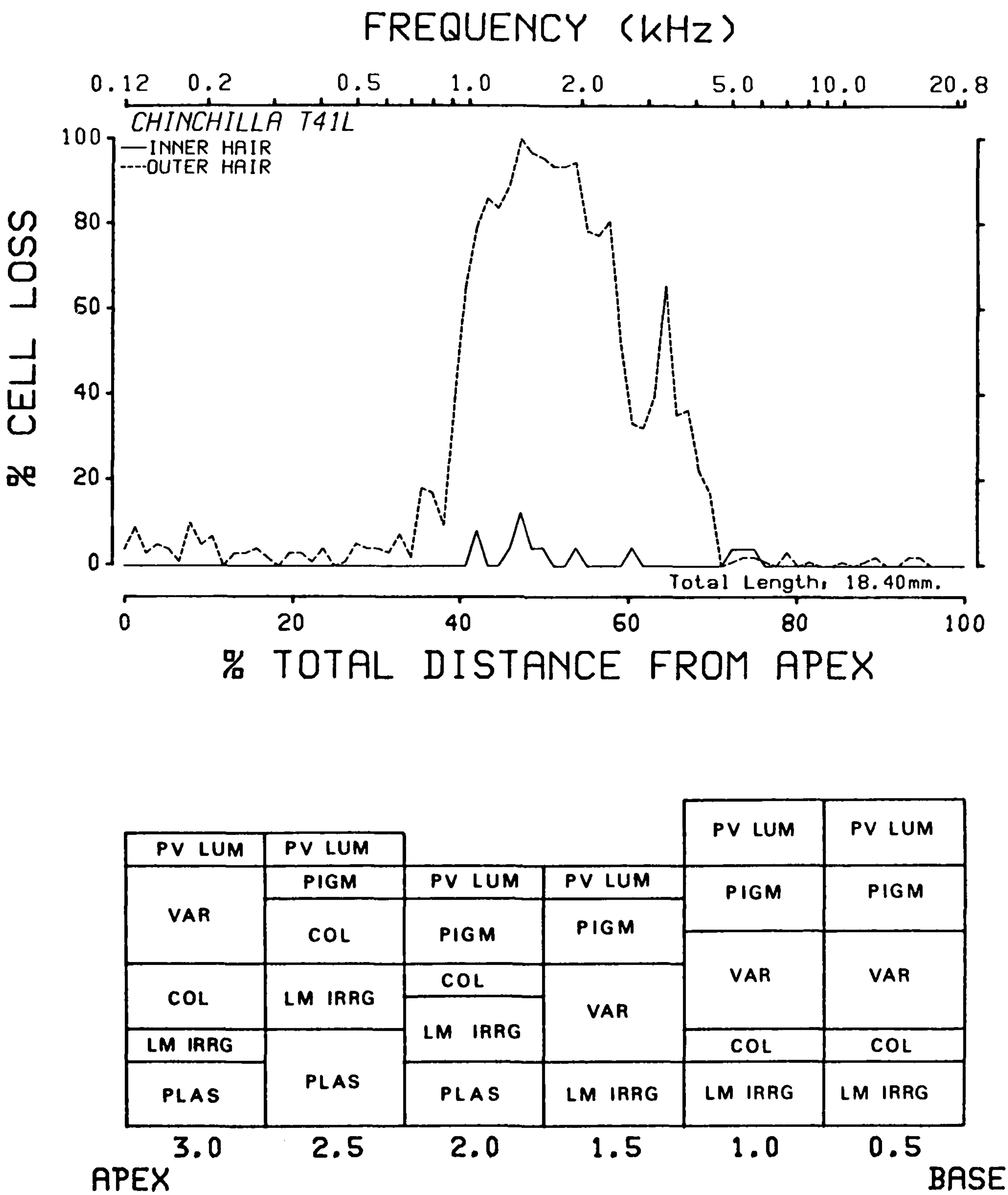
FREQUENCY (kHz)
0.12 0.2 0.5 1.0 2.0 5.0 10.0 20.8
CHINCHILLA T41L
—INNER HAIR
----OUTER HAIR
% CELL LOSS
0 20 40 60 80 100
Total Length, 18.40mm.
0 20 40 60 80 100
% TOTAL DISTANCE FROM APEX
PV LUM
VAR
COL
LM IRRG
PLAS
PV LUM
PIGM
COL
LM IRRG
PLAS
PV LUM
PIGM
COL
LM IRRG
PLAS
PV LUM
PIGM
VAR
LM IRRG
PV LUM
PIGM
VAR
COL
LM IRRG
PV LUM
PIGM
VAR
COL
LM IRRG
3.0 2.5 2.0 1.5 1.0 0.5
APEX
BASE

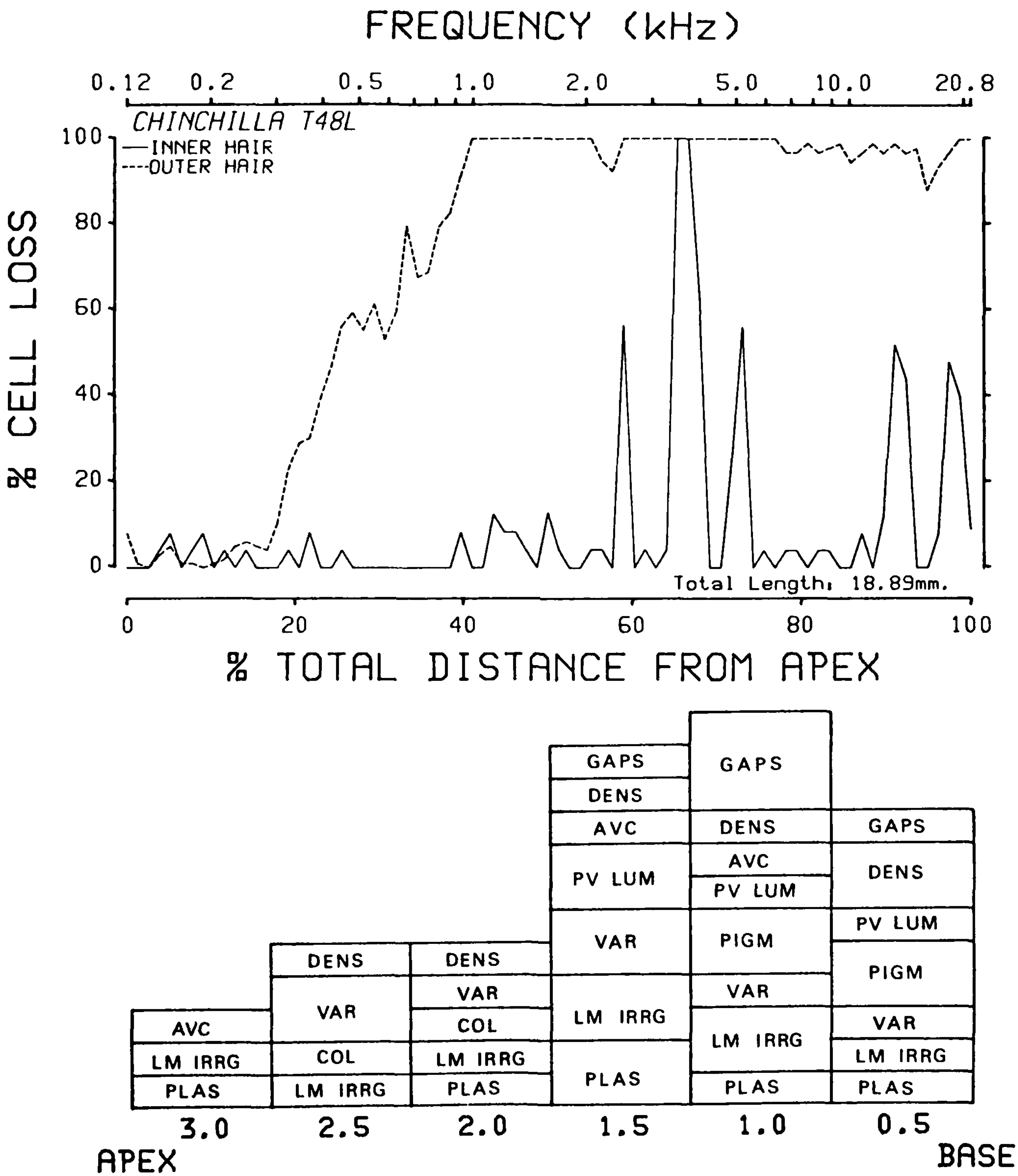
FREQUENCY (kHz)
0.12 0.2 0.5 1.0 2.0 5.0 10.0 20.8
CHINCHILLA T48L
—INNER HAIR
----OUTER HAIR
% CELL LOSS
100 80 60 40 20 0
Total Length: 18.89mm.
0 20 40 60 80 100
% TOTAL DISTANCE FROM APEX
AVC
LM IRRG
PLAS
DENS
VAR
COL
LM IRRG
DENS
VAR
COL
LM IRRG
PLAS
GAPS
DENS
AVC
PV LUM
VAR
LM IRRG
PLAS
GAPS
DENS
AVC
PV LUM
PIGM
VAR
LM IRRG
PLAS
GAPS
DENS
PV LUM
PIGM
VAR
LM IRRG
PLAS
3.0 2.5 2.0 1.5 1.0 0.5
APEX
BASE

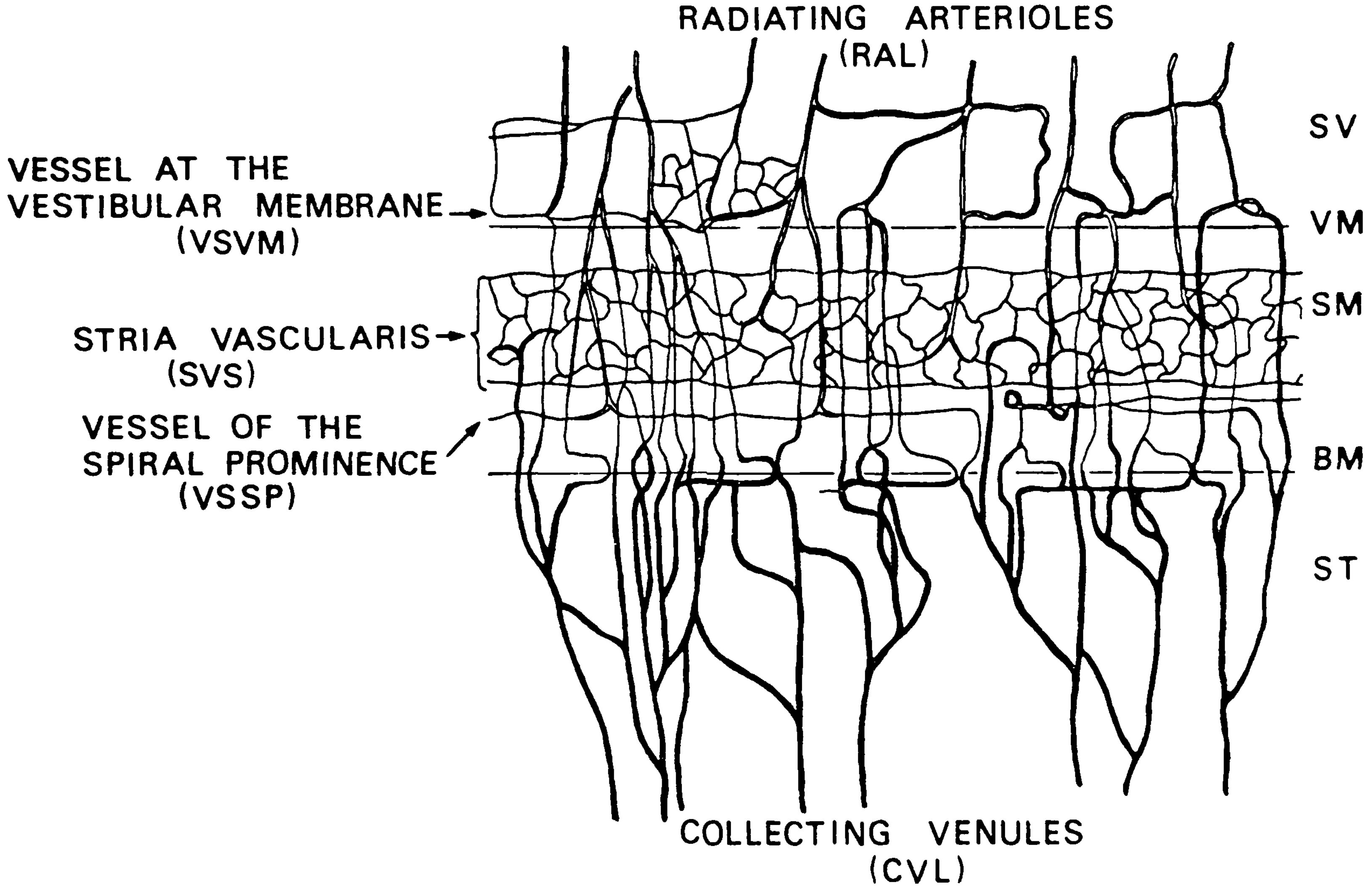
RADIATING ARTERIOLES
(RAL)
SV
VESSEL AT THE
VESTIBULAR MEMBRANE
(VSVM)
VM
SM
STRIA VASCULARIS
(SVS)
VESSEL OF THE
SPIRAL PROMINENCE
(VSSP)
BM
ST
COLLECTING VENULES
(CVL)

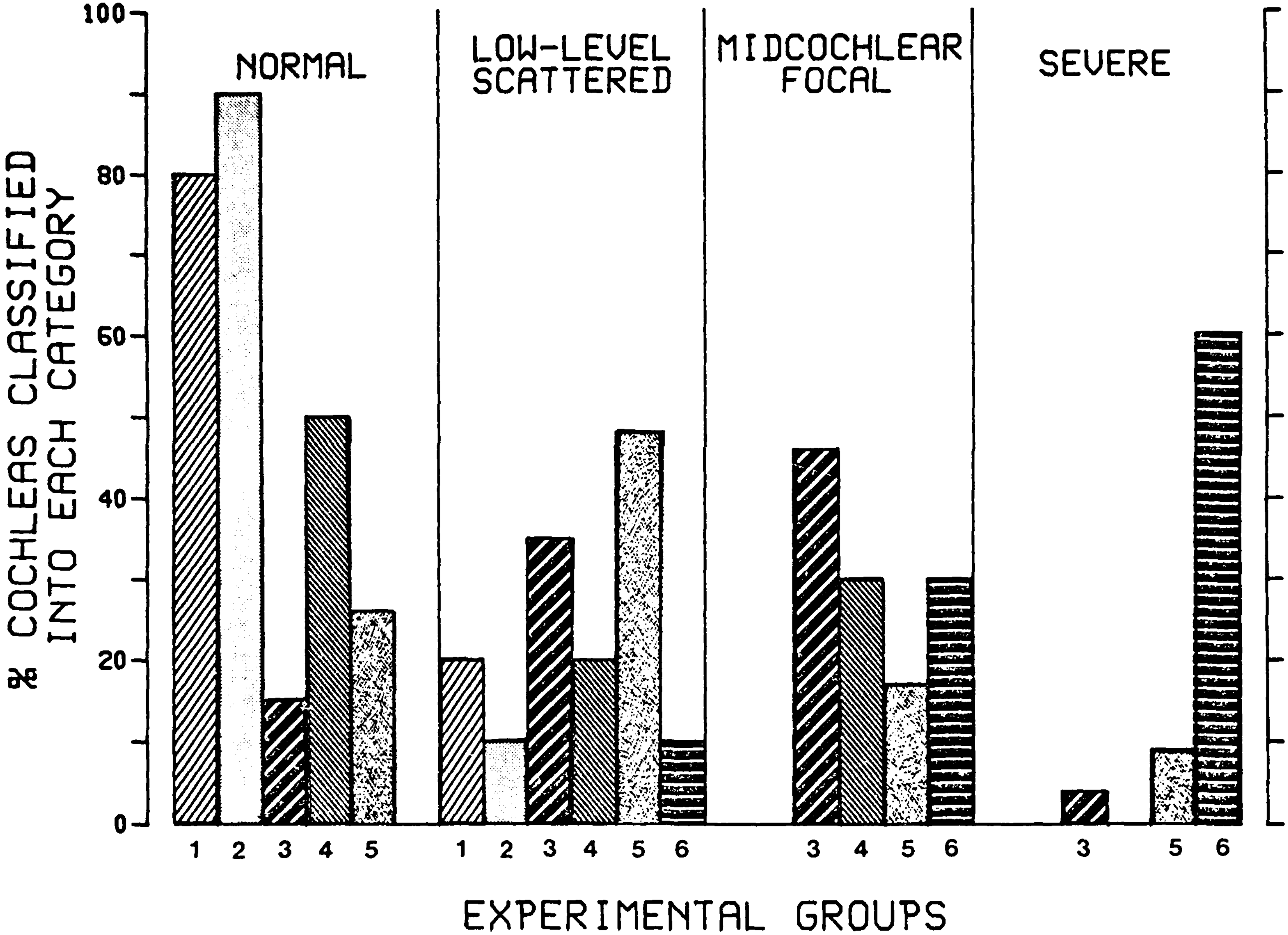

% COCHLEAS CLASSIFIED INTO EACH CATEGORY
100
80
60
40
20
0
NORMAL
LOW-LEVEL SCATTERED
MIDCOCHLEAR FOCAL
SEVERE
1 2 3 4 5
1 2 3 4 5 6
3 4 5 6
3 5 6
EXPERIMENTAL GROUPS

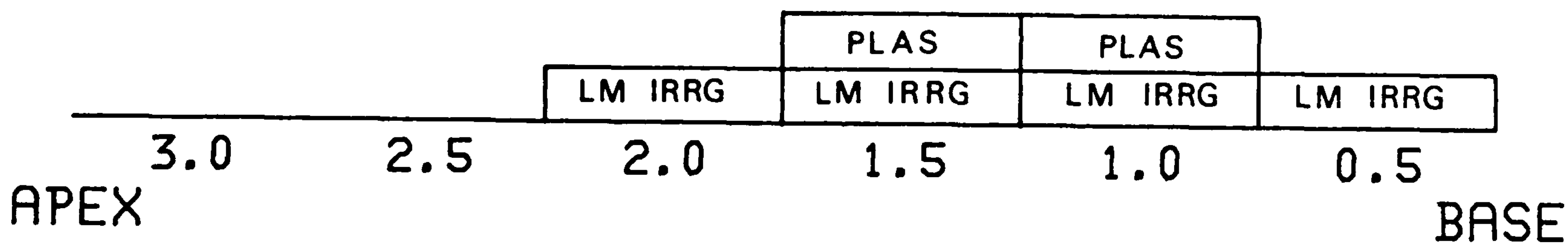
PLAS
PLAS
LM IRRG
LM IRRG
LM IRRG
LM IRRG
3.0
2.5
2.0
1.5
1.0
0.5
APEX
BASE

END

10-86

DTIC